NASA CR- 132735

Reacting Fluids Laboratory
Department of Chemical Engineering
Louisiana State University

COUPLED RADIATING SHOCK LAYERS WITH FINITE RATE CHEMISTRY EFFECTS

(NASA-CR-132735) COUPLED RADIATING SHOCK LAYERS WITH FINITE RATE CHEMISTRY EFFECTS. PART 2: ANALYSIS OF THE INTERACTION OF ABLATING PROTECTION SYSTEMS AND STAGNATION REGION HEATING (Louisiana State Univ.)
N75-30213
Unclas
G3/13 33058

Final Report, Part II on
NASA GRANT NGR 19-001-059

Analysis of the Interaction of Ablating Protection Systems and Stagnation Region Heating

by

Ralph W. Pike, Co-principal Investigator
Richard C. Farmer, Co-principal Investigator
John F. Balhoff, [illegible]aduate Associate

1975

for

Langley Research Center
National Aeronautics and Space Administration

June 1, 1975
Baton Rouge, Louisiana

PREFACE

This is the fourth in a series of final reports and completes the documentation of research on NASA Grant NGR 19-001-059. It also served as the Ph.D. dissertation for John F. Balhoff.

COUPLED RADIATING SHOCK LAYERS
WITH FINITE RATE CHEMISTRY EFFECTS

A Dissertation

Submitted to the Graduate Faculty of the
Louisiana State University and
Agricultural and Mechanical College
in partial fulfillment of the
requirements for the degree of
Doctor of Philosophy

in

The Department of Chemical Engineering

by

John Frederick Balhoff
B.S.Ch.E., Louisiana State University, 1970
M.S.Ch.E., Louisiana State University, 1972
May, 1975

ACKNOWLEDGEMENTS

This research was performed under the direction of Dr. Ralph W. Pike, Professor of Chemical Engineering at Louisiana State University. His encouragement and guidance are gratefully acknowledged.

Appreciation is also expressed to the National Aeronautics and Space Administration's Langley Research Center which sponsored this research and, especially to James N. Moss, Grant Monitor, for his helpful discussions on numerical problems encountered in this research.

An acknowledgement is extended to the Charles E. Coates Memorial Fund of the L.S.U. Foundation for funds to pay a portion of the typing cost of the dissertation and to the L.S.U. Computer Research Center for the use of their facilities during the course of this research.

Special thanks are given to friends Simon Hacker, Hazel LaCoste, Suresh Vora and countless others who unselfishly gave their help and friendship when it was most needed. Thanks are also extended to Mona Davis who typed the manuscript.

TABLE OF CONTENTS

Page

ACKNOWLEDGEMENTS ii

LIST OF TABLES vi

LIST OF FIGURES viii

ABSTRACT xii

CHAPTER

I INTRODUCTION AND BACKGROUND 1
 Introduction 1
 The Problems of Atmospheric Entry 1
 The Charring Ablator 7
 Flow Field Interaction 10
 Summary 14
 References 15

II A REVIEW OF RADIATING AND NONEQUILIBRIUM FLOW FIELDS 17
 Introduction 17
 Radiating Solutions 17
 Nonequilibrium Chemistry Solutions 35
 Summary 43
 References 45

III DEVELOPMENT OF THE THIN SHOCK LAYER EQUATIONS . . . 50
 Introduction 50
 The Physical Environment 51
 The Conservation Equations 55
 The Thin Shock Layer Equations 61
 Nondimensionalized and Transformed Equations . . . 63
 Boundary and Initial Conditions 68
 Boundary Conditions at the Bow Shock 68
 Boundary Conditions at the Ablator Surface 71
 Initial Conditions 81
 Shock Geometry 88
 Quasilinearization of Shock Equations 90
 Summary 93
 References 95

CHAPTER Page

IV TRANSPORT, THERMODYNAMIC, RADIATION AND KINETIC PROPERTIES 97

Introduction. 97
Chemical Kinetics 98
Transport Properties. 103
Thermodynamic Properties 109
Radiation Properties. 112
Summary 115
References 119

V NUMERICAL IMPLEMENTATION OF THE SHOCK LAYER EQUATIONS. 121

Introduction 121
Coupled Ablation Flow Field Analysis 122
Numerical Solution of the Conservation Equations. . 124
Global Continuity 127
Calculation of $\partial\eta/\partial x$ 129
y-Momentum Equation 130
Boundary Conditions 131
Stability of the Energy Equation. 137
Damping Coefficients 148
Shock Standoff Distance 149
Initial Profiles. 154
Iteration Sequence 156
Convergence 159
Summary 162
References. 164

VI RESULTS OF THE SHOCK LAYER ANALYSIS. 165

Introduction. 165
Stagnation Region Heating 166
Comparison with Other Stagnation Line Investigators 175
Around the Body Results 182
Radiation-Chemical Reactions Interaction 195
Species Boundary Conditions 214
Computation Time and Core Usage 219
Summary 223
References 224

VII CONCLUSIONS AND RECOMMENDATIONS. 226

Conclusions 226
Recommendations 228

NOMENCLATURE. 229

APPENDIX Page

A ENERGY TRANSFER IN THE CHAR ZONE 234

Introduction 234
Development of the Char Zone Analysis 235
Padé Numerical Integration Technique. 242
Energy Equation Solution. 246
Results of the Char Analysis 247
Summary 255
References 258

B MODELING SUBLIMATION OF A CHARRING ABLATOR 259

Introduction. 259
Model Description 259
Results of Analysis 264
Conclusions 267
References 269

C POLYNOMIAL COEFFICIENTS FOR THERMODYNAMIC PROPERTIES 270

D USERS INSTRUCTIONS FOR CRAC COMPUTER PROGRAM 274

E CRAC SOURCE DECK, SAMPLE INPUT, AND SAMPLE OUTPUT. . 284

VITA 446

LIST OF TABLES

TABLE		Page
3.1	Nondimensional Thin Shock Layer Equations	65
4.1	Shock Layer Reactions with Kinetic Coefficients	101
4.2	Additional Ablation Product and Combustion Reactions	104
4.3	Additional Air and Hydrogen Combustion Reactions	105
4.4	Empirical Constants for Viscosity Correlation	106
4.5	Empirical Constants for Thermal Conductivity Correlation	108
4.6	Collision Parameters Employed in the Current Study	110
4.7	Species Considered in LRAD Radiation Model	116
5.1	Curve Fit Coefficients for Heat Conducted through the Surface of a Phenolic Nylon Ablator	134
5.2	Compositions at the Surface of a Phenolic Nylon Ablator	136
5.3	Insensitivity of Heating to Convergence of Shock Standoff Distance	153
5.4	Nodal Convergence in Tangential Direction	161
6.1	Freestream and Ablator Conditions for Cases Studied in the Present Investigation	167
6.2	Heating Rate Results for Cases Studied in the Present Investigation	169
6.3	Comparison of Moderate Heating Rate Results	176
6.4	Comparison of Severe Heating Rate Results	179

TABLE Page

6.5 Frequency Factors for Three Finite Rate Cases for Selected Reactions in the Shock Layer 197

6.6 Species Composition at the Ablator Surface 217

6.7 Elemental Composition of a Phenolic Nylon Ablator 218

A.1 Curve Fit Coefficients for Heat Conducted through the Surface of a Phenolic Nylon Ablator 250

A.2 Species Compositions at the Char-Decomposition Zone Interface. 252

A.3 Species Compositions at the Ablator Surface on the Char and Flowfield Sides. 254

A.4 Chemical Reactions Occurring in the Char Layer . . 256

B.1 Accomodation Coefficients and Arrhenius Coefficients for Vapor Pressure of C_1, C_2, and C_3 261

B.2 Representative Pyrolysis Product Composition of 40% (by weight) Nylon - 60% (by weight) Phenolic Resin Ablative Composite 263

C.1 Polynomial Coefficients for Thermodynamic Property Correlations 271

D.1 CRAC Input Variables 279

D.2 Description of CRAC Subroutines 282

LIST OF FIGURES

FIGURE		Page
1.1	Expected Earth Entry Velocities for Several Planetary Missions	2
1.2	Peak Stagnation Point Heating Rates	3
1.3	Flight Regimes	5
1.4	Schematic of Ablator Energy Absorption Mechanisms	8
1.5	Heat Rejection Mechanisms for a Phenolic Nylon, Blunt Body Ablator	8
1.6	Illustration of Charring-Ablator and Flowfield Interaction	11
1.7	Illustration of Heat Transfer Mechanisms in Ablating Thermal Protection Systems	13
2.1	The Effect of Mass Injection on Surface Flux Reduction	24
2.2	Computation Time for Various Numbers of Chemical Species	37
3.1	Flight Regimes	53
3.2	Body-Oriented Coordinate System	58
3.3	Resolution of Velocity Components in a Body Oriented Coordinate System	69
3.4	Illustration of Flowfield Coupling and Quasi-steady Ablator Response	80
4.1	Spectral Absorption Coefficient of Air-Carbon Phenolic Ablation Products Mixture for P=1 and T=16,000°K	114
4.2	Comparison of Dimensionless Radiative Heating Rates	117

FIGURE Page

5.1 Simplified Flow Diagram of Coupled Shock Layer Analysis 123

5.2 Crank Nicolson Finite Difference Grid 125

5.3 Ablator Heating Response vs. Mass Loss Rate 133

5.4 Coupling of the Shock Layer to the Ablator by a Surface Energy Balance 138

5.5 Dimensionless Blowing Rate Profile Around the. . . . 139 Body

5.6 Dimensionless Heating Rate Profile Around the Body-Coupled 140

5.7 Instability of the Temperature Form of the Energy Equation 142

5.8 Illustration of the Effect of Temperature Variations Upon Radiative Flux Divergence. 143

5.9 Stable Enthalpy Profiles Using Enthalpy Form of the Energy Equation 145

5.10 Stable Temperature Profiles Using Enthalpy Form of the Energy Equation. 146

5.11 Variation in Equilibrium Chemistry Temperature Profiles from Iteration to Iteration Using the Temperature Form of the Energy Equation 147

5.12 Convergence of Shock Angle, ε, Around the Body . . . 151

5.13 Convergence of Shock Shape Profile Around the Body 152

5.14 Dimensionless Temperature Profile for Initial Estimate at Stagnation Line 157

5.15 Iteration Sequence of Shock Layer Analysis 158

6.1 Stagnation Heating Rate at a Phenolic Nylon Ablator Surface Along Reentry Trajectory 168

6.2 Reentry Trajectory for Present Investigation 170

6.3 Effectiveness of Heat Absorption Mechanisms for a Phenolic Nylon Ablator Along the Reentry Trajectory 173

FIGURE Page

6.4 Mass Loss Rate at the Stagnation Line of a Phenolic Nylon Ablator Along the Reentry Trajectory 174

6.5 Dimensionless Blowing Rate Profile Around the Body 185

6.6 Dimensionless Heating Rate Profile for Case 1 - Coupled. 186

6.7 Dimensionless Heating Rate Profile for Case 2 - Coupled 187

6.8 Dimensionless Heating Rate Profile for Case 3 - Coupled 188

6.9 Dimensionless Heating Rate Profile for Case 4 - Coupled 189

6.10 Ablator Surface Temperature Profiles for Cases Studied 191

6.11 Dimensionless Temperature Profiles for the Stagnation Line and Downstream 192

6.12 Comparison of Investigators 193

6.13 Comparison of Flux Divergence Profiles for Various Kinetic Models 200

6.14 Species Profiles for "Fast Perturbation" Kinetics Case at the Stagnation Line 201

6.15 Species Profiles for "Slow Perturbation" Kinetics Case at the Stagnation Line 202

6.16 Species Profiles for "Best" Kinetics Case at the Stagnation Line 203

6.17 Species Profiles for Equilibrium Chemistry at the Stagnation Line 204

6.18 Effects of Carbon Atom and Molecular Radiative Coupling on the Temperature Profile and Radiative Heating 206

6.19 Species Profiles for Nonequilibrium Chemistry at a Severe Heating Load at the Stagnation Line 211

FIGURE Page

6.20 Species Profiles for Equilibrium Chemistry
at a Severe Heating Load at the Stagnation
Line 213

6.21 Comparison of Radiative Flux Divergence
Profiles for Severe Heating Rate Conditions
of Equilibrium and Finite Rate Analyses 215

6.22 Comparison of Radiative Flux Divergence
Profiles for Equilibrium and Nonequilibrium
Walls at the Stagnation Line 220

A.1 Flow in the Char Zone 236

A.2 Ablator Heating Response vs. Mass Loss Rate 248

A.3 Decomposition Zone Heat Absorption Rate 251

A.4 Temperature at Char-Decomposition Zone
Interface 253

B.1 Comparison of the Hertz-Knudsen Analysis
with Other Investigators 265

B.2 Predominant Carbon Vapor Species From the
Sublimation of a Charring Phenolic Nylon
Ablator 268

D.1 CRAC Overlay Structure 277

ABSTRACT

The conservation equations that describe the mass, momentum, and energy transfer in the shock layer around an ablating blunt body were developed and placed into numerical solution form. Effects of line and continuum radiation along with finite rate chemistry were considered. Sixteen chemical reactions with 19 chemical species were included in the analysis, and 12 of these species were employed in the radiative flux divergence calculation. The shock layer was coupled to a phenolic-nylon charring ablator through a surface energy balance.

The resulting conservation equations were a set of parabolic integro-partial differential equations which were quasilinearized and solved using the Crank-Nicolson implicit numerical technique. The partial differential equations required two sets of boundary conditions and one set of initial conditions. The boundary conditions were specified at the shock using the Rankine-Hugoniot relations and conditions at the ablator were determined by employing the nonequilibrium Hertz-Knudsen equation for sublimation and surface energy balance. The stagnation line equations are a set of ordinary integro-differential equations which supply the initial conditions for the analysis. The same boundary conditions were employed at the stagnation line as for the shock layer solution.

Results are presented for coupled solutions at six key points along a reentry trajectory for the stagnation line. Four of these six

solutions were continued around-the-body. A study was also performed to determine the uncertainty in radiative heating due to the uncertainty in chemical kinetic data.

On the basis of this research, it was concluded that the numerical solution of the quasilinearized conservation equations yielded stable and accurate solutions to the nonequilibrium, radiating shock layer surrounding a blunt reentry body. These nonequilibrium solutions, when compared to equilibrium solutions at comparable conditions yielded consistently lower wall radiative heating rates. The difference was most pronounced at low heating rates (e.g. 121 BTU/sq. ft-sec for nonequilibrium) where the equilibrium results were 190% higher. At higher heating rates (~2000 BTU/sq. ft-sec) the equilibrium results were found to be generally less than 20% higher than nonequilibrium. The species profiles for low heating rates differed significantly especially in the air layer from the nonequilibrium and equilibrium analyses whereas the species profiles for the high heating rate cases were very similar.

For the around-the-body analyses, it was observed that one nondimensional blowing profile along the ablator surface was sufficient for all four cases to adequately couple the shock layer with the ablator response. The coupling between ablator and shock layer was found to differ by only 16% for the worst case.

The choice of species boundary conditions at the ablator wall does not greatly affect the shock layer solution. The surface heating rate was found to differ by only 4% for the case of a nonequilibrium wall versus an equilibrium wall. However, the choice of species boundary conditions at the shock does appear to affect the solution. The species composition at the shock were assumed to be equilibrium. In light of the results of this investigation, the assumption of equilibrium appears to be inaccurate (especially at low heating rates) and further study is recommended in this area.

One of the major problems encountered in this study was the tremendous amount of computer time necessary. Over 100 hours of computer time on an IBM 360/65 computer was required. The specification of a correct shock standoff distance did not alter the heating rate analysis, but the amount of computer time was found to decrease significantly when the converged shock standoff distance was used. It is felt that more study is needed in the area of shock standoff calculations.

CHAPTER I

INTRODUCTION AND BACKGROUND

Introduction

Aerodynamic heating is one of the most severe problems encountered by a reentry vehicle when returning from interplanetary missions. A reentry vehicle with a blunt body configuration and having a charring ablative heat shield has been found to be the most effective design for combatting this problem. This chapter discusses the advantages of the blunt body configuration over other alternatives and presents a detailed description of the processes which occur in a charring ablator and its surrounding flow field environment. The description includes a comprehensive overview of the intricate heat and mass transport mechanisms involved in the ablative heat shield and the shock heated air layer flowing over the reentry capsule.

The Problem of Atmospheric Entry

A reentry vehicle encounters extreme heating during hyperbolic atmospheric entry when utilizing aerodynamic braking. This heating is a result of applying the frictional resistance of the atmosphere to decrease the speed of the vehicle. Since kinetic energy ($KE = MV^2/2$) is a function of the square of the velocity, it is necessary to know the ranges of relevant velocities for manned missions. In Figure 1.1 these ranges for flights to the planets and and the ranges encountered by Apollo are given. Notice that Apollo

Figure 1.1

Expected Earth Entry Velocities for Several Planetary Missions

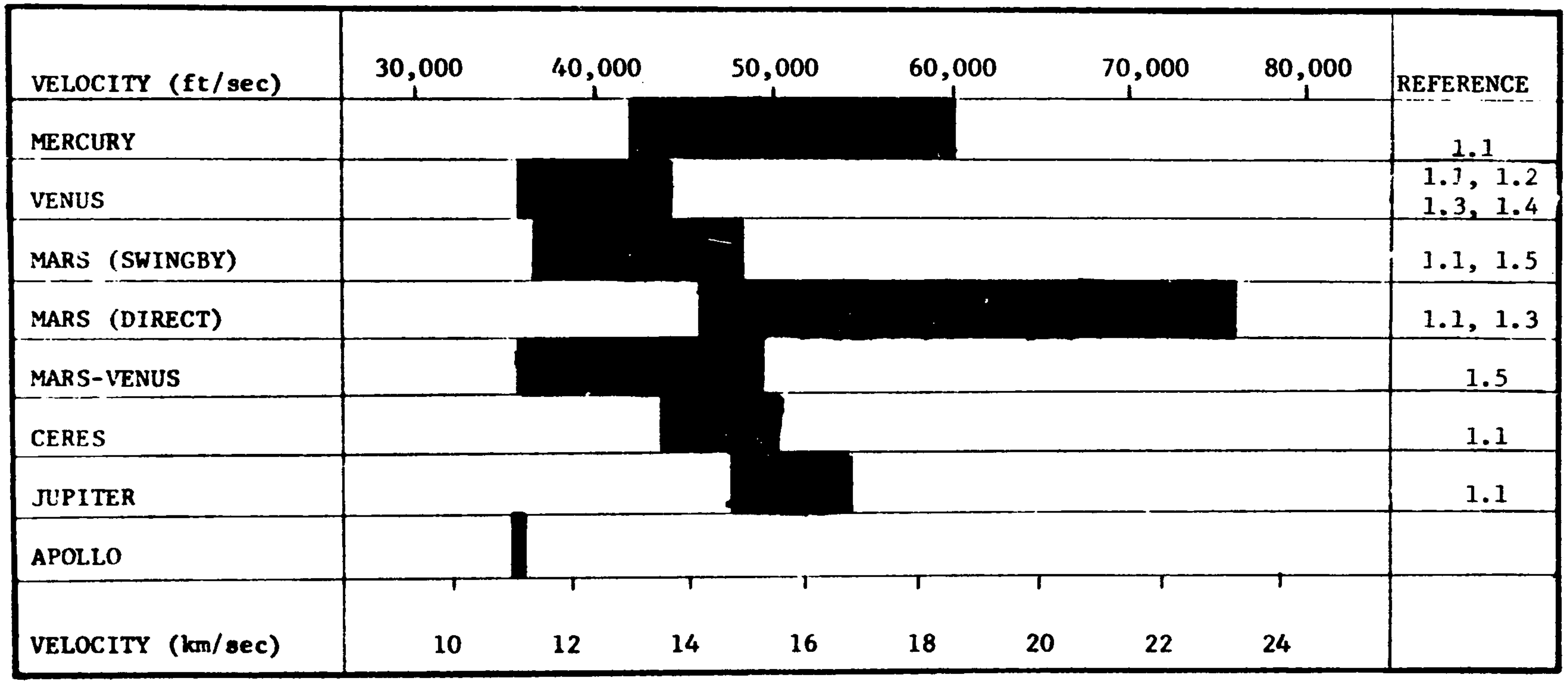

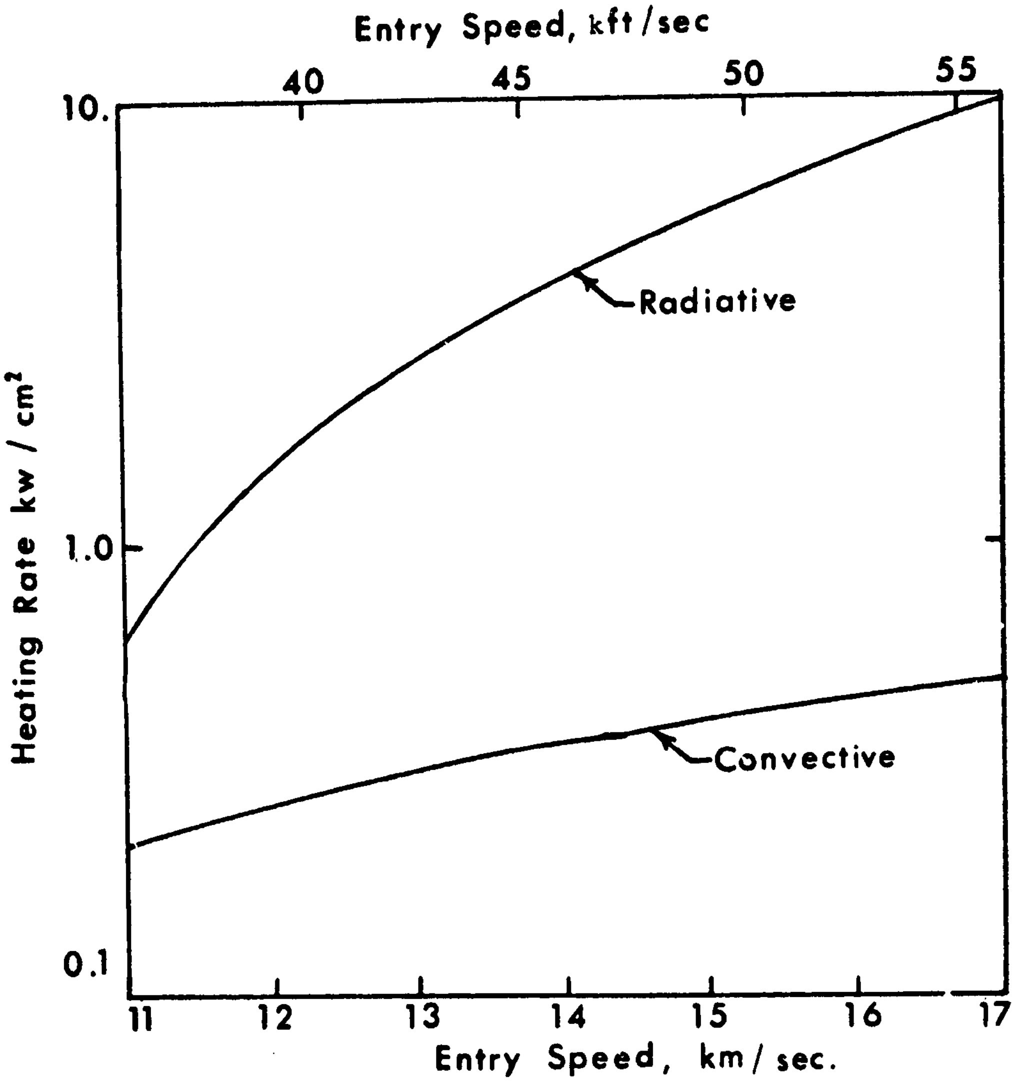

Figure 1.2. Peak Stagnation Point Heating Rates (Ref. 1.1).

has the lowest return velocity range. This kinetic energy upon renetry is transformed into thermal energy and a bow shock wave is formed. Passing through the shock wave, the air is heated as it flows over the heat shield of the reentry vehicle. The air layer then transfers a portion of this heat to the surface of the space capsule primarily by convection and radiation. The relative importance of convective and radiative heating can be seen in Figure 1.2. Note that radiation heat transfer becomes increasingly important as the reentry velocity increases. Thus, it is extremely important to have a reasonable description of the radiative transport mechanisms for return from planetary missions where the velocities are much higher than Apollo. In Figure 1.3, the region where radiative heat transfer is significant is shown.

The alternative to aerodynamic braking would be to slow down the vehicle by using reverse thrust. Since the return velocity is of the same magnitude as the launch velocity, the reverse thrust method requires the same amount of fuel for reentry, therefore doubling the fuel requirement and adding unnecessary weight. In terms of weight efficiency for entry deceleration, an ablation protection system requires 10 to 50 times less entry vehicle weight than would be required by the reverse thrust method (Ref. 1.7). Excessive weight on a return capsule is quite prohibitive since it has been estimated that each kilogram carried throughout a manned planetary mission can represent between 300 and 1000 kg on the launch pad (Ref. 1.1). On this basis, excess weight cannot be tolerated especially in the return phase of the mission and reverse thrust becomes unsuitable.

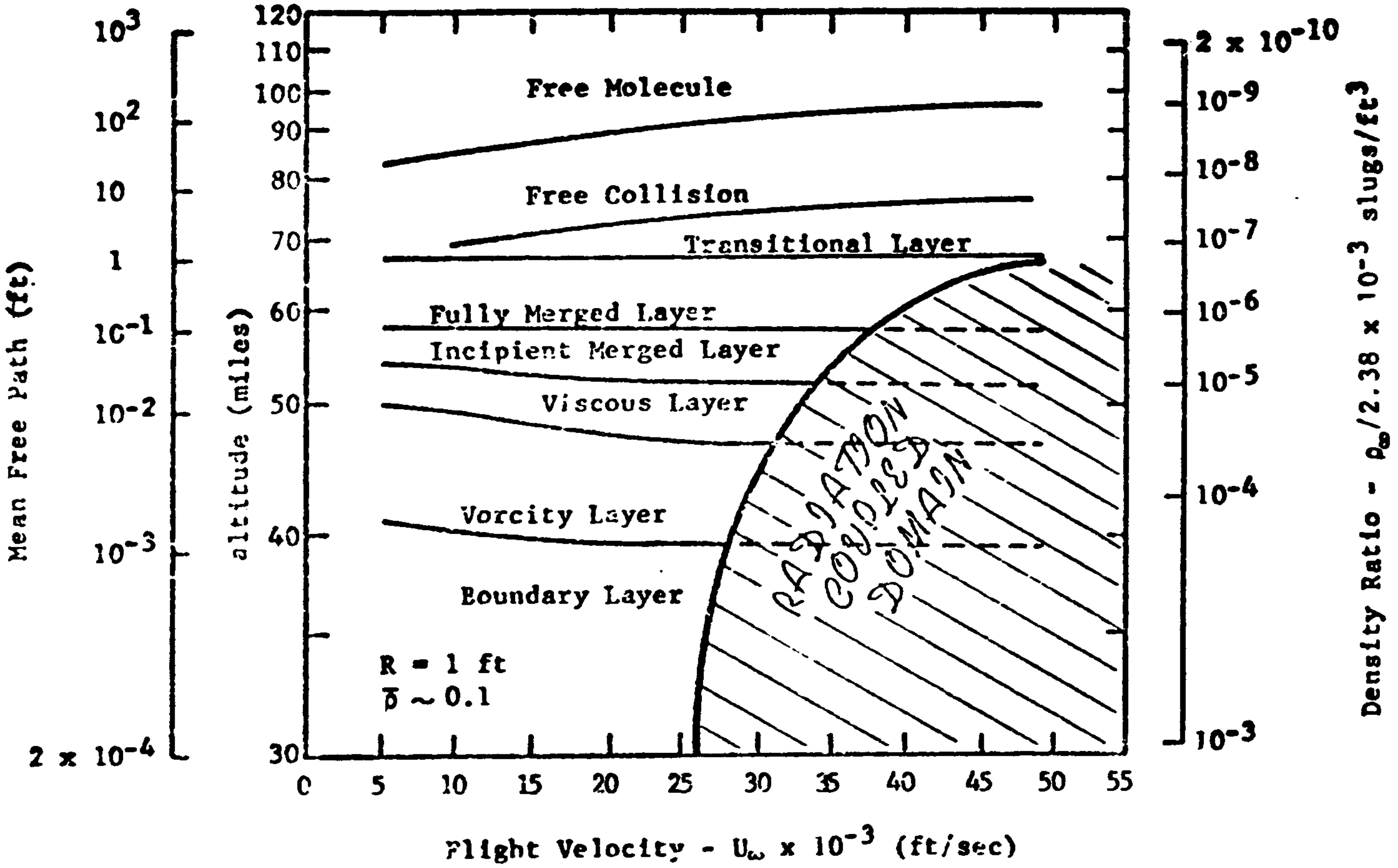

Figure 1.3. Flight Regimes (Modified from Ref. 1.6)

First it was thought that a slender body would be the logical design. The slender body does have the smallest aerodynamic drag. However, this shape produces a weak, attached shock wave and a large percentage of the heat generated on reentry is absorbed by the body. Slender body configurations are best suited for ballistic missiles and supersonic flow applications where low heating loads are experienced for short durations (Ref. 1.8).

The blunt or high drag configuration is more applicable to reentry of space vehicles since these have a much larger fraction of the total energy transfer to the atmosphere. An extremely strong, detached shock wave is formed around the blunted vehicle causing a major portion of the energy to be absorbed by the air flowing between the shock wave and the vehicle surface. This energy is then carried away in the wake behind the craft. The shock heated layer surrounding the vehicle becomes progressively hotter during the course of reentry causing dissociation and ionization of the air. Heat is transferred by convection and radiation to the capsule surface from the shock layer. The amount of heat transferred to the space craft is enough to cause surface temperatures of the order of 3600°K. This high temperature occurs despite the fact that most of the heat has been diverted away from the craft by using the blunt body configuration. The space capsule cannot survive these temperatures unless an efficient thermal protection system is used. The answer to heat shielding of reentry vehicles was the charring ablator which is discussed subsequently.

The Charring Ablator

To dissipate the tremendous amount of heat that is generated at reentry, several methods were suggested (Ref. 1.9, 1.10, 1.11). These are (1) Heat Sink, (2) Radiation Cooling, (3) Transpiration Cooling, (4) Convection Cooling, (5) Film Cooling, and (6) Ablative Cooling. The most important of these is ablative cooling since it combines the advantages of all of the other methods. The combination of wide range of application with high reliability made the system extremely successful.

The charring ablator is a special type of ablator with qualities which make it a superb heat shielding material. The charring ablator utilized several mechanisms to reduce the heat transferred to the interior of the space craft. This type of ablator is normally made up of a composite virgin plastic such as phenolic resin and carbon or phenolic resin and nylon. As shown in Figure 1.4, the virgin material of these composites decomposes when subjected to intense heating and forms a porous carbon matrix along with pyrolysis gases which flow through and react in this porous carbon matrix. The carbon surface is removed by chemical reactions, sublimation and is eroded away by the shearing force in the shock layer (spallation). The pyrolysis gases flow through the char, reacting with themselves and the char layer and finally are injected into the boundary layer at the surface.

The ablative process is an intricate, complex, and yet orderly transfer of heat and mass. The important mechanisms involved are (a) heat conduction into the material and storage by its effective heat capacity, (b) heat absorption by the heat capacity of the

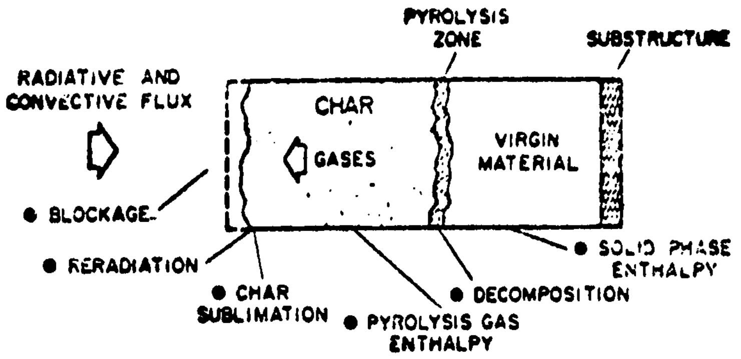
PYROLYSIS ZONE
SUBSTRUCTURE
RADIATIVE AND CONVECTIVE FLUX
CHAR
GASES
VIRGIN MATERIAL
● BLOCKAGE
● RERADIATION
● CHAR SUBLIMATION
● PYROLYSIS GAS ENTHALPY
● DECOMPOSITION
● SOLID PHASE ENTHALPY

Figure 1.4. Schematic of Ablator Energy Absorption Mechanisms.

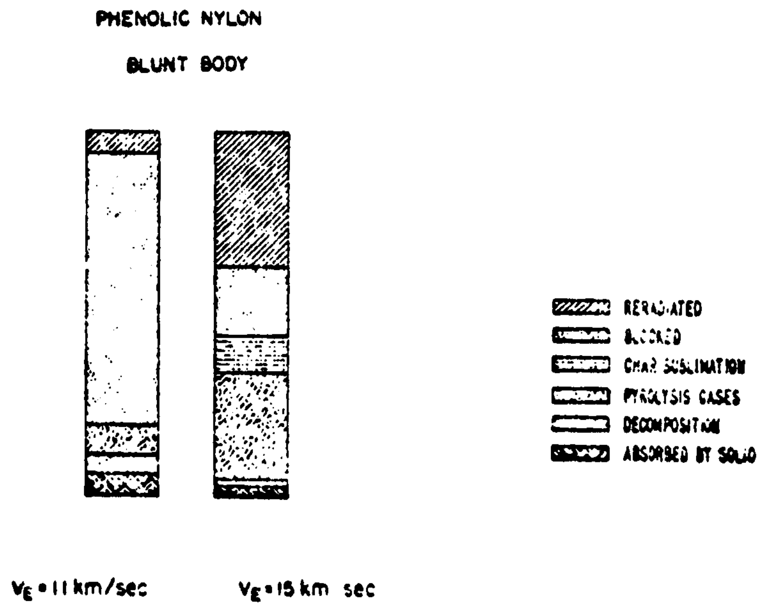

Figure 1.5. Heat Rejection Mechanisms for a Phenolic Nylon, Blunt Body Ablator.

pyrolysis gases, (c) primarily endothermic reactions of the gases (homogeneous and heterogeneous), (d) sublimation and surface reactions, (e) surface reradiation, (f) blowing into the shock layer by the pyrolysis gases, and (g) blockage of shock layer radiation by ablation species. This flow of pyrolysis gases through the char layer gives the charring ablator the added effect of transpiration cooling.

The degradation of the primary pyrolysis gases when flowing through the char into smaller molecules has two very important effects (1) decomposition is endothermic, because heat is consumed in the breaking of chemical bonds, and (2) the overall heat capacity of the smaller molecules is larger than that of the original decomposition products.

It is essential for the ablator to have a low thermal conductivity, a high thermal capacity, and a high heat of sublimation. The superiority of the charring ablator over subliming and melting ablators is largely due to its ability to reradiate substantial quantities of energy from the surface. The surface of the char possesses a high-emissivity; and, at high temperatures, reradiation is one of the most important energy absorbing mechanisms for charring ablators. For most carbonaceous materials, a reasonable assumption is constant emmisivity and constant absorptivity (absorption is important when considering radiating shock layers). The values of emissivity and absorptivity are not necessarily equal, though, due to the fact that the radiation and reradiation normally involve different wave-length ranges (Ref. 1.12).

One of the outstanding features of an ablator is that it not only absorbs heat, but through the injection of gaseous ablation products, it also modifies the adjacent boundary layer and greatly reduces the level of aerodynamic convective heating. These injected gases have the additional property of being good radiation absorbers, thus reducing the radiative heat transferred to the surface. More will be said about these two phenomena in the following section when discussing the flow field interaction.

The relative importance of the various heat rejection mechanisms is shown in Figure 1.5 for two entry velocities of 11 km/sec and 15 km/sec. Only the energy which reaches the ablator surface is considered, therefore the reduction of convective and radiative heating by gaseous injection is not included. At the higher velocity of 15 km/sec, the heat rejection modes of reradiation, char sublimation, and pyrolysis gas heat capacity and reactions become increasingly significant.

Flow Field Interaction

The ablator must be described in its proper environment in order to visualize the physical phenomena occuring. In the case of a reentry vehicle with an ablative heat shield, this environment is a shock heated shock layer shown schematically in Figure 1.6. At the outer edge of the shock layer, shock heated atmospheric gases (~15,000°K) move primarily by convection toward the stagnation point, where diffusive and viscous mechanisms become predominant. The region in the immediate vicinity of the stagnation point is thus referred to as the diffusion or viscous layer. The region between the bow shock and the diffusion layer is called the air layer and the ablation layer is located between the diffusion zone and the

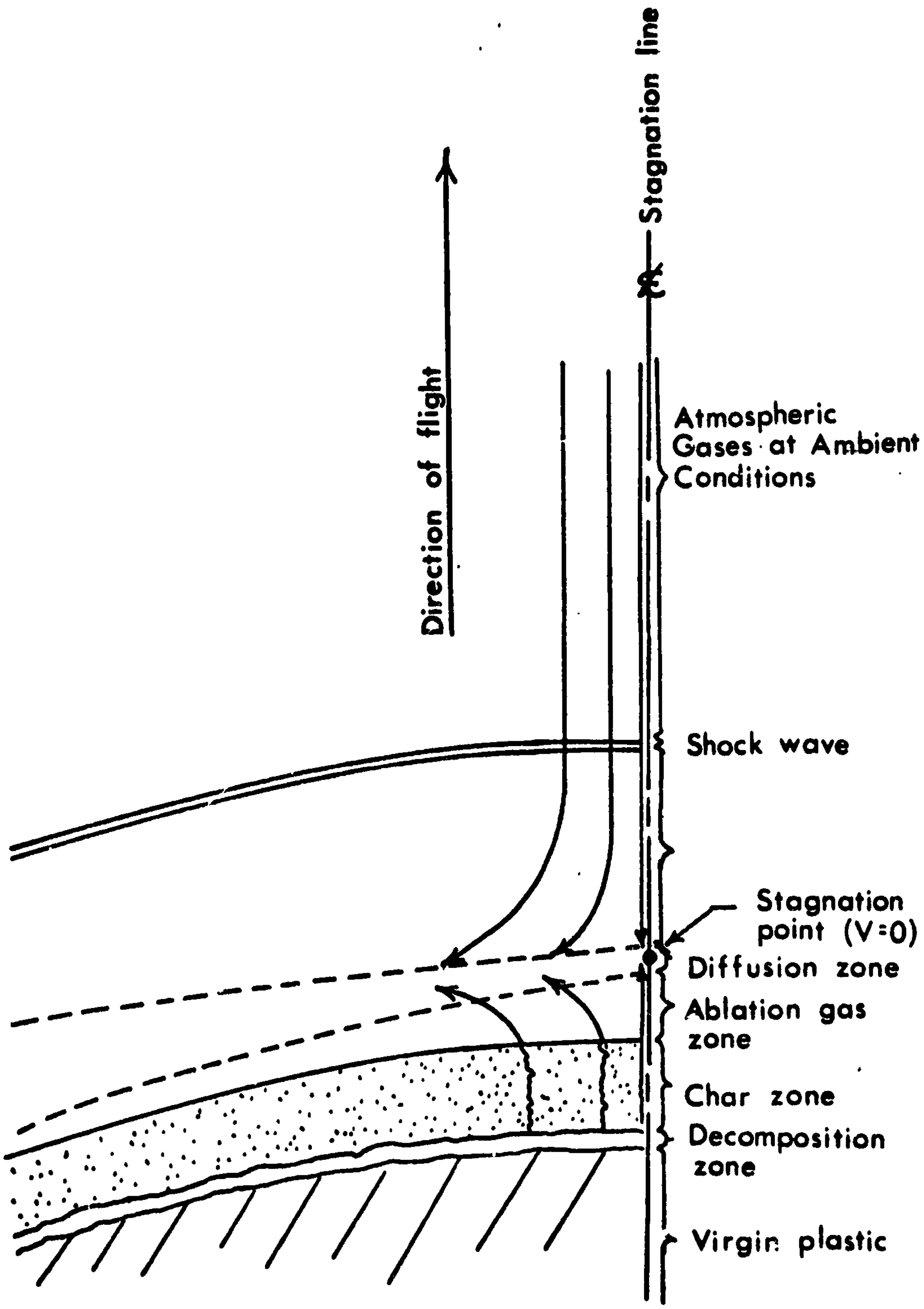
Stagnation line
℄
Direction of flight
Atmospheric Gases at Ambient Conditions
Shock wave
Stagnation point (V=0)
Diffusion zone
Ablation gas zone
Char zone
Decomposition zone
Virgin plastic

Figure 1.6. Illustration of Charring-Ablator and Flowfield Interaction.

ablator. As in the air layer, convective effects also predominate in the ablation layer.

Although simply depicted in Figure 1.6, the overall process is extremely complex and presents a significant challenge to an accurate mathematical analysis. The major difficulties are describing the radiative heating, the chemical reactions, and the interaction between the flow field and the ablator. In Figure 1.7 the modes of heat transfer in the shock layer are illustrated along with the interactions with the ablator surface. The following discussion describes these heat transfer modes and the coupling that exists between the flow field and the ablator.

In the air layer the predominant radiation effect is emission which occurs in all directions. The radiant heat emitted away from the body through the bow shock, is absorbed by the ambient air and is called precursor radiation. This effect increases the free stream enthalpy, thus elevating the temperatures in the shock layer. The radiative flux toward the body is partially absorbed in the ablation layer, increasing the temperature of the gases in this region. The radiant energy that is transmitted through this layer is then absorbed by the solid char surface where part is reradiated back into the shock layer and the remaining is conducted through the char to the decomposition zone. In the ablator the energy is absorbed by primarily endothermic reactions in the char zone and the decomposition of the polymer. The remaining fraction of energy is finally conducted through the virgin material to the substructure.

Heat is also transported to the vehicle by convection and conduction, but radiation is by far the most important mode of heat

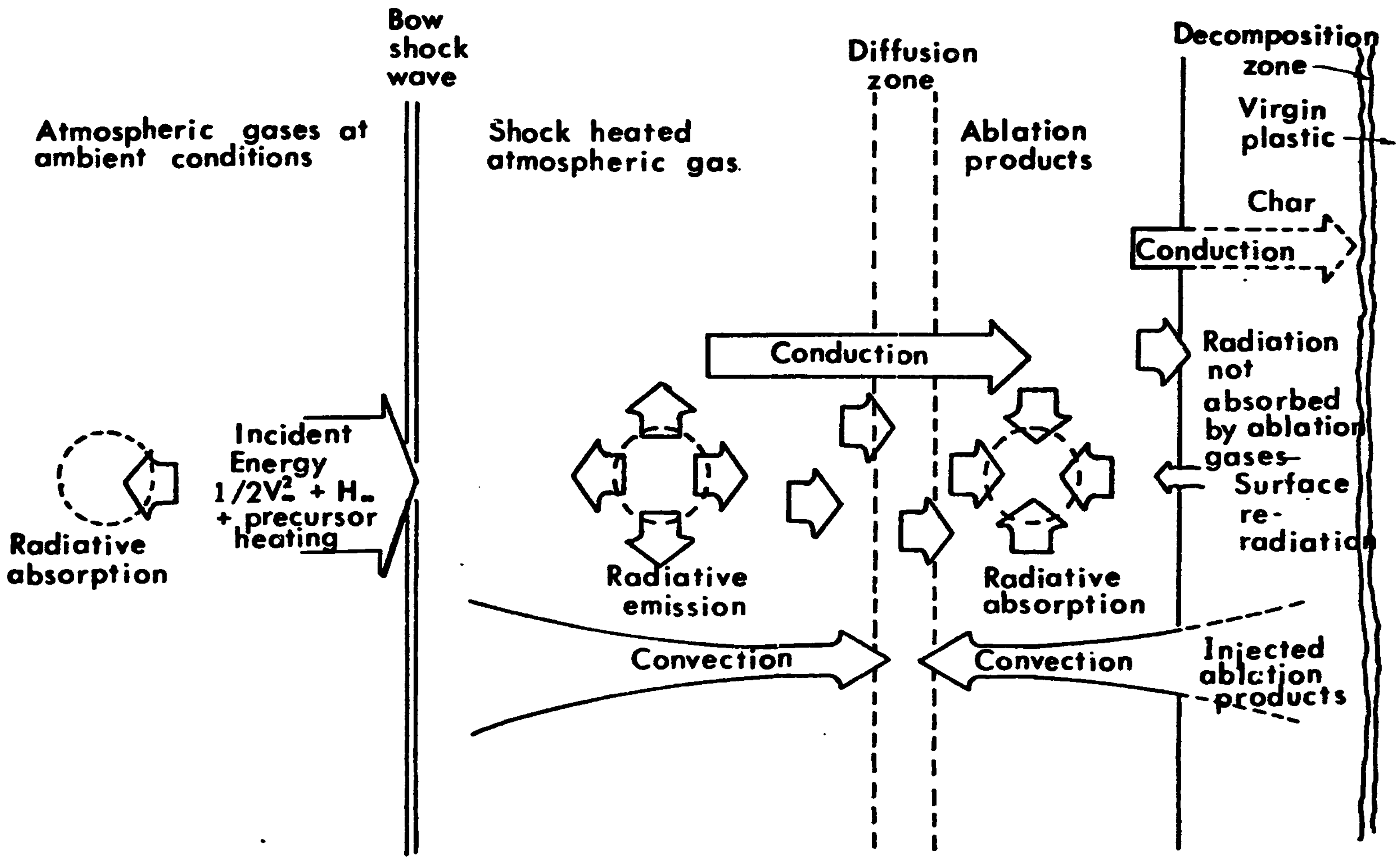
Bow
shock
wave
Atmospheric gases at ambient conditions
Radiative absorption
Incident Energy 1/2V²∞ + H∞ + precursor heating
Shock heated atmospheric gas.
Radiative emission
Convection
Diffusion zone
Conduction
Ablation products
Radiative absorption
Convection
Decomposition zone
Virgin plastic
Char
Conduction
Radiation not absorbed by ablation gases
Surface re-radiation
Injected ablation products

Figure 1.7. Illustration of Heat Transfer Mechanisms in Ablating Thermal Protection Systems.

transfer. The foregoing discussion has described the intimate coupling of ablator and flow field. The necessity exists, therefore, to accurately describe the major transport mechanisms in the shock layer and ablator including their coupling effects.

Summary

The ablator and its interaction with the surrounding flow field has been shown to be a very complicated process of mass and heat transport. The ablator and its associated flow field have been studied by many investigators who have made various assumptions about chemistry, heat transfer, and momentum transfer. The state of the art has reached a point where most of the analyses have assumed either equilibrium chemistry or no radiation heat transfer. Very few have actually coupled the response of the ablator to the flow field and those that do have used equilibrium chemistry models.

This research was undertaken to develop an analysis which incorporates the effects of finite rate chemistry, coupling of the flow field to a charring phenolic nylon ablator, and detailed line and continuum radiation heat transfer. The analysis is formulated to describe a reentering blunt vehicle typical of manned interplanetary missions.

A comprehensive overview of the work that has been done in the area of the shock heated flow field is given in the following chapter. The discussion will cover all of the recent pertinent work on nonequilibrium and radiation blunt body flows.

REFERENCES

1.1 Syvertson, C. A., "Research Problems in Atmospheric Entry and Landing for Manned Planetary Missions," NASA TM D-4977 (January 1969).

1.2 Stewart, J. D. and D. H. Greenshields, "Entry Vehicles for Space Programs," Journal of Spacecraft and Rockets, Vol. 6, No. 10 (October 1969), pp. 1089-1102.

1.3 Allen, Julian H., "Hypersonic Aerodynamic Problems of the Future," in The High Temperature Aspects of Hypersonic Flow, ed. by W. C. Nelson (Pergamon Press, MacMillan Co., New York, New York), 1964, pp. 1-42.

1.4 Jaworski, W. and R. G. Nagler, "A Parametric Analysis of Venus Entry Heat Shield Requirements," Jet Propulsion Laboratory Tech. Report No. 32-1468, (California Inst. of Tech., Pasadena, Calif. 1970).

1.5 Willis, E. A., Jr. and J. A. Padrutt, "Round-Trip Trajectories with Stopovers at Both Mars and Venus," NASA TN D-5758 (April 1970).

1.6 Edelman, R. K. and D. Fortune, "Mixing and Combustion in the Exhaust Plumes of Rocket Engines Burning RP1 and Liquid Oxygen," TR-631 General Applied Science Laboratories, Inc., Nov. 1966.

1.7 Eggers, A. J. and N. B. Cohen, "Progress and Problems in Atmospheric Entry," Proceedings of the XVI th International Aero. Congress, Gauthier-Villars, Paris, 1965.

1.8 April, Gary C., "Evaluation of the Energy Transfer in the Char Zone During Ablation," Ph.D Dissertation, Louisiana State University, Baton Rouge, La. (1969).

1.9 Penner, S. S. and O. P. Sharma, "Ablation with Radiant Heating," Zeitschrift fur Flugwissen-schafter, 14, pp. 169-179, 1966.

1.10 Kelley, J. B. and M. R. L'Ecuyer, "Transpiration Cooling - Its Theory and Application," Report No. TM-66-5, Jet Propulsion Center, Purdue University, Contract NSG-592, N66-30856, (June, 1966).

1.11 Steverding, B. and V. A. Nieberlein, "Ablation for Heat Shielding," Chemical Engineering, 72, pp. 163-168, (July 19, 1965).

1.12 Walbert, G. D. and E. M. Sullivan, "Ablative Heat Shields for Planetary Entries - A Technology Review," Presented at ASTM/IES/AIAA Space Simulation Conference, September 14-16, 1970.

CHAPTER II

A REVIEW OF RADIATING AND NONEQUILIBRIUM FLOW FIELDS

Introduction

In the past decade, numerous investigations of flow fields surrounding blunt reentry vehicles have been performed to determine the heating rates encountered by such vehicles. Various degrees of detail have been incorporated into the modeling of the flow field processes. The momentum, energy, and species equations have undergone assumptions pertaining to the viscous, conducting, radiating, and chemical nature of the flow. Radiating solutions have developed from the initial gray emission simplifications to continum models and further to detailed line and continum models. Chemical models of frozen, equilibrium, and nonequilibrium chemistry have emerged with nonequilibrium being the realistic and most difficult analysis. At each stage of development, more understanding was gained and accordingly computation time increased. In this chapter the best currently available studies involving radiating and nonequilibrium flow will be discussed -- first the radiating analysis, then the nonequilibrium analysis.

Radiating Solutions

Radiative energy transport becomes an exceedingly important mode for heat transfer at high velocity entries and low altitudes. Many investigators have attempted to define the important mechanisms involved in this radiative transport. A review is given below of the significant investigations performed in contributing to the current state-of-art prediction of radiative heat transfer. The analyses are split into direct methods which calculate a shock shape from a given body shape and inverse methods which use a specified shock shape and determine the body shape.

Direct Methods: One of the first efforts by Lockheed Missiles & Space Company to model the shock layer processes was by Wilson and Hoshizaki (Ref. 2.1) who attempted the relatively simple problem of inviscid and radiating flow using the optically thin approximation. The major effort by this group has been in assessing the important mechanisms of radiative transport. This first effort used an integral method to solve the conservation equations and the analysis applied away from the stagnation point. Later, Hoshizaki and Wilson (Ref. 2.2) extended their work to include viscous effects. This analysis was for a viscous, radiating but nonabsorbing gas in the shock layer. Hoshizaki and Wilson studied the effect of radiation cooling for a 30° hemisphere-cone and showed that the loss of energy in the shock layer by radiation reduced both the radiative and convective heat transfer. Solutions were presented for heating around the body which showed that the reduction of heating rate persists far from the stagnation line. The momentum and energy equations were solved using an integral method in which the tangential velocity and enthalpy profiles were represented by fifth and sixth-order polynomials respectively. Solutions were obtained for air only which eliminated the need to solve the species equations. The numerical solution proceeded by first obtaining a solution at the stagnation point. The coefficients of the polynomials of tangential velocity and enthalpy were determined by using the boundary conditions at the wall and shock and the assumption that the shock was concentric. The solution proceeded downstream with an initial estimate for shock shape. This was compared to the output shock shape and a new estimate was then made. Iterations were performed until convergence was attained for the shock shape.

The third effort by Hoshizaki and Wilson (Ref. 2.3) was a major step forward in complexity by eliminating the assumption of an optically thin shock layer and accounted for the spectral behavior of the continuum absorption and emission radiative processes. The numerical method differed from the previous investigation by employing a combined finite difference-integral method. The solutions to the momentum and species continuity equations were obtained in an approximate manner by means of an integral method. The velocity and concentration profiles resulting from the approximate solution were then used to solve the energy equation by means of a modified finite difference method (Ref. 2.4). This analysis included the effects of injected ablation products which were assumed to have thermodynamic and transport properties identical to those of air. The injected gas was assumed to be inert within the context that no chemical reactions between ablation products and air were allowed. Solutions were obtained at the stagnation line and around the body. Iterations were made around the body as in Ref. 2.2 until the shock shape had converged. The primary purpose of this investigation was to determine the effect of self-absorption on the radiative and convective heating. Numerical results obtained showed that self-absorption reduced the radiative heating by an order of magnitude but had little effect on convective heating.

The complex chemical equilibrium which results from injection of realistic ablation products into the shock layer was considered by Hoshizaki and Lasher (Ref. 2.5). In this analysis the shock layer chemical equilibrium composition was calculated using the FEMP computer program (from Ref. 2.4) which minimizes free energy given a specified temperature and pressure. According to Wilson (Ref. 2.6), "the use of FEMP, along with an even more detailed accounting of spectral radiative transport, raised a computational cost barrier which has since prevented the application of the direct finite difference analysis away from the stagnation point," Hoshizaki and Lasher (Ref. 2.5) state, therefore, that although around the body analyses can, in principle, be performed, only stagnation point solutions were obtained. The solution of the momentum equation was obtained using the Karman-Pohlhausen integral method and splitting the flow field in two parts - ablation layer and air layer. The ablation layer was terminated when ablation injected species comprised approximately 1% of the gas mixture. The velocity at the air-ablation interface was matched to combine the two solutions.

The analysis of Hoshizaki and Lasher included radiative emission and absorption, radiation cooling, and coupling between convection and radiation. Only continuum radiation was considered - lines for atomic and ionic species were not considered. The infinite slab, one dimensional approximation to the radiative flux was used which is tantamount to saying that gradients of temperature and density in the stream-wise direction are negligible. Wilson (Ref. 2.7) later studied the effects of the infinite slab prediction and found it to be quite reasonable. Numerical results showed that absorption by ablation products reduced the radiative surface flux by almost a factor of two. This result was in contrast to an earlier paper by Howe and Sheaffer (Ref. 2.8) who found that mass additions enhanced, rather than reduced, the radiative flux to the surface. Hoshizaki and Lasher claimed that this result was due to Howe and Sheaffer's gray gas approximation. It was also shown that atomic carbon was the principal absorber and that the ablation product molecules play a minor role in determining the radiative flux.

Chin (Ref. 2.9) investigated radiation transport in the stagnation region of an ablating body with an invisicid, nonconducting flow model. The gas in the shock layer was assumed to be in thermodynamic equilibrium and at quasi-steady state. The flow field was assumed to have an interface between the ablation products and the shock-layer air. The stagnation region air layer and ablation layer were analyzed by means of similarity transformations with a continuity of pressure across the interface. The wall was assumed to be at the equilibrium sublimation temperature corresponding to the surface pressure. The ablator is coupled to the flow field by performing the following surface energy balance.

$$v_w = (q_w - \sigma T_w^4)/\rho_w \Delta H_v \qquad [2.1]$$

where: v_w = velocity of injected gases into shock layer

q_w = heat flux toward surface from shock layer

σT_w^4 = energy reradiated by surface

ρ_w = density of injected gases

ΔH_v = heat of ablation

A heating rate, q_w, was assumed and then updated until the flow field solution corresponded to the surface energy balance.

The radiation transport in the analysis attempted to introduce the effect of lines on the radiative surface heat flux. Only nitrogen lines were included and the ablation layer was modeled with a continuum approximation. Chin also made perturbation studies of the radiative properties to examine radiative uncertainties. Chin's results indicated that the ablation layer was very effective in reducing wall heat flux (41%) and that self-absorption and energy-loss effects reduced the sensitivity of the wall radiative flux to environmental variables and to uncertainties in radiative properties.

In order to remove major deficiencies in the treatment of the momentum equation due to the integral technique used in Refs. 2.5 and 2.10, Wilson (Ref. 2.11) solved the momentum equation in finite difference form. This method permitted solutions to "massive" blowing problems and placed all three conservation equations in the same solution form. The opacity data in the radiative transport model was extended to include atomic line transitions of H and C species. Thus, transport through the ablation product gases was more complete than in previous published studies. Finally, the inclusion of continuum and line opacity data for the He atoms permitted the solution to be applied to both Earth and Jovian entry (RATRAP from Ref. 2.12).

In comparing his results with Chin (Ref. 2.9), Wilson found that Chin's solution overpredicted the effectiveness of radiative blocking. This result was due to the omission of C and H lines by Chin (only N lines were included in Ref. 2.9). Wilson showed that Chin's inviscid solution compared closer to a continuum only calculation as shown in Figure 2.1. The result of this research demonstrated that, unlike the situation with convective heating, massive blowing was ineffective in achieving a major reduction in the surface radiative flux. These conclusions held not only for earth entry but particularly for Jovian entry when predominately carbon species comprised the ablation product gases.

The end result of the work of Hoshizaki, Wilson and Lasher is the "VISC Code" reported in Ref. 2.6. In this investigation, the simplifying but nonessential gas dynamic approximations that $\rho\mu$ = constant and the construction of an inner inviscid layer were removed. The results used a completely variable $\rho\mu$ as well as a technique for integrating the conservation equations toward both the shock and wall from the interior shock layer point where the stream function passes through zero. The radiative transport subroutine was further extended to include wall emission/reflection terms. The previously employed analytic method (Ref. 2.13) for obtaining the flux divergence due to lines was dropped and replaced by a direct numerical differencing of the line flux. The code was used to obtain heating predictions for reentry into the earth's atmosphere and for probe entry into the atmospheres of Jupiter and Venus.

Another group to study radiation transport in the shock layer (stagnation line only) was that of Rigdon, Dirling, and Thomas of McDonnell Douglas Corporation. Rigdon et al. (Ref. 2.14 and 2.15) solved the viscous stagnation line equations using an initial value

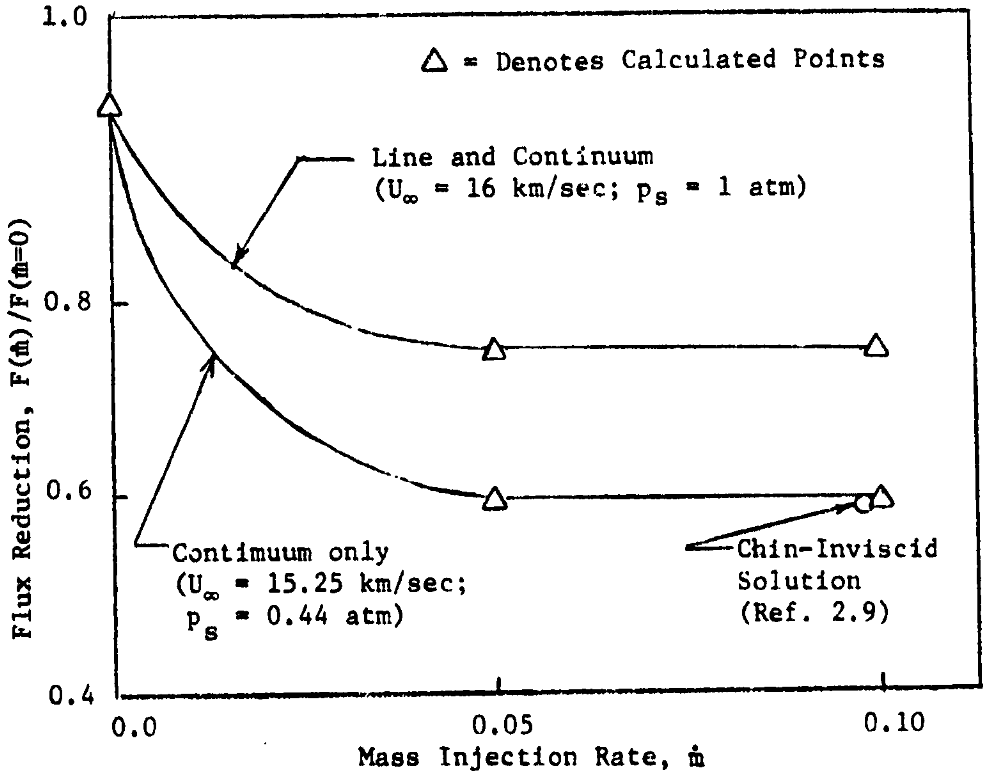

Figure 2.1. The Effect of Mass Injection on Surface Flux Reduction (Ref. 2.11)

(marching) finite difference technique. The solution was started at the stagnation point and proceeded in both directions (toward the wall and toward the shock), and the initial slope (at the stagnation point) was iterated on until the boundary conditions at both the wall and shock were satisfied. This technique was used in order to avoid the numerical problems associated with marching techniques that start the solution at a wall with mass injection where the slope is close to zero. Difficulties arose from trying to maintain numerical precision when taking differences between numbers of the same size.

Rigdon, et al. (Ref. 2.15) used a binary diffusion coefficient based on the C-N interaction and demonstrated that the choice of binary diffusion coefficient was not critical in the prediction of wall heating rates. The species equations were solved by assuming that ablation species were diffusing into air species and the mixture was in chemical equilibrium. In Ref. 2.15 the effect of injection of ablation species were considered. This was an extension of previous work of Rigdon et al. (Ref. 2.14) where only air blowing was studied. The effects of the thermodynamic and transport properties of ablation products on the heat flux at the wall was investigated, and radiation preheating of ambient air (precursor radiation) was considered. For these solutions the radiative transfer was computed using the detailed spectral radiative properties of both air and ablation products including atomic line transitions.

Comparison of the detailed solutions of Rigdon, et al. (Ref. 2.15) with other less exact methods, e.g., line grouping, showed a necessity for retaining full spectral detail in the description of the radiative properties. Furthermore, the thermodynamic properties of the ablation products must be peroperly described. Results showed that precursor radiation increases the wall heat flux by less than 10% for entry velocities up to 55,000 feet per second and shock layer pressures of approximately one atmosphere.

NASA's Langley Research Center has done some extensive investigation of the radiating flow around blunt reentry bodies (Refs. 2.16 - 2.20). All of these investigations are restricted to the chemical equilibrium flow.

The inviscid, radiating, nonadiabatic flow field equations were solved by Suttles (Ref. 2.19) using an approximate computational scheme in which a method of integral relations was applied. The method was used for a one-strip approximation with an equilibrium-air gas model. A frequency dependent, self-absorbing radiation model was employed which accounted for atomic-line radiation as well as the important continuum radiation processes. This work was an extension of the work of Garrett, et al. (Ref. 2.21) who used the integral relations approach to a nonradiating flow field. Mass injection at the surface was not included. Comparison were made to the stagnation solutions of Olstad (Ref. 2.22) and Callis (Ref. 2.23). Suttles showed that the nonadiabatic solution resulted in significantly reduced enthalpies and temperatures, increased densities, and decreased shock standoff distance. Suttles concluded that although the approximate method did not produce all details of the flow, it did yield a good description of the flow field through quantities such as shock standoff distance and flow properties at the body surface.

A combined chemical equilibrium chemistry flow field and ablation study was performed by Smith et al. (Ref. 2.16) for a blunt body reentering earth's atmosphere. Three interacting regions were distinguished: inviscid air layer, ablation boundary layer, and charring carbon phenolic heat shield. The outer air layer was analyzed as an inviscid region using a one strip integral method. The inner ablation layer was analyzed using two techniques. For small ablation rates a boundary layer solution was used; whereas for large ablation rates (where the boundary layer solution was unstable) an integral method was used. No radiation coupling between air and ablation layers was considered. The radiation model used was that of Wilson and Hoshizaki (Ref. 2.10) which included various line and continuum mechanisms for atoms, ions and molecules excluding line mechanisms for C and H atoms. Heating rates for the stagnation region and around the body along a trajectory were presented. Coupling of the ablator to the flow field was accomplished in a similar manner to Chin (Ref. 2.9) in which the mass loss rate was determined by a surface energy balance. An equilibrium enthalpy of ablation was used along with surface reradiation of energy (the surface was assumed to be at the equilibrium sublimation temperature). Results were compared to Chin and indicated a smaller blockage of radiation (22% compared to 46%) due to the ablation layer. A similar result was found when compared to Rigdon et al. (Ref. 2.15) who predicted 55% blockage by the ablation layer. The conclusion was that the differences occurred due to the differences in radiative transport models of the three investigations.

In a recent study by Sutton (Ref. 2.18), the fully coupled radiating gas flow about an ablating planetary entry body was applied to Venusian entries. The method of solution coupled an inviscid flow solution and a boundary layer solution (laminar or turbulent) in which the divergence of the radiative flux was included in the energy equation for the solution of each gas layer. The treatment of radiation included molecular band, continuum, and line transitions with a detailed frequency dependence of the absorption coefficient. The species equations were solved in elemental form with chemical equilibrium being assumed. Results showed that the radiative flux toward the body was attenuated in the boundary layer at downstream regions of the body as well as at the stagnation point. The results were the same even when radiation absorption by ablation products was taken into account. The radiative heating rates along the downstream regions were shown to exceed stagnation point values under certain conditions. Blockage of radiation was found to be 10% to 20% for nominal entry conditions but radiation blockage as large as 30% resulted at higher velocities.

In an investigation by Garrett, et al. (Ref. 2.21), the viscous shock layer equations in the stagnation region were solved using an implicit finite difference sheme. The flow field was assumed to be in thermodynamic and chemical equilibrium. The radiation model used was the computer code RATRAP (Ref. 2.24) which accounted for both continuum and line radiation exchange. The species equation was solved by assuming ablation products diffusing into air species as a binary system. The assumption of the binary diffusion model was evaluated by comparing heating rate results for two cases. One case assumed the binary diffusion coefficient to be that of hydrogen-nitrogen diffusion and the other to be that of carbon-nitrogen diffusion. The results showed that a maximum difference of 3 percent occurred in the radiative heat flux which indicated that the assumption of a binary diffusion model was valid for the conditions examined.

For massive blowing cases, damping of the enthalpy profile was required to keep the solution stable. A damping factor of 0.5 was found to be the most efficient when considering the trade-off of computer time and stability. Garrett et al. improved on the stability of their solution by using a windward differencing technique instead of central differencing. Oscillations in the enthalpy and species solutions were removed by use of windward differencing.

Comparison by Garret (Ref. 2.21) with other investigations (Ref. 2.9, 2.15, 2.16, 2.19, 2.25) demonstrated lower wall radiative heating rates for carbon phenolic ablation. The results indicated that the ablation products were highly effective in blocking the incident radiation from the high temperature outer layer of the shock. For blowing rates of 0.1 and 0.2, typical reductions in radiative heat flux at the wall ranged from 34 to 39 percent of the values for no blowing.

Engel et al. (Ref. 2.26) concluded from the results of Refs. 2.27 and 2.28 that the energy and species equations could be simplified by setting the diffusion term equal to zero. This assumption yielded a step function for the elemental mass fractions where ablation elemental mass fractions were used from the wall to the stagnation point and air elemental compositions were used in the region from stagnation point to the shock. The species compositions were then calculated assuming thermo-chemical equilibrium. The thin shock layer, stagnation line equations were solved including line and continuum radiation from air and ablation species. The flow field was coupled to a phenolic nylon ablator by assuming the ablator surface to be at its sublimation temperature and the heat absorbed to be that by quasi-steady ablation - similar to the coupling by Chin (Ref. 2.19) and Smith _et al._ (Ref. 2.16). An implicit finite difference scheme was used to solve the energy and momentum quasi-linearized equations.

Engel's results indicated that the continuum contribution to the surface radiative heat flux is essentially unchanged by increasing the ablation rate above about 5% of the freestream blowing rate. Molecular absorption of radiant energy in the ablation layer was found to contribute significantly to the reduction of wall heating rates (52% for the case studied).

Contemporary with the study performed by Engel was an investigation by Esch (Ref. 2.28) to determine, primarily, the effect of assuming binary diffusion. Esch's investigation differed from Engel in that he solved the species equations with the diffusion term included. The radiation model was identical to Engel's. Comparison of binary diffusion results with multicomponent diffusion results led to the conclusion that binary diffusion was sufficient to describe the shock layer process if an appropriate value of the diffusion coefficient was selected. He used the binary coefficient based on H-C_2H_2 interaction. The effect of using air thermodynamic and transport properties, instead of including ablation products, was also investigated by Esch. Detailed transport properties were found to be unimportant but inclusion of thermodynamic properties of ablation products proved to alter the radiative wall heating rate significantly. These results are supported by the findings of Rigdon et al. (Ref. 2.15) and Garrett et al. (Ref. 2.21).

Inverse Methods: In solutions which use inverse methods, the shock shape is given and the body shape is to be determined. The shock shape can then be adjusted until the desired body shape is found. The disadvantage of this technique is that, in general, one would like to specify body shape directly (the direct method). Unfortunately, shock shape is somewhat insensitive to body shape. Therefore, different body configurations could have the same shock shape and the inverse method does not always work effectively.

Some success has been achieved using inverse methods. Chou (Ref. 2.29) performed an inverse solution using locally nonsimilar solutions for a radiating shock layer about smooth axisymmetric bodies. In this method, nonsimilar terms in the governing equations were defined as dependent variables; model equations were derived for these variables. Solutions were presented for nonblowing bodies and compared with the Blasius type series solution of Chou and Blake (Ref. 2.30). Excellent agreement was found. Blowing solutions were also obtained (constant blowing around the body), but these cases did not consider radiative transport and no diffusion mechanism was taken into account. Therefore, the injected gas was assumed to be the same as that of the freestream. Results indicated that blowing solutions were more difficult to obtain than nonblowing solutions since the blowing cases were not presented for points very far downstream of the stagnation region. Another limitation was that only continuum radiation was considered.

In a later report by Chou (Ref. 2.31), the restriction of no blowing for radiative heating cases was removed. In addition the simplifications of constant transport properties and continuum radiation only were also removed. The same locally nonsimilar method was used. Ablation products were allowed to diffuse into the shock layer and the governing equations were modified to allow mass injection rates (carbon injection) to vary with distance around the body. The shock layer was assumed to be in thermo-chemical equilibrium and the FEMP, Free Energy Minimization, computer program (Ref. 2.4) was used to determine the equilibrium composition. Molecular band and atomic line, as well as continuum radiation, was considered. Comparisons were made with the adiabatic inviscid flows of Olstad (Ref. 2.32) and Schneider (Ref. 2.33) and the viscous, nonradiating flow of Davis and Flugge-Lotz (Ref. 2.34).

Chou's results showed good agreement with the work reported in Refs. 2.32, 2.33, and 2.34. A sample calculation was made for a typical Jovian entry which indicated a 40% reduction in total radiative flux at the stagnation point due to carbon gas injection when compared to the nonblowing case. The reduction increased to about 70% of the stagnation line value at about four body nose radii downstream. The radiative flux reduction indicates that most of the radiative energy is absorbed by the injected carbon gas and dumped into the wake. An examination of the spectral distribution of the radiative flux revealed that most of the flux reduction occured in molecular bands of C_2 and C_3.

A companion report to Ref. 2.31 was Ref. 2.35 which is a user's manual for the SL4 computer code. The report describes the input and output for the inverse shock layer solution of Chou. The code also provides a basis for obtaining predictions of the surface heating to a body entering any planetary atmosphere at hyperbolic velocities.

In an inverse solution by Olstad (Ref. 2.32) an attempt was made to study the effects of radiation on the flow about smooth symmetric bodies downstream of the stagnation point. Previously Olstad had only presented stagnation region solutions (Refs. 2.22 and 2.36). In the analysis, a simplified flowfield technique developed by Maslen (Ref. 2.37) was modified to account for radiation and large blowing. The radiative transport model included effects of atomic lines and continuum radiation. Blowing was studied for cases of cold air injection, thus only air thermodynamic, transport, and radiative properties were required.

At some point not too large a distance downstream of the stagnation point, the flow direction in the shock layer is nearly parallel to the shock. Maslen (Ref. 2.37) took advantage of this situation to derive a simplified system of equations which adequately describe the flow and thermodynamic properties in the shock layer for an inviscid, nonreacting, nonradiating gas for a given shock shape. The most important step in the derivation was the transformation to the von Mises plane and the subsequent uncoupling of the normal momentum equation from the other equations. Using a modified form of Maslen's method, Olstad studied the effect of cold air blowing on radiative heating. He found that in the stagnation region blowing was quite effective in reducing the radiative heating to the body surface. However, downstream of the stagnation region, where the radiative heat flux from the hot shock layer decreased, re-emission from the blown layer became increasingly important compared with absorption. Thus the effectiveness of the blown layer decreased and finally became negative, so that the presence of the blown layer actually increased the radiative heating to the body surface downstream of the body station where blowing ceased. Olstad's results must be evaluated in the light of the system under study, i.e., only air blowing was considered and ablation products with different radiative, transport, and thermodynamic properties could very well invalidate the conclusions reached (e.g. Chou, Ref. 2.31).

Falanga and Sullivan (Ref. 2.25) presented an inverse solution for an inviscid shock layer flow about a blunt body. The model included nongray radiative transfer and only considered equilibrium air flow. The technique had the restriction that the shock shape had to be analytic and the solution was only applicable to the subsonic flow region in the shock layer. No blowing from the body was considered. Results compared favorably with the direct method of Rigdon et al. (Ref. 2.15) and the analysis of Callis (Ref. 2.23) who used a time-asymptotic technique.

More recently Sutton and Falanga (Ref. 2.38) published results for the entry of a blunt vehicle into a Venusian atmosphere of 90% carbon dioxide and 10% nitrogen. In this analysis only stagnation region heating results were obtained, but ablation product injection and a boundary layer adjacent to the body were included. Again nongray radiation was accounted for and fully coupled solutions were presented (i.e. radiative coupling and ablator-flow field coupling). A high density phenolic nylon ablator was considered in the investigation. Results indicated that ablation products reduced radiative heating by as much as 35% for high velocity entries (11 km/sec) and that the boundary layer also significantly reduced the radiative heating (20-30%). For entry velocities below about 10 km/sec, it appeared that the inviscid layer solution gave reasonable estimates of radiative heating.

Nonequilibrium Chemistry Solutions

The preceding discussion has been centered on analyses that have sought primarily to describe the important radiative heating phenomena that occur in high temperature shock layers. None of these analyses have considered the effect of nonequilibrium chemistry on the flow field solution. At best equilibrium chemistry was included in some of the previously discussed investigations. This section will attempt to describe some of the important work that has been done in the area of nonequilibrium or finite rate chemistry analyses. In general these studies do not include the effects of radiative heat transport.

Blottner (Refs. 2.39 - 2.43) has done extensive work in the investigation of nonequilibrium flows, especially for boundary layer flows. In an early work by Blottner (Ref. 2.41), the investigation of a viscous nonequilibrium-ionized air boundary layer was performed. Seven air species (O_2, N_2, O, N, NO, NO^+, e-) and 11 chemical reactions were considered. The equations were transformed with the Mangler and Howarth-Dorodnitsyn transformation in order to obtain them in a form more appropriate for numerical solution. The resulting partial differential equations were then solved using an implicit finite difference shceme. Results were given for slender vehicles entering at 22,000 feet per second at altitudes of 100,000 feet and 150,000 feet. For distances 15 feet downstream from the tip and for conditions considered, none of the chemical reactions were near equilibrium. No mass injection at the wall was included in this analysis.

Blottner published an excellent survey paper on finite difference methods for the solution of the boundary layer equations (Ref. 2.39) in 1970. The paper presented a technique for solving the boundary layer equations for a multicomponent flow with finite chemical reactions. The technique was developed in an effort to attain a method that would solve the governing equations when many chemical species exist in the flow. The solution technique involved the quasilinearization of the equations, uncoupling them, placing them in finite difference form, and solving the resulting tri-diagonal matrices. Blottner found this technique superior in computational efficiency as can be seen from Figure 2.2 to the fully coupled solution. When the equations are fully coupled, the program storage requirements and the computation time increase rapidly as more species are included. Since a matrix inversion must be performed in the fully coupled solution and computation time is proportional to the cube of the matrix size (number of species), large chemical systems become prohibitive. On the other hand, the uncoupled method results in solution times which are approximately proportional to the number of species.

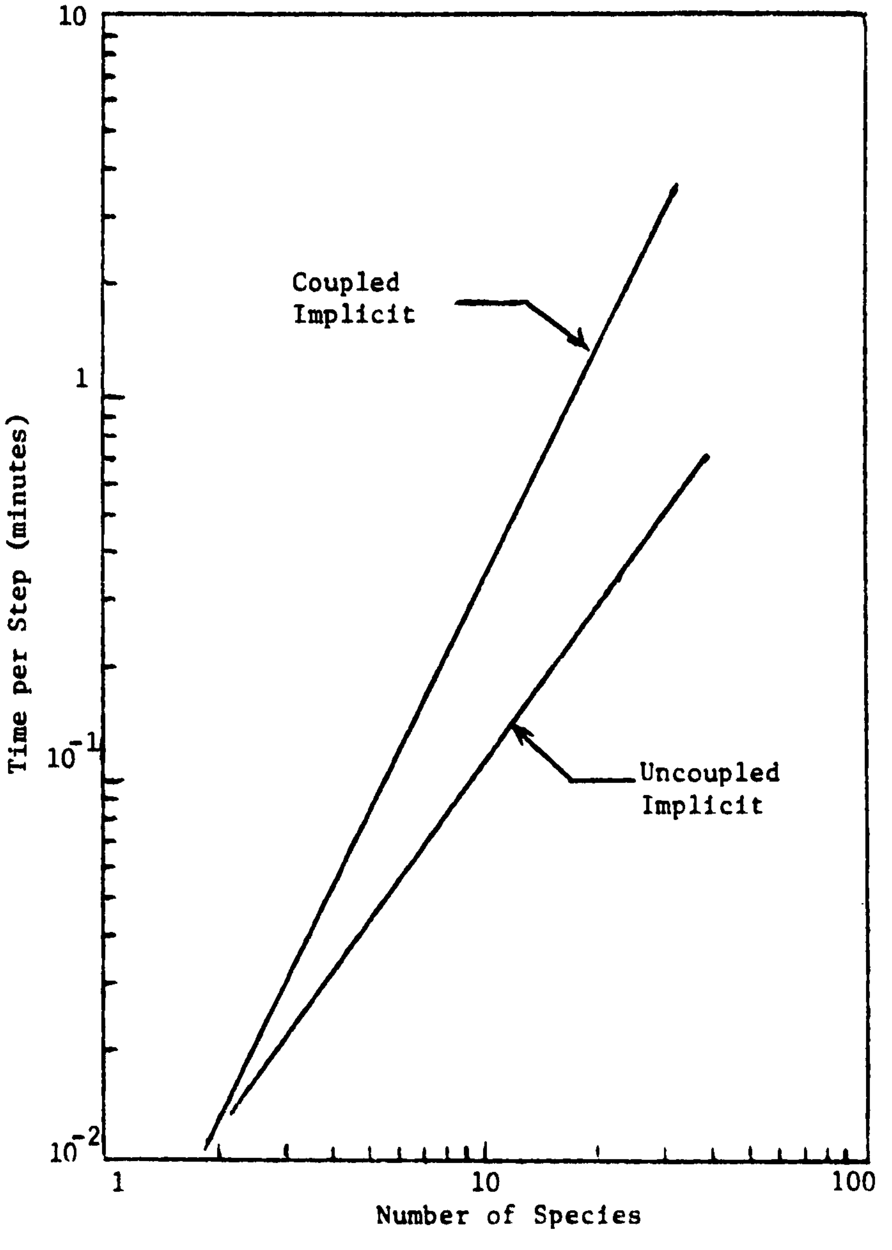

Figure 2.2. Computation Time for Various Numbers of Chemical Species (Binary Diffusion) (Ref. 2.39).

The finite differenced equations were written with a parameter "Θ" which can vary between 0.0 and 1.0, where Θ is 0 for explicit methods, 1/2 for Crank-Nicolson method and 1 for the Standard Implicit method. Blottner used $\Theta = 1/2$ or the Crank-Nicolson difference scheme because the accuracy is of second order compared to first order accuracy for the standard implicit. The explicit scheme was not used since unstable solutions invariably occur when this method is used on boundary layer problems. The boundary conditions for the boundary layer equations were presented by Blottner and placed into the finite difference formulation also. In this analysis, Blottner considered the effect of an ablator injecting mass into the boundary layer. The initial conditions (stagnation line equations) for solution were developed in Ref. 2.42 by Blottner. These ordinary differential equations were treated in the same manner as the partial differential equations which describe the boundary layer.

Results were obtained by Blottner for binary and multicomponent diffusion which showed differences which were almost indistinguishable. The surface boundary conditions employed in the study were such that the wall was either noncatalytic, or fully catalytic. For the case of the non-catalytic wall the mass injection rate and and diffusion rate of air species to the surface was zero. A fully catalytic recombination surface for air is defined as a wall where every dissociated and ionized species that strikes the surface is converted to a molecular species due to heterogeneous reactions. Comparison of catalytic to noncatalytic solutions showed negligible differences in temperature and velocity profiles but about a 20%

difference was found in the boundary layer thickness (noncatalytic being higher).

For the solution with a noncatalytic wall, oscillations were obtained with Crank-Nicolson (θ equal to 0.5) method. To avoid this problem, the standard implicit method with θ equal to 1.0 was employed. The results were compared with θ equal to 0.5 and 1.0, and the results were in close agreement downstream. Near the tip (first few inches) there was a difference between the predictions of the two methods for the mass fraction of the species, with the implicit method giving the more accurate results. This type of stability problem has also been observed by Moore (Ref. 2.44) and was corrected by using the standard implicit scheme for the first grid point away from the wall.

In a summary report (Ref. 2.43) Blottner et al. prepared a user's manual for the boundary layer - shock layer computer program that evolved from their work. In the report additional improvements were made in the numerical schemes. Initial profiles can be obtained by the program and variable step sizes across the layer are possible. Results are presented for various boundary layer and shock layer solutions and three example runs are given for input and output of the program which demonstrate its flexibility. One of the major improvements in this version of the program was the capability to handle arbitrary body shapes.

Davis (Refs. 2.45 and 2.46) presented solutions for the viscous flow in the shock layer about reentering vehicles at moderate to high Reynolds number. Shock and wall slip conditions were included in the boundary conditions and were shown to be important for low

Reynolds number cases. The flow field was described by one consistent set of equations which are the thin shock layer equations as Blottner used (Ref. 2.43). The gas was assumed to be a perfect gas so that no chemical reactions occurred and the species continuity equations did not need to be solved.

Davis used a numerical scheme similar to Blottner (Ref. 2.39) and developed the variable step size finite differencing used in Ref. 2.43. Starting with the assumption that the thin shock layer equations applied and that the shock was concentric to the body, the solution proceeded from the stagnation point to points downstream. The thin shock layer assumption is tantamount to omitting normal velocity terms in the normal momentum equations. These assumptions were then removed by making successive iterations around the body using a corrected shock shape and normal components of velocity in the normal momentum equation.

The addition of chemical reactions in the shock layer was later investigated by Davis (Ref. 2.47). In this analysis a chemically reacting binary mixture of oxygen atoms and molecules was considered. Flows past hyperboloids with one inch nose radius asymtotic far downstream to cones of 60°, 45°, and 20° were investigated at altitudes of 100 to 250 thousand feet and an entry velocity of 20,000 feet per second. The calculations extended 25 nose radii downstream and considered both catalytic and noncatalytic wall boundary conditions. No mass injection at the wall boundary was considered.

Before the calculations were made downstream, Davis performed several stagnation-region solutions to determine what effect rates of chemical reaction given by various authors (Refs. 2.48-2.52) would have on the solution. Typical results showed that there was about a factor of four between the lowest and highest atom concentration profiles. For the remainder of the work, Davis used the rate data of Bortner (Ref. 2.49).

The wall catalyticity had little effect of skin friction and wall pressure distribution, but had a sizable effect on heat transfer. The wall catalyticity was also shown to have little effect on velocity and temperature profiles in all cases. Davis found by comparing equilibrium concentrations to nonequilibrium calculations that at 100,000 feet the outer inviscid flow was essentially in equilibrium at the stagnation-point, but was not a few nose radii downstream. Caution should be taken, therefore, in using stagnation-point solutions to determine when equilibrium conditions are reached.

In a study that followed Davis, Moss (Ref. 2.53) extended Davis's model (Ref. 2.47) to include multicomponent effects. This investigation studied the effects of chemistry models (frozen, equilibrium, or nonequilibrium) on the flow field solution, the effect of multicomponent diffusion, wall catalyticity, and mass injection. The numerical solution technique was identical to that of Davis (Ref. 2.47) and the body studied was a 45° hyperboloid.

Moss's results indicated that the chemistry models substantially influenced flow parameters and surface transport. Heat transfer rates were higher for both frozen and equilibrium than for nonequilibrium (e.g. 54% higher for equilibrium in the stagnation region). Wall catalyticity also had an effect of increasing heat transfer rates for nonequilibrium cases. The effect of multicomponent diffusion was shown to be negligibly different from the binary diffusion assumption which agrees with the results of Blottner (Ref. 2.39) and Esch (Ref. 2.28).

Moss considered mass injection of air, water, and ablation products into the shock layer. Only for the case of air injection was nonequilibrium chemistry attempted. Equilibrium solutions were obtained for water and ablation injection. The effect of that mass injection had on heat transfer rates decreased as the injection rate increased. Also, the effect that mass injected in the stagnation region had on the flow field decreased very rapidly downstream. Water was found to be the most effective in reducing heat transfer rates for the injectants considered.

Adams et al. (Ref. 2.54) presented results for chemical nonequilibrium inviscid and laminar viscous flow over spherically blunted cone geometrics. The calculations were made for flight velocities and altitudes where radiative transport was negligible. The chemistry was restricted to air species and injected species of argon, helium, or carbon dioxide. Multicomponent diffusion was discussed; however, no results were presented. For the cases studied, the influence of a noncatalytic wall with mass injection significantly reduced the convective heat transfer.

Using an approximate inverse solution, Grose (Ref. 2.55) presented results for the inviscid nonequilibrium flow in the shock layer about a vehicle in hypersonic flight. Cases were run for Earth, Martian, and Venusian atmospheric entry. The method used a von Mises transformation to place the equations in the form of the stream function similar to Olstad (Ref. 2.32). A large number of reactions and/or species was easily handled. The gas model permitted consideration of vibrational relaxation, dissociation, recombination, ionization, electronic excitation, and vibration-dissociation coupling. The method had the advantage of being able to solve the subsonic and supersonic portions of the flow field whereas many flow field solutions require the use of two methods for the two regimes. The primary advantage of the method was that computing time was small (79 seconds to about 14 minutes). One disadvantage was that approximations were crude close to the stagnation point where peak heating generally occurs.

Summary

The studies reviewed represent the best currently available. Unfortunately the radiating solutions are for equilibrium chemistry flow fields at best. On the other hand the nonequilibrium solutions are presented for cases in which radiation is not a dominant heat transfer mechanism. None of the analyses reviewed incorporate both the effects of radiative transport and nonequilibrium chemistry. With the exception of Chin (Ref. 2.9), Smith et al. (Ref. 2.16), Esch (Ref. 2.28), and Engel (Ref. 2.27), the solutions neglect the coupling of the flow field to the body whereby a surface energy balance is maintained.

As can be seen, no single analysis includes all of the important effects of radiative heating, nonequilibrium chemistry, and ablator coupling. It was the main purpose of this research, therefore, to incorporate all these effects using a computational scheme which is reasonable, accurate and rapid. The model developed includes radiative transport with various line and continuum contributions, nonequilibrium chemistry, and is coupled to a phenolic nylon ablator.

In Chapter 3, the equations that describe this system are developed and placed into a form suitable for numerical solution.

REFERENCES

2.1 Wilson, K. H. and H. Hoshizaki, "Inviscid, Nonadiabatic Flow About Blunt Bodies," AIAA Journal, 3, pp. 67-74, 1965.

2.2 Hoshizaki, H. and K. H. Wilson, "Viscous, Radiating Shock Layer About a Blunt Body," AIAA J., Vol. 3, No. 9, Sept. 1965, p. 1614-1622.

2.3 Hoshizaki, H. and K. H. Wilson, "Convective and Radiation Heat Transfer During Superorbital Entry," AIAA J., 5 (1), 25 (Jan. 1967).

2.4 Smith, A.M.O. and N.A. Jaffe, "General Method for Solving the Laminar Nonequilibrium Boundary-Layer Equations of a Dissociating Gas," AIAA Journal, 4, 611-620 (1966).

2.5 Hoshizaki, H. and L. E. Lasher, "Convective and Radiative Heat Transfer to an Ablating Body," AIAA J., 6 (8), pp. 1441-1449, (Aug., 1968).

2.6 Wilson, K. H., "The VISC Cose - A User's Manual," NASA CR-2237, March, 1973.

2.7 Wilson, K. H., "Evaluation of One-dimensional Approximations for Radiative Transport in Blunt Body Shock Layers," NASA CR-1990, March, 1972.

2.8 Howe, J. T. and Y. S. Sheaffer, "Mass Addition in the Stagnation Region for Velocities Up to 50,000 Feet Per Second," TR R-207, Aug. 1964, NASA.

2.9 Chin, J. H., "Radiation Transport for Stagnation Flows Including the Effect of Lines and Ablation Layer," AIAA Paper No. 68-664, Fluid and Plasma Dynamics Conference (Los Angeles, Cal.), June 24-26, 1968.

2.10 Wilson, K. H. and H. Hoshizaki, "Effect of Ablation Product Absorption and Line Transistions on Shock Layer Radiative Transport," NASA CR-1264, 1969.

2.11 Wilson, K. H., "Massive Blowing Effects on Viscous, Radiating, Stagnation-Point Flow," AIAA Paper No. 70-203, Eighth Aerospace Sciences Meeting (New York, N. Y.), January 19-21, 1970.

2.12 Wilson, K. H. and R. Greif, "Radiation Transport in Atomic Plasmas," Journal of Quantitative Spectroscopy Research & Technology, Vol. 8, 1968, pp. 1061-1086.

2.13 Wilson, K. H., "Stagnation Point Analysis of Coupled Viscous-Radiating Flow with Massive Blowing," NASA CR-1548, June 1970.

2.14 Rigdon, W. S., R.B. Dirling, Jr., and M. Thomas, "Radiative and Convective Heating During Atmospheric Entry," NASA CR-1170, September, 1968.

2.15 Rigdon, W. S., R. B. Dirling, and M. Thomas, "Stagnation Point Heat Transfer During Hypervelocity Atmospheric Entry," NASA CR-1462, 1970.

2.16 Smith, G. L., J. T. Suttles and E. M. Sullivan, "Viscous Radiating Flow Field on an Ablating Blunt Body," AIAA Paper No. 70-218, Eighth Aerospace Sciences Meeting, (New York, New York), January 19-21, 1970.

2.17 Garrett, B. L., G. L. Smith, and J. N. Perkins, "An Implicit Finite Difference Solution to the Viscous Shock Layer, Including the Effects of Radiation and Strong Blowing," NASA TR R-388, November 1972.

2.18 Sutton, K., "Fully Coupled Nongray Radiating Gas Flows with Ablation Product Effects About Planetary Entry Bodies," AIAA Paper No. 73-672, (Palm Springs, California), July 16-18, 1973.

2.19 Suttles, J. T., "A Method of Integral Relations Solution for Radiating, Nonadiabatic, Inviscid Flow Over a Blunt Body," NASA TN D-5480, October, 1969.

2.20 Garrett, L. B., "An Implicit Finite Difference Solution to the Viscous Radiating Shock Layer with Strong Blowing," Ph.D. dissertation, North Carolina State University, Raleigh, North Carolina, 1971.

2.21 Garrett, L. B., J. T. Suttles and J. N. Perkins, "A Modified Method of Integral Relations Approach to the Blunt-Body Equilibrium Air Flow Field, Including Comparisons with Inverse Solutions," NASA TN D-5434, September, 1969.

2.22 Olstad, W. B., "Blunt-Body Stagnation - Region Flow with Nongray Radiation Heat Transfer - A Singular Perturbation Solution," NASA TR R-295, 1968.

2.23 Callis, L. B., "Solutions of Blunt-Body Stagnation - Region Flow with Nongray Emission and Absorption of Radiation by a Time-Asymtotic Technique," NASA TR R-299, 1969.

2.24 Wilson, K. H. "RATRAP - A Radiation Transport Code," 6-77-67-12, Lockheed Missiles and Space Co., March 14, 1967.

2.25 Falanga, R. A. and E. M. Sullivan, "An Inverse-Method Solution for Radiating, Nonadiabatic, Equilibrium Inviscid Flow Over a Blunt Body," NASA TN D-5907, August 1970.

2.26 Engel, C. D., R. C. Farmer, and R. W. Pike, "Ablation and Radiation Coupled Viscous Hypersonic Shock Layers," AIAA Journal, 11 (8), pp. 1174-1181, August 1973.

2.27 Engel, C. D., "Ablation and Radiation Coupled Viscous Hypersonic Shock Layers," Ph.D. dissertation, Louisiana State University, Baton Rouge, Louisiana (1971).

2.28 Esch, D. D., "Stagnation Region Heating of a Phenolic-Nylon Ablator During Return from Planetary Missions," Ph.D. dissertation, Louisiana State University, Baton Rouge, Louisiana (1971).

2.29 Chou, Y. S., "Locally Nonsimilar Solutions for Radiating Shock Layer about Smooth Axisymmetric Bodies," NASA CR 1989, March 1972.

2.30 Chou, Y. S. and L. H. Blake, "Thin Radiating Shock Layer About a Blunt Body," NASA CR-1547, March 1970.

2.31 Chou, Y. S., "Radiative Coupled Viscous Flow with Massive Blowing," NASA CR-2236, March 1973.

2.32 Olstad, W. B., "Nongray Radiating Flow about Smooth Symmetric Bodies," AIAA Journal, 9, (1), pp. 122-130, January 1971.

2.33 Schneider, W., "A Uniformly Valid Solution for the Hypersonic Flow Past Blunted Bodies," Journal of Fluid Mechanics, Vol. 31, Part 2, 1968, pp. 379-415.

2.34 Davis, R. T. and I. Fluggi-Lotz, "Second Order Boundary-Layer Effects in Hypersonic Flow Past Axisymmetric Blunt Bodies," J. Fluid Mech., Vol. 20, 1964, pp. 593-623.

2.35 Chou, Y. S., "SL4 Code - A User's Manual," NASA CR-2235, March 1973.

2.36 Olstad, W. B., "Stagnation-Point Solutions for Inviscid Radiating Shock Layers," NASA TN D-5792, June 1970.

2.37 Maslen, S. H., "Inviscid Hypersonic Flow Past Smooth Symmetric Bodies," AIAA Journal, 2 (6), pp. 1055-1061, June 1964.

2.38 Sutton, K. and R. A. Falanga, "Stagnation Region Radiative Heating with Steady-State Ablation During Venus Entry," JSR, 10 (2), pp. 155-157, February 1973.

2.39 Blottner, F. G., "Finite Difference Methods of Solution of Bloundary Layer Equations," AIAA J., 8, (2), Feb. 1970.

2.40 Blottner, F. G., "Similar and Nonsimilar Solutions of the Nonequilibrium Laminar Boundary Layer," AIAA Journal, 1 (9), pp. 2156-2157, September 1963.

2.41 Blottner, F. G., "Nonequilibrium Laminar Boundary-Layer Flow of Ionized Air," AIAA Journal, 2 (11), pp. 1921-1927, November 1964.

2.42 Blottner, F. G., "Viscous Shock Layer at the Stagnation Point with Nonequilibrium Air Chemistry," AIAA Journal 7, (12), pp. 2281-2288, December 1969.

2.43 Blottner, F. G., M. Johnson and M. Ellis, "Chemically Reacting Viscous Flow Program for Multi-Component Gas Mixtures," SC-RR-70-754, Sandia Laboratories, (Albuquerque, New Mexico), December 1971.

2.44 Moore, J. A., "Chemical Nonequilibrium of Viscous Flows," Ph.D. dissertation, State Univ. of New York at Buffalo, May 1967.

2.45 Davis, R. T., "The Hypersonic Fully Viscous Shock-Layer Problem," SC-RR-68-840, Sandia Laboratories, December 1968.

2.46 Davis, R. T., "Numerical Solution of the Hypersonic Viscous Shock-Layer Equations," AIAA Journal, 8 (5), pp. 843-851, May 1970.

2.47 Davis, R. T., "Hypersonic Flow of a Chemically Reacting Binary Mixture Past a Blunt Body," AIAA Paper No. 70-805, Third Fluid and Plasma Dynamics Conference (Los Angeles, Cal.), June 29-July 1, 1970.

2.48 Bortner, M. H. and J. A. Golden, "A Critique on Reaction Rate Constants Involved in the Chemical System of High Temperature Air," General Electric TIS R-61SD023, 1961.

2.49 Bortner, M. H., "A Review of Rate Constants of Reactions in Re-entry Flow Fields," General Electric TIS R-68SD13, 1968.

2.50 Chung, P. M. and A. D. Anderson, "Dissociative Relaxation of Oxygen Over an Adiabatic Flat Plate at Hypersonic Mach Numbers," NASA TN D-140, 1960.

2.51 Cresswell, J., B. Kaplan, R. Porter, and C. Sarkos, "Material Effects of Low Temperature Ablators on Hypersonic Wake Properties of Slender Bodies," General Electric TIS 67SD255, 1967.

2.52 Hall, G. J., A. W. Eschenroeder, and P. V. Marrone, "Blunt-Nosed Inviscid Airflows with Coupled Nonequilibrium Processes," J. Aerospace Sciences, Vol. 29, pp. 1038-1051, 1962.

2.53 Moss, N. N., "Solutions for Reacting and Nonreacting Viscous Shock Layers with Multicomponent Diffusion and Mass Injection, Ph.D. dissertation, Virginia Polytechnic Institute and State University, Blacksburg, Virginia (1971).

2.54 Adams, J. G., C. H. Lewis, H. S. Brahensky, et. al., "Nonequilibrium, Mass Transfer, and Viscous Interaction on Spherically

Blunted Cones at Hypersonic Conditions," AEDC-TR-69-237, Arnold Engineering Development Center, Jan. 1970.

2.55 Grose, W. L., "A Thin-Shock-Layer Solution for Nonequilibrium, Inviscid Hypersonic Flows in Earth, Martian, and Venusian Atmospheres," NASA TN D-6529, Decmeber 1971.

CHAPTER III

DEVELOPMENT OF THE THIN SHOCK LAYER EQUATIONS

Introduction

In this chapter the governing equations for the radiating, chemically reacting, viscous flow around a blunt body are developed, transformed, and placed into solution form. A more detailed development of these equations, including an order of magnitude analysis is given by Engel et al. (Ref. 3.1). Engel's development is a complete derivation of the thin shock layer equations from general transport equations which includes intermediate formulations of varying degrees of rigor. The assumptions inherent at each stage of development are clearly stated. This chapter omits some of the tedious mathematical details of the derivation while retaining most of the logical step-by-step procedure used in obtaining the set of equations necessary to describe the flow field around an ablating blunt body.

The thin shock layer equations, which model the flow of the multicomponent gas in the shock heated region of the ablator, are a set of parabolic partial integro-differential equations. By nature, parabolic differential equations require one set of initial conditions and two sets of boundary conditions. In the shock layer, the initial conditions are given by the stagnation line equations, and the two boundary conditions are given by the Rankine-Hugoniot equations at the bow shock and the mass and energy balances at the ablator surface. The stagnation line equations are simply the thin shock layer equations reduced to ordinary integro-differential equations at the axis of symmetry on the body. The Rankine-Hugoniot equations at the shock and the surface balances at the ablator surface insure conservation of mass, energy, and momentum across these boundaries. Since the initial and boundary conditions are a very integral part of the shock layer solution, this chapter treats the derivation of these equations in some detail.

In order to attain a more feasible coordinate system for solution, the blunt body equations are transformed by the Dorodnitsyn transformation. This transformation is an independent variable transformation which allows for a stretching of the normal body coordinate near the body utilizing the variation in density across the shock. The solution in this form allows for easier numerical solution.

Finally, a general form for numerical solution of the set of parabolic partial differential equations is developed and presented. In Chapter V the equations in this form are finite differenced and arranged in the form for numerical solution.

The Physical Environment

It becomes necessary in the development of any mathematical model to make simplifying assumptions to the general conservation equations in order to obtain a set of equations that is more feasible to solve. These simplifying assumptions are determined only by understanding the physical system to be modeled and by assessing the magnitude of the terms in the general conservation equations. An assessment of this sort will provide, not only a basis for omitting from the equations terms of neglible consequence, but will also provide a means of estimating the magnitude of terms impossible or too difficult to evaluate at this stage of technological development. A knowledge of the importance of these various terms indicates which uncertain parameters are most necessary to study.

In order to determine the proper mathematical model to describe the flow field around a blunt body moving at hypersonic velocities, the behavior of the gas the vehicle will encounter must be investigated. In Figure 3.1 based on the work of Reference 3.2 the flight regimes are presented which are encountered by a body during atmospheric entry. The regimes can be grouped into two gasdynamic domains-continuum and noncontinuum. Hayes and Probstein (Ref. 3.2) demonstrates the continuum can be divided into five regimes: (1) classical boundary layer, (2) vorticity interaction, (3) fully viscous, (4) incipient merged layer, and (5) fully merged layer. The general conservation equations can be used to describe the gas flow over a body in these continuum regimes. A brief description of these five continuum regimes follows (Ref. 3.1):

1. Boundary layer regime: The classical boundary layer equations are a valid approximation of the viscous effects for high Reynolds numbers corresponding to lower altitudes. Viscous effects dominate near the wall in a region which is small compared to the shock layer thickness. Vorticity generated by the shock curvature is therefore negligible, having no effect on the boundary layer flow.
2. Vorticity interaction becomes important at lower Reynolds numbers where shock generated vorticity becomes significant in respect to viscous effects near the body. Here the

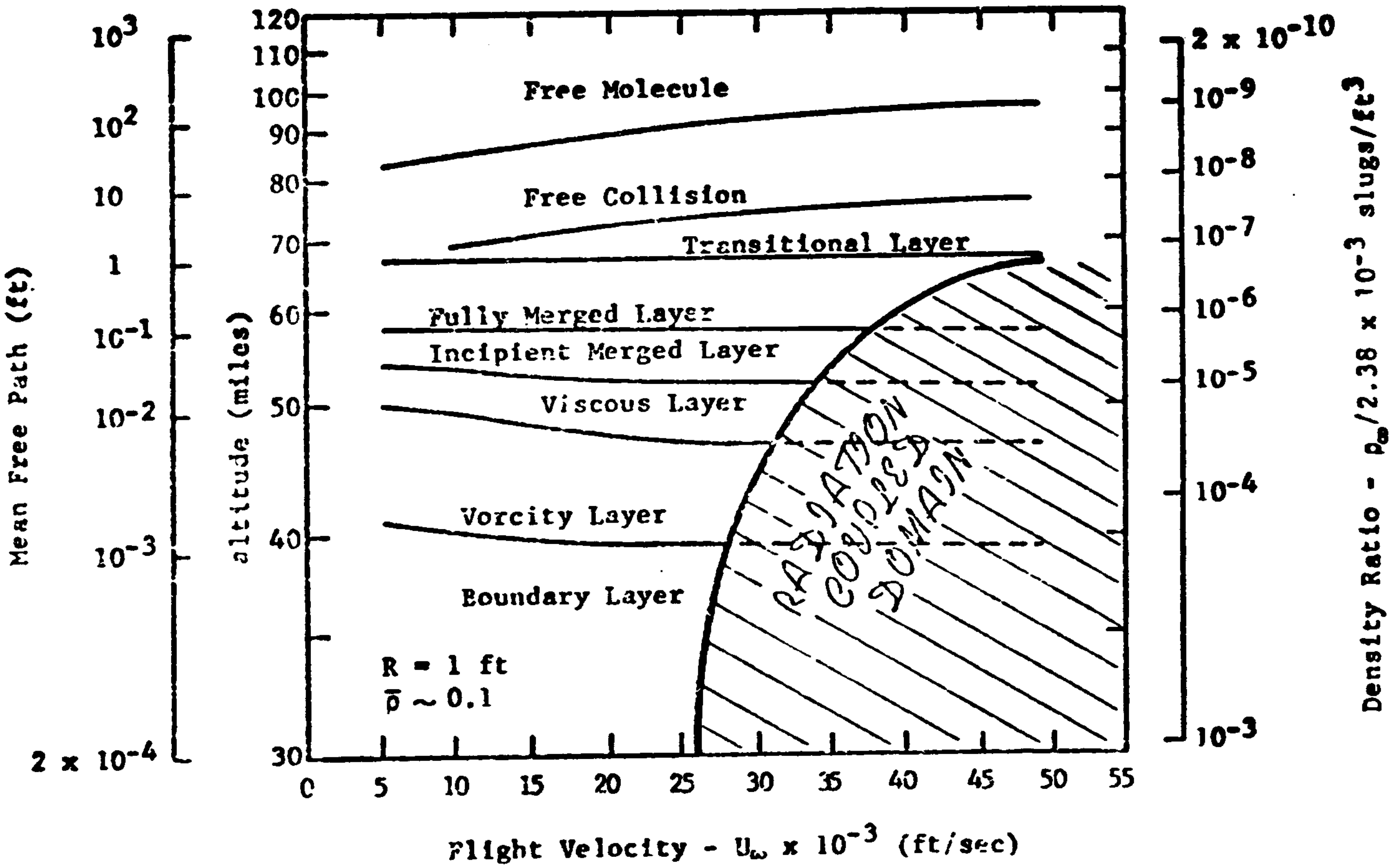

Figure 3.1. Flight Regimes (Modified from Ref. 3.4).

outer region of the shock layer, usually considered the inviscid layer, becomes coupled through momentum transport to the higher shear region near the body, usually thought of as the boundary layer. The high shear region near the body is also larger than experienced at higher Reynolds numbers.

3. Viscous layer regime: Viscous effects from the body interaction are spread through the shock layer. This occurs at lower Reynolds numbers and correspondingly higher altitudes than the vorticity interaction regime. Viscous dissipation at the shock is still small in comparison to dissipation at the body. This condition is true as long as the ratio of the mean free path behind the shock over the shock layer thickness is much smaller than the square root of the density ratio across the shock wave (Ref. 3.2). This implies that the Rankine-Hugoniot shock wave equations are valid for determination of the shock layer boundary conditions.
4. Incipient merged layer regime: The incipient merged layer begins when dissipative effects at the shock are significant. The shock wave is thin relative to the shock layer thickness but the Rankine-Hugoniot relations must be modified to account for viscous effects at the shock boundary.
5. Fully merged layer regime: At higher altitudes and low Reynolds numbers, a distinct shock does not exist. The free stream mean free path over the major body radius is approximately one or less. The flow behaves continuously from the free stream to the body. Above this altitude

range continuum concepts are no longer applicable, and the flow goes through a transition to free molecular flow.

The foregoing discussion of the five continuum flow regimes follows the reasoning of Hayes and Probstein (Ref. 3.2) under the assumption that radiative energy transport and ablative mass injection were negligible. In the present development, these two effects are of primary importance. Figure 3.1 shows the flight regimes where radiative heating to a one-foot body becomes significant. For the most part, significant ablation rates are also encountered in these regimes when using present day charring ablators such as phenolic carbon and phenolic nylon. Engel et al. (Ref. 3.1) concludes that these same mechanisms for momentum transport hold true when radiation and ablation are present, therefore the basic characteristics of the shock layer are unchanged in these regimes.

The basic conservation equations are appropriate to describe the flow of a continuum reacting and radiating gas mixture over a blunt surface when thermal equilibrium exists. For the present work, a reduced set of equations will be determined which describes the flow in the shock layer over a blunt body when the outer boundary of the shock layer is a shock wave described by the Rankine-Hugoniot equations. Thus, the equations governing the flow in the shock layer will be applicable to the three higher Reynolds number regimes. It is in these three regimes where the heating rates to a vehicle's surface are the most significant.

The Conservation Equations

The conservation equations can now be written in general vector-tensor notation. The statement of these equations is given by

Engel et al. (Ref. 3.1) in time independent vector form as follows:

Global Continuity:

$$\overline{\nabla} \cdot \rho\overline{V} = 0 \qquad [3.1]$$

Species Continuity:

$$\overline{\nabla} \cdot (\rho_i\overline{V}) + \overline{\nabla} \cdot \overline{J}_i = \omega_i \qquad [3.2]$$

Momentum:

$$\rho(\overline{V}\cdot\overline{\nabla})\ \overline{V} + \overline{\nabla} \cdot (\overline{\overline{\tau}} - \overline{\overline{I}}P) = 0 \qquad [3.3]$$

Energy:

$$\rho(\overline{V}\cdot\overline{\nabla})\ H + \overline{\nabla}\cdot(\overline{q}_D + \overline{q}_R) - \overline{\nabla}\cdot(\overline{\overline{\tau}}) \cdot \overline{V} = 0 \qquad [3.4]$$

where the radiation pressure tensor and external force field terms have been omitted from the energy and momentum equations.

In order to describe the flow over blunt bodies, moving at hypersonic velocities, it is found convenient to state the conservation equations in orthogonal body oriented coordinate systems. The type of body under consideration, i.e. three dimensional, axisymmetric or two-dimensional, determines the stretching functions which are used in transforming the equations from general vector-tensor notation into a usable coordinate system. The classes of bodies considered in this development are axisymmetric and two dimensional which have the same stretching functions therefore the same form of the equations. The statement of the body oriented shock layer equations is given below (after Engel, Ref. 3.1):

Global Continuity:

$$\frac{\partial}{\partial x} (\rho u r^A) + \frac{\partial}{\partial y} (\tilde{\kappa} r^A \rho v) = 0 \qquad [3.5]$$

Species Continuity:

$$\frac{\partial}{\partial x} (r^A \rho C_i u) + \frac{\partial}{\partial y} (\tilde{\kappa} r^A \rho C_i v) = - \frac{\partial}{\partial x} (r^A J_{i,x})$$

$$- \frac{\partial}{\partial y} (\tilde{\kappa} r^A J_{i,y}) + \tilde{\kappa} r^A \omega_i \qquad [3.6]$$

x-momentum:

$$\rho r^A u \frac{\partial u}{\partial x} + \rho \tilde{\kappa} r^A v \frac{\partial v}{\partial y} - \rho \kappa r^A uv + r^A \frac{\partial P}{\partial x}$$

$$- \frac{\partial}{\partial x} (r^A \tau_{xx}) - \frac{\partial}{\partial y} (\tilde{\kappa} r^A \tau_{xy}) - r^A \kappa \tau_{xy} + \tau_{zz} \frac{\partial r^A}{\partial x} = 0 \qquad [3.7]$$

y-momentum:

$$\rho r^A u \frac{\partial v}{\partial x} + \rho \tilde{\kappa} r^A v \frac{\partial v}{\partial y} - \rho \kappa r^A u^2 + \tilde{\kappa} r^A \frac{\partial P}{\partial y}$$

$$- \frac{\partial}{\partial x} (r^A \tau_{xy}) - \frac{\partial (\tilde{\kappa} r^A \tau_{yy})}{\partial y} + \kappa r^A \tau_{xx} + \tilde{\kappa} \tau_{zz} \frac{\partial r^A}{\partial y} \qquad [3.8]$$

Energy:

$$\rho r^A u \frac{\partial H}{\partial x} + \rho \tilde{\kappa} r^A v \frac{\partial H}{\partial y} = - \frac{\partial}{\partial x} (r^A q_{D,x}) - \frac{\partial}{\partial y} (\tilde{\kappa} r^A q_{D,y})$$

$$- \frac{\partial}{\partial x} (r^A q_{R,x}) - \frac{\partial}{\partial y} (\tilde{\kappa} r^A q_{R,y}) + \frac{\partial}{\partial x} [r^A u \tau_{xx} + r^A v \tau_{xy}]$$

$$+ \frac{\partial}{\partial y} [\tilde{\kappa} r^A u \tau_{xy} + \tilde{\kappa} r^A v \tau_{yy}] = 0 \qquad [3.9]$$

where κ is the local body curvature and r is defined in Figure 3.2. Using Figure 3.2, the following relationships may be found

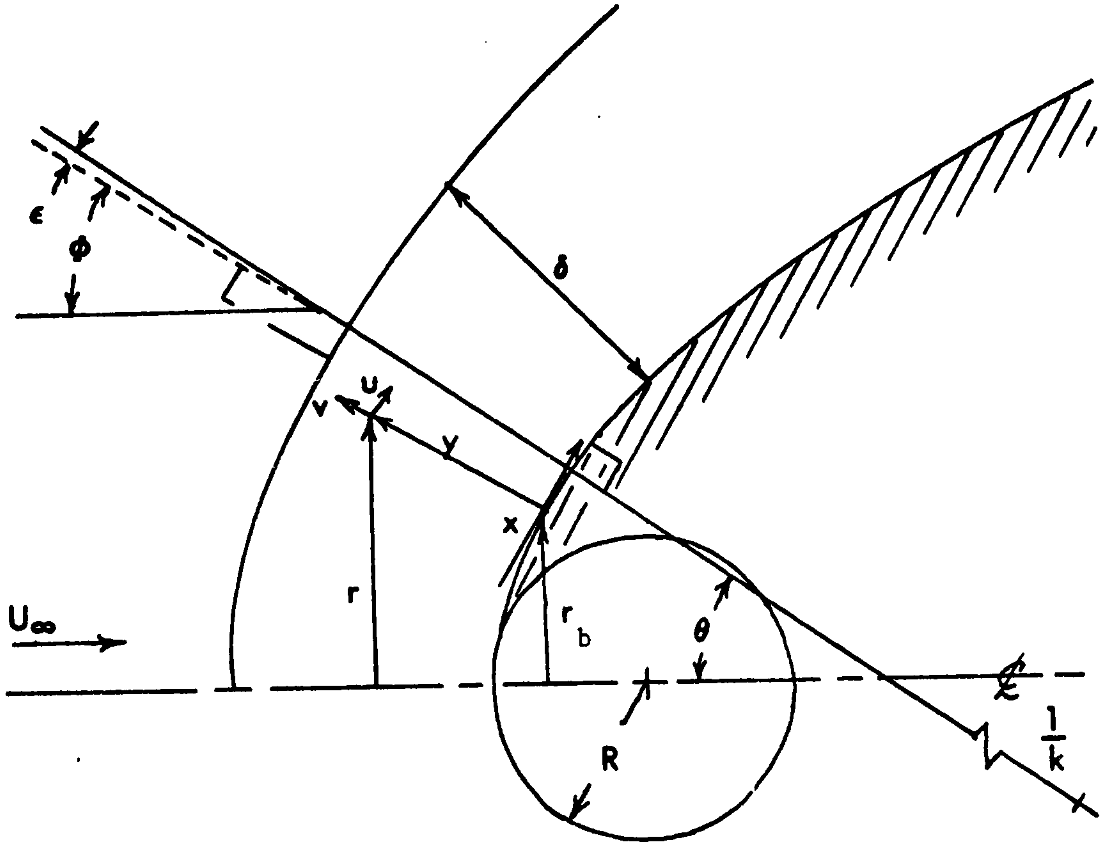

ϵ
ϕ
δ
u
v
y
x
r
r_b
θ
U_∞
℄
R
$\frac{1}{k}$

$$\tan\epsilon = \frac{d\delta}{(1 + k\delta)\ dx} \qquad \frac{d\theta}{dx} = k(x)$$

$$\delta = \int_0^x (1 + k\delta)\ \tan\epsilon dx + \delta_o$$

$$\theta = \int_0^x k\ (x)\ dx$$

Figure 3.2. Body-Oriented Coordinate System.

$$r = r_b + y \sin \Theta \qquad [3.10]$$

$$dr = \sin \Theta \, dy + \tilde{\kappa} \cos \Theta \, dx \qquad [3.11]$$

where

$$\tilde{\kappa} = 1 + \kappa y \qquad [3.12]$$

$$A = 0 \quad , \quad \text{two dimensional}$$

$$A = 1 \quad , \quad \text{axisymmetric} \qquad [3.13]$$

Defining the diffusional mass flux vectors, $\overline{J}_i$, and the heat flux vectors, $\overline{q}_D$, yields

$$\overline{J}_i = \overline{J}_i^{(D)} + \overline{J}_i^{(T)} ; \; \overline{q} = \overline{q}_D + \overline{q}_R \qquad [3.14]$$

The components (neglecting force and pressure mass diffusion) are Concentration diffusion:

$$J_{i,x}^{(D)} = \frac{n_T^2}{\rho RT} \sum_{j=1}^{n} M_i M_j D_{ij} \left(Y_i \sum_{\substack{k=1 \\ k \neq j}}^{n} \left(\frac{\partial G_i}{\partial Y_k}\right)_{\substack{T, V, Y_i \\ i \neq j,k}} \frac{1}{\tilde{\kappa}} \frac{\partial Y_k}{\partial x} \right) \qquad [3.15]$$

$$J_{i,y}^{(D)} = \frac{n_T^2}{\rho RT} \sum_{j=1}^{n} M_i M_j D_{ij} \left(Y_i \sum_{\substack{k=1 \\ k \neq j}}^{n} \left(\frac{\partial G_i}{\partial Y_k}\right)_{\substack{T, V, Y_i \\ i \neq j,k}} \frac{\partial Y_k}{\partial y} \right) \qquad [3.16]$$

Thermal diffusion:

$$J_{i,x}^{(T)} = - \frac{D_i^T}{\tilde{\kappa}} \frac{\partial \ln T}{\partial x} \qquad [3.17]$$

$$J_{i,y}^{(T)} = - D_i^T \frac{\partial \ln T}{\partial y} \qquad [3.18]$$

Diffusional heat flux:

$$q_{D,x} = - \frac{k}{\tilde{\kappa}} \frac{\partial T}{\partial x} + \sum h_i J_{i,x} - \frac{P}{N^2} \sum_i \sum_{j \neq i} \frac{N_i}{m_i} \frac{D_i^T}{D_{ij}} \left(\frac{J_{j,x}}{\rho_j} - \frac{J_{i,x}}{\rho_i} \right) \qquad [3.19]$$

$$q_{D,y} = - k \frac{\partial T}{\partial y} + \sum h_i J_{iy} - \frac{P}{N^2} \sum_i \sum_{j \neq i} \frac{N_i}{m_i} \frac{D_i^T}{D_{ij}} \left(\frac{J_{j,y}}{\rho_j} - \frac{J_{i,y}}{\rho_i} \right) \qquad [3.20]$$

Radiative heat flux:

$$q_{R,x} = \int_{x(\bar{r}_o)}^{x(\bar{r}_1)} \int_o^\infty \alpha_v \left(4\Pi \; B_v - \int_o^{4\Pi} I_v \; (\bar{r}) d\Omega \right) d\nu \tilde{\kappa} dx \qquad [3.21]$$

$$q_{R,y} = \int_{y(\bar{r}_o)}^{y(\bar{r}_1)} \int_o^\infty \alpha_v \left(4\Pi \; B_v - \int_o^{4\Pi} I_v \; (\bar{r}) d\Omega \right) d\nu \; dy \qquad [3.22]$$

In the momentum and the energy equations, the components of the stress tensor are:

$$\tau_{xx} = \frac{\lambda}{\tilde{\kappa} r^A} \left(\frac{\partial}{\partial x} (r^A u) + \frac{\partial}{\partial y} (\tilde{\kappa} r^A v) \right)$$

$$+ \frac{2\mu}{\tilde{\kappa}} \left(\frac{\partial u}{\partial x} + \kappa v \right) \qquad [3.23]$$

$$\tau_{yy} = \frac{\lambda}{\tilde{\kappa} r^A} \left(\frac{\partial}{\partial x} (r^A u) + \frac{\partial}{\partial y} (\tilde{\kappa} r^A v) \right) + 2\mu \frac{\partial v}{\partial y} \qquad [3.24]$$

$$\tau_{zz} = \frac{\lambda}{\tilde{\kappa} r^A} \left(\frac{\partial}{\partial x} (r^A u) + \frac{\partial}{\partial y} (\tilde{\kappa} r^A v) \right.$$

$$+ 2\mu \left[\frac{u}{\tilde{\kappa} r^A} \frac{\partial r^A}{\partial x} + \frac{v}{r^A} \frac{\partial r^A}{\partial y} \right) \qquad [3.25]$$

$$\tau_{xy} = \tau_{yx} = \mu \left(\frac{1}{\tilde{\kappa}} \frac{\partial v}{\partial x} + \frac{\partial u}{\partial y} - \frac{\kappa}{\tilde{\kappa}} u \right) \qquad [3.26]$$

The statement of these vector and tensor components completes the set of conservation equations expressed in body-oriented, orthogonal coordinates. These equations are subsequently simplified by an order of magnitude analysis, yielding a much more manageable set of equations called the thin shock layer equations.

The Thin Shock Layer Equations

The statement was made earlier that the basic conservation equations were to be used for the flow of a continuum reacting and radiating gas mixture over a blunted surface when thermodynamic equilibrium exists. It was also stated that a reduced set of equations could be used which would describe the flow when the outer boundary of the shock layer is a shock wave described by the Rankine-Hugoniot relations. This set of equations is called the thin shock layer equations and is arrived at by an order of magnitude analysis in which all terms of order one [1] are retained (Ref. 3.1). Further simplifications can be made by neglecting the shock layer thickness in comparison to the local body radius. This implies

$$\kappa \rightarrow 0, \quad \tilde{\kappa} \rightarrow 1, \text{ and } r^A \rightarrow r_b^A \qquad [3.27]$$

Applying these limits and dropping terms using an order of magnitude analysis gives

Global Continuity:

$$\frac{\partial}{\partial x} (r_b^A \rho u) + r_b^A \frac{\partial}{\partial y} (\rho v) = 0 \qquad [3.28]$$

Species Continuity:

$$\frac{\partial}{\partial x} (r_b^A \rho \ell C_i u) + r_b^A \frac{\partial}{\partial y} (\rho C_i v) = -r_b \frac{\partial}{\partial y} (J_{i,y}) + r_b \, \omega_i \qquad [3.29]$$

x-momentum:

$$\rho u \frac{\partial u}{\partial x} + \rho v \frac{\partial u}{\partial y} = - \frac{\partial P}{\partial x} + \frac{\partial}{\partial y} \left(\mu \frac{\partial u}{\partial y} \right) \qquad [3.30]$$

y-momentum:

$$\frac{\partial P}{\partial y} = \frac{\kappa}{\tilde{\kappa}} \rho u^2 \qquad [3.31]$$

Energy:

$$\rho u \frac{\partial H}{\partial x} + \rho v \frac{\partial H}{\partial y} = \frac{\partial}{\partial y} \left(\frac{k \partial T}{\partial y}\right) - \frac{\partial}{\partial y} \left\{ \sum_i h_i J_{i,y} - \frac{P}{N^2} \sum_i \sum_{j \neq i} \frac{N_i}{m_i} \frac{D_i^T}{\mathbb{D}_{ij}} \left(\frac{J_{i,y}}{\rho_j} - \frac{J_{i,y}}{\rho_i} \right) \right\} - \frac{\partial q_{R,y}}{\partial y} + \frac{\partial}{\partial y} \left(\mu u \frac{\partial u}{\partial y}\right) \qquad [3.32]$$

The shock layer equations 3.28 to 3.32 are now rewritten with some changes noted. The global continuity and the two momentum equations are unchanged. The global continuity is removed from the species equation, and the energy equation is written with enthalpy and temperature as the principle dependent variable. Furthermore, the resulting temperature form of the energy equation was obtained by subtracting the momentum equation, substituting the right hand side of the species equation from the left hand side and assuming binary diffusion. Thermal diffusion is also neglected. The resulting set of dimensional asixymmetric (A=1) shock layer equations is

Global Continuity:

$$\frac{\partial}{\partial x} (\rho \; u \; r_b) + r_b \frac{\partial}{\partial y} (\rho v) = 0 \qquad [3.33]$$

Species Continuity:

$$\rho u \frac{\partial C_i}{\partial x} + \rho v \frac{\partial C_i}{\partial y} = \frac{\partial}{\partial y} (\rho D_{12} \frac{\partial C_i}{\partial y}) + \omega i \qquad [3.34]$$

x-momentum:

$$\rho u \frac{\partial u}{\partial x} + \rho v \frac{\partial u}{\partial y} = - \frac{\partial P}{\partial x} + \frac{\partial}{\partial y} (\mu \frac{\partial u}{\partial y}) \qquad [3.30]$$

y-momentum

$$\frac{\partial P}{\partial y} = \frac{\kappa}{\tilde{\kappa}} \rho u^2 \qquad [3.31]$$

Energy (Enthalpy):

$$\rho u \frac{\partial H}{\partial x} + \rho v \frac{\partial H}{\partial y} = \frac{\partial}{\partial y} (k \frac{\partial T}{\partial y}) - \frac{\partial}{\partial y} \sum h_i J_{i,y} - \frac{\partial q_{R,y}}{\partial y}$$

$$+ \frac{\partial}{\partial y} (\mu u \frac{\partial u}{\partial y}) \qquad [3.35]$$

Energy (Temperature):

$$\rho u C_p \frac{\partial T}{\partial x} + \rho v C_p \frac{\partial T}{\partial y} = - \sum h_i \omega_i + u \frac{\partial P}{\partial x}$$

$$+ \frac{\partial}{\partial y} (k \frac{\partial T}{\partial y}) - \frac{\partial q_R}{\partial y} + \mu (\frac{\partial u}{\partial y})^2 + \sum C_{pi} \rho D_{12} \frac{\partial C_i}{\partial y} \frac{\partial T}{\partial y} \qquad [3.36]$$

These equations are in dimensional form and body oriented coordinates. In the following section these equations are nondimensionalized and an independent variable transformation is performed.

Nondimensionalized and Transformed Equations

The thin shock layer equations 3.30, 3.31, 3.33, 3.34, 3.35 and 3.36 can be nondimensionalized by using the following dimensionless variables which are appropriate to the problem under consideration.

$$x = \frac{x^*}{R^*} \qquad y = \frac{y^*}{R^*} \qquad u = \frac{u^*}{U_\infty^*} \qquad v = \frac{v^*}{U_\infty^*}$$

$$\rho = \frac{\rho^*}{\rho_{s,o}} \qquad \mu = \frac{\mu^*}{\mu_{s,o}^*} \qquad P = \frac{P^*}{\rho_{so}^* U_\infty^{*2}} \qquad \delta = \frac{\delta^*}{R^*}$$

$$r_b = \frac{r_b^*}{R^*} \qquad \kappa = \kappa^* R^* \qquad k = \frac{k^* T_{s,o}^*}{R^* \rho_{s,o}^* U_\infty^{*3}} \qquad T = \frac{T^*}{T_{s,o}^*}$$

$$h = \frac{h^*}{1/2 U_\infty^{*2}} \qquad \omega_i = \frac{R^* \omega_i^*}{\rho_{s,o}^* U_\infty^*} \qquad C_p = \frac{C_p^* T_{s,o}^*}{1/2 \; U_\infty^{*2}}$$

$$\tilde{\kappa} = 1 + \kappa y \qquad Re_s = \frac{\rho_{s,o}^* U_\infty^* R^*}{\mu_{s,o}^*} \qquad Sc = \frac{\mu_{s,o}^*}{\rho_{s,o}^* D_{12}^*}$$

$$\mathbb{E} = \frac{\mathbb{E}^* \rho^*}{\rho_{s,o}^* U_\infty^{*3}} \qquad \text{where } \mathbb{E}^* = \frac{\partial q_R^*}{\partial y^*}$$

The dimensional variables used in the preceding section for the thin shock layer equations are denoted by a superscript asterisk (*) in this discussion. The nondimensional variables have no superscript, and the nondimensional quantities for Reynolds number (Re_s) and Schmit (Sc) number have been incorporated. The resulting form of the shock layer equations in nondimensional form is shown in Table 3.1.

These equations can now undergo an independent variable transformation of the Dorodnitzn type. The Dorodnitzn transformation reduces the effect of a large variation in density in the body normal coordinate by incorporating the density in the transformed normal coordinate. The new independent variables now become

Table 3.1

Nondimensional Thin Shock Layer Equations

Global Continuity:

$$\frac{\partial}{\partial x}(\rho u r_b) + r_b \frac{\partial}{\partial y}(\rho v) = 0 \qquad [3.37]$$

Species Continuity:

$$\rho u \frac{\partial C_i}{\partial x} + \rho v \frac{\partial C_i}{\partial y} = \frac{1}{Re_s} \frac{\partial}{\partial y}\left(\frac{\mu}{S_c} \frac{\partial C_i}{\partial y}\right) + \omega_i \qquad [3.38]$$

x-momentum:

$$\rho u \frac{\partial u}{\partial x} + \rho v \frac{\partial u}{\partial y} = -\frac{\partial P}{\partial x} + \frac{1}{Re_s} \frac{\partial}{\partial y} \left(\mu \frac{\partial u}{\partial y}\right) \qquad [3.39]$$

y-momentum:

$$\frac{\partial P}{\partial y} = \frac{\kappa}{\bar{\kappa}} \rho \, u^2 \qquad [3.40]$$

Energy (Enthalpy):

$$\rho u \frac{\partial h}{\partial x} + \rho v \frac{\partial h}{\partial y} + 2\rho \; (u^2 \frac{\partial u}{\partial x} + uv \frac{\partial v}{\partial x} + v^2 \frac{\partial v}{\partial y} + vu \frac{\partial u}{\partial y}$$

$$= 2 \frac{\partial}{\partial y}\left(\frac{k}{C_p} \frac{\partial h}{\partial y}\right) - 2 \frac{\partial}{\partial y}\left(\frac{k}{C_p} \sum h_i \frac{\partial C_i}{\partial y}\right) + \frac{1}{Re_s} \sum \frac{\mu}{Sc} \frac{\partial C_i}{\partial y} \frac{\partial h_i}{\partial y}$$

$$+ \frac{1}{Re_s} \sum h_i \frac{\partial}{\partial y}\left(\frac{\mu}{Sc} \frac{\partial C_i}{\partial y}\right) - 2 \; \mathbb{E} \frac{2}{Re_s} \; \frac{\partial}{\partial y}\left(\mu u \frac{\partial u}{\partial y}\right) \qquad [3.41]$$

Energy (Temperature):

$$\rho u \, C_p \frac{\partial T}{\partial x} + \rho v \, C_p \frac{\partial T}{\partial y} = \sum h_i \, \omega_i + 2u \frac{\partial P}{\partial x}$$

$$+ 2 \frac{\partial}{\partial y}\left(k \frac{\partial T}{\partial y}\right) - 2 \, \mathbb{E} + \frac{2\mu}{Re_s}\left(\frac{\partial u}{\partial y}\right)^2 + \frac{\mu}{Re_s}\left(\sum \frac{C_{pi}}{Sc} \frac{\partial C_i}{\partial y}\right)\frac{\partial T}{\partial y} \qquad [3.42]$$

$$\xi = x \tag{3.43}$$

$$\eta = \frac{\int_0^y \rho \, dy}{\int_0^\delta \rho \, dy} \qquad \frac{\int_0^y \rho \, dy}{\tilde{\delta}} \tag{3.44}$$

where δ is the shock standoff distance, and $\tilde{\delta}$ is the transformed shock standoff distance which is used to normalize the variable η from 0 to 1. The derivatives become

$$\frac{\partial}{\partial x} = \frac{\partial}{\partial \xi} + \frac{\partial \eta}{\partial x} \frac{\partial}{\partial \eta} \tag{3.45}$$

$$\frac{\partial}{\partial y} = \frac{\rho}{\tilde{\delta}} \frac{\partial}{\partial \eta} \tag{3.46}$$

When the new independent variables are introduced and the transformations are applied, the nondimensional shock layer equations become the following in the transformed plane:

Global Continuity:

$$\frac{1}{r_b} \frac{\partial}{\partial \xi} (\rho u r_b) + \frac{\partial \eta}{\partial x} \frac{\partial}{\partial \eta} (\rho u) + \frac{\rho}{\tilde{\delta}} \frac{\partial}{\partial \eta} (\rho v) = 0 \tag{3.47}$$

Species Continuity:

$$\rho u \frac{\partial C_i}{\partial \xi} + \rho u \frac{\partial \eta}{\partial x} \frac{\partial C_i}{\partial \eta} + \frac{\rho^2 v}{\tilde{\delta}} \frac{\partial C_i}{\partial \eta} =$$

$$\frac{\rho}{Re_s \delta^2} \frac{\partial}{\partial \eta} \left(\frac{\rho \mu}{S_c} \frac{\partial C_i}{\partial \eta} \right) + \omega_i \tag{3.48}$$

x-momentum:

$$\rho u \frac{\partial u}{\partial \xi} + \rho u \frac{\partial \eta}{\partial x} \frac{\partial u}{\partial \eta} + \frac{\rho^2 v}{\tilde{\delta}} \frac{\partial u}{\partial \eta} = - \frac{\partial P}{\partial \xi} - \frac{\partial \eta}{\partial x} \frac{\partial P}{\partial \eta}$$

$$+ \frac{\rho}{Re_s \tilde{\delta}^2} \frac{\partial}{\partial \eta} (\rho \mu \frac{\partial u}{\partial \eta}) \qquad [3.49]$$

y-momentum:

$$\frac{\partial P}{\partial \eta} = \frac{\kappa}{\tilde{\kappa}} \tilde{\delta} u^2 \qquad [3.50]$$

Energy (Enthalpy):

$$\rho u \frac{\partial h}{\partial \xi} + \rho u \frac{\partial \eta}{\partial x} \frac{\partial h}{\partial \eta} + \rho v \frac{\rho}{\tilde{\delta}} \frac{\partial h}{\partial \eta} + 2\rho (u^2 \frac{\partial u}{\partial \xi} + u^2 \frac{\partial \eta}{\partial x} \frac{\partial u}{\partial \eta}$$

$$+ vu \frac{\partial v}{\partial \xi} + vu \frac{\partial \eta}{\partial x} \frac{\partial v}{\partial \eta} + \frac{\rho v^2}{\tilde{\delta}} \frac{\partial v}{\partial \eta} + \frac{\rho vu}{\tilde{\delta}} \frac{\partial u}{\partial \eta}) =$$

$$\frac{2\rho}{\tilde{\delta}^2} \frac{\partial}{\partial \eta} (\frac{\rho k}{C_p} \frac{\partial h}{\partial \eta}) - \frac{2\rho}{\tilde{\delta}^2} \frac{\partial}{\partial \eta} (\frac{\rho k}{C_p} \sum h_i \frac{\partial Ci}{\partial \eta}) +$$

$$\frac{\rho}{Re_s \tilde{\delta}^2} \sum (\frac{\rho \mu}{Sc}) \frac{\partial C_i}{\partial \eta} \frac{\partial h_i}{\partial \eta} + \frac{\rho}{Re_s \tilde{\delta}^2} \sum h_i \frac{\partial}{\partial \eta} (\frac{\rho \mu}{Sc} \frac{\partial C_i}{\partial \eta})$$

$$- 2 \mathbb{E} + \frac{2\rho}{Re_s \tilde{\delta}^2} \frac{\partial}{\partial \eta} (\rho \mu u \frac{\partial u}{\partial \eta}) \qquad [3.51]$$

Energy (Temperature):

$$\rho u C_p \frac{\partial T}{\partial \xi} + \rho u C_p \frac{\partial \eta}{\partial x} \frac{\partial T}{\partial \eta} \rho^2 \frac{v}{\tilde{\delta}} C_p \frac{\partial T}{\partial \eta} = \sum h_i \omega_i$$

$$+ 2u \frac{\partial P}{\partial \xi} + 2u \frac{\partial \eta}{\partial x} \frac{\partial P}{\partial \eta} + \frac{2\rho}{\tilde{\delta}^2} \frac{\partial}{\partial \eta} (\rho k \frac{\partial T}{\partial \eta}) - 2 \mathbb{E}$$

$$+ \frac{2\rho^2 \mu}{Re_s \tilde{\delta}^2} \left(\frac{\partial u}{\partial \eta} \right)^2 + \frac{\rho^2 \mu}{Re_s \tilde{\delta}^2} (\sum \frac{C_{pi}}{S_c} \frac{\partial C_i}{\partial \eta}) \frac{\partial T}{\partial \eta} \qquad [3.52]$$

This nondimensional, transformed set of equations is a set of parabolic partial differential equations which needs two sets of boundary conditions and one set of initial conditions. The formulation of the boundary and initial conditions will now be discussed.

Boundary and Initial Conditions

The parabolic nature of the thin shock layer equations mathematically requires initial conditions as well as boundary conditions in order to obtain a solution. The entry vehicle axis of symmetry is the appropriate location of the starting line for zero angle of attack problems and provides the initial conditions for the shock equations. The determination of conditions along this line, called the stagnation line, is a major and important problem in itself. The stagnation line solution also requires the same two sets of boundary conditions as the shock layer solution. Consequently, development of the method to obtain these initial conditions (i.e. stagnation line solution) is delayed until after the boundary conditions are established. The boundary conditions are specified at the bow shock and at the ablator surface.

Boundary Conditions at the Bow Shock

If the shock geometry is known, the Rankine-Hugoniot equations can be used to obtain the shock boundary conditions. The development of these equations in curvilinear coordinates follows directly from Ref. 3.5. The dimensional Rankine-Hugoniot equations written in body oriented coordinates (See Figures 3.2 and 3.3) are:

$$v_s = U_\infty^* \sin\phi \sin\varepsilon - \bar{\rho}\, U_\infty^* \cos\phi \cos\varepsilon \qquad [3.53]$$

$$u_s = U_\infty^* \sin\phi \cos\varepsilon + \bar{\rho}\, U_\infty^* \cos\phi \sin\varepsilon \qquad [3.54]$$

$$P_s^* + \rho_s^* \,(\bar{\rho} U_\infty^* \cos\phi)^2 = P_\infty^* + \rho_\infty^* \,(U_\infty^* \cos\phi)^2 \qquad [3.55]$$

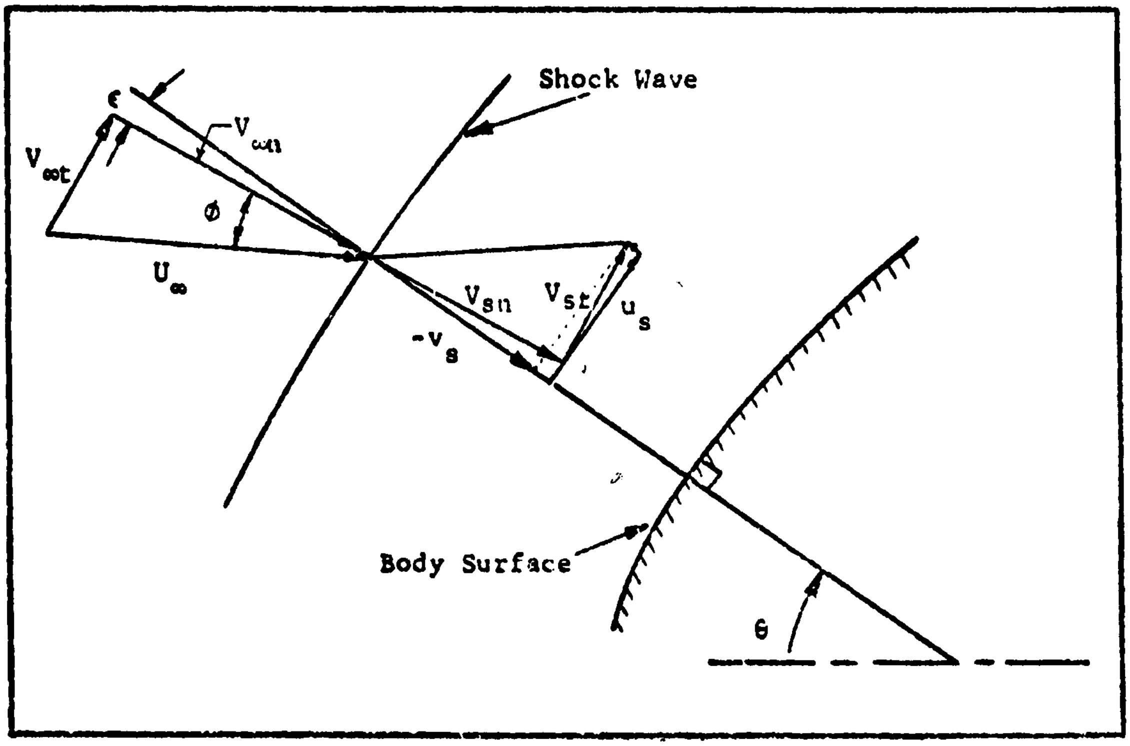
Shock Wave
ϵ
$V_{\infty n}$
$V_{\infty t}$
ϕ
U_∞
V_{sn}
V_{st}
u_s
$-v_s$
Body Surface
θ

Fig. 3.3. Resolution of Velocity Components in a Body Oriented Coordinate System

$$h_s^* = \frac{U_\infty^{*2}}{2} - \frac{1}{2}(u_s^{*2} + v_s^{*2}) + h_\infty^* \qquad [3.56]$$

The tangential velocity is negligible near the stagnation line thus reducing Equation 3.56 to

$$h_s^* = \frac{1}{2} U_\infty^{*2}(1 - \bar{\rho}^2) \cos^2 \phi + h_\infty^* \qquad [3.57]$$

Nondimensionalizing Equations 3.53 through 3.57 and dropping P_∞^* and h_∞^* which are of order $(\bar{\rho}^2)$ yields the following shock boundary conditions:

$$v_s = \sin \phi \sin \varepsilon - \bar{\rho} \cos \phi \cos \varepsilon \qquad [3.58]$$

$$u_s = \sin \phi \cos \varepsilon + \bar{\rho} \cos \phi \sin \varepsilon \qquad [3.59]$$

$$P_s = (1-\bar{\rho}) \cos^2 \phi \qquad [3.60]$$

$$h_s = (1-\bar{\rho}^2) \cos^2 \phi \qquad [3.61]$$

or

$$h_s = 1 - (u_s^2 + v_s^2) \qquad [3.62]$$

where the following nondimensionalization convention has been used.

$$v = \frac{v^*}{U_\infty^*}, \quad u = \frac{u^*}{U_\infty^*}, \quad h = \frac{h^*}{1/2\; U_\infty^{*2}}, \quad P = \frac{P^*}{\rho_\infty^* U_\infty^{*2}}, \quad \bar{\rho} = \frac{\rho_\infty^*}{\rho_s^*}$$

The preceding Rankine-Hugoniot relations were obtained by performing mass, energy, and momentum balances across a thin shock wave. These relations now enable us to write the shock boundary conditions at $y = \delta$.

$$u = u_s$$

$$v = v_s$$

$$P = P_s$$

$$h = h_s$$

$$C_i = C_{i,s}\ (P_s,\ h_s)\ \text{(Assuming chemical equilibrium)}$$

$$I_\nu^-\ (\tau_{\nu,s}) = 0 \qquad [3.63]$$

The Rankine-Hugoniot equations provide expressions for u_s, v_s, P_s, and h_s. The equation of state and free stream elemental mass fraction provides the post shock species mass fractions assuming chemical equilibrium. The specific intensity coming through the shock towards the body is specified as zero. It is noted that, in total, four boundary conditions are required for the energy equation because of its integro-differential nature. Thus, two boundary conditions, enthalpy and specific intensity, have been specified at the shock.

Boundary Conditions at the Ablator Surface

In order to specify the conditions at the ablator boundary, surface balances of mass, momentum, and energy are required. In connection with these balances, an evaluation is required of the surface removal mechanisms: sublimation, chemical reactions, and erosion. The purpose of this section is to integrate the various surface phenomena through which flow field calculations and the ablator response calculations are coupled. In Appendix A, the quasi-steady state equations that describe the ablator response are presented along with results from numerical solutions. The arrangement of the surface species and energy balances into a form suitable—for coupling of the flow field to the ablator response is given in Appendix B. This development in Appendix B is based on the assumption that sublimation is the major surface removal mechanism.

The boundary conditions for this investigation can be derived in either of two ways. The first technique consists of simply formulating a physical balance across the boundaries of the system. The second technique involves the use of the flow field equations themselves, which are integrated across the system boundaries and then contracted by taking the limit as the spacial increment approaches zero. Both of these methods should yield the same results. In this development both of these methods will be employed. The first method has the advantage that the physical significance of each term in the resulting equation is more readily evident. The integration technique will assure that all of the necessary terms have been included.

Species Boundary Conditions: At the char surface the following general surface balance is known to exist:

$$\left\{\begin{array}{l}\text{convective flux}\\ \text{of species i on}\\ \text{the char side}\\ \text{of the interface}\end{array}\right\} + \left\{\begin{array}{l}\text{diffusive flux of}\\ \text{species i on the}\\ \text{char side of the}\\ \text{interface}\end{array}\right\} + \left\{\begin{array}{l}\text{all contributions}\\ \text{to the net flux}\\ \text{of species i due}\\ \text{to the surface}\\ \text{phenomena}\end{array}\right\}$$

$$= \left\{\begin{array}{l}\text{convective flux of}\\ \text{species i on flow}\\ \text{field side of the}\\ \text{interface}\end{array}\right\} + \left\{\begin{array}{l}\text{diffusive flux of}\\ \text{species i on flow}\\ \text{field side of the}\\ \text{interface}\end{array}\right\} \qquad [3.64]$$

or

$$\rho^{*} v^{*} C_i^{-} + J_i^{*-} + S_i^{*} = \rho\overset{*}{v}^{*} C_i^{+} J_i^{*+} \qquad [3.65]$$

Nondimensionalizing by $\overset{*}{\rho}_{s,o}$ and U_∞^* gives

$$\rho v\, C_i^- + J_i^- + S_i = \rho v\, C_i^+ + J_i^+ \qquad [3.66]$$

The surface generation, S_i, can now be quantitatively defined and the remaining terms of the equation verified by examining the integral derivation of the species surface balance from the nondimensional shock layer species continuity equation. Equation 3.38 is now rewritten as

$$\rho u \frac{\partial C_i}{\partial x} + \rho v \frac{\partial C_i}{\partial y} = -\frac{\partial J_i}{\partial y} + \omega_i \qquad [3.67]$$

where J_i has been substituted back into the equation. Equation 3.67 can be further simplified when we realize that a no slip stipulation at the surface implies that $u = 0$ which gives

$$\rho v \frac{dC_i}{dy} = -\frac{dJ_i}{dy} + \omega_i \qquad [3.68]$$

The generation term in this equation can be expressed as the sum of contributing effects

$$\omega_i = \omega_{i_{homo}} + \omega_{i_{het}} + \omega_{i_{subl}} \qquad [3.69]$$

where $\omega_{i_{homo}}$ is the net generation of species i by means of homogeneous chemical reactions, $\omega_{i_{het}}$ is the net generation by heterogeneous reactions, and $\omega_{i_{subl}}$ is the rate of formation of gaseous species by sublimation.

Each of the previous terms represents a generation of mass of species i by reaction per unit time per unit volume. For the ablator this unit volume contains both gas and solid. Thus if R_i^* is the rate of formation of species i by heterogeneous reaction per unit of solid surface, A^*_r, then $\omega^*_{i_{het}}$ is given by the following equation

$$\omega^*_{i_{het}} = \frac{R^*_i A^*_r}{A^* \Delta y^*} \qquad [3.70]$$

The ratio of $A^*_r/A^*\Delta y^*$ represents the concentration of surface area, i.e., the available surface area per unit volume of the reacting system.

In the subsequent steps of this analysis Equation 3.68 will be integrated across the char interface a distance of Δy^* which will define the thickness of a control volume of cross-sectional area A^* which contains a total reactive surface area A^*_r. Equation 3.70 can be written in non-dimensional form by the following manipulations.

$$\omega_{i_{het}} = \left(\frac{R^*_i A^*_r}{A^* \Delta y^*}\right)\left(\frac{R^*}{\rho^*_{s,o} U^*_\infty}\right) = \frac{R_i A^*_r}{A^* \Delta y} \qquad [3.71]$$

This equation can also be conveniently expressed in terms of char porosity, ϵ_p (volume of voids per unit volume), which for an isotropic material is equal to $(A^* - A^*_r)/A^*$. Thus,

$$\omega_{i_{het}} = R_i \frac{(1 - \epsilon_p)}{\Delta y} \qquad [3.72]$$

In a similar manner the sublimation term can be derived as,

$$\omega_{i_{subl}} = \left(\frac{\int^*_i A^*_r}{A^* \Delta y^*}\right)\left(\frac{R^*}{\rho^*_{s,o} U^*_\infty}\right) = \int_i \frac{(1 - \epsilon_p)}{\Delta y} \qquad [3.73]$$

where $\int^*_i$ is the mass rate of sublimation per unit area of solid surface.

Following the above procedure, the homogeneous reaction rate term can be written as

$$\omega_{i_{homo}} = (\omega^*_{i_{homo}} \epsilon_p) \left(\frac{R^*}{\rho^*_{s,o} U^*_\infty}\right) \qquad [3.74]$$

where $\omega^*_{i,homo}$ is the net rate of formation of species i in the gas phase.

Having now defined, quantitatively, the total generation term in the species continuity equation, the integration technique will be used to define f_i in terms of ω_i. Equation 3.68 can be integrated as follows:

$$\int_{y-}^{y+} \rho v \frac{dC_i}{dy}\, dy = -\int_{y-}^{y+} \frac{dJ_i}{dy}\, dy + \int_{y-}^{y+} (\omega_{i_{homo}} + \omega_{i_{het}} + \omega_{i_{subl}})\, dy \qquad [3.75]$$

Substituting Equations 3.72 and 3.74 into the above gives:

$$\int_{y-}^{y+} \rho v\, d\, C_i = -\int_{y-}^{y+} d\, J_i + \int_{y-}^{y+} \omega_{i_{homo}}\, dy + \int_{y-}^{y+} \frac{(R_i + f_i)(1-\epsilon_p)}{\Delta y}\, dy \qquad [3.76]$$

Integrating the above equation noting that ρv is a constant gives

$$\rho v\, C_i^+ - \rho v\, C_i^- = J_i^- + J_i^+ + \omega_{i_{homo}} \Delta y + (R_i + f_i)(1-\epsilon_p) \qquad [3.77]$$

Taking the limit as $\Delta y \to 0$ and rearranging gives:

$$\rho v\, C_i^- + J_i^- + (R_i + f_i)(1-\epsilon_p) = \rho v\, C_i^+ + J_i^+ \qquad [3.78]$$

Comparing the above equation with Equation 3.66 confirms our previous surface balance and defines S_i, the dimensionless surface generation term, as:

$$S_i = (R_i + \int_i)(1-\varepsilon_p) \qquad [3.79]$$

Although Equation 3.78 is completely rigorous for all species which may exist either in the flow field or the char, a more specific interpretation of this equation can be arrived at for various types of species which can be grouped into distinct categories. For example: pyrolysis gases (excluding carbon), carbon gas, all remaining gases, and finally the solid carbon. A more complete treatment of how these various categories are handled is given in Appendix B.

Energy Boundary Conditions: Starting with Equation 3.32 the energy balance at the surface will be developed in a fashion analogous to the preceding one for the species equations. Equation 3.32 is the energy equation in a dimensionless form. This equation becomes (omitting thermal diffusion)

$$\rho u \frac{\partial H}{\partial x} + \rho v \frac{\partial H}{\partial y} = \frac{\partial}{\partial y} [k \frac{\partial T}{\partial y} - \sum h_i J_i] - \frac{\partial q_{R,y}}{\partial y}$$

$$+ \frac{\partial}{\partial y} (\mu u \frac{\partial u}{\partial y}) \qquad [3.80]$$

Again noting that the tangential velocity, u, equals zero at the surface, Equation 3.80 reduces to

$$\rho v \frac{dH}{dy} = \frac{d}{dy} (k \frac{dT}{dy}) - \frac{d}{dy} \sum h_i \; J_i - \frac{\partial q_{R,y}}{dy} \qquad [3.81]$$

Integrating the above equation across the char surface gives

$$\rho v H^+ - \rho v H^- = [k \frac{dT^+}{dy} - \sum h_i J_i^+ + q_R^-] - [k \frac{dT^-}{dy} - \sum h_i J_i^- + q_R^+] \qquad [3.82]$$

The above equation can be placed in a more convenient form using the following equations. The equation for the total enthalpy is

$$H = h + \frac{\overline{V}^2}{2} \qquad [3.83]$$

and, using the definition of the static enthalpy it can be written in terms of the mass fraction, C_i, and enthalpy per unit mass of i, h_i.

$$H = \sum h_i C_i + \frac{\overline{V}^2}{2} \qquad [3.84]$$

Using the above relationships and noting that kinetic energy terms are small compared to the enthalpy terms and can be deleted, the left hand side of Equation 3.82 can be written as

$$\rho v \sum h_i C_i^+ - \rho v \sum h_i C_i^- \qquad [3.85]$$

The terms on the right hand side of Equation 3.82 will now be evaluated. Considering the first bracketed term on the right hand side of Equation 3.82, all three terms in this bracket are to be evaluated in the flow field and will be retained. The first term is the conductive heat flux, the second is the diffusive energy flux, and the third, q_R^-, is the energy radiated to the surface from the flow field. In the second bracketed term the only terms of importance are the conduction of energy into the char $(k\frac{dT^-}{dy})$

and the energy radiated by the surface (q_R^+). The resulting equation after substituting in these relations becomes

$$\rho v \sum h_i \left(C_i^+ - C_i^-\right) + k \frac{dT}{dy}^- - q_{RR} = k \frac{dT}{dy}^+ - \sum h_i J_i^+ - q_R \qquad [3.86]$$

where q_R is the energy radiated by the flow field to the surface and q_{RR} is the energy radiated by the surface toward the flow field. The terms with the superscript (-) are evaluated with an ablator response analysis described in Appendices A and B. The terms with the superscript (+) are evaluated in the flow field analyses.

The above form of the surface energy balance shows the coupling between the compositions, mass fluxes and surface temperature. Thus a simultaneous solution of the species surface balances and the energy surface balance is required.

Momentum Boundary Conditions: If a no slip condition is imposed at the ablator surface, the tangential velocity, u, is zero for all x at y = 0. This boundary condition has been used in the previous species and energy surface balance derivations. This condition can also be used in the determination of the surface pressure from the y-momentum equations, Equation 3.31, yielding

$$\frac{dP}{dy} = 0 \qquad [3.87]$$

Integrating Equation 3.87 gives the simple result

$$P^+ = P^- \qquad [3.88]$$

which states that the pressures on both sides of the surface are equal when considering terms in the y-momentum equation that are first order accurate.

Global Continuity Boundary Condition: The global continuity equation is a statement of the conservation of mass and is a first order partial differential equation. The solution of this equation requires the specification of the normal velocity at the surface. More normally the mass injection rate is specified (ρv). Figure 3.4 shows that the flow of gases $(\rho_g v_g)$ to the surface along with the rate of solid addition $(\rho_c v_r)$ is equal to the total mass injection rate, $(\rho v)_{wall}$. This same conclusion can be arrived at by solving the global continuity equation, Equation 3.37, at the surface

$$\frac{d}{dy}(\rho v) = 0 \qquad [3.89]$$

which upon integrating becomes

$$\rho v|^{-} = \rho v|^{+} \qquad [3.90]$$

or

$$\rho_g v_g + \rho_c v_r = \rho v_{wall} \qquad [3.91]$$

The terms $\rho_g v_g$ and $\rho_c v_r$ are determined from the ablator response characteristics.

In summary, the derivation of the wall boundary conditions has been completed by applying surface mass, energy, and momentum balances. These balances describe the interaction of the ablator with the flow field. Appendix A develops the equations which describe the ablator response and Appendix B shows the coupling

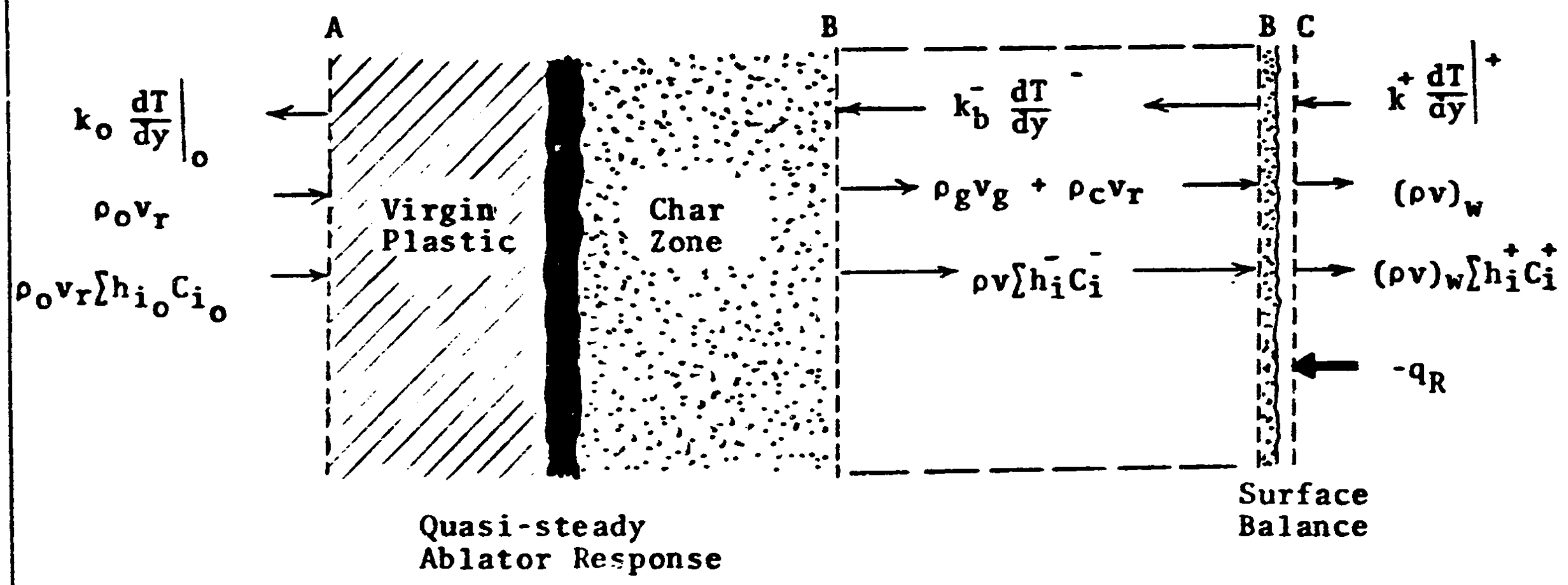
A
B
B C
$k_o \frac{dT}{dy}\Big|_o$
$\rho_o v_r$
$\rho_o v_r \sum h_{i_o} C_{i_o}$
Virgin Plastic
Char Zone
$k_b^- \frac{dT}{dy}^-$
$\rho_g v_g + \rho_c v_r$
$\rho v \sum \bar{h}_i \bar{C}_i$
$k^+ \frac{dT}{dy}\Big|^+$
$(\rho v)_w$
$(\rho v)_w \sum h_i^+ C_i^+$
$-q_R$
Quasi-steady Ablator Response
Surface Balance

Figure 3.4. Illustration of Flowfield Coupling and Quasi-steady Ablator Response.

that exists between the species and energy surface balances. The behavior of the flow field is governed by the shock layer equations along with its boundary conditions and initial conditions. To complete the flow field specification, the initial conditions will now be discussed.

Initial Conditions

In order to obtain initial values for the shock layer solution, a reduced set of thin shock-layer equations must be solved at $x = 0$ along y, the stagnation line (see Figure 3.2). The solution of this set of equations is important because any distributional shock layer solution, due to its parabolic nature, is only as valid as its initial values.

The solution of the stagnation line equations by direct methods has been approached in two ways. The work of Ho and Probstein (Ref. 3.6) typifies the stagnation region solutions which use expansions of the dependent variables in x to obtain the stagnation and near stagnation line equations. The work of Hoshizaki and Wilson (Ref. 3.7) typifies the stagnation line solutions which determine the stagnation line equations by formally taking the limit of the terms in the shock layer equations at $x = 0$ using symmetry conditions. The latter method is used in this analysis.

Engel (Ref. 3.8) develops the stagnation line equations by a detailed derivation from the thin shock layer equations. The global continuity, species continuity, and energy equations are reduced by taking limits and noting that at $x = 0$, $u = 0$, the species and energy equations become ordinary differential equations. The x-momentum equation yields a trivial solution in its unaltered form, therefore the x-momentum equation is differentiated with respect to x and its limiting form along the stagnation line is determined.

The normal curvature effects are dropped and only first order terms are kept. The resulting equations are

Global Continuity:

$$2 \frac{\partial u}{\partial x} = \frac{-1}{\rho} \frac{\partial}{\partial y} (\rho v) \qquad [3.92]$$

Species Continuity:

$$\rho v \frac{\partial C_i}{\partial y} = \frac{-\partial}{\partial y} (J_{i,y}) + \omega_i \qquad [3.93]$$

x-momentum:

$$\frac{\partial}{\partial y} [\mu \frac{\partial}{\partial y} (\frac{\partial u}{\partial y})] - \rho v \frac{\partial}{\partial y} (\frac{\partial u}{\partial x}) + \rho (\frac{\partial u}{\partial x})^2 + (\frac{\partial^2 P}{\partial x^2})_{x=0} = 0 \qquad [3.94]$$

y-momentum:

$$\frac{\partial P}{\partial y} = 0 \qquad [3.95]$$

Energy (Enthalpy):

$$\rho v \frac{\rho}{\delta} \frac{dh}{d\eta} + \frac{2(\rho v)}{\tilde{\delta}} \frac{dv}{d\eta} = \frac{2\rho}{\tilde{\delta}} \frac{d}{d\eta} \left(\rho \frac{k}{C_p} \frac{dh}{d\eta}\right)$$

$$- \frac{2\rho}{\tilde{\delta}^2} \frac{d}{d\eta} \left(\rho \frac{k}{C_p} \sum h_i \frac{dC_i}{d\eta}\right) + \frac{\rho}{Re_s \tilde{\delta}^2} \sum \frac{(\rho\mu)}{Sc} \frac{dC_i}{d\eta} \frac{dh_i}{d\eta}$$

$$+ \frac{\rho}{Re_s \tilde{\delta}^2} \sum h_i \frac{d}{d\eta} \left(\frac{\rho\mu}{Sc} \frac{dC_i}{d\eta}\right) - 2 \mathbb{E} \qquad [3.96]$$

Energy (Temperature):

$$\rho v \, C_p \frac{dT}{dy} = - \sum h_i \, \omega_i + \frac{d}{dy} (k \frac{dT}{dy}) - \frac{dq_R}{dy}$$

$$+ \sum C_{pi} \, J_i \frac{dT}{dy} \qquad [3.97]$$

Using the nondimensional quantities given previously, the global continuity and momentum equations can be placed in dimensionless form as follows:

Global Continuity:

$$2 \frac{\partial u}{\partial x} = - \frac{1}{\rho} \frac{\partial}{\partial y} (\rho v) \qquad [3.98]$$

x-momentum:

$$\frac{1}{Re_s} \frac{\partial}{\partial y} (\mu \frac{\partial}{\partial y} (\frac{\partial u}{\partial x})) - \rho v \frac{\partial}{\partial y} (\frac{\partial u}{\partial x}) - \rho (\frac{\partial u}{\partial x})^2$$

$$- \frac{\partial^2 P}{\partial x^2} = 0 \qquad [3.99]$$

y-momentum:

$$\frac{\partial P}{\partial y} = 0 \qquad [3.100]$$

Species Continuity:

$$\rho v \frac{dC_i}{dy} = - \frac{1}{Re_s} \frac{dJ_i}{dy} + \omega_i \qquad [3.101]$$

Energy (Enthalpy):

$$\rho v \frac{\partial h}{\partial y} + 2\rho v^2 \frac{\partial v}{\partial y} = 2 \frac{\partial}{\partial y} (\frac{k}{C_p} \frac{\partial h}{\partial y}) - 2 \frac{\partial}{\partial y} (\frac{k}{C_p} \sum h_i \frac{\partial C_i}{\partial y}$$

$$+ \frac{1}{Re_s} \sum \frac{\mu}{Sc} \frac{\partial C_i}{\partial y} \frac{\partial h_i}{\partial y} + \frac{1}{Re_s} \sum h_i \frac{\partial}{\partial y} (\frac{\mu}{Sc} \frac{\partial C_i}{\partial y}) - 2 \mathbb{E} \qquad [3.102]$$

Energy (Temperature):

$$\rho v C_p \frac{dT}{dy} = \sum h_i \omega_i + 2 \frac{d}{dy} (k \frac{dT}{dy}) - 2 E$$

$$+ \frac{\mu}{Pe_s} \sum C_{pi} J_i \frac{dT}{dy} \qquad [3.103]$$

The second derivative of pressure term in the x-momentum equation can be evaluated at the shock using the Rankine-Hugoniot equations if $\frac{\partial P}{\partial y}$ is assumed zero. This pressure term is

$$\frac{\partial^2 P}{\partial x^2} = - 2 \bar{\rho} (1-\bar{\rho}) \left(\frac{\partial \phi}{\partial x}\right)^2 \qquad [3.104]$$

For a concentric shock $\frac{\partial \phi}{\partial x} = 1$. The concentric shock assumption is usually rather good for hypersonic flow, however in this derivation $\frac{\partial \phi}{\partial x}$ will be treated as a parameter and thus will be left general. Substituting this term into the momentum equation yields

$$\frac{1}{Re_s} \frac{\partial}{\partial y} (\mu \frac{\partial}{\partial y} (\frac{\partial u}{\partial x})) - \rho v \frac{\partial}{\partial y} (\frac{\partial u}{\partial x}) - \rho (\frac{\partial u}{\partial x})^2$$

$$+ 2 \bar{\rho} (1 - \bar{\rho}) (\frac{\partial \phi}{\partial x})^2 = 0 \qquad [3.105]$$

To obtain a more classical form of the momentum equation, a velocity function is defined

$$f' = \frac{\partial u}{\partial x} / \frac{\partial u_{s,o}}{\partial x} = \lim_{x \to o} \frac{u}{u_s} = \text{a function of } y \qquad [3.106]$$

where

$$\frac{\partial u_{s,o}}{\partial x} = \frac{\partial \phi}{\partial x} + \bar{\rho} \frac{\partial \varepsilon}{\partial x} \qquad [3.107]$$

from the Rankine-Hugoniot equations. Substituting into the momentum equation yields

$$\frac{1}{Re_s} \frac{\partial}{\partial y} (\mu \frac{\partial f'}{\partial y}) - \rho v \frac{\partial f'}{\partial y} - \rho \frac{\partial u_{s,o}}{\partial x} (f')^2$$

$$+ \frac{2 \bar{\rho} (1-\bar{\rho})}{\partial u_{s,o} / \partial x} (\frac{\partial \phi}{\partial x})^2 = 0 \qquad [3.108]$$

The stagnation line equations can now be transformed using the

Dorodnitzn transformation as was used for the thin shock layer equations. For this transformation, Equations 3.43 through 3.46 are applied

$$\xi = x \qquad [3.43]$$

$$\eta = \frac{\int_0^y \rho\, dy}{\tilde{\delta}} \qquad [3.44]$$

$$\frac{\partial}{\partial x} = \frac{\partial}{\partial \xi} + \frac{\partial \eta}{\partial x}\frac{\partial}{\partial \eta} \qquad [3.45]$$

$$\frac{\partial}{\partial y} = \frac{\rho}{\tilde{\delta}}\frac{\partial}{\partial \eta} \qquad [3.46]$$

where $\partial\eta/\partial x$ equals zero at the stagnation line. The resulting transformed equations are

Global Continuity:

$$2\frac{\partial u}{\partial \xi} = -\frac{1}{\tilde{\delta}}\frac{\partial}{\partial \eta}(\rho v) \qquad [3.109]$$

Species Continuity:

$$\frac{\rho v}{\tilde{\delta}}\frac{dC_i}{d\eta} = \frac{1}{Re_s\tilde{\delta}^2}\frac{d}{d\eta}\left(\frac{\rho\mu}{S_c}\frac{dC_i}{d\eta}\right) + \frac{\omega_i}{\rho} \qquad [3.110]$$

Velocity function:

$$f' = \frac{\partial u/\partial\xi}{\partial u_{s,o}\partial\xi} = \frac{\frac{-1}{2\tilde{\delta}}\frac{\partial}{\partial \eta}(\rho\, v)}{\frac{\partial u_{s,o}}{\partial \xi}} = \frac{\partial f}{\partial \eta} \qquad [3.111]$$

x-momentum:

$$\frac{d}{d\eta}\left(\rho\mu\frac{df'}{d\eta}\right) - \rho v\, Re_s\tilde{\delta}\frac{df'}{d\eta} +$$

$$\frac{Re_s\,\tilde{\delta}}{\mu\left(\frac{\partial u_{s,o}}{\partial \xi}\right)}\left[\,2\bar{\mu}\,(1-\bar{\rho})\left(\frac{\partial \Phi}{\partial \xi}\right)^2 - \mu\left(\frac{\partial u_{s,o}}{\partial \xi}f'\right)^2\right] = 0 \qquad [3.112]$$

y-momentum:

$$\frac{dP}{d\eta} = 0 \qquad [3.113]$$

Energy (Enthalpy):

$$\rho v \frac{\rho}{\tilde{\delta}} \frac{\partial h}{\partial \eta} + 2 \frac{\rho^2 v^2}{\tilde{\delta}} \frac{\partial v}{\partial \eta} = \frac{2\rho}{\tilde{\delta}^2} \frac{\partial}{\partial \eta} \left(\rho \frac{k}{C_p} \frac{\partial h}{\partial \eta}\right) - \frac{2\rho}{\tilde{\delta}^2} \frac{\partial}{\partial \eta}$$

$$\left(\frac{\rho k}{C_p} \sum h_i \frac{\partial C_i}{\partial \eta}\right) + \frac{\rho}{Re_s \, \tilde{\delta}^2} \sum \left(\frac{\rho\mu}{Sc}\right) \frac{\partial C_i}{\partial \eta} \frac{\partial h_i}{\partial \eta} +$$

$$\frac{\rho}{Re_s \, \tilde{\delta}^2} \sum h_i \frac{\partial}{\partial \eta} \left(\frac{\rho\mu}{Sc} \frac{\partial C_i}{\partial \eta}\right) - 2\,\mathbb{E} \qquad [3.114]$$

Energy (Temperature):

$$\frac{\rho v \, C_p}{\tilde{\delta}} \frac{dT}{d\eta} = \sum h_i \left(\frac{\omega_i}{\rho}\right) + \frac{2}{\tilde{\delta}^2} \frac{d}{d\eta} \left(\rho k \frac{dT}{d\eta}\right)$$

$$- \frac{2\,\mathbb{E}}{\rho} + \frac{\rho\mu}{Re_s \, \tilde{\delta}^2} \sum \frac{C_{pi}}{Sc} \frac{dC_i}{d\eta} \frac{dT}{d\eta} \qquad [3.115]$$

Integrating Equation 3.111 yields

$$\rho v = -2 \left(\frac{\partial u_{s\rho}}{\partial \xi}\right) \tilde{\delta} f \qquad [3.116]$$

Equation 3.116 can be used to eliminate ρv from the x-momentum equation. This procedure results in a third order nonlinear ordinary differential equation.

$$(\rho\mu f'')' + \left[2 \, Re_s \, \tilde{\delta}^2 \left(\frac{\partial u_{s,\rho}}{\partial \xi}\right)\right] f f'' +$$

$$\frac{Re_s \, \tilde{\delta}^2}{\left(\frac{\partial u_{s\rho}}{\partial \xi}\right)} \left[\frac{2\bar{\rho}\,(1-\bar{\rho})}{\rho} \left(\frac{\partial \phi}{\partial \xi}\right)^2 - \left(\frac{\partial u_{s,\rho}}{\partial \xi}\right)^2 (f')^2\right] = 0 \qquad [3.117]$$

The boundary conditions for this equation are

$$f' = 1 \qquad \text{at} \qquad \eta = 1$$

$$f' = 0 \qquad \text{at} \qquad \eta = 0$$

$$f = fw = \frac{-(\rho v)_w}{2\tilde{\delta}\,(\partial u_{s,o}/\partial \xi)} \qquad \text{at} \qquad \eta = 0 \qquad [3.118]$$

In addition, Equation 3.116 has a boundary condition imposed on it to determine the transformed standoff distance, $\tilde{\delta}$.

$$f = f_s = \frac{-(\rho v)_s}{2\tilde{\delta}(\frac{\partial u_{s,o}}{\partial \xi})} \qquad \text{at} \qquad \eta = 1 \qquad [3.119]$$

The momentum equation can be reduced to a first and a second order equation by defining

$$\zeta = \frac{f'}{\tilde{\delta}} \qquad [3.120]$$

and substituting into Equation 3.117

$$(\rho\mu)\zeta'' + [2\,Re_s\,\tilde{\delta}^2\,(\frac{\partial u_{s,o}}{\partial \xi})f + (\rho\mu)']\,\zeta'$$

$$-\,Re_s\,\tilde{\delta}^3\,(\frac{\partial u_{s,o}}{\partial \xi})\zeta^2 = -(\frac{2\,Re_s\,\tilde{\delta}\,\bar{\rho}\,(1-\bar{\rho})}{\rho\,(\frac{\partial u_{s,o}}{\partial \xi})})\,(\frac{\partial \phi}{\partial \xi})^2 \qquad [3.121]$$

The resulting boundary conditions for Equation 3.121 are:

$$\zeta = 0 \qquad \text{at} \qquad \eta = 0$$

$$\zeta = 1/\tilde{\delta} \qquad \text{at} \qquad \eta = 1 \qquad [3.122]$$

Equations 3.120 and 3.121 can now be solved simultaneously to give ζ and f. Equation 3.119 can then be solved for the transformed standoff distance, $\tilde{\delta}$.

The foregoing discussion of the stagnation line equations completes the formulation for the initial conditions needed in the solution of the thin shock layer equations. The boundary conditions for the energy and species stagnation line equations are the very same as those discussed for the shock layer equations, i.e. the Rankine-Hugoniot relations and the surface balances. The shock layer solution requires one more piece of information to be completely specified - the shock geometry. The following section describes the geometrical relation necessary in determining shock shape.

Shock Geometry

There are three methods which may be used to determine the shock shape and pressure distribution around the body. First, the technique used in Reference 3.9 and 3.10 and others can be used. The shock shape is specified *a priori* from which the wall pressure distribution is calculated as the solution proceeds around the body. An output shock shape is calculated from the geometrical relation (Ref. 3.11).

$$\varepsilon = \tan^{-1} [(d\delta/d\xi)/(1 + \kappa\delta)] \qquad [3.123]$$

where δ is calculated as a result of the x-momentum solution. This output angle is compared with the input angle and if the input and output meet a specified tolerance, the solution is said to be converged.

The second technique of predicting shock shape involves specifying a wall pressure distribution *a priori*. Preferably this distribution is known from experimental data for hypersonic Mach numbers. The change in pressure due to radiation coupling is justifiably neglected (Ref. 3.9), and a shock shape is also assumed. The shock layer equations are solved around the body and the calculated and input pressure distributions are compared. The shock shape is then numerically adjusted according to the pressure differences. This calculation is repeated until satisfactory pressure convergence is obtained.

The third technique involves a simultaneous solution of the geometric relation

$$\delta = \int_0^{\xi} (1 + \kappa\xi) \tan \varepsilon \, d\xi + \delta_0 \qquad [3.124]$$

with the shock layer equations. The pressure behind the shock and the pressure at the surface are calculated as part of the thin shock layer solution. Only one around the body iteration is required for this technique.

The first two techniques have been implemented in a modified version of the computer program described in Reference 3.9 and 3.10. Unfortunately both of these techniques have severe limitations. The first method consumes a large amount of computer time because many around the body iterations are necessary to insure convergence. In addition, each estimate of shock shape must be made by hand. The second method also consumes a ~~great deal~~ of computer time for the same reason - too many iterations. The second technique does have the advantage over the first that the input and output pressures are smooth allowing an automatic update of the shock shape by the computer. However, this technique does not necessarily satisfy the geometrical differential equation, Equation 3.124.

Engel (Ref. 3.8) concludes, therefore, that since the first two techniques are subject to undesirable limitation, the third technique should be implemented.

This section concludes the development of the mathematical equations which describe the shock layer surrounding a reentering blunt vehicle. The solution of these mathematical equations is taken up in Chapter V where a numerical procedure is developed which requires that the thin shock layer and stagnation line equations first be linearized. The linearization of these equations, therefore, is carried out in the next section.

Quasilinearization of Shock Equations

The differential equations can be made linear in the unknown variables by performing a Taylor series expansion and truncating after the first derivative term of the Taylor series. Coupling between the equations is eliminated in this analysis because computer storage becomes excessive with many chemical species. Coupling between the equations is required for the quasilinearization technique as defined by Bellman and Kulaba (Ref. 3.12), but the uncoupled procedure is shown to be computationally superior by Blottner (Ref. 3.13). Therefore, the present scheme uncouples the conservation equations.

The thin shock layer equations and the stagnation line equations, with the exception of global continuity and y-momentum, can be written in the following general form

$$\frac{\partial^2 W}{\partial \eta^2} + \alpha_1 \frac{\partial W}{\partial \eta} + \alpha_2 W + \alpha_3 + \alpha_4 \frac{\partial W}{\partial \xi} = 0 \qquad [3.125]$$

where α_1, α_2, α_3, and α_4 are the linearized coefficients for $W = \zeta$, $W = u$, $W = C_i$, $W = H$, and $W = T$. These coefficients are as follows

x momentum (stagnation line, $W = \zeta$)

$$\alpha_1 = \frac{2\,Re_s\,\tilde{\delta}^2}{\rho\mu}\left(\frac{\partial\,u_{s,o}}{\partial\xi}\right)f + \frac{(\rho\mu)'}{\rho\mu}$$

$$\alpha_2 = -\frac{2\,Re_s\,\tilde{\delta}^3}{\rho\mu}\left(\frac{\partial\,u_{s,o}}{\partial\xi}\right)\zeta$$

$$\alpha_3 = 2Re_s\tilde{\delta}\left[\frac{\bar{\rho}\,(1-\bar{\rho})}{\rho^2\mu\,\left(\frac{\partial u_{s,o}}{\partial\xi}\right)}\left(\frac{\partial\phi}{\partial\xi}\right)^2 + \frac{\tilde{\delta}^2}{2\rho\mu}\left(\frac{\partial u_{s,o}}{\partial\xi}\right)\zeta^2\right] \qquad [3.126]$$

$$\alpha_4 = 0$$

x-momentum (shock layer, $W = u$)

$$\alpha_1 = \frac{1}{\rho\mu}\left[\,(\rho\mu)' - Re_s\,\tilde{\delta}\,\rho v - Re_s\,\tilde{\delta}^2\,u\,\frac{\partial\eta}{\partial x}\,\right]$$

$$\alpha_2 = \frac{-Re_s\tilde{\delta}^2}{\rho\mu}\left[\frac{\partial u}{\partial\xi} + \frac{\partial\eta}{\partial x}\,\frac{\partial u}{\partial\eta} + \frac{2\tilde{\delta}u}{\rho}\,\frac{\partial\eta}{\partial x}\,\right]$$

$$\alpha_3 = \frac{Re_s\tilde{\delta}^2}{\rho\mu}\left[\,u\,\frac{\partial u}{\partial\xi} - \frac{1}{\rho}\,\frac{\partial P}{\partial\xi} + u\,\frac{\partial\eta}{\partial x}\,\frac{\partial u}{\partial\eta} + \frac{u^2\tilde{\delta}}{\rho}\,\frac{\partial\eta}{\partial x}\right]$$

$$\alpha_4 = -\frac{Re_s\,\tilde{\delta}^2 u}{\rho\mu} \qquad [3.127]$$

Species Continuity, $W = C_i$

$$\alpha_1 = \frac{1}{\beta}\left[\,\beta' - Re_s\,\tilde{\delta}\,\rho v - Re_s\,\tilde{\delta}^2\,u\,\frac{\partial\eta}{\partial x}\,\right]$$

$$\alpha_2 = \frac{Re_s\,\tilde{\delta}^2}{\beta}\,\frac{\partial}{\partial C_i}\left(\frac{\omega_i}{\rho}\right)$$

$$\alpha_3 = \frac{Re_s \tilde{\delta}^2}{\beta} \left[\frac{\omega_i}{\rho} - \left(\frac{\partial}{\partial C_i} \left(\frac{\omega_i}{\rho}\right)\right) C_i \right] \qquad [3.128]$$

$$\alpha_4 = \frac{-Re_s \tilde{\delta}^2 u}{\beta}$$

where

$$\beta = \rho\mu / Sc \qquad [3.129]$$

Energy (Enthalpy): W = h

$$\alpha_1 = \frac{C_p}{\rho k} \left[\frac{\partial}{\partial \eta} \left(\frac{C_p}{\rho k}\right) - \frac{u\tilde{\delta}^2}{2} \frac{\partial \eta}{\partial x} - \frac{\rho v \tilde{\delta}}{2} \right]$$

$$\alpha_2 = 0$$

$$\alpha_3 = \frac{C_p}{\rho k} \left\{ \left(\frac{\rho\mu}{2ScRe_s} - \frac{\rho k}{C_p}\right) \sum \frac{\partial C_i}{\partial \eta} \frac{\partial h_i}{\partial \eta} + \left| \frac{1}{2\ Re_s} \frac{\partial}{\partial \eta} \left(\frac{\rho\mu}{Sc}\right) - \frac{\partial}{\partial \eta} \left(\frac{\rho k}{C_p}\right) \right| \right.$$

$$\sum h_i \frac{\partial C_i}{\partial \eta} + \left(\frac{\rho\mu}{2\ Re_s S_c} - \frac{\rho k}{C_p}\right) \sum h_i \frac{\partial^2 C_i}{\partial \eta^2} - \frac{\tilde{\delta}^2}{\rho} \, |E$$

$$+ \frac{1}{Re_s} \left(\frac{\partial}{\partial \eta} \left(\rho\mu u\right) \frac{\partial u}{\partial \eta} + \rho\mu u \frac{\partial^2 u}{\partial \eta^2}\right) -$$

$$\tilde{\delta}^2 \left| \ u^2 \frac{\partial u}{\partial \xi} + \left(u^2 \frac{\partial \eta}{\partial x} + \frac{\rho v u}{\tilde{\delta}}\right) \frac{\partial u}{\partial \eta} + uv \frac{\partial v}{\partial \xi} + \right.$$

$$\left. \left(uv \frac{\partial \eta}{\partial x} + \frac{\rho v^2}{\tilde{\delta}}\right) \frac{\partial v}{\partial \eta} \ \right| \qquad [3.130]$$

$$\alpha_4 = \frac{-u\ C_p \tilde{\delta}^2}{2\rho k}$$

Energy (Temperature): W = T

$$\alpha_1 = \frac{1}{\rho k} \left| (\rho k)' - \frac{\rho v \tilde{\delta} C_p}{2} + \frac{\rho\mu}{2\ Re_s} \sum C_p \frac{\partial C_i}{\partial \eta} \right.$$

$$- \frac{u\ C_p\ \tilde{\delta}^2}{2} \frac{\partial \eta}{\partial x}$$

$$\alpha_2 = \frac{\tilde{\delta}^2}{2\rho k} [\sum (C_{pi}(\frac{\omega_i}{\rho}) + h_i \frac{\partial}{\partial T} (\frac{\omega_i}{\rho}))] T_{s,o}$$

$$\alpha_3 = \frac{\tilde{\delta}^2}{2\rho k} [\sum h_i(\frac{\omega_i}{\rho}) + \frac{2u}{\rho} \frac{\partial P}{\partial \xi} + \frac{\tilde{\delta} u^3}{\rho} \frac{\partial \eta}{\partial x} - 2 \frac{\mathbb{E}}{\rho}$$

$$+ \frac{2 \rho \mu}{Re_s} (\frac{\partial u}{\partial \eta})^2] - \alpha_2 T$$

$$\alpha_4 = -u\, C_p\, \tilde{\delta}^2/2\rho k \qquad [3.131]$$

Equations 3.125 through 3.131 can be used to numerically solve the shock layer problem. The species and energy equations can be applied at the stagnation line simply by noting that the tangential velocity, u, equals zero, thus making α_4 zero along with terms in the energy equation that contain the normal derivative of u. Chapter V treats these equations further by placing them in finite difference form and describing the numerical solution procedure.

Summary

The thin shock layer equations have been derived from the general conservation equations in vector-tensor notation. The resulting partial integro-differential equations require two sets of boundary conditions and one set of initial conditions due to their parabolic nature. The boundary conditions are given at the bow shock by the Rankine-Hugoniot relations and at the ablator surface by the surface balances. The initial conditions were derived from the thin shock layer equations by taking the limit as x approached zero which yields the stagnation line equations (along the line of symmetry). The shock layer equations were then nondimensionalized, transformed, and quasilinearized for ease of numerical solution.

In order to solve the final set of equations, thermodynamic, transport, kinetic, and radiation properties must be known. The next chapter describes how these properties are obtained and gives the values used in the solution of the equations. In Chapter V the quasilinearized shock layer equations are finite differenced and the method of solution, stability, and results of numerical experimentation are demonstrated.

REFERENCES

3.1 Engel, C. D., D. D. Esch, R. C. Farmer and R. W. Pike, "Formulation, Derivation and Development of the Analysis of Interaction of Ablating Protection Systems and Stagnation Region Heatings", NASA CR-66931, 1970.

3.2 Hayes, W. D. and R. F. Probstein, *Hypersonic Flow Theory* 2nd Ed., Ch. 5, Academic Press, New York (1966).

3.3 Probstein, R. F., "Shock Wave and Flow Field Development in Hypersonic Reentry," *Am. Rocket Soc. Journal*, *31*, pp. 184-194 (Feb. 1961).

3.4 Edelman, R. K. and D. Fortune, "Mixing and Combustion in the Exhaust Plumes of Rocket Engines Burning RP1 and Liquid Oxygen," TR-631 General Applied Science Laboratories, Inc., Nov. 1966.

3.5 Spradley, L. W. and C. D. Engel, "Formulation of a Method for Predicting Coupled Convective and Radiative Heat Transfer About A Blunt Body", NASA CR-61200 (April, 1968).

3.6 Ho, H. T. and R. F. Probstein, "The Compressible Viscous Shock Layer in Rarefied Hypersonic Flow", in *Rarefied Gas Dynamics*, ed. L. Talbot, Academic Press, New York (1961).

3.7 Hoshizaki, H. and K. H. Wilson, "Convective and Radiation Heat Transfer During Superorbital Entry," *AIAA Jour.*, *5* (1), 25 (January, 1967).

3.8 Engel, C. D., "Ablation and Radiation Coupled Viscous Hypersonic Shock Layers," Ph.D. dissertation, Louisiana State University, Baton Rouge, Louisiana (1971).

3.9 Spradley, L. W. and C. D. Engel, "The Effects of Shock Layer Radiation and Viscous Coupling in the Total Heating Rate to a Reentering Blunt Body," NASA CR-61224, April, 1968.

3.10 Spradley, L. W. and C. D. Engel, "A Computer Program for Predicting Coupled Convective and Radiative Heat Transfer to a Body During Superorbital Reenetry," LMSC/HREC A791350, Lockheed Missiles & Space Company, Huntsville, Alabama, (May, 1968).

3.11 Hoshizaki, H. and K. H. Wilson, "Viscous, Radiating Shock Layer About a Blunt Body," *AIAA J.* *3*, No. 9, Sept. 1965, pp. 1614-1622.

3.12 Bellman, R. E. and R. E. Kulaba, *Quasilinearization and Nonlinear Boundary-Value Problems*, American Elsevier, New York, 1965.

3.13 Blottner, F. G., "Finite Difference Methods of Solution of Boundary Layer Equations," *AIAA Jour.*, 8, (2), (February, 1970), pp. 193-205.

CHAPTER IV

TRANSPORT, THERMODYNAMIC, RADIATION, AND KINETIC PROPERTIES

Introduction

In the previous chapter the conservation equations were developed into a form that will be finite differenced and placed into numerical solution form in the following chapter. However, first the coefficients in these equations contain not only the dependent variables, but also transport and thermodynamic properties along with generation terms of mass and energy which must be evaluated. The production or generation of mass is described by the chemical kinetics of the multicomponent reacting system. The generation terms for energy include that due to chemical reaction and that due to radiative heat flux.

It is important to have an accurate description of these terms in order to have a valid mathematical model. In general, the transport and thermodynamic properties and the chemical and radiation generation terms are functions of temperature, pressure, and chemical composition. Theoretical values of the transport and thermodynamic properties for pure components are curve fit and used in correlation formulas to predict mixture values. These curve fits allow a reasonably fast method of computation in contrast to the more rigorous theoretical computations which are extremely time consuming. This chapter is devoted to presenting the form to be used in the numerical computation of the transport, thermodynamic, kinetic, and radiation properties of a multicomponent system. The numerical values for the curve fits and kinetic equations are given in tabular form for the ablating-flow field system under consideration.

Chemical Kinetics

The generation of mass in the species equation and the generation of heat in the temperature form of the energy equation are given by the reaction kinetics of the system. The reaction rate is a function of density, temperature, and mixture composition.

$$\omega_i = \omega_i \; (\rho, \; T, \; C_i) \qquad [4.1]$$

The rate is given by the Law of Mass Action as

$$\omega_i = \sum_{j=1}^{M} \nu''_{ij} \; \frac{k_{rj}}{\rho M_i} \; \prod_{k=1}^{n} \left(\rho \frac{C_k}{M_k} \right)^{\nu''_{kj}} - \sum_{j=1}^{M} \nu'_{ij} \; \frac{k_{fj}}{\rho M_i} \prod_{k=1}^{n} \left(\rho \frac{C_k}{M_k} \right)^{\nu'_{kj}} \qquad [4.2]$$

where n is the number of species present and M is the total number of chemical reactions. The coefficients k_{fj} and k_{rj} are the forward and reverse rate constants respectively for the jth reaction and are taken as a function of temperature only. The forward rate constant has the form

$$k_{fj} = A_{fj} T^{S_{fj}} \exp \left[\; -E_{fj} / \vert RT \; \right] \qquad [4.3]$$

where A_{fj} is referred to as the frequency factor and E_{fj} is known as the activation energy. A_{fj}, S_{fj}, and E_{fj} are constants for each reaction. The reverse rate constants can be determined from the equilibrium constant, K_{eq}, for elementary reactions using the following relation

$$k_{rj} = k_{fj}/K_{eq_j} \qquad [4.4]$$

The stoichiometric coefficients ν''_{ij} and ν'_{ij} are defined by the following expression for the jth chemical reaction equation

$$\sum_{i=1}^{n} \nu'_{ij} R_i \rightleftarrows \sum_{i=1}^{n} \nu''_{ij} P_i \qquad j = 1, \ldots, M \qquad [4.5]$$

where R_i and P_i are the chemical symbols of the reactants and products respectively.

Also appearing in the quasilinearized species equation, Equation 3.128 is the reaction rate linearized with respect to species "i". The quasilinearized form of the energy equation, Equation 3.131, requires the reaction rate linearized with respect to temperature. These quantities can be derived from Equation 4.2 and are expressed as follows:

$$\frac{\partial}{\partial C_i}\left(\frac{\omega_i}{\rho}\right) = \sum_{j=1}^{M} (\nu''_{ij})^2 \, k_{rj} \, C_i^{(\nu''_{ij}-1)} \prod_{\substack{k=1 \\ k\neq i}}^{n} \left(\rho \frac{C_k}{M_k}\right)^{\nu''_{kj}}$$

$$- \sum_{j=1}^{M} (\nu'_{ij})^2 \, k_{fj} \, C_i^{(\nu'_{ij}-1)} \prod_{\substack{k=1 \\ k\neq i}}^{n} \left(\rho \frac{C_k}{M_k}\right)^{\nu'_{kj}} \qquad [4.6]$$

and

$$\frac{\partial}{\partial T}\left(\frac{\omega_i}{\rho}\right) = \sum_{j=1}^{M} \nu''_{ij} \left(\frac{s_{rj}}{T} + \frac{E_{rj}}{RT^2} \right) k_{rj} \prod_{k=1}^{n} \left(\rho \frac{C_k}{M_k}\right)^{\nu'_{kj}}$$

$$- \sum_{j=1}^{M} \nu'_{ij} \left(\frac{s_{fj}}{T} + \frac{E_{rj}}{RT^2} \right) k_{fj} \prod_{k=1}^{n} \left(\rho \frac{C_k}{M_k}\right)^{\nu'_{kj}} \qquad [4.7]$$

These partial derivatives can be analytically evaluated if the chemical kinetics of the system are known and used in the numerical solution of the species and energy equations for the shock layer.

The problem now rests in the specification of the chemical kinetics that describe the shock layer. There are innumerable possible chemical reactions that can take place among the air and ablation product species that are present in the shock layer adjacent to an ablating blunt body. However, to be able to solve the transport equations, a set of important chemical reactions must be selected that accurately describe the chemistry of the reactions of ablation products and air species. This information is stored in the form of a computer implemented data management file which presently contains several thousand reactions.

It was necessary to examine this extensive set of reactions to arrive at a listing of most probable reactions. These probable reactions were selected from the kinetic data management system. This set represented a total of 44 reactions involving 28 species. Currently, it is not possible to consider a solution of the transport equations with this many species and reactions. Therefore, this preliminary list was then re-examined for key reactions to represent the chemical system. The selection was based on the species anticipated to have the largest compositions and presumably, therefore, dominate the energy absorption of the system. These 16 key reactions among 19 species are given in Table 4.1 along with the recommended values of the rate constants. The forward rate constant listed was the best experimental value or was computed theoretically. The reverse rate constant was computed using Equation 4.4

Table 4.1

Shock Layer Reactions with Kinetic Coefficients

$k_f = \exp [A + B \ln T - C \times 1000/T]$

$K_{eq}^{(a)} = \exp [D - E \times 1000/T]$

Reaction	A	B	C	D	E	Source
1. $N_2 + M \rightleftarrows 2N + M$*	48.35	-1.5	112.5	3.07	114.3	5.7
2. $O + M \rightleftarrows O^+ + e^- + M$	28.66	0.5	156.5	-5.33	165.9	5.8
3. $N + M \rightleftarrows N^+ + e^- + M$	28.70	0.5	166.5	-3.69	175.7	5.8
4. $H_2 + M \rightleftarrows 2H + M$	42.73	-0.8	51.5	0.94	51.2	5.8
5. $CN + M \rightleftarrows C + N + M$	46.84	-1.0	65.9	2.06	93.8	5.9
6. $C_2H + H \rightleftarrows C_2 + H_2$	26.83	0.5	17.5	0.33	14.6	5.10
7. $CO + M \rightleftarrows C + O + M$	45.89	-1.0	129.0	3.58	127.0	5.9
8. $CO + N \rightleftarrows CN + O$	30.40	0.5	35.0	1.55	33.4	5.10
9. $C_2 + M \rightleftarrows 2C + M$	31.84	0.5	70.5	1.28	70.7	5.11

* M is a third body

Table 4.1 (Cont'd)

	Reaction	A	B	C	D	E	Source
10.	$C + M \rightleftarrows C^+ + e^- + M$	32.97	0.5	130.7	-5.11	136.3	5.11
11.	$HCN + M \rightleftarrows CN + H + M$	31.84	0.5	60.0	3.97	72.4	(b)
12.	$C_2H + M \rightleftarrows C_2 + H + M$	31.84	0.5	70.0	1.00	64.0	(b)
13.	$C_2H_2 + M \rightleftarrows C_2H + H + M$	31.84	0.5	58.5	2.28	54.8	(b)
14.	$C_3 + M \rightleftarrows C_2 + C + M$	31.84	0.5	95.0	4.14	78.7	(b)
15.	$C_3H + M \rightleftarrows C_2H + C + M$	31.84	0.5	41.5	5.08	80.9	(b)
16.	$C_4H + M \rightleftarrows C_3H + C + M$	31.84	0.5	36.5	1.02	67.0	(b)

(a) K_{eq}, equilibrium constant, computed using the method of free energy minimization

(b) Kinetic data estimated employing Ref. 5.12.

assuming the equilibrium constant could be expressed in the form, $K_{eq} = \exp\,[A+B/T]$ for the temperature range from 3000°K to 15000°K. The system shown in Table 4.1 includes 16 chemical reactions with 19 species.

In Table 4.2 the previously omitted ablation product and combustion reactions are given. Shown in Table 4.3 are the additional air and hydrogen combustion reactions. Some kinetic data is available for these; but, as a matter of convenience, it has not been included.

Transport Properties

Generally, investigators in the area of shock layer solutions have resorted to the classical Chapman-Enskog kinetic theory relations for estimation of the required transport properties. The modification of these relationships to account for polyatomic, reacting mixtures results in very cumbersome equations. In some cases there are simplifications which can be applied without substantial loss in accuracy. At this point, it becomes desirable to optimize between accuracy and computation time. A wide variety of methods for estimating these properties has been developed in just this manner. In this section, a formulation is provided from which an optimum method to accurately compute high temperature transport properties with reasonable computational convenience is presented. These properties, along with comparisons with other investigators, are developed in more detail by Esch et al. (Ref. 4.1). The following discussion is based on Esch's work.

Viscosity: The relationship employed for the prediction of mixture viscosity is the commonly used Buddenberg-Wilke correlation (Ref. 4.2).

Table 4.2. Additional Ablation Product and Combustion Reactions

CH_4, CH_3, CH_2, CH Reactions

1. $CH_4 \rightleftarrows CH_3 + H$
2. $CH_4 \rightleftarrows CH_2 + H_2$
3. $CH_3 \rightleftarrows CH_2 + H$
4. $CH_2 \rightleftarrows CH + H$
5. $CH_2 + H \rightleftarrows CH + H_2$
6. $CH \rightleftarrows C + H$
7. $C + H_2 \rightleftarrows CH + H$
8. $CH_2 + O \rightleftarrows CO + H_2$

CN Reactions

1. $2CN \rightleftarrows C_2 + N_2$
2. $CN + O \rightleftarrows N + CO$

C_2H_2, C_2H Reactions

1. $C_2H_2 + H \rightleftarrows C_2H + H_2$
2. $C_2H_2 + O \rightleftarrows CH_2 + CO$
3. $C_2H_2 + OH \rightleftarrows C_2H + H_2O$
4. $C_2H + H \rightleftarrows C_2 + H_2$
5. $C_2H + O \rightleftarrows CH + CO$

Other Reactions

1. $C_4H \rightleftarrows C_3H + C$
2. $C_3H \rightleftarrows C_2H + C$
3. $C_2 + H \rightleftarrows C + CH$

Table 4.3. Additional Air and Hydrogen Combustion Reactions

Air Reactions

1. $O_2 + M \rightleftarrows 2O + M$
2. $N_2 + M \rightleftarrows N^+ + e^- + M$
3. $NO + M \rightleftarrows N + O + M$
4. $NO + O \rightleftarrows O_2 + N$
5. $N_2 + O \rightleftarrows NO + N$
6. $N + O \rightleftarrows NO^+ + e^-$

Hydrogen Combustion Reactions

1. $H + O_2 \rightleftarrows OH + O$
2. $O + H_2 \rightleftarrows OH + H$
3. $OH + H_2 \rightleftarrows H_2O + H$
4. $2OH \rightleftarrows H_2O + O$
5. $H + OH + M \rightleftarrows H_2O + M$
6. $H + O + M \rightleftarrows OH + M$

The mixture viscosity is calculated from the pure component viscosities with the relation

$$\mu = \sum_{i=1}^{n} \frac{Y_i \ \mu_i}{\sum_{j=1}^{n} Y_j \quad \Phi_{ij}} \qquad [4.8]$$

The coefficients Φ_{ij} are a function of the pure component viscosities and molecular weight ratios.

$$\Phi_{ij} = \frac{1}{\sqrt{8}} \left(1 + \frac{M_i}{M_j} \right)^{-1/2} \left[1 + \left(\frac{\mu_i}{\mu_j} \right)^{1/2} \left(\frac{M_j}{M_i} \right)^{1/4} \right]^2 \qquad [4.9]$$

where the pure component viscosity in this analysis is calculated by the second order polynomial curve fit

$$\mu_i = a_i + b_i T + c_i T^2 \qquad [4.10]$$

The above curve fit is obtained using the data from theoretical predictions (Refs. 4.3-4.7). This curve fit can then be used for computer inplementation. A summary for the empirical constants required for Equation 4.10 is given in Table 4.4.

Thermal Conductivity: Mixture thermal conductivity is calculated in the same manner as mixture viscosity

$$k = \sum_{i=1}^{n} \frac{Y_i \ k_i}{\sum_{j=1}^{n} Y_j \ \Phi_{ij}} \qquad [4.11]$$

where k is the frozen mixture thermal conductivity and Φ_{ij} is defined by Equation 4.9. As with the viscosity, the pure component thermal conductivities were obtained from the theoretical predictions of Refs. 4.3-4.7. Examination of the data revealed that a

Table 4.4
Empirical Constants for Viscosity Correlation

$$\mu_i = a_i + b_i T + c_i T^2 \ \frac{\text{lbm}}{\text{ft-sec}} \qquad \text{(Ref. 4.1)}$$

Species	$a \times 10^5$	$b \times 10^7$	$c \times 10^{12}$	Temperature Range (°K)
O_2	1.693	0.1496	-0.2276	2,000-10,000
N_2	0.970	0.1613	-0.1916	2,000-10,000
O	1.519	0.1875	-0.2228	2,000-10,000
N	0.253	0.2206	-0.3737	2,000-10,000
O^+	0.0	0.0500	-0.1000	8,000-15,000
N^+	0.0	0.0500	-0.1000	8,000-15,000
e^-	0.0	0.0500	-0.1000	8,000-15,000
C	1.997	0.1772	-0.3378	5,000-10,000
H	0.294	0.0889	-0.0811	4,000-10,000
H_2	-0.079	0.0791	-0.0886	4,000-10,000
CO	2.404	0.1363	-0.2184	4,000- 9,000
C_3	2.019	0.1179	-0.1655	1,000- 5,000
CN	2.404	0.1363	-0.2184	4,000- 9,000
C_2H	2.404	0.1363	-0.2184	4,000- 9,000
C_2H_2	1.396	0.0842	-0.6939	1,000- 5,000
C_3H	2.019	0.1179	-0.1655	1,000- 5,000
C_4H	2.019	0.1179	-0.1655	1,000- 5,000
HCN	1.378	0.0965	-0.0948	1,000- 5,000
C_2	1.931	0.1393	-0.2575	4,000- 9,000
C^+	0.0	0.0500	-0.1000	8,000-15,000

linear fit would be satisfactory for accurate correlation.

$$k_i = a_i + b_i T \qquad [4.12]$$

A summary of the coefficients required for Equation 4.12 is presented in Table 4.5.

Binary Diffusion Coefficients: In view of the multiplicity of binary interactions required, it was decided that the following Chapman-Enskog equation for the prediction of binary diffusion coefficients would be used (Ref. 4.8).

$$D_{ij} = \frac{28.28 \times 10^{-7}\ T^{3/2}}{P\ \sigma_{ij}^2\ \Omega_{ij}^{(1,1)}} \left(\frac{M_i + M_j}{2\ M_i\ M_j}\right)^{1/2} \frac{ft^2}{sec} \qquad [4.13]$$

where $\sigma_{ij} = (\sigma_i + \sigma_j)/2$, the quantities σ_i and σ_j being the collision diameters of the interacting species. The quantity, $\Omega_{ij}^{(1,1)}$, is the Leonard-Jones collison integral for diffusion as determined by the following empirical equation

$$\Omega_{ij}^{(1,1)} = 1.061\ (T_{ij}^{*})^{-1.56} \qquad [4.14]$$

These constants were obtained from a curve fit of the Leonard-Jones potential as reported by Hirschfelder in Ref. 4.8 for $10 \leq T_{ij}^{*} \leq 1000$ which includes all species and temperatures considered in the current study. The quantity T_{ij}^{*} is computed as

$$T_{ij}^{*} = \frac{T}{\epsilon_{ij/k}} \qquad [4.15]$$

where $\epsilon_{ij} = \sqrt{\epsilon_i \epsilon_j}$, ϵ_i and ϵ_j being the characteristic interaction energies of species i and j.

Table 4.5

Empirical Constants for Thermal Conductivity Correlation

$k_i = a + bT$ (BTU/ft-sec-°R) (Ref. 4.1)

Species	a x 10^5	b x 10^8	Temperature Range (°K)
O_2	1.019	0.4901	2,000-10,000
N_2	0.654	0.6457	2,000-10,000
O	1.250	0.7092	2,000-10,000
N	1.281	0.8593	2,000-10,000
O^+	26.0	0.0	8,000-15,000
N^+	26.0	0.0	8,000-15,000
e^-	26.0	0.0	8,000-15,000
C	2.506	0.7479	5,000-10,000
H	2.496	5.129	4,000-10,000
H_2	3.211	5.344	4,000-10,000
CO	0.859	0.6233	1,000- 5,000
C_3	0.630	0.5804	1,000- 5,000
CN	0.859	0.6233	2,000-10,000
C_2H	1.126	0.7439	1,000- 5,000
C_2H_2	1.126	0.7439	1,000- 5,000
C_3H	0.630	0.5804	1,000- 5,000
C_4H	0.630	0.5804	1,000- 5,000
HCN	0.486	0.8714	1,000- 5,000
C_2	0.859	0.6233	1,000- 5,000
C^+	26.0	0.0	8,000-15,000

Values for the collision parameters, σ_i and $\varepsilon_{i/k}$ for O_2, N_2, C, H, H_2, CO, CN, C_2H_2, HCN, and C_2, were obtained from Svehla (Ref. 4.6). Since no data was available for C_3, C_2H, C_3H, and C_4H, it was necessary to develop correlations based upon similar species. Esch (Ref. 4.1) developed the following correlation structures for the prediction of the collision parameters of the above light hydrocarbon species.

Collision Diameter:

$$\sigma_i = 2.69 + 0.0514\, M_i \qquad [4.16]$$

Interaction Energy (C_n molecules):

$$\varepsilon_{i/k} = -17.0 + 4.02\, M_i \qquad [4.17]$$

Interaction Energy (C_nH_n molecules):

$$\varepsilon_{i/k} = -105. + 12.4\, M_i \qquad [4.18]$$

The collision parameters for O, N, O^+, N^+, and e^- were estimated from the theoretically determined binary diffusion coefficients reported by Yun, Weissman, and Mason (Ref. 4.3) and by Yos (Ref. 4.7). The behavior of C^+ was then assumed to be similar to that of N^+. A summary of the collision parameters employed in the present study is given in Table 4.6.

Thermodynamic Properties

The thermodynamic properties of heat capacity and enthalpy appear in the energy equation of the thin shock layer equations. Data for thermodynamic properties was obtained from References 4.9-4.13. In Reference 4.13 the appropriate species for the shock layer are presented with polynomial fits for a range of temperature of 300°K

Table 4.6.

Collision Parameters Employed in the Current Study

Species	M_i	σ_i	ε_i/k
O_2	32.000	3.467	106.7
N_2	28.016	3.798	71.4
O	16.000	7.990	106.7
N	14.008	7.940	71.4
O^+	16.000	14.220	106.7
N^+	14.008	14.930	71.4
e^-	5.486×10^{-4}	14.930	71.4
C	12.001	3.385	30.6
H	1.008	2.708	37.0
H_2	2.016	2.827	59.7
C_3	36.033	4.450	128.0
CN	26.019	3.856	75.0
C_2H	25.030	3.880	205.0
C_2H_2	26.038	4.033	231.8
C_3H	37.041	4.600	356.0
C_4H	49.052	5.210	504.0
HCN	27.027	3.630	469.1
C_2	24.022	3.913	78.8
C^+	12.011	15.000	30.6

to 15000°K. The heat capacity of species "i" is expressed in terms of temperature in the following form

$$\frac{C_{pi}}{R} = a_1 + a_2T + a_3T^2 + a_4T^3 + a_5T^4 \qquad [4.19]$$

The coefficients a_1 through a_5 are given in Appendix C for the shock layer chemistry constituents. In addition to heat capacity data, enthalpy is required. The enthalpy of species "i" is obtained from the relation

$$h_i = \int_{298}^{T} C_{pi}\, dT + h^{\circ}_{i_{298}} \qquad [4.20]$$

where $h^{\circ}_{i_{298}}$ is the enthalpy of formation of species "i". The polynomial form for enthalpy follows directly from the integration of Equation 4.20 by substituting in the heat capacity from Equation 4.19.

$$\frac{h_i}{RT} = a_1 + \frac{a_2T}{2} + \frac{a_3T^2}{3} + \frac{a_4T^3}{4} + \frac{a_5T^4}{5} + \frac{a_6}{T} \qquad [4.21]$$

The mixture values of heat capacity and enthalpy have the simple relationship

$$C_p = \sum_{i=1}^{n} Y_i\, C_{pi} \qquad [4.22]$$

and

$$h = \sum_{i=1}^{n} Y_i\, h_i \qquad [4.23]$$

where C_p is the frozen total heat capacity and h is the total static enthalpy.

Radiation Properties

Radiating shock layer analyses can be catagorized by means of the radiation transport model employed, i.e. whether the gas is treated as transparent, gray, or nongray. In a transparent gas, fluid elements are assumed to emit locally but not absorb radiative energy. Both gray and nongray gas fluid elements locally emit and absorb some of the incident radiative intensity that originates from the other fluid elements in the shock layer. However, the effect of this self-absorption differs markedly between a gray gas and a nongray gas. The gas absorption coefficient is independent of wavelength for the gray gas assumption, whereas the nongray gas model includes the wavelength variation of the gas absorption coefficient, either approximately or in detail. The nongray model is the most realistic treatment for atmospheric reentry although it is also by far the most time-consuming computationally. In addition, each of the three categories can be subdivided according to whether or not the gas dynamic flow field is assumed to be coupled with the radiative energy transport. If no coupling is assumed, the computation of local flow field variables neglects local emission or absorption of radiation, and the radiative energy flux is subsequently calculated by integration over the resulting (nonradiating) flow field density and temperature profiles. The more realistic case is that of radiative gas dynamic coupling, where the fact that the flow field variables depend on radiative emission is accounted far.

It is not intended to present a complete mathematical formulation of the radiative gas dynamics in this section since a formulation of this type is given in detail by Engel (Ref. 4.14).

The following discussion will be more qualitative and will attempt to justify the radiation model used in this analysis by comparing results with other investigators. The present analysis is a nongray radiation model which is coupled to the flow field variables.

The radiative flux divergence ($\partial q_R/\partial y$) appearing in Equation 3.35 is defined as follows (Ref. 4.15):

$$\frac{\partial q_R}{\partial y} = \int_0^\infty \int_0^{4\Pi} \alpha(y, \nu) \, [B\,(y, \nu) - I\,(y, \nu, \Omega)] \, d\Omega d\nu \qquad [4.24]$$

where q_R = the radiative flux in the normal direction from the body,

$\alpha(y,\nu)$ = volumetric absorption coefficient,

$B(y,\nu)$ = Plankian radiation intensity,

$I(y,\nu,\Omega)$ = radiation intensity,

$d\Omega$ = solid angle about the unit vector $\bar{\Omega}$,

ν = frequency.

With given temperature and species profiles, Equation 4.24 can be evaluated theoretically. However, due to the discontinuous nature of the absorption coefficients, numerical integration is a formidable task. Typical absorption coefficient distributions are shown in Figure 4.1 to illustrate the extent of this problem (Ref. 4.16).

To overcome the numerical difficulties associated with the integration of such distributions, the frequency range is sub-divided into regions (bands) in which the discontinuous variations are averaged. Continuum radiation bands are used to represent wide regions of continuous radiation while line bands are used to model the effects of the various discontinuous (line) contributions. The use of more bands obviously leads to a more accurate representation of

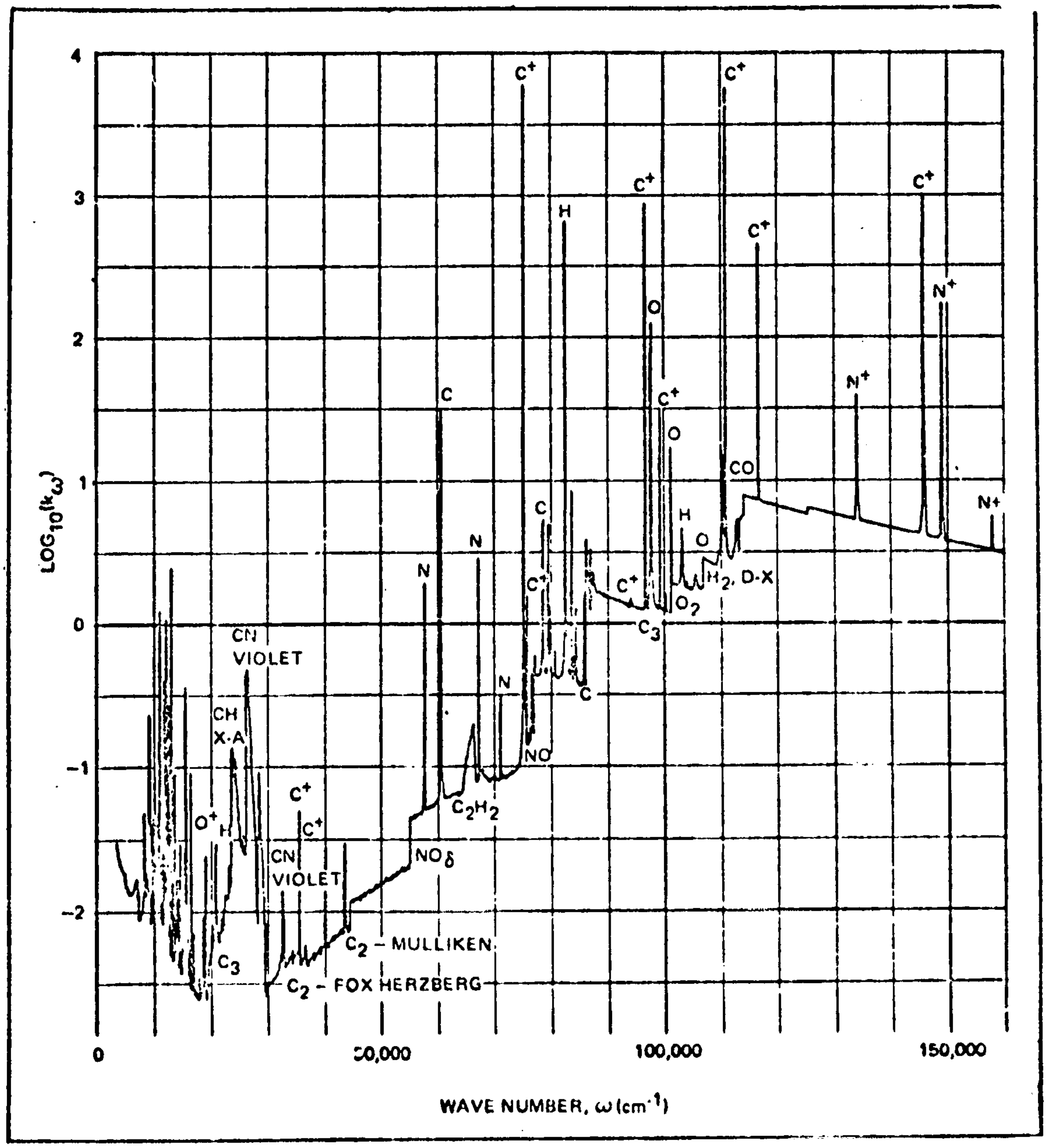

Figure 4.1. Spectral Absorption Coefficient of Air-Carbon Phenolic Ablation Products Mixture for P = 1 and T = 16,000°K (Ref. 4.19).

the radiative process. However, in developing radiation models for computer implementation, some compromise must be reached between computer time and the number of bands.

The radiation model used in the present work is a revision (Engel, Ref. 4.14) of a coupled line and continuum model originally developed by Wilson (Ref. 4.15). This model provides a useful tool for evaluating the radiation flux and the radiative flux divergence across a slab of gas containing both air and ablation species.

The existing program (LRAD) contains twelve continuum frequency bands and nine line bands. A comparison with a more detailed model (RATRAP) in Reference 4.17, demonstrated that the existing analysis predicted total heat flux values to within 5%. The species considered in the model used in the current study are shown in Table 4.7.

The radiation model was included in reduced form (air species only) in a program called VISRADI which was developed by Spradley and Engel (Ref. 4.18). Figure 4.2 presents a comparison of dimensionless radiative heating rates as a function of free stream velocity by several investigators. For this no mass injection case the comparison is quite reasonable. All investigators reported on this figure have line and continuum radiation calculations for air at the stagnation line. Although this case does not contain the effects of ablation species, it is a standard for comparison of computational techniques.

Summary

The terms in the thin shock layer equations have now been completely specified. This chapter has presented the values to be

Table 4.7

Species Considered in LRAD Radiation Model

Continuum and Lines	Continuum
C	CO
H	C_2
N	C_3
O	O_2
	H_2
	N_2
	C_2H
	e^-

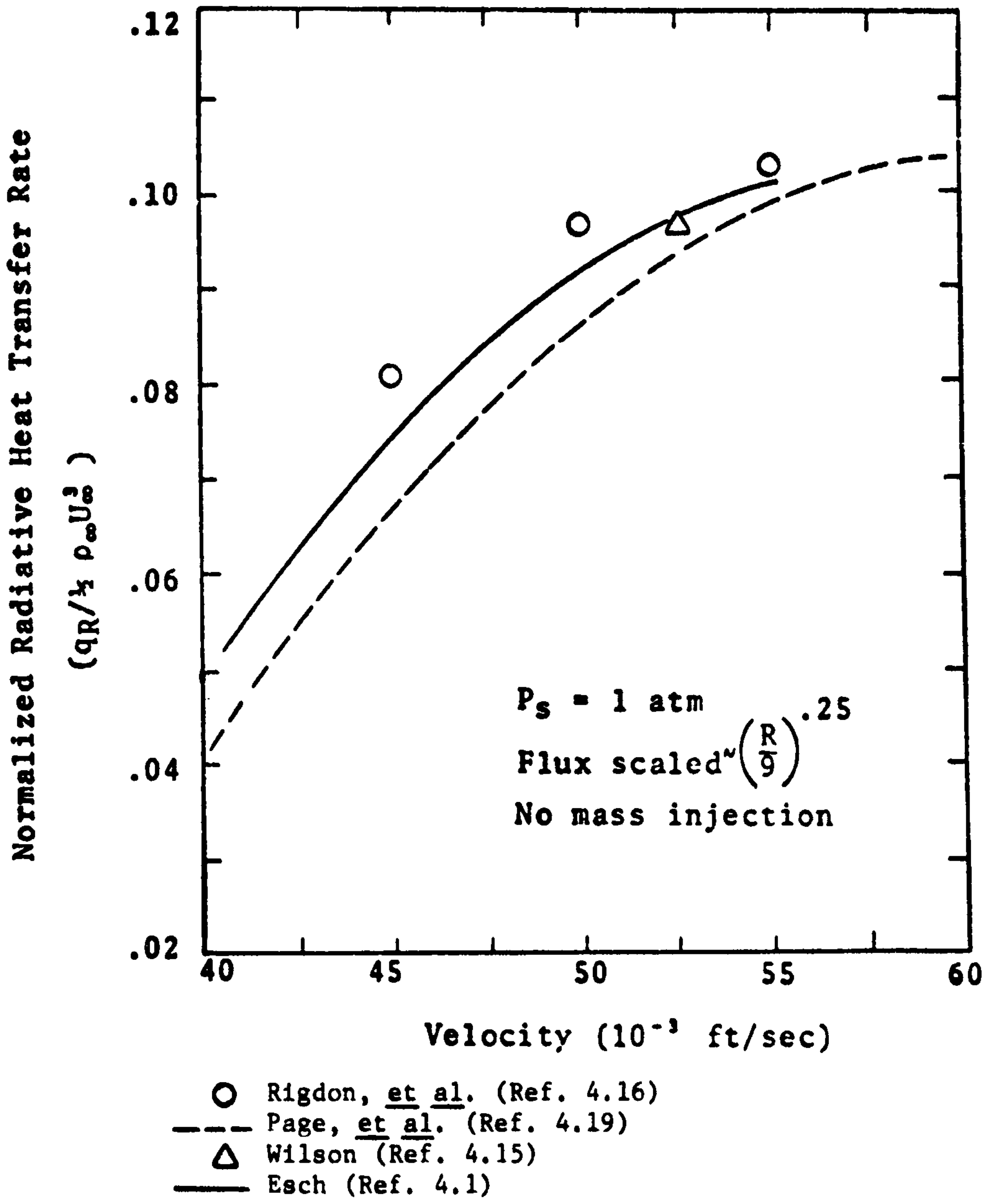

Figure 4.2. Comparison of Dimesnionless Radiative Heating Rates.

used for the transport properties, viscosity, thermal conductivity, and binary diffusion coefficients; the thermodynamic properties, heat capacity and enthalpy; and the production terms, chemical production and radiative energy production. With these properties known, it is now possible to solve the complete simultaneous set of shock layer equations along with their initial and boundary conditions. In Chapter V these equations, as given in linearized form in Chapter III, are finite differenced, and they are placed in numerical solution form.

REFERENCES

4.1 Esch, D. D., "Stagnation Region Heating of a Phenolic-Nylon Ablator During Return from Planetary Missions," Ph.D. dissertation, Louisiana State University, Baton Rouge, Louisiana (1971).

4.2 Buddenberg, J. W. and C. R. Wilke, *Ind. Eng. Chem.*, *41*, pp. 1345-1347 (1949).

4.3 Yun, Kwank-Sik, S. Weissman, and E. A. Mason, "High Temperature Transport Properties of Dissociating Nitrogen and Dissociating Oxygen," *Phys. Fluids 5*, 672 (1962).

4.4 Lasher, L. E., "The Effect of Carbon Gas Injection (Graphite Ablation) on the Stagnation Point Compressible Boundary Layer," Masters thesis, Cornell University, Ithaca, New York (1965).

4.5 Valderslice, J. F., *et al.*, "High-Temperature Transport Properties of Dissociating Hydrogen," *Phys. Fluids 5*, 155 (1962).

4.6 Svahla, R. S., "Estimated Viscosities and Thermal Conductivities of Gases at High Temperatures," NASA TR R-132 (1962).

4.7 Yos, J. M., "Transport Properties of Nitrogen, Hydrogen, Oxygen, and Air to 30,000°K," AVCO RAD Technical Memorandum 63-7, (1963) as cited by Hoshizaki, *op cit*.

4.8 Hirschfelder, J. O., C. F. Curtiss, and R. B. Bird, *Molecular Theory of Gases and Liquids*, 2nd printing, corrected with notes added, John Wiley and Sons, Inc., New York (1964).

4.9 Browne, W. G., "Thermodynamic Properties of Some Atoms and Atomic Ions," General Electric Company, MSVD Engr. Physics Tech. Memo. No. 2 (May 14, 1962).

4.10 Browne, W. G., "Thermodynamic Properties of Some Diatoms and Diatomic Ions," General Electric Co. MSVD Engr. Physics Tech. Memo. 8, (May 14, 1962).

4.11 Browne, W. G., "Thermodynamic Properties of the Species CN, C_2, C_3, C_2N_2, and C^-," General Electric MSVD Engr. Physics Tech. Memo., No. 9, (May 14, 1962).

4.12 Browne, W. G., "Thermodynamic Properties of Some Ablation Products from Plastic Heat Shields in Air," General Electric Co. MSVD Engr.Physics Tech.Memo. No. 11, (March 15, 1964).

4.13 Esch, D. D., A. Siripong, and R. W. Pike, "Thermodynamic Properties in Polynomial Form for Carbon, Hydrogen, Nitrogen, and Oxygen Systems from 300°K to 15,000°K," NASA RFL-TR-70-3, 1970.

4.14 Engel, C. D., "Ablation and Radiation Coupled Viscous Hypersonic Shock Layers," Ph.D. dissertation, Louisiana State University, Baton Rouge, Louisiana (1971).

4.15 Wilson, K. H., "Stagnation Point Analysis of Coupled Viscous-Radiating Flow with Massive Blowing," LMSC-687209, April 1969.

4.16 Rigdon, W. S., R. B. Dirling, and M. Thomas, "Stagnation Point Heat Transfer During Hypervelocity Atmospheric Entry," NASA CR-1462, 1970.

4.17 Wilson, K. H. and H. Hoshizaki, "Effect of Ablation Product Absorption and Line Transitions on Shock Layer Radiative Transport," NASA CR-1264, 1969.

4.18 Spradley, L. W. and C. D. Engel, "A Computer Program for Predicting Coupled Convective and Radiative Heat Transfer to a Body During Superorbital Reentry," LMSC/HREC A791350, Lockheed, Missiles & Space Company, Huntsville, Alaba, May 1968.

4.19 Page, W. A., et al., "Radiative Transport in Inviscid Nonadiabatic Stagnation-Region Shock Layers," AIAA Paper No. 68-784, AIAA 3rd Thermophysics Conference, June 1968.

CHAPTER V

NUMERICAL IMPLEMENTATION OF THE SHOCK LAYER EQUATIONS

Introduction

In Chapter III the thin shock layer equations were developed into a general quasilinearized form suitable for numerical solution. The coefficients (α's) in these equations are functions of the local temperature, composition, and pressure. The transport, thermodynamic, kinetic, and radiative properties of the system required for complete description of these coefficients were discussed in the previous chapter. The general quasilinear equations are a set of parabolic partial differential equations which can be solved by an appropriate finite difference technique. The numerical finite differenced form is presented in this chapter along with a discussion of stability, convergence, and general computational experience. The numerical technique uncouples the finite differenced equations and results in a tridiagonal matrix which can be solved efficiently using the Thomas Algorithm.

Detailed results are presented in the following chapter using the numerical scheme described in this chapter for heating rates to an ablation protection system typical of reentry from planetary missions.

Coupled Ablation Flow Field Analysis

A simplified flow diagram of the overall flow field-ablation analysis, as developed in this study, is given in Figure 5.1. The analysis is initiated at the stagnation line or line of symmetry on an axisymmetric body of arbitrary shape. The major input data consist of free-stream velocity (U_∞), free-stream density (ρ_∞) which is indicative of altitude, body radius (R), and mass injection rate (RVW). Initial estimates of all other variables and profiles are automatically developed by the program unless the user overrides them. The parameter, mass injection rate (RVW), is varied until the heating rate from flow field to ablator surface agrees with the energy absorbed and reradiated by the ablator - in essence, satisfying a surface energy balance for a fully coupled solution. The results are punched out on cards for the stagnation line at the free-stream conditions specified.

The analysis proceeds around the body by using the results from the stagnation line as initial conditions. The ablator mass loss rate profile is specified as a function of distance around the body which also determines surface heating rate and surface temperature from the surface energy balance. When the correct mass loss rate profile has been selected, this fact will be reflected by a matching heating rate profile from the flow field.

The program first determines boundary conditions at the bow shock and the ablator surface. Thermodynamic, transport, and radiation properties are then calculated using assumed temperature, pressure, and composition profiles. Subsequently the shock layer equations are solved yielding profiles of pressure from the

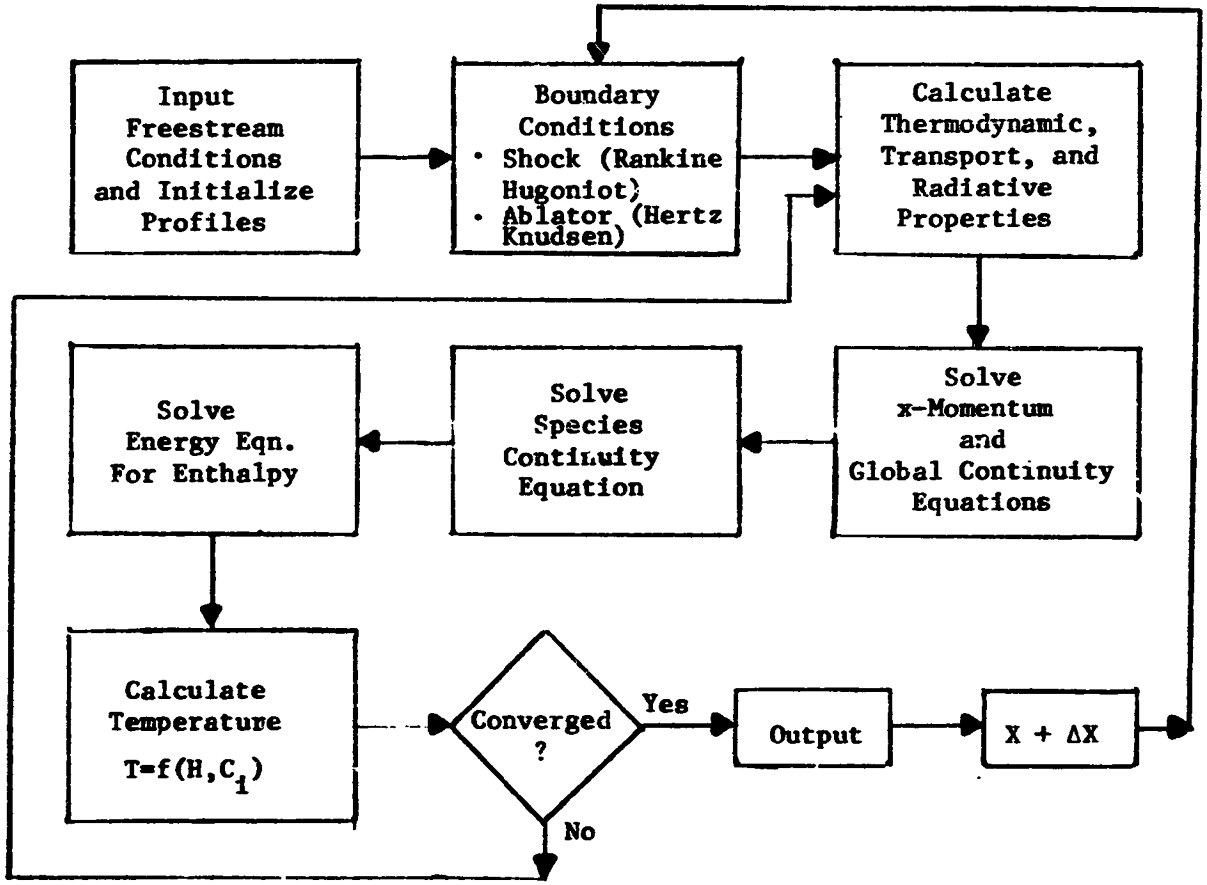
Input Freestream Conditions and Initialize Profiles
Boundary Conditions
• Shock (Rankine Hugoniot)
• Ablator (Hertz Knudsen)
Calculate Thermodynamic, Transport, and Radiative Properties
Solve x-Momentum and Global Continuity Equations
Solve Species Continuity Equation
Solve Energy Eqn. For Enthalpy
Calculate Temperature T=f(H,C1)
Converged ?
Yes
No
Output
X + ΔX

Figure 5.1. Simplified Flow Diagram of Coupled Shock Layer Analysis.

y-momentum equation, tangential velocity (or velocity function, f$'$) from the x-momentum equation, normal velocity from global continuity, composition from species continuity, and temperature (or enthalpy) from the energy equation. The shock layer equations have been uncoupled during the finite differencing procedure and coupling is then achieved by iteration until all profiles are converged simultaneously. The finite difference procedures used to solve the flow field equations are presented in the following sections.

Numerical Solutions of the Conservation Equations

The general qualilinearized form for the x-momentum, species continuity, and energy equations was given in Chapter III as

$$-\frac{\partial^2 W}{\partial \eta^2} + \alpha_1 \frac{\partial W}{\partial \eta} + \alpha_2 W + \alpha_3 + \alpha_4 \frac{\partial W}{\partial \xi} = 0 \qquad [3.125]$$

where α_4 equals zero along the stagnation line and W is the dependent variable. Using a three point, variable step size, finite difference approximation at (s-2) points (Fig. 5.2) across the flow field, the numerical form of the equations becomes

$$\bar{\bar{A}} \cdot \bar{W} = \bar{B} \qquad [5.1]$$

where $\bar{\bar{A}}$ is a tridiagonal matrix of order (s-2). This form readily lends ~~itself~~ to numerical solution by a tridiagonal matrix inversion algorithm (Ref. 5.1). The matrix has the form

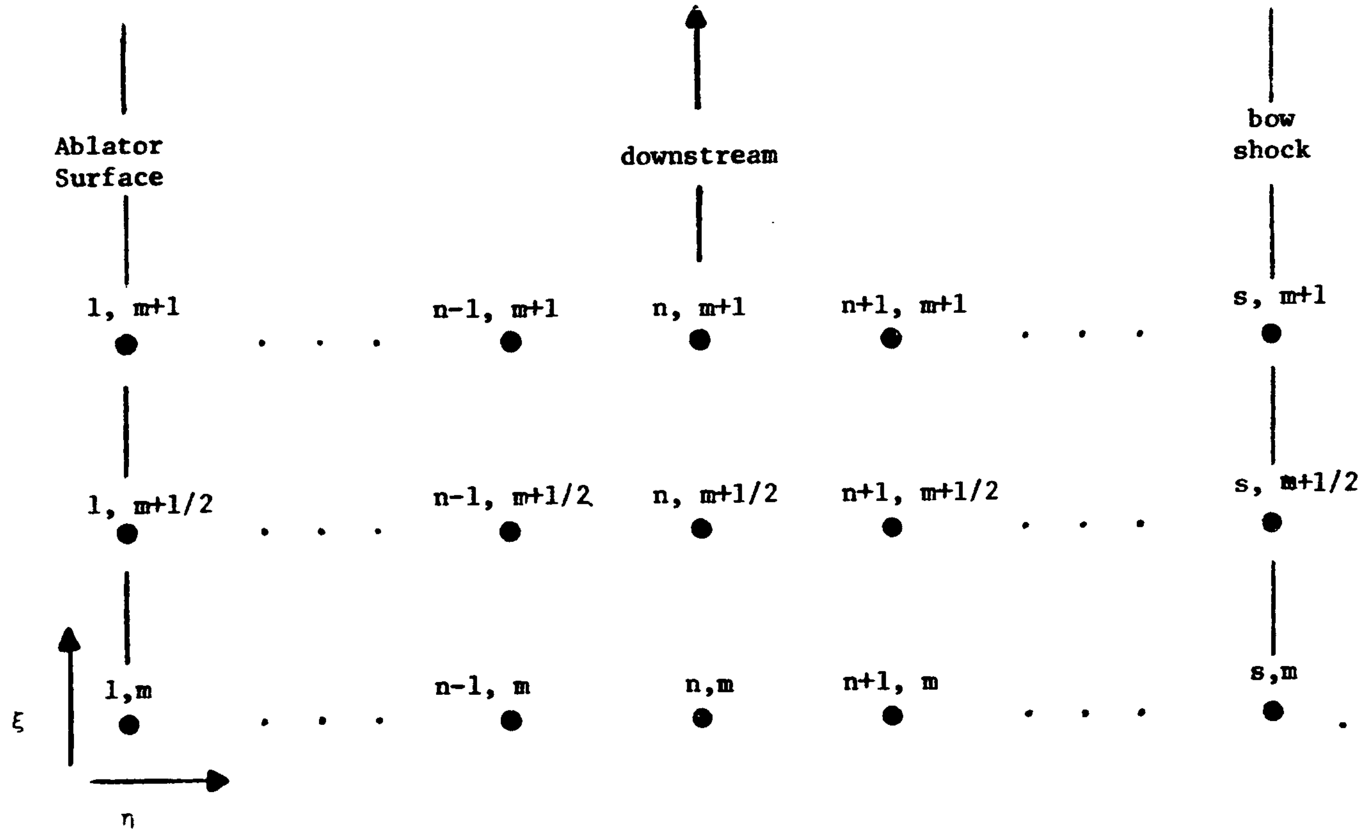
Ablator Surface
downstream
bow shock
1, m+1
n-1, m+1
n, m+1
n+1, m+1
s, m+1
1, m+1/2
n-1, m+1/2
n, m+1/2
n+1, m+1/2
s, m+1/2
1,m
n-1, m
n,m
n+1, m
s,m
ξ
η

Figure 5.2. Crank Nicolson Finite Difference Grid.

$$\begin{bmatrix} B_1 & C_1 & & & & \\ A_2 & B_2 & C_2 & & & \\ & A_3 & B_3 & C_3 & & \\ & \cdot & \cdot & \cdot & & \\ & & \cdot & \cdot & \cdot & \\ & & & A_{s-2} & B_{s-2} & C_{s-2} \\ & & & & A_{s-1} & B_{s-1} \end{bmatrix} \begin{bmatrix} W_2 \\ W_3 \\ W_4 \\ \cdot \\ \cdot \\ W_{s-2} \\ Ws\text{-}1 \end{bmatrix} = \begin{bmatrix} D_1 - A_1 W_1 \\ D_2 \\ D_3 \\ \cdot \\ \cdot \\ D_{s-2} \\ D_{s-1} - C_{s-1} W_s \end{bmatrix} \qquad [5.2]$$

The coefficients A_n, B_n, C_n and D_n have the following values.

$$A_n = \Theta\,({H^2}_n + \alpha_1 H'_n)$$

$$B_n = \Theta\,({G^2}_n + \alpha_1\, G'_n + \alpha_2) + \alpha_4/\Delta\xi \qquad [5.3]$$

$$C_n = \Theta\,({F^2}_n + \alpha_1\, F'_n)$$

$$D_n = \frac{(\Theta-1)}{\Theta}\,[A_n W^m_{n-1} + B_n W^m_n + C_n W^m_{n+1}] - \alpha_3 + \frac{\alpha_4}{\Theta\Delta\xi}$$

where Θ is a parameter which will yield the various finite difference schemes as given below:

$$\Theta \begin{cases} 0 & \text{Explicit} \\ 1/2 & \text{Crank Nicolson} \\ 1 & \text{Implicit} \end{cases}$$

and the F, G, and H coefficients are obtained from the three point finite difference formulae (Ref. 5.2).

$$\frac{\partial W}{\partial \eta} = F_n^{'} W \quad + G_n^{'} W_n + H_n^{'} W_{n-1} \qquad [5.4]$$

$$\frac{\partial^2 W}{\partial \eta^2} = F_n^2 W_{n+1} G_n^2 W_n + H_n^2 W_{n-1} \qquad [5.5]$$

The shock layer is divided with a variable grid size $\Delta\eta$ and $\Delta\xi$ in which the subscript n refers to the η or normal coordinate and the superscript m refers to the ξ or tangential coordinate. The tridiagonal matrix is solved for the dependent W variables at the $(m+1)^{th}$ body station.

To complete the system of Eqs. (5.2), the boundary conditions are included as follows:

$$B_1 W_2^{m+1} + C_1 W_3^{m+1} = D_1 - A_1 W_1^{m+1}$$

$$A_{s-1} W_{s-2}^{m+1} + B_{s-1} W_{s-1}^{m+1} = D_{s-1} - C_{s-1} W_s^{m+1} \qquad [5.6]$$

where W_1^{m+1} is the boundary condition at the ablator surface and W_s^{m+1} is the boundary condition of the shock. These boundary conditions were discussed in some detail in Chapter III.

Global Continuity

The global continuity equation is a first order partial differential equation which has one form downstream of the stagnation line and a limiting form at the stagnation line. The downstream form is

$$\frac{1}{r_b} \frac{\partial}{\partial \xi} (\rho u r_b) + \frac{\partial \eta}{\partial X} \frac{\partial}{\partial \eta} (\rho u) + \frac{\rho}{\delta} \frac{\partial}{\partial \eta} (\rho v) = 0 \qquad [5.8]$$

and the limiting form at the stagnation line is

$$2\,\frac{\partial u}{\partial \xi} = -\,\frac{1}{\tilde{\delta}}\,\frac{\partial}{\partial \eta}\,(\rho v) \qquad [5.9]$$

Both of these forms can be solved readily for ρv by integrating yielding

$$\rho v = (\rho v)_w - \int_o^{\eta} \frac{\tilde{\delta}}{\rho}\left[\frac{1}{r_b}\,\frac{\partial}{\partial \xi}\,(\rho u r_b) + \frac{\partial \eta}{\partial X}\,\frac{\partial}{\partial \eta}\,(\rho u)\right] d\eta \qquad [5.10]$$

and

$$\rho v = (\rho v)_w - 2\int_o^{\eta} \tilde{\delta}\left(\frac{\partial u}{\partial \xi}\right) d\eta \qquad [5.11]$$

Numerically this integration is carried out quite satisfactorily by a simple trapezoidal scheme. The transformed standoff distance, $\tilde{\delta}$, is computed at the stagnation line and around the body using the respective global continuity equations in the following manner

$$\tilde{\delta} = -\,\frac{(\rho v)_s - (\rho v)_w}{\int_o^1 f'\,d\eta}\ \text{(stagnation)} \qquad [5.12]$$

and

$$\tilde{\delta} = -\,\frac{(\rho v)_s - (\rho v)_w}{\int_o^1 \frac{1}{\rho}\left[\frac{1}{r_b}\,\frac{\partial}{\partial \xi}\,(\rho u r_b) + \frac{\partial \eta}{\partial x}\,\frac{\partial}{\partial \eta}\,(\rho u)\right] d\eta} \qquad [5.13]$$

The integrals for Eqs. 5.12 and 5.13 are identical to those in 5.10 and 5.11 and are obtained by using the trapezoidal rule integration. This computed value of $\tilde{\delta}$ is then compared to the assumed value and a new value is estimated. The calculation is repeated until convergence of $\tilde{\delta}$ is achieved (<0.1%). The actual standoff distance is then computed from the flow field as

$$\delta = \tilde{\delta} \int_{o}^{1} \frac{d\eta}{\rho} \qquad [5.14]$$

Again, the integral is evaluated using the simple trapezoidal scheme.

The standoff distance around the body can be calculated by the following geometrical relationship (trapezoidal integration)

$$\delta^{m+1} = \int_{o}^{\xi m+1} (1 + \kappa\delta) \tan \varepsilon \, d\xi \qquad [5.15]$$

The value of δ from the flow field calculation and the geometrical relation can then be compared to indicate if numerical convergence has been obtained on shock standoff distance. In practice, an ε profile is assumed and the geometrical relation is integrated using this assumed profile. The ε profile is then updated until input shock shape (geometrical relation) and the output shock shape (flow field calculation) agree within about 2%.

Calculation of $\partial\eta/\partial x$

The value, $\partial\eta/\partial x$, appears in the conservation equations and must therefore be evaluated. The term can be expanded as follows using the chain rule

$$\frac{\partial\eta}{\partial x} = \frac{\partial\eta}{\partial y} \frac{\partial y}{\partial x} \qquad [5.16]$$

where

$$\frac{\partial\eta}{\partial y} = \frac{\rho}{\delta} \qquad [5.17]$$

since by definition

$$d\eta = \frac{\rho}{\tilde{\delta}}\, dy \qquad [5.18]$$

The term $\partial y/\partial x$ can be evaluated numerically as

$$\frac{\partial y}{\partial x} = \frac{y^{m+1} - y^{m}}{\Delta x} \qquad [5.19]$$

y^{m+1} is approximated using

$$y^{m+1} \simeq \frac{y^{m}}{\delta^{m}}\, \delta^{m+1} \qquad [5.20]$$

where δ^m and δ^{m+1} are evaluated from the geometrical relation, Eq. 5.15.

y-Momentum Equation

The final partial differential equation to be solved is the y-momentum equation for pressure along the normal coordinate. This equation is actually an ordinary differential equation when the thin shock layer approximation is made as in this study. The transformed y-momentum equation becomes

$$\frac{dP}{d\eta} = \tilde{\kappa}\, u^2 \qquad [5.21]$$

Upon integrating

$$P(\eta) = P_s - \int_1^{\eta} \tilde{\kappa}\, u^2 d\eta \qquad [5.22]$$

which can be solved by a simple trapezoidal method as was the global continuity.

The conservation equations have thus been specified as to their numerical solution form. Now a discussion of how the boundary conditions are incorporated follows.

Boundary Conditions

The boundary conditions must be specified at two points since the conservation equations are second order parabolic equations. The conditions for this system are given at the shock and the ablator surface. First, the method of determining shock boundary conditions will be discussed followed by the boundary specification at the ablator surface.

Shock boundary conditions: The conditions at the shock are determined by using the Raukine-Hugoniot equations (Eqns. 3.58-3.62). Chemical equilibrium is assumed at the shock and an initial guess of density ratio across the shock wave is made. From the density ratio, enthalpy can be calculated from the Rankine-Hugoniot relations. Temperature is determined from the enthalpy, and the density ratio can then be calculated using equilibrium air compositions (from the equilibrium air subroutine, GAS). This density ratio is then compared with the assumed density ratio. This value is then updated until convergence is obtained ($<0.5\%$). When density ratio is known, the shock pressure, the normal velocity, and the tangential velocity can be determined from the Rankine-Hugoniot relations. The temperature and species compositions are products of the chemical equilibrium calculation.

Ablator surface conditions: The boundary conditions at the ablator surface are a little more complicated to evaluate than the shock boundary conditions. The material response is actually determined from the solution to a set of nonlinear ordinary differential equations which describes the ablation of the plastic composite heat shield. In this research a Padé approximation numerical technique (CHAR) was used to describe the flow of decomposition gases through the charred heat shield. The technique is described in Appendix A along with a discussion of results and their eventual incorporation in the overall analysis. Essentially, the analysis yields heat conducted at the surface of the ablator as a function of mass loss rate and surface temperature as shown in Figure 5.3.

The results are input into the flow field analysis as

$$q_{cond} = a_1 T^3 \rho v + a_2 T^2 \sqrt{\rho v} + a_3 T^3 \sqrt{\rho v} + a_4 \rho v \qquad [5.23]$$

Coefficients for a_1, a_2, a_3, and a_4 are given in Table 5.1 where T and ρv are evaluated at the surface.

The overall analysis is initiated at the stagnation line with an assumed value of mass loss rate (ρv). From this assumed value of mass loss rate, the surface temperature (T) can be calculated using the Hertz-Knudsen equation as described in Appendix B.

$$T = f(\rho v, P) \qquad [5.24]$$

The pressure is determined at the shock from the Rankine-Hugoniot equations. The wall pressure is equivalent to the shock pressure at the stagnation line since the thin shock layer assumption has been assumed valid.

Boundary conditions have been established for energy ($T = T_w$),

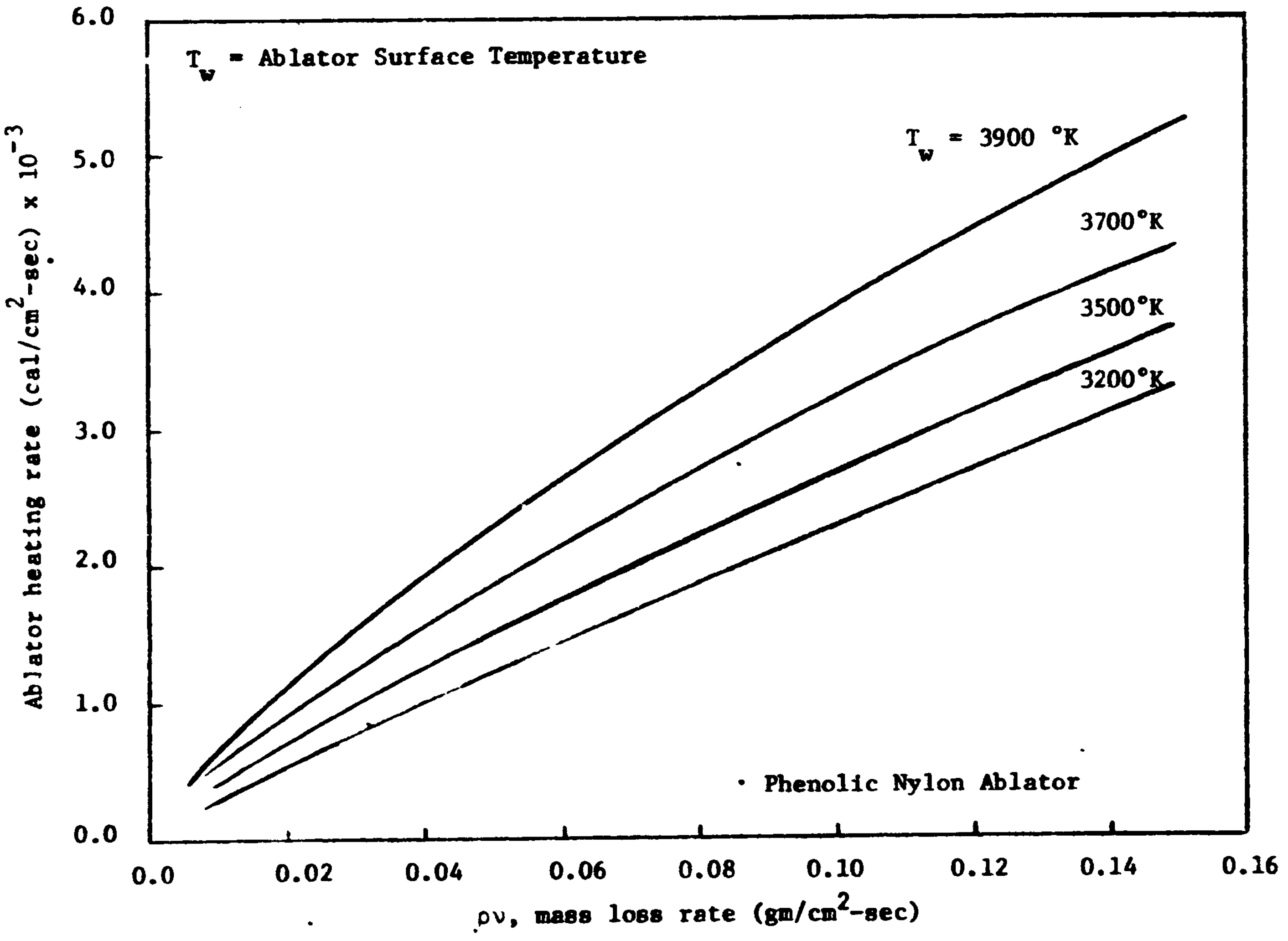

Figure 5.3. Ablator Heating Response vs. Mass Loss Rate.

Table 5.1

Curve Fit Coefficients for Heat Conducted Through the Surface of a Phenolic Nylon Ablator

$(q = a_1T^3\ \rho v + a_2T^2\ \sqrt{\rho v} + a_3T^3\ \sqrt{\rho v} + a_4\ \rho v)$

	q in * cal/sq cm-sec	q in † BTU/sq ft-sec
a_1	0.9292×10^{-8}	0.1674×10^{-7}
a_2	-0.1292×10^{-3}	-0.3330×10^{-3}
a_3	0.4268×10^{-7}	0.1099×10^{-6}
a_4	0.1516×10^{4}	$0.273x \times 10^{4}$

* T is temperature in °K
ρv is mass loss rate in gm/sq cm-sec
† T is temperature in °K
ρv is mass loss rate in lbm/sq ft-sec

x-momentum ($f'=0$), and global continuity ($\rho v=\rho v_w$). The wall values of species composition remain to be specified. This specification is made using constant values of wall composition. The values chosen were determined from the CHAR program at conditions considered typical of the ablator surface during planetary reentry (3600°K and 0.04 lbs/ sq. ft.-sec. mass loss rate) and are given in Table 5.2.

The stagnation line solution can now be determined since the problem has been completely specified. The solution of the shock layer equations yields a value of heating rate (radiative + conductive + diffusive) from flow field to ablator surface. This value must be equivalent to the energy absorbed by the ablator surface by conduction, sublimation phase change and energy reradiated by the surface, q_w.

$$q_w = q_{cond} + q_{subl} + q_{RR} \qquad [5.25]$$

The first term, q_{cond}, is attained by evaluating Eq. 5.23 for the conduction through the surface. The heat absorbed by sublimation phase change, q_{subl}, is simply the heat of sublimation, ΔH_{vap} ($\sim 4.4 \times 10^3$ BTU/lb), multiplied by the mass loss rate of solid carbon, $(\rho v)_c$

$$q_{subl} = 4.4 \times 10^3 \, (\rho v)_c \qquad [5.26]$$

and the energy reradiated by the char surface is found by applying the Stephan-Boltzmann equation with an emmissivity, ε, of 0.66 (Ref. 5.3).

Table 5.2

Compositions at the Surface of a Phenolic Nylon Ablator*

(Surface Temperature = 3600°K,
Pressure = 1 atm, Mass Loss Rate = .04 lbm sq ft-sec)

	Component	Mass Fraction	Mole Fraction
1	H_2	0.04135	0.2745
2	H	0.0221	0.2934
3	C_2H_2	0.0589	0.0301
4	C	0.3695	0.1363
5	C_2	0.0422	0.0233
6	C_3	0.0211	0.0233
7	C_2H	0.1388	0.0737
8	C_3H	1×10^{-10}	-
9	C_4H	1×10^{-10}	-
10	CO	0.257	0.1219
11	O	0.292×10^{-8}	-
12	N_2	0.04951	0.0235
13	HCN	1×10^{-10}	-
14	CN	1×10^{-10}	-
15	N	1×10^{-10}	-
16	N^+	1×10^{-10}	-
17	O^+	1×10^{-10}	-
18	C^+	1×10^{-10}	-
19	O_2	1×10^{-10}	-
20	e^-	1×10^{-10}	-

---

* Calculated using CHAR program described in Appendix A.

$$q_{RR} = \varepsilon\sigma T^4 = 3.3 \times 10^{-12}\ T^4 \qquad [5.27]$$

where q_{RR} is the reradiated energy expressed in BTU/sq ft-sec and T is the surface temperature expressed in °K.

The surface heating rates from the flow field solution and Eq. 5.25 can then be compared. If they differ, then a new value of mass loss rate must be assumed and the procedure repeated. A typical solution progression is shown in Figure 5.4. Normally a reasonably (within 2%) coupled flow field-surface solution can be obtained in three attempts in this manner at the stagnation line.

The solution downstream of the stagnation region is coupled by assuming an initial mass loss rate profile and comparing heating rates as at the stagnation line. In Figure 5.5 a typical mass loss profile is shown and in Figure 5.6, the corresponding heating rates are given. The mass loss rate profile is updated until coupling is achieved at all points downstream of the stagnation region.

Stability of the Energy Equation

The energy equation was found to present the most severe stability problems of all the conservation equations. Two forms of the energy equation were presented in Chapter III - the temperature formulation and the enthalpy formulation. Unsurmountable problems with stability were encountered when attempting to use the temperature form whereas the enthalpy form gave excellent results when properly "tuned". A discussion of both methods follows.

Temperature form: The temperature form of the energy equation proved to be quite unsatisfactory for reasons of extreme instability. Initially it was believed that the temperature formulation

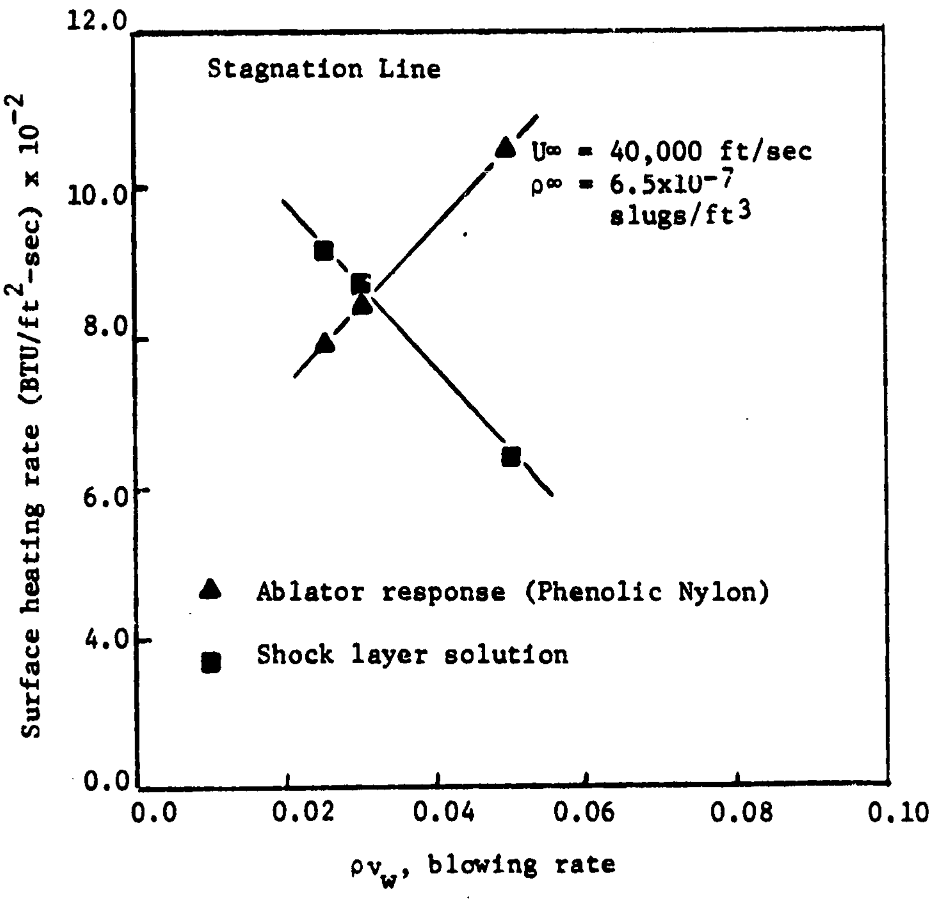

Figure 5.4. Coupling of the Shock Layer to the Ablator by a Surface Energy Balance.

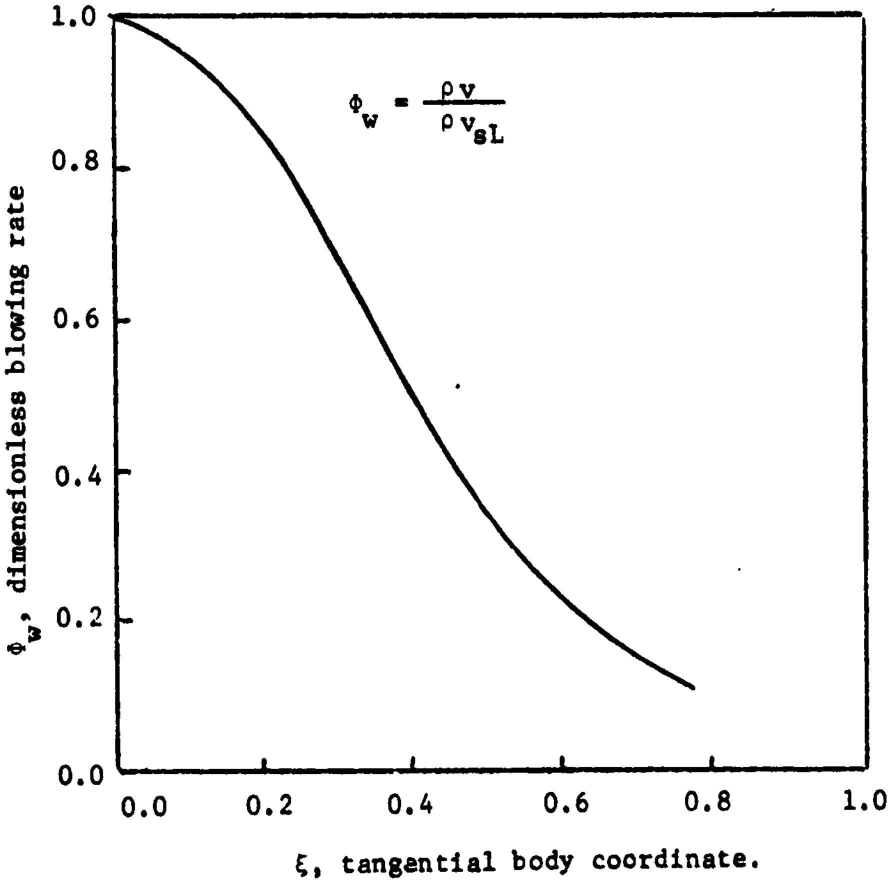

Figure 5.5. Dimensionless Blowing Rate Profile Around the Body.

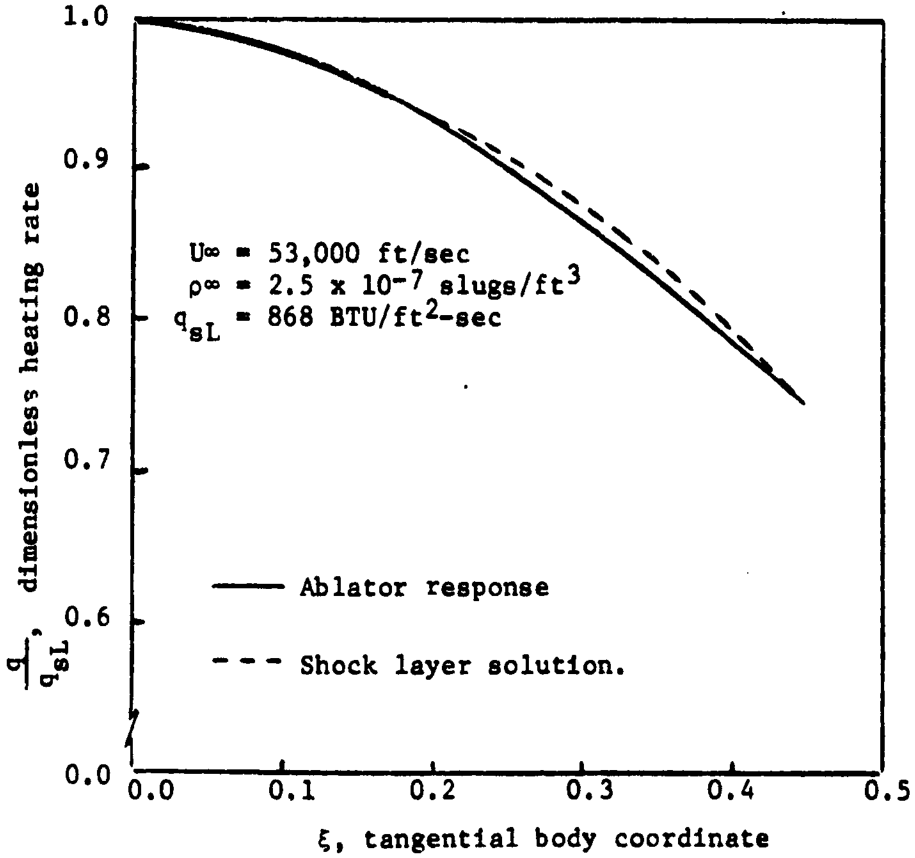

Figure 5.6. Dimensionless Heating Rate Profile Around the Body - Coupled.

would be more desirable than the enthalpy form since temperature is a direct result of the solution of the tridiagonal matrix. In the enthalpy formulation, the tridiagonal matrix solution yields enthalpy which must then be converted to temperature using an iteration scheme with species compositions at each nodal point. The temperature formulation, however, rapidly goes unstable with disastrous oscillations which create havoc on thermodynamic, transport, kinetic, and radiative properties. Within a few iterations the temperature goes negative at some nodal points and at other points, the shock temperature is greatly exceeded. The first few iterations with the energy equation in the temperature form are shown in Figure 5.7. All attempts to dampen these oscillations were unsuccessful.

The probable reason for this instability in the temperature formulation might be in the quasilinearized chemical production term

$$\alpha_2 = \frac{\partial}{\partial T} (\Sigma\, h_i \frac{\omega_i}{\rho}) \qquad [5.28]$$

This quasilinearized term should technically include the radiative flux divergence contribution along with the chemical production term. Unfortunately, there is no convenient analytical expression for the partial of radiative flux with respect to temperature. In an attempt to include the quasilinearized radiative flux divergence into α_2, the flux divergence term was numerically differentiated. The radiative flux divergence is highly nonlinear as depicted in Figure 5.8. In fact with a slight variation in temperature profile,

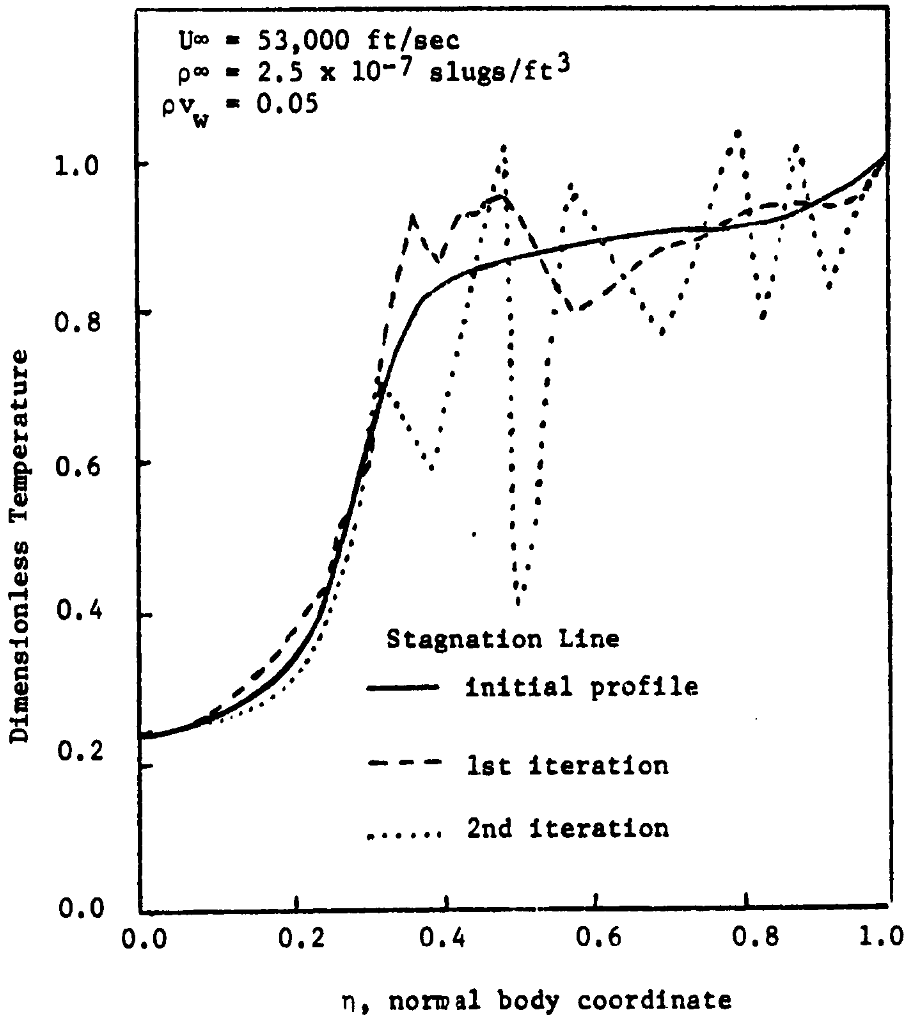

Figure 5.7. Instability of the Temperature Form of the Energy Equation.

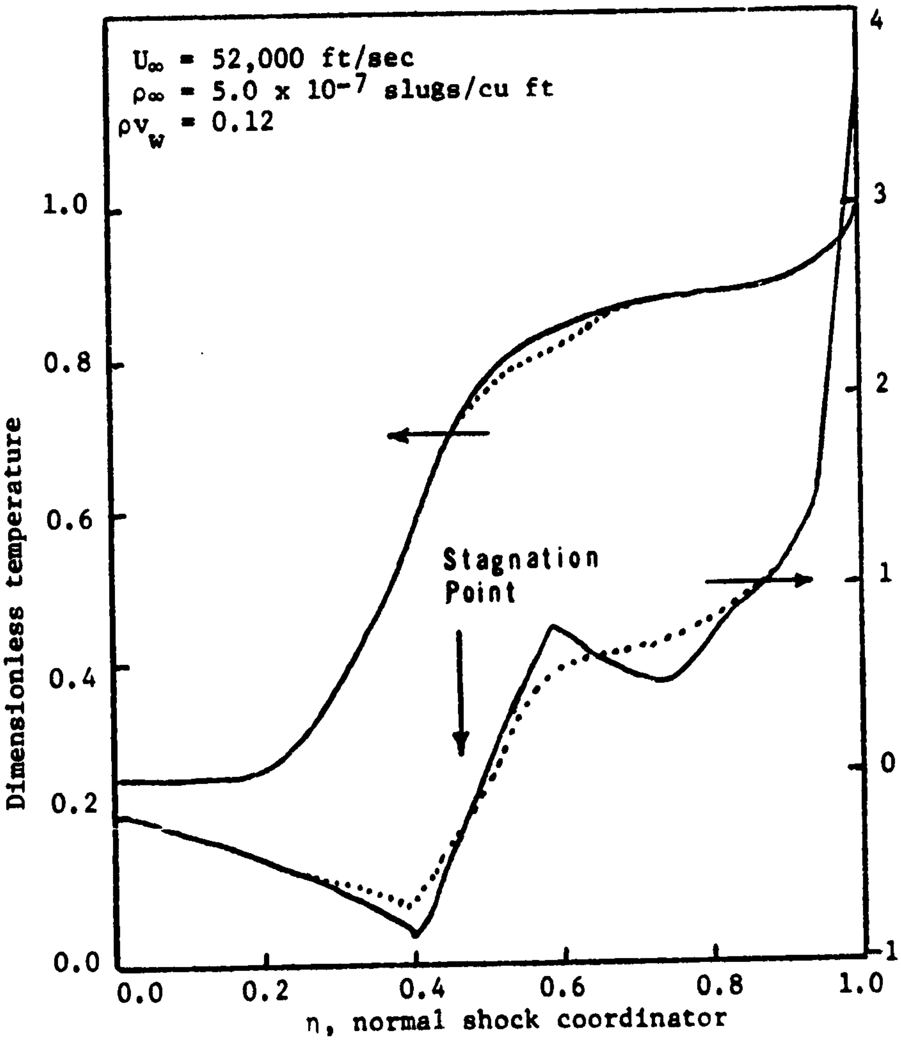

Figure 5.8. Illustration of the Effect of Temperature Variations Upon Radiative Flux Divergence.

the radiative flux divergence changes dramatically inside the flow field. This extreme nonlinearity led to a very unstable numerical differentiation; and, therefore, a very unstable numerical solution of the energy equation.

With the quasilinearized part of the radiative flux term being excluded, α_2 is left with only the chemical production term. The problem with this arrangement is that the primary energy production in the flow field is not due to chemical reactions but to radiation. The resulting situation appeared to place undue emphasis on chemical production which provided for an unstable energy equation formulation. The energy equation in enthalpy form circumvents these problems as discussed below.

Enthalpy form: When the energy equation is solved in its enthalpy form (Eq. 3.130), the result is a quite stable solution. In Figure 5.9 the consecutive enthalpy profiles obtained from using the enthalpy formulations are presented. In Figure 5.10 the temperature profiles which correspond to the enthalpy profiles are presented. The results very clearly show a smooth, stable behavior of the solution.

Comparing the enthalpy formulation of this work with the temperature formulation (equilibrium chemistry model) of Esch (Ref. 5.4) demonstrates the superior stability of the enthalpy formulation (Fig. 5.11). Esch reported that when several iterations were performed the solution sometimes became unstable enough that it could not recover. The profile was then manually adjusted and the solution continued. In the present enthalpy formulation, manual adjustment

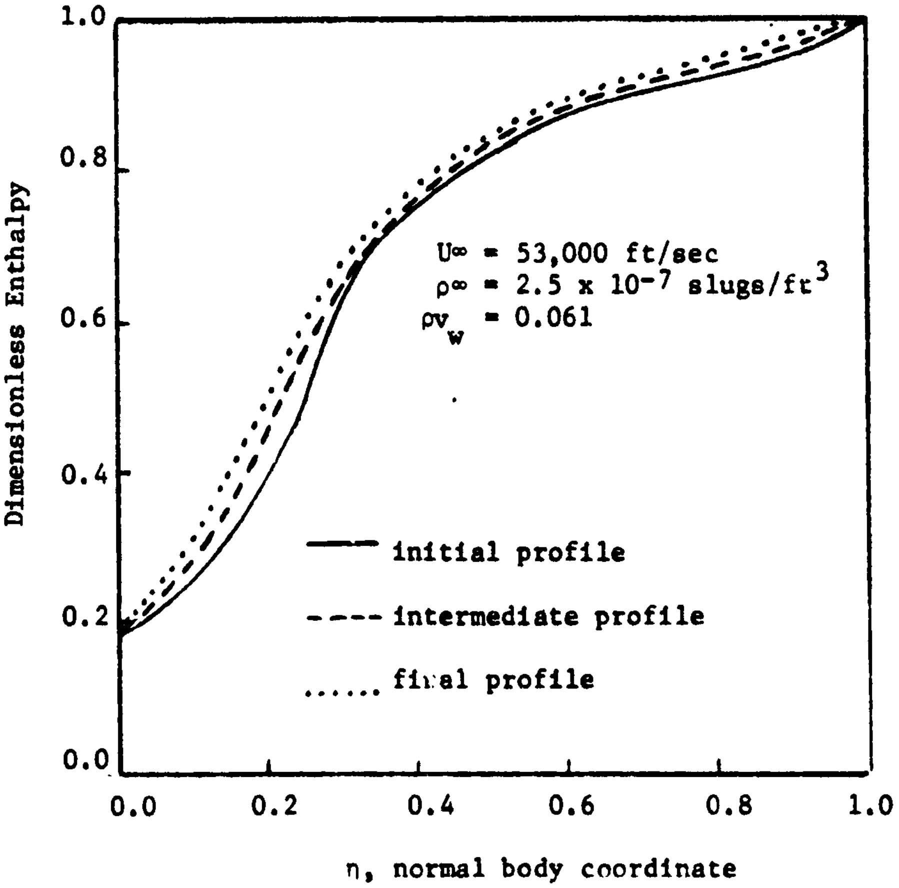

Figure 5.9. Stable Enthalpy Profiles Using Enthalpy Form of the Energy Equation.

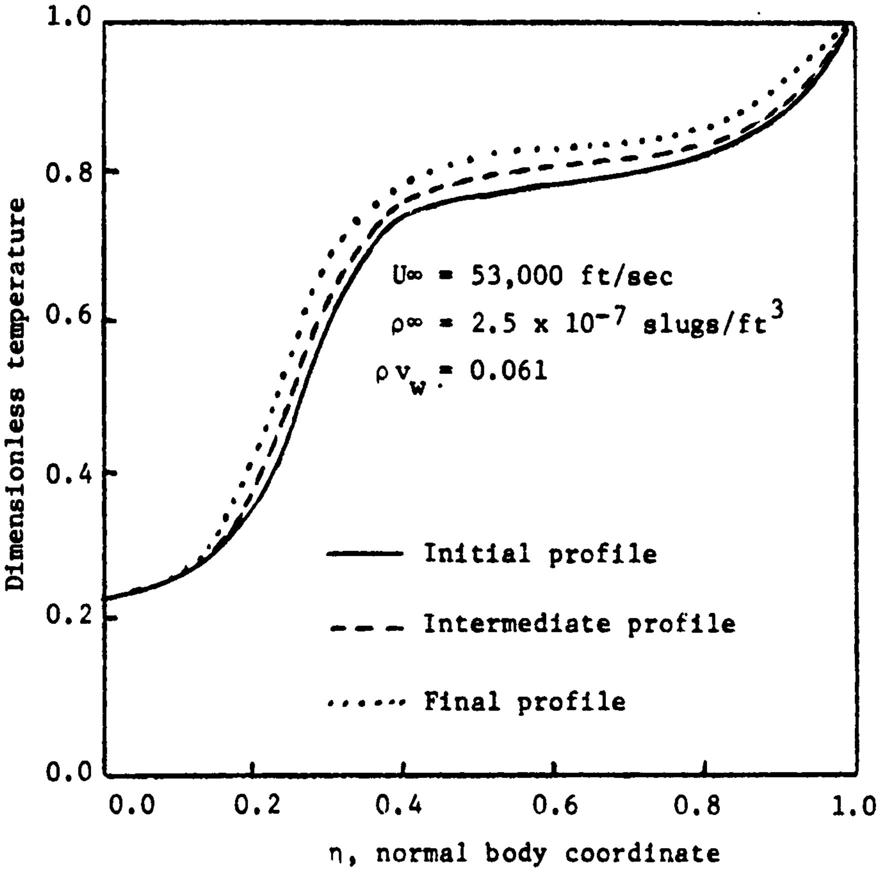

Figure 5.10. Stable Temperature Profiles Using Enthalpy Form of the Energy Equation.

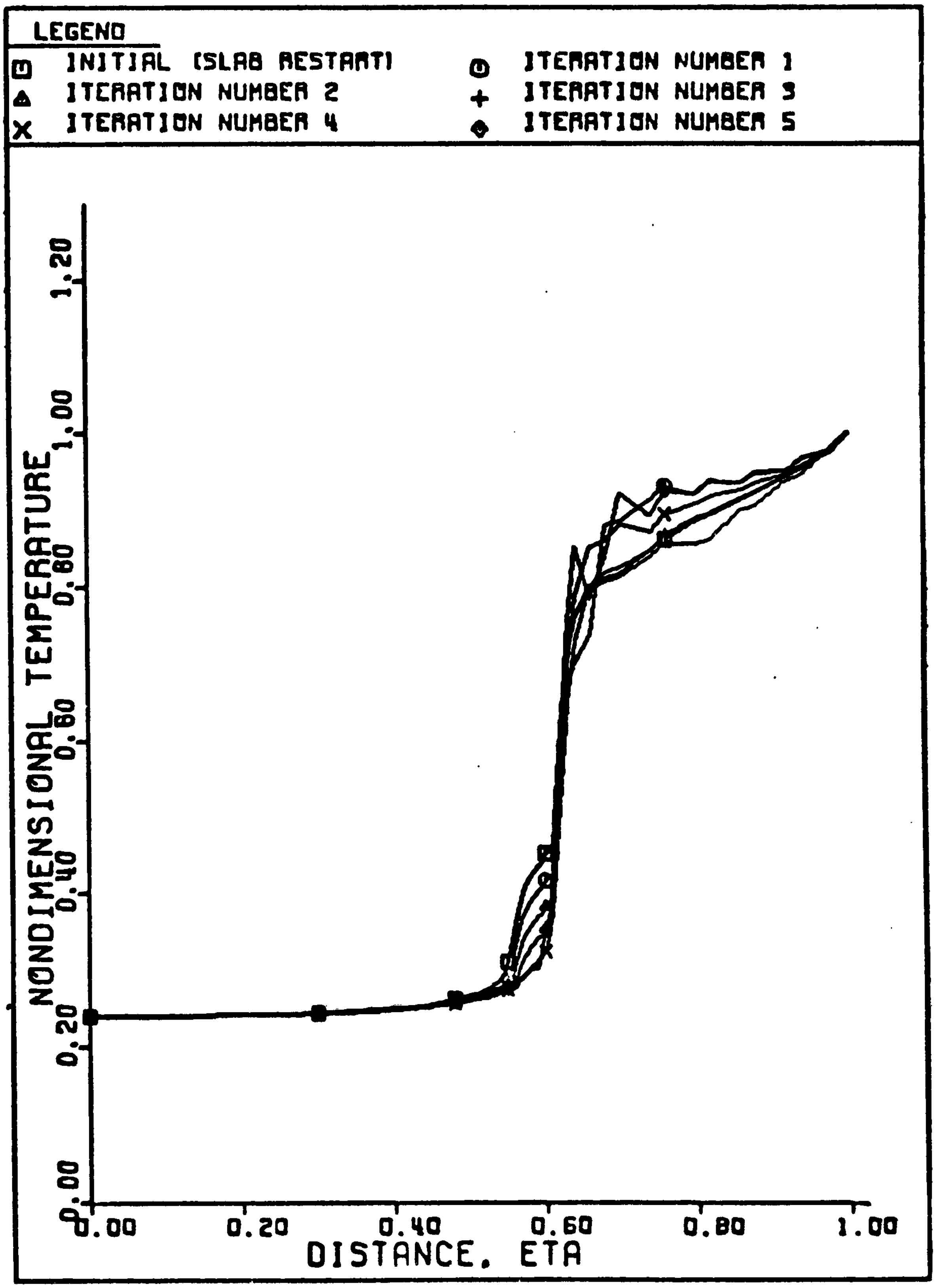

Figure 5.11. Variation in Equilibrium Chemistry Temperature Profiles from Iteration to Iteration Using the Temperature Form of the Energy Equation. (Esch, Ref. 5.4)

was not found necessary. Damping of successive iterations was, however, required as described in the next section.

Damping Coefficients

The conservation equations, especially the energy equation, can be made more stable by the use of damping coefficients. The solution is thus permitted to vary only slowly from the initial guessed profile. Damping was achieved by using ith iteration values and calculated values of the profiles in the following manner

$$W^{i+1} = d\,W_{calc} + (1-d)\,W^{i} \qquad [5.29]$$

where the damping coefficient, d, is between 0.0 and 1.0 and can be different for each conservation equation. For fast response (rapid convergence), the damping coefficient should approach 1.0. This cannot always be done in practice since stability sometimes becomes a severe problem. In case of instability, the lower value of damping coefficient must be utilized. The best value of damping coefficient can only be determined by numerical experimentation with the specific case and the specific conservation equation in question. The most sensitive equation by far in this study was the energy equation due to its extreme nonlinear production terms of radiation and chemical reaction. For cases in which radiative heating was not severe, damping values of 0.5 on enthalpy yielded reasonably stable solutions, but when radiative heating became predominant, the damping coefficient had to be reduced to 0.25.

The species continuity equations are heavily dependent upon temperature since temperature appears in the Arrhenius form of the chemical production terms. Due to the sensitivity that the species exhibited on temperature, convergence was often difficult to attain (although stability was no problem) unless the temperature was damped with the very low coefficient of 0.1. The best results were obtained when a damping coefficient of 0.25 was used to bring the solution close to convergence. The damping coefficient was then reduced to 0.1 to eliminate small oscillations in the temperature profile which caused corresponding but slightly more pronounced oscillations in the species profiles. Solutions could then be obtained in which all profiles were converged to within 0.5%.

The "best" damping coefficients for the x-momentum and species continuity equations were found to be 1.0. The damping coefficient used for the enthalpy profile was 0.5 (this value directly affects the temperature profile since the temperature is calculated from enthalpy). Besides damping coefficients on these profiles, a damping coefficient was applied to the calculation of the transformed shock standoff distance, $\tilde{\delta}$ (from global continuity), as follows

$$\tilde{\delta}^{i+1} = d\,\tilde{\delta}_{calc} + (1-d)\,\tilde{\delta}^{i} \qquad [5.30]$$

The value of the damping coefficient used for $\tilde{\delta}$ for 0.5. The use of this damping coefficient on transformed standoff distance increased stability and made convergence more rapid.

Shock Standoff Distance

The calculation of shock standoff is not as simple as it would appear at first glance. The calculation of standoff distance from the geometrical relation of Equation 5.15 requires the specification of the angle, ε, which is the difference between the body angle and the shock angle (refer to Fig. 3.2). This angle is also used in the calculation of the boundary conditions at the shock with the Rankine-Hugoniot relations. These shock boundary conditions in turn alter the flow field solution significantly thus altering the value of shock standoff distance calculated from Equation 5.14.

In Figure 5.12 two ε angle profiles are shown as a function of distance around the body. The corresponding shock standoff distances as computed from Equations 5.14 and 5.15 are shown in Figure 5.13. The different ε angle profiles create only a minor change in the solution of the geometrical relation (Eq. 5.15) but the same difference in profiles causes a drastic change in standoff distance as computed from the flow field solution, Equation 5.14. This sensitivity of the flow field shock standoff distance calculation to input ε profile causes difficult convergence problems. Because of the difficulty associated with achieving a converged shock standoff profile, the convergence criteria was not as stringent as for the rest of the flow field parameters. A difference of about 2 to 3% was considered acceptable.

In order to determine the sensitivity of the overall solution on the correct shock standoff distance, the heating rate profiles were compared for the two profiles. Results in Table 5.3 using the two profiles in Figure 5.12 yielded heating rate profiles that differed by only 0.5% at a body station of $\xi = 0.7$. This result

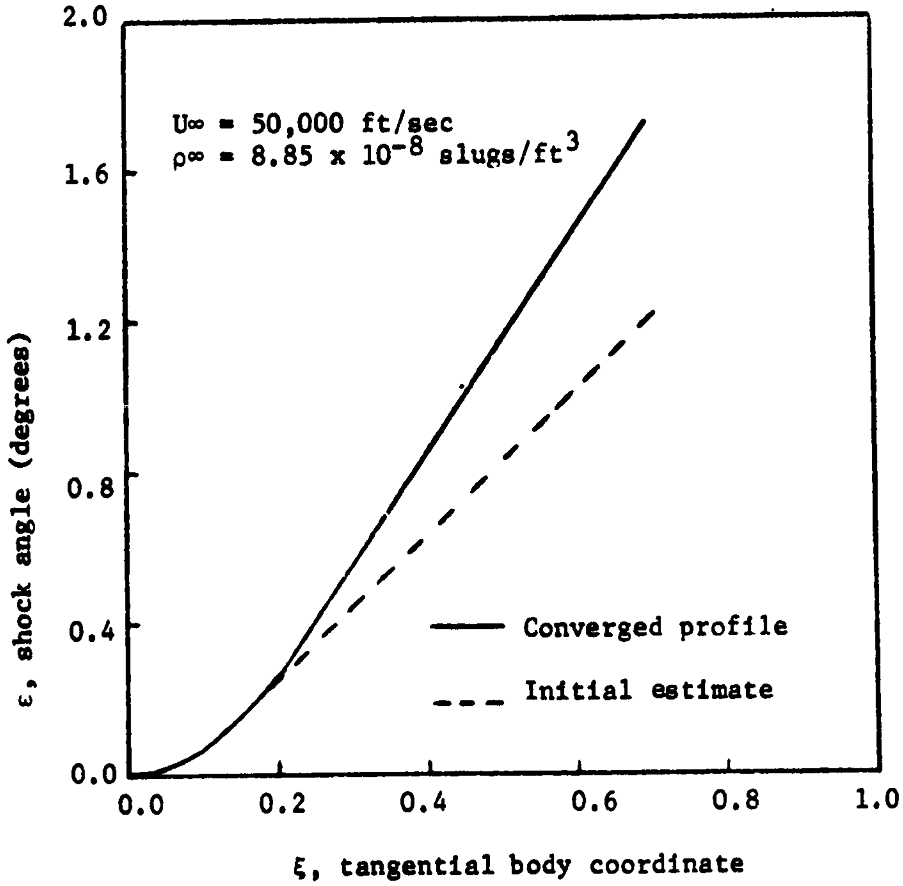

Figure 5.12. Convergence of shock angle, ε, Around the Body.

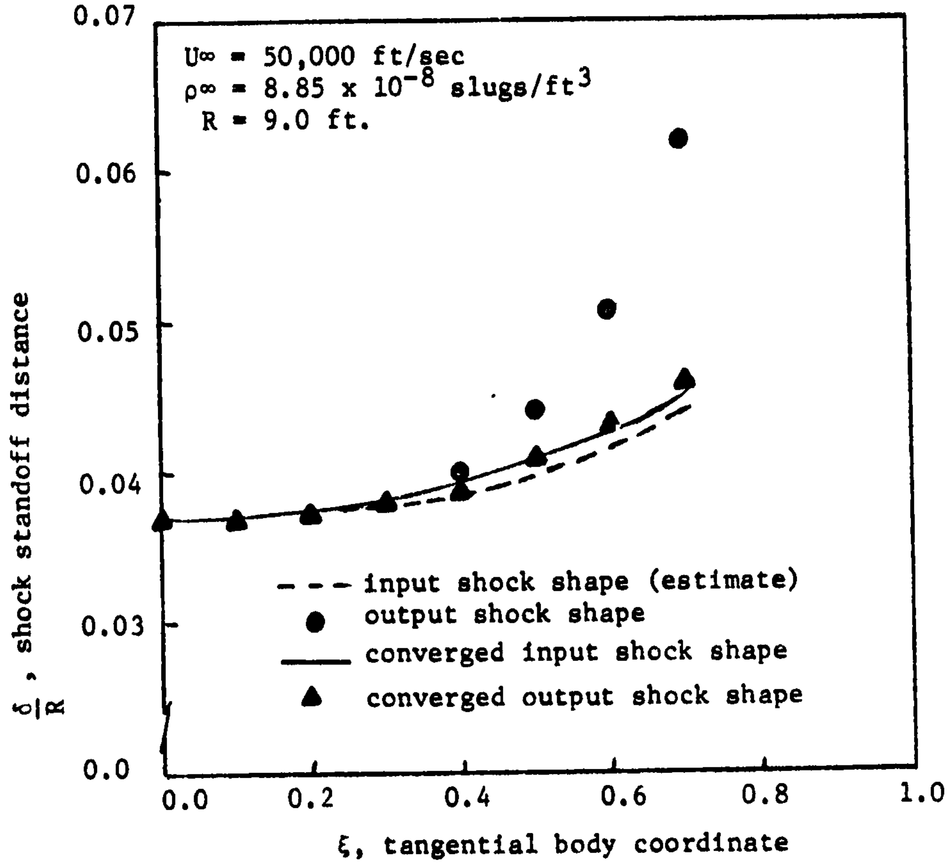

Figure 5.13. Convergence of shock shape profile around the body.

Table 5.3

Insensitivity of Heating Rate to Convergence of Shock Standoff Distance, δ

U_∞ = 50,000 ft/sec ρ_∞ = 8.85 x 10^{-8} slugs/cu ft	Heating Rate (BTU/sq ft - sec)	
ξ	δ converged	δ not converged
0.0	182.2	182.2
0.2	163.1	163.1
0.4	114.5	114.3
0.6	58.1	58.0
0.8	24.2	24.0

indicates that the solution is essentially insensitive to shock standoff distance.

The specification of the shock stand-off distance does appear to affect the speed of convergence. When the incorrect angle profile was used, the solution took 150 minutes of computer time (IBM 360/65) to reach a body station of $\xi = 0.6$; and when the correct angle profile was used, the solution time took only 120 minutes of computer time to reach a body station of $\xi = 0.9$.

The results from this study indicated that a highly accurate profile of shock angle was not completely necessary for an accurate solution of the heat load on the ablation heat shield. Comparable results were obtained by Moss (Ref. 5.5). However, the closer one can approximate the correct profile, the seemingly more efficient is the utilization of computer time. Using this result as a basis, therefore, relatively little emphasis was placed on convergence of shock standoff distance.

Initial Profiles

The specification of initial profiles was made along the stagnation line using the following

$$\rho v = \eta^2[(\rho v)_s - (\rho v)_w] + (\rho v)_w \qquad [5.31]$$

$$f' = \eta \qquad [5.32]$$

$$C_i = \begin{cases} C_{i_w} & \rho v < 0 \\ C_{i_\delta} & \rho v > 0 \end{cases} \qquad [5.33]$$

$$\frac{T - T_w}{T_\delta - T_w} = \frac{T' - T_w'}{T_\delta' - T_w'} \qquad [5.34]$$

where T' is an internally guessed profile for nondimensional temperature as shown in Figure 5.14. This profile can be input by the user if a better idea of its shape is known. In all cases studied, it was found that the solution converged satisfactorily using the temperature profile in Figure 5.14.

It was found from experience that the species profile estimates in Equation 5.33 yielded negative values which when used to calculate temperature from enthalpy, yielded an unstable temperature profile. This problem was solved by iterating a number of times with the species continuity equation alone (no energy or momentum) and using absolute values of species composition. The species profiles eventually lined-out and the solution could proceed normally. A satisfactory number of iterations was found to be 50.

The initial guesses of profiles downstream of the stagnation line are determined as follows

$$\left.\frac{v - v_w}{v_s - v_w}\right)_{\xi_{m+1}} = \left.\frac{v - v_w}{v_s - v_w}\right)_{\xi_m} \qquad [5.35]$$

$$f'(\xi_{m+1}) = f'(\xi_m) \qquad [5.36]$$

$$C_i\ (\xi_{m+1}) = C_i\ (\xi_m) \qquad [5.37]$$

$$\left.\frac{T - T_w}{T_\delta - T_w}\right)_{\xi_{m+1}} = \left.\frac{T - T_w}{T_\delta - T_w}\right)_{\xi_m} \qquad [5.38]$$

The solution iterates at each body station until convergence is attained and then proceeds to the m+1th body station with initial guesses as given in Equations 5.35 - 5.38.

Interation Sequence

The iteration scheme used in this study is shown in Figure 5.15. With initial estimates of the flow field variables the radiative flux divergence was computed in LRAD. The normal and tangential velocity profiles along with the transformed shock standoff distance were then computed by converging simultaneously on the global continuity, x-momentum, and y-momentum equations. Convergence was assumed when the tangential velocity profile change by less than 0.5% and the transformed shock standoff distance changed by less than 0.1%.

The species continuity equations (SPECIE) were then solved with five consecutive iterations. These multiple iterations were found necessary to stabilize the solution since it appears that the species equations have a much slower response than the energy equation. If the species solution is not allowed to keep pace with the energy solution, stability problems are encountered when the temperature profile is computed from enthalpy and species profiles. The problem soon compounds itself and the solution wanders

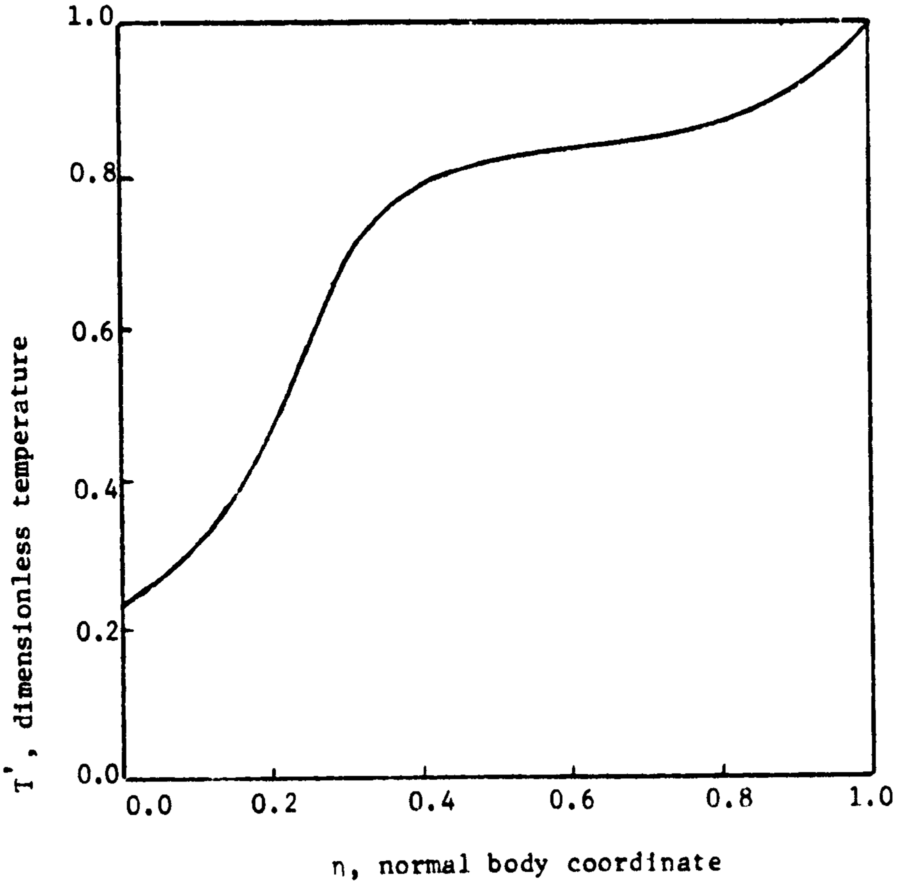

Figure 5.14. Dimensionless Temperature Profile for Initial Estimate at Stagnation Line.

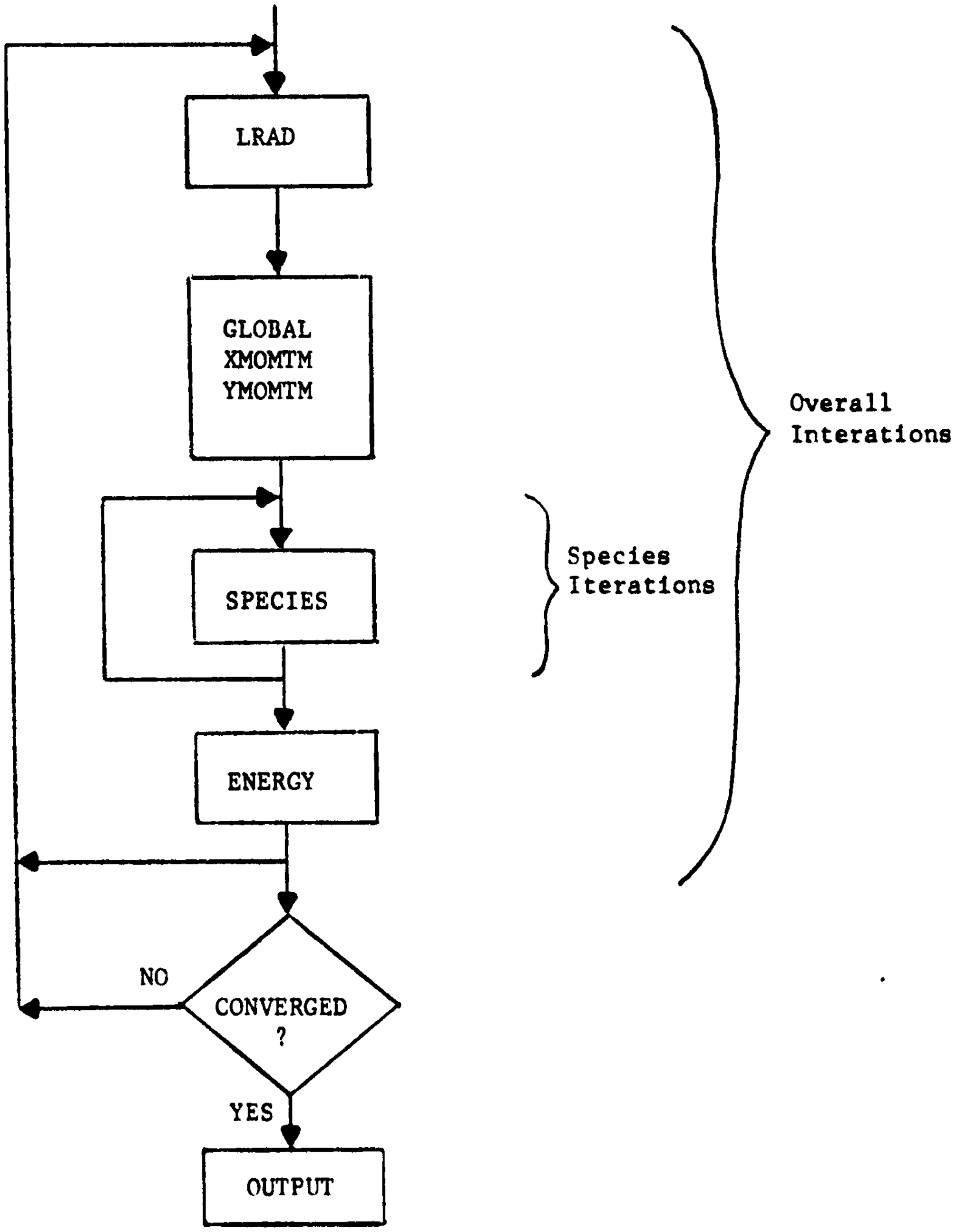
LRAD
GLOBAL
XMOMTM
YMOMTM
SPECIES
ENERGY
NO
CONVERGED
?
YES
OUTPUT
Overall
Interations
Species
Iterations

Fig. 5.15. Iteration Sequence of Shock Layer Analysis

into oblivion. Five iterations on species continuity for every iteration on energy proved quite satisfactory.

The energy equation (ENERGY) was then solved in enthalpy form. The enthalpy profile thus obtained was used in conjunction with the species profiles to determine a temperature profile. This cycle of x-momentum, y-momentum, global, species, and energy was repeated five times using the same radiative flux divergence profile in the energy equation. The flux divergence profile was then updated and the sequence repeated until convergence of the overall analysis was achieved.

Convergence

Convergence must be satisfied on two levels -- first, the solution must agree from one iteration to the next, and second, the number of nodal points used must be sufficient to give the true solution. Both of these convergence criteria are discussed below.

Iteration convergence: Initially, an attempt was made to require all the profiles to be within 0.5% of each other on consecutive iterations before converged was assumed. Computer time using this convergence criteria, however, became astronomical. An alternate convergence criteria was then used which stipulated that heat flux from flow field to ablator agreed within 0.5% on consecutive iterations. The heating rate, after all, is the factor that determines the rate at which the ablator loses mass - the direct purpose of this research. Reasonable computation time was experienced using this convergence criteria.

Nodal convergence: The shock layer equations are a set of parabolic partial differential equations in two dimensions. The finite difference grid, therefore, has two spacings - one the normal coordinate and the other the tangential coordiante. Convergence must be demonstrated for both coordinates. The finite difference grid system was shown schematically in Figure 5.2 where n is the normal coordinate nodal point and m is the tangential coordinate nodal point.

Convergence was verified in the tangential direction by halving the stepsize from $\Delta\xi = 0.2$ to $\Delta\xi = 0.1$ and the heating rate profile was examined (since this is the most important variable in the analysis, and it determines mass loss rate for the ablator). This profile was used for the convergence criteria, and the heating rate profiles differed by less than 1% for the two stepsizes investigated at a body station of $\xi = 0.8$ as indicated by the comparison of results in Table 5.4. This result implied that convergence had been attained so a step size of $\Delta\xi = 0.05$ was used in all subsequent analyses.

Esch (Ref. 5.4) showed convergence along the stagnation line by approximately halving the step size (126 points versus 59 points). He demonstrated that the profiles of dependent variables remained essentially the same. The flow field analysis by Esch was very similar to the present flow field analysis in that it was the solution of the reacting, radiating, viscous flow equations. The present analysis also used the same numerical technique as used by Esch. The major differences are that Esch's analysis was only for the stagnation line, it used equilibrium chemistry, and it

Table 5.4

Nodal Convergence in Tangential Direction

U_∞ = 50,000 ft/sec

ρ_∞ = 8.85 x 10^{-8} slugs/cu ft

Heating Rate Results

BTU/sq ft.-sec

ξ	$\Delta\xi$ = 0.1	$\Delta\xi$ = 0.2
0.0	182.2	182.2
0.2	163.1	163.0
0.4	114.5	113.8
0.6	58.1	57.8
0.8	24.2	24.0

solved the energy equation in temperature form. The present analysis applied to the entire flow field in which nonequilibrium chemistry was employed, and the energy equation was solved in its enthalpy form. These differences did not significantly alter the validity of the numerical solution, but they did significantly affect computational time and core requirements. Convergence was therefore established by calling upon the Lax equivalence theorem (Ref. 5.6). This theorem states: "Given a properly posed initial boundary value problem and a finite difference approximation to it that satisfies the consistency condition, then stability is the necessary and sufficient condition for convergence." The finite difference equation is said to be consistent (compatible) with the differential equation if the local truncation errors tend to zero as $h, k \to 0$. The explicit and Crank Nicolson formulae are compatible (Ref. 5.6). Since the Crank Nicolson method was used in this analysis, and stability had been achieved, it can be argued that convergence has been attained based on the Lax equivalence theorem.

Summary

The numerical formulation of shock layer equations has been specified in this chapter. Using the α coefficients developed in Chapter III and the flow field properties (thermodynamic, transport, kinetic, and radiative) developed in Chapter IV, results can be achieved for a wide variety of cases.

In this chapter numerical incorporation of the boundary conditions was discussed along with stability, convergence, and numerical experience with the numerical techniques. It was concluded that the energy equation could be most easily solved in its enthalpy formulation with proper use of damping coefficients. The temperature formulation of the energy equation leads to a highly unstable solution which appears impossible to control. Convergence to a true solution was shown by calling upon the Lax Equivalence Theorem. The shock standoff distance demonstrated severe sensitivity to shock angle, ε, but this was shown to have an insignificant effect on the overall analysis.

The next chapter will use the numerical procedures presented in this chapter and investigate heating rates and mass loss rates for the flow field around an ablating blunt body (phenolic-nylon ablator).

References

5.1 Conte, S. O., Elementary Numerical Analysis, McGraw-Hill Book Co., New York (1965).

5.2 Davis, R. T., "Numerical Solution of the Hypersonic Viscous Shock-Layer Equations," AIAA Journal, 8 (5), pp. 843-851, May 1970.

5.3 Pope, R. B., "Measurement of the Total Surface Emittance of Charring Ablators," AIAA Journal, Vol. 5, No. 12, (1967), pp. 2285-2287.

5.4 Esch, D. D., "Stagnation Region Heating of a Phenolic-Nylon Ablator During Return from Planetary Missions," PhD dissertation, Louisiana State University, Baton Rouge, Louisiana (1971).

5.5 Moss, J. N., "Solutions for Reacting and Nonreacting Viscous Shock Layers with Multicomponent Diffusion and Mass Injection," PhD dissertation, Virginia Polytechnic Institute and State University, Blacksburg, Virginia (1971).

5.6 Ames, Williams F., Numerical Methods for Partial Differential Equations, Barnes & Noble, Inc., New York, N.Y., pp. 61-62, (1969).

5.7 Bahn, G. S., "Reaction Rate Compilation for the H-O-N System", p. 23, Gordon and Breach Science Publication, New York (1968).

5.8 Pike, R. W., "Evaluation of the Literature for Chemical Reaction Rates for the Decomposition Products from Charring Ablators," Langley Working Paper, LWP-181, NASA (Jan. 21, 1966).

5.9 Menees, G. P. and R. L. McKenzie, "A Simplified Chemical Model for Estimating Non-Equilibrium Radient Emission of CN (Violet) in Shock-Heated Mixtures of CO_2 and N_2," AIAA J., 6 (3), 554 (March 1968).

5.10 Davies, William O., "Radiative Energy Transfer on Entry Into Mars and Venus," Rept. No. IITRI-T200-13, IIT Research Institute, Chicago, Illinois, Dec. 1965.

5.11 Allen, C. W., Astrophysical Quantities, Second edition, University of London, Athlone Press, 1963.

5.12 Semenov, N. N., Some Problems of Chemical Kinetics and Reativity, Vol. I, Pergamon Press, New York, p. 2, 1958.

CHAPTER VI

RESULTS OF THE SHOCK LAYER ANALYSIS

Introduction

The ground work has been laid in the foregoing chapters for the results presented in this chapter. All the assumptions pertinent to obtaining the results presented here were discussed in Chapter III where the conservation equations which describe the flow-field were developed. The species and momentum conservation equations have the form of a set of parabolic partial differential equations and the energy equation takes the form of an integro - partial differential equation. In Chapter IV, the thermodynamic, transport, and radiative properties of the flow field were discussed along with the chemical reactions taking place in the flow field. This work was based on the development of a useful analytical tool to be applied in the determination of the heating load on a manned reentry space vehicle. This reentry vehicle is to be equipped with a heat shield made of a phenolic nylon composite capable of sustaining velocities of earth entry on return from planetary missions such as Mars. Typically, a reentering spacecraft will make contact with the earth's thin upper atomosphere at about 55,000 feet per second. When the craft encounters the denser air at low altitudes, it will be slowed by the frictional drag of the atmosphere thus reducing its kinetic energy.

The results presented in this chapter will be for six key points along the reentry trajectory. The reentry body was taken to have a spherical shape with a nine (9.0) foot radius which is typical of the Apollo spacecraft. Heating rates were determined at the stagnation line for these six cases and downstream heating was determined for four of these six cases - all of which were coupled to the ablator by a surface energy balance. These six cases required more than 100 hours of IBM 360/65 CPU time. A study of chemical reaction rates in the flow field was also performed which demonstrated a marked effect on the heating load on the ablator.

After the stagnation line heating rate results are presented in this chapter, a comparison of the stagnation line is made with several other investigators. Around the body results are then presented followed by a discussion of chemical reactions in the shock layer. The chapter closes with a discussion of computer limitations and other difficulties encountered in the analysis.

Stagnation Region Heating

The stagnation line solution is important, not only because this is normally the region of peak heating, but also because this solution is required as initial conditions for the solution of the flow field around-the-body. Conditions for the six coupled stagnation line cases run for this investigation are given in Table 6.1. Heating rate results are shown in Figure 6.1 and Table 6.2 for these cases. The trajectory along which these conditions exist is shown in Figure 6.2. All six cases were coupled to the ablator by a surface energy balance as described in Chapter III.

Table 6.1

Freestream and Ablator Conditions for Cases Studied in the Present Investigation

Case	Altitude (ft)	U_∞ (ft/sec)	ρ_∞ (slugs/ft^3)	Surface * Temperature (°K)	Mass Loss Rate * (lbm/sq ft-sec)
1	247,000	55,000	7.5×10^{-8}	3390	0.005
2	218,000	53,000	2.5×10^{-7}	3576	0.026
3	199,500	52,000	5.0×10^{-7}	3741	0.102
4	193,000	50,000	6.5×10^{-7}	3781	0.135
5	193,000	45,000	6.5×10^{-7}	3685	0.059
6	193,000	40,000	6.5×10^{-7}	3605	0.026

* Stagnation line quantities.

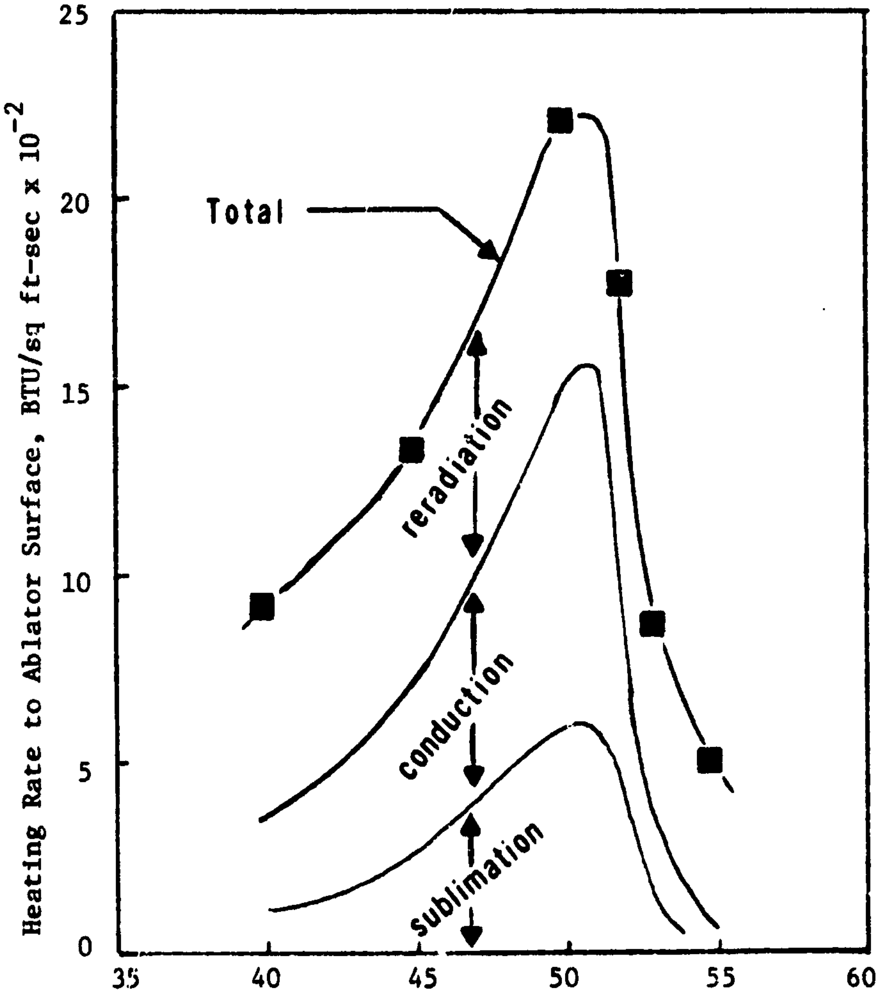

U_∞, Entry Velocity (Kfps)

Figure 6.1. Stagnation Heating Rate at a Phenolic Nylon Ablator Surface Along a Reentry Trajectory.

Table 6.2

Stagnation Line Heating Rate Results for Cases Investigated

Case	Heating Rate, BTU/sq ft-sec							
	Ablator Surface				Shock Layer			
	q^{1}_{RR}	q^{2}_{c}	q^{3}_{s}	q^{4}_{T}	q^{5}_{R}	q^{2}_{c}	q^{6}_{D}	q^{4}_{T}
1	436	48	22	506	153	255	93	501
2	540	214	115	868	671	156	49	876
3	646	716	451	1813	1793	-36	25	1782
4	674	926	600	2200	2232	-72	33	2193
5	609	450	262	1320	1266	39	45	1350
6	558	225	116	899	649	199	75	923

1. q_{RR} is energy reradiated from char surface

2. q_c is energy transport by conduction

3. q_s is energy absorbed by sublimation phase change

4. q_r is total energy

5. q_R is radiative energy transmitted from the shock layer to the surface

6. q_D is energy transport by diffusion

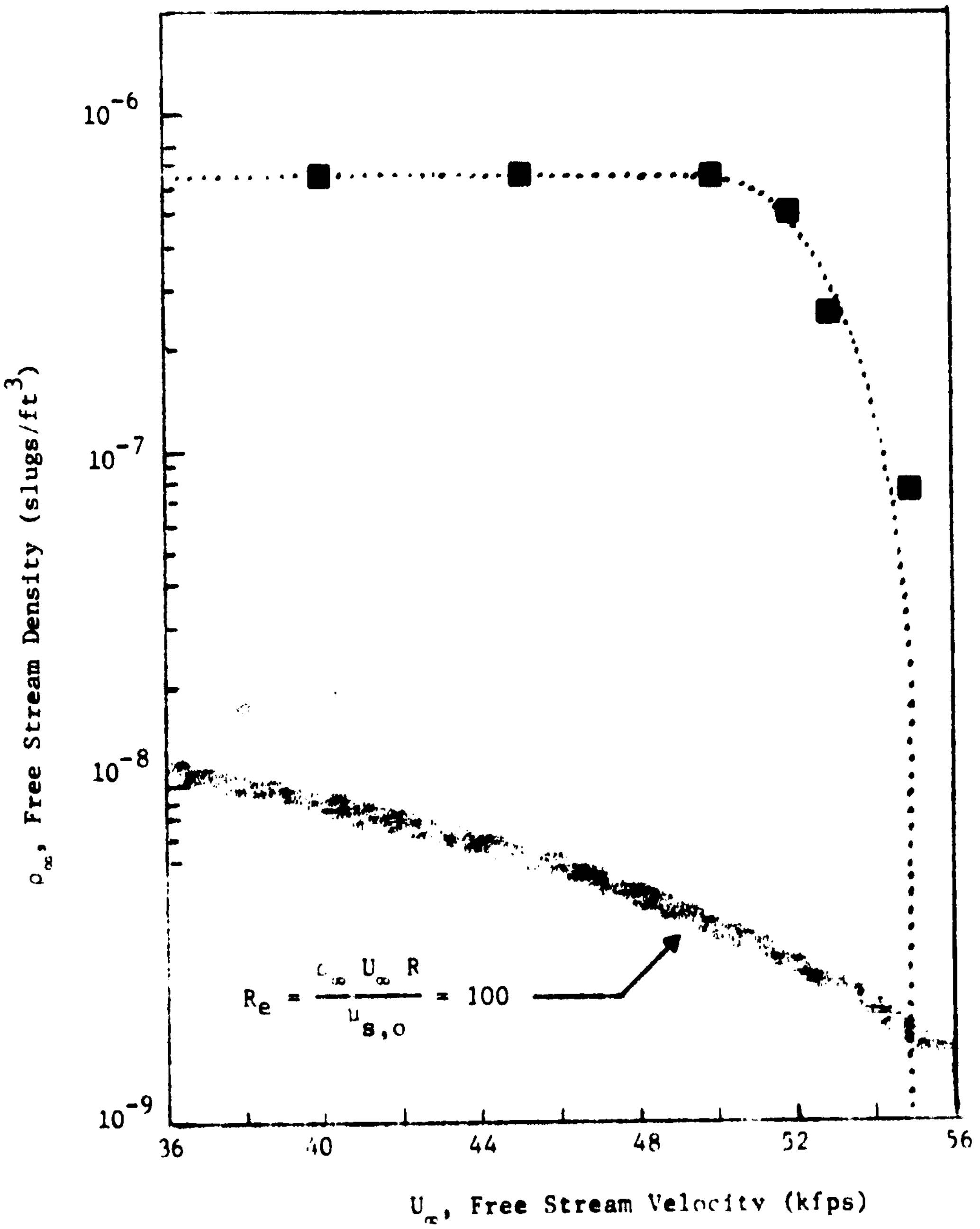

Figure 6.2. Reentry Trajectory for Present Investigation.

Note in Figure 6.1 that, as the vehicle first encounters the earth's atmosphere at a high rate of speed (55,000 feet per second), the heating load on the protective heat shield is low. As reentry proceeds, the capsule slows down but the load on the heat shield attains a maximum at around 50,000 to 51,000 feet per second. The heating rate then decreases as the capsule is slowed further. The reason for this phenomenon is that the upper atmosphere first encountered at around 247,000 feet is an extremely low density layer (7.5 x 10^{-8} slugs/c.ft.). The amount of frictional heat developed in this region is therefore only minor and the capsule is slowed only slightly. However, as the vehicle encounters the denser earth atmosphere at lower altitudes, the frictional heating becomes more intense. On this trajectory the capsule is slowed from 53,000 feet per second to 50,000 feet per second while traversing densities of 2.5 x 10^{-7} to 6.5 x 10^{-7} slugs per cubic foot. At an altitude of 193,000 feet where the density is 6.5 x 10^{-7} slugs per cubic foot, the capsule is then slowed rapidly to a point where the heating load becomes much less severe. Results show that the stagnation heating rate is only 900 BTU/sq. ft.-sec. at a velocity of 40,000 feet per second and an atmospheric density of 6.5 x 10^{-7} slugs per cubic foot -- 41% of the heating rate at 50,000 feet per second. The heating rate will fall off even more as the capsule slows further at this same density (see trajectory curve of Figure 6.2).

In Figure 6.1 the primary heat absorption mechanisms of conduction and sublimation of carbon along with reradiated energy are shown for the energy reaching the ablator surface. The magnitude of all the heat absorption mechanisms increases as total heat absorption increases but the fraction of energy accomodated by each mechanism changes through the trajectory.

At the low heat load conditions experienced at 55,000 ft/sec., for example, sublimation only accounts for 4% of the heat absorbed, (Figure 6.3), conduction accounts for about 11% and reradiation is the dominant heat transfer mechanism in reradiating 85% of the heat reaching the ablator surface. Conversely, as the heat load increases, the fraction of energy reradiated decreases and the mechanisms of conduction and sublimation account for a much more substantial portion of the heat absorption. For instance, at the maximum heating rate conditions experienced during the trajectory (about 50,000 ft/sec. and 193,000 feet), the energy reradiated is only 30% of the total energy reaching the capsule surface. Conduction and sublimation account for 42% and 28% respectively at these peak heating conditions. This fact means that the heat shield is losing mass at a much faster rate. The mass loss rate is shown in Figure 6.4. It is seen to be characteristically similar to the heat load profile.

These stagnation line results are the first attempt made which incorporate both nonequilibrium chemistry and detailed line and continuum radiative transport in the calculation at severe heat loads. Until now all analyses performed have been for equilibrium or non-radiating flow. The results depict the solution along a typical reentry trajectory for manned interplanetary missions. Points were chosen on the trajectory which represent typical heat loads on an ablative heat shield at the stagnation point. Previously

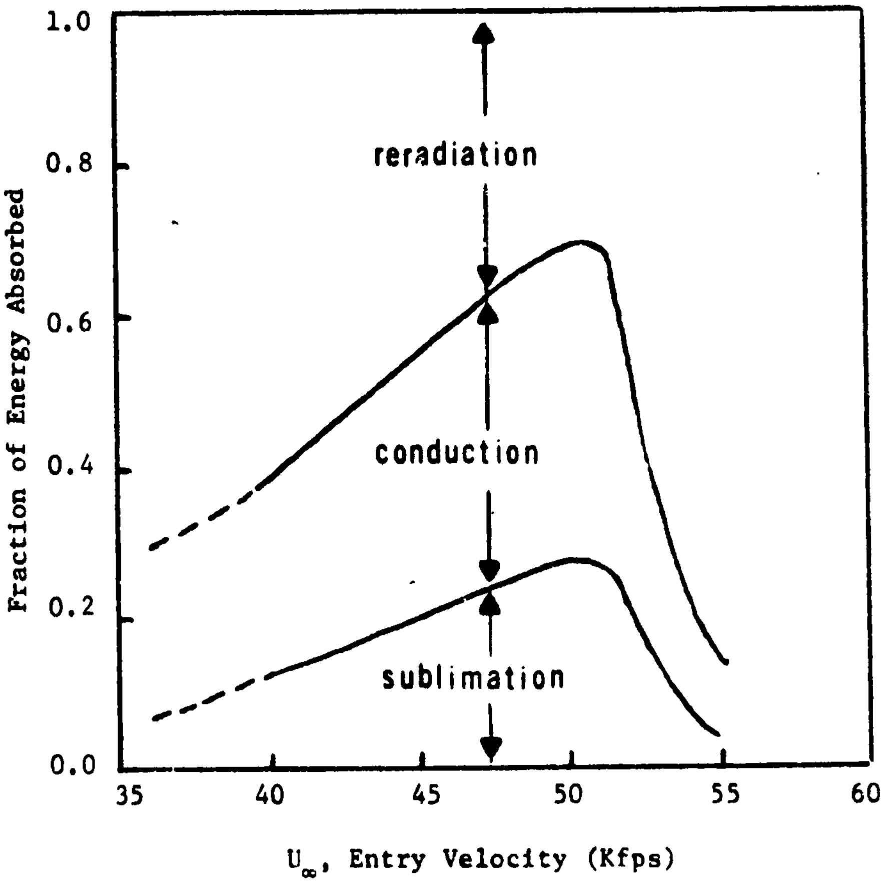

Figure 6.3. Effectiveness of Heat Absorption Mechanisms for a Phenolic Nylon Ablator Along the Reentry Trajectory.

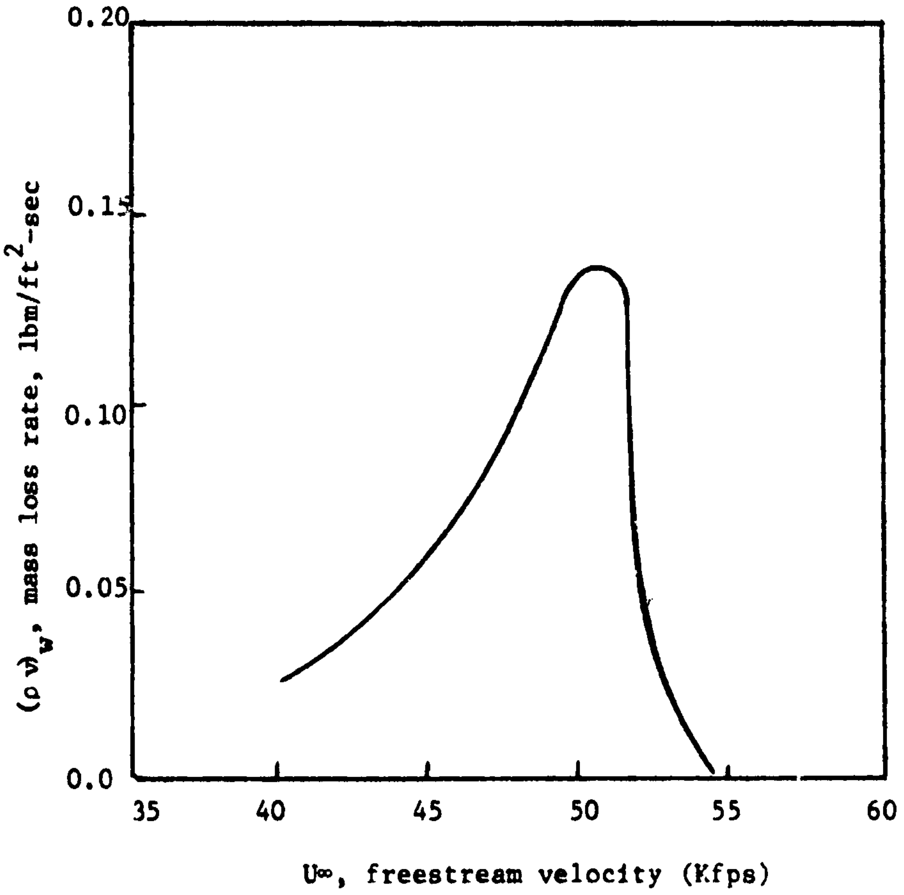

Figure 6.4. Mass Loss Rate at the Stagnation Line of a Phenolic Nylon Ablator Along the Reentry Trajectory.

analyses were performed along similar trajectories using the simpler equilibrium chemistry approximations. Nonequilibrium analyses were generally not attempted in this regime since the results are not accurate when radiation heating is not included. This analysis is also the first to couple a nonequilibrium shock layer to a nonequilibrium charring ablator.

The following section shows a comparison of the heating results from the present investigation with equilibrium results from previous investigators. A comparison is also made with a low heating load case of Perez (Ref. 6.1) which included nonequilibrium chemistry and radiative heating.

Comparison with Other Stagnation Line Investigators

In Table 6.3 is a list of results for the present investigation along with a comparison with previous investigators for conditions of low radiative heating to the ablator. These results are shown for the stagnation line with a phenolic-nylon ablator.

The present investigation used finite rate chemistry whereas, with the exception of one case run by Perez (Ref. 6.1), the rest of the analyses assumed equilibrium chemistry. The reason for this comparison with equilibrium chemistry is that there are no other finite rate analyses including radiative heat transfer. The only conditions for which a direct comparison can be made with Esch (Ref. 6.2), Engel (Ref. 6.3), and Perez (Ref. 6.1) is a freestream velocity of 50,000 feet per second, a freestream density of 8.85×10^{-8} slugs per cubic foot, and a blowing rate of 5% of freestream with a phenolic nylon ablator.

Table 6.3

Comparison of Moderate Heating Rate Results at the Stagnation Line (Phenolic Nylon Ablator)

$U_\infty = 50{,}000$ ft/sec, $\rho_\infty = 8.85 \times 10^{-8}$ slugs/ft^3, $\rho v_w = 0.05$

Reference	Chemistry	q_R (BTU/ft^2-sec)
Present investigation	Nonequilibrium	121
Perez (Ref. 6.1)	Nonequilibrium	121
Perez (Ref. 6.1)	Equilibrium	340
Esch (Ref. 6.2)	Equilibrium	349
Engel (Ref. 6.3)	Equilibrium	305

To verify the validity of the present analysis a comparison was made with the nonequilibrium results of Perez (Ref. 6.1). Both analyses predict 121 BTU/sq ft-sec for the case shown in Table 6.3 which is excellent agreement. The analysis of Perez can be validated by comparing his equilibrium results at these same conditions to the work of Esch (Ref. 6.2) and Engel (Ref. 6.3). His radiative heating results (q_R = 340 BTU/sq ft-sec) compare very faborably with the analyses of Esch (q_R = 349 BTU/sq ft-sec), and Engel (q_R = 304 BTU/sq ft-sec). Perez used identical equilibrium and nonequilibrium numerical solutions of the conservation equation to those of Esch and Engel except for the solution of the species equations. Actually, a comparison with Esch is more meaningful since in both these analyses the species equations were actually solved whereas Engel used a step function model of elemental compsoition across the diffusion zone (discussed in Chapter II).

Perez's equilibrium results differ with Esch by less than 3% for a very favorable agreement. However Perez's equilibrium results are about 190% higher than the nonequilibrium results. This was the first time nonequilibrium chemistry and radiative heating effects were included simultaneously in a shock layer solution. The results show that nonequilibrium chemistry effects can significantly effect the heating rate to a phenolic nylon ablator during reentry.

Direct comparisons between investigators are difficult if not impossible at high heat loads for several reasons. Analyses have been performed for widely different radiation and chemistry models, and different ablator composites. The result is that lack of agreement is not only probable but expected.

For higher heating loads at denser atmospheric conditions, the results from Case 3 of the present investigation were used for comparison with equilibrium analyses of other investigators as shown in Table 6.4. The blowing rate of $\rho v_w = 0.1$ shown in Table 6.4 was a case run in the process of attempting to couple Case 3 to the ablator. It should be noted that the results reported in Table 6.4 are for solutions which are not coupled to the ablator by a surface energy balance with the exception of Chin (Ref. 6.4). At 52,000 feet per second, this case has a higher freestream velocity than the other cases shown at 50,000 feet per second but because of the lower freestream density (5.0×10^{-7} slugs per cubic foot), the kinetic energy is within 7% of the cases run at 5.3×10^{-7} slugs per cubic foot which means that the energy absorbed in both cases should be the same order of magnitude. This is the case, and Chin obtained 1445 BTU/ft ^{2} sec as compared to 1820 BTU/ft ^{2} sec in this work.

The nonequilibrium results at these high heating rates could be postulated to compare quite faborably with equilibrium analyses since it is theorized that equilibrium is approached at these severe (high temperature) conditions. The radiative heating results of Garrett (Ref. 6.5) at a blowing rate of 0.1, $q_R = 2455$ BTU/sq ft-sec, are about 35% higher than the heating results of the present investigation at the same blowing rate, $q_R = 1820$ BTU/sq ft-sec. Although the nonequilibrium heating rate is appreciably lower than equilibrium for this case, the difference is much less than the previous low heating rate case (35% vs 190% difference). This fact lends

Table 6.4

Comparison of Severe Heating Rate Results at the Sttagnation Line

U_∞ (kfps)	ρ_∞ (slugs/ft^3) x 10^{-7}	ρv_w	q_R (BTU/ft^2-sec)	Ablator	References
52	5.0	0.1	1820	PN*	Present investigation
50	5.3	0.1	2455	CP	Garrett et al. (Ref. 6.5)
50	5.3	0.2	2253	CP	Garrett et al. (Ref. 6.5)
50	5.3	0.2	2350	CP	Rigdon et al. (Ref. 6.6)
50	5.3	0.2	2856	CP	Smith et al. (Ref. 6.7)
50	4.5	0.2	1816	PN	Esch (Ref. 6.2)
50	4.5	0.2	1661	PN	Engel (Ref. 6.3)
50	3.45	0.076	1445	CP	Chin (Ref. 6.4)
50	3.45	0.076	1925	CP	Smith et al. (Ref. 6.7)
50	3.45	0.076	1423	CP	Garrett et al. (Ref. 6.5)

PN = Phenolic Nylon, CP = Carbon Phenolic

* Nonequilibrium

credibility to the assumption that equilibrium chemistry can be used as an accurate approximation at the higher heating rates.

The equilibrium analyses of Garrett (Ref. 6.5) predicts a radiative heating rate of 2253 BTU/sq ft-sec at a reentry velocity of 50,000 feet per second, an atmospheric density of 5.3 x 10^{-7} slugs per cubic foot, and a wall blowing rate of 0.2. Rigdon, et al. (Ref. 6.6) attained similar results in predicting a radiative heating rate of 2350 BTU/sq ft-sec at these same conditions. The difference in these two analyses is only about 4%. In contrast to these results, Smith, et al. (Ref. 6.7) studied these identical conditions and determined a radiative heating rate of 2856 BTU/sq ft-sec which is 22% greater than either Garrett or Rigdon, et al. The major reason for this discrepancy appears to be the radiation model used by these investigators. Smith, et al. have neglected to include atomic line absorption for the highly absorbing carbon species. This fact accounts for the over-prediction of heating rate by Smith, et al.

A comparison of the present nonequilibrium results with Garrett and Rigdon, et al. shows that the nonequilibrium prediction is about 24% lower than these equilibrium results. A greater difference is seen between the nonequilibrium case and Smith, et al. but the reason for this is that carbon atomic lines were included in the nonequilibrium radiation analyses whereas Smith, et al. omitted this absorption mechanism in his analysis.

A comparison of the present results with the equilibrium analyses of Esch (Ref. 6.2) and Engel (Ref. 6.3) are also shown in Table 6.4. Flight conditions for the equilibrium runs were 50,000 feet per second, 4.5×10^{-7} slugs per cubic foot, and 0.2 blowing rate. Again these flight conditions differ from the nonequilibrium case but are close enough for comparison purposes. The radiative heating rate predicted by Engel was 1661 BTU/sq ft-sec which is 8.7% lower than the 1820 BTU/sq ft-sec from the present analysis. Esch determined the radiative heating rate to be 1816 BTU/sq ft-sec yielding only a 0.2% difference. The comparison with Esch is more realistic since he actually solved the equilibrium species continuity equations whereas Engel assumed a step function of elemental compositions across the stagnation point. The fact that blowing rates are different (0.2 for equilibrium and 0.1 for present nonequilibrium) does not affect the results very significantly (probably less than 10%) since Engel demonstrated in a parametric study that the effect of increased blowing rate above 0.1 is not very great on radiative heating. The agreement between the present analysis and Esch is then seen to be excellent despite the differences in conditions.

The results presented at 50,000 feet per second, 3.45×10^{-7} slugs per cubic foot, and 0.076 blowing rate were included for completeness. These conditions are much less stringent than the 52,000 feet per second, 5.0×10^{-7} slugs per cubic foot, and 0.1 blowing rate for the nonequilibrium case. The radiative heating rates of Chin (Ref. 6.4), 1445 BTU/sq ft-sec, and Garrett, et al., 1423 BTU/sq ft-sec, are very close to each other in contrast to the 1925 BTU/sq ft-sec predicted by Smith, et al. The kinetic energy for the equilibrium cases is seen to be 36% lower than the nonequilibrium case (1820 BTU/sq ft-sec) but the heating rates are only about 25% lower for Chin and Garrett, et al., and 5.8% higher for Smith, et al. Again the reason for the large discrepancy between Smith, et al. and other investigators is believed to be due to differences in radiation data.

In summarizing, radiative heating predictions from the present nonequilibrium investigation are identical to those of Perez (Ref. 6.1) who did a nonequilibrium study at 50,000 feet per second and 8.85 x 10^{-8} slugs per cubic foot. Perez's numerical solution was verified by comparing his equilibrium results at these same conditions to the equilibrium results of Esch (Ref. 6.2) and Engel (Ref. 6.3) yielding less than 11% difference with Engel and less than 3% difference with Esch.

At higher heat load conditions, comparisons were made with equilibrium solutions at slightly different conditions. In general the results from the present investigation agree quite well considering the fact that equilibrium and nonequilibrium chemistry were used and flight conditions were not identical. Heating rate predictions for nonequilibrium chemistry in the present investigation is consistently lower than equilibrium predictions by other investigations. This phenomenon is due to the differences in species profiles across the shock layer as will be shown later in a discussion on kinetics.

Around the Body Results

Six coupled solutions were obtained at the stagnation line using nonequilibrium chemistry and were presented in Figure 6.1 and Tables 6.1 and 6.2. Of these six cases, four cases were continued downstream using the stagnation line results as initial conditions. The shock layer, was coupled to the ablator surface at all points around-the-body using the blowing rate profile. Heating rate profiles could then be compared with ablator response heating rates to insure a coupled solution. Only four of the six stagnation line cases were run because of the immense computer time required. For instance, Case 4 took four hours of CPU time to reach a downstream point of $\xi = 0.30$. A more complete discussion of computer time is provided at the end of the chapter.

In Figure 6.5 a plot of nondimensional blowing rate versus around the body distance is presented. The blowing rate is nondimensionalized with the stagnation line blowing rate, $(\rho v)\ \xi = 0$. Dimensionless heating rates are presented in Figures 6.6 through 6.9 for cases 1 through 4 using the blowing rate profile in Figure 6.5. The heating rate is nondimensionalized with the stagnation heating rate, q_{SL}, for convenience. The ablator-flow field coupling was found to be excellent, differing by less than 3% along the wall using the one generalized blowing rate profile with the exception of Case 1 where the flow field and ablator solutions diverge downstream of the stagnation line where a difference of 16.3% was observed. The blowing rate profile could have been altered until the ablator-flow field solutions matched for Case 1 but this would have required more computer time (approximately four to six hours of IBM/360/65 CPU time). The expense of the computer time was deemed too great in view of the fact that Case 1 is not a high heating rate case since the stagnation line heating rate is only 22% of the maximum heating rate investigated (Case 4). In addition, the difference in heating rate at the downstream point of $\xi = 0.45$ between ablator and shock layer solutions is only 16.3% which is not that great a deviation.

The shock layer results for the various cases run were obtained farther downstream for some than others. The reason for this is that some cases are more difficult computationally than others and therefore computer time becomes a major factor. The high heating rate cases of Case 3 and Case 4 were the most time consuming. For Case 3, a downstream value of $\xi = 0.35$ was reached, where for Case 4, a downstream value of only 0.30 was reached. Over four hours of computer time was used for each of these cases to reach these downstreams points. The heating rate severity appears to be a measure of the computational difficulty.

An interesting result of the around the body analysis is that one blowing rate profile can be used to describe all of the points on the reentry trajectory reasonably satisfactorily. What this means is that given the mass injection rate at the stagnation line, an estimate of the downstream mass loss rate can be made using Figure 6.5. The total mass injection rate, $\dot{m}$, can be estimated using the following relationship

$$\dot{m} = (\rho v)_{SL} \; 2\pi \int_0^{\xi} \phi_w \; \xi \; d\xi$$

which is the mass flux from the ablator integrated over the ablator surface area. The mass flux at the stagnation line $(\rho v)_{SL}$, can be determined from Figure 6.4 and the nondimensionalized mass flux around the body, ϕ_w, is the function in Figure 6.5. The value of the integral is a constant. By knowing the time elapsed at each point along the trajectory, the total mass loss for reentry, m, can

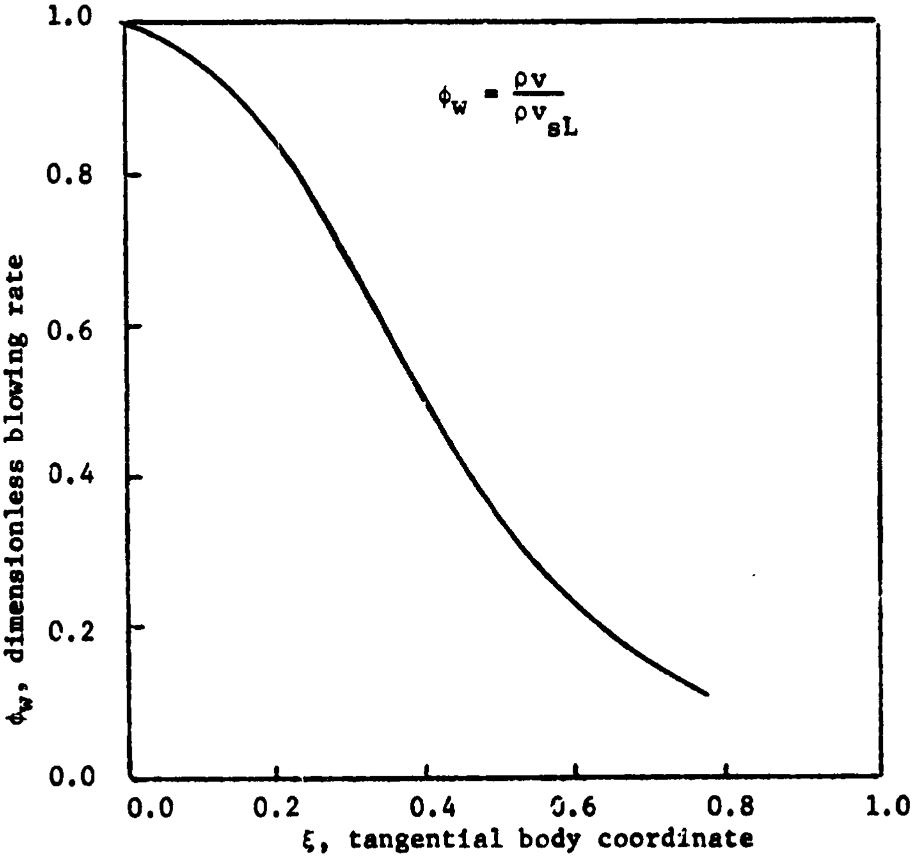

Figure 6.5. Dimensionless Blowing Rate Profile Around the Body.

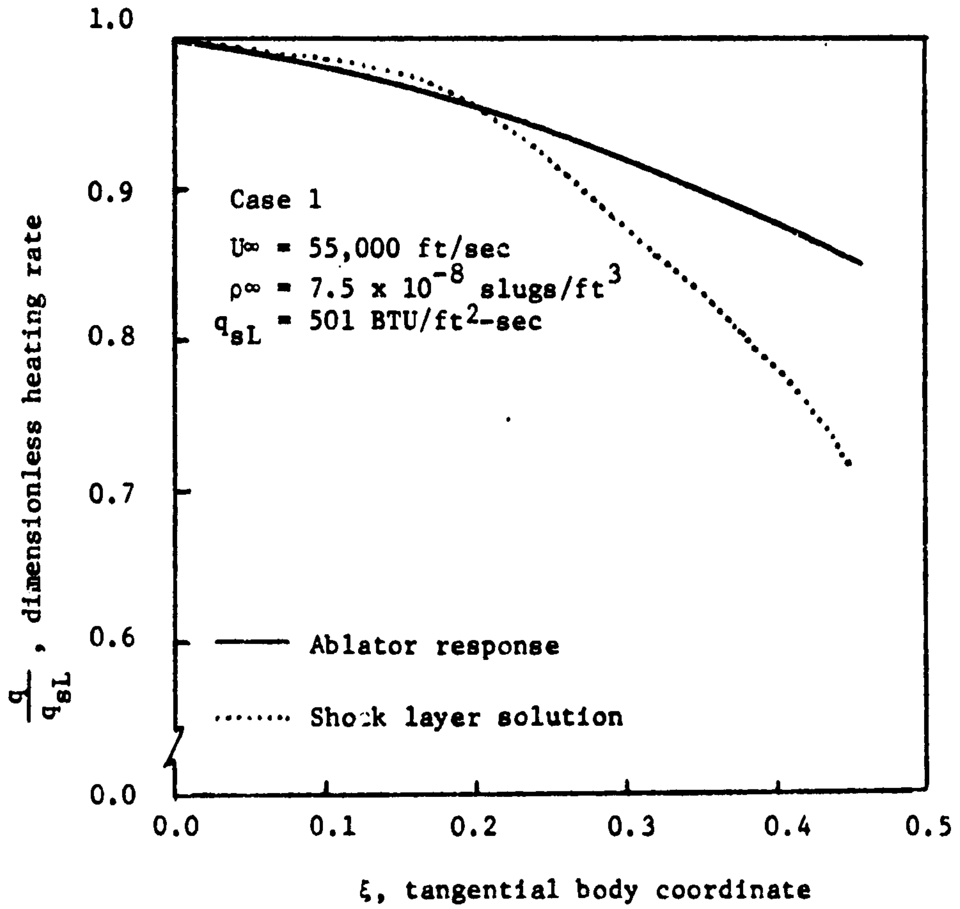

Figure 6.6. Dimensionless Heating Rate Profile For Case 1 - Coupled

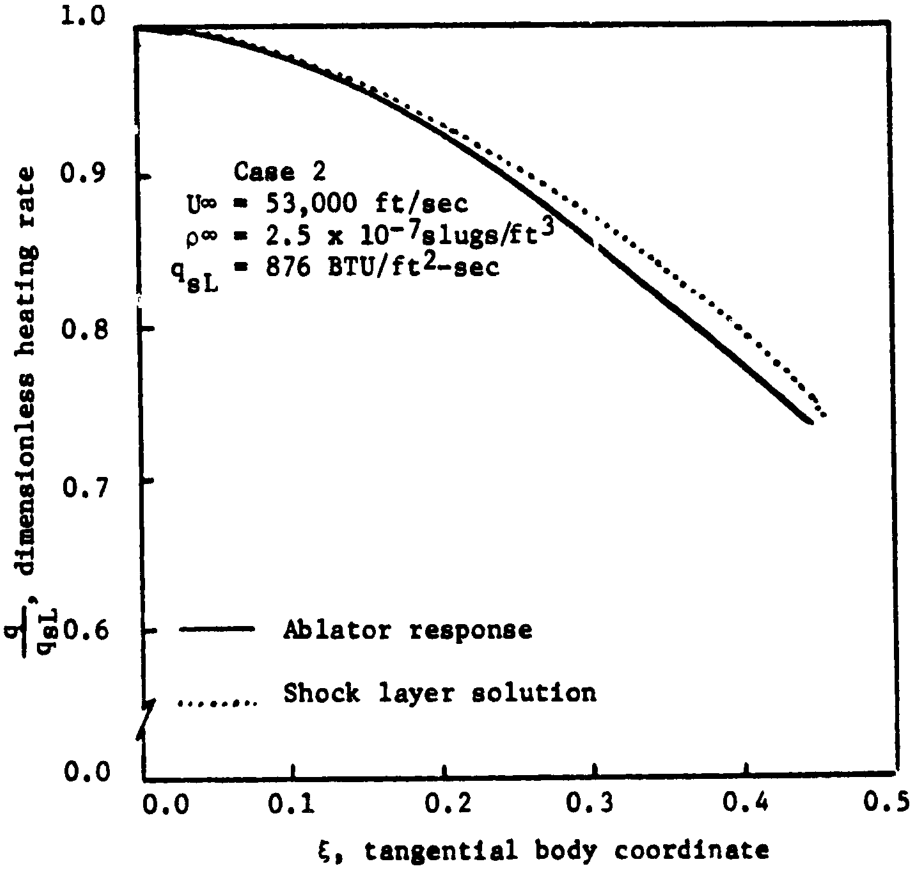

Figure 6.7. Dimensionless Heating Rate Profile for Case 2 - Coupled.

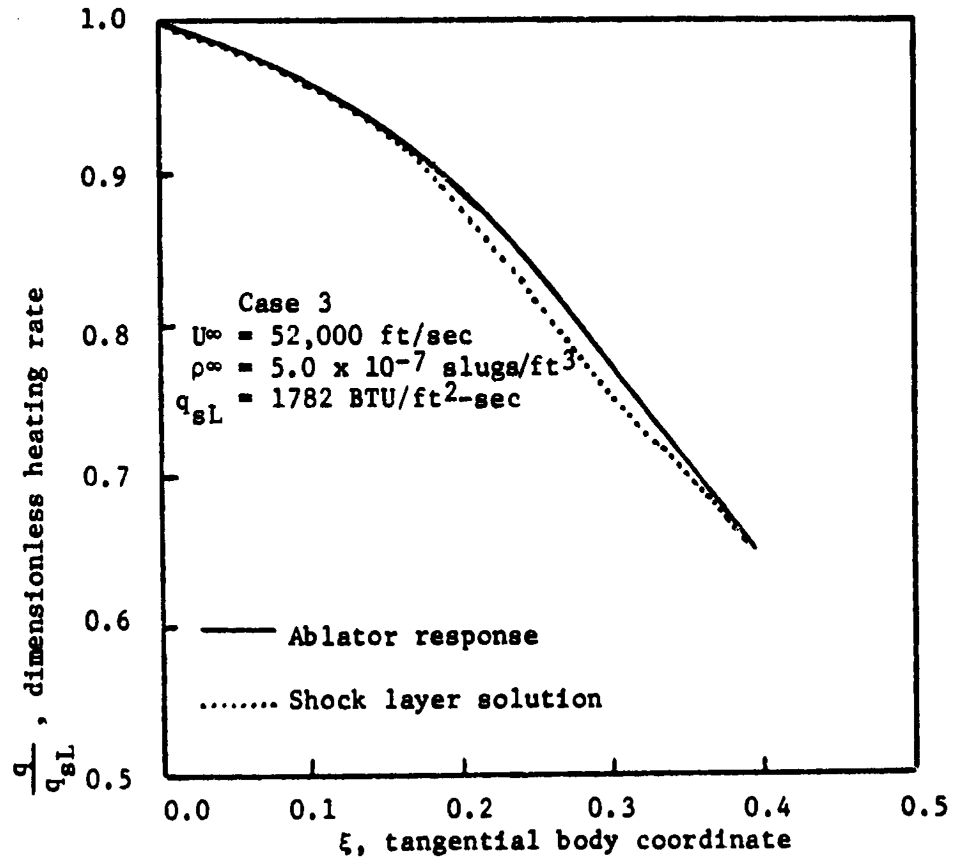

Figure 6.8. Dimensionless Heating Rate Profile for Case 3 - Coupled

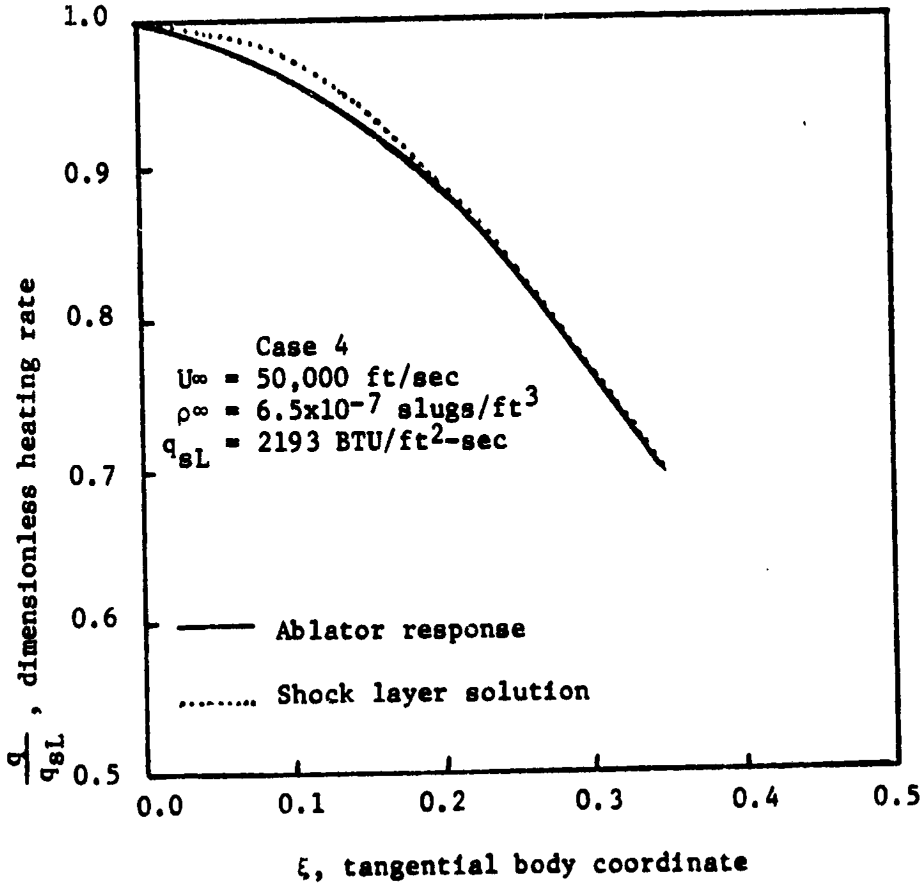

Figure 6.9. Dimensionless Heating Rate Profile for Case 4 - Coupled.

be estimated as

$$m = \int_o^t \dot{m}\, dt$$

or

$$m = 2\pi \int_o^{\xi} \phi_w \xi \, d \xi \int_o^t (\rho v)_{SL} \, dt$$

The result of the solution of the integral equation is the total mass loss from the ablative heat shield from the stagnation point to a radius ξ between initial contact with earth's upper atmosphere and some elapsed time "t". All that is required now is a time plot for the trajectory and the solution could be completed.

In Figure 6.10 the wall surface temperature profiles are shown for the four around the body cases. These surface temperatures were calculated using the Hertz-Knudsen analysis described in Appendix B. The wall temperature is seen to decrease gradually as the solution progresses downstream. This decrease in temperature is due to the two factors of decreased surface pressure and decreased heating rate.

Temperature profiles for stagnation line and downstream points $\xi = 0.30$ and $\xi = 0.45$ are presented in Figure 6.11 for Case 3. The profiles are very similar although the temperature gradient at the wall increases slightly as the solution proceeds downstream. The same kind of results were obtained for the other cases.

A comparison of around the body heating results is given in Figure 6.12 between Case 4 of the present analysis and those of Chou and Blake (Ref. 6.8) and Smith et al. (Ref. 6.7). The comparison is made at different conditions shown in the figure but the heating rate has been nondimensionalized with the stagnation line

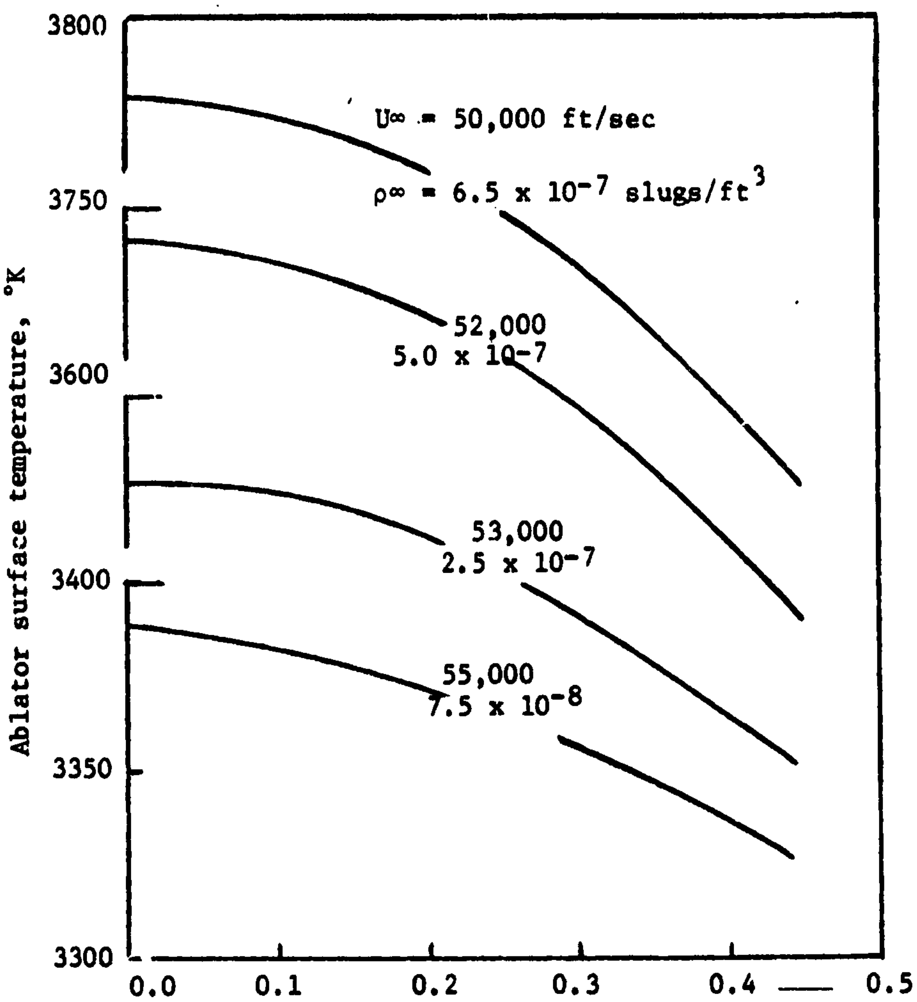

Figure 6.10. Ablator surface temperature profiles for cases studied.

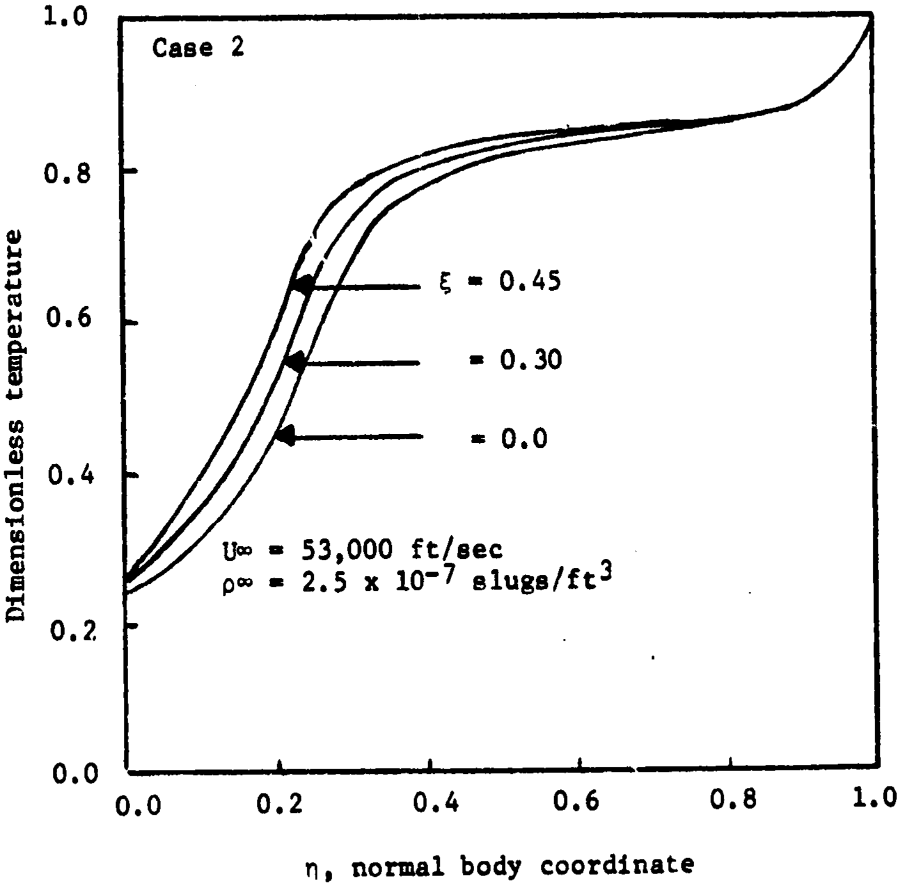

Figure 6.11. Dimensionless Temperature Profiles for the Stagnation Line and Downstream.

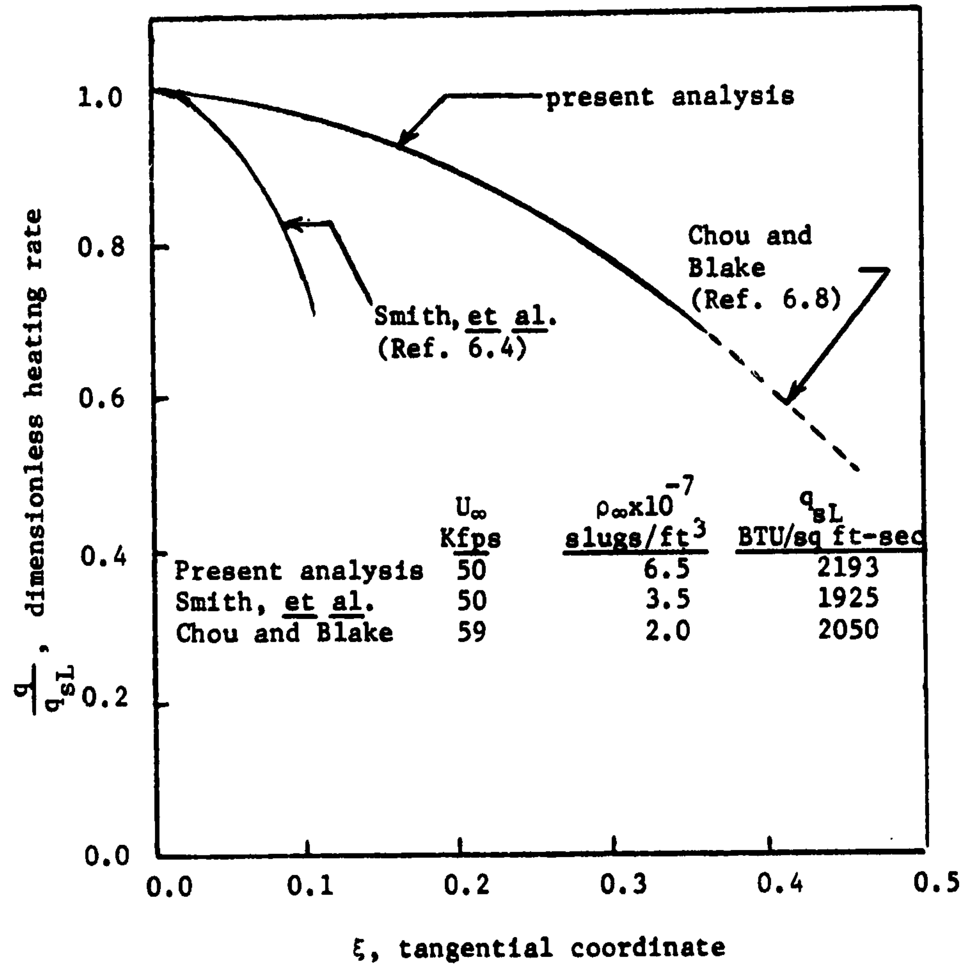

	U_∞ Kfps	$\rho_\infty x10^{-7}$ slugs/ft^3	q_{sL} BTU/sq ft-sec
Present analysis	50	6.5	2193
Smith, *et al.*	50	3.5	1925
Chou and Blake	59	2.0	2050

Figure 6.12. Comparison of Dimensionless Heating Rates Around the Body

heating rate. The results of Chou and Blake and the present analysis are identical as the solution proceeds downstream (with the results of Chou and Blake extending farther downstream). In contrast to these results, Smith et al. predicts a much more rapid decrease in heating rate away from the stagnation line. The heating rate has already been reduced to 70% of the stagnation line value at $\xi = 0.1$ whereas the present analysis along with Chou and Blake do not decrease to 70% until a body station of $\xi = 0.35$ is reached. Differences occur in radiation properties included for the three analyses, along with differences in numerical solutions, and chemistry (nonequilibrium for the present analysis vs. equilibrium for the others). It is not clear which of these effects or what combination of these effects causes the similarities and differences in results presented. It is somewhat surprising that Chou and Blake and the present analysis agree so well actually since the analysis of Chou and Blake did not include wall blowing.

These around the body results are the first to be presented for a reentering space vehicle whith the inclusion of finite rate chemistry and line and continuum radiation. Although some previous investigators have coupled their flow fields to the ablator, this is the first attempt to couple a nonequilibrium flow field to a nonequilibrium ablator. Previous investigators have used equilibrium sublimation models to yield temperature and species concen tration at the surface. The present investigation employed the nonequilibrium Hertz-Knudsen sublimation model described in Appendix B and the nonequilibrium char analysis described in Appendix A to determine surface boundary conditions and further couple them with the flow field by an energy balance. The results presented have been for the stagnation point and around the body for points along a typical reentry trajectory from planetary missions. These results make feasible a realistic estimate of the total mass loss during reentry and therefore provide the necessary information for calculation of the ablator heat shield thickness.

Radiation - Chemical Reactions Interaction

The results presented in the previous sections for stagnation line and around-the-body solutions were based on a set of chemical reactions and chemical species for the flow field given in Table 4.1. The choice of species and chemical reactions to include was based upon equilibrium and nonequilibrium considerations along with computer limitations. The choice of these reactions and species was discussed briefly in Chapter IV but the choice of kinetic data is an altogether different problem.

Although the reactions for the flow field had been chosen, the task of deciding what kinetic data to use remained. For some reactions data was reported by several investigators - sometimes in disagreement with one another. Other reactions had data from only one source, and for still others there was no data. When one source of data was found, this was used; but when many were found, the one that appeared to be most reputable was used. The most difficult case was when no data was found. In this instance the data had to be estimated from theory.

For estimated data, two constants had to be evaluated in the rate constant shown below - the frequency factor, k_o, and the activation energy, E.

$$k = k_o \; T^{1/2} \exp \left[-E/RT\right]$$

Initially no rate data was found for the reactions listed in Table 6.5. These are nine out of a total of 16 reactions and these nine are ablation species reactions. For these nine reactions the frequency factor was calculated using collision theory (Ref. 6.10) and the activation energy was estimated using the method of Semenov (Ref. 6.9). The activation energy estimation appeared quite satisfactory since the estimated values agreed with data when it was available.

The collision theory frequency factor, however, was often orders of magnitude different from published data. In Table 6.5 three sets of frequency factors are labled best, fast perturbation, and slow pertubation. Chronologically, the first values used were the fast perturbation frequncy factors which were calculated when collision theory was applied in error. When the frequency factor calculation was corrected, the slow perturbation values were achieved. Data was subsequently found in the literature for the first three reactions in Table 6.5 (Refs. 6.10, 6.11) which was not in agreement with the estimated frequncy factors ($\sim 10^{14}$ vs 10^{10}). Based on the data for these three reactions the decision was made to alter all of the nine collision theory frequency factors from 10^{10} to 10^{14}. The values thus obtained were decided to be the best frequency factor estimates available and were used for all coupled stangation line and around the body results.

Table 6.5

Frequency Factors for Three Finite Rate Cases
for Selected Reactions of Ablation Species in the Shock Layer

Reaction	Frequency Factor, log k_o		
	Best Kinetics	Slow Perturbation	Fast Pertubation
$CO + N \rightleftarrows CN + O$	13.2	10.0	18.9
$C_2 + M \rightleftarrows 2C + M$	13.8	10.1	19.0
$C + M \rightleftarrows C^+ + e^- + M$	14.3	10.1	19.0
$HCN + M \rightleftarrows CN + H + M$	13.8	10.0	18.9
$C_2H + M \rightleftarrows C_2 + H + M$	13.8	10.0	18.9
$C_2H_2 + M \rightleftarrows C_2H + H + M$	13.8	10.0	18.9
$C_3 + M \rightleftarrows C_2 + C + M$	13.8	10.0	18.9
$C_3H + M \rightleftarrows C_2H + C + M$	13.8	10.0	18.9
$C_4H + M \rightleftarrows C_3H + C + M$	13.8	10.0	18.9

As a consequence of these changes a collection of results were in hand with different values of the frequency factor for nine of the 16 reactions. This information was used to give an estimate of the effects of uncertainty of kinetic data on radiative heating. Three sets of data were available at moderate heating conditions of 50,000 feet per second, 8.85×10^{-8} slugs per cubic foot, a wall blowing rate of 5% of freestream, and a wall surface temperature of 3450°K at the stagnation line. The ablator was a phenolic-nylon composite. These conditions and ablator were the same as those studied by Esch (Ref. 6.2) who used an equilibrium chemistry model. The study was extended to include a comparison of the best kinetics with equilibrium at more severe heating conditions.

It would have been more desirable to conduct a parameter study on all frequency factors and activation energies. However, since one case requires approximately 60 minutes of computer time it was felt that the available results would serve this purpose. In all, these runs required three hours of computer time.

Moderate heating conditions in ablation layer: For the case of moderate heating to a phenolic nylon ablator, the freestream conditions of 50,000 feet per second and 8.85×10^{-8} slugs per cubic foot were used. Wall blowing rate was 5% of freestream blowing and wall surface temperature was 3450°K. All three non-equilibrium chemistry cases were investigated and compared to chemical equilibrium of Esch (Ref. 6.2).

The basis of comparison is the radiative heating rate arriving at the ablator surface since this is the most important parameter in design of thermal protection systems. It will be shown that as a result of variations in species concentration profiles in the shock layer for the different frequency factors of nine reactions the radiative heating can be appreciably altered. In the ablation layer the important species appears to be the highly absorbing carbon atom.

In Figure 6.13 the radiative flux divergence profiles are shown for the three reaction rate sets investigated and the equilibrium results of Esch (Ref. 6.2). The radiative wall heating rates for the cases are also shown in Figure 6.13 - best (121 BTU/sq ft-sec), slow (160), fast (90), and equilibrium (349). In Figures 6.14, 6.15, and 6.16 are the species profiles for the finite rate cases and equilibrium species porfiles are presented in Figure 6.17.

The interaction between species and radiative heating in the ablation layer is quite pronounced. Note that there is a trend in radiative flux divergence profiles near the stagnation point (η=0.1 to η= 0.4) for the four cases presented. The equilibrium model (the infinitely fast reaction rate) demonstrates a large dip in this region, the fast kinetics perturbation dips slightly less, the best kinetics shows no dip at all, and the slow kinetics perturbation actually reaches a local maximum in the stagnation region. The results indicate that, at increasingly faster reaction rates, the radiative flux divergence drops off due to some absorption mechanism in the stagnation region. For an explanation of this phenomenon, inspection of the species profiles in Figures 6.14 through 6.17 is helpful. Notice in particular the carbon atom profiles for the four cases. Both equilibrium and the fast kinetics pertubation show high peak mass fractions of carbon atom (~0.5 to ~0.6). The best kinetics case shows a moderate peak for carbon atom (mass fraction

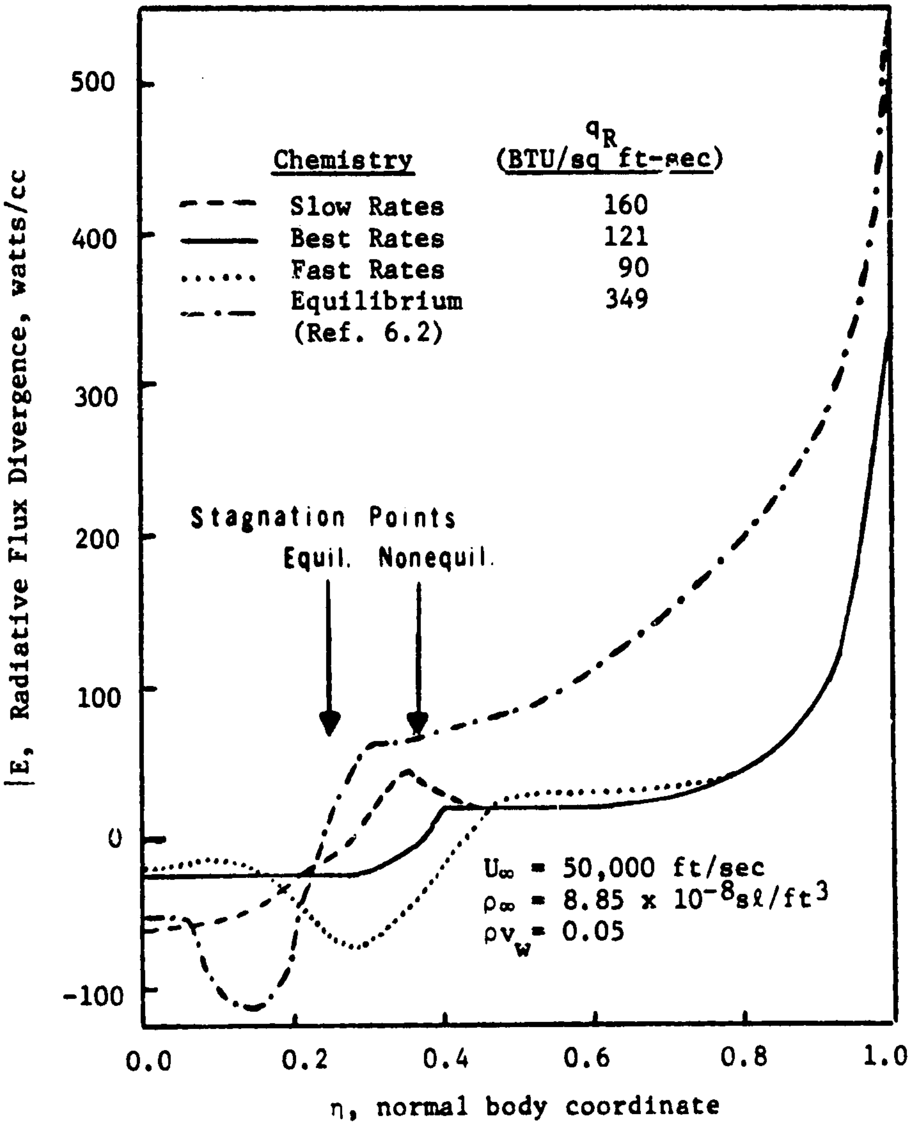

Figure 6.13. Comparison of Flux Divergence Profiles for Various Chemistry Models at the Stagnation Line.

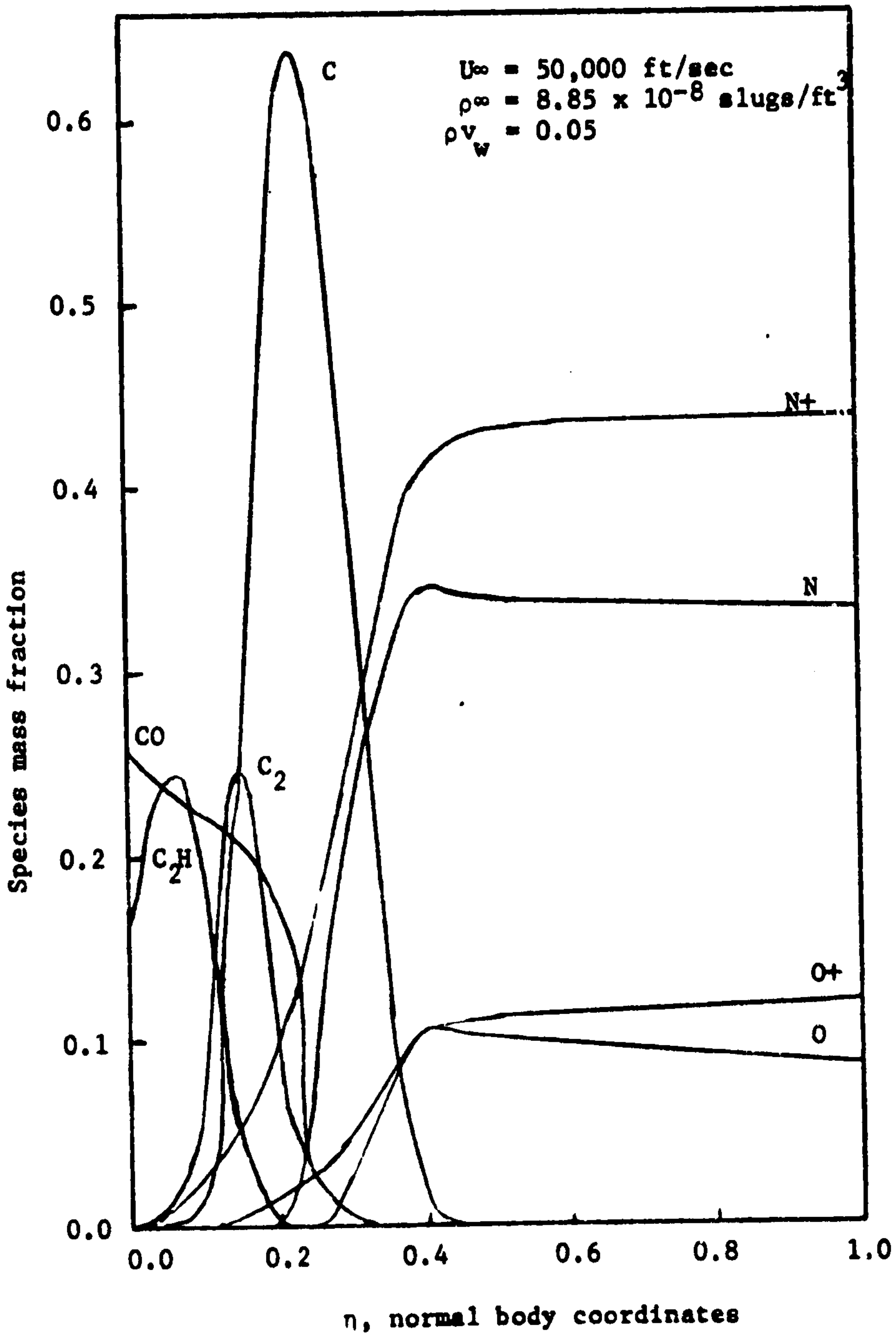

Figure 6.14. Species Profiles for "Fast Perturbation" Kinetics Case at the Stagnation Line.

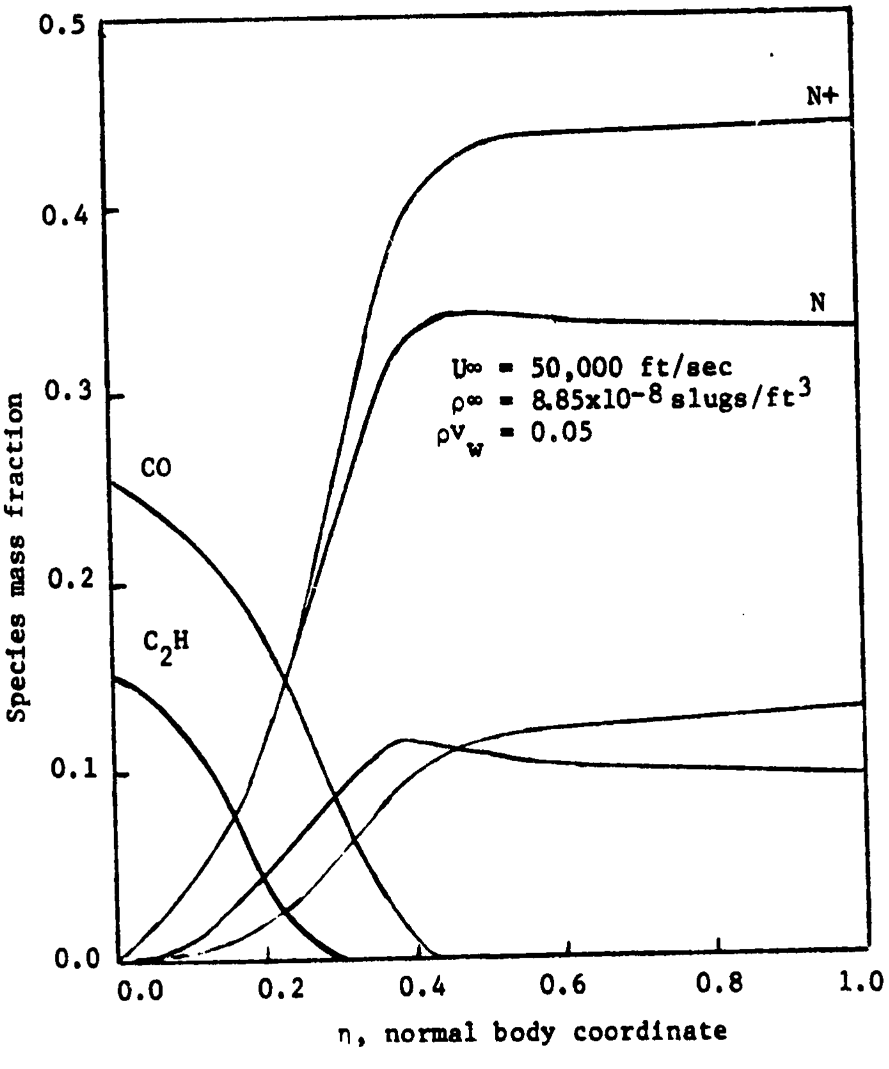

Figure 6.15. Species Profiles for "Slow Perturbation" Kinetics Case at the Stagnation Line.

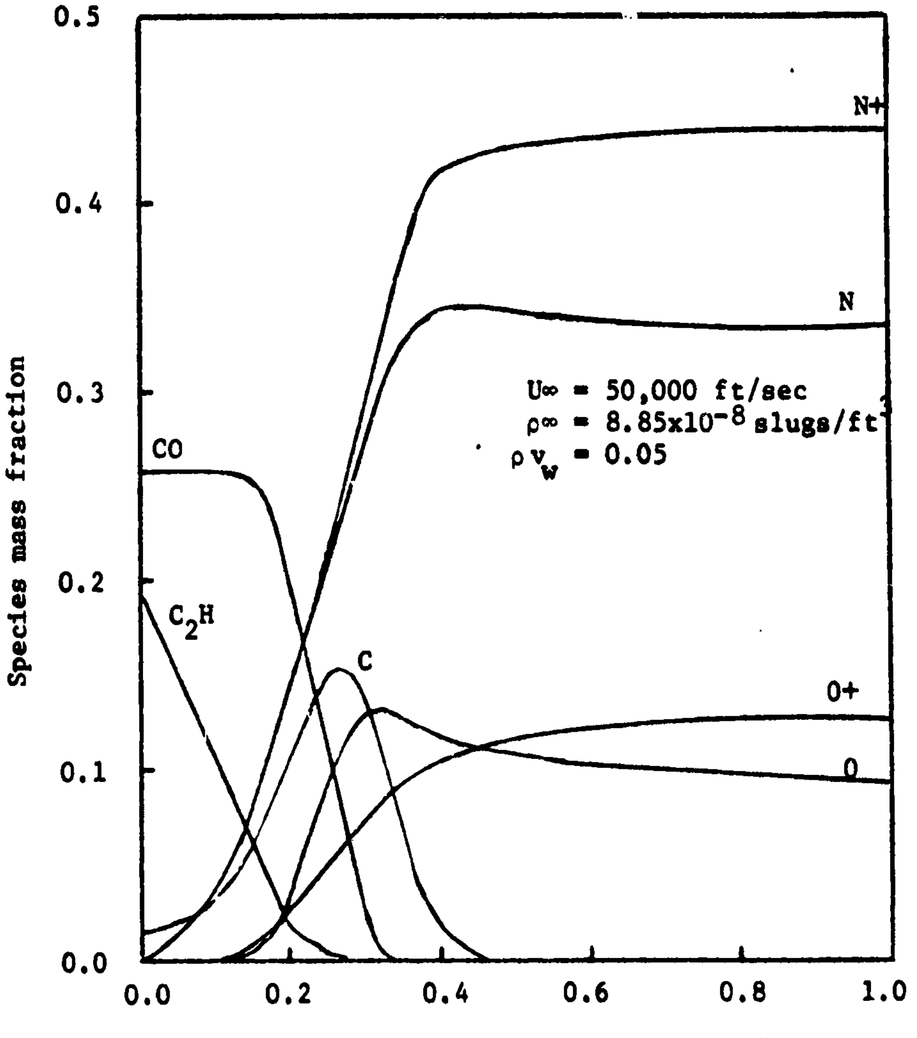

Figure 6.16. Species Profiles for "Best" Kinetics Case at the Stagnation Line.

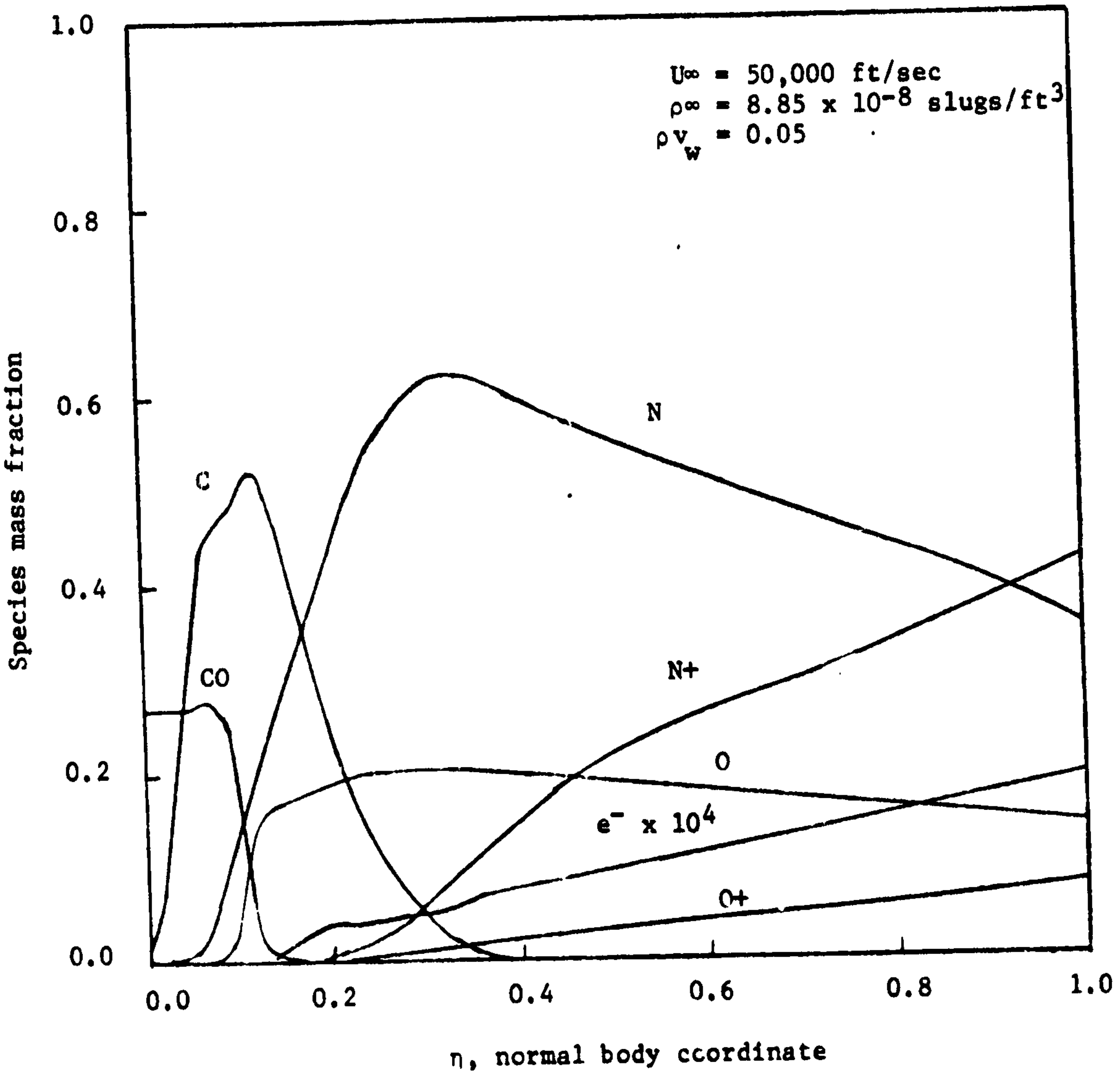

Figure 6.17. Species Profiles for Equilibrium Chemistry at the Stagnation Line (Esch, Ref. 6.2)

of 0.15), and in the slow perturbation kinetics case there was not a significant concentration of carbon atom anywhere within the shock layer. The key to explain the nature of the radiative flux divergence profiles near the stagnation point is these carbon atom profiles. Carbon is a highly absorbing species in this temperature range, therefore, high concentrations result in significant reductions in radiative heating as evidenced by the results presented in Figure 6.13. For the three kinetics models, the heating rate increases (90 BTU/sq ft-sec for fast, 121 for best, 160 for slow) as the reaction rate is decreased. The exception to the rule is the infinitely fast rate of equilibrium which has the highest heating rate, 349 BTU/sq ft-sec. This discrepancy will be discussed in the following section.

The importance of carbon atom radiative absorption can be corroborated with the results of Engel (Ref. 6.3). In Figure 6.18 are the temperature profiles and radiative heating rates obtained by Engel for three cases at the same conditions. The first case included all species in the radiative flux divergence calculation (1661 BTU/sq ft-sec), the second case excluded carbon atom (2530 BTU/sq ft-sec), and the third case omitted molecules (2605 BTU/sq ft-sec). The effect of which species are included in the radiation calculation are seen to have a dramatic effect on radiative heating at the ablator surface. Of special significance is the increased heating effect when carbon atom is omitted allowing a 52% increase. The same type of effect is realized with respect to slow and fast perturbation kinetics of the present investigation. By slowing down the reaction rate to a point where no atomic carbon is produced

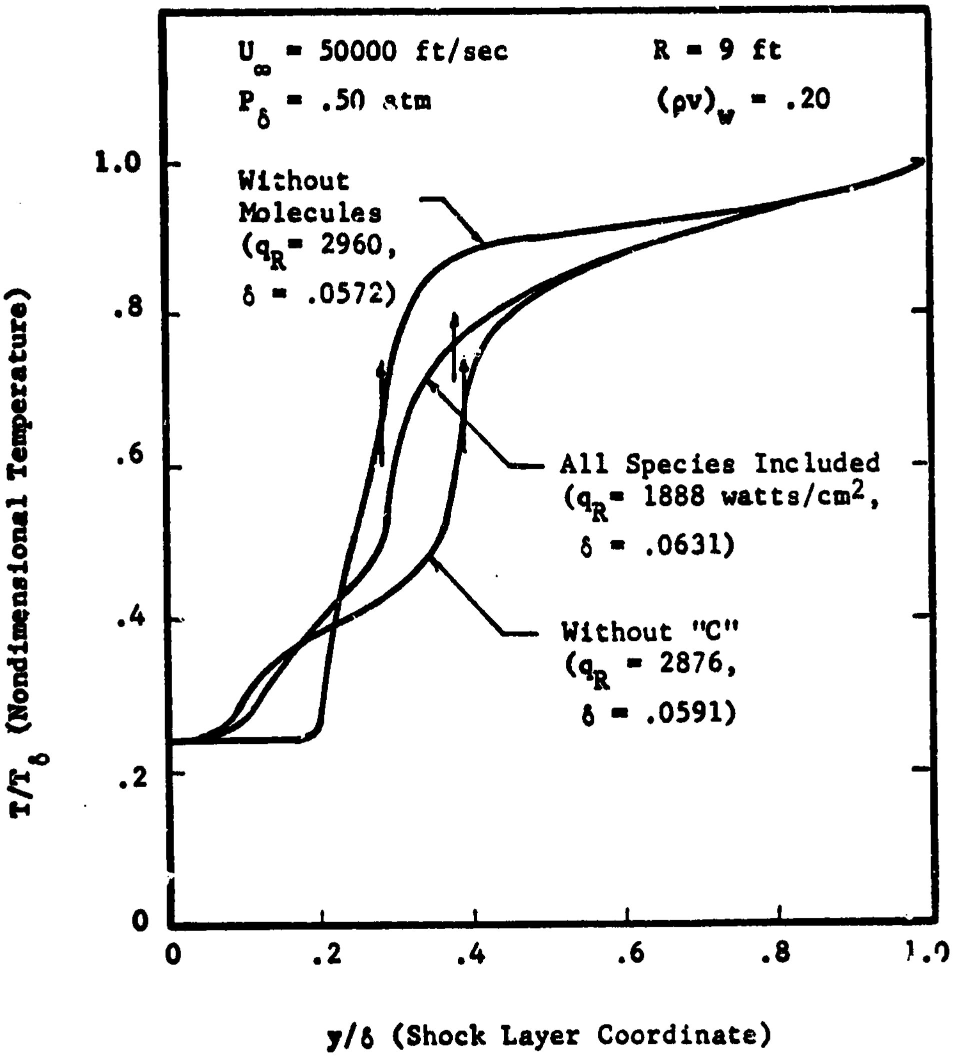

Figure 6.18. Effects of Carbon Atom and Molecular Radiative Coupling on the Temperature Profile and Radiative Heating (Ref. 6.3).

(slow perturbation kinetics, 160 BTU/sq ft-sec), a 78% higher heating rate is observed than the fast perturbation kinetics, 90 BTU/sq ft-sec. The best kinetics case, with an intermediate buildup of atomic carbon, results in an intermediate heating rate, 121 BTU/sq ft-sec.

In summary, the three kinetics cases of the present investigation and the equilibrium analysis of Esch follow a pattern in their ablation layer species profiles with atomic carbon increasing as reaction rate increases. The radiative flux divergence profiles of these cases reflect this trend near the stagnation point by demonstrating a significant reduction for cases where the highly absorbing carbon atom is present in high concentrations. The radiative heating rates of the three kinetics cases of the present investigation also reflect this trend by increasing as atomic carbon decreases corresponding to a decrease in reaction rate. The exception to this trend in heating rate is the equilibrium results which show the highest radiative heating rate although the atomic carbon concentration is high for this infinitely fast reaction rate. The reasons for the apparent contradiction are discussed in the following section.

Moderate heating conditions in air layer: In Figure 6.17 the species profiles from Esch's (Ref. 6.2) equilibrium analysis were presented. As disucssed above, these results compare well with the results of the fast finite rate analysis in the ablation layer. Note, however, that the species mass fraction profiles in the air layer for chemical equilibrium are very much different than any of the finite rate analyses (Compare Figure 6.16 with Figures 6.13, 6.14

and 6.15). There appears to be little reaction occurring in the air layer for the nonequilibrium analysis (Figures 6.14, 6.15, and 6.16) if one inspects the flat nature of the N, N^+, O and O^+ profiles. The N^+ and O^+ ion concentration levels remain high until they reach the diffusion zone near the stagnation point indicating no reactions are proceeding in the air layer. The equilibrium analysis of Esch produced species profiles as shown in Figure 6.17. The mass fractions of ionic species N^+ and O^+ decrease from shock to stagnation point much faster for equilibrium than for nonequilibrium. The equilibrium mass fractions of atomic species N and O compensate by increasing readily. In other words; at equilibrium reactions take place which alter the species profiles in the air layer. If the shock layer were truly near chemical equilibrium, the finite rate reactions would reflect this by occurring fast enough to experience similar profiles to the equilibrium profiles. They do not; therefore, one can conclude from these results that equilibrium is not a valid assumption even for this hot outer air layer -- at least at these conditions (50,000 feet per second and 8.85 x 10^{-8} slugs per cubic foot) and a nonequilibrium shock calculation should be performed.

The postulate that the shock wave is not at equilibrium,as assumed, is substantiated by the work of Carlson (Ref. 6.12). Carlson did a nonequilibrium calculation across the shock wave using an air chemistry model. He states that a high degree of chemical and thermal nonequilibrium can exist for low pressure conditions as in this study. The conclusion is made that these effects cannot be neglected if accurate solutions are desired. Zeldovich et al.

(Ref. 6.13) explains that it is not until 20,000°K that rapid atomic dissociation is achieved, and the rate of single ionization is still considered a slow mechanism at this time. Slow refers to a process which requires a large number of gas kinetic collisions. When the pressure is reduced, the number of collisions is reduced. The result is that the shock wave is only in partial equilibrium and probably has only achieved atomic dissociation at best.

The radiative heating implications are evident when an inspection is made of these species mass fractions in light of the radiative properties. The air layer is a predominantly emitting zone. The species that exist in the air layer are N, N^+, O, O^+, and e^- of which radiative properties exist for N, O, and e^-. In the equilibrium case (q_R = 349 BTU/sq ft-sec) the emitting species of N and O atoms are present in higher concentrations than in the nonequilibrium cases (q_R = 160 BTU/sq ft-sec). The concentrations of the nonemitting N^+ and O^+ ions and the emitting electron are present in high concentrations for the nonequilibrium cases. This shift from nitrogen and oxygen atom radiative properties to electron radiative properties for equilibrium and nonequilibrium respectively appears to have a significant effect on the radiative heating. Equilibrium predicts 190% higher radiative heating than nonequilibrium best kinetics. The result is a lower net radiative heating (emission) when the air layer is highly ionized.

In Figure 6.13 the radiative heating differences of the various chemistry models were dramatically demonstrated. The three nonequilibrium models show similarity in the vicinity of the air layer for both species profiles and radiative flux divergence. The equilibrium model, on the other hand, depicts a much greater positive flux divergence in the air layer thus demonstrating its widely different species composition in this air layer (atomic rather than ionic).

The apparent paradox that equilibrium has the highest heating rate (349 BTU/sq ft-sec) and fast kinetics has the lowest heating rate (90 BTU/sq ft-sec) can now be explained. The reason for this is that "fast" applies only to some select reactions. These reactions all pertain to species in the ablation layer. Therefore, the air layer is practically unaffected by changes made for the three kinetics cases. This is the reason the radiative flux divergence and species profiels are almost identical in the air layer for the kinetics cases of the present investigation. The equilibrium analysis, in contrast, is seen to be dominated by the radiation from the air layer (Figure 6.13).

Severe heating rate conditions: In Figure 6.19 is a plot of species profiles at the stagnation line for the coupled solution of a severe heating rate case (Case 3) run using the frequency factors from the best kinetics case in Table 6.5. In this case a freestream velocity of 52,000 feet per second and a freestream density of 5.0×10^{-7} slugs per cubic foot were used. The radiative heating rate at the ablator surface for the coupled solution was 1782 BTU/ sq ft-sec with a blowing rate of 12% of freestream. A comparison was made with an equilibrium case of Esch (Ref. 6.2) run at 50,000 feet per second, 4.5×10^{-7} slugs per cubic foot, and a blowing rate of 20% of freestream. The radiative heating rate for this case was 1816 BTU/sq ft-sec. These conditions are not exactly the

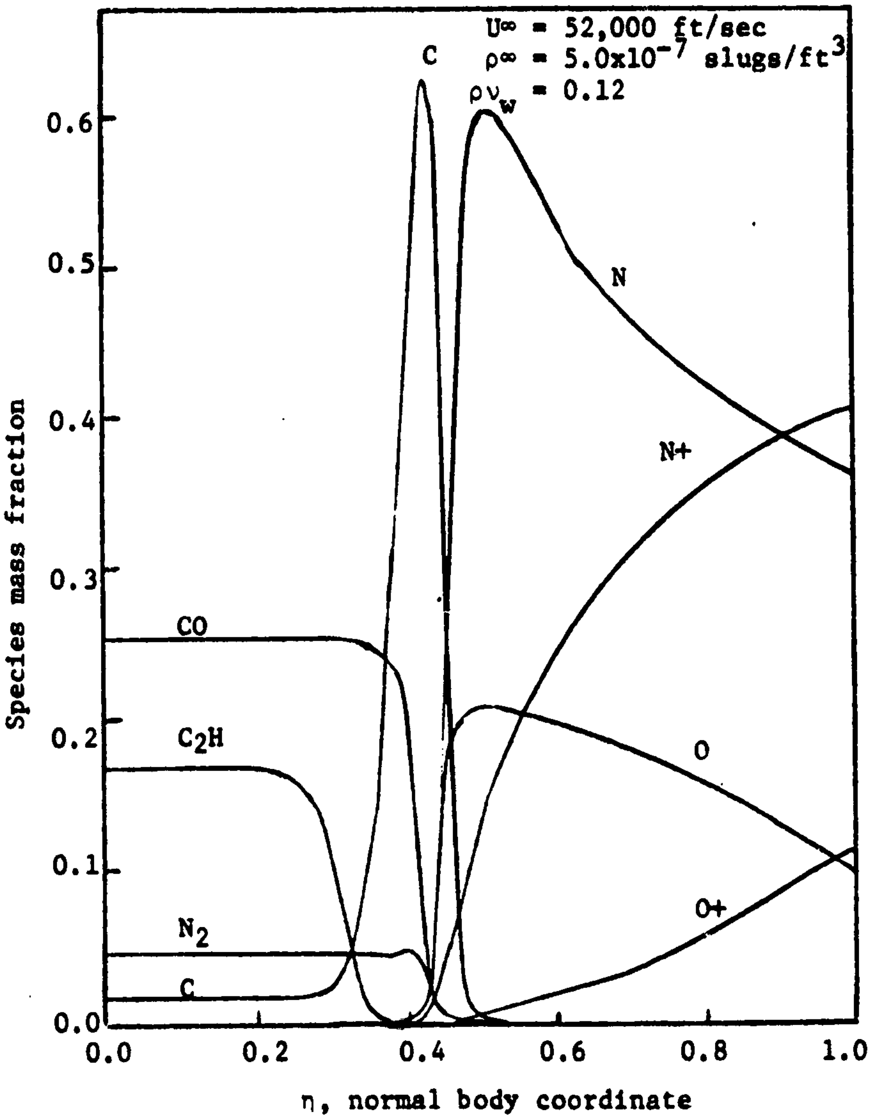

Figure 6.19. Species Profiles for Nonequilibrium Chemistry at a Severe Heating Load at the Stagnation Line.

same as the finite rate conditions, but they are close enough for comparative purposes.

A plot of species mass fraction profiles for Esch's equilibrium case is shown in Figure 6.20. The stagnation point of the non-equilibrium analysis (Case 3) in Figure 6.18 is about $\eta = 0.4$ whereas Esch's equilibrium analysis has a stagnation point displaced further toward the shock ($\eta = 0.6$). The reason for the difference in stagnation points is that Case 3 has a blowing rate of 12% and Esch assumed a blowing rate of 20%. Other than this difference the species profiles are remarkably similar -- even in the air layer where the moderate heating rate analysis showed a great deal of difference (Figures 6.16 and 6.17). For both the severe heating rate cases, atomic nitrogen and oxygen build up in concentration from shock to stagnation point and ionic species N^+ and O^+ decrease in this region. At the stagnation point itself, the concentration of all air species decreases due to diffusion. In the ablation layer the major species again have very similar profiles. Flat profiles are observed for CO, C_2H, and N_2. Carbon atom attains a peak of about 0.6 mass fraction at the stagnation point and drops off rapidly on either side.

For years investigators have postulated that at high heating load conditions, the shock layer approaches chemical equilibrium and could therefore be modeled as such. The results presented here for the severe heating case only support this contention. The conditions in the hot outer air layer (14,500°K) are such that reactions occur fast enough to compare with equilibrium. The reason for this result is a combination of both high temperature

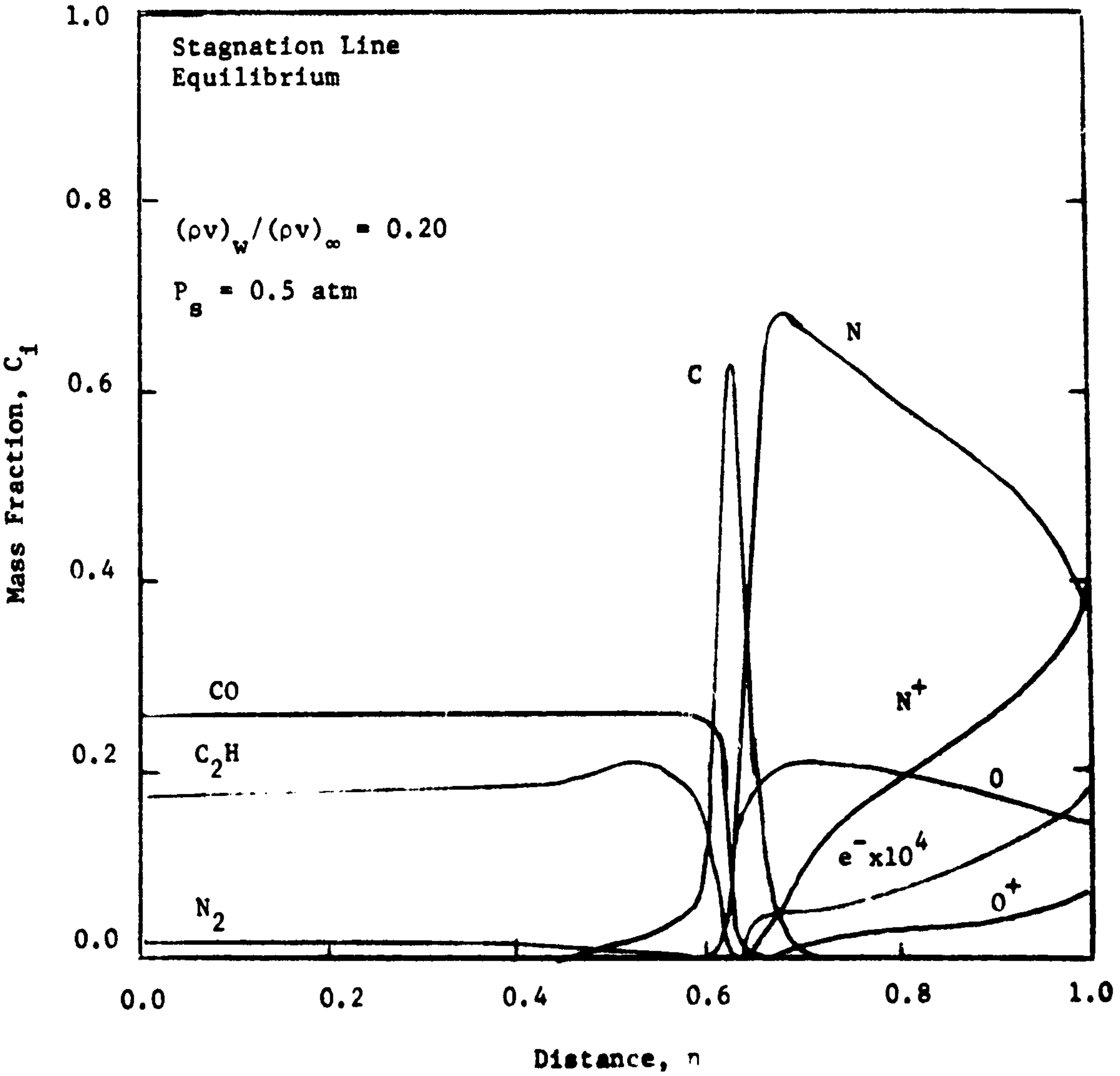

Figure 6.20. Species Profiles for Equilibrium Chemistry at a Severe Heating Load at the Stagnation Line. (Esch, Ref. 6.2)

and post shock pressure (0.5 atm). For the moderate heating cases discussed earlier, the post shock pressure was only 0.1 atm and the shock temperature was 13,000°K. Since the phenomenological reaction rate expression has a collision theory temperature dependence and is proportional to the product of the partial pressures, the thermodynamic variables of temperature and pressure are very important to the finite rate chemistry. The combined effect of high temperature and high pressure provides sufficiently fast chemical reaction rates that the shock layer approaches equilibrium at severe heat loads.

The radiative flux divergence profiles of these two cases are presented in Figure 6.21. The profiles are very similar showing a characteristic dip in the stagnation region and increasing rapidly in the air layer. The dip in flux divergence for Case 3 is closer to the ablator since the stagnation point is closer to the ablator (due to a 12% vs 20% blowing rate). The radiative heating rates for the equilibrium (1816 BTU/aq ft-sec) and the nonequilibrium (1782 BTU/sq ft-sec) differ by only 2% demonstrating excellent agreement.

Species Boundary Conditions

At the shock wave chemical equilibrium air is normally assumed to provide boundary conditions at the shock. This assumption is often a good one especially at high heat loads (as discussed in the previous section). However, the boundary conditions at the ablator are most likely different from equilibrium. In Appendices A and B a nonequilibrium char layer analysis and the nonequilibrium Hertz-Knudsen

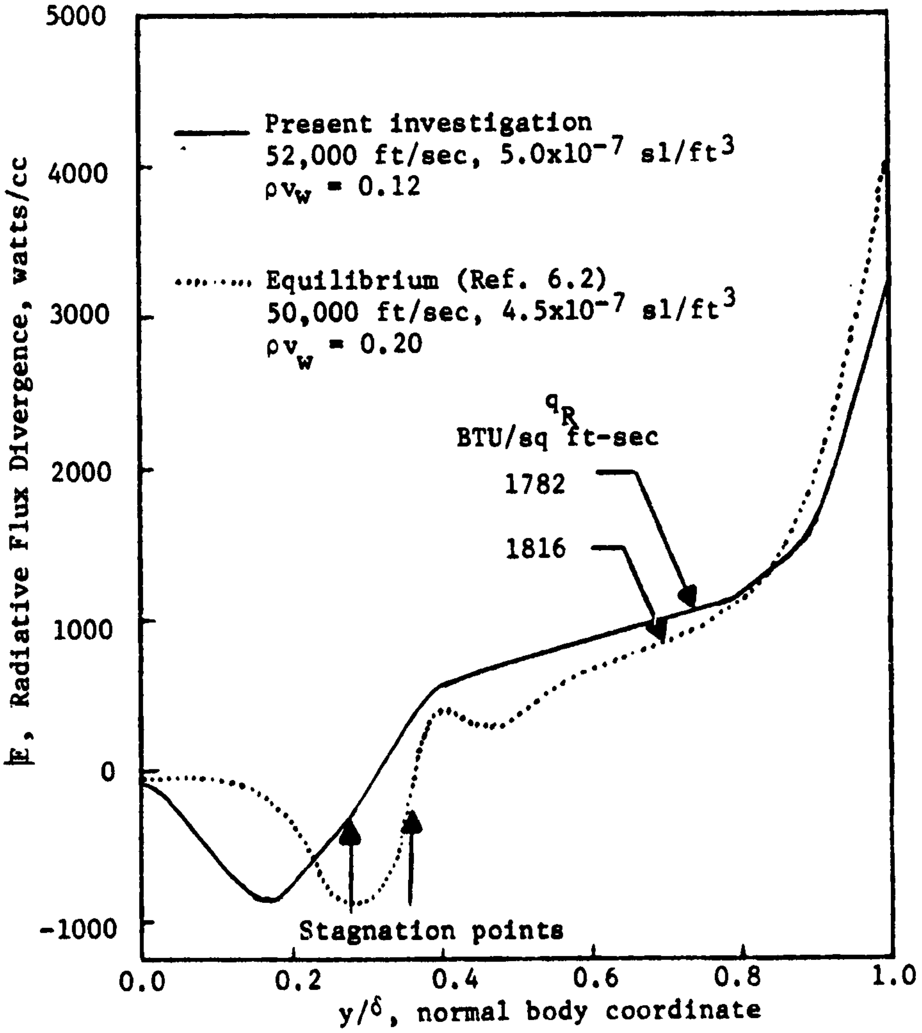

Figure 6.21. Comparison of Radiative Flux Divergence Profiles for Severe Heating Rate Conditions of Equilibrium and Finite Rate Analyses.

equation are used to determine the conditions at the ablator surface. Ablator surface compositions of twenty species vary as functions of surface temperature, pressure, and blowing rate. To couple species compositions from the nonequilibrium ablator analyses to the shock layer or even their results would be a formidable task in itself. Based on the results presented in this section and the tremendous computational simplification involved, one nonequilibrium set of ablator surface mass fractions was used for all coupled stagnation line and around the body results. The conditions that these species compositions were obtained from were a surface temperature of 3600°K, a surface pressure of 1.0 atmosphere, and a mass loss rate of 0.04 lbs/sq ft-sec.

To evaluate the effect of this simplification on radiative heating rates two cases were investigated for the following conditions -- freestream velocity of 50,000 feet per second, freestream density of 8.85 x 10^{-8} slugs per cubic foot, and a wall blowing rate of 5% of freestream. The frequency factors of the best kinetics in Table 6.5 were used and coupling of shock layer to ablator surface was not attempted. The compositions chosen for the study are shown in Table 6.6. One case is equilibrium compositions at 3450°K for a phenolic-nylon ablator with an elemental composition shown in Table 6.7. The other case used the nonequilibrium values at 3600°K, 1.0 atmosphere, and 0.4 mass loss rate achieved from the nonequilibrium analyses described in Appendices A and B.

The radiative heating rates were 125 and 121 BTU/sq ft-sec for nonequilibrium and equilibrium ablator boundary conditions respectively. The radiative flux divergence profiles for the two cases are

Table 6.6

Species Composition at the Ablator Surface

Component	Composition (mass fraction)	
	Equilibrium	Nonequilibrium
1. O_2	4.81×10^{-15}	1.00×10^{-10}
2. N_2	5.37×10^{-2}	4.95×10^{-2}
3. O	9.74×10^{-8}	1.00×10^{-10}
4. N	9.44×10^{-5}	1.00×10^{-10}
5. O^+	1.66×10^{-20}	1.00×10^{-10}
6. N^+	5.72×10^{-18}	1.00×10^{-10}
7. e^-	1.13×10^{-9}	1.00×10^{-10}
8. C	1.34×10^{-2}	2.11×10^{-2}
9. H	3.86×10^{-2}	2.21×10^{-2}
10. H_2	1.36×10^{-2}	4.13×10^{-2}
11. CO	2.69×10^{-1}	2.57×10^{-1}
12. C_3	8.17×10^{-2}	3.69×10^{-1}
13. CN	7.79×10^{-2}	1.00×10^{-10}
14. C_2H	1.65×10^{-1}	1.39×10^{-1}
15. C_2H_2	1.67×10^{-2}	5.89×10^{-2}
16. C_3H	1.30×10^{-1}	1.00×10^{-10}
17. C_4H	8.42×10^{-2}	1.00×10^{-10}
18. HCN	3.10×10^{-2}	1.00×10^{-10}
19. C_2	2.47×10^{-2}	4.22×10^{-2}
20. C^+	1.43×10^{-11}	1.00×10^{-10}

Table 6.7

Elemental Composition of a Phenolic Nylon Ablator

Element	Elemental Composition (mass fraction)
Carbon	0.7303
Hydrogen	0.0729
Nitrogen	0.0496
Oxygen	0.1472

shown in Figure 6.22. They compare almost identically along the shock layer with the exception of a slight difference near the surface which is expected. The difference in radiative heating rates is only 3.2% which is definitely within the accuracy of the calculation. If the extreme case of equilibrium at the surface varies so little from the nonequilibrium conditions used, then the true nonequilibrium values should differ even less. Based on the insensitivity of the analysis to the wall boundary conditions, it was decided to use the one simplified set of compositions in Table 6.6.

Computation Time and Core Usage

The stagnation line and around the body results that have been presented in this chapter represent a sizeable amount of computer time and core usage. The computer utilized in this study was an IBM 360/65 and the program was compiled on the FORTRAN H-compiler for maximum computational optimization. The total size of the program was about 252K bytes which was overlayed down to 186K bytes. The radiation package, LRAD, developed by Engel (Ref. 6.3) was itself 96K (overlayed from 104K bytes) of the 186K. The computer time usage was in the order of 100 hours of actual CPU time with about 60 hours being used on stagnation line solutions alone.

The major time consumption calculations were radiation (LRAD) which took 1.5 minutes per pass and the species solutions which took 20 seconds per pass. The LRAD calculation included line and continuum radiative properties for twelve ionic, atomic, and molecular species. This same calculation took 2.5 minutes by Esch

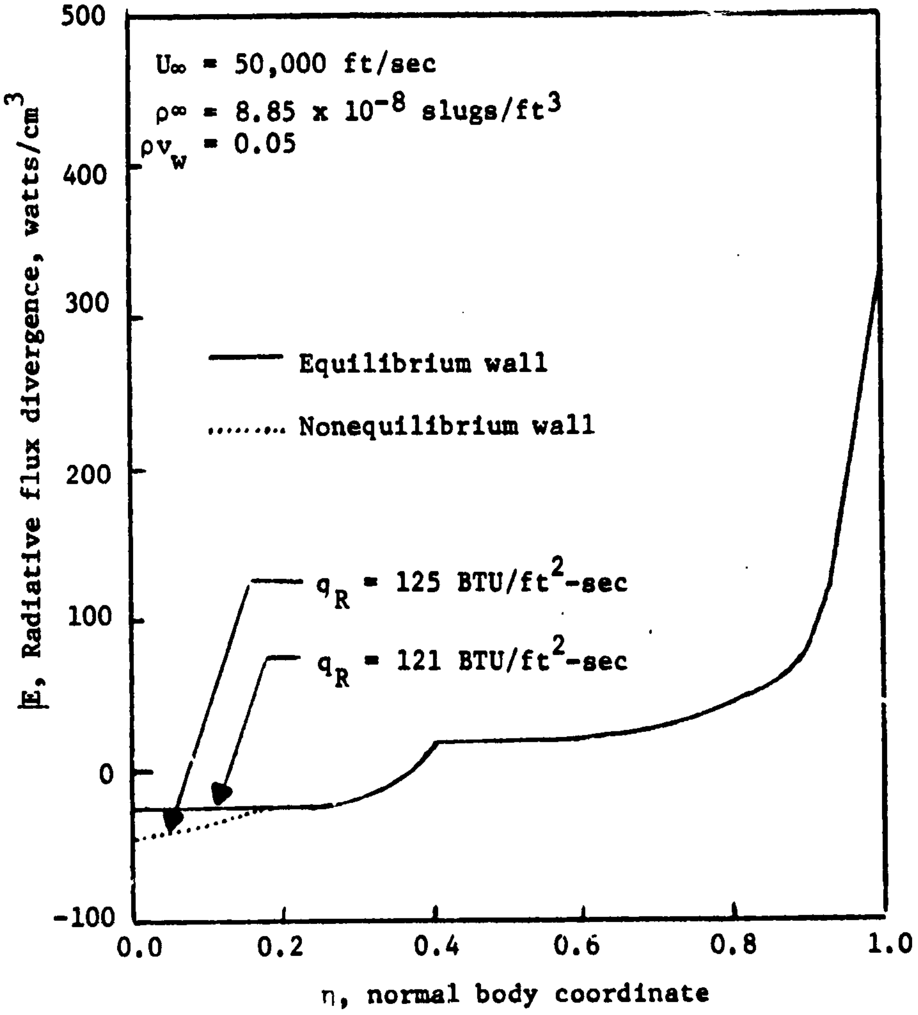

Figure 6.22. Comparison of Radiative Flux Divergence Profiles for Equilibrium and Nonequilibrium Walls at the Stagnation Line.

(Ref. 6.2) when using the same computer but the FORTRAN G compiler instead of the FORTRAN H compiler. Since there were 20 species, it took 20 seconds of total time to solve the species conservation equations taking approximately one second per species. The iteration scheme employed in this study called for many more solutions to the species equations than the radiation flux divergence in LRAD, therefore the total time utilized in the species solution was about three times the LRAD calculation.

The total time for a major iteration loop was about 8 minutes. The total time for stagnation line uncoupled solutions took anywhere from 0.5 hours to about 6 hours. In comparison the same case that took Perez (Ref. 6.1) about 30 hours of CPU time only took 40 minutes for the present investigation. The savings in computer time is believed to come from different initialization, iteration scheme, and efficiency in programming. The initialization of species profiles, for example, was achieved by using flat or frozen flow compositions from shock and ablator to the stagnation point. Since chemical reactions were slow for this case especially in the air layer, the initially assumed compositions were close from the start. Perez, on the other hand, assumed equilibrium profiles and iterated until the profiles became flat. For other cases Perez's initialization scheme may prove more advantageous. For a coupled stagnation line solution, at least three stagnation line solutions had to be run so typical coupled solutions required in the order of 10 hours for completion.

The around the body solutions required differing amounts of time depending on the severity of heating rate. Usually the more severe heating rates took longer to reach the same distance around the body as a less severe case. For instance Case 1 (q_R = 153 BTU/sq ft-sec) took about 2.5 hours to reach a point of $\xi = 0.45$ whereas Case 4 (q_R = 2232 BTU/sq ft-sec) only reached a point of $\xi = 0.30$ after 4.0 hours (see Figures 6.5 and 6.6).

One reason for long computation time in the around the body solution was the shock standoff distance, δ. If the calculated value was very different than the input value, convergence on all the conservation equations was very difficult (especially momentum). When the input shock standoff distance was altered to yield a more realistic value, the heating rates were essentially unchanged but the computation time decreased significantly -- sometimes by a factor of two. This result was discussed in Chapter V and it was decided that since heating rates remained unchanged, the input shock standoff distance would only be altered to improve the convergence rate of the conseravtion equations. No real attempt was made to obtain absolute convergence of the shock stanoff distance.

The important point to be made from these results is that shock layer solutions do require large amounts of computer time and core. Although the analysis was diligently trimmed to reduce both time and core usage, the expense is still seen to be phenomenal. Such small inputs as shock standoff distance or iteration scheme can greatly alter the CPU time required. Further improvements in such things to reduce this computational expense should be studied in the future.

Summary

An investigation of the performance of a phenolic-nylon ablator has been made for flight conditions characteristic of return from planetary flight. The conclusions and recommendations resulting from this study are presented in the following chapter.

REFERENCES

6.1 Perez, G., "Finite-Rate Chemistry Effects Upon Convective and Radiative Heating of an Atmospheric Entry Vehicle," Ph.D. dissertation, Louisiana State University, Baton Rouge, Louisiana (1974).

6.2 Esch, D. D., "Stagnation Region Heating of a Phenolic-Nylon Ablator During Return from Planetary Missions," Ph.D. dissertation, Louisiana State University, Baton Rouge, Louisiana (1971).

6.3 Engel, C. D., "Ablation and Radiation Coupled Viscous Hypersonic Shock Layers," Ph.D. dissertation, Louisiana State University, Baton Rouge, Louisiana (1971).

6.4 Chin, J. H. "Radiation Transport for Stagnation Flows Including the Effect of Lines and Ablation Layer," *AIAA* Paper No. 68-664, Fluid and Plasma Dynamics Conference (Los Angeles, Calf.), June 24-26, 1968.

6.5 Garrett, L. B., G. L. Smith, and J. N. Perkins, "An Implicit Finite Difference Solution to the Viscous Shock Layer, Including the Effects of Radiation and Strong Blowing," NASA TR R-388, November 1972.

6.6 Rigdon, W. S., R. B. Dirling, and M. Thomas, "Stagnation Point Heat Transfer During Hypervelocity Atmopheric Entry," NASA CR-1462, 1970.

6.7 Smith, G. L., J. T. Suttles, and E. M. Sullivan, "Viscous Radiating Flow Field on an Ablating Blunt Body," *AIAA* Paper No. 70-218, Eighth Aerospace Sciences Meeting (New York, New York), January 19-21, 1970.

6.8 Chou, Y. S. and L. H. Blake, "Thin Radiating Shock Layer About a Blunt Body," NASA CR-1547, March 1970.

6.9 Semenov, N. N., *Some Problems of Chemical Kinetics and Reactivity*, Vol. I, Pergamon Press, New York, p. 2, 1958.

6.10 Davies, William O., "Radiative Energy Transfer on Entry Into Mars and Venus," Report No. IITRI-T200-13, IIT Research Institute, Chicago, Illinois, December 1965.

6.11 Allen, C. W., *Astrophysical Quantities*, Second edition, University of London, Athlone Press, 1963.

6.12 Carlson, L. A., "Radiative-Gasdynamic Coupling and Nonequilibrium Effects behind Reflected Shock Waves," *AIAA J.*, *9* (5), May 1971, 858-864.

6.13 Zeldovich, Y. B., Y. P. Raizer, Physics of Shock Waves and High Temperature Hydrodynamic Phenomena, Vol. II, ed. W. D. Hayes and R. F. Probstein, Academic Press, New York and London, p. 489-90 (1967).

CHAPTER VII

CONCLUSIONS AND RECOMMENDATIONS

Conclusions

Based upon the results of the present investigation, the following conclusions are drawn:

1. The numerical solution of the conservation equations were found to yield stable and accurate solutions to the nonequilibrium, radiating shock layer surrounding a blunt reentry body.

2. Nonequilibrium results, when compared to equilibrium results at comparable conditions, yield consistently lower wall heating rates.

   (a) The largest differences in equilibrium and nonequilibrium heating rates occurred at low head load conditions. This fact was due to the inability of the finite rate reactions in air to proceed as fast as these conditions at equilibrium. The air layer species profiles in this layer were very different for equilibrium and nonequilibrium thus drastically changing the radiant emission back to the ablator wall.

   (b) The nonequilibrium heating rate, although lower than equilibrium, did approach the equilibrium prediction for high heat load conditions. The reactions did proceed fast enough in these cases to yield near equilibrium species profiles resulting in similar radiative emission.

3. One normalized around-the-body blowing rate profile was sufficient to adequately couple all the cases studied on the trajectory (coupling required a surface energy balance on the ablator).

4. The specification of equilibrium boundary conditions at the shock wave may be an invalid assumption; especially for low heating rate conditions since the air layer is itself far from chemical equilibrium at these conditions.

5. An incorrect estimate of input shock stand-off distance in the around-the-body solutions does not appreciably affect the coupled surface heating rate around-the-body but can increase computer time quite significantly.

6. The choice of species wall boundary conditions does not greatly affect the shock layer solution. For heating rate at the surface there was a 4% difference in heating rate between nonequilibrium and equilibrium wall cases.

7. Computer time for the stagnation line and around-the-body analyses is large (over 100 hours) for the radiating, nonequilibrium chemistry model used. The radiation calculation (LRAD) and the convergence of the species conservation equations were the major time consuming steps.

8. The temperature form of the energy conservation equation is extremely unstable for the shock layer system with finite rate chemistry and radiation. The enthalpy form of the energy equation is quite stable and converges satisfactorily when the proper damping coefficients are chosen.

Recommendations

Considering the conclusions presented above, it is recommended that:

1. Nonequilibrium predictions should be employed when low heating rate conditions are involved (<1500 BTU/sq. ft.-sec). Equilibrium models are sufficient for high heat load conditions (>1500 BTU/sq. ft.-sec).

2. For a conservative estimate of the mass loss rate for the phenolic nylon ablator, equilibrium predictions should be used throughout since this will overpredict the mass loss.

3. One representative set of species compositions should be used at the ablator surface to reduce the computational difficulty and computer time required. The difference in radiative heating was shown to be small (4%) for the cases investigated.

4. An investigation should be performed to determine the effect of doing a finite rate analysis across the bow shock. The equilibrium assumption was shown to be in error at low heat load conditions.

5. The numerical analysis in its present form is extremely computer time sensitive to the specification of this profile around-the-body. A more satisfactory method of solution should be found for shock standoff distance calculation.

6. The enthalpy form of the energy equation should be preferred to the temperature form since the enthalpy form is much more stable.

NOMENCLATURE

English

B_v	Planckian radiation intensity (m/t^2 x no. of particles)
C_i	Mass fraction (mass of i/unit mass of fluid) $C_i = \frac{\rho_i}{\rho} \frac{Y_i M_i}{M} = \frac{n_i M_i}{\rho}$, $\sum_i C_i = 1$
C_p	Specific heat at constant pressure (L^2/t^2 x T)
D_{ij}	Multicomponent diffusion coefficient (L^2/t)
D_{i_T}	Effective multicomponent diffusion coefficient (L^2/t)
D_i	Thermal diffusion coefficient (m/L x t)
D_{ij}	Binary diffusion coefficient (L^2/t)
E	Stagnation internal energy (mL^2/t^2)
$\mathbb{E}$	Radiative flux divergence (m/L x t^2)
$\overline{\overline{e}}$	Strain tensor (1/t)
f'	Velocity function, u/u_s
G_j	Gibbs free energy (mL^2/t^2 x mole of j)
H	Total enthalpy, $H = h + \overline{V}^2/2$
h	Static enthalpy, $h = Q + P/\rho$ (L^2/t^2), also Planck's constant
$\overline{J}_i$	Mass flux vector of species i (m/L^2 x t)
k	Ordinary coefficient of thermal conductivity (mL/t^3 x T)
k_c	Boltzmann's constant (mL^2/t^2T)
k_b	Bulk thermal conductivity (mL/t^3 x T)
M_i	Molecular weight of species i (mass of i/mole of i)
m_i	Mass of i (m)

n	Number density (particles/L^3)
n_i	Molal volume (moles of i/L^3)
n_t	Molal density (total moles/L^3)
P	Static pressure ($m/L \times t^2$) or (F/L^2)
P_r	Prandtl number, $C_p\mu/k$
$\bar{\bar{P}}$	Radiative stress tensor ($m/L \times t^2$)
Q	Internal energy per unit mass, including chemical energy (L^2/t^2)
$\bar{q}_R$	Radiative heat flux vector defined by (m/t^3) or ($E/L^2 \times t$)
q_c	Convective energy flux to a surface (m/t^3)
q_R	Radiative energy flux to a surface (m/t^3)
$\bar{q}_D$	Diffusional energy flux vector (m/t^3)
R	Body nose radius (L)
R_{e_s}	Reynolds number, $\rho_{\delta,0}U_\infty R/\mu_{s,0}$
R_i	Mass rate of formation of species i by heterogeneous reactions (m/tL^2)
$\mathbb{R}$	Universal gas constant ($mL^3/t^2 \times T \times$ no. of moles)
r	Cylindrical body radius
S_i	Total surface generation of species i ($m/t\ L^2$)
T	Thermodynamic temperature (T)
t	Time (t)
U_∞	Freestream velocity (L/t)
x	Body oriented coordinate
y	Body oriented coordinate
Y_i	Mole fraction of species i, $Y = n_i/n_t$, $\sum_i Y_i = 1$

Greek

α	Sublimation accommodation coefficient
α_v	Volumetric absorption coefficient, effective (L^2 x no. of particles/L^3)
∇	Del operator (1/L)
δ	Shock detachment distance (L)
$\tilde{\delta}$	Transformed shock detachment distance
ε	Difference between the body and shock angle $\varepsilon = \Theta - \phi$ (radians)
ε_ρ	Volume of voids per unit volume
η	Dorodnitzyn variable
Θ	Body angle (radians)
I_v	Spectral radiation intensity (m/t^2 x no. of particles x no. of steardians)
$\bar{\bar{I}}$	Unit tensor
κ	Absorption coefficient (L^2 x no. of particles/L^3)
κ	Local body curvature (1/L)
$\tilde{\kappa}$	$1 + \kappa y$
λ	$(\tilde{\mu} - 2/3\ \mu)$ (m/L x t)
M	$\sum_i Y_i M_i$ mean molecular weight of the mixture (m of mixture/ mole of mixture)
μ	Ordinary viscosity (m/L x t)
$\tilde{\mu}$	Bulk viscosity (m/L x t)
ν	Frequency (1/t)
ρ	Density (m/L^3), $\rho = n_t M$
ρ_i	Partial density of species i, $\rho_i = n_i M_i$ (m of i/L^3)
$\bar{\rho}$	Density ratio across shock ρ_∞ / ρ_s

σ	Radiative absorption cross section (L^2)
τ_ν	Optical depth at frequency ν
$\bar{\bar{\tau}}$	Viscous stress tensor ($m/L \times t^2$)
ϕ	Shock angle (radians)
$\bar{\Omega}_1$	Unit vector in the direction of photon propagation
Ω	Solid angle (stearadians)
Ω_{ij}	Collision integral of colliding species i and j
ω_i	Generation of species i ($m/L^3 \times t$)
u	Component of $\bar{V}$ in the ξ_1 direction (parallel to body surface) (L/t)
$\bar{V}$	Velocity vector, $u\bar{i} + v\bar{j} + w\bar{k}$ (L/t)
v	Component of $\bar{V}$ in the direction normal to the body surface (L/t)

Subscripts

i	Species i
w	Wall quantities
o	Stagnation line quantities
∞	Freestream conditions
s,δ	Quantities immediately behind the shock

Superscripts

D	Diffusion
A	0 or 1 denoting two-dimensional or axisymetric respectively (an exponent)
T	Thermal
*	Denotes dimensional variables
o	Standard state quantity

.. Evaluated on char side of ablator interface

+ Evaluated on flow field side of ablator interface

APPENDIX A

ENERGY TRANSFER IN THE CHAR ZONE

Introduction

An important step in the development of a coupled solution for the heat transfer in the flow field of a reentry body, is the description of the ablator itself. For the phenolic nylon ablator studied in this investigation, there are two zones of interest in the ablator - the decomposition zone and the char zone. This section will concentrate on the solution of the conservation equations in the char zone since this is the zone of most significant heat and mass transfer. For results of the phenomena occurring in the decomposition zone, the work of del Valle (Ref. A.1) was used.

The solution of the char zone conservation equations requires a specification of the thermodynamic and transport properties for the species involved along with a set of chemical reactions which occur at the conditions present. For this information the work of del Valle (Ref. A.1) was again used as a basis.

The problem of using del Valle's results directly as input to the flow field was a severe shortcoming in the numerical technique used. The conditions studied in del Valle's work allowed the use of fourth order Runge-Kutta for numerical solution of the energy and species equations. Unfortunately, these conditions were for the case where chemical reactions were not very rapid. The conditions required for a coupled solution to the flow field surrounding the ablator during planetary return have much faster chemical reaction rates. The step size for the Runge-Kutta integration became so small (in order to insure stability) that computation time became excessive and accuracy became questionable (due to round off errors). A new, absolutely stable numerical technique was then used which was many times faster than Runge-Kutta. This implicit technique is called the Padé integration scheme.

In this section a brief development of the one-dimensional conservation equations that describe the char zone will be presented. This development will be followed by a discussion of the Padé integration scheme and numerical solution of the energy and species equations. Finally, results will be given which were used in the coupled shock layer-phenolic nylon ablator solutions of this study.

Development of the Char Zone Analysis

To predict the energy transferred in the char zone, the equations of change are written to apply to one-dimensional flow in the char zone. Using a quasi-steady state approximation, the point of view is taken of an observer moving with the negative of the surface recession velocity. This is illustrated in Figure A.1 which shows schematically the virgin plastic, pyrolysis gases, and char. The point at which thermal degradation of the plastic is initiated is taken as $z = 0$.

The material balance relating the virgin plastic flow with the flow of pyrolysis gases and degrading solid in the combined decomposition char zone was written by Stroud (Ref. A.2) as

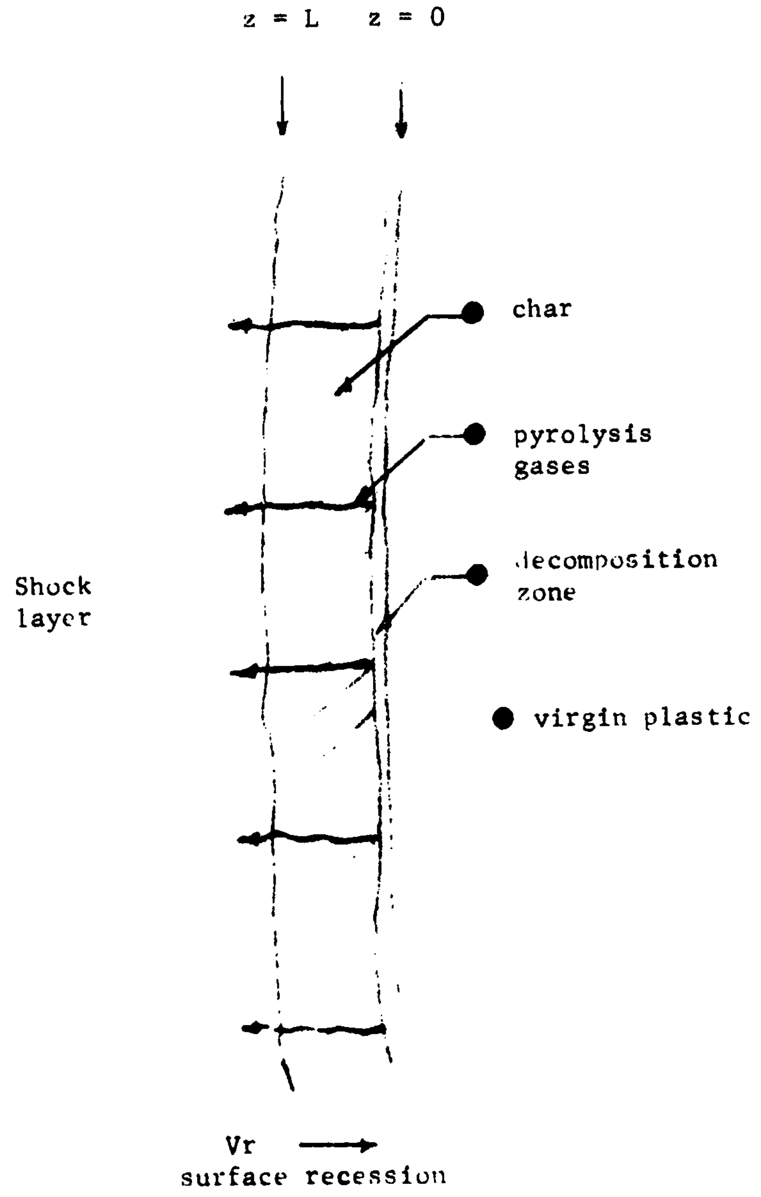
z = L
z = 0
char
pyrolysis gases
decomposition zone
Shock layer
virgin plastic
Vr
surface recession

Figure A.1. Flow in the Char Zone

$$\rho_o v = w + \rho v \qquad [1]$$

where w is the total gas mass flux, v is the surface recession velocity, and ρ_o and ρ are the virgin and degrading solid densities respectively. This assumes one-dimensional flow, quasi-steady state, and that the bulk volume of the char is the same as that of the virgin plastic. All of these have experimental justification. The composition of the gases generated by the decomposition of the virgin plastic composites must be known to be able to accurately predict the energy absorbed due to chemical reactions in the char zone. As illustrated in Figure A.1, these pyrolysis products enter the char zone and exit through the front surface of the char, at $Z = L$. Changes in the mass flux of the various species within the char occur as a result of chemical reactions at finite chemical reaction rates.

The particular restrictions and assumptions made in the formation of the combined zone analysis are presented below and have been justified by del Valle in Ref. A.1.

(1) Flow of pyrolysis gases is quasi-steady and one dimensional.

(2) Pyrolysis products behave as a perfect gas mixture.

(3) Thermal equilibrium between the pyrolysis gas products and the char is attained.

(4) PV work and viscous dissipation are neglible.

(5) Diffusional transport is negligible.

(6) Virgin material, char and gas physical properties are variable.

(7) For momentum transfer in the char zone the modified form of Darcy's Law was used.

The application of the above restrictions to the general equations for flow fo the pyrolysis gases in the char zone is now discussed.

Species Continuity Equation: Referring to Figure A-1 the species continuity equation for the ith component of a gas mixture for flow through a porous medium is (Ref. A.3)

$$\frac{D\rho_i}{Dt} = -\rho_i \; (\nabla \cdot u) - (\nabla \cdot J_i) + R_i$$

where ρ_i is the concentration, J_i, the mass flux by diffusion, R_i, the rate of generation of chemical species i and u is the velocity of the pyrolysis products within the pores.

For steady, one dimensional flow of gases with the above restrictions Equation (2) reduces to

$$\frac{d}{dz} (\rho_i u) = R_i \qquad [3]$$

If the mass flow rate of pyrolysis gases do not lose or gain by chemical reaction, Equation (3) becomes, summing over all the gas species:

$$\sum_{i=1}^{n} \frac{d}{dz} (\rho_i u) = 0 \qquad [4]$$

However, if the mass flow rate of pyrolysis gases changes due to carbon deposition, Equation (4) becomes:

$$\sum_{i=1}^{n} \frac{d}{dz} (\rho_i u) = -R_c \qquad [5]$$

where R_c is the amount of carbon deposition. If we define W_p as the mass flux of pyrolysis gases based on the cross-sectional area of voids in the char, $\sum_{i=1}^{n} \rho_i u$, (units of $lbs/ft^2{}_{voids}$ -sec) Equation (5) becomes:

$$\frac{dW_p}{dz} = \sum_{i=1}^{n} \frac{d}{dz} (\rho_i u) = -R_c \qquad [6]$$

Equation (6) says that any change of the mass flux of pyrolysis gases is due to the loss or gain of carbon by chemical reaction of the pyrolysis gases with the char.

Momentum Equation: The momentum equation for flow through porous media was formulated by H. P. G. Darcy in 1856 (Ref. A.4). Darcy's Law is:

$$u = \frac{\alpha}{\varepsilon\mu} (\nabla P - \rho g) \qquad [7]$$

Applying this equation to a one-dimensional, horizontal flow through a porous char layer and solving for the pressure gradient gives:

$$-\frac{dP}{dz} = \frac{\mu}{\alpha} (u\varepsilon) \qquad [8]$$

This equation is valid at low gas flow velocities within the porous medium. However, at high gas velocities it is necessary to to add a term to account for the inertial effects. This additional term leads to a modified form of Darcy's Law:

$$-\frac{dP}{dz} = \frac{\mu}{\alpha}\,(u\varepsilon) + \beta\rho\,(u\varepsilon)^2 \qquad [9]$$

Multiplying both sides of Equation (9) by the gas density, ρ, followed by substitution of the ideal gas equation of state ($\rho = PM_w/RT$) on the left hand side of the Equation (9), can be written in the following form

$$-\frac{M_w P}{RT}\frac{dP}{dz} = \rho(\mu/\alpha)\,(u\varepsilon) + \beta\rho^2\,(u\varepsilon)^2 \qquad [10]$$

If we define W as the total mass flux of pyrolysis gases based on the total area, we have that:

$$W = W_p = \varepsilon\rho u \qquad [11]$$

Therefore, substitution of Equation (11) into Equation (10) results after rearrangement:

$$-PdP = \frac{RT}{M_w}\,(\mu/\alpha)\,W + \beta\,(W)^2 \qquad [12]$$

Integration of Equation (12) between the front surface pressure ($P = P_L$ at $Z = L$) and any point within the char layer, (P at z), results in an integral equation for the pressure distribution in the char.

$$P = (-P_L^2 + 2R[\int_z^L(\mu/\alpha)\,W(T/M_w)dz + \int_z^L\beta(T/M_w)\,(W)^2\,dz)]^{1/2} \qquad [13]$$

In this equation all parameters that vary with temperature (hence, char distance) are left under the integral signs. These parameters are calculated by polynomials in temperature and from the solution of the energy equation.

Energy Equation. To formulate the equation that describes the energy transfer in the char zone, the energy equation for the gas and for the solid are written separately. They are later combined considering that the gas and solid are at the same temperature at any cross section in the flow; that is in thermal equilibrium.

The one dimensional, steady state energy equation for a gas mixture containing n species in reacting gas flow through porous media is

$$W \bar{C}p \frac{dT}{dz} = \varepsilon \frac{d}{dz} \left(k_g \frac{dT}{dz}\right) - \varepsilon \sum_{i=1}^{n} H_i R_i \qquad [14]$$

Similarly, the energy equation for the solid in the char zone simplified for the same restrictions to the following form:

$$(1-\varepsilon) C_p \rho v \frac{dT}{dz} = (1-\varepsilon) \frac{d}{dz} \left(k_c \frac{dT}{dz}\right) + (1-\varepsilon) H_c R_c \qquad [15]$$

The total energy transferred in the char zone is formed by adding Equations (14) and (15) and by using the definition of W of Equation (11):

$$[\varepsilon \bar{C}pWp + (1-\varepsilon) C_p \rho v] \frac{dT}{dz} = \frac{d}{dz} \left(k_e \frac{dT}{dz}\right) - \sum_{i=1}^{n+1} H_i \bar{R}_i \qquad [16]$$

where k_e represents an effective thermal conductivity defined as:

$$k_e = \varepsilon \bar{k}_g + (1-\varepsilon) k_c \qquad [17]$$

where $\overline{k}_g$ is the thermal conductivity of the flowing pyrolysis gases and k_c that of the solid matrix.

In addition the term $\sum_{i=1}^{n+1} H_i \overline{R}_i$ is defined as:

$$\sum_{i=1}^{n+1} H_i \overline{R}_i = \varepsilon \sum_{i=1}^{n} H_i R_i + (1-\varepsilon) H_c R_c \qquad [18]$$

The above represents the energy absorbed by the chemical reactions on a "total volume" basis. The solution of the energy equation, Equation (16), gives the temperature distribution in the char zone.

Padé Numerical Integration Technique

A system of n first order ordinary differential equations (ODE's) can be expressed in general form as:

$$\dot{y}\,(t) = f\,(t,y) \quad ; \quad y(t_o) = y_o \qquad [19]$$

where y is a vector valued function of t, and f is a vector valued function of t and y. Given the initial vector y_o, the system of ODE's is to be numerically integrated over the time domain (t_o, t_f).

A class of stable integration formulas can be derived by using known properties of linear ODE's. A numerical method of solution is termed stable if an error, once introduced, decreases from step to step. It can be shown that for a stable solution the eigenvalues of the matrix $[\partial f_i/\partial y_j]$ have negative real parts (see Ref. A.5). These formulas, while directly applicable to a system of linear ODE's, may be applied to systems of non-linear differential equations by linearizing at each step. Even considering the additional computer time necessary to linearize the equations, the total time needed to solve a complete problem is much less than required by any standard method (Ref. A.6).

Consider a system of n linear ODE's with constant coefficients:

$$\dot{y}\ (t) = A\ y\ (t) + b \qquad [20]$$

the formal solution of this equation a t = h is

$$y(h) = \exp\ (hA)\ \ [y_o + A^{-1}\ b] - A^{-1}\ b \qquad [21]$$

where

$$\exp\ (hA) = I + hA + \frac{1}{2}\ (hA)^2 + \ldots$$

In Equation 21, the exponential term can be approximated in numerous ways, and the form of the approximation will determine whether the procedure is stable. A convenient method of approximating any function is the rational approximation, which can be derived using the Padé transformation of the power series. If P and Q are polynomial of degree p and q, respectively, the exponential is represented as

$$e^{hA} = Q^{-1}P + E\ (hA)$$

The rational approximation agrees with the power series of exp (hA) for at least p + q + 1 terms and the residual error is denoted by E(hA). The polynomials P and Q for the exponential function (Ref. A.7) are given by

$$P = \sum_{k=0}^{p} \frac{(p + q - k)!\, p!}{(p + q)!\, k!\, (p - k)!} (hA)^k$$

$$Q = \sum_{k=0}^{q} \frac{(p + q - k)!\, q!}{(p + q)!\, k!\, (q - k)!} (-hA)^k$$

Substituting the rational approximation into Equation (21) yields the desired integration formula:

$$y(h) = Q^{-1} P \, [y_o + A^{-1} b] - A^{-1} b$$

Or rearranging the terms,

$$y(h) = Q^{-1} \, [Py_o + (P - Q) \, A^{-1} b] \qquad [22]$$

Equation (22) includes numerous types of single step integration methods and not all of these methods are stable. The Euler method, which has been shown to be partially stable is a special case of Equation (22) with $Q = I$ and $P = I + hA$ ($q = 0$ and $p = 1$). In this section only the stable procedures are of interest and for these methods $q \geq p$. Of particular interest are those methods where the diagonal ($p = q$) of the Padé table is used. Such methods are called Padé integration procedures or rational approximation methods. For the cases $p = q = 1$ and $p = q = 2$, the following expressions are obtained from Equation (22):

$$y(h) = (I - \frac{1}{2} hA)^{-1} \, [(I + \frac{1}{2} hA) \, y_o + hb] + O(h^3) \qquad [23a]$$

$$y(h) = [I - \frac{1}{2} hA + \frac{1}{12} (hA)^2]^{-1} [(I + \frac{1}{2} hA + \frac{1}{12} (hA)^2)y_o + hb] + O(h^5) \quad [23b]$$

The truncation errors are $O(h^3)$ and $O(h^5)$, respectively.

The Padé integration method is directly applicable to linear systems of ordinary differential equations. Some additional steps are required to apply the method to chemical kinetic equations, which are represented by Equation (19). The non-linear system of equations can be reduced to the form Equation (20) by expanding the function f in a Taylor's Series and neglecting terms which are second order and higher:

$$\dot{y} = f(t_o,y_o) + \frac{\partial f}{\partial y} (t_o,y_o)\Delta y + O(\Delta y^2) \quad [24]$$

where $\Delta y = y - y_o$ and $\frac{\partial f}{\partial y} (t_o,y_o)$ denotes the matrix A in Equation (20) with elements

$$a_{ij} = \frac{\partial f_i}{\partial y_j}$$

The indices i and j denote the i^{th} and j^{th} elements in the f and y vectors, respectively. Hence grouping terms as in Equation (20)

$$\dot{y} = \frac{\partial f}{\partial y} (t_o,y_o)y + (f(t_o,y_o) - \frac{\partial f}{\partial y} (t_o,y_o)y_o) + O(\Delta y^2) \quad [25]$$

The phenomenological kinetic rate expression represents the function f_i which must be expanded in a Taylor's Series as shown in Equation (24). In terms of the functions f_i the elements of the matrix, A, and vector, b, are

$$a_{ij} = \frac{\partial f_i}{\partial y_j} \quad [26]$$

$$b_i = f_i(t_o, y_o) - \sum_{k=1}^{n} a_{ik} (y_o)_k \qquad [27]$$

where the index i denotes the species production equation, the index j denotes the species, and $(y_o)_k$ is an element of the vector of species at time t_o.

The Padé integration routine used in this analysis assumes that y(0)=0. This assumption simplifies Eqs. (23) and the linearized system is then conveniently expressed in terms of Δy as

$$(I - \frac{1}{2} hA + KA^2) \Delta y = hb \qquad [28]$$

where K = 0 for a second order integration scheme and $K=h^2/12$ for a fourth order integration scheme. By permitting K to be specified as an input, either the second order or fourth order methods can be conveniently selected. In cases where the higher order scheme offers no great advantages, the elimination of the calculation of the matrix A^2 can save an appreciable amount of computer time.

The species equations are "stiff" and therefore need to be solved using the numerically stable Padé scheme instead of the more conventional Runge-Kutta method. The energy equation, however, is not "stiff" and its solution can be performed using Runge-Kutta as described below.

Energy Equation Solution

The solution of the energy equation was perfommed using a standard fourth order Runge-Kutta integration technique. Actually, the energy equation was solved as two simultaneous equations in

$\frac{dT}{dz}$ and T by taking Equation (16) and expanding as follows:

$$[\varepsilon CpWp + (1-\varepsilon)\ \bar{C}_p\ \rho v)\ \frac{dT}{dz} = k_e\ \frac{d^2T}{dz^2} + \frac{dk_e}{dz}\ \frac{dT}{dz} - \sum_{i=1}^{\ell}\ H_i\bar{R}_i \qquad [28]$$

where the term $\frac{dk_e'}{dz}$ can be further expanded as

$$\frac{dk_e}{dz} = \frac{dk_e}{dT}\ \frac{dT}{dz} \qquad [29]$$

using the chain rule. This yields the following result

$$k_e\ \frac{d^2T}{dz^2} = [\varepsilon CpWp + (1-\varepsilon)\ \bar{C}_p\rho v + \frac{dk_e}{dT}\ \frac{dT}{dz} + \sum_{i=1}^{\ell}\ H_i\bar{R}_i]\frac{dT}{dz} \qquad [30]$$

or when divided by k_e

$$\frac{d^2T}{dz^2} = \frac{1}{k_e}\ [\varepsilon C_pW_p + (1-\varepsilon)\ \bar{C}_p\ \rho v + \frac{dk_e}{dT}\ \frac{dT}{dz} + \sum_{i=1}^{\ell}\ H_i\bar{R}_i]\ \frac{dT}{dz} \qquad [31]$$

Equation (31) is a second order nonlinear differential equation in T which can be considered two first order in T and $y = \frac{dT}{dz}$. The two equations are

$$\frac{dy}{dz} = f(T,y) \qquad [32]$$

and

$$\frac{dT}{dz} = y \qquad [33]$$

The standard fourth order Runge-Kutta integration formula can then be applied to the simultaneous equations.

Results of the Char Analysis

The results of the analysis in the char layer are presented in Fig. A.2. Heating rates are given as a function of ablator mass

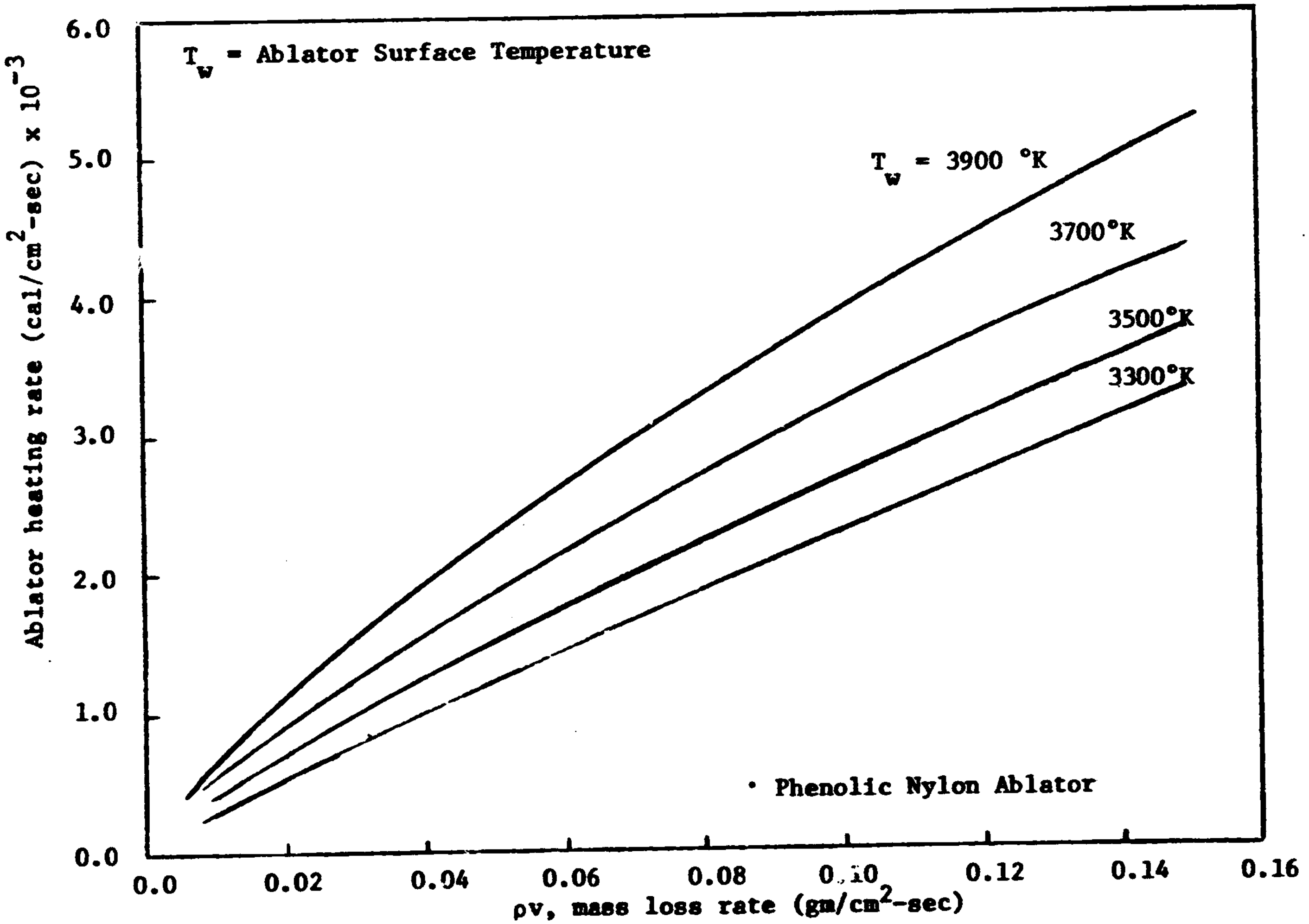

Figure A.2. Ablator Heating Response vs. Mass Loss Rate.

loss rates with ablator surface temperature as a parameter. The heating rates are typical of those encountered during reentry from planetary missions. These curves were curve fit using a linear regression program from SAS (Statistical Analysis System developed at North Carolina State University, Ref. A.8). The equation used to fit the curves was:

$$q = a_1 T^3 \rho v + a_2 T^2 \sqrt{\rho v} + a_3 T^3 \rho v + a_4 \rho v \qquad [34]$$

where the coefficients a_1 to a_4 are given in Table A.1.

The energy and species equations needed boundary conditions for these results. For the energy equation, the heat flux from the decomposition zone was used (from an extension of Ref. A.1). This heat flux from the decomposition zone is a function of mass loss rate as depicted in Figure A.3. This heat flux was the value when the solution of the decomposition zone species equations showed the correct mass ratio of char to pyrolysis gases. The mass fractions of gases and char entering the char layer are given in Table A.2. By using this criteria for the specification of the interface, continuity was achieved between the decomposition zone and the char. The heat flux allows the initial specification of dT/dz. Also required in the solution of the energy equation is the temperature at decomposition zone-char zone interface (shown in Figure A.4).

Each species equation needs the specification of initial composition at the back surface. The values used in this analysis are the same as used in Ref. A.1. and are presented in Table A.2. The values of species compositions as they exit the char surface are shown in Table A.3 for conditions of mass loss rate of 0.04 lbm/sq

Table A.1

Curve Fit Coefficients for Heat Conducted through the Surface of a Phenolic Nylon Ablator

$$(q = a_1 T^3 \rho v + a_2 T^2 \sqrt{\rho v} + a_3 T^3 \sqrt{\rho v} + a_4 \rho v)$$

	q in * cal/sq. cm-sec	q in † BTU/sq. ft-sec
a_1	0.9292×10^{-8}	0.1674×10^{-7}
a_2	-0.1292×10^{-3}	-0.3330×10^{-3}
a_3	0.4268×10^{-7}	0.1099×10^{-6}
a_4	0.1516×10^{4}	0.2732×10^{4}

* T is temperature in °K

ρv is mass loss rate in gm/sq cm-sec

† T is temperature in °K

ρv is mass loss rate in lbm/sq ft-sec

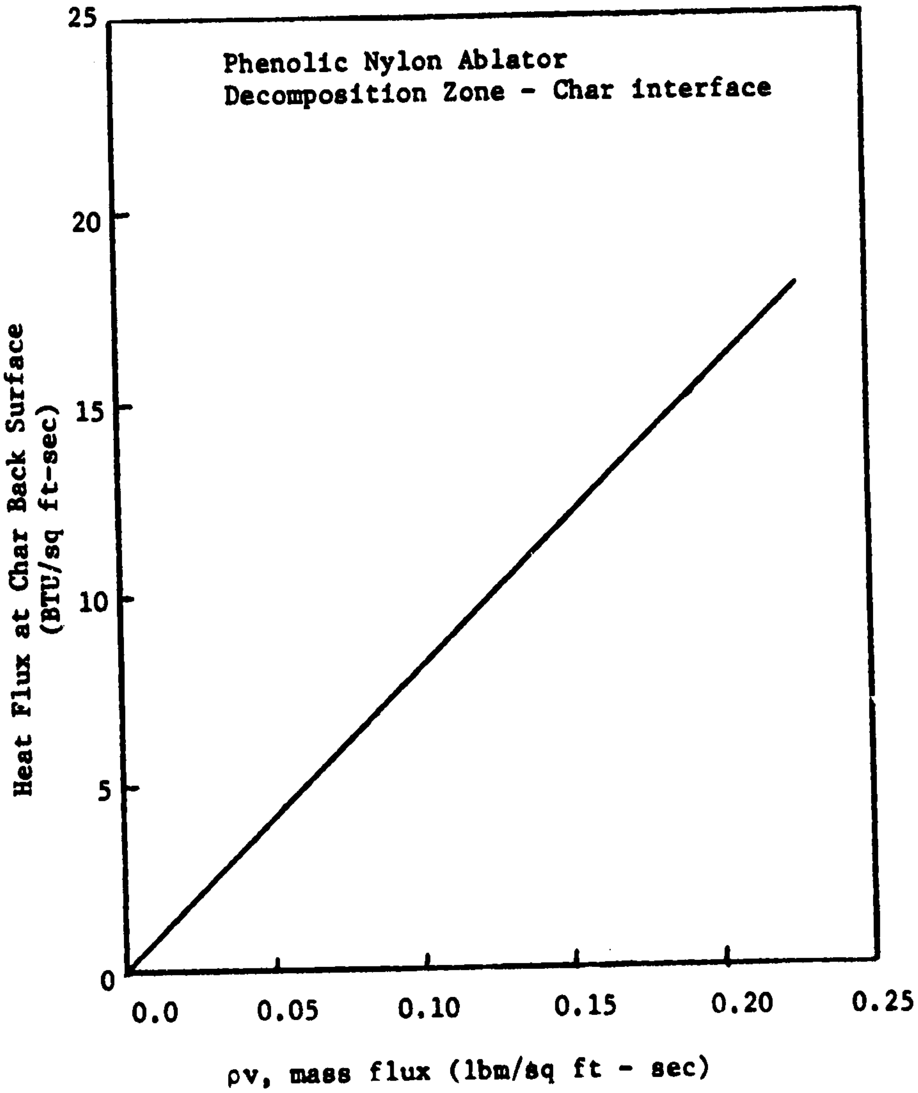

Figure A.3. Decomposition Zone Heat Absorption Rate.

Table A.2

Species Compositions at the Char Zone - Decomposition Zone Interface

Component	Composition (Mass Percent)
H_2	3.03
CH_4	3.87
C_2H_2	3.89
C_2H_4	3.90
C_2H_6	0.65
C_6H_6	2.59
C_6H_5OH	23.18
CO	4.18
CO_2	4.62
H_2O	5.65
N_2	4.96
Carbon (solid)	39.48
Total	100.00%

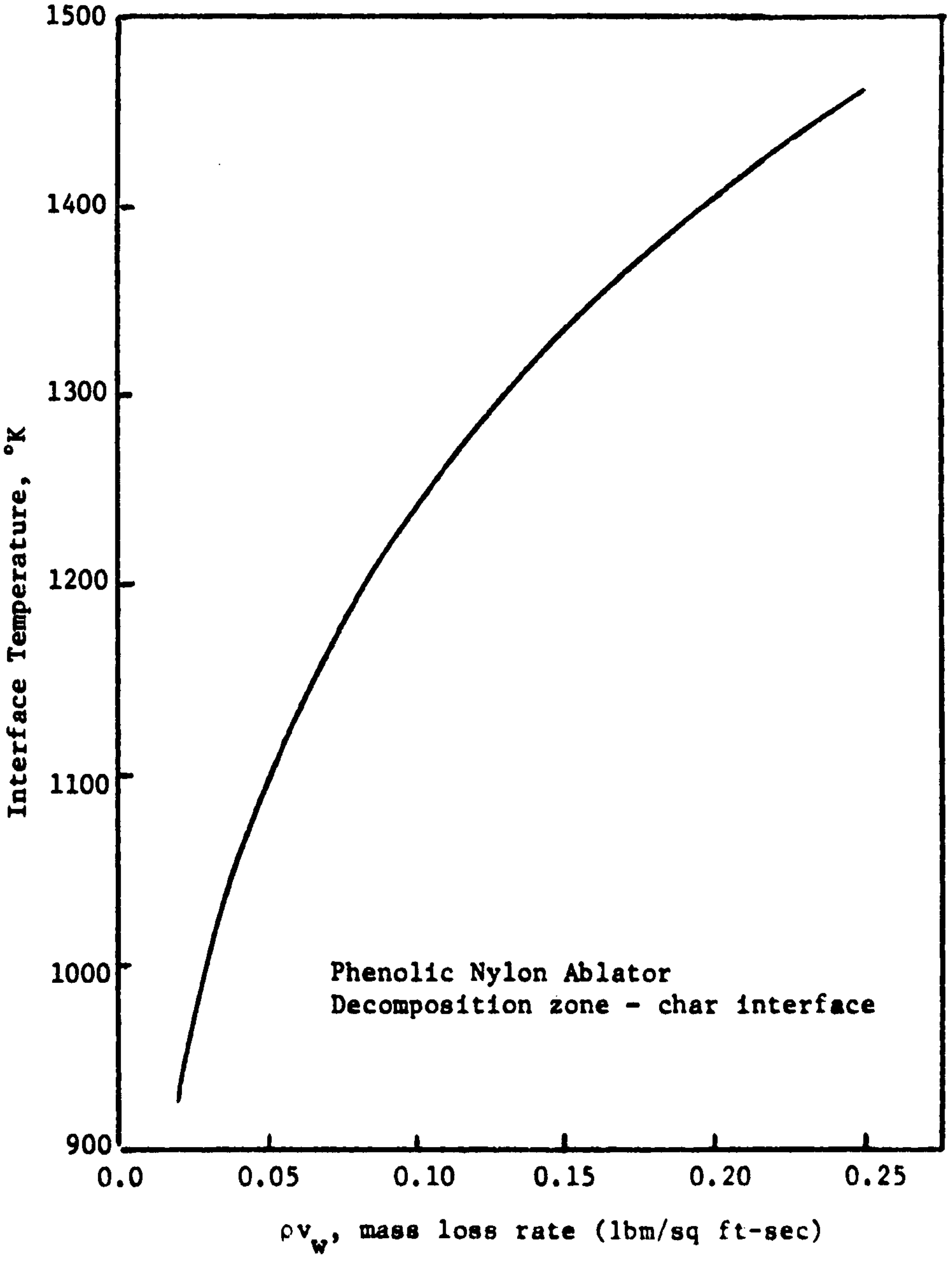

Figure A.4. Temperature at Char-Decomposition Zone Interface as a Function of Mass Loss Rate.

Table A.3

Species Compositions at the Ablator Surface on the Char and Flowfield Sides

Component	Species Composition (Mass Percent)	
	Char Side	Flowfield Side
H_2	3.81	4.14
C_2H_2	5.96	5.89
CO	25.70	25.70
N_2	4.96	4.96
C_2H	11.80	13.88
H	2.88	2.21
CH_4	0.08	*
CH_3	0.32	*
CH_2	3.10	*
Carbon (solid)	42.11	*
C	*	36.95
C_2	*	4.22
C_3	*	2.11
C_3H	*	1×10^{-10}
C_4H	*	1×10^{-10}
O	*	1×10^{-10}
HCN	*	1×10^{-10}
CN	*	1×10^{-10}
N	*	1×10^{-10}
N^+	*	1×10^{-10}
O^+	*	1×10^{-10}
C^+	*	1×10^{-10}
O_2	*	1×10^{-10}
e^-	*	1×10^{-10}

* Species not considered present on this side.

ft - sec and surface temperature of 3600°K. These conditions are typical of those encountered by a re-entering vehicle from planetary missions. Also shown in Table A.3 are the species compositions modified to agree with the species considered in the flow field. The only species of any reasonable concentration that were omitted from ablator surface to flow field were CH_2 and CH_3. The reason this was done was the equilibrium considerations show that these species do not exist in the shock layer. To reduce the number of species in the shock layer and thus reduce the computation time the species were assumed to instantaneously react to carbon solid, C(s), and hydrogen, H_2. These values were used in the flow field analysis in order to eliminate the complexity of curve fitting all the compositions as functions of temperature and mass loss rate.

The reactions considered important in the char layer are given in Table A.4 along with kinetic data. A detailed discussion of the criteria for reaction selection and composition at the decomposition zone interface is given in Ref. A.1. The set of 15 reactions shown in Table A.4 are a result of applying this criteria for reaction selection. The procedure bases its selection on thermodynamic and kinetic consideration along with initial gas composition.

Summary

The conservation equations for the description of one dimensional char zone layer flow were presented in this section. The char was assumed to be degraded from a phenolic-nylon composition (40 wt. % nylon, 60 wt. % phenolic) at quasi-steady state. The pyrolysis gases were assumed to be in thermal equilibrium with the porous char

Table A.4

Chemical Reactions Occurring in the Char Zone

CH_4	$\rightleftarrows$	$CH_2 + H_2$
CH_4	$\rightleftarrows$	$CH_3 + H$
$2CH_3$	$\rightleftarrows$	$C_2 H_6$
C_2H_6	$\rightleftarrows$	$C_2 H_4 + H_2$
C_2H_4	$\rightleftarrows$	$C_2 H_2 + H_2$
$C_2 H_2$	$\rightleftarrows$	$C_2H + H$
$C(s) + H_2O$	$\rightleftarrows$	$CO + H_2$
$C(s) + CO_2$	$\rightleftarrows$	$2 CO$
$H_2 + M$	$\rightleftarrows$	$2 H + M$
$H_2O + M$	$\rightleftarrows$	$OH + H + M$
CO_2	$\rightleftarrows$	$CO + O$
$H + CO_2$	$\rightleftarrows$	$CO + OH$
$C_6 H_5 OH$	$\rightleftarrows$	$H_2O + C_6 H_6$
$C_6 H_6$	$\rightleftarrows$	$3 C_2 H_2$

matrix and diffusional transport was considered neglible. The non-equilibrium species equations required numerical solution by an absolutely stable technique such as the Padé integration which was described in this section.

Heating rate results as a function of surface temperature and mass loss rate were curve fit using SAS (Statistical Analysis System). These heating rates can then be used as input to the flow field solution as a wall boundary condition. The other wall boundary conditions obtained from the char analysis are the species mass fractions. Due to the complexity of inputing compositions as a function of temperature and mass loss rate into the flow field, constant values of composition were used. These values were those obtained at a surface temperature of 3600°K and 0.04 lbm/sq ft sec -- conditions typical of planetary re-entry.

Fifteen chemical reactions and 19 species were included in the numerical solution. These reactions and species were identical to those used by del Valle (Ref. A.1). Selection of these was based on thermodynamic and kinetic considerations as discussed by del Valle.

Appendix B further specifies the wall boundary conditions by applying the Hertz-Knudsen equation to the char surface which relates surface temperature to wall pressure and mass loss rate.

References

A.1 del Valle, E. G., PhD dissertation, Louisiana State University (1975).

A.2 Stroud, C. W., "A Study of the Chemical Reaction Zone in Charring Ablators During Thermal Degradation," Paper 33b, National Meeting of the AIChE, Dallas, Texas (February 6-9, 1966).

A.3 Bird, R. B., W. E. Stewart, and E. N. Lightfoot, Transport Phenomena, John Wiley and Sons, Inc. New York, 828-30 (1960).

A.4 Koh, J.C.Y., E. P. del Casal, R. W. Evans, and V. Deriugin, "Fluid Flow and Heat Transfer in High temperature Porous Matrices for Transpiration Cooling," Technical Report AFFDL-TR066-70, The Boeing Company, 207 pages (May 1966).

A.5 Magnus, D. E. and H. S. Schechter, "Analysis of Error Growth and Stability for the Numerical Integration of the Equations of Chemical Kinetics." GASL TR-607, June 1966.

A.6 Magnus, D., and H. Schechter, "Analysis and Application of the Padé Approximation for the Integration of Chemical Kinetic Equations," TR-642, GASL, (March 1967).

A.7 Varga, R. S., "On Higher Order Stable Implicit Methods for Solving Parabolic Partial Differential Equations," J. Math. Physics, Vol. 40, pp. 220-331.

A.8 Ban, A. J. and J. H. Goodnight, A Users Guide to the Statistical Analysis System, Department of Statistics, North Carolina State University, Raleigh, North Carolina (August, 1972).

APPENDIX B

ON MODELING SUBLIMATION OF A CHARRING ABLATOR

Introduction

The determination of the sublimation rate of carbon for a char forming ablative heat shield is necessary to fully describe the material response to aerodynamic heating. This sublimation rate is required in the surface mass and energy balances which give the interaction of the flow field and the ablator.

The sublimation model that is used in this analysis and compared to other investigators is based on the Hertz-Knudsen equation. The basic equation originally given by Hertz in 1882 (Ref. B.1) relates in the mass of molecules striking a unit area per unit time to the pressure and temperature of the gas. The theoretical model is shown to compare quite favorably with arc-jet experimental data and demonstrates its usefulness by its accuracy and simplicity.

Model Description

The Hertz equation represents the condensation of a solid and is:

$$\dot{m}_c = \alpha \frac{A_r}{A} P \left(\frac{M}{2\pi RT}\right)^{\frac{1}{2}} \qquad [1]$$

In the equation, α is the fraction of molecules which strike the surface that condense and is referred to as an "accomodation coefficient." The ratio of available surface area, A_r, to the surface of total cross sectional area, A, is included in the equation, and for a perfect surface such as the fact of a crystal, A_r equals A. In the case of rough or porous surfaces, the value of A_r will generally not be the same as A. Equation B.1 is a modification of the simple kinetic theory relation and gives the gross rate of condensation of the solid.

At equilibrium, the condensation rate is equal to the vaporization rate, and the pressure is equal to the equilibrium vapor pressure of the solid. This approach to solid vaporization was first suggested and experimentally verified by Knudsen (Ref. B.2) in 1915. The gross rate of evaporization is:

$$\dot{m}_v = \alpha \frac{A_r}{A} P_{vap} \left(\frac{M}{2\pi RT}\right)^{\frac{1}{2}} \qquad [2]$$

For non-equilibrium such as the case where the subliming material is continually removed, the net rate of evaporation is given by the well known Hertz-Knudsen equation [Ref. B.3].

$$\dot{m} = \dot{m}_v - \dot{m}_c = \alpha \frac{A_r}{A} \left(\frac{M}{2\pi RT}\right)^{\frac{1}{2}} (P_{vap} - P) \qquad [3]$$

The previous equation can be extended for vaporization of a solid into a mixture of gases by simply replacing the total pressure, P, with partial pressure of the vaporizing component, P_i.

$$\dot{m}_i = \alpha_i (1 - \varepsilon) \left(\frac{M_i}{2\pi RT}\right)^{\frac{1}{2}} (P_{i,\,vap} - P_i) \qquad [4]$$

Here the effective area ratio A_r/A is approximated by $(1 - \varepsilon)$ where ε is the char porosity.

Carbon Species: Studies (Ref. B.4) have shown that the three primary constituents of vaporizing carbon are C_1, C_2, and C_3. These species have Arrhenius dependence of vapor pressure on temperature of the form $\log P_i = a_i + b_i/T$. The accomodation coefficients, α_i, along with the Arrhenius vapor pressure coefficients (Ref. B.5) are given in Table B.1.

Table B.1

Accomodation Coefficients and Arrhenius Coefficients for Vapor Pressure of C_1, C_2 and C_3 (Ref. B.5)

Species	Accomodation Coefficient, α_i	$\log P_{i,vap} = a_i - b_i \times 10^4/T$	
		a_i	b_i
C_1	0.37	8.14	3.72
C_2	0.34	9.69	4.23
C_3	0.08	9.81	4.03

Surface Mass Balance: The general species mass balance at the surface of the ablator includes convective flux to and away from the surface ($\rho v C_i$), diffusive flux to and away from the surface (J_i) and surface generation by chemical reaction (ω_i). The species mass balance is stated as follows:

$$\rho v C_i^- + \omega_i + J_i^- = \rho v C_i^+ + J_i^+ \qquad [5]$$

In the region where the rate of sublimation is significant, reaction controlled or diffusion controlled surface chemical reactions will not occur (Ref. B.6). Also diffusion will not be important when the convective terms are large as is the case for the high heating rates encountered during manned return from planetary missions. The result is a porous char (solid carbon matrix) vaporizing into the gaseous species C_1, C_2, and C_3. Also flowing through this porous matrix are the transpiring gases from the pyrolysis zone of the ablator. The composition of the pyrolysis gases was reported in error in Ref. B.6 for a phenolic-nylon ablator and corrected values are given in Table B.2. This table also includes a typical final composition of the pyrolysis gases at the surface after flowing through and reacting with the char as computed by a finite rate analysis, an extension of the work in Ref. B.7.

Combining the Hertz-Knudsen equation, Eq. B.4, with the surface mass balance for these previously described conditions for i being C_1, C_2, or C_3, the mass flux of these gaseous carbon species injected into the shock layer is given by

$$\rho v C_i^+ = \alpha_i \, (1-\varepsilon) \left(\frac{M_i}{2\pi RT}\right)^{\frac{1}{2}} (P_{i,vap} - P_i^+) \qquad [6]$$

Table B.2
Representative pyrolysis product composition of 40% (by weight) Nylon - 60% (by weight) phenolic resin ablative composite

Component	Composition of Pyrolysis Gases (Mass Percent) Decomposition Zone	Composition of Pyrolysis Gases (Mass Percent) Ablator Surface
H_2	3.03	3.81
CH_4	3.87	0.08
C_2H_2	3.89	5.96
C_2H_4	3.90	*
C_2H_6	0.65	*
C_6H_6	2.59	*
C_6H_5OH	23.18	*
CO	4.18	25.70
CO_2	4.62	*
H_2O	5.65	*
N_2	4.96	4.96
CH_3	*	0.32
CH_2	*	3.10
C_2H	*	11.80
H	*	2.88
Carbon (solid)	39.48	42.11
Total	100.00%	100.00%

Element	Elemental Composition (mass percent)
C	73.03
H	7.29
N	4.96
O	14.72
Total	100.00%

* Concentration is less than 0.01%.

or in terms of the total pressure at the surface

$$\rho v C_i^+ = \alpha_i(1 - \epsilon) \left(\frac{M_i}{2\pi RT}\right)^{\frac{1}{2}} (P_{i,vap} - C_i^+ P\bar{M}/M_i) \qquad [7]$$

Equation B.7 can be solved for the mass fraction of the gaseous carbon species C_i^+ leaving the surface as:

$$C_i^+ = B\, P_{i,vap}/(\rho v + B\bar{M}P/M_i) \qquad [8]$$

where

$$B = \alpha_i(1 - \epsilon) \left(\frac{M_i}{2\pi RT}\right)^{\frac{1}{2}} \qquad [9]$$

Finally a total mass balance on carbon says that all carbon coming to the surface as a solid leaves as a vapor.

$$C(s) = \sum_{i=1}^{3} C_i^+ \qquad [10]$$

This does not include the possibility of erosion as a surface removal mechanism, but erosion could be readily included if important.

Using Equations B.8, 9, and 10 and the data in Tables B.1 and B.2, the mass flux at the surface can be computed as a function of surface temperature. Also the composition of C_1, C_2 and C_3 in the gases injected into the shock layer are determined.

Results of the Analysis

In Figure B.1 a comparison is shown between our calculations suing the Hertz-Knudsen equation and the results from Bishop and DiCristina (Ref. B.8) for a phenolic-carbon ablator. The porosity used in the Hertz-Knudsen equation was 0.2 which was the value given by Clayton et al. (Ref. B.9) for carbon-phenolic. The results

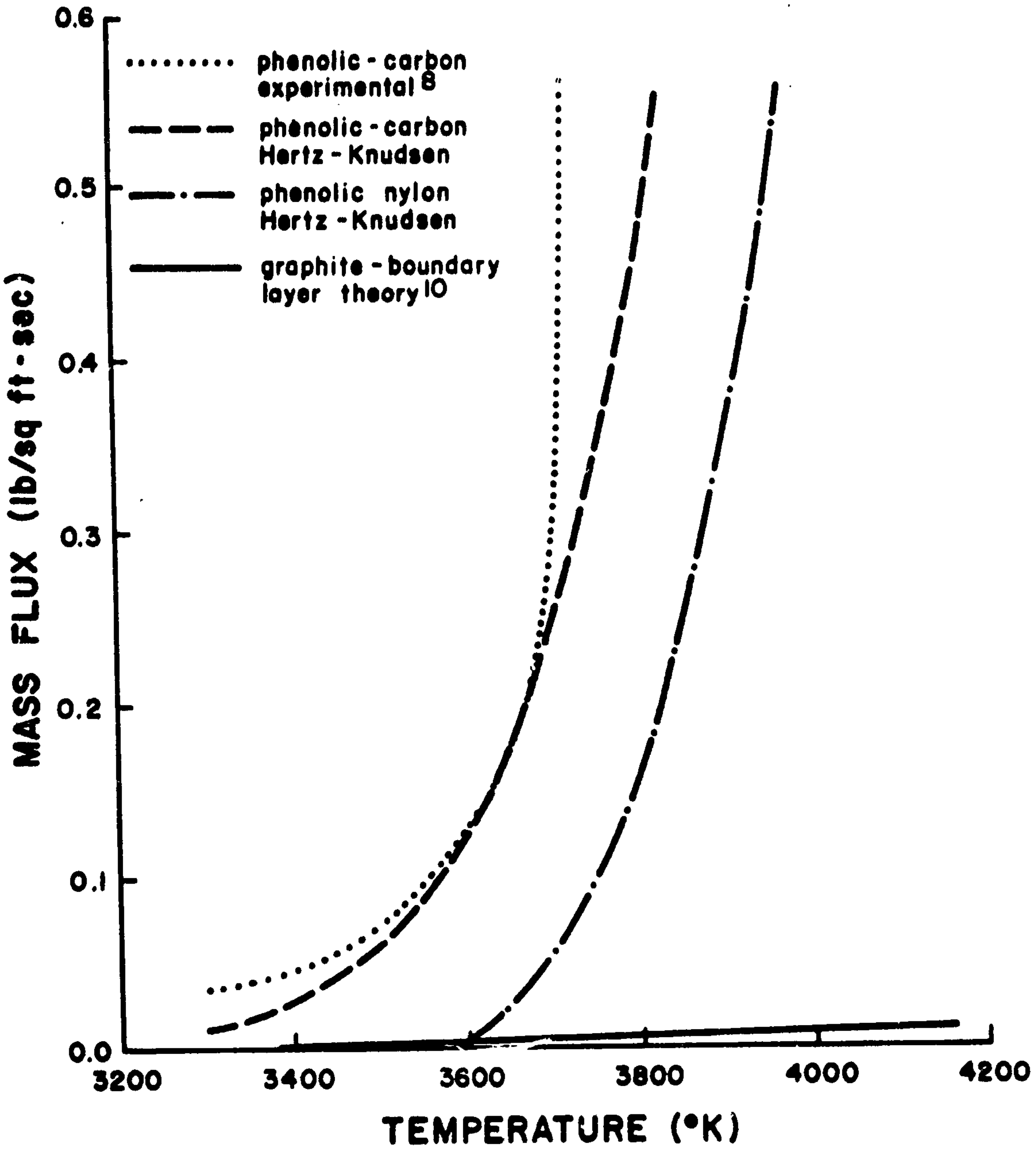

Figure B.1. Comparison of the Hertz-Knudsen Analysis with Other Investigators.

reported by Bishop and DiCristina (Ref. B.8) were obtained from arc jet experimental data for phenolic-carbon in the sublimation regime. The theoretical predictions of the Hertz-Knudsen sublimation model correspond quite well with the experimental curve except for some divergence at higher surface temperatures. Bishop and DiCristina stated in their paper that their curve would break less sharply if their surface temperature data had been corrected for the pyrometer error due to "significant nose curvature over the specimen area". Taking this fact into account, excellent agreement between the Hertz-Knudsen theoretical approach and the results from arc jet experimental work would be obtained.

Also shown in Figure B.1 are the results reported by Scala and Gilbert (Ref. B.10). These results were obtained using an equilibrium chemistry boundary layer analysis to predict the sublimation rate of graphite. These results differ greatly from both the Hertz-Knudsen predictions and the data of Bishop and DiCristina. The difference could be due to the fact that Scala and Gilbert's analysis assumed equilibrium between the graphite and the carbon vapor phase. Applying the Hertz-Knudsen analysis for graphite ablation gave essentially the same results as for the phenolic carbon. In the graphite analysis the porosity is zero, and there is no flow of pyrolysis products. These two effects shift the curve in opposite directions, and thus the graphite curve is essentially the same as that for carbon-phenolic which would correspond to Scala and Gilbert's results.

To demonstrate the difference that porosity can make on the mass flux, the Hertz-Knudsen analysis was applied to a phenolic-nylon ablator with a porosity of 0.8. Referring to Figure B.1, increasing porosity has the effect of raising the surface temperature for a given mass flux.

In Figure B.2, the carbon species compositions for the phenolic-nylon ablator are given, and this shows that C_3 is the predominant component that is obtained from the subliming char. This result agrees with Palmer and Shelef (Ref. B.4) who report that C_3 becomes the primary constituent at these temperatures.

Conclusions

The Hertz-Knudsen analysis has been shown to accurately predict the sublimation rate from a charring ablator. Porosity was shown to have a significant effect on the surface temperature - an increase in porosity results in an increase in surface temperature. The predominant carbon species in the vapor was C_3 which agreed with previous investigations.

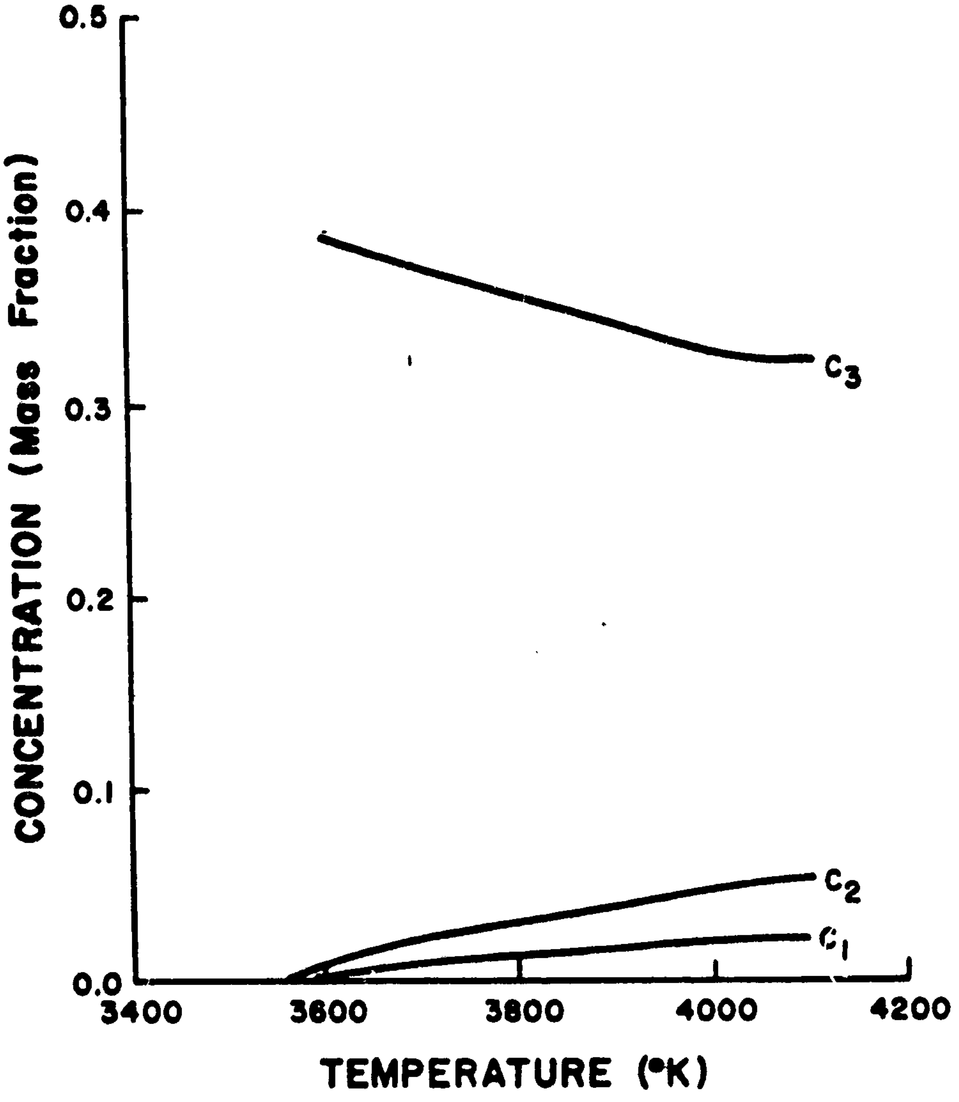

Figure B.2. Predominant Carbon Vapor Species from the Sublimation of a Phenolic Nylon Ablator.

REFERENCES

B.1. Somorhai, G.A., "Studies of the Sublimation Mechanism of Solids," in Advances in High Temperature Chemistry, ed. by Leroy Eyring. New York: Academic Press, 1969, Vol. 2, p. 205.

B.2. Knudsen, Martin, "Die Maximale Verdampfungsgeschwindigkeit des Quiksilbers," Ann. Phy., 47, 697 (1915).

B.3. Schrage, Robert W., A Theoretical Study of Interphase Mass Transfer, Columbia University Press, New York, p. 36, 1953.

B.4. Palmer, H. B. and Mordecai Shelef, "Vaporization of Carbon," in Chemistry and Physics of Carbon, ed. by P. L. Walker, Jr., New York: Marcel Dekker, Inc., 1968, Vol. 4, p. 85 f.

B.5. Thorn, R. J. and G. H. Winslow, "Vaporization Coefficient of Graphite and Composition of Equilibrium Vapor," J. Chem. Phys, 26, (1), 186 (1957).

B.6. Pike, R. W., G. C. April, E. G. del Valle, and S. Hacker, "On Methods for Determining the Composition of Pyrolysis Products from Ablative Composites," JSR, 7 (10), pp. 1250-1253 (October 1970).

B.7. April, G. C., R. W. Pike, E. G. del Valle, "Modeling Reacting Gas Flow in the Char Layer of an Ablator," AIAA Journal, 9 (6), pp. 1113-1119, (June 1971).

B.8. Bishop, W. M. and V. DiCristina, "The Combustion and Sublimation of Carbon at Elevated Temperatures," AIAA Paper No. 68-759, Third Thermophysics Conf. (Los Angeles, California), June 24-26, 1968.

B.9. Clayton, W. A., T. J. Fabish, J. F. Lagedrost, "Thermal Conductivity of Phenolic-Carbon Chars," AFML TR 69-313, (December 1969).

B.10. Scala, S. M. and L. M. Gilbert, "Sublimation of Graphite at Hypersonic Speeds," AIAA Journal, 3 (9), 1635-1644, (1965).

APPENDIX C

POLYNOMIAL COEFFICIENTS FOR THERMODYNAMIC PROPERTIES

The thermodynamic properties of heat capacity, C_p°, and enthalpy, H_T°, are discussed in Chapter IV where it is stated that these variables are satisfactorily represented by a polynomial fit such as

Heat Capacity:

$$\frac{C_p^\circ}{\mathbb{R}} = A_1 + A_2T + A_3T^2 + A_4T^3 + A_5T^4$$

Enthalpy:

$$\frac{H_T^\circ}{\mathbb{R}T} = A_1 + \frac{A_2T}{2} + \frac{A_3T^2}{3} + \frac{A_4T^3}{4} + \frac{A_5T^4}{5} + \frac{A_6}{T}$$

The determination of these coefficients is discussed by Esch (Ref. C.1) and are presented in Table C.1. For each species two ranges of temperature were fit — 1000 - 7000°K and 5000°K - 18,000°K The overlapping of the temperature ranges was necessary to overcome accuracy limitations at the extremes of the fit.

Table C.1

POLYNOMIAL COEFFICIENTS FOR THERMODYNAMIC PROPERTY CORRELATIONS

Species	A1	A2	A3	A4	A5	A6	A7	T*
C+	0.2609E 01	-0.1393E-03	0.5359E-07	-0.1037E-10	0.6345E-15	0.2168E 06	0.3709E 01	L
	0.2528E 01	0.4969E-05	-0.7026E-09	0.1134E-11	-0.3476E-16	0.2168E 06	0.4133E 01	H
H	0.2500E 01	-0.8243E-06	0.6421E-09	-0.1720E-12	0.1457E-16	0.2547E 05	-0.4612E 00	L
	0.3034E 01	-0.1776E-02	0.6013E-06	-0.7819E-10	0.3482E-14	0.2547E 05	-0.8598E 01	H
N+	0.2727E 01	-0.2820E-03	0.1103E-06	-0.1551E-10	0.7847E-15	0.2254E 06	0.3645E 01	L
	0.2499E 01	-0.3725E-05	0.1147E-07	-0.1102E-11	0.3072E-16	0.2254E 06	0.4950E 01	H
O+	0.2491E 01	0.2762E-04	-0.1881E-07	0.3307E-11	-0.1028E-15	0.1879E 06	0.4424E 01	L
	0.2944E 01	-0.4108E-03	0.9156E-07	-0.5948E-11	0.1190E-15	0.1879E 06	0.1750E 01	H
E-	0.2500E 01	0.3440E-06	-0.1954E-09	0.3937E-13	-0.2573E-17	-0.7450E 03	-0.1173E 02	L
	0.2508E 01	-0.6332E-05	0.1364E-08	-0.1094E-12	0.2934E-17	-0.7450E 03	-0.1208E 02	H
C	0.2612E 01	-0.2030E-03	0.1095E-06	-0.1695E-10	0.8550E-15	0.8542E 05	0.4144E 01	L
	0.2141E 01	0.3219E-03	-0.5498E-07	0.3604E-11	-0.5564E-16	0.8542E 05	0.6874E 01	H
CN	0.3411E 01	0.4897E-03	0.1003E-06	-0.3473E-10	0.2361E-14	0.4745E 05	0.4746E 01	L
	0.3473E 01	0.7337E-03	-0.9088E-07	0.4847E-11	-0.1018E-15	0.5420E 05	0.4152E 01	H
CO	0.3254E 01	0.9698E-03	-0.2647E-06	0.3037E-10	-0.1177E-14	-0.1434E 05	0.4875E 01	L
	0.3366E 01	0.8027E-03	-0.1968E-06	0.1940E-10	-0.5549E-15	-0.1434E 05	0.4263E 01	H
C2	0.4443E 01	-0.2885E-03	0.3036E-06	-0.6244E-10	0.3315E-14	0.9787E 05	-0.1030E 01	L
	0.4026E 01	0.4657E-03	-0.7026E-07	0.4666E-11	-0.1142E-15	0.9787E 05	0.1030E 01	H
C2H	0.3485E 01	0.3563E-02	-0.1237E-05	0.1866E-09	-0.1013E-13	0.5809E 05	0.4784E 01	L
	0.5307E 01	0.8966E-03	-0.1378E-06	0.9251E-11	-0.2278E-15	0.5809E 05	-0.5288E 01	H

*Temperature Range L = 1000-6000°K, H = 6000-15,000°K

(continued)

Table C.1 (Cont'd)

Species	A1	A2	A3	A4	A5	A6	A7	T*
C2H2	0.3891E 01	0.5717E-02	-0.1957E-05	0.2931E-09	-0.1565E-13	0.2590E 05	0.6520E 00	L
	0.6789E 01	0.1503E-02	-0.2295E-06	0.1534E-10	-0.3763E-15	0.2590E 05	-0.1530E 02	H
C3	0.4002E 01	0.3541E-02	-0.1318E-05	0.2064E-09	-0.1144E-13	0.9423E 05	0.2020E 01	L
	0.2213E 02	-0.1759E-01	0.5565E-05	-0.6758E-09	0.2825E-13	0.9423E 05	-0.1021E 03	H
C3H	0.3365E 01	0.6200E-02	-0.2265E-05	0.3717E-09	-0.2262E-13	0.6283E 05	0.3467E 01	L
	0.3365E 01	0.6200E-02	-0.2265E-05	0.3717E-09	-0.2262E-13	0.6283E 05	0.3467E 01	H
C4H	0.5874E 01	0.7403E-02	-0.2729E-05	0.4437E-09	-0.2637E-13	0.7605E 05	-0.4010E 01	L
	0.5874E 01	0.7403E-02	-0.2729E-05	0.4437E-09	-0.2637E-13	0.7605E 05	-0.4010E 01	H
HCN	0.3654E 01	0.3444E-02	-0.1258E-05	0.2169E-09	-0.1430E-13	0.1442E 05	0.2373E 01	L
	0.3654E 01	0.3444E-02	-0.1258E-05	0.2169E-09	-0.1430E-13	0.1442E 05	0.2373E 01	H
H2	0.3358E 01	0.2794E-03	0.9372E-07	-0.2948E-10	0.2141E-14	-0.1018E 04	-0.3546E 01	L
	0.3363E 01	0.4656E-03	-0.5127E-07	0.2802E-11	-0.4905E-16	-0.1018E 04	-0.3716E 01	H
N	0.2474E 01	0.9097E-04	-0.7314E-07	0.2218E-10	-0.1485E-14	0.5609E 05	0.4300E 01	L
	0.2746E 01	-0.3909E-03	0.1338E-06	-0.1151E-10	0.3369E-15	0.5609E 05	0.2872E 01	H
C	0.2670E 01	-0.1970E-03	0.7193E-07	-0.8931E-11	0.4002E-15	0.2915E 05	0.4504E 01	L
	0.2548E 01	-0.5952E-04	0.2701E-07	-0.2738E-11	0.9380E-16	0.2915E 05	0.5049E 01	H
N2	0.3221E 01	0.9678E-03	-0.2907E-06	0.3938E-10	-0.2200E-14	-0.1043E 04	0.4320E 01	L
	0.3727E 01	0.4684E-03	-0.1140E-06	0.1154E-10	-0.3253E-15	-0.1043E 04	0.1294E 01	H
C2	0.3416E 01	0.1151E-02	-0.3726E-06	0.6186E-10	-0.3666E-14	-0.1044E 04	0.5393E 01	L
	0.3721E 01	0.4254E-03	-0.2835E-07	0.6600E-12	-0.5186E-17	-0.1044E 04	0.3254E 01	H

*Temperature Range   L = 1000-6000°K, H = 6000-15,000°K

REFERENCES

C.1 Esch, D. D., "Stagnation Region Heating of a Phenolic-Nylon Ablator During Return from Planetary Missions," Ph.D. Dissertation, Louisiana State University, Baton Rouge, Louisiana (1971).

APPENDIX D

USERS INSTRUCTIONS FOR CRAC COMPUTER PROGRAM

Introduction

The purpose of this appendix is to describe the procedure for using the Coupled, Radiating, and Chemically reacting shock layer computer program (CRAC). This program consists of a numerical solution of the viscous thin shock layer equations presented in Chapter III coupled to a phenolic nylon ablator by the equations presented in Appendix A. A general description of the overall logic and the details of the numerical solutions were given in Chapter V.

The program CRAC has been written in such a way that a minimum of input is required for the solution of any given problem. The required input is a specification of freestream velocity, freestream density, and body nose radius. From this input, the flow field profiles are calculated for a blowing rate of 5% of freestream. A namelist option is provided in the input which allows the specification of a number of critical variables (such as blowing rate, surface temperature, etc.) and critical profiles if the user has a good idea of their values. If no value is input, the program internally estimates all variables and profiles.

The program outputs boundary condition information at wall and shock including ablator heating response for the assumed blowing rate. The shock layer solution provides temperature, pressure, density, velocity, species fractions, and radiative flux divergence profiles along with flow field physical property profiles of thermal conductivity, viscosity and heat capacity. The heat flux from shock layer to ablator surface is also output for comparison with the ablator heating response. The ablator heating response is calculated by the program using the analysis and results presented in Appendices A and B. When these are equal, the solution has been coupled as discussed in Chapter V.

CRAC has been set up to be as versatile as possible with subroutines that can be altered or replaced to provide more sophistication, different ablators, different atmospheres, etc. For instance, if a different ablator is desired, subroutine BCWALL can be replaced to reflect the material response for the new ablator. If a different body shape is needed (the assumed shape is spherical), subroutine SHAPE can be replaced. The subroutines are listed below with their description which may require alteration for application to a different system.

BCWALL - Wall boundary conditions (a function of the ablator)

BLOCK DATA - Species, thermodynamic, and transport property fits, and initial guesses

FGH - Finite difference method

FG2 - Kinetic production rates of species (chemical reactions)

GAS - Freestream gas equilibrium model

LRAD - Radiation properties of flow field species

SHAPE - Body shape

The program solves the shock layer equations about a blunt body and always starts at $\xi = 0$, the stagnation line. The program will handle solutions in an arbitrary freestream where the velocity, density, and species mass fraction define the environment.

In the iteration procedure employed to obtain the initial profiles, the stagnation line momentum is solved first. followed by an iteration on the species equations. The energy equation is not solved in this initialization step. This iteration is stopped when NOE iterations (internally set at NOE = 50 but can be changed by namelist option) have been performed. The solution then proceeds to the stagnation line iteration scheme. The radiative flux divergence is solved first using the initial profiles. Then MI iterations (internally set at MI = 5) are performed on the shock layer stagnation line equations using the initial profiles from above. An iteration of the species equations within this larger iteration is possible depending on the value of MIS (internally set at MIS = 5).

In the iteration procedure it is often necessary to weigh the calculated solution with the assumed solution as was discussed in Chapter V. The damping values used for this are HDAMP for enthalpy, TDAMP for termperature, CDAMP for mass fractions, FDAMP for the momentum solution, and DDAMP for the transformed shock stand off distance, $\tilde{\delta}$. The appropriate values to employ depend on the case being run and can be determined only from experience. Internally set values are given in Table D.1.

A description of input variables is given in Table D.1 and a brief description of each of the subprograms included in the computer code is given in Table D.2. Finally, a diagram of the program overlay structure used on the IBM system 360/65 is presented in Figure D.1

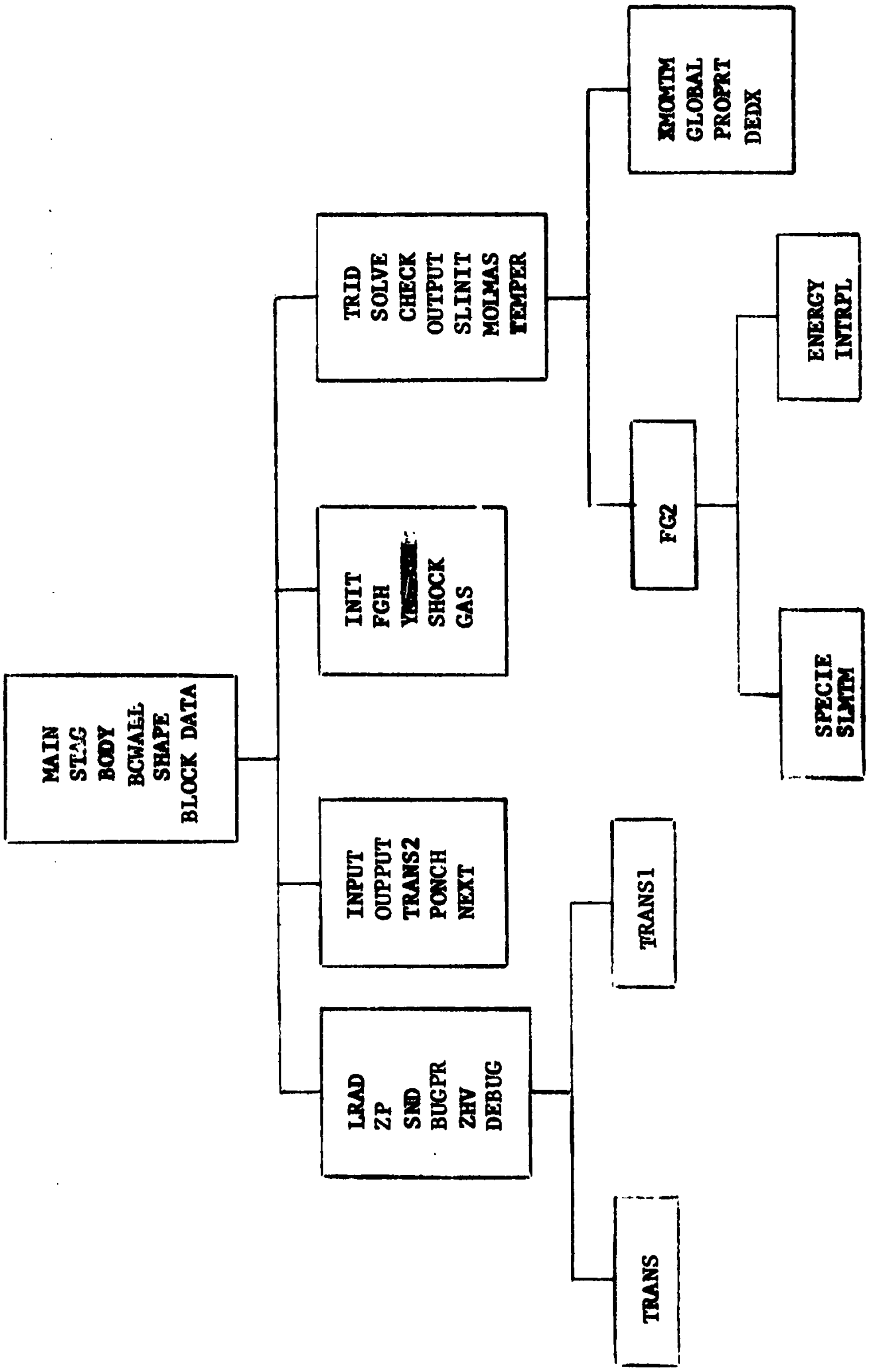
MAIN
STAG
BODY
BCWALL
SHAPE
BLOCK DATA
LRAD
ZP
SND
BUGPR
ZHV
DEBUG
INPUT
OUPPUT
TRANS2
PONCH
NEXT
INIT
FGH
SHOCK
GAS
TRID
SOLVE
CHECK
OUTPUT
SLINIT
MOLMAS
TEMPER
TRANS
TRANS1
FG2
SPECIE
SLMTM
ENERGY
INTRPL
XMOMTM
GLOBAL
PROPRT
DEDX

Figure D.1. CRAC overlay Structure

which reduces considerably the core requirements (from 250K bytes down to 186K bytes). This overlay allows the whole program to be run totally in high speed core.

Table D.1

CRAC Input Variables

CARD I

Title Card

Fortran Variable	Format	Columns	Description
TITLE	18A4	1-72	Any description information desired

CARD 2

Fortran Variable	Format	Columns	Description
UINF	E10.1	1-10	Freestream velocity in ft/sec
RINF	E10.1	11-20	Freestream density in slugs/ft^3
R	E10.1	21-30	Body radius, ft.
ISTART	I5	31-35	Program code 0 = initial start-up at stagnation line using only namelist input 1 = initial start-up at stagnation line using input deck from another run 2 = continuation of stagnation line solution using punched data deck 3 = around the body solution using punched, converged stagnation line solution data

Table D.1 (continued)

Namelist Option

Variable	Variable Type	
NETA	Integer	Number of points along the coordinate normal to the body [59]*
MI	Integer	Number of iterations made with conservation equations for each pass through LRAD radiation flux divergence calculation [5]
MIS	Integer	Number of internal iterations on the species equations [5]
MAXE	Integer	Maximum number of iterations for enthalpy-temperature calculation [10]
MAXM	Integer	Maximum number of iterations for the momentum equation [10]
NTIME	Integer	Minutes of CPU time remaining when user wishes to have program stop and punch output deck [0]
IDGD	Integer	Debug printout on $\tilde{\delta}$ [0] 0 = no output (defalut value) 2 = debug output
IDGF	Integer	Debug printout on x-momentum equation [0]
IDGH	Integer	Debug printout on enthalpy equation [0]
IDGT	Integer	Debug printout on temperature equation [0]
IDGS	Integer	Debug printout on species equation [0]
IDEBUG	Integer	Debug printout on stagnation line x-momentum equation [0]
CDAMP	Real	Damping coefficient for species [1.0]
DDAMP	Real	Damping coefficient for $\tilde{\delta}$ [0.5]
HDAMP	Real	Damping Coefficient for enthalpy [0.5]

*[] Default value internally set

Table D.1 (continued)

Variable	Variable Type	
TDAMP	Real	Damping coefficient for temperature [0.25]
TPRCT	Real	Convergence tolerance on enthalpy-temperature calculation [0.01]
FPRCT	Real	Convergence tolerance on stagnation x-momentum equation [0.005]
PDTIL	Real	Convergence tolerance on $\tilde{\delta}$ [0.001]
TWOLD	Real	Estimate of surface temperature, °K [3600°K]
RVW	Real	Ablator blowing rate [0.05]
CWALL	Real Vector	Species mass fractions at ablator surface
RVN	Real Vector	Estimate of blowing rate around the body normalized to the stagnation value
DXI	Real	Tangential coordinate stepsize [0.05]
ETA	Real Vector	Normal coordinate nodal points
T	Real Vector	Estimate of temperature profile
IAB	Integer	Number of points in vectors RVN and EPSN [20]
EPSN	Real Vector	Estimate of ε profile around the body
XIN	Real Vector	Coordinate points for EPSN and RVN

Table D.2

Description of CRAC Subroutines

Subroutine	Description
MAIN	Driver Program
INPUT	Reads in all necessary data
STAG	Driver program for stagnation line solution
SLINIT	Initialization routine for stagnation line
BODY	Driver program for around the body solution
SHAPE	Routine to calculate body and shock angles for a specified body shape (spherical)
BCWALL	Calculates ablator surface temperature, and ablator surface heating for a specified blowing rate and wall pressure
SHOCK	Calculates density ratio at the shock, shock temperature, pressure, and species mass fractions
GLOBAL	Routine to solve the global continuity equation around the body
SLMTM	Solution of the stagnation line x-momentum equation
XMOMTM	Solution of the around the body x-momentum equation
YMOMTM	Solution of the y-momentum equation
SPECIE	Solution of the species equations
ENERGY	Solution of the energy equation in enthalpy form
TEMPR	Temperature-enthalpy iteration to obtain temperature profile from the enthalpy profile
DEDX	Calculation of shock standoff distance, δ and $\partial n/\partial x$
MOLMAS	Changes species concentration from moles i/mass total to mass fraction and vice versa
GAS	Calculates chemical equilibrium for air species along with thermodynamic and transport properties

Table D.2 (continued)

Subroutine	Description
FG2	Calculates chemical production terms and linearized chemical production terms for species conservation equation
LRAD, TRANS, SND, ZP, BUGPR, ZHV, & TRANS 1, TRANS 2	Calculates radiative flux divergence for specified temperature, pressure, and composition profiles
SOLVE	Takes α coefficients calculated in conservation subroutines XMOMTM, SPECIE, and ENERGY and sets up tradiagonal matrix for TRID
TRID	Solves the tridiagonal matrix
FGH	Finite difference coefficients
CHECK	Routine to check for converged solutions of profiles
INTRPL	Lagrange interpolation scheme
OUPPUT	Prints output for shock layer solution
OUTPUT	Debug output of intermediate profiles
PONCH	Punches solution on cards
BLOCK DATA	Contains thermodynamic and transport property data along with initialization data

APPENDIX E

CRAC SOURCE DECK, SAMPLE INPUT, AND SAMPLE OUTPUT

```
C                         C R A C
C
C     COUPLED RADIATING AND CHEMICALLY REACTING SHOCK LAYER
C           BY  JOHN FREDERICK BALHOFF          FEB  1975
C
C          AROUND  THE  BODY  SOLUTION
C
C
      CALL  INPUT
      CALL  INIT
      CALL  STAG
      CALL  BODY
      CALL  EXIT
      END
      SUBROUTINE INIT
C
      COMMON/HOFF1/F1( 60).F2( 60).G1(60).G2(60) .H1 (60).H2(60)
      COMMON /FRSTRM/ U INF. RINF. UINF2. R . RE. LXI. ITM. IEM. NETA
      COMMON/PROP1/PI( 60).RHO( 60).  T(60).AMW(60).C  (20.60).EC(5.60)
      COMMON/NUMBER/NSP.NNS.NE.NC
      COMMON /NON/RDZ.MUDZ.RMDZ.AKNF.HNF.CPNF
      COMMON/MIKE/ NETA1.NETA2.PNF.WNF.RHOD.DP.TS.UD.VD.RW.RWO.EPS,PHI
      COMMON /BILL/ KODE(20).KOPT(10).CSHOCK(20)
      COMMON /VEL/  F(60).FC( 60).Z(60).V(60)
      COMMON /DEL/  DELTA.DTIL.DTILS
      COMMON /DICK/  Q( 60).QD(60)
      COMMON/EQ2/AA( 20.5).ICODE(20)
      COMMON/EQ3/IA( 20.5)
C
      NETA1=NETA-1
      NETA2=NETA-2
      UINF2 = UINF*UINF
      PNF=2116./RDZ/UINF2
      WNF   = R/UINF
      RHOD=RDZ*32.174
      DO 5 K=1.NSP
      C(K.NETA) = CSHOCK(K)
    5 CONTINUE
      CALL RADIN
      DO15 M=1.NE
      DO15 I=1.NSP
      AA(I.M) = IA(I.M)
   15 CONTINUE
      Q(1) = 0.0
      Q(NETA) = 1.0
      DO 35 J=2.NETA1
      Q(J) = Z(J-1)*DTIL
      CALL FGH (J.F1(J).G1(J).H1(J))
      CALL FGH2(J.F2(J).G2(J).H2(J))
   35 CONTINUE
```

```
      RETURN                                                            INIT 370
      END                                                               INIT 380
      SUBROUTINE INPUT
C
C
C     **  ROUTINE TO READ AND PRINT ALL INPUT DATA  **
C
C
      COMMON /CONV/ FPRCT,TPRCT,DDAMP,TDAMP,PDTIL
      COMMON/CONV1/HDAMP,FDAMP,CDAMP
      COMMON /DEL/ DELTA,DTIL,DTILS
      COMMON /FRSTRM/ U INF, RINF, UINF2, R , RE, LXI, ITM, IEM, NETA
      COMMON /MAIM/KEEP,MAXE,MAXM,MAXD,IDEBUG,MCONV,ECONV,DCONV,LT,IAB
      COMMON /NON/RDZ,MUDZ,RMDZ,AKNF,HNF,CPNF
      COMMON/PROP1/PI(60),RHO(60), T(60),AMW(60),C (20,60),CC(5,60)
      COMMON/PROP2/  MU(60),RM(60), AK(60)
      COMMON/PROP3/CPS(20,60),HS(20,60),CP (60),HM(60)
      COMMON /RFLUX/ E(60),IRAD,ITYPE
      COMMON /VEL/ F(60),FC(60),Z(60),V(60)
      COMMON /RH/ DUD,DPHI,TD,RZB,PD,HD,HTOTAL
      COMMON/WALL/RVW,PRW,TWOLD,FLUX(20),CWALL(20),ECWALL(5)
      COMMON /YL/ETA(60),YOND(60)
      COMMON/TIT/TITLE(18)
C
C
      COMMON/EQ1/AI(20), BI(20), CI(20), DI(20), EI(20), FI(20), GI(20),
     X           AII(20),BII(20),CII(20),DII(20),EII(20),FII(20),GII(20)
      COMMON/EQ2/AA(20,5),ICODE(20)
      COMMON/EQ3/IA(20,5)
      COMMON/ID/SP(20),EL(5)
      COMMON/WT/SMW(20),AWT(5)
      COMMON/NUMBER/NSP,NNS,NE,NC
      COMMON/SP1/SS,TOL,NDBUG
      COMMON/JFB/ IPN
      COMMON/MIKE/ NETA1,NETA2,PNF,WNF,RHOD,DP,TS,UD,VD,RW,RWO,EPS,PHI
      COMMON/JOHN/ UO(60),U(60),DU(60),VO(60),RO(60),DNDX(60),DTLA,DTILO
      COMMON /BILL/ NODE(20),ISTART,IDGD,IDGF,IDGH,IDGT,IDGS,
     X  MI,NOE,NTIME,MIS
```

```
      COMMON/GUESS/TG1(60),TG2(60)                                      INPU 370
      COMMON/BOB/ XI,DXI,YL                                             INPU 380
      COMMON /GEORGE/ EPSN(30),XIN(30),QWN(30)                          INPU 390
C                                                                       INPU 400
      REAL  MU,MUDZ                                                     INPU 410
      LOGICAL MCONV,ECONV,DCONV                                         INPU 420
      DATA END /'END '/                                                 INPU 430
      NAMELIST/ENTRY/ NETA,TS,RW,EPS,IRAD,IDEBUG,TG2,IDGD,IDGF,IDGH,    INPU 440
     X     IDGT,IDGS,RVW,MAXE,TWOLD,CC,TOL,CWALL,ISTART,MI,NOE,NTIME,MISINPU 450
     X    ,HDAMP,TDAMP,CDAMP,XIF,XIN,EPSN,QWN,IAB,DXI,ETA               INPU 460
C                                                                       INPU 470
C     **  INPUT  FORMATS  **                                            INPU 480
C                                                                       INPU 490
  100 FORMAT (18A4,2I4)                                                 INPU 500
C CARD 1 -------------------------------------------------------------- INPU 510
      READ (5,100) TITLE                                                INPU 520
      READ(5,10) UINF,RINF,R,ISTART                                     INPU 530
   10 FORMAT(3E10.3,I5)                                                 INPU 540
      IF (ISTART .EQ. 0) GO TO 1000                                     INPU 550
C        ****    RE-START    ****                                       INPU 560
C                                                                       INPU 570
      READ(5,1801)  FPRCT,TPRCT,DDAMP,TDAMP,PDTIL,HDAMP                 INPU 580
      READ(5,1801) DELTA,DTIL,DTILS                                     INPU 590
      READ(5,1802)     U INF, RINF, UINF2, R  , RE, ITM, IEM, NETA      INPU 600
      READ(5,1803) KEEP,MAXE,MAXM,MAXD,IDEBUG,MCONV,ECONV,DCONV,LT,IAB  INPU 610
      READ(5,1801)RDZ,MUDZ,RMDZ,AKNF,HNF,CPNF                           INPU 620
      READ(5,1804)  NSP,NNS,NE,NC                                       INPU 630
      READ(5,1801) (PI(J),RHO(J),T(J),J=1,NETA)                         INPU 640
      READ (5,1801)(AMW(J),J=1,NETA)                                    INPU 650
      READ(5,1801) ((C(I,J),J=1,NETA),I=1,NSP)                          INPU 660
       READ(5,1801)( HM(J),J=1,NETA)                                    INPU 670
      READ(5,1801)  (E(J),J=1,NETA)                                     INPU 680
      READ(5,1804) IRAD,ITYPE                                           INPU 690
      READ(5,1801)DUD,DPHI,TD,RZB,PD,HD,HTOTAL                          INPU 700
      READ (5,1801)(F(J),FC(J),Z(J),V(J),J=1,NETA)                      INPU 710
      READ(5,1801)RVW,PRW,TWOLD                                         INPU 720
      READ(5,1801) (CWALL(I),I=1,NSP)                                   INPU 730
      READ(5,1801) (ECWALL(K),K=1,NE)                                   INPU 740
      READ(5,1801) (ETA(J),YOND(J),J=1,NETA)                            INPU 750
       READ(5,715)NDBUG,IAB,TOL                                         INPU 760
      READ (5,1801)((CC(K,J),J=1,NETA),K=1,NE)                          INPU 770
      READ(5,1801) XI,RW,TS,U(NETA)                                     INPU 780
 1801 FORMAT(6E13.5)                                                    INPU 790
 1802 FORMAT(5E12.5,3I3)                                                INPU 800
 1803 FORMAT(5I5,3L3,2I5)                                               INPU 810
 1804 FORMAT(4I4)                                                       INPU 820
  715  FORMAT(2I5,E15.6)                                                INPU 830
C                                                                       INPU 840
 1000 READ(5,ENTRY)                                                     INPU 850
C                                                                       INPU 860
C         ****    PRINT DATA    ****                                    INPU 870
C                                                                       INPU 880
      RETURN                                                            INPU 890
      END                                                               INPU 900
      SUBROUTINE STAG
C
      COMMON /FRSTRM/ U INF, RINF, UIMF2, R , RE, LXI, ITM, IEM, NETA
      COMMON/NUMBER/NSP,NNS,NE,NC
      COMMON/BOB/ XI,DXI,YL
      COMMON /BILL/ NODE(20),ISTART,IDGD,IDGF,IDGH,IDGT,IDGS,
     X  MI,NOE,NTIME,MIS
C
      IF( ISTART .GT. 2) RETURN
      CALL  SHAPE
      CALL  SHOCK
      CALL  BCWALL
      CALL  SLINIT
      CALL  NEXT
    1 CONTINUE
      CALL  PROPRT (NSP,1,NETA)
      CALL  LRAD
      DO 100 IEM=1,MI
      CALL  SLMTM
      DO 15 I=1,MIS
      CALL  SPECIE (KODS)
   15 CONTINUE
      CALL  PROPRT (NSP,1,NETA)
      CALL  ENERGY (KODE)
      IF(KODS.GT.3 .AND. KODE.GT.4) GO TO 1000
  100 CONTINUE
 1000 CALL  GUPPUT (N)
      GO TO 1
      END
      SUBROUTINE BODY
      COMMON/BOB/ XI.DXI.YL
      COMMON/NUMBER/NSP.NNS.NE.NC
      COMMON /FRSTRM/ U INF. RINF. UINF2. R . RE. LXI. ITM. IEM. NETA
      COMMON /BILL/ NODE(20).ISTART.IDGD.IDGF.IDGH.IDGT.IDGS.
     X  MI.NOE.NTIME.MIS
    1 CONTINUE
      XI = XI + DXI
      CALL SHAPE
      CALL SHOCX
      CALL BCWALL
      CALL NEXT
      CALL CEDX
      CALL YMOMTM
    2 CONTINUE
      CALL PROPRT (NSP.1.NETA)
      CALL LRAD
      DO 100 IEM=1.MI
    6 CONTINUE
      YL=0.5
      CALL XMOMTM (KODE)
      CALL YMOMTM
      YL = 1.0
      CALL GLOBAL (KOD )
      IF(KOD .LT. 5 .OR. KODE .LT. 5) GO TO 6
      YL=1.0
      DO 25 I=1.MIS
      CALL SPECIE (KODS)
   25 CONTINUE
      CALL PROPRT (NSP.1.NETA)
      CALL ENERGY (KODT)
      IF(KODS.GT.3 .AND. KODT.GT.4) GO TO 1000
  100 CONTINUE
C
C
 1000 CALL OUPPUT (N)
```

```
      GO TO (1,2), N                                                    BODY 370
      END                                                               BODY 380
      SUBROUTINE NEXT
C
C        ROUTINE TO DETERMINE GUESSES FOR PROFILES AT THE M + 1
C        BODY STATION USING THE PROFILES AT THE MTH STATION
C
      COMMON/TOM/ SC(60),TO(60),PR(60),TE(60)
      COMMON/JTB/ CO(60,20),RED,RED2
      COMMON/NUMBER/NSP,NNS,NE,NC
      COMMON/PROP1/PI(60),RHO(60), T(60),AMW(60),C (20,60),EC(5,60)
      COMMON /RH/ DUD,DPHI,TD,RZB,PD,HD,MTOTAL
      COMMON /FRSTRM/ U INF, RINF, UINF2, R , RE, LXI, ITM, IEM, NETA
      COMMON/MIKE/ NETA1,NETA2,PNF,WNF,RHOD,DP,TS,UD,VD,RW,RWO,EPS,PHI
      COMMON /VEL/ F(60),FC(60),Z(60),V(60)
      COMMON/JOHN/ UO(60),U(60),DU(60),VO(60),RO(60),DNDX(60),DTLA,DTILO
      COMMON /DEL/ DELTA,DTIL,DTILS
      COMMON /YL/ETA(60),YOND(60),YO(60)
      COMMON /RFLUX/ E(60),IRAD,ITYPE
      COMMON/DON/ PO(60),EO(60),HMO(60)
      COMMON/PROP3/CP(20,60),H(20,60),CPM(60),HM(60)
      COMMON /DICK/ Q(60),QO(60)
      COMMON/WALL/RVW,PRW,TWOLD,FLUX(20),CWALL(20),ECWALL(5)
C
      DTILO = DTIL
      DTLA=DTIL
      T1 = TWOLD/TS
      TDO = T(NETA)*TS
      TW = T(1)
      TWO = TW*TS
      RHO1 = PI(1)*AMW(1)/TWOLD/1.3157/32.174
      V1 = RVW*RINF/RHO1
      VDO = V(NETA)
      VO1 = V(1)
      FP = 0.0
      DO 5 I=1,NETA
      TO(I)=T(I)
      QO(I) =Q(I)
      UD(I) = FP*U(NETA)                                                NEXT 370
      U(I) = FP*UD                                                      NEXT 380
      FP = Z(I)*DTIL                                                    NEXT 390
      IF (I.EQ.NETA-1) FP = 1.0                                         NEXT 400
      T(I) = T1 + (T(I)-TW) * (TD-TWOLD) / (TDO-TWO)                    NEXT 410
      TE(I)=T(I)                                                        NEXT 420
      RO(I) = RHO(I)                                                    NEXT 430
      VO(I) = V(I)                                                      NEXT 440
      V(I) = V1 + (V(I)-VO1)*(VD-V1)/(VDO-VO1)                          NEXT 450
      HMO(I) = HM(I)                                                    NEXT 460
      PO(I) = PI(I)                                                     NEXT 470
      EO(I) = E(I)                                                      NEXT 480
      YO(I) = YOND(I)                                                   NEXT 490
      DO 5 J=1.NSP                                                      NEXT 500
      CO(I.J) = C(J.I)                                                  NEXT 510
    5 CONTINUE                                                          NEXT 520
      RETURN                                                            NEXT 530
      END                                                               NEXT 540
      SUBROUTINE SHAPE                                                  SHAP  10
      COMMON/JOHN/ UD( 60).U(60).DU(60).VD(60).RD(60).DNDX(60).DTLA.DTILOSHAP  20
      COMMON /FRSTRM/ U INF. RINF. UINF2. R . RE. LXI. ITM. IEM. NETA   SHAP  30
      COMMON/PROP1/PI(60).RHO(60). T(60).AMW(60).C (20.60).EC(5.60)     SHAP  40
      COMMON /DEL/ DELTA.DTIL.DTILS                                     SHAP  50
      COMMON /YL/ETA(60).YOND(60).YD(60)                                SHAP  60
      COMMON/MIKE/ NETA1.NETA2.PNF.WNF.RHOD.DP.TS.UD.VD.RW.RWD.EPS.PHI  SHAP  70
      COMMON/BOB/ XI.DXI.YL                                             SHAP  80
      COMMON /MAIN/KEEP.MAXE.MAXM.MAXD.IDEBUG.MCONV.ECONV.DCONV.LT.IAB  SHAP  90
      COMMON /GEORGE/ EPSN(30).XIN(30).RVN(30)                          SHAP 100
      DATA DELT /0.0/                                                   SHAP 110
      EPS=0.0                                                           SHAP 120
      IF(XI .EQ. 0.0) GO TO 20                                          SHAP 130
      DTHT = 0.025                                                      SHAP 140
      DTHT = .01                                                        SHAP 150
      XID = XI - DXI                                                    SHAP 160
      IF(DELT .EQ.0.0) DELT = DELTA                                     SHAP 170
      DELTO = DELT                                                      SHAP 180
    1 XIDA = XID + DTHT/2.                                              SHAP 190
      CALL  INTRPL (XIDA.XIN.EPSN.IAB.EPS)                              SHAP 200
      DELT = DELT + DTHT*TAN(EPS)                                       SHAP 210
      XID = XID + DTHT                                                  SHAP 220
      IF(XID .LE. XI) GO TO 1                                           SHAP 230
      DTHT = XI - XID                                                   SHAP 240
      XIDA = XID + DTHT/2.                                              SHAP 250
      CALL  INTRPL (XIDA.XIN.EPSN.IAB.EPS)                              SHAP 260
      DELT = DELT + DTHT*TAN(EPS)                                       SHAP 270
      CALL  INTRPL (XI  .XIN.EPSN.IAB.EPS)                              SHAP 280
      WRITE (6.100) DELT.DELTA.EPS                                      SHAP 290
  100 FORMAT(5X.'DELTA (GEO) ='.F10.7.5X.'DELTA (FF) ='.F10.7.5X.'EPS (RSHAP 300
     XAD) ='.F10.7)                                                     SHAP 310
      DO 5 I=1.NETA                                                     SHAP 320
      DNDX(I) = RHO(I)/DTIL*( YOND(I)*(DELT - DELTO)/DELTA/DXI)         SHAP 330
    5 CONTINUE                                                          SHAP 340
   20 CONTINUE                                                          SHAP 350
      PHI = XI - EPS                                                    SHAP 360
      THT = XI                                                          SHAP 370
      RWC = RW                                                          SHAP 380
      RW  = SIN(THT)                                                    SHAP 390
      RETURN                                                            SHAP 400
      END                                                               SHAP 410
      SUBROUTINE SHOCK
C
C        THIS SUBROUTINE DETERMINES THE BOUNDARY CONDITIONS AT THE
C        SHOCK USING THE RANKINE HUGONIOT RELATIONS
C
      COMMON /RH/ DUD,DPHI,TD,RZB,PD,HD,HTOTAL
      COMMON/BOB/ XI,DXI,YL
      COMMON /FRSTRM/ U INF, RINF, UINF2, R , RE, LXI, ITM, IEM, NETA
      COMMON/PROP1/PI(60),RHO(60), T(60),AMW(60),C (20,60),EC(5,60)
      COMMON /NON/RDZ,MUDZ,RMDZ,AKNF,HNF,CPNF
      COMMON/MIKE/ NETA1,NETA2,PNF,WNF,RHOD,DP,TS,UD,VD,RW,RWO,EPS,PHI
      COMMON/TIT/TITLE(18)
C
C        CALCULATION OF PRESSURE AND ENTHALPY FROM R-H RELATIONS
C
      PD = PD
      ITER = 0
    1 PD = (1.-RZB)*COS(PHI)**2*RINF*UINF2/2116.
      PI(NETA) = PD
      VD= SIN(PHI)*SIN(EPS) - RZB*COS(PHI)*COS(EPS)
      UD= SIN(PHI)*COS(EPS) + RZB*COS(PHI)*SIN(EPS)
      HD = (1.-RZB*RZB)*COS(PHI)**2*UINF2/(2.*778.*32.174)
      HD = (1. - UD*UD - VD*VD)*UINF2/(2.*778.*32.174)
      CALL GAS (NETA)
      RZB1 = RINF/RDZ/RHO(NETA)
      TEST = ABS((RZB-RZB1)/RZB)
      IF(TEST.LT.0.005) GO TO 1000
      ITER = ITER + 1
      IF( ITER .GT. 10) GO TO 1000
      RZB = (RZB+RZB1)/2.
      GO TO 1
C
 1000 CONTINUE
      RZB = (RZB + RZB1)/2.
C
C        CONVERGED ON DENSITY RATIO (RZB)
```

```
C        NOW CALCULATE VELOCITIES FROM R-H RELATIONS                    SHOC 370
C                                                                       SHOC 380
C                                                                       SHOC 390
C        CALCULATE SPECIES COMPOSITION AT SHOCK THRU CHEMEQ             SHOC 400
C                                                                       SHOC 410
      WRITE(6.130) TITLE                                                SHOC 420
      WRITE(6.135) XI                                                   SHOC 430
      WRITE(6.140)                                                      SHOC 440
      WRITE(6.150) TD.VD.PD.UD.PHI.EPS                                  SHOC 450
  130 FORMAT('1'.///.18A4.6(/))                                         SHOC 460
  135 FORMAT(20X.'BOUNDARY CONDITIONS AT     XI  ='.F6.2.///)           SHOC 470
  140 FORMAT('0'.48X.'BOW SHOCK CONDITIONS'.//)                         SHOC 480
  150 FORMAT(20X.'SHOCK TEMPERATURE (OK)    ='.F10.0.8X.                SHOC 490
     X   'NORMAL VELOCITY          ='.F10.4./.                          SHOC 500
     X        20X.'SHOCK PRESSURE (ATM)     ='.F10.4.8X.                SHOC 510
     X   'TANGENTIAL VELOCITY      ='.F10.4./.                          SHOC 520
     X        20X.'SHOCK ANGLE. PHI (RAD)   ='.F10.4.8X.                SHOC 530
     X   'ANGLE EPS (RAD)          ='.F10.4./////)                      SHOC 540
      RETURN                                                            SHOC 550
      END                                                               SHOC 560
      SUBROUTINE BCWALL
C
C        THIS SUBROUTINE CALCULATES BLOWING RATE AT THE ABLATOR SURFACE
C        FOR A GIVEN SURFACE TEMPERATURE AND PRESSURE
C
      COMMON /BILL/ NODF(20),ISTART,IDGD,IDGF,IDGH,IDGT,IDGS,
     X  MI,NOF,NTIME,KOPT
      COMMON/MIKE/ NETA1,NETA2,PNF,WNF,RHOD,DP,TS,UD,VD,RW,RWO,EPS,PHI
      COMMON /YL/ETA(60),YOND(60)
      COMMON/WALL/RVW,PRW,TWOLD,FLUX(20),CWALL(20),ECWALL(5)
      COMMON /VEL/ F(60),FC(60),Z(60),V(60)
      COMMON/PROP1/PI(60),RHO(60), T(60),AMW(60),C (20,60),CC(5,60)
      COMMON /FRSTRM/ U INF, RINF, UINF2, R , RE, LXI, ITM, IEM, NETA
      COMMON /NON/RDZ,MUDZ,RMDZ,AKNF,HNF,CPNF
      COMMON /DEL/ DELTA,DTIL,DTILS
      COMMON /MAIM/KEEP,MAXE,MAXM,MAXD,IDEBUG,MCONV,ECONV,DCONV,LT,IAB
      COMMON/BOB/ XI,DXI,YL
      COMMON /GEORGE/ EPSN(30),XIN(30),RVN(30)
      DIMENSION A(3),D(3),E(3),XMW(3)
      DATA A /0.37,0.34,0.08/
      DATA XMW/12.,24.,36./
      DATA D  /8.21,9.64,10.25/
      DATA E  /-3.75,-4.27,-4./
      DATA EP,RR,AM/0.8,1.215E-4,13.3/
      DATA A1,A2,A3,A4 /1.674065E-8,-.333005F-3,10.99963E-8,2731.659/
C
      TL  =0.0
      TW  =TWOLD
      NETA1 = NETA - 1
C
C        INITIAL GUESS FOR BLOWING RATE OF CARBON SOLID
      IF (XI .EQ. 0.0) PRW = RVW
      CALL INTRPL (XI,XIN,RVN,IAD,RVW)
      RVW = RVW * PRW
      RVCC = RVW*RINF*UINF*32.174 * 0.4328
C
```

```
C         CALCULATION OF SURFACE PRESSURE FROM YMCMTM EQ.                BCWA 370
C                                                                        BCWA 380
      P = PI(NETA)                                                       BCWA 390
      IF (ISTART .LT. 3) GO TO 1                                         BCWA 400
      FP = DTIL                                                          BCWA 410
      DO 15 I=1,NETA1                                                    BCWA 420
      J = NETA - I                                                       BCWA 430
      DETA = ETA(J+1) - ETA(J)                                           BCWA 440
      P = P - DTIL *(FP*UD)**2*DETA/PNF                                  BCWA 450
      IF(J .GT. 1) FP = Z(J-1)*DTIL                                      BCWA 460
   15 CONTINUE                                                           BCWA 470
C                                                                        BCWA 480
    1 RVC =0.0                                                           BCWA 490
      PI(1) = P                                                          BCWA 500
      RV = RVCC/.4328                                                    BCWA 510
      DO 5 I=1,3                                                         BCWA 520
      PVP = 10.**(D(I) + E(I)/TW*1.E4)                                   BCWA 530
      EVP = A(I)*(1. - FP)*SQRT(XMW(I)/RR/TW)                            BCWA 540
      BT  = AM*P/XMW(I)                                                  BCWA 550
      CG  = EVP/(RV + BT*EVP)*PVP                                        BCWA 560
      RVC = RVC + RV*CG                                                  BCWA 570
    5 CONTINUE                                                           BCWA 580
C                                                                        BCWA 590
C         CHECK TO SEE IF HERTZ-KNUDSEN EQ. IS CONVERGED                 BCWA 600
C                                                                        BCWA 610
      ABD =      (RVCC - RVC)/RVCC                                       BCWA 620
      ABSD = ABS(ABD)                                                    BCWA 630
      IF(ABSD .LT. 0.001) GO TO 20                                       BCWA 640
      IF ( TL .GT. 0.0 ) GO TO 10                                        BCWA 650
      TL = TW                                                            BCWA 660
      RVCL = RVC                                                         BCWA 670
      TW = TW + 10.*ABD/ABSD                                             BCWA 680
      GO TO 1                                                            BCWA 690
   10 TWOLD = TW                                                         BCWA 700
      TW = TW + (TW-TL)/(RVC-RVCL)*(RVCC-RVC)                            BCWA 710
      TL = TWOLD                                                         BCWA 720
      RVCL = RVC                                                        BCWA 730
      GO TO 1                                                           BCWA 740
   20 TWOLD = TW                                                        BCWA 750
C                                                                       BCWA 760
C        CALCULATE HEAT ABSORBED & RERADIATED BY ABLATOR                BCWA 770
C                                                                       BCWA 780
      T3 = TW*TW*TW                                                     BCWA 790
      SRV = SQRT(RV)                                                    BCWA 800
C        HEAT ABSORBED BY CARBON SUBLIMING (BTU/FT2-SEC)                BCWA 810
C                                                                       BCWA 820
      QSUBL = 4440.*RV                                                  BCWA 830
C                                                                       BCWA 840
C        HEAT CONDUCTED THRU CHAR (BTU/FT2-SEC)                         BCWA 850
C                                                                       BCWA 860
      QCOND = A1*RV*T3 + A2*SRV*TW*TW + A3*SRV*T3 + A4*RV               BCWA 870
C                                                                       BCWA 880
C        ENERGY RERADIATED BY CHAR SURFACF WITH FMISSIVITY OF C.66      BCWA 890
C                                                                       BCWA 900
      QRR   = 3.3E-12*T3*TW                                             BCWA 910
C                                                                       BCWA 920
C        TOTAL HEAT FLUX ACCOMODATED BY ABLATOR (BTU/FT2-SEC)           BCWA 930
C                                                                       BCWA 940
      QT = QCOND + QRR + QSUBL                                          BCWA 950
C                                                                       BCWA 960
      RVW = RV/RINF/UINF/32.174                                         BCWA 970
      WRITE (6,100)                                                     BCWA 980
      WRITE(6,110) TW,QCOND,P,QSUBL,RVW,QRR,RV,QT                       BCWA 990
  100 FORMAT(1H ,50X,'ABLATOR SURFACE',//)                              BCWA1000
  110 FORMAT(20X,'SURFACE TEMPERATURE (OK) =',F10.0,8X,                 BCWA1010
     X    'QCOND (BTU/FT2-SFC)      =',F10.0,/,                         BCWA1020
     X        20X,'SURFACE PRFSSURF (ATM)   =',F10.4,8X,                BCWA1030
     X    'QSUBL (BTU/FT2-SEC)      ='F10.0,/,                          BCWA1040
     X        20X,'BLOWING RATE             =',F10.4,8X,                BCWA1050
     X    'QRR (BTU/FT2-SEC)        =',F10.0,/,                         BCWA1060
     X        20X,'MASS LOSS (LB/FT2-SEC)   =',F10.4,8X,                BCWA1070
     X    'QTOTAL (BTU/FT2-SEC)     =',F10.0)                           BCWA1080
```

```
      IF(RVC .EQ. 0.0) CALL EXIT                                        BCWA1090
      RETURN                                                            BCWA1100
      END                                                               BCWA1110
```

```
INCLUDE FOHLAB(GLOBAL,CHECK,INPUT2,XMOMTM,PONCH,MOLMAS,DEDX)
INCLUDE FOHLAB(GAS,FG2,TRID,DATA,SOLVE,SLMTM,OUPPUT,YMOMTM)
INCLUDE FOHLAB(NEXT,SHOCK,SPECIE,INTRPL,TEMPR,PROPRT,ENERGY)
INCLUDE FOHLAB(SLINIT,FGH,MAIN,SHAPE,CHEMEQ)
INCLUDE FOHLAB(WALL)
INCLUDE FOHLAB(LRAD)
ENTRY MAIN
OVERLAY ONE
INSERT TRID,SOLVE,CHECK,MOLMAS,SLINIT,OUTPUT,TEMPR
OVERLAY TWO
INSERT FG2
OVERLAY THREE
INSERT SPECIF,SLMTM
OVERLAY THREE
INSERT ENERGY,INTRPL
OVERLAY TWO
INSERT XMOMTM,GLOBAL,PROPRT,DEDX
OVERLAY ONE
INSERT INPUT,OUPPUT,TRANS2,PONCH,NEXT
OVERLAY ONE
INSERT SHOCK
OVERLAY FIVE
INSERT CHEMEQ,THERMC,MATINV
OVERLAY FIVE
INSERT GAS
OVERLAY ONE
INSERT LRAD,ZP,SND,BUGFR,ZHV
INSERT DBUG
OVERLAY FOUR
INSERT TRANS
OVERLAY FOUR
INSERT TRANS1
```

```
                  C A S E  2      53.C00 FT/SEC      2.5E-7 SLUGS/CU FT
  53000.          2.5E-7          9.     0
   &ENTRY
   &END
```

```
      SUBROUTINE SLINIT                                                 SLIN  10
C                                                                       SLIN  20
C        ROUTINE TO GUESS INITIAL VALUES AT THE STAGNATION LINE FOR     SLIN  30
C        COLD START                                                     SLIN  40
C                                                                       SLIN  50
      COMMON/HOFF1/F1(60),F2(60),G1(60),G2(60),H1(60),H2(60)            SLIN  60
      COMMON/JOHN/ UD(60),U(60),DU(60),VD(60),RO(60),DNDX(60),DTLA,DTILOSLIN  70
      COMMON/MIKE/ NETA1,NETA2,PNF,WNF,RHOD,DP,TS,UD,VD,RW,RWO,EPS,PHI  SLIN  80
      COMMON /YL/ETA(60),YOND(60)                                       SLIN  90
      COMMON /RH/ DUD,DPHI,TD,RZB,PD,HD,HTOTAL                          SLIN 100
      COMMON/WALL/RVW,PRW,TWOLD,FLUX(20),CWALL(20),ECWALL(5)            SLIN 110
      COMMON /VEL/ F(60),FC(60),Z(60),V(60)                             SLIN 120
      COMMON /RFLUX/ E(60),IRAD,ITYPE                                   SLIN 130
      COMMON/PROP2/  MU(60),RM(60), AK(60)                              SLIN 140
      COMMON/PROP1/PI(60),RHO(60), T(60),AMW(60),C (20,60),CC(5,60)     SLIN 150
      COMMON /NON/RDZ,MUDZ,RMDZ,AKNF,HNF,CPNF                           SLIN 160
      COMMON /MAIN/KEEP,MAXE,MAXM,MAXD,IDEBUG,MCONV,ECONV,DCONV,LT,IAB  SLIN 170
      COMMON /FRSTRM/ U INF, RINF, UINF2, R , RE, LXI, ITM, IEM, NETA   SLIN 180
      COMMON /DEL/ DELTA,DTIL,DTILS                                     SLIN 190
      COMMON/BOB/ XI,DXI,YL                                             SLIN 200
      COMMON/GUESS/ TG1(60),TG2(60)                                     SLIN 210
      COMMON/NUMBER/NSP,NNS,NE,NC                                       SLIN 220
      COMMON /BILL/ NODE(20),ISTART,IDGD,IDGF,IDGH,IDGT,IDGS,           SLIN 230
     X  MI,NOE,NTIME,KOPT                                               SLIN 240
      COMMON/WT/SMW(20),AWT(5)                                          SLIN 250
      REAL  MU,MUDZ                                                     SLIN 260
      LOGICAL MCONV,ECONV,DCONV                                         SLIN 270
C                                                                       SLIN 280
      IF(ISTART .GT. 1) RETURN                                          SLIN 290
      TS = TD                                                           SLIN 300
      CALL PROPRT (NSP,NETA,NETA)                                       SLIN 310
      RDZ  = RHO(NETA)                                                  SLIN 320
      AKNF = 1.8*778.28*TS/(RDZ*UINF*UINF2*R)                           SLIN 330
      CPNF = 1.8*778.28*TS*32.174*2./UINF2                              SLIN 340
      HNF  =  2.*778.28   *32.174   /UINF2                              SLIN 350
      MUDZ = MU(NETA)                                                   SLIN 360
      RMDZ = RM(NETA)
      WNF  = R/UINF
      PNF=2116./RDZ/UINF2
      RHOD=RDZ*32.174
      RHO(NETA) = 1.0
C
C        ** GUESS DELTA AND DTIL **
C
      IF(DELTA .EQ. 0.0) DELTA = 0.78*RZB
      IF(DTIL  .EQ. 0.0) DTIL = 1.1*DELTA + 1.2*RVW
C
C        ** CALCULATE REYNOLDS NO. **
C
      RE = RDZ*R*UINF*32.174/MUDZ
C
      DEPS = 0.0
      DPHI = 1. - DEPS
      DUD = DPHI + RZB*(1. - DPHI)
      FD  = RZB/(2.*DUD*DTIL)
      FW  = -RVW*FD
      TW  = TWOLD/TS
      TWP = TG2(1)
      DO 5 I=1,NETA
      T(I) = 1.-(1.-TG2(I))*(1.-TW)/(1.-TWP)
      PI(I) = PD
      E(I)  = 0.0
      F(I)  = (FD - FW)*ETA(I)**2 + FW
      V(I)  = -2.*F(I)*DTIL/RHO(I)
      Z(I)  = ETA(I+1)/DTIL
      YOND(I) = 0.0
      IF(ISTART .GT. 0) GO TO 5
      AM  = 0.0
      DO 15 K=1,NSP
      C(K,I) = C(K,NETA)
      IF(V(I) .GT. 0.0) C(K,I) = CWALL(K)
      AM  = AM + C(K,I)/SMW(K)
```

```
 15 CONTINUE                                                            SLIN 730
    AMW(I) = 1./AM                                                      SLIN 740
  5 CONTINUE                                                            SLIN 750
    DO 35 I=2,NETA1                                                     SLIN 760
    CALL FGH (I,F1(I),G1(I),H1(I))                                      SLIN 770
 35 CONTINUE                                                            SLIN 780
    KODE=0                                                              SLIN 790
    CALL PROPRT (NSP,1,NETA)                                            SLIN 800
    DO 25 I=1,NOE                                                       SLIN 810
    IF(KODE .LT. 2) GO TO 40                                            SLIN 820
    CALL PROPRT (NSP,1,NETA)                                            SLIN 830
    CALL SLMTM                                                          SLIN 840
 40 CALL SPECIE (KODE)                                                  SLIN 850
    IF(KODE .GT. 4) RETURN                                              SLIN 860
 25 CONTINUE                                                            SLIN 870
    DO 45 I=2,NETA1                                                     SLIN 880
    CALL FGH (I,F1(I),G1(I),H1(I))                                      SLIN 890
 45 CONTINUE                                                            SLIN 900
    RETURN                                                              SLIN 910
    END                                                                 SLIN 920
```

```
      SUBROUTINE GAS (KODE )                                            GAS  10
C                                                                       GAS  20
C     **   THERMODYNAMIC AND TRANSPORT PROPERTIES OF AIR **             GAS  30
C     **  REFERENCE NASA TR R-50 **                                     GAS  40
C                                                                       GAS  50
C  THE FOLLOWING PROPERTIES ARE CALCULATED                              GAS  60
C              TEMPERATURE AT WHICH PROPERTIES ARE WANTED (T) IN DEG R GAS  70
C              PRESSURE AT WHICH PROPERTIES ARE WANTED (P) IN LB/IN**2 GAS  80
C              RATIO OF SPECIFIC HEATS (GAMMA) IN DIMENSIONLESS        GAS  90
C              SPECIFIC HEAT AT CONSTANT PRESSURE (CP) IN BTU/LB-DEG R GAS 100
C              ABSOLUTE VISCOSITY (V) IN LB/FT-SEC                     GAS 110
C              PRANDTL NUMBER (PR) IN DIMENSIONLESS                    GAS 120
C              THERMAL CONDUCTIVITY (XK) IN BTU/FT-SEC-DEG R           GAS 130
C              PRESSURE (P) IN ATMOSPHERES                             GAS 140
C              DENSITY (DEN) IN LB/FT**3                               GAS 150
C               ENTHALPY (H) IN BTU/LB                                 GAS 160
C               ENTROPY (S) IN BTU/LB-DEG R                            GAS 170
C               COMPRESSIBILITY (Z) IN DIMENSIONLESS                   GAS 180
C               SPEED OF SOUND (SOS) IN FT/SEC                         GAS 190
C               SPECIFIC HEAT AT CONSTANT VOLUMN (CV) IN BTU/LB-DEG R  GAS 200
C               ENTROPY (S) IN FT**2/SEC**2                            GAS 210
C               VELOCITY (VEL) IN FT/SEC                               GAS 220
C               PRESSURE (P) IN LBS/FT**2                              GAS 230
C               MACH NUMBER (M) IN DIMENSIONLESS                       GAS 240
C                                                                       GAS 250
C                                                                       GAS 260
C NOMENCLATURE  1=OXYGEN MOLECULES, 2=NITROGEN MOLECULES, 3=OXYGEN ATMOSGAS 270
C              4=NITROGEN ATMOS, 5=OXYGEN IONS, 6=NITROGEN IONS         GAS 280
C              7=ELECTRONS                                              GAS 290
C                                                                       GAS 300
C                                                                       GAS 310
      COMMON /FRSTRM/ U INF, RINF, UINF2, R , RE, LXI, ITM, IEM, NETA   GAS 320
      COMMON /NON/RDZ,MUDZ,RMDZ,AKNF,HNF,CPNF                           GAS 330
      COMMON/PROP1/PI(60),RHO(60),TI(60),AMW(60),C (20,60),CC(5,60)     GAS 340
      COMMON/PROP2/  MU(60),RM(60), AK(60)                              GAS 350
      COMMON/PROP3/CPS(20,60),HS(20,60),CPT(60),HM(60)                  GAS 360
      COMMON /RH/ DUD.DPHI.TD.RZB.PD.HD.HTOTAL                          GAS  370
      COMMON/WALL/RVW.PRW.TWOLD.FLUX(20).CWALL(20).ECWALL(5)            GAS  380
      COMMON/MIKE/ NETA1.NETA2.PNF.WNF.RHOD.DP.TZ.UD.VD.RW.RWO.EPS.PHI  GAS  390
      REAL  MU.MUDZ                                                     GAS  400
      LOGICAL MCONV.GCONV.SCONV                                         GAS  410
      DATA GASC /49721.7/                                               GAS  420
C                                                                       GAS  430
C                                                                       GAS  440
      DO 2000 I=KODE.NETA                                               GAS  450
      T = TI(I) * TZ                                                    GAS  460
      P = PI(I)                                                         GAS  470
C                                                                       GAS  480
C THE FOLLOWING PART OF PROGRAM USES PRESSURE IN ATMOSPHERES            GAS  490
C AND TEMPERATURE IN DEG K                                              GAS  500
C                                                                       GAS  510
      ITER=0                                                            GAS  520
C                                                                       GAS  530
C     **  TEMPERATURE - ENTHALPY ITERATION  **                          GAS  540
C                                                                       GAS  550
 900  CONTINUE                                                          GAS  560
      ITER=ITER+1                                                       GAS  570
      IF(T.LT.100.) T=100.                                              GAS  580
      A1=11390./T                                                       GAS  590
      A2=18990./T                                                       GAS  600
      A3=2270./T                                                        GAS  610
      A4=3390./T                                                        GAS  620
      A5=228./T                                                         GAS  630
      A6=326./T                                                         GAS  640
      A7=22800./T                                                       GAS  650
      A8=48600./T                                                       GAS  660
      A9=27700./T                                                       GAS  670
      A10=41500./T                                                      GAS  680
      A11=38600./T                                                      GAS  690
      A12=58200./T                                                      GAS  700
      A13=70.6/T                                                        GAS  710
      A14=188.9/T                                                       GAS  720
      A15=22000./T                                                      GAS  730
      A16=47000./T                                                      GAS  740
      A17=67900./T                                                      GAS  750
      A18=2270./(4.*T)                                                  GAS  760
      A19=TANH(A18)                                                     GAS  770
      A20=3390./(4.*T)                                                  GAS  780
      A21=TANH(A20)                                                     GAS  790
      TT=1./T                                                           GAS  800
      TSQ=T**2                                                          GAS  810
      TSQRT=T**.5                                                       GAS  820
      A22=112.2222/T                                                    GAS  830
      A23=T/59000.                                                      GAS  840
      A24=T/113200.                                                     GAS  850
      A25=T/75400.                                                      GAS  860
      AA1=EXP(-A1)                                                      GAS  870
      AA2=EXP(-A2)                                                      GAS  880
      AA3=EXP(A3)                                                       GAS  890
      AA4=EXP(A4)                                                       GAS  900
      AA5=EXP(-A5)                                                      GAS  910
      AA6=EXP(-A6)                                                      GAS  920
      AA7=EXP(-A7)                                                      GAS  930
      AA8=EXP(-A8)                                                      GAS  940
      AA9=EXP(-A9)                                                      GAS  950
      AA10=EXP(-A10)                                                    GAS  960
      AA11=EXP(-A11)                                                    GAS  970
      AA12=EXP(-A12)                                                    GAS  980
      AA13=EXP(-A13)                                                    GAS  990
      AA14=EXP(-A14)                                                    GAS 1000
      AA15=EXP(-A15)                                                    GAS 1010
      AA16=EXP(-A16)                                                    GAS 1020
      AA17=EXP(-A17)                                                    GAS 1030
C  CALCULATING ENERGIES PER COMPONENT OF GAS MIXTURE ABOVE              GAS 1040
C  REFERENCE ENERGIES.                                                  GAS 1050
       E1=2.5+((2.*AA1*A1+AA2*A2)/(3.+2.*AA1+AA2))+(A3/(AA3-1.))        GAS 1060
      ET=2.5+ (A4/(AA4-1.))                                             GAS 1070
      E3=1.5+((3.*AA5*A5+AA6*A6+5.*AA7*A7+AA8*A8)/(5.+3.*AA5+AA6+5.*AA7+GAS 1080
     1AA8))                                                             GAS 1090
      E4=1.5+((10.* AA9*A9+6.*AA10*A10)/(4.+10.*AA9+6.*AA10))           GAS 1100
      E5=1.5+((10.*AA11*A11+6.*AA12*A12)/(4.+10.*AA11+6.*AA12))         GAS 1110
      E6=1.5+((3.*AA13*A13+5.*AA14*A14+5.*AA15*A15+AA16*A16+5.*AA17*A17)GAS 1120
     1/(1.+3.*AA13+5.*AA14+5.*AA15+AA16+5.*AA17))                       GAS 1130
      E7=1.5                                                            GAS 1140
C TOTAL ENERGY PER COMPONENT OF GAS MIXTURE                             GAS 1150
      EN1=E1                                                            GAS 1160
      EN2=ET                                                            GAS 1170
      EN3=E3+29500./T                                                   GAS 1180
      EN4=E4+56600./T                                                   GAS 1190
      EN5=E5+187500./T                                                  GAS 1200
      EN6=E6+225400./T                                                  GAS 1210
      EN7=E7                                                            GAS 1220
C LOGS OF PARTITION FUNCTIONS                                           GAS 1230
      TL1=ALOG(T)*3.5                                                   GAS 1240
      TL2=ALOG(T)*2.5                                                   GAS 1250
      EQ1=TL1+.11+ALOG((3.+2.*AA1+AA2)/(1.-(1.0/AA3)))                  GAS 1260
      EQ2=TL1-.42-ALOG((1.-(1.0/AA4)))                                  GAS 1270
      EQ3=TL2+.5+ALOG((5.+3.*AA5+AA6+5.*AA7+AA8))                       GAS 1280
       EQ4=TL2+.3+ALOG((4.+10.*AA9+6.*AA10))                            GAS 1290
      EQ5=TL2+.5+ALOG((4.+10.*AA11+6.*AA12))                            GAS 1300
       EQ6=TL2+.3+ALOG((1.+3.*AA13+5.*AA14+5.*AA15+AA16+5.*AA17))       GAS 1310
      EQ7=TL2-14.24                                                     GAS 1320
C EQUILIBRIUM CONSTANS FOR CHEMICAL REACTIONS                           GAS 1330
      EK1=-59000./T+2.*EQ3-EQ1                                          GAS 1340
      EK2=-113200./T+2.*EQ4-EQ2                                         GAS 1350
      EK3=-158000./T+EQ5+EQ7-EQ3                                        GAS 1360
      EK4=-168800./T+EQ6+EQ7-EQ4                                        GAS 1370
      CCC=-79.9                                                         GAS 1380
      IF(EK1.LE.CCC) EK1=-79.9                                          GAS 1390
      IF(EK2.LE.CCC) EK2=-79.9                                          GAS 1400
      IF(EK3.LE.CCC) EK3=-79.9                                          GAS 1410
      IF(EK4.LE.CCC) EK4=-79.9                                          GAS 1420
      XK1=EXP(EK1)                                                      GAS 1430
      XK2=EXP(EK2)                                                      GAS 1440
      XK3=EXP(EK3)                                                      GAS 1450
      XK4=EXP(EK4)                                                      GAS 1460
      XK34= .2*XK3+.8*XK4                                               GAS 1470
      EE1=(-0.8+(.64+.8*(1.+((4.*P)/XK1)))**0.5)/(2.*(1.+4.*P/XK1))     GAS 1480
      EE2=(-0.4+(.16+3.84*(1.+(4.*P)/(XK2)))**0.5)/(2.*(1.+4.*P/XK2))   GAS 1490
      EE3= 1./(( 1.+P/XK34)**.5)                                        GAS 1500
      IF(EE1.GT..19999)EE1 = .19999                                     GAS 1510
      IF(EE2.GT..79999)EE2 = .79999                                     GAS 1520
      IF(EE3.GT..99999)EE3 = .99999                                     GAS 1530
C COMPRESSIBILITY (Z) DIMENSIONLESS                                     GAS 1540
      Z=1.+EE1+EE2+2.*EE3                                               GAS 1550
C COMPONENT MOL FRACTIONS IN AIR                                        GAS 1560
      X1=(.2-EE1)/Z                                                     GAS 1570
      X2=(.8-EE2)/Z                                                     GAS 1580
      X3=(2.*EE1-.4*EE3)/Z                                              GAS 1590
      X4=(2.*EE2-1.6*EE3)/Z                                             GAS 1600
      X5= .4*EE3/Z                                                      GAS 1610
      X6= 1.6*EE3/Z                                                     GAS 1620
      X7= 2.*EE3/Z                                                      GAS 1630
      IF(X1.LE.0.)  X1=1.E-20                                           GAS 1640
      IF(X2.LE.0.)  X2=1.E-20                                           GAS 1650
      IF(X3.LE.0.)  X3=1.E-20                                           GAS 1660
      IF(X4.LE.0.)  X4=1.E-20                                           GAS 1670
      IF(X5.LE.0.)  X5=1.E-20                                           GAS 1680
      IF(X6.LE.0.)  X6=1.E-20                                           GAS 1690
      IF(X7.LE.0.)  X7=1.E-20                                           GAS 1700
C ENERGY PER MOL OF INITIALLY UNDISSOCIATED AIR-DIMENSIONLESS           GAS 1710
      ER= Z*(X1*EN1+X2*EN2+X3*EN3+X4*EN4+X5*EN5+X6*EN6+X7*EN7)          GAS 1720
C ENTHALPY PER INITIAL MOL OF AIR-DIMENSIONLESS                         GAS 1730
      HR=ER+Z                                                           GAS 1740
C ENTHALPY PER INITIAL MOL OF AIR (H) IN BTU/LB                         GAS 1750
      H=HR*T*.12348                                                     GAS 1760
      IF(KODE.LT.NETA) GO TO 1000                                       GAS 1770
      HRATO=.5*(H-HD)/H                                                 GAS 1780
      AHR  = ABS( HRATO )                                               GAS 1790
      IF(AHR .LE. 0.0010) GO TO 999                                     GAS 1800
      IF(ITER .GT.1) GO TO 203                                           GAS 1810
      TP=T                                                               GAS 1820
      HP=HRATO                                                           GAS 1830
      T = T *(1. - HRATO )                                               GAS 1840
      IF(ITER .LT. 15) GO TO 900                                         GAS 1850
  203 CONTINUE                                                           GAS 1860
      TS=T*(1.0-HRATO)                                                   GAS 1870
      IF(HRATO*HP .LT.0.0) TS=.5*(T+TP)                                  GAS 1880
      TP=T                                                               GAS 1890
      T=TS                                                               GAS 1900
      HP=HRATO                                                           GAS 1910
      IF(ITER .LT. 15) GO TO 900                                         GAS 1920
      WRITE(6.200) T.H.HT                                                GAS 1930
  200 FORMAT(39H1TEMPERATURE-ENTHALPY DID NOT CONVERGE /3E15.6)          GAS 1940
C     CALL OUTPUT(4)                                                     GAS 1950
      STOP                                                               GAS 1960
  999 CONTINUE                                                           GAS 1970
      TD = T                                                             GAS 1980
C                                                                        GAS 1990
 1000 CONTINUE                                                           GAS 2000
C ENTROPY PER INITIAL MOL OF AIR-DIMENSIONLESS                           GAS 2010
      D1=EQ1+E1+1.                                                       GAS 2020
      D2=EQ2+ET+1.                                                       GAS 2030
      D3=EQ3+E3+1.                                                       GAS 2040
      D4=EQ4+E4+1.                                                       GAS 2050
      D5=EQ5+E5+1.                                                       GAS 2060
      D6=EQ6+E6+1.                                                       GAS 2070
      D7=EQ7+E7+1.                                                       GAS 2080
C TOTAL ENTROPY                                                          GAS 2090
      SR=Z*(X1*D1+X2*D2+X3*D3+X4*D4+X5*D5+X6*D6+X7*D7)-Z*(X1*ALOG(X1) +  GAS 2100
     1X2*ALOG(X2)+X3*ALOG(X3)+X4*ALOG(X4)+X5*ALOG(X5)+X6*ALOG(X6)+X7*    GAS 2110
     2ALOG(X7))-Z*ALOG(P)                                                GAS 2120
C ENTROPY PER INITIAL MOL OF AIR (S) IN BTU/LB-DEG R                     GAS 2130
      S    =SR*0.0686                                                    GAS 2140
C SPECIFIC HEAT AT CONSTANT VOLUME-CV                                    GAS 2150
      FF1=3.+2.*AA1+AA2                                                  GAS 2160
      CV1=2.5+((2.*AA1*A1*A1+AA2*A2*A2)/FF1)-(((2.*AA1*A1+AA2*A2)/FF1)**GAS 2170
     12.)+((.25*A3*A3)/(((2.*A19)/(1.-A19*A19))**2))                    GAS 2180
      CV2=2.5+((.25*A4*A4)/(((2.*A21)/(1.-A21*A21))**2))                GAS 2190
      CV3=1.5+((3.*AA5*A5*A5+AA6*A6*A6+5.*AA7*A7*A7+AA8*A8*A8)/(5.+3.*AAGAS 2200
     15+AA6+5.*AA7+AA8))-((E3-1.5)**2.)                                 GAS 2210
      CV4=1.5+((10.*AA9*A9*A9+6.*AA10*A10*A10)/(4.+10.*AA9+6.*AA10))    GAS 2220
     1-((E4-1.5)**2.)                                                   GAS 2230
      CV5=1.5+((10.*AA11*A11*A11+6.*AA12*A12*A12)/(4.+10.*AA11+6.*AA12))GAS 2240
     1-((E5-1.5)**2.)                                                   GAS 2250
      CV6=1.5+((3.*AA13*A13*A13+5.*AA14*A14*A14+5.*AA15*A15*A15+AA16*A16GAS 2260
     1*A16+5.*AA17*A17**2)/(1.+3.*AA13+5.*AA14+5.*AA15+AA16+5.*AA17))-((GAS 2270
     2E6-1.5)**2.)                                                      GAS 2280
      CV7=1.5                                                           GAS 2290
C LOGARITHMIC DERIVATIVES                                                GAS 2300
      CK1=TT*(59000./T+2.*E3-E1)                                        GAS 2310
      CK2=TT*(113200./T+2.*E4-ET)                                       GAS 2320
      CK3=TT*(158000./T+E5+E7-E3)                                       GAS 2330
      CK4=TT*(168800./T+E6+E7-E4)                                       GAS 2340
      CK34=.2*CK3+.8*CK4                                                GAS 2350
      PK1= CK1+TT                                                       GAS 2360
      PK2= CK2+TT                                                       GAS 2370
      PK3= CK3+TT                                                       GAS 2380
      PK4= CK4+TT                                                       GAS 2390
      PK34=0.2*PK3+0.8*PK4                                              GAS 2400
C PARTIAL DERIVATIVES REQUIRED FOR CP                                     GAS 2410
      DE1P=(PK1*EE1*(1.+EE1)*(.2-EE1))/(.8*(.5-EE1))                    GAS 2420
      DE2P=(PK2*EE2*(1.2+EE2)*(.8-EE2))/(.4*(4.8-EE2))                  GAS 2430
      DE3P=.5*PK34*EE3*(1.-EE3**2)                                      GAS 2440
      DZX1P=-DE1P                                                       GAS 2450
      DZX2P=-DE2P                                                       GAS 2460
      DZX3P=2.*DE1P - .4*DE3P                                           GAS 2470
      DZX4P=2.*DE2P-1.6*DE3P                                            GAS 2480
      DZX5P=.4*DE3P                                                     GAS 2490
      DZX6P=1.6*DE3P                                                    GAS 2500
      DZX7P=2.* DE3P                                                    GAS 2510
C EQUATION FOR SPECIFIC HEAT AT CONSTANT PRESSURE                         GAS 2520
```

```
      CPF=Z*(X1*(CV1+1.)+X2*(CV2+1.)+X3*(CV3+1.)+X4*(CV4+1.)+X5*(CV5+1.  GAS 2530
     1)+X6*(CV6+1.)+X7*(CV7+1.))                                        GAS 2540
      CPR = CPF +            T*(DZX1P*(EN1+1.)+DZX2P*(EN2+1.)+DZX3P*(EGAS 2550
     3N3+1.)+DZX4P*(EN4+1.)+DZX5P*(EN5+1.)+DZX6P*(EN6+1.)+DZX7P*(EN7+1.)GAS 2560
     4)                                                                 GAS 2570
      CPF = CPR                                                         GAS 2580
C SPECIFIC HEAT AT CONSTANT  PRESSURE (CP) IN BTU/LB-DEG R              GAS 2590
      CP=CPR*.0686                                                      GAS 2600
      CPF = CPF*.0686                                                   GAS 2610
C DENSITY (DEN) IN LB/FT**3                                             GAS 2620
C IF REAL GAS EQUATION OF STATE IS TO BE APPLIED USE                    GAS 2630
C FOR PERFECT GAS LAW THE COMPRESSIBILITY FACTOR IS  Z = 1              GAS 2640
      DEN=22.03703*P/T /Z                                               GAS 2650
C **TRANSPORT PROPERTIES**                                              GAS 2660
C COLLISION CROSS SECTIONS                                              GAS 2670
      S2=31.4*1.E-16*(1.+(112./T))                                      GAS 2680
      SI2=(S2/3.1415927)**.5                                            GAS 2690
      SI4=(1.11676-(.01490* ALOG(1.-(1.-A23) **.5))-(.23654* ALOG       GAS 2700
     1(1.-(1.-A24)**.5))-(.11582* ALOG(1.-(1.-A25)**.5)))*1.0E-8        GAS 2710
      S4=3.1415927*(SI4)**2                                             GAS 2720
      SI24=(SI2+SI4)/2.                                                 GAS 2730
      S24=3.1415927*(SI24)**2                                           GAS 2740
      S47=9.40*1.0E-14/TSQRT                                            GAS 2750
      FI=ALOG(1.042*1.0E-7*TSQ*(P*X7 )**(-.5))                          GAS 2760
      S7=8.55644*1.0E-6*(1./TSQ)*FI                                     GAS 2770
      SIP4=(1.11676-(.0149*ALOG(1.-(1.-2.*A23)**.5))-(.23654*ALOG(1.-(1.GAS 2780
     1-2.*A24)**.5))-(.11582* ALOG(1.-(1.-2.*A25)**.5)))*1.0E-8         GAS 2790
      SP4=3.145927*(SIP4)**2                                            GAS 2800
      SIP24=(SI2+SIP4)/2.                                               GAS 2810
      SP24=3.145927*SIP24**2                                            GAS 2820
C COMPONENT MOL FRACTIONS FOR INDEPENDENT REACTIONS                     GAS 2830
      F1=1.+EE1                                                         GAS 2840
      F2=1.2+EE2                                                        GAS 2850
      F3=1.+EE3                                                         GAS 2860
      X1OD=(.2-EE1)/F1                                                  GAS 2870
      X2OD=.8/F1                                                        GAS 2880
      X30D=2.*EE1/F1                                                    GAS 2890
      X2ND=(.8-EE2)/F2                                                  GAS 2900
      X3ND=.4/F2                                                        GAS 2910
      X4ND=2.*EE2/F2                                                    GAS 2920
      X4I=(1.-EE3)/F3                                                   GAS 2930
      X6I=EE3/F3                                                        GAS 2940
C MEAN FREE PATH RATIOS                                                 GAS 2950
      SS1=S24/S2                                                        GAS 2960
      SS2=S4/S2                                                         GAS 2970
      SS3=S7/S2                                                         GAS 2980
      SS4=S47/S2                                                        GAS 2990
      FP10D=X10D+X20D*.9660918 +X30D*SS1*.8164966                       GAS 3000
      FP20D=X10D*1.032796+X20D+X30D*SS1*.8528029                        GAS 3010
      FP30D=X10D*1.154701*SS1+X2ND*SS1*1.128152+X30D*SS2                GAS 3020
      FP2ND=X2ND+X4ND*SS1*.8164966+X3ND*SS1*.8528029                    GAS 3030
      FP3ND=X2ND*SS1*1.128152+X4ND*SS2*.9660918+X3ND*SS2                GAS 3040
      FP4ND=X2ND*SS1*1.154701+X4ND*SS2+X3ND*SS2*1.032796                GAS 3050
      FP4I=X4I*SS2+X6I*SS2                                              GAS 3060
      FP6I=X4I*SS2+X6I*SS3                                              GAS 3070
      FP7I=X4I*SS4*1.414186+X6I*SS3*1.414186+X6I*SS3                    GAS 3080
C VISCOSTITES OF THE COMPONENTS FOR THE DIFFERENT REACTIONS              GAS 3090
      V10D=1.054093*X10D*1./FP10D                                       GAS 3100
      V20D=.9860133*X20D*1./FP20D                                       GAS 3110
      V30D=.745356*X30D*1./FP30D                                        GAS 3120
      V2ND=.9860133*X2ND*1./FP2ND                                       GAS 3130
      V3ND=.745356*X3ND*1./FP3ND                                        GAS 3140
      V4ND=.6972167*X4ND*1./FP4ND                                       GAS 3150
      V4I=.6972167*X4I*1./FP4I                                          GAS 3160
      V6I=.6972167*X6I*1./FP6I                                          GAS 3170
      V7I=.4367848*1.0E-2*X6I*1./FP7I                                   GAS 3180
      VROD=V10D+V20D+V30D                                               GAS 3190
      VRND=V2ND+V3ND+V4ND                                               GAS 3200
      VRI=V4I+V6I+V7I                                                   GAS 3210
      F4=EE2/(.2-EE1+EE2)                                               GAS 3220
      F5=2.*EE3/(.8-EE2+2.*EE3)                                         GAS 3230
      VR=VROD+(F4*(VRND-VROD))+(F5*(VRI-VRND))                          GAS 3240
```

```
C TOTAL VISCOSITY (V) IN LB/FT-SEC                                      GAS 3250
      V=VR*.9841838*1.0E-6*TSQRT/(1.+A22)                               GAS 3260
C CONDUCTIVITY DUE TO MOLECULAR COLLISIONS FOR DIFFERENT REACTIONS      GAS 3270
      G1=.2105263*CV1+.4736842                                          GAS 3280
      G2=.2105263*CV2+.4736842                                          GAS 3290
      G3=.2105263*CV3+.4736842                                          GAS 3300
      G4=.2105363*CV4+.4736842                                          GAS 3310
      G5=.2105363*CV6+.4736842                                          GAS 3320
      G6=.2105363*CV7+.4736842                                          GAS 3330
      XKNOD=(V1OD*.9*G1)+(V2OD*1.028571*G2)+(V3OD*1.8*G3)               GAS 3340
      XKNND=(V2ND*1.028571*G2)+(V3ND*1.8*G3)+(V4ND*2.057143*G4)         GAS 3350
      XKNI=(V4I*2.057143*G4)+(V6I*2.057143*G5)+(V7I*52416.0*G6)         GAS 3360
      XKN=XKNOD+(F4*(XKNND-XKNOD))+(F5*(XKNI-XKNND))                    GAS 3370
C CONDUCTIVITY DUE TO CHECMICAL REACTIONS FOR THE DIFFERENT REACTIONS   GAS 3380
      XKROD=(.178637*(T*PK1)**2)/((SP24/(1.732051*S2))*(((X3OD+2.*X1OD) GAS 3390
     1**2)/(X3OD*X1OD))+(4.*X2OD/X3OD))+(X2OD/(1.414214*X1OD)))         GAS 3400
      XKRND=(.178637*(T*PK2)**2)/((SP24/(1.732051*S2))*((((X4ND+2.*X2ND)GAS 3410
     1**2)/(X4ND*X2ND))+(X3ND/X2ND)) +(SP4*2.*X3ND/(S2*X4ND)))          GAS 3420
      XKR1=(.178637*(T*PK34)**2)/(((.5*SP4/S2)+(.4347826*1.0E-2*S47/S2))GAS 3430
     1*((X4I+X6I)**2)/(X4I*X6I))                                        GAS 3440
      XKOD=XKNOD+XKROD                                                  GAS 3450
      XKND=XKNND+XKRND                                                  GAS 3460
      XKI=XKNI+XKR1                                                     GAS 3470
      XKR=XKOD+(F4*(XKND-XKOD))+(F5*(XKI-XKND))                         GAS 3480
C TOTAL THERMAL CONDUCTIVITY (XK) IN BTU/FT-SEC-DEG R                   GAS 3490
      XK=XKR*((.3206522*1.0E-6*TSQRT)/(1.+A22))                         GAS 3500
C PRANDTL NUMBER (PR) DIMENSIONLESS                                     GAS 3510
      PRN = .2105263 * CPR * VR / XKR                                   GAS 3520
      IF(I.EQ. 1) PRW = PRN                                             GAS 3530
C FORM REQUIRED BY CALL STATEMENT                                       GAS 3540
C                                                                       GAS 3550
C     **  RHO UNITS SLUGS/FT**3                                         GAS 3560
C     **  MU UNITS LBM/FT-SEC                                           GAS 3570
C     **  RW UNITS LBF**2 SEC**3/FT**6                                  GAS 3580
C                                                                       GAS 3590
      MU (I) = V                                                        GAS 3600
      RHO(I)=DEN/32.174                                                 GAS 3610
      RM(I)=RHO(I)*MU(I )/32.174                                        GAS 3620
      AK(I) = XK                                                        GAS 3630
      CPT(I) = CPF                                                      GAS 3640
C *** CALCULATE  THE MEAN MOLECULAR WT. ***                              GAS 3650
      REAL = 25050.*S    *Z / SR                                        GAS 3660
      AMW(I)= GASC / REAL                                               GAS 3670
C MASS FRACTIONS                                                        GAS 3680
      C(1.I) = X1    *32.00/AMW(I)                                      GAS 3690
      C(2.I) = X2    *28.00/AMW(I)                                      GAS 3700
      C(3.I) = X3    *16.00/AMW(I)                                      GAS 3710
      C(4.I) = X4    *14.C0/AMW(I)                                      GAS 3720
      C(5.I) = X5    *16.00/AMW(I)                                      GAS 3730
      C(6.I) = X6    *14.00/AMW(I)                                      GAS 3740
      C(7.I) = X7    /(1820.*AMW(I))                                    GAS 3750
C SPECIES ENTHALPY PER INITIAL MOLE OF AIR IN BTU/LB OF I               GAS 3760
      HS(1.I) = (Z*X1*EN1/C(1.I) +Z)*T*.12348                           GAS 3770
      HS(2.I) = (Z*X2*EN2/C(2.I) +Z)*T*.12348                           GAS 3780
      HS(3.I) = (Z*X3*EN3/C(3.I) +Z)*T*.12348                           GAS 3790
      HS(4.I) = (Z*X4*EN4/C(4.I) +Z)*T*.12348                           GAS 3800
      HS(5.I) = (Z*X5*EN5/C(5.I) +Z)*T*.12348                           GAS 3810
      HS(6.I) = (Z*X6*EN6/C(6.I) +Z)*T*.12348                           GAS 3820
      HS(7.I) = (Z*X7*EN7/C(7.I) +Z)*T*.12348                           GAS 3830
 2000 CONTINUE                                                          GAS 3840
C                                                                       GAS 3650
C                                                                       GAS 3860
      DO 40 I=KODE.NETA                                                 GAS 3870
C                                                                       GAS 3880
C     **  NONDIMENSIONALIZE  RHO  AND  MU  **                           GAS 3890
C                                                                       GAS 3900
      RHO(I) = RHO(I)/RDZ                                               GAS 3910
      MU(I) = MU(I)/MUDZ                                                GAS 3920
      RM(I) =RM(I)/RMDZ                                                 GAS 3930
      AK(I) = AK(I)*AKNF                                                GAS 3940
      CPT(I) = CPT(I)*CPNF                                              GAS 3950
C NONDIMENSIONAL SPECIES ENTHALPY                                       GAS 3960
```

```
      HS(1,I) = HS(1,I)*HNF                                             GAS 3970
      HS(2,I) = HS(2,I)*HNF                                             GAS 3980
      HS(3,I) = HS(3,I)*HNF                                             GAS 3990
      HS(4,I) = HS(4,I)*HNF                                             GAS 4000
      HS(5,I) = HS(5,I)*HNF                                             GAS 4010
      HS(6,I) = HS(6,I)*HNF                                             GAS 4020
      HS(7,I) = HS(7,I)*HNF                                             GAS 4030
C                                                                       GAS 4040
C                                                                       GAS 4050
 40   CONTINUE                                                          GAS 4060
  100 FORMAT(1X,9E14.6)                                                 GAS 4070
      RETURN                                                            GAS 4080
      END                                                               GAS 4090
      SUBROUTINE BCWALL                                                 BCWA  10
C                                                                       BCWA  20
C        THIS SUBROUTINE CALCULATES BLOWING RATE AT THE ABLATOR SURFACE BCWA  30
C        FOR A GIVEN SURFACE TEMPERATURE AND PRESSURE                   BCWA  40
C                                                                       BCWA  50
      COMMON /BILL/ NODE(20),ISTART,IDGD,IDGF,IDGH,IDGT,IDGS,           BCWA  60
     X  MI,NOE,NTIME,KOPT                                               BCWA  70
      COMMON/MIKE/ NETA1,NETA2,PNF,WNF,RHOD,DP,TS,UD,VD,RW,RWO,EPS,PHI  BCWA  80
      COMMON /YL/ETA(60),YOND(60)                                       BCWA  90
      COMMON/WALL/RVW,PRW,TWOLD,FLUX(20),CWALL(20),ECWALL(5)            BCWA 100
      COMMON /VEL/ F(60),FC(60),Z(60),V(60)                             BCWA 110
      COMMON/PROP1/PI(60),RHO(60), T(60),AMW(60),C (20,60),CC(5,60)     BCWA 120
      COMMON /FRSTRM/ U INF, RINF, UINF2, R , RE, LXI, ITM, IEM, NETA   BCWA 130
      COMMON /NON/RDZ,MUDZ,RMDZ,AKNF,HNF,CPNF                           BCWA 140
      COMMON /DEL/ DELTA,DTIL,DTILS                                     BCWA 150
      COMMON /MAIM/KEEP,MAXE,MAXM,MAXD,IDEBUG,MCONV,ECONV,DCONV,LT,IAB  BCWA 160
      COMMON/BOB/ XI,DXI,YL                                             BCWA 170
      COMMON /GEORGE/ EPSN(30),XIN(30),RVN(30)                          BCWA 180
      DIMENSION A(3),D(3),E(3),XMW(3)                                   BCWA 190
      DATA A /0.37,0.34,0.08/                                           BCWA 200
      DATA XMW/12.,24.,36./                                             BCWA 210
      DATA C  /8.21,9.64,10.25/                                         BCWA 220
      DATA E  /-3.75,-4.27,-4./                                         BCWA 230
      DATA EP,RR,AM/0.8,1.215E-4,13.3/                                  BCWA 240
      DATA A1,A2,A3,A4 /1.674065E-8,-.333005E-3,10.99963E-8,2731.659/   BCWA 250
C                                                                       BCWA 260
      TL =0.0                                                           BCWA 270
      TW =TWOLD                                                         BCWA 280
      NETA1 = NETA - 1                                                  BCWA 290
C                                                                       BCWA 300
C        INITIAL GUESS FOR BLOWING RATE OF CARBON SOLID                 BCWA 310
      IF (XI .EQ. 0.0) PRW = RVW                                        BCWA 320
      CALL INTRPL (XI,XIN,RVN,IAB,RVW)                                  BCWA 330
      RVW = RVW * PRW                                                   BCWA 340
      RVCC = RVW*RINF*UINF*32.174 * 0.4328                              BCWA 350
C                                                                       BCWA 360
```

```
C        CALCULATION OF SURFACE PRESSURE FROM YMOMTM EQ.                BCWA 370
C                                                                       BCWA 380
      P = PI(NETA)                                                      BCWA 390
      IF (ISTART .LT. 3) GO TO 1                                        BCWA 400
      FP = DTIL                                                         BCWA 410
      DO 15 I=1,NETA1                                                   BCWA 420
      J = NETA - I                                                      BCWA 430
      DETA = ETA(J+1) - ETA(J)                                          BCWA 440
      P = P - DTIL *(FP*UD)**2*DETA/PNF                                 BCWA 450
      IF(J .GT. 1) FP = Z(J-1)*DTIL                                     BCWA 460
   15 CONTINUE                                                          BCWA 470
C                                                                       BCWA 480
    1 RVC =0.0                                                          BCWA 490
      PI(1) = P                                                         BCWA 500
      RV = RVCC/.4328                                                   BCWA 510
      DO 5 I=1,3                                                        BCWA 520
      PVP = 10.**(D(I) + E(I)/TW*1.E4)                                  BCWA 530
      EVP = A(I)*(1. - EP)*SQRT(XMW(I)/RR/TW)                           BCWA 540
      BT  = AM*P/XMW(I)                                                 BCWA 550
      CG  = EVP/(RV + BT*EVP)*PVP                                       BCWA 560
      RVC = RVC + RV*CG                                                 BCWA 570
    5 CONTINUE                                                          BCWA 580
C                                                                       BCWA 590
C        CHECK TO SEE IF HERTZ-KNUDSEN EQ. IS CONVERGED                 BCWA 600
C                                                                       BCWA 610
      ABD =      (RVCC - RVC)/RVCC                                      BCWA 620
      ABSD = ABS(ABD)                                                   BCWA 630
      IF(ABSD .LT. 0.001) GO TO 20                                      BCWA 640
      IF ( TL .GT. 0.0 ) GO TO 10                                       BCWA 650
      TL = TW                                                           BCWA 660
      RVCL = RVC                                                        BCWA 670
      TW = TW + 10.*ABD/ABSD                                            BCWA 680
      GO TO 1                                                           BCWA 690
   10 TWOLD = TW                                                        BCWA 700
      TW = TW + (TW-TL)/(RVC-RVCL)*(RVCC-RVC)                           BCWA 710
      TL = TWOLD                                                        BCWA 720
      RVCL = RVC                                                        BCWA 730
      GO TO 1                                                           BCWA 740
   20 TWOLD = TW                                                        BCWA 750
C                                                                       BCWA 760
C        CALCULATE HEAT ABSORBED & RERADIATED BY ABLATOR                BCWA 770
C                                                                       BCWA 780
      T3 = TW*TW*TW                                                     BCWA 790
      SRV = SQRT(RV)                                                    BCWA 800
C        HEAT ABSORBED BY CARBON SUBLIMING (BTU/FT2-SEC)                BCWA 810
C                                                                       BCWA 820
      QSUBL = 4440.*RV                                                  BCWA 830
C                                                                       BCWA 840
C        HEAT CONDUCTED THRU CHAR (BTU/FT2-SEC)                         BCWA 850
C                                                                       BCWA 860
      QCOND = A1*RV*T3 + A2*SRV*TW*TW + A3*SRV*T3 + A4*RV               BCWA 870
C                                                                       BCWA 880
C        ENERGY RERADIATED BY CHAR SURFACE WITH EMISSIVITY OF 0.66      BCWA 890
C                                                                       BCWA 900
      QRR   = 3.3E-12*T3*TW                                             BCWA 910
C                                                                       BCWA 920
C        TOTAL HEAT FLUX ACCOMODATED BY ABLATOR (BTU/FT2-SEC)           BCWA 930
C                                                                       BCWA 940
      QT = QCOND + QRR + QSUBL                                          BCWA 950
C                                                                       BCWA 960
      RVW = RV/RINF/UINF/32.174                                         BCWA 970
      WRITE (6,100)                                                     BCWA 980
      WRITE(6,110) TW,QCOND,P,QSUBL,RVW,QRR,RV,QT                       BCWA 990
  100 FORMAT(1H ,50X,'ABLATOR SURFACE',//)                              BCWA1000
  110 FORMAT(20X,'SURFACE TEMPERATURE (OK) =',F10.0,8X,                 BCWA1010
     X   'QCOND (BTU/FT2-SEC)     =',F10.0,/,                           BCWA1020
     X        20X,'SURFACE PRESSURE (ATM)    =',F10.4,8X,               BCWA1030
     X   'QSUBL (BTU/FT2-SEC)     ='F10.0,/,                            BCWA1040
     X        20X,'BLOWING RATE              =',F10.4,8X,               BCWA1050
     X   'QRR (BTU/FT2-SEC)       =',F10.0,/,                           BCWA1060
     X        20X,'MASS LOSS (LB/FT2-SEC)    =',F10.4,8X,               BCWA1070
     X   'QTOTAL (BTU/FT2-SEC)    =',F10.0)                             BCWA1080
```

```
      IF(RVC .EQ. 0.0) CALL EXIT                                        BCWA1090
      RETURN                                                            BCWA1100
      END                                                               BCWA1110
      SUBROUTINE SLMTM
C
C -----THIS SUBROUTINE SOLVES THE MOMENTUM EQUATION AS A
C       SECOND ORDER EQUATION AND A FIRST ORDER EQUATION -----
      COMMON /CONV/ FPRCT.TPRCT.DDAMP.TDAMP.PDTIL
      COMMON /DEL/ DELTA.DTIL.DTILS
      COMMON /FRSTRM/ U INF. RINF. UINF2. R . RE. LXI. ITM. IEM. NETA
      COMMON /MAIM/KEEP.MAXE.MAXM.MAXD.IDEBUG.MCONV.ECONV.DCONV.LT.IAB
      COMMON /NON/RDZ.MUDZ.RMDZ.AKNF.HNF.CPNF
      COMMON/PROP1/PI(60).RHO(60). T(60).AMW(60).C (20.60).EC(5.60)
      COMMON/PROP2/  MU(60).RM(60). AK(60)
      COMMON/PROP3/CPS(20.60).HS(20.60).CP (60).HM(60)
      COMMON /RFLUX/ E(60).IRAD.ITYPE
      COMMON /RH/ DUD.DPHI.TD.RZB.PD.MD.HTOTAL
      COMMON/VECTOR/ CA(60).CB(60).CC(60).B(60)
      COMMON /VEL/ F(60).FC(60).Z(60).V(60)
      COMMON/WALL/RVW.PRW.TWOLD.FLUX(20).CWALL(20).ECWALL(5)
      COMMON /YL/ETA(60).YOND(60)
      LOGICAL MCONV.ECONV.DCONV
      REAL*8 CA.CB.CC.B
C
C----- INITIALIZED QUANTITIES -----
C
      MCONV = .FALSE.
      DTILS = DTIL
      ITM = 1
      N = NETA -2
      L = NETA-1
      AA3 = RZB*(1.-RZB)*DPHI**2/DUD
      AAA3 = AA3
      DTILS2 = DTILS
      IF(IEM.GT.3) DTIL=.5*(DTIL+DTILS2)
C
C
C-----Z''+A1*Z'+A2*Z=A3
C     COMPUTE A1.A2.A3
```

```
   14 CONTINUE                                                            SLMT 370
C----- BOUNDARY CONDITIONS -----                                          SLMT 380
C                                                                         SLMT 390
      RED = RE*DTIL                                                       SLMT 400
      RED2 = 2.*RED*DTIL*DUD                                              SLMT 410
      DTIL2 = DTIL*DTIL                                                   SLMT 420
      FD = RZB/(2.*DUD*DTIL)                                              SLMT 430
      FD = RZB/(2.*DUD*DTIL)*RHO(NETA)                                    SLMT 440
      FW = -RVW*FD                                                        SLMT 450
      F(1) = FW                                                           SLMT 460
      B(L) = 1./DTIL                                                      SLMT 470
      ITER = 1                                                            SLMT 480
   15 CONTINUE                                                            SLMT 490
      SUM = 0.0                                                           SLMT 500
      ZP = 1.0                                                            SLMT 510
      DO 35 I=1,N                                                         SLMT 520
      J = NETA-I                                                          SLMT 530
      ZA = (ZP + Z(J-1))/2.                                               SLMT 540
      DETA = ETA(J+1) - ETA(J)                                            SLMT 550
      SUM = SUM + DTIL2*Z(J-1)**2*DETA/    DUD*DTIL                       SLMT 560
      CC(J-1) = SUM                                                       SLMT 570
      ZP = Z(J-1)                                                         SLMT 580
   35 CONTINUE                                                            SLMT 590
      II = 1                                                              SLMT 600
      DO 20 I=1,N                                                         SLMT 610
      AA3 = AAA3 + CC(I)                                                  SLMT 620
      DET=ETA(I+1)-ETA(I)                                                 SLMT 630
      DETN=ETA(I+2)-ETA(I+1)                                              SLMT 640
      D1  =  DETN*(DETN+DET)                                              SLMT 650
      D2  =  DETN*DET                                                     SLMT 660
      D3  =  DET*(DETN+DET)                                               SLMT 670
      RMP = DET*RM(I+2)/D1 +(DETN-DET)*RM(I+1)/D2 -DETN*RM(I)/D3          SLMT 680
      A1 = (RED2*F(I+1) +RMP)/RM(I+1)                                     SLMT 690
      A2 = -RED2*DTIL*Z(I)/RM(I+1)                                        SLMT 700
      A3 = -2.*RED*( AA3/(RHO(I+1)*RM(I+1))                               SLMT 710
     1              +DTIL2  *DUD*Z(I)**2/(2.*RM(I+1)) )                   SLMT 720
```

```
C                                                                       SLMT 730
C-----CA*Z(N-1)+CB*Z(N)+CC*Z(N+1)=B                                     SLMT 740
C      COMPUTE CA,CB,CC                                                 SLMT 750
       CA(II) =(2.-A1*DETN)/D3                                          SLMT 760
       CB(I)=A1*(DETN-DET)/D2-2./D2+A2                                  SLMT 770
       CC(I)=(2.+A1*DET)/D1                                             SLMT 780
       B(I)=A3                                                          SLMT 790
       II = I                                                           SLMT 800
   20  CONTINUE                                                         SLMT 810
       B(N)=B(N)-CC(N)/DTIL                                             SLMT 820
C                                                                       SLMT 830
       CALL TRID (N)                                                    SLMT 840
C                                                                       SLMT 850
C-----INTEGRATE FIRST ORDER EQUATION-----                               SLMT 860
       FC(1)=FW                                                         SLMT 870
       SUM=FW+ (B(1)+FW)*(ETA(2)-ETA(1))*DTIL/2.                        SLMT 880
       FC(2)=SUM                                                        SLMT 890
       DO 30 K=3,NETA                                                   SLMT 900
       SUM=SUM+DTIL*(B(K-1)+B(K-2))*(ETA(K) -ETA(K-1))/2.               SLMT 910
  30   FC(K) = SUM                                                      SLMT 920
C                                                                       SLMT 930
C-----CHECK FOR CONVERGENCE                                             SLMT 940
C                                                                       SLMT 950
       DO 40 K=2,NETA                                                   SLMT 960
       PRCT=ABS((FC(K)-F(K))/F(K))                                      SLMT 970
       IF (PRCT.GT.FPRCT) GO TO 50                                      SLMT 980
   40  CONTINUE                                                         SLMT 990
       GO TO 90                                                         SLMT1000
   50  CONTINUE                                                         SLMT1010
       ITER=ITER+1                                                      SLMT1020
       DO 60 K=1,NETA                                                   SLMT1030
   60  F(K)=FC(K)                                                       SLMT1040
       DO 65 I=1,N                                                      SLMT1050
   65  Z(I)=B(I)                                                        SLMT1060
       IF(ITER.GE.MAXM ) GO TO 90                                       SLMT1070
       GO TO 15                                                         SLMT1080
   90 CONTINUE                                                              SLMT1090
C                                                                           SLMT1100
C----- COMPUTE NEW DTIL -----                                               SLMT1110
C                                                                           SLMT1120
      DTILC = (FD-FW)*DTIL/(F(NETA)-FW)                                     SLMT1130
      PRCT = ABS((DTIL-DTILC)/DTIL)                                         SLMT1140
      IF(ITM.GT.MAXM) GO TO 160                                             SLMT1150
      ITM = ITM +1                                                          SLMT1160
      IF(PRCT.LE.PDTIL) GO TO 150                                           SLMT1170
      DTIL = DTIL +DDAMP*(DTILC-DTIL)                                       SLMT1180
      GO TO 14                                                              SLMT1190
 150  CONTINUE                                                              SLMT1200
      DTIL = DTIL+ DDAMP*(DTILC -DTIL)                                      SLMT1210
      MCONV = .TRUE.                                                        SLMT1220
C                                                                           SLMT1230
C CHECK MOMENTUM-ENERGY CONVERGENCE                                         SLMT1240
      PRCT = ABS((DTIL-DTILS)/DTILS)                                        SLMT1250
      IF(PRCT.LE.PDTIL) DCONV = .TRUE.                                      SLMT1260
 160  CONTINUE                                                              SLMT1270
C                                                                           SLMT1280
      DO 170 K=1,NETA                                                       SLMT1290
 170  V(K) = -FC(K)*DTIL*2./RHO(K)                                          SLMT1300
C DEBUG OUTPUT                                                              SLMT1310
      IF(IDEBUG.EQ. 0) RETURN                                               SLMT1320
      WRITE(6,102) ITER,ITM                                                 SLMT1330
 102  FORMAT( 10X,2I3/)                                                     SLMT1340
      WRITE(6,100) DTIL,DTILC                                               SLMT1350
      WRITE(6,101)                                                          SLMT1360
  101 FORMAT(6X,'ETA',12X,'F',12X,'FC',12X,'RHO',12X,'RM',12X,'VS',12X,     SLMT1370
     1 'V')                                                                 SLMT1380
      DO 120 K=1,NETA                                                       SLMT1390
      VS=-FC(K)*DTIL*UINF*2./RHO(K)                                         SLMT1400
      WRITE(6,100) ETA(K),F(K),FC(K),  RHO(K),RM(K),VS ,V(K)                SLMT1410
  100 FORMAT( 1X,9E14.6)                                                    SLMT1420
  120 CONTINUE                                                              SLMT1430
      WRITE(6,103)                                                          SLMT1440
```

```
103 FORMAT(6X,'ETA',13X,'Z',13X,'B',12X,2HF')                           SLMT1450
    DO 121 I=1,N                                                          SLMT1460
    U=B(I)*DTIL                                                           SLMT1470
    WRITE(6,100) ETA(I+1),Z(I),B(I),U                                     SLMT1480
121 CONTINUE                                                              SLMT1490
    RETURN                                                                SLMT1500
    END                                                                   SLMT1510
```

```
      SUBROUTINE DEDX
C
C        THIS SUBROUTINE CALCULATES THE SHOCK STNDOFF DISTANCE, DELTA
C        AND THE PARTIAL OF ETA WITH RESPECT TO X, DNDX
C
      COMMON/JOHN/ UO(60).U(60).DU(60).VO(60).RO(60).DNDX(60).DTLA.DTILO
      COMMON/BOB/ XI.DXI.YL
      COMMON /FRSTRM/ U INF. RINF. UINF2. R . RE. LXI. ITM. IEM. NETA
      COMMON/PROP1/PI(60).RHO(60). T(60).AMW(60).C (20.60).EC(5.60)
      COMMON /DEL/ DELTA.DTIL.DTILS
      COMMON /YL/ETA(60).YOND(60).YO(60)
C
      YA  = 0.0
      DO 15 J=2.NETA
      I=J-1
      DETA = ETA(J) - ETA(J-1)
      YA = YA + DTIL*DETA*(1./RHO(I) + 1./RHO(J))/2.
      YOND(J) = YA
   15 CONTINUE
      DELTA = YOND(NETA)
      RETURN
      END
      SUBROUTINE SOLVE(BC1,BC2,WO)
C
C        THIS SUBROUTINE SOLVES THE PARTIAL DIFFERENTIAL EQUATION
C
C              W'' + A1*W' + A2*W + A3 + A4*W'(X) = 0
C
      COMMON /FRSTRM/ U INF, RINF, UINF2, R , RE, LXI, ITM, IEM, NETA
      COMMON/HOFF1/F1(60),F2(60),G1(60),G2(60),H1(60),H2(60)
      COMMON/VECTOR/ SUB(60),DIAG(60),SUP(60),B(60)
      DIMENSION WO(1)
      COMMON/BOB/ XI,DXI,YL
      REAL*8 SUB,DIAG,SUP,B
      NETA2=NETA-2
      DO5 I=1,NETA2
      J=I+1
      A1= SUB(I)
      A2= DIAG(I)
      A3= SUP(I)
      A4= B(I)
      CA = (H2(J)+A1*H1(J))*YL
      DIAG(I)= (G2(J)+A1*G1(J)+A2)*YL
      SUP(I) = (F2(J)+A1*F1(J))*YL
      B(I)   = A4*WO(J)/DXI-(1-YL)/YL*(CA*WO(I)+ SUP(I)*WO(J+1)
     X           +DIAG(I)*WO(J)) - A3
      DIAG(I)=DIAG(I)+A4/DXI
      IF(I.EQ.1) GO TO 4
      SUB(I-1)=CA
      GO TO 5
    4 A = CA
    5 CONTINUE
      B(1)   = B(1) - A*BC1
      B(NETA2)=B(NETA2) - SUP(NETA2)*BC2
      CALL TRID (NETA2)
      RETURN
      END
      SUBROUTINE YMOMTM
C
C        THIS ROUTINE SOLVES THE THIN SHOCK LAYER Y-MOMENTUM EQUATION
C        FOR THE PRESSURE
C
      COMMON/MIKE/ NETA1,NETA2,PNF,WNF,RHOD,DP,TS,UD,VD,RW,RWO,EPS,PHI
      COMMON /YL/ETA(60),YOND(60),YO(60)
      COMMON/JOHN/ UO(60),U(60),DU(60),VO(60),RO(60),DNDX(60),DTLA,DTILO
      COMMON /FRSTRM/ U INF, RINF, UINF2, R , RE, LXI, ITM, IEM, NETA
      COMMON/PROP1/PI(60),RHO(60), T(60),AMW(60),C (20,60),EC(5,60)
      COMMON /DEL/ DELTA,DTIL,DTILS
      COMMON /VEL/ F(60),FC(60),Z(60),V(60)
      COMMON/BOB/ XI,DXI,YL
C
      DO 15 I=1,NETA1
      J = NETA - I
      DETA = ETA(J+1) - ETA(J)
      UA = (U(J)+U(J+1))/2.
      PI(J) = PI(J+1) - DTIL*UA*UA*DETA/PNF
   15 CONTINUE
      RETURN
      END
      SUBROUTINE XMOMTM(KODE)                                           XMOM  10
C                                                                       XMOM  20
C        THIS ROUTINE SOLVES THE X-MOMENTUM EQUATION FOR THE TANGENTIAL XMOM  30
C        VELOCITY (U) FOR THE RADIATING. CHEMICALLY REACTING. VISCOUS   XMOM  40
C        FLOW IN THE SHOCK LAYER ABOUT A BLUNT BODY                     XMOM  50
C                                                                       XMOM  60
      COMMON /FRSTRM/ U INF. RINF. UINF2. R . RE. LXI. ITM. IEM. NETA   XMOM  70
      COMMON/PROP1/PI(60).RHO(60). T(60).AMW(60).C (20.60).EC(5.60)     XMOM  80
      COMMON/PROP2/  MU(60).RM(60). AK(60)                              XMOM  90
      COMMON/JOHN/ UO(60).U(60).DL(60).VO(60).RO(60).DNDX(60).DTLA.DTILOXMOM 100
      COMMON /VEL/ F(60).FC(60).Z(60).V(60)                             XMOM 110
      COMMON /DEL/ DELTA.DTIL.DTILS                                     XMOM 120
      COMMON/HOFF1/F1(60).F2(60).G1(60).G2(60).H1(60).H2(60)            XMOM 130
      COMMON/VECTOR/ SUB(60).DIAG(60).SUP(60).B(60)                     XMOM 140
      COMMON/JTB/ CO(60.20).RED.RED2                                    XMOM 150
      COMMON/BOB/ XI.DXI.YL                                             XMOM 160
      COMMON/MIKE/ NETA1.NETA2.PNF.WNF.RHOD.DP.TS.UD.VD.RW.RWO.EPS.PHI  XMOM 170
      COMMON/CON/ PO(60)                                                XMOM 180
      COMMON/CONV1/HDAMP.FDAMP.CDAMP                                    XMOM 190
      COMMON /BILL/ NODE(20).ISTART.IDGD.IDGF.IDGH.IDGT.IDGS            XMOM 200
      REAL*8 SUB.DIAG.SUP.B                                             XMOM 210
C                                                                       XMOM 220
      DTLA = YL*DTIL +  (1-YL)*DTILO                                    XMOM 230
      RED = RE*DTLA                                                     XMOM 240
      RED2 = RED*DTLA                                                   XMOM 250
      DO 5 I=1.NETA2                                                    XMOM 260
      J=I+1                                                             XMOM 270
      RHOA= YL*RHO(J) + (1-YL)*RO(J)                                    XMOM 280
      VA  = YL*V(J)    + (1-YL)*VO(J)                                   XMOM 290
      DP = (PI(J)-PO(J))*PNF/DXI                                        XMOM 300
      DRM=H1(J)*RM(J-1)+G1(J)*RM(J)+F1(J)*RM(J+1)                       XMOM 310
      UA = YL*U(J) + (1-YL)*UO(J)                                       XMOM 320
      DU(J)=(U(J)-UO(J))/DXI                                            XMOM 330
      DUN = H1(J)*U(I)+G1(J)*U(J)+F1(J)*U(J+1)                          XMOM 340
      DUN= YL*DUN + (1-YL)*(H1(J)*UO(I)+G1(J)*UO(J)+F1(J)*UO(J+1))      XMOM 350
C                                                                       XMOM 360
```

```
C        CALCULATION OF A1                                                XMOM 370
      SUB(I) =DRM/RM(J)-RED*RHOA*VA/RM(J)                                 XMOM 380
     X           -RED2*UA*DNDX(J)/RM(J)                                   XMOM 390
C                                                                         XMOM 400
C        CALCULATION OF A2                                                XMOM 410
      DIAG(I)=-RED2*DU(J)/RM(J)                                           XMOM 420
     X           -RED2*DNDX(J)*DUN/RM(J)                                  XMOM 430
     X           -2.*RED2*DTLA*UA*DNDX(J)/RHOA/RM(J)                      XMOM 440
C                                                                         XMOM 450
C        CALCULATION OF A3                                                XMOM 460
      SUP(I) =RED2/RM(J)*(UA   *DU(J)-DP/RHOA)                            XMOM 470
     X           +RED2*DNDX(J)*UA*(DUN + UA*DTLA/RHOA)/RM(J)              XMOM 480
C                                                                         XMOM 490
C        CALCULATION OF A4                                                XMOM 500
      B(I)   =-RED2*UA  /RM(J)                                            XMOM 510
    5 CONTINUE                                                            XMOM 520
      CALL SOLVE(0.0,U(NETA),UO)                                          XMOM 530
      CALL CHECK(U,B,KODE,IDGF,'U    ',FDAMP)                             XMOM 540
      RETURN                                                              XMOM 550
      END                                                                 XMOM 560
      SUBROUTINE GLOBAL (KODE)
C
C        SOLUTION TO THE GLOBAL CONTINUITY EQUATION FOR 'V' PROFILE
C        USING THE 'U' FORM OF THE GLOBAL CONT. EQUATION
C        THE TRANSFORMED STANDOFF DISTANCE. DTIL. IS ALSO CALCULATED
C
      COMMON/WALL/RVW.PRW.TWOLD.FLUX(20).CWALL(20).ECWALL(5)
      COMMON /NON/RDZ.MUDZ.RMDZ.AKNF.HNF.CPNF
      COMMON/VECTOR/ SUB(60).DIAG(60).SUP(60).B(60)
      COMMON /DEL/ DELTA.DTIL.DTILS
      COMMON /VEL/ F(60).FC(60).Z(60).V(60)
      COMMON/PROP1/PI(60).RHO(60). T(60).AMW(60).C (20.60).EC(5.60)
      COMMON /FRSTRM/ U INF. RINF. UINF2. R . RE. LXI. ITM. IEM. NETA
      COMMON/HOFF1/F1(60).F2(60).G1(60).G2(60).H1(60).H2(60)
      COMMON/JOHN/ UO(60).U(60).DU(60).VO(60).RO(60).DNDX(60).DTLA.DTILO
      COMMON/JTB/ CO(60.20).RED.RED2
      COMMON/BOB/ XI.DXI.YL
      COMMON /YL/ETA(60).YOND(60).YO(60)
      COMMON/MIKE/ NETA1.NETA2.PNF.WNF.RHOD.DP.TS.UD.VD.RW.RWO.EPS.PHI
      COMMON /CONV/ FPRCT.TPRCT.DDAMP.TDAMP.PDTIL
      COMMON /BILL/ NODE(20).ISTART.IDGD.IDGF.IDGH.IDGT.IDGS
      REAL *8 SUB.SUP.DIAG.B
C
C
      DTILC = DTIL
      RWA = YL*RW      + (1-YL)*RWO
      IDN =0
    1 SUM=0.0
      TERM1 = -RHO(1)*V(1)/DTIL
      TERM1 = 0.0
      TERM2 = 0.0
      TERM3 = 0.0
      DO 15 J=1.NETA1
      I = J+1
      DETA= ETA(I) - ETA(J)
      UA  = YL*U(J)    + (1-YL)*UO(J)
      VA   = YL*V(J)    + (1-YL)*VO(J)                                 GLOB 370
      RHOA= YL*RHO(J) + (1-YL)*RO(J)                                   GLOB 380
      ROA = YL*RHO(I) + (1-YL)*RO(I)                                   GLOB 390
      ROAA= (RHOA + ROA)/2.                                            GLOB 400
      DRU = (ROA*(YL*U(I) + (1-YL)*UO(I)) - RHOA*UA)/DETA              GLOB 410
      UAP = YL*U(I)     + (1-YL)*UO(I)                                 GLOB 420
      UAA = (UA     + UAP)/2.                                          GLOB 430
      DNX = (DNDX(I) + DNDX(J))/2.                                     GLOB 440
      TERM1 = TERM1 +    DETA/ROAA*                                    GLOB 450
     1       (RHO(J)*U(J)-RO(J)*UO(J) + RHO(I)*U(I)-RO(I)*UO(I))/DXI/2. GLOB 460
      TERM2=TERM2+ DETA*UAA*(RW-RWO)/RWA/DXI                           GLOB 470
      TERM3 = TERM3 + DNX*DRU*DETA/ROAA                                GLOB 480
      SUM1 = SUM                                                       GLOB 490
      SUM = (TERM1 + TERM2 + TERM3)                                    GLOB 500
      IF(IDN.EQ.0) GO TO 15                                            GLOB 510
      TERM = SUM - SUM1                                                GLOB 520
      V(I) = (-(1-YL)*VO(I) + (RHOA*VA - DTIL*TERM)/ROA)/YL            GLOB 530
   15 CONTINUE                                                         GLOB 540
      IF(IDN.EQ.1) GO TO 25                                            GLOB 550
      DTIL =  - (RHO(NETA)*VD - RHO(1)*V(1))/SUM                       GLOB 560
      TEST = (DTIL - DTILC)/DTIL                                       GLOB 570
      KODE = 5                                                         GLOB 580
      IF(ABS(TEST).GT. PDTIL) KODE = 0                                 GLOB 590
      DTIL = DDAMP*DTIL + (1.-DDAMP)*DTILC                             GLOB 600
      IDN = 1                                                          GLOB 610
      GO TO 1                                                          GLOB 620
   25 CONTINUE                                                         GLOB 630
      IF(IDGD.GT.0)                                                    GLOB 640
     XWRITE(6.100) DTIL.DTILO.DELTA                                    GLOB 650
      IF(IDGD.GT.0)                                                    GLOB 660
     XWRITE(6.100) TERM1.TERM2.TERM3                                   GLOB 670
  100 FORMAT(1H0.15X.'DTIL ='.3E16.6)                                  GLOB 680
      RETURN                                                           GLOB 690
      END                                                              GLOB 700
      SUBROUTINE SPECIE (KOD)
C
C        THIS ROUTINE SOLVES THE SPECIES EQUATIONS FOR RADIATING,
C        CHEMICAL NONEQUILIBRIUM,VISCOUS FLOW IN A SHOCK LAYER ABOUT
C        A BLUNT BODY
C
      COMMON/JOHN/ UO(60),U(60),DU(60),VO(60),RO(60),DNDX(60),DTLA,DTILO
      COMMON/HOFF1/F1(60),F2(60),G1(60),G2(60),H1(60),H2(60)
      COMMON /FRSTRM/ U INF, RINF, UINF2, R , RE, LXI, ITM, IEM, NETA
      COMMON/PROP1/PI(60),RHO(60), T(60),AMW(60),C (20,60),EC(5,60)
      COMMON /VEL/ F(60),FC(60),Z(60),V(60)
      COMMON/VECTOR/ SUB(60),DIAG(60),SUP(60),B(60)
      COMMON/NUMBER/NSP,NNS,NE,NC
      COMMON/CK/ISN(20),XWT(19)
      COMMON/FOG/ AII,BB,CC
      COMMON/JTB/ CO(60,20),RED,RED2
      COMMON /RH/ DUD,DPHI,TD,RZB,PD,HD,HTOTAL
      COMMON/ID/SP(20),EL(5)
      COMMON /NON/RDZ,MUDZ,RMDZ,AKNF,HNF,CPNF
      COMMON/TOM/ SC(60),TO(60)
      COMMON/MIKE/ NETA1,NETA2,PNF,WNF,RHOD,DP,TS,UD,VD,RW,RWO,EPS,PHI
      COMMON/BOB/ XI,DXI,YL
      COMMON /DEL/ DELTA,DTIL,DTILS
      DIMENSION DRO(60),Y(20),FT(60)
      COMMON /BILL/ KODE(20),ISTART,IDGD,IDGF,IDGM,IDGT,IDGS
      COMMON/CONV1/HDAMP,FDAMP,CDAMP
      REAL*8 SUB,DIAG, SUP,B
      REAL MUDZ
C
      KOD = 5
      DTLA = YL*DTIL +  (1-YL)*DTILO
      RED = RE*DTLA
      RED2 = RED*DTLA
      CALL MASMOL (NSP,NETA)
      DO 15 K=1,NSP
      KK=ISN(K)
      IF(IEN.GT.1 .AND. KODE(KK).GT.4) GO TO 15                         SPEC 370
      DO 5 I=1,NETA2                                                    SPEC 380
      J=I+1                                                             SPEC 390
      DO 25 L=1,NSP                                                     SPEC 400
      C(ISN(L),J)= ABS(C(ISN(L),J))                                     SPEC 410
      Y(L)= YL*C(ISN(L),J) + (1-YL)*CO(J,ISN(L))                        SPEC 420
   25 CONTINUE                                                          SPEC 430
      TA = YL*T(J) + (1-YL)*TO(J)                                       SPEC 440
      UA = YL*U(J) + (1-YL)*UO(J)                                       SPEC 450
      VA  = YL*V(J)    + (1-YL)*VO(J)                                   SPEC 460
      RHOA= YL*RHO(J) + (1-YL)*RO(J)                                    SPEC 470
      CALL FG2(Y,RHOD*RHOA,TS*TA,K)                                     SPEC 480
      DSC = F1(J)*SC(J+1) + G1(J)*SC(J) + H1(J)*SC(I)                   SPEC 490
C                                                                       SPEC 500
C        CALCULATION OF A1                                              SPEC 510
      SUB(I) =( DSC-RED*RHOA*VA - RED2*UA*DNDX(J))/SC(J)                SPEC 520
C                                                                       SPEC 530
C        CALCULATION OF A2                                              SPEC 540
      DIAG(I)=RED2*AII*WNF/SC(J)                                        SPEC 550
C                                                                       SPEC 560
C        CALCULATION OF A3                                              SPEC 570
      SUP(I) =RED2*(CC-AII*Y(K))*WNF/SC(J)                              SPEC 580
C                                                                       SPEC 590
C        CALCULATION OF A4                                              SPEC 600
      B(I)    =-RED2*UA/SC(J)                                           SPEC 610
    5 CONTINUE                                                          SPEC 620
C                                                                       SPEC 630
      CALL SOLVE (C(KK,1),C(KK,NETA),CO(1,KK))                          SPEC 640
      DO 45 I=1,NETA                                                    SPEC 650
      FT (I)=C(KK,I)                                                    SPEC 660
   45 CONTINUE                                                          SPEC 670
      CALL CHECK (FT,B,KODE(KK),IDGS,SP(KK),CDAMP)                      SPEC 680
      DO 55 I=1,NETA                                                    SPEC 690
      C(KK,I)=  FT(I)                                                   SPEC 700
   55 CONTINUE                                                          SPEC 710
      KOD = AMINO (KOD,KODE(KK))                                        SPEC 720
   15 CONTINUE                                                                  SPEC 730
      IF(IDGS.GT.0)                                                             SPEC 740
     XWRITE (6,100) (SP(I),KODE(I),I=1,NSP)                                     SPEC 750
  100 FORMAT((2X,10(A4,I2,4X)))                                                 SPEC 760
      CALL MOLMAS (NSP,NETA)                                                    SPEC 770
      RETURN                                                                    SPEC 780
      END                                                                       SPEC 790
      SUBROUTINE MOLMAS (K.N)                                           MOLM  10
      COMMON/PROP1/PI(60).RHO(60). T(60).AMW(60).C (20.60).EC(5.60)     MOLM  20
      COMMON/WT/SMW(20).AWT(5)                                          MOLM  30
      COMMON/JTB/ CO(60.20).RED.RED2                                    MOLM  40
      DO 5 J=1.N                                                        MOLM  50
      AM=0.0                                                            MOLM  60
      SUM=0.0                                                           MOLM  70
      DO 15 I=1.K                                                       MOLM  80
      AM = AM + C(I.J)                                                  MOLM  90
      C(I.J)=C(I.J)*SMW(I)                                              MOLM 100
      SUM=SUM + C(I.J)                                                  MOLM 110
   15 CONTINUE                                                          MOLM 120
      DO 35 I=1.K                                                       MOLM 130
      C(I.J)=C(I.J)/SUM                                                 MOLM 140
      CO(J.I)=CO(J.I)*SMW(I)                                            MOLM 150
   35 CONTINUE                                                          MOLM 160
      AMW(J)=1./AM                                                      MOLM 170
    5 CONTINUE                                                          MOLM 180
      RETURN                                                            MOLM 190
      ENTRY MASMOL (K.N)                                                MOLM 200
      DO 25 J=1.N                                                       MOLM 210
      DO 25 I=1.K                                                       MOLM 220
      C(I.J)=C(I.J)/SMW(I)                                              MOLM 230
      CO(J.I)=CO(J.I)/SMW(I)                                            MOLM 240
   25 CONTINUE                                                          MOLM 250
      RETURN                                                            MOLM 260
      END                                                               MOLM 270
      SUBROUTINE ENERGY (KODE)
C
C        THIS ROUTINE SOLVES THE ENTHALPY FORM OF THE ENERGY EQUATION
C        FOR THE RADIATING. CHEMICALLY REACTING. VISCOUS FLOW IN A
C        SHOCK LAYER ABOUT A BLUNT BODY
C
      COMMON/DON/ PO(60).EO(60).HMO(60)
      COMMON/BOB/ XI.DXI.YL
      COMMON/MIKE/ NETA1.NETA2.PNF.WNF.RHOD.DP.TS.UD.VD.RW.RWD.EPS.PHI
      COMMON/PROP2/VISM(60).RM(60).TCM(60)
      COMMON/JTB/ CO(60.20).RED.RED2
      COMMON /VEL/ F(60).FC(60).Z(60).V(60)
      COMMON/HOFF1/F1(60).F2(60).G1(60).G2(60).H1(60).H2(60)
      COMMON/TOM/ SC(60).TO(60).PR(60).TE(60)
      COMMON/JOHN/ UO(60).U(60).DU(60).VO(60).RO(60).DNDX(60).DTLA.DTILO
      COMMON/NUMBER/NSP.NNS.NE.NC
      COMMON /NON/RDZ.MUDZ.RMDZ.AKNF.HNF.CPNF
      COMMON/VECTOR/ SUB(60).DIAG(60).SUP(60).B(60)
      COMMON/PROP1/PI(60).RHO(60). T(60).AMW(60).C (20.60).EC(5.60)
      COMMON /FRSTRM/ U INF. RINF. UINF2. R . RE. LXI. ITM. IEM. NETA
      COMMON /DEL/ DELTA.DTIL.DTILS
      COMMON/PROP3/CP(20.60).H(20.60).CPM(60).HM(60)
      COMMON /RFLUX/ E(60).IRAD.ITYPE
      COMMON/CONV1/HDAMP.FDAMP.CDAMP
      COMMON /BILL/ NODE(20).ISTART.IDGD.IDGF.IDGH.IDGT.IDGS
      REAL *8 SUB.SUP.DIAG.B
C
      IF ( KODE .GT. 4 .AND. IEM .GT. 1 ) RETURN
      DTLA = YL*DTIL +  (1-YL)*DTILO
      DTIL2 = DTLA*DTLA
C
            EMA = YL*E(1) + (1-YL)*EO(1)
      EP = E(2)
      EA  =  YL*EP + (1-YL)*EO(2)
      DO 15 I=1.NETA2
      J = I+1
      EP = E(J+1)                                                       ENER 370
      EPA = YL*EP + (1-YL)*EO(J+1)                                      ENER 380
      HMM = YL*HM(I) + (1-YL)*HMO(I)                                    ENER 390
      HMP = YL*HM(J+1) + (1-YL)*HMO(J+1)                                ENER 400
      VA  = YL*V(J)    + (1-YL)*VO(J)                                   ENER 410
      UA = YL*U(J) + (1-YL)*UO(J)                                       ENER 420
      RHOA= YL*RHO(J) + (1-YL)*RO(J)                                    ENER 430
      S1 = 0.0                                                          ENER 440
      S2 = 0.0                                                          ENER 450
      S3 = 0.0                                                          ENER 460
      DO 25 K=1,NSP                                                     ENER 470
      DH  = F1(J)*H(K,J+1) + G1(J)*H(K,J) + H1(J)*H(K,I)                ENER 480
      DC1 = F1(J)*C(K,J+1) + G1(J)*C(K,J) + H1(J)*C(K,I)                ENER 490
      DC2 = F2(J)*C(K,J+1) + G2(J)*C(K,J) + H2(J)*C(K,I)                ENER 500
      S1 = S1 + DC1*DH                                                  ENER 510
      S2 = S2 + H(K,J)*DC1                                              ENER 520
      S3 = S3 + H(K,J)*DC2                                              ENER 530
   25 CONTINUE                                                          ENER 540
      DPR = F1(J)*PR(J+1) + G1(J)*PR(J) + H1(J)*PR(I)                   ENER 550
      DSC = F1(J)*SC(J+1) + G1(J)*SC(J) + H1(J)*SC(I)                   ENER 560
      DRM = F1(J)*RM(J+1) + G1(J)*RM(J) + H1(J)*RM(I)                   ENER 570
      DVN = F1(J)* V(J+1) + G1(J)* V(J) + H1(J)* V(I)                   ENER 580
      DUN = F1(J)* U(J+1) + G1(J)*U (J) + H1(J)* U(I)                   ENER 590
      DUN2= F2(J)* U(J+1) + G2(J)* U(J) + H2(J)* U(I)                   ENER 600
      DVN = YL*DVN + (1-YL)*(F1(J)*VO(J+1)+G1(J)*VO(J)+H1(J)*VO(I))     ENER 610
      DUN = YL*DUN + (1-YL)*(F1(J)*UO(J+1)+G1(J)*UO(J)+H1(J)*UO(I))     ENER 620
      DUN2= YL*DUN2+ (1-YL)*(F2(J)*UO(J+1)+G2(J)*UO(J)+H2(J)*UO(I))     ENER 630
      UP =(U(J) - UO(J))/DXI                                            ENER 640
      DV =(V(J) - VO(J))/DXI                                            ENER 650
C        SC(J) = RM/SC                                                  ENER 660
      S1 = S1*(SC(J)/RE/2. - PR(J))                                     ENER 670
      S3 = S3*(SC(J)/RE/2. - PR(J))                                     ENER 680
      S2 = S2*(DSC/RE/2.    - DPR)                                      ENER 690
      S4 = ((RM(J)*DUN + UA*DRM )*DUN + RM(J)*UA*DUN2)/RE               ENER 700
      S5 = DTIL2*(UA*UA*UP +(UA*UA*DNDX(J)+RHOA*VA*UA/DTLA)*DUN         ENER 710
     X     + VA*UA*DV + (VA*UA*DNDX(J) + RHOA*VA*VA/DTLA)*DVN)          ENER 720
```

```
C                                                                        ENER 730
C                                                                        ENER 740
C        CALCULATION OF A1                                               ENER 750
      SUB(I) = (DPR - UA*DTIL2*DNDX(J)/2. - RHOA*VA*DTLA/2.)/PR(J)      ENER 760
C                                                                        ENER 770
C        CALCULATION OF A2                                               ENER 780
      DIAG(I)= (EPA -EMA)/(HMP - HMM)/PR(J)*(-   DTIL2/RHOA)           ENER 790
      DIAG(I)= 0.0                                                       ENER 800
C                                                                        ENER 810
C        CALCULATION OF A3                                               ENER 820
      SUP(I) = ( S1 + S2 + S3 - DTIL2*EA/RHOA + S4 - S5 )/PR(J)         ENER 830
     X    - DIAG(I)*HM(J)                                                ENER 840
C                                                                        ENER 850
C        CALCULATION OF A4                                               ENER 860
      B(I)    = -DTIL2*UA/PR(J)/2.                                       ENER 870
      EMA = EA                                                           ENER 880
      EA  = EPA                                                          ENER 890
   15 CONTINUE                                                           ENER 900
C                                                                        ENER 910
      CALL  SOLVE (HM(1),HM(NETA),HMO)                                   ENER 920
      CALL  CHECK (HM,B,KODE,IDGH,'ENTH',HDAMP)                          ENER 930
      CALL  TEMPR                                                        ENER 940
      RETURN                                                             ENER 950
      END                                                                ENER 960
      SUBROUTINE TEMPR
C
C        THIS ROUTINE DETERMINES THE TEMPERATURE PROFILE GIVEN
C        A STSTIC ENTHALPY PROFILE AND SPECIES PROFILES
C
      COMMON/PROP3/CP(20.60).H(20.60).CPM(60).HM(60)
      COMMON /FRSTRM/ U INF. RINF. UINF2. R . RE. LXI. ITM. IEM. NETA
      COMMON/PROP1/PI(60).RHO(60). T(60).AMW(60).C (20.60).EC(5.60)
      COMMON/VECTOR/ SUB(60).DIAG(60).SUP(60).B(60)
      COMMON/MIKE/ NETA1.NETA2.PNF.WNF.RHOD.DP.TS.UD.VD.RW.RWO.EPS.PHI
      COMMON/NUMBER/NSP.NNS.NE.NC
      COMMON /MAIN/KEEP.MAXE.MAXM.MAXD.IDEBUG.MCONV.ECONV.DCONV.LT.IAB
      COMMON /CONV/ FPRCT.TPRCT.DDAMP.TDAMP.PDTIL
      COMMON /BILL/ NODE(20).ISTART.IDGD.IDGF.IDGH.IDGT.IDGS
      COMMON /YL/ETA(60).YOND(60)
      REAL *8 SUB.SUP.DIAG.B
C
      DO 15 J=2.NETA1
      TC = T(J)
      B(J-1) = HM(J)
C
      K = 0
   10 CALL PROPRT (NSP.J.J)
      K = K + 1
      DTT = (B(J-1) - HM(J))/CPM(J)
      T(J) = T(J) + DTT
      DTT = DTT/T(J)
C
      IF(K .GT. MAXE) GO TO 30
      IF(ABS(DTT).GT. TPRCT) GO TO 10
      GO TO 20
   30 WRITE(6.200) MAXE.J.TC.T(J)
  200 FORMAT(2X.'*** MAXIMUM NO. OF ITERATIONS('.I3.') EXCEEDED FOR TEMP
     XERATURE - ENTHALPY AT ETA POINT'.I3./.5X.'TOLD='.F10.4.3X.'TNEW='.
     X  F10.4)
   20 B(J-1) = T(J)
```

```
      DIFF = (T(J) - TC)/TC                                             TEMP 370
      IF(ABS(DIFF) .GT. 0.03) B(J-1) = TC + .03*TC*ABS(DIFF)/DIFF       TEMP 380
      T(J) = TC                                                         TEMP 390
   15 CONTINUE                                                          TEMP 400
      CALL CHECK (T,B,KODE,IDGT,'TEMP',TDAMP)                           TEMP 410
      RETURN                                                            TEMP 420
      END                                                               TEMP 430
      SUBROUTINE PROPRT(NSP,NI,NF)                                      PROP  10
C * * * * * * * * * * * * * * * * * * * * * * * * * * * * * * * * * * * PROP  20
C                                                                       PROP  30
C      SUBROUTINE FOR THE CALCULATION OF THERMODYNAMIC AND TRANSPORT    PROP  40
C      PROPERTIES                                                       PROP  50
C                                                                       PROP  60
C      NOMENCLATURE....                                                 PROP  70
C            Y(I)...MOLE FRACTION OF COMPONENT I                        PROP  80
C            C(I,N)...MASS FRACTION OF COMPONENT I AT POINT N           PROP  90
C            T1........TEMPERATURE, DEG. K                              PROP 100
C            CP(I).....SPECIES SPECIFIC HEAT, CAL/GMOLE OF I-K          PROP 110
C            CPM(N)....MIXTURE SPECIFIC HEAT, CAL/GMOLE OF M-K          PROP 120
C            H(I)......SPECIES ENTHALPY, CAL/GMOLE OF I                 PROP 130
C            HM(N).....MIXTURE ENTHALPY, CAL/GMOLE OF M                 PROP 140
C            VIS(I)....SPECIES VISCOSITY, LBM/FT-SEC                    PROP 150
C            VISM(N)...MIXTURE VISCOSITY, LBM/FT-SEC                    PROP 160
C            TC(I).....SPECIES THERMAL CONDUCTIVITY, BTU/FT-SEC-DEG. R  PROP 170
C            TCM(N)...MIXTURE  THERMAL CONDUCTIVITY, BTU/FT-SEC-DEG. R  PROP 180
      COMMON /BLOCK1/V1(20),V2(20),V3(20)                               PROP 190
      COMMON/BLOCK3/K1(20),K2(20)                                       PROP 200
      COMMON/EQ1/AI(20), BI(20), CI(20), DI(20), EI(20), FI(20), GI(20),PROP 210
     X        AII(20),BII(20),CII(20),DII(20),EII(20),FII(20),GII(20)   PROP 220
      COMMON /FRSTRM/ U INF, RINF, UINF2,RAD, RE, LXI, ITM, IEM,NETA    PROP 230
      COMMON/PROP1/PI(60),RHO(60),T(60),AMW(60),C (20,60),CC(5,60)      PROP 240
      COMMON/PROP2/VISM(60),RM(60),TCM(60)                              PROP 250
      COMMON/PROP3/CP(20,60),H(20,60),CPM(60),HM(60)                    PROP 260
      COMMON/WT/SMW(20),AWT(5)                                          PROP 270
      COMMON /RH/ DUD,DPHI,TD,RZB,PD,HD,HTOTAL                          PROP 280
      COMMON /NON/RDZ,MUDZ,RHDZ,AKNF,HNF,CPNF                           PROP 290
      COMMON/TOM/ SC(60),TD(60),PR(60)                                  PROP 300
      COMMON/MIKE/ NETA1,NETA2,PNF,WNF,RHOD,DP,TS,UD,VD,RW,RWO,EPS      PROP 310
      COMMON/JOHN/ UO(60),U(60),DU(60),VO(60),RO(60),DNDX(60),DTLA,DTELUPROP 320
      COMMON/BOB/ XI,DXI,YL                                             PROP 330
      DIMENSION PHI(20,20),YPHI(20),Y(20),TC(20),VIS(20)                PROP 340
      DIMENSION SAMW(2)                                                 PROP 350
      REAL  MU,MUDZ,K1,K2                                               PROP 360
      DATA R /1.98716/
C
      DO500N=NI,NF
      TA = YL*T(N) + (1-YL)*TO(N)
      T1=TA*TS
      T2=T1*T1
      T3=T2*T1
      T4=T3*T1
      T5=T4*T1
      DO150I=1,NSP
      IF(T1.GT.6000.)GOTO 50
      CP(I,N)=( AI(I)+ BI(I)*T1+ CI(I)*T2+ DI(I)*T3+ EI(I)*T4)*R
      H(I,N)=( AI(I)*T1+ BI(I)*T2/2.+ CI(I)*T3/3.+ DI(I)*T4/4.
     X                  + EI(I)*T5/5.+ FI(I))*R
      GOTO 100
   50 CP(I,N)=(AII(I)+BII(I)*T1+CII(I)*T2+DII(I)*T3+EII(I)*T4)*R
      H(I,N)=(AII(I)*T1+BII(I)*T2/2.+CII(I)*T3/3.+DII(I)*T4/4.
     X                  +EII(I)*T5/5.+FII(I))*R
  100 IF(NF.NE.NETA) GO TO 150
      Y(I)=C(I,N)*AMW(N)/SMW(I)
      VIS(I)=(V1(I) + V2(I)*T1 + V3(I)*T2)*1.0E-05
      TC(I)=(K1(I)+K2(I)*T1)*1.0E-5
  150 CONTINUE
      IF(NF.NE.NETA) GO TO 500
C-----CALCULATE PHI(I,J) PARAMETERS FOR MIXTURE PROPERTIES....
C
      DO200 I=1,NSP
      DO200J=1,NSP
      VIS12=SQRT(VIS(I)/VIS(J))
      SMW14=(SMW(J)/SMW(I))**.25
      PHI(I,J)=.354*((1.+VIS12*SMW14)**2)/SQRT(1.+SMW(I)/SMW(J))
  200 CONTINUE
C
C-----CALCULATION OF MIXTURE PROPERTIES...
C
      DO250I=1,NSP
      YPHI(I)=0.0                                                       PROP 730
      DO250J=1.NSP                                                      PROP 740
  250 YPHI(I)=YPHI(I) + Y(J)*PHI(I.J)                                   PROP 750
      VISM(N)=0.0                                                       PROP 760
      TCM(N) = 0.                                                       PROP 770
      DO300I=1.NSP                                                      PROP 780
      IF(Y(I).LT.1.E-5) GO TO 300                                       PROP 790
      VISM(N)=VISM(N)+Y(I)*VIS(I)/YPHI(I)                               PROP 800
  300 TCM(N) = TCM(N) + Y(I)*TC(I)/YPHI(I)                              PROP 810
      RHO(N) = PI(N)*AMW(N)/T(N)/TS/RDZ/1.3157/32.174                   PROP 820
      RHOA= YL*RHO(N) + (1-YL)*RO(N)                                    PROP 830
      D=8.128E-8*T1**1.659/PD                                           PROP 840
      SC(N) = VISM(N)/RHOA/RHOD/D                                       PROP 850
  500 CONTINUE                                                          PROP 860
C                                                                       PROP 870
C----- NONDIMENSIONALIZE QUANTITIES -----                               PROP 880
C                                                                       PROP 890
      DO 550 N=NI.NF                                                    PROP 900
      CPM(N) = 0.                                                       PROP 910
      HM(N) = 0.                                                        PROP 920
      DO 555I=1.NSP                                                     PROP 930
      CP(I.N) = CP(I.N)*CPNF/SMW(I)                                     PROP 940
      H(I.N) = H(I.N)*HNF*1.80/SMW(I)                                   PROP 950
      CPM(N) = CPM(N) + CP(I.N)*C(I.N)                                  PROP 960
      HM(N) = HM(N) + H(I.N)*C(I.N)                                     PROP 970
  555 CONTINUE                                                          PROP 980
      IF(NF.NE.NETA) GO TO 550                                          PROP 990
      VISM(N) = VISM(N)/MUDZ                                            PROP1000
      TCM(N) = TCM(N)*AKNF                                              PROP1010
      RHOA= YL*RHO(N) + (1-YL)*RO(N)                                    PROP1020
      RM(N)=RHOA*VISM(N)                                                PROP1030
      SC(N) = RM(N)/SC(N)                                               PROP1040
      PR(N) = RHOA*TCM(N)/CPM(N)                                        PROP1050
  550 CONTINUE                                                          PROP1060
      RETURN                                                            PROP1070
      END                                                               PROP1080
      SUBROUTINE TRID (M)                                               TRID  10
C**** TRID --TRIDIAGONAL EQUATION SOLVER  OBTAINED FROM CONTE P-184 *** TRID  20
C      SUBROUTINE SOLVES AX = B FOR THE VECTOR X (WHERE A IS TRIDIAGONALTRID  30
C      M = ORDER OF SYSTEM                                              TRID  40
C      SUP = SUPER DIAGONAL OF A                                        TRID  50
C      SUB = SUB DIAGONAL OF A                                          TRID  60
C      DIAG = MAIN DIAGONAL OF A                                        TRID  70
C      B = CONSTANT VECTOR                                              TRID  80
C      SUP AND DIAG ARE DESTROYED                                       TRID  90
C      SOLUTION VECTOR IS RETURNED IN B                                 TRID 100
C                                                                       TRID 110
      COMMON/VECTOR/ SUB(60),DIAG(60),SUP(60),B(60)                     TRID 120
      REAL*8 SUB,DIAG,SUP,B                                             TRID 130
C                                                                       TRID 140
      N = M                                                             TRID 150
      NN = N -1                                                         TRID 160
      SUP(1) = SUP(1)/DIAG(1)                                           TRID 170
      B(1) = B(1)/DIAG(1)                                               TRID 180
      DO 10 I=2,N                                                       TRID 190
      II = I -1                                                         TRID 200
C------DECOMPOSE A TO FORM A = LU WHERE L IS LOWER TRIANGULAR,          TRID 210
C       AND U IS UPPER TRIANGULAR ---------                             TRID 220
      DIAG(I) = DIAG(I) - SUP(II)*SUB(II)                               TRID 230
      IF(I .EQ.  N) GO TO 10                                            TRID 240
      SUP(I) = SUP(I) / DIAG(I)                                         TRID 250
C------COMPUTE Z WHERE LZ = B                                           TRID 260
   10 B(I) = (B(I) - SUB(II) *B(II))/ DIAG(I)                           TRID 270
C------COMPUTE X BY BACK SUBSTITUTION WHERE UX = Z                      TRID 280
      DO 20 K =1,NN                                                     TRID 290
      I = N - K                                                         TRID 300
   20 B(I) = B(I) -SUP(I) *B(I+1)                                       TRID 310
      RETURN                                                            TRID 320
      END                                                               TRID 330
      SUBROUTINE CHECK (W.B.KODE.IDG.SP.FR)
C
C        THIS ROUTINE CHECKS TO SEE IF THE SOLUTION OF A PROFILE 'W'
C        IS CONVERGED
C
C        W = GUESSED PROFILE
C        B = CALCULATED PROFILE
C        FR = WEIGHTING FRACTION
C        IDG =  DEBUG OUTPUT.IDG.GT.1 YIELDS W AND B PROFILES OUTPUT
C        KODE = CONVERGENCE CODE
C        KOCE = 0 . FAR FROM CONVERGENCE
C        KODE = 5 . CONVERGED
C        SP = VARIABLE NAME
C
      COMMON /FRSTRM/ U INF. RINF. UINF2. R . RE. LXI. ITM. IEM. NETA
      DIMENSION W(1).B(1)
      REAL*8 B
      DATA TOL1.TOL2.TOL3.TOL4/.05..025..01..005/
      NETA2=NETA-2
      KODE=5
      IF(IDG.GT.1) CALL OUTPUT (W.B.SP.NETA2)
      DO 5 I=1.NETA2
      IF(W(I+1).EQ.0.0) GO TO 6
      ABD=(B(I)-W(I+1))/W(I+1)
      AB =ABS(ABD)
      IF(W(I+1).LT.1.E-6.AND.B(I).LT.1.E-6) GO TO 6
      GO TO (4.4.3.2.1).KODE
    1 IF(AB.GT.TOL4) KODE=4
    2 IF(AB.GT.TOL3) KODE=3
    3 IF(AB.GT.TOL2) KODE=2
    4 IF(AB.GT.TOL1) KODE=1
    6 W(I+1) = FR*B(I) + (1-FR)*W(I+1)
    5 CONTINUE
      RETURN
      END
      SUBROUTINE OUTPUT(W,B,SP,N)
C
C        DEBUG OUTPUT FOR GUESSED(W) AND CALCULATED(B) VALUES OF 'SP'
C
      DIMENSION W(1),B(1)
      REAL*8 B
C
      WRITE(6,110) SP
  110 FORMAT(1H0,5X,A4,//)
      I=1
      WRITE(6,100)I,W(I)
      M=N+1
      L=M+1
      WRITE(6,100) (J,W(J),B(J-1),J=2,M),L,W(L)
  100 FORMAT((10X,3(I5,2E16.7)))
      RETURN
      END
      SUBROUTINE FG2 (Y.RHOA.TN.K)                                               FG2   10
C--------ORCER OF SPECIES ISO                                                    FG2   20
C         CO          C          C2          C3          C+         C2H        CN FG2   30
C          1          2           3           4           5           6         7 FG2   40
C        HCN         H2           H          N2           N          N+         O FG2   50
C          8          9          10          11          12          13        14 FG2   60
C         O+         E-        C2H2         C3H         C4H                       FG2   70
C         15         16          17          18          19                       FG2   80
      COMMON/FOG/AII      .B      .C     .                T                        FG2   90
      DIMENSION Y(19).T1(5)                                                      FG2  100
      DIMENSION RHO(2).QK(16.2).PL(16.10). RATES(3.16).EQK(16)                   FG2  110
      DATA R/82.05/                                                              FG2  120
      DATA RATES/                                                                FG2  130
C        KINETIC COEFFICIENTS FOR CASE 1                                         FG2  140
     1   .4352597E 02.   .5000000E 00.   .3500000E 05.   .2683251E 02.           FG2  150
     2   .5000000E 00.   .1761263E 05.   .4835429E 02.  -.1500000E 01.           FG2  160
     3   .1131738E 05.   .4272747E 02.  -.8200000E 00.   .5193211E 05.           FG2  170
     4   .2866064E 02.   .5000C00E 00.   .1575073E 06.   .2870602E 02.           FG2  180
     5   .5000000E 00.   .1675716E 06.   .4684016E 02.  -.1000000E 01.           FG2  190
     6   .6632414E 05.   .4357476E 02.   .5000000E 00.   .6038617E 05.           FG2  200
     7   .4369782E 02.   .5000C00E 00.   .7045053E 05.   .4369782E 02.           FG2  210
     8   .5C00000E 00.   .5887682E C5.   .4588918E 02.  -.1000000E 01.           FG2  220
     9   .1297799E 06.   .4374912E 02.   .5000000E 00.   .9561144E 05.           FG2  230
     A   .4367655E 02.   .5000000E 00.   .7052980E 05.   .4368724E 02.           FG2  240
     1   .5000000E 00.   .1307138E 06.   .4369782E 02.   .5000000E 00.           FG2  250
     2   .8303098E 05.   .4369782E 02.   .5000000E 00.   .7296662E 05/           FG2  260
      DIMENSION E1(95).E2(95).E3(34).E(16.7.2)                                   FG2  270
      EQUIVALENCE (E(1.1.1).E1(1))                                               FG2  280
      DATA E1/                                                                   FG2  290
     1 0.3530E 00. 0.1816E 01. 0.1727E 01. 0.1642E 01. 0.2321E 01.               FG2  300
     2 0.2753E 01. 0.1675E 01. 0.2257E 01. 0.3458E 01. 0.2094E 01.               FG2  310
     3 0.2028E 01. 0.3053E 01. 0.7810E 00. 0.2497E 01. 0.2132E 01.               FG2  320
     4 0.7030E 00.-0.7681E-03.-0.3571E-02.-0.8059E-03.-0.2810E-03.               FG2  330
     5 0.2250E-03.-0.3726E-03.-0.6017E-03.-0.2955E-02.-0.3852E-02.               FG2  340
     6-0.2155E-02.-0.1370E-02.-0.4032E-02.-0.1175E-03. 0.6404E-04.               FG2  350
     7-0.2840E-02.-0.1406E-02. 0.5153E-06. 0.1634E-05. 0.1344E-06.               FG2  360
     8-0.9244E-07,-0.9094E-07, 0.1884E-06,-0.6914E-07, 0.1359E-05,      FG2  370
     9 0.1541E-05, 0.7206E-06, 0.4461E-06, 0.1731E-05,-0.8460E-07,      FG2  380
     A-0.5011E-07, 0.1138E-05, 0.5735E-06,-0.9618E-10,-0.2783E-09,      FG2  390
     1 0.4980E-11, 0.2914E-10, 0.1275E-10,-0.3765E-10, 0.3996E-10,      FG2  400
     2-0.2518E-09,-0.2492E-09,-0.1067E-09,-0.5622E-10,-0.2858E-09,      FG2  410
     3 0.2854E-10, 0.6619E-11,-0.2020E-09,-0.8895E-10, 0.5427E-14,      FG2  420
     4 0.1617E-13,-0.9780E-15,-0.2112E-14,-0.5056E-15, 0.2271E-14,      FG2  430
     5-0.2991E-14, 0.1668E-13, 0.1406E-13, 0.5735E-14, 0.2436E-14,      FG2  440
     6 0.1621E-13,-0.2197E-14,-0.2271E-15, 0.1335E-13, 0.4609E-14,      FG2  450
     7 0.3485E 05, 0.1329E 05, 0.1132E 06, 0.5196E 05, 0.1580E 06,      FG2  460
     8 0.1686E 06, 0.9406E 05, 0.5850E 05, 0.6525E 05, 0.5766E 05,      FG2  470
     9 0.1289E 06, 0.8906E 05, 0.7297E 05, 0.1306E 06, 0.8068E 05/      FG2  480
      EQUIVALENCE (E(16,6,1),E2(1))                                     FG2  490
      DATA E2/                                                          FG2  500
     1 0.7220E 05, 0.7500E-01,-0.8961E 01, 0.4274E 01, 0.2626E 01,      FG2  510
     2-0.1181E 02,-0.1238E 02, 0.3698E 01, 0.1912E 01,-0.6335E 01,      FG2  520
     3 0.3671E 01, 0.3773E 01, 0.1034E 01, 0.9378E 01,-0.1216E 02,      FG2  530
     4 0.5461E 01, 0.1162E 02,-0.9100E-01,-0.1852E 01, 0.1765E 01,      FG2  540
     5 0.4505E 01, 0.2904E 01, 0.2261E 01, 0.1414E 01, 0.3753E 01,      FG2  550
     6 0.2653E 01, 0.2452E 01, 0.1323E 01,-0.1596E 02, 0.2560E 00,      FG2  560
     7 0.2895E 01, 0.3483E 01, 0.2320E 00, 0.2624E-03, 0.1831E-02,      FG2  570
     8-0.1250E-02,-0.4018E-02,-0.3576E-03, 0.3808E-03,-0.8027E-03,      FG2  580
     9-0.4486E-02,-0.2187E-02,-0.2382E-02,-0.5403E-03, 0.1840E-01,      FG2  590
     A 0.1581E-03,-0.3234E-03,-0.4981E-02,-0.8811E-03,-0.8699E-09,      FG2  600
     1-0.5850E-06, 0.3816E-06, 0.1254E-05, 0.6591E-07,-0.1210E-06,      FG2  610
     2 0.1697E-06, 0.1768E-05, 0.6688E-06, 0.6930E-06, 0.1688E-06,      FG2  620
     3-0.5690E-05,-0.3970E-07, 0.4932E-07, 0.2072E-05, 0.4090E-06,      FG2  630
     4-0.5441E-11, 0.7641E-10,-0.3536E-10,-0.1592E-09,-0.3159E-11,      FG2  640
     5 0.1070E-10,-0.1315E-10,-0.2902E-09,-0.8277E-10,-0.8428E-10,      FG2  650
     6-0.1859E-10, 0.6841E-09, 0.2542E-11,-0.2579E-11,-0.3588E-09,      FG2  660
     7-0.6840E-10, 0.2100E-15,-0.3417E-14, 0.1003E-14, 0.7013E-14,      FG2  670
     8 0.2813E-16,-0.3032E-15, 0.3831E-15, 0.1768E-13, 0.3596E-14,      FG2  680
     9 0.3630E-14, 0.5931E-15,-0.2842E-13, 0.2920E-17, 0.2381E-16/      FG2  690
      EQUIVALENCE (E(15,5,2),E3(1))                                     FG2  700
      DATA E3/                                                          FG2  710
     1 0.2234E-13, 0.3694E-14, 0.4160E 05, 0.1329E 05, 0.1132E 06,      FG2  720
     2 0.5196E 05, 0.1580E 06, 0.1686E 06, 0.8731E 05, 0.6525E 05,
     3 0.6525E 05, 0.5766E 05, 0.1289E 06, 0.8906E 05, 0.7297E 05,
     4 0.1306E 06, 0.8068E 05, 0.7220E 05, 0.2066E 01, 0.1126E 02,
     5 0.4450E 01,-0.1348E 02,-0.1538E 02,-0.1000E 02, 0.5594E 01,
     6-0.6819E 01,-0.2220E 01, 0.1504E 01, 0.7660E 01, 0.1101E 03,
     7 0.1266E 02,-0.1481E 02,-0.1881E 01, 0.1435E 02/
      IF (K.LT. 20) GO TO 5
      AII=0.0
      C  =0.0
      RETURN
    5 CONTINUE
C        RHOA= DENSITY (LBM/FT3)
      RHOB= .031085*RHOA
      RHO(1)=.515362*RHOB
      RHO(2)=RHO(1)*RHO(1)
      X=0.
      DO 6 I=1, 19
    6 X=X+Y(I)
      IF(ABS((TN-T)/TN)-.0001)20,20,10
   10 T=TN
      T1(1) = T
      DO12M=2,4
   12 T1(M) = T1(1)*T1(M-1)
      T1(5) = ALOG(T1(1))
      RT = R*T
      L=1
      IF(T1(1).GT.6000.)L=2
      DO 18 I=1, 16
      QK(I,1)=T**RATES(2,I)* EXP(RATES(1,I)-RATES(3,I)/T)
      QK(I,2) = E(I,1,L)*(1.-T1(5))-E(I,2,L)*T1(1)/2.-E(I,3,L)*T1(2)/6.
     X-E(I,4,L)*T1(3)/12.-E(I,5,L)*T1(4)/20.+E(I,6,L)/T1(1)-E(I,7,L)
      EQK(I) = EXP(-QK(I,2))
      QK(I,2) = QK(I,1)/ EQK(I)
      IF(I.GT.2)QK(I,2) = RT*QK(I,2)
   18 CONTINUE
   20 PL(  1,  1) = QK(  1,  1)*RHO(1)*Y( 12)
```

```
      INC = 0                                                           FG2 1090
      PL(  1.  2) = QK(  1.  1)*RHO(1)*Y(  1)                           FG2 1100
      PL(  1.  6) = QK(  1.  2)*RHO(1)*Y( 14)                           FG2 1110
      PL(  1.  7) = QK(  1.  2)*RHO(1)*Y(  7)                           FG2 1120
      PL(  2.  1) = QK(  2.  1)*RHO(1)*Y( 10)                           FG2 1130
      PL(  2.  2) = QK(  2.  1)*RHO(1)*Y(  6)                           FG2 1140
      PL(  2.  6) = QK(  2.  2)*RHO(1)*Y(  9)                           FG2 1150
      PL(  2.  7) = QK(  2.  2)*RHO(1)*Y(  3)                           FG2 1160
      PL(  3.  1) = QK(  3.  1)*RHO(1)*X                                FG2 1170
      PL(  3.  6) = 2.*QK(  3.  2)*RHO(2)*Y( 12)*X                      FG2 1180
      PL(  3.  5) = QK(  3.  1)*RHO(1)*Y( 11)                           FG2 1190
      PL(  3. 10) = QK(  3,  2)*RHO(2)*Y( 12)*Y( 12)                    FG2 1200
      PL(  4.  1) = QK(  4.  1)*RHO(1)*X                                FG2 1210
      PL(  4.  6) = 2.*QK(  4.  2)*RHO(2)*Y( 10)*X                      FG2 1220
      PL(  4.  5) = QK(  4.  1)*RHO(1)*Y(  9)                           FG2 1230
      PL(  4. 10) = QK(  4.  2)*RHO(2)*Y( 10)*Y( 10)                    FG2 1240
      PL(  5.  1) = QK(  5.  1)*RHO(1)*X                                FG2 1250
      PL(  5.  6) = QK(  5.  2)*RHO(2)*Y( 16)*X                         FG2 1260
      PL(  5.  7) = QK(  5.  2)*RHO(2)*Y( 15)*X                         FG2 1270
      PL(  5.  5) = QK(  5.  1)*RHO(1)*Y( 14)                           FG2 1280
      PL(  5. 10) = QK(  5.  2)*RHO(2)*Y( 15)*Y( 16)                    FG2 1290
      PL(  6.  1) = QK(  6.  1)*RHO(1)*X                                FG2 1300
      PL(  6.  6) = QK(  6.  2)*RHO(2)*Y( 16)*X                         FG2 1310
      PL(  6.  7) = QK(  6.  2)*RHO(2)*Y( 13)*X                         FG2 1320
      PL(  6.  5) = QK(  6.  1)*RHO(1)*Y( 12)                           FG2 1330
      PL(  6. 10) = QK(  6.  2)*RHO(2)*Y( 13)*Y( 16)                    FG2 1340
      PL(  7.  1) = QK(  7.  1)*RHO(1)*X                                FG2 1350
      PL(  7.  6) = QK(  7.  2)*RHO(2)*Y( 12)*X                         FG2 1360
      PL(  7.  7) = QK(  7.  2)*RHO(2)*Y(  2)*X                         FG2 1370
      PL(  7.  5) = QK(  7.  1)*RHO(1)*Y(  7)                           FG2 1380
      PL(  7. 10) = QK(  7.  2)*RHO(2)*Y(  2)*Y( 12)                    FG2 1390
      PL(  8.  1) = QK(  8.  1)*RHO(1)*X                                FG2 1400
      PL(  8.  6) = QK(  8.  2)*RHO(2)*Y( 10)*X                         FG2 1410
      PL(  8.  7) = QK(  8.  2)*RHO(2)*Y(  7)*X                         FG2 1420
      PL(  8.  5) = QK(  8.  1)*RHO(1)*Y(  8)                           FG2 1430
      PL(  8. 10) = QK(  8.  2)*RHO(2)*Y(  7)*Y( 10)                    FG2 1440
      PL(  9.  1) = QK(  9.  1)*RHO(1)*X                                FG2 1450
      PL(  9.  6) = QK(  9.  2)*RHO(2)*Y( 10)*X                         FG2 1460
      PL(  9.  7) = QK(  9.  2)*RHO(2)*Y(  3)*X                         FG2 1470
      PL(  9.  5) = QK(  9.  1)*RHO(1)*Y(  6)                           FG2 1480
      PL(  9. 10) = QK(  9.  2)*RHO(2)*Y(  3)*Y( 10)                    FG2 1490
      PL( 10.  1) = QK( 10.  1)*RHO(1)*X                                FG2 1500
      PL( 10.  6) = QK( 10.  2)*RHO(2)*Y( 10)*X                         FG2 1510
      PL( 10.  7) = QK( 10.  2)*RHO(2)*Y(  6)*X                         FG2 1520
      PL( 10.  5) = QK( 10.  1)*RHO(1)*Y( 17)                           FG2 1530
      PL( 10. 10) = QK( 10.  2)*RHO(2)*Y(  6)*Y( 10)                    FG2 1540
      PL( 11.  1) = QK( 11.  1)*RHO(1)*X                                FG2 1550
      PL( 11.  6) = QK( 11.  2)*RHO(2)*Y( 14)*X                         FG2 1560
      PL( 11.  7) = QK( 11.  2)*RHO(2)*Y(  2)*X                         FG2 1570
      PL( 11.  5) = QK( 11.  1)*RHO(1)*Y(  1)                           FG2 1580
      PL( 11. 10) = QK( 11.  2)*RHO(2)*Y(  2)*Y( 14)                    FG2 1590
      PL( 12.  1) = QK( 12.  1)*RHO(1)*X                                FG2 1600
      PL( 12.  6) = QK( 12.  2)*RHO(2)*Y(  2)*X                         FG2 1610
      PL( 12.  7) = QK( 12.  2)*RHO(2)*Y(  3)*X                         FG2 1620
      PL( 12.  5) = QK( 12.  1)*RHO(1)*Y(  4)                           FG2 1630
      PL( 12. 10) = QK( 12.  2)*RHO(2)*Y(  3)*Y(  2)                    FG2 1640
      PL( 13.  1) = QK( 13.  1)*RHO(1)*X                                FG2 1650
      PL( 13.  6) = 2.*QK( 13.  2)*RHO(2)*Y(  2)*X                      FG2 1660
      PL( 13.  5) = QK( 13.  1)*RHO(1)*Y(  3)                           FG2 1670
      PL( 13. 10) = QK( 13.  2)*RHO(2)*Y(  2)*Y(  2)                    FG2 1680
      PL( 14.  1) = QK( 14.  1)*RHO(1)*X                                FG2 1690
      PL( 14.  6) = QK( 14.  2)*RHO(2)*Y( 16)*X                         FG2 1700
      PL( 14.  7) = QK( 14.  2)*RHO(2)*Y(  5)*X                         FG2 1710
      PL( 14.  5) = QK( 14.  1)*RHO(1)*Y(  2)                           FG2 1720
      PL( 14. 10) = QK( 14.  2)*RHO(2)*Y(  5)*Y( 16)                    FG2 1730
      PL( 15.  1) = QK( 15.  1)*RHO(1)*X                                FG2 1740
      PL( 15.  6) = QK( 15.  2)*RHO(2)*Y( 2)*X                          FG2 1750
      PL( 15.  7) = QK( 15.  2)*RHO(2)*Y( 6)*X                          FG2 1760
      PL( 15.  5) = QK( 15.  1)*RHO(1)*Y(18)                            FG2 1770
      PL( 15. 10) = QK( 15.  2)*RHO(2)*Y( 6)*Y( 2)                      FG2 1780
      PL( 16.  1) = QK( 16.  1)*RHO(1)*X                                FG2 1790
      PL( 16.  6) = QK( 16.  2)*RHO(2)*Y( 2)*X                          FG2 1800
      PL( 16,  7) = QK( 16,  2)*RHO(2)*Y(18)*X                          FG2 1810
      PL( 16,  5) = QK( 16,  1)*RHO(1)*Y(19)                            FG2 1820
      PL( 16, 10) = QK( 16,  2)*RHO(2)*Y(18)*Y( 2)                      FG2 1830
      GO TO (31,32,33,34,35,36,37,38,39,40,41,42,43,44,45,46,47,48,49),KFG2 1840
31    AA          = PL( 11, 10) - PL( 11,  5)                           FG2 1850
      AII     = AA      -PL(1,1)- PL(11,1)                              FG2 1860
      GO TO 90                                                          FG2 1870
32    BB=    PL(  7,  6)+   PL(  7, 10)+   PL( 11,  6)+   PL( 11, 10)   FG2 1880
      BB=BB+   PL( 12,  7)+   PL( 12, 10)+2.*PL( 13,  6)+2.*PL( 13, 10) FG2 1890
      AA=    PL(  7,  5)+   PL( 11,  5)+   PL( 12,  5)+2.*PL( 13,  5)   FG2 1900
      AA=AA+   PL( 14, 10) + PL(15, 5) + PL(16, 5)                      FG2 1910
      BB=BB+   PL( 14,  1)+   PL( 14,  5) + PL(15,10) + PL(15, 7)       FG2 1920
      BB=BB+   PL( 16,10) + PL(16, 7)                                   FG2 1930
      AII         = AA - BB                                             FG2 1940
      GO TO 90                                                          FG2 1950
33    AA=    PL(  9,  5)+   PL( 12,  5)+   PL( 13, 10)                  FG2 1960
      BB=    PL(  9, 10)+   PL( 12, 10)+   PL( 13,  5)                  FG2 1970
      AA          = AA - BB                                             FG2 1980
      AII         = AA          - PL(  2,  6) - PL(  9,  6) - PL( 12,  6) FG2 1990
     1 - PL( 13,  1)                                                    FG2 2000
      GO TO 90                                                          FG2 2010
34    AA=    PL( 12, 10)                                                FG2 2020
      BB=    PL( 12,  5)                                                FG2 2030
      AA          = AA - BB                                             FG2 2040
      AII         = AA          - PL( 12,  1)                           FG2 2050
      GO TO 90                                                          FG2 2060
35    BB=    PL( 14, 10)                                                FG2 2070
      AA=    PL( 14,  5)                                                FG2 2080
      AA          = AA - BB                                             FG2 2090
      AII         = AA          - PL( 14,  6)                           FG2 2100
      GO TO 90                                                          FG2 2110
36    AA=    PL(  9, 10)+   PL( 10,  5) + PL( 15,  5)                   FG2 2120
      BB=    PL(  9,  5)+   PL( 10, 10) + PL( 15, 10) + PL( 15,  6)     FG2 2130
      AA          = AA - BB                                             FG2 2140
      AII         = AA          - PL(  2,  1) - PL(  9,  1) - PL( 10,  6) FG2 2150
      GO TO 90                                                          FG2 2160
```

```
37 AA=    PL(  7, 10)+   PL(  8,  5)                                      FG2 2170
   BB=    PL(  7,  5)+   PL(  8, 10)                                      FG2 2180
   AA            = AA - BB                                                FG2 2190
   AII           = AA          - PL(  1,  6) - PL(  7,  1) - PL(  8,  6) FG2 2200
   GO TO 90                                                               FG2 2210
38 AA=    PL(  8, 10)                                                     FG2 2220
   BB=    PL(  8,  5)                                                     FG2 2230
   AA            = AA - BB                                                FG2 2240
   AII           = AA          - PL(  8,  1)                              FG2 2250
   GO TO 90                                                               FG2 2260
39 AA=    PL(  4, 10)                                                     FG2 2270
   BB=    PL(  4,  5)                                                     FG2 2280
   AA            = AA - BB                                                FG2 2290
   AII           = AA          - PL(  2,  7) - PL(  4,  1)                FG2 2300
   GO TO 90                                                               FG2 2310
40 BB=    PL(  2,  2)+2.*PL(  4,  6)+2.*PL(  4, 10)+   PL(  8,  7)      FG2 2320
   BB=BB+   PL(  8, 10)+   PL(  9,  7)+   PL(  9, 10)+   PL( 10,  7)   FG2 2330
   AA=2.*PL(  4,  5)+   PL(  8,  5)+   PL(  9,  5)+   PL( 10,  5)      FG2 2340
   BB=BB+   PL( 10, 10)                                                   FG2 2350
   AII           = AA - BB                                                FG2 2360
   GO TO 90                                                               FG2 2370
41 AA=    PL(  3, 10)                                                     FG2 2380
   BB=    PL(  3,  5)                                                     FG2 2390
   AA            = AA - BB                                                FG2 2400
   AII           = AA          - PL(  3,  1)                              FG2 2410
   GO TO 90                                                               FG2 2420
42 BB=    PL(  1,  2)+2.*PL(  3,  6)+2.*PL(  3, 10)+   PL(  6,  1)      FG2 2430
   AA=2.*PL(  3,  5)+   PL(  6, 10)+   PL(  7,  5)                        FG2 2440
   BB=BB+   PL(  6,  5)+   PL(  7,  7)+   PL(  7, 10)                     FG2 2450
   AII           = AA - BB                                                FG2 2460
   GO TO 90                                                               FG2 2470
43 AA=    PL(  6,  5)                                                     FG2 2480
   BB=    PL(  6, 10)                                                     FG2 2490
   AA            = AA - BB                                                FG2 2500
   AII           = AA          - PL(  6,  6)                              FG2 2510
   GO TO 90                                                               FG2 2520
```

```
44 AA=    PL(  5, 10)+    PL( 11,  5)                                            FG2 2530
   BB=    PL(  5,  5)+    PL( 11, 10)                                            FG2 2540
   AA            = AA - BB                                                       FG2 2550
   AII           = AA          - PL(  1,  7) - PL(  5,  1) - PL( 11,  7)         FG2 2560
   GO TO 90                                                                      FG2 2570
45 AA=    PL(  5,  5)                                                            FG2 2580
   BB=    PL(  5, 10)                                                            FG2 2590
   AA            = AA - BB                                                       FG2 2600
   AII           = AA          - PL(  5,  6)                                     FG2 2610
   GO TO 90                                                                      FG2 2620
46 AA=    PL(  5,  5)+    PL(  6,  5)+    PL( 14,  5)                            FG2 2630
   BB=    PL(  5, 10)+    PL(  6, 10)+    PL( 14, 10)                            FG2 2640
   AA            = AA - BB                                                       FG2 2650
   AII           = AA          - PL(  5,  7) - PL(  6,  7) - PL( 14,  7)         FG2 2660
   GO TO 90                                                                      FG2 2670
47 AA            = PL( 10, 10) - PL( 10,  5)                                     FG2 2680
   AII           = AA          - PL( 10,  1)                                     FG2 2690
   GO TO 90                                                                      FG2 2700
48 AA        = PL(15,10) - PL(15, 5) + PL(16, 5) - PL(16,10)                     FG2 2710
   AII       =AA       - PL(15, 1) - PL(16, 6)                                   FG2 2720
   GO TO 90                                                                      FG2 2730
49 AA         = PL(16,10) - PL(16, 5)                                            FG2 2740
   AII        = AA        - PL(16, 1)                                            FG2 2750
90 PL(  1,  1)=Y(  1)*PL(  1,  1)                                                FG2 2760
   PL(  1,  6)=Y(  7)*PL(  1,  6)                                                FG2 2770
   PL(  2,  1)=Y(  6)*PL(  2,  1)                                                FG2 2780
   PL(  2,  6)=Y(  3)*PL(  2,  6)                                                FG2 2790
   PL(  3,  1)=Y( 11)*PL(  3,  1)                                                FG2 2800
   PL(  3,  6)=Y( 12)*PL(  3,  6)/2.                                             FG2 2810
   PL(  4,  1)=Y(  9)*PL(  4,  1)                                                FG2 2820
   PL(  4,  6)=Y( 10)*PL(  4,  6)/2.                                             FG2 2830
   PL(  5,  1)=Y( 14)*PL(  5,  1)                                                FG2 2840
   PL(  5,  6)=Y( 15)*PL(  5,  6)                                                FG2 2850
   PL(  6,  1)=Y( 12)*PL(  6,  1)                                                FG2 2860
   PL(  6,  6)=Y( 13)*PL(  6,  6)                                                FG2 2870
   PL(  7,  1)=Y(  7)*PL(  7,  1)                                                FG2 2880
```

```
      PL(  7,  6)=Y(  2)*PL(  7,  6)                                    FG2 2890
      PL(  8,  1)=Y(  8)*PL(  8,  1)                                    FG2 2900
      PL(  8,  6)=Y(  7)*PL(  8,  6)                                    FG2 2910
      PL(  9,  1)=Y(  6)*PL(  9,  1)                                    FG2 2920
      PL(  9,  6)=Y(  3)*PL(  9,  6)                                    FG2 2930
      PL( 10,  1)=Y( 17)*PL( 10,  1)                                    FG2 2940
      PL( 10,  6)=Y(  6)*PL( 10,  6)                                    FG2 2950
      PL( 11,  1)=Y(  1)*PL( 11,  1)                                    FG2 2960
      PL( 11,  6)=Y(  2)*PL( 11,  6)                                    FG2 2970
      PL( 12,  1)=Y(  4)*PL( 12,  1)                                    FG2 2980
      PL( 12,  6)=Y(  3)*PL( 12,  6)                                    FG2 2990
      PL( 13,  1)=Y(  3)*PL( 13,  1)                                    FG2 3000
      PL( 13,  6)=Y(  2)*PL( 13,  6)/2.                                 FG2 3010
      PL( 14,  1)=Y(  2)*PL( 14,  1)                                    FG2 3020
      PL( 14,  6)=Y(  5)*PL( 14,  6)                                    FG2 3030
      PL( 15,  1)=Y( 18)*PL( 15,  1)                                    FG2 3040
      PL( 15,  6)=Y(  6)*PL( 15,  6)                                    FG2 3050
      PL( 16,  1)=Y( 19)*PL( 16,  1)                                    FG2 3060
      PL( 16,  6)=Y( 18)*PL( 16,  6)                                    FG2 3070
  191 GO TO (51,52,53,54,55,56,57,58,59,60,61,62,63,64,65,66,67,68,69),KFG2 3080
   51 AA=   PL(  1,  6)+   PL( 11,  6)                                  FG2 3090
      BB=   PL(  1,  1)+   PL( 11,  1)                                  FG2 3100
      B       = AA - BB                                                 FG2 3110
      GO TO 95                                                          FG2 3120
   52 BB=   PL(  7,  6)+   PL( 11,  6)+   PL( 12,  6)+2.*PL( 13,  6)    FG2 3130
      AA=   PL(  7,  1)+   PL( 11,  1)+   PL( 12,  1)+2.*PL( 13,  1)    FG2 3140
      AA=AA+   PL( 14,  6) + PL(15, 1) + PL(16, 1)                      FG2 3150
      BB=BB+   PL( 14,  1) + PL(15, 6) + PL(16,6)                       FG2 3160
      B       = AA - BB                                                 FG2 3170
      GO TO 95                                                          FG2 3180
   53 AA=   PL(  2,  1)+   PL(  9,  1)+   PL( 12,  1)+   PL( 13,  6)    FG2 3190
      BB=   PL(  2,  6)+   PL(  9,  6)+   PL( 12,  6)+   PL( 13,  1)    FG2 3200
      B       = AA - BB                                                 FG2 3210
      GO TO 95                                                          FG2 3220
   54 AA=   PL( 12,  6)                                                 FG2 3230
      BB=   PL( 12,  1)                                                 FG2 3240
      B        = AA - BB                                                          FG2 3250
      GO TO 95                                                                    FG2 3260
   55 AA=   PL( 14,  1)                                                           FG2 3270
      BB=   PL( 14,  6)                                                           FG2 3280
      B        = AA - BB                                                          FG2 3290
      GO TO 95                                                                    FG2 3300
   56 AA=   PL(  2,  6)+   PL(  9,  6)+   PL( 10,  1) + PL( 15,  1)               FG2 3310
      BB=   PL(  2,  1)+   PL(  9,  1)+   PL( 10,  6) + PL( 15,  6)               FG2 3320
      B        = AA - BB                                                          FG2 3330
      GO TO 95                                                                    FG2 3340
   57 AA=   PL(  1,  1)+   PL(  7,  6)+   PL(  8,  1)                             FG2 3350
      BB=   PL(  1,  6)+   PL(  7,  1)+   PL(  8,  6)                             FG2 3360
      B        = AA - BB                                                          FG2 3370
      GO TO 95                                                                    FG2 3380
   58 AA=   PL(  8,  6)                                                           FG2 3390
      BB=   PL(  8,  1)                                                           FG2 3400
      B        = AA - BB                                                          FG2 3410
      GO TO 95                                                                    FG2 3420
   59 AA=   PL(  2,  1)+   PL(  4,  6)                                            FG2 3430
      BB=   PL(  2,  6)+   PL(  4,  1)                                            FG2 3440
      B        = AA - BB                                                          FG2 3450
      GO TO 95                                                                    FG2 3460
   60 AA=   PL(  2,  6)+2.*PL(  4,  1)+   PL(  8,  1)+   PL(  9,  1)              FG2 3470
      BB=   PL(  2,  1)+2.*PL(  4,  6)+   PL(  8,  6)+   PL(  9,  6)              FG2 3480
      AA=AA+   PL( 10,  1)                                                        FG2 3490
      BB=BB+   PL( 10,  6)                                                        FG2 3500
      B        = AA - BB                                                          FG2 3510
      GO TO 95                                                                    FG2 3520
   61 AA=   PL(  3,  6)                                                           FG2 3530
      BB=   PL(  3,  1)                                                           FG2 3540
      B        = AA - BB                                                          FG2 3550
      GO TO 95                                                                    FG2 3560
   62 AA=   PL(  1,  6)+2.*PL(  3,  1)+   PL(  6,  6)+   PL(  7,  1)              FG2 3570
      BB=   PL(  1,  1)+2.*PL(  3,  6)+   PL(  6,  1)+   PL(  7,  6)              FG2 3580
      B        = AA - BB                                                          FG2 3590
      GO TO 95                                                                    FG2 3600
```

```
                                                                        FG2 3610
   63 AA=   PL(  6,  1)                                                 FG2 3620
      BB=   PL(  6,  6)                                                 FG2 3630
      B       = AA - BB                                                 FG2 3640
      GO TO 95                                                          FG2 3650
   64 AA=   PL(  1,  1)+    PL(  5,  6)+    PL( 11,  1)                 FG2 3660
      BB=   PL(  1,  6)+    PL(  5,  1)+    PL( 11,  6)                 FG2 3670
      B       = AA - BB                                                 FG2 3680
      GO TO 95                                                          FG2 3690
   65 AA=   PL(  5,  1)                                                 FG2 3700
      BB=   PL(  5,  6)                                                 FG2 3710
      B       = AA - BB                                                 FG2 3720
      GO TO 95                                                          FG2 3730
   66 AA=   PL(  5,  1)+    PL(  6,  1)+    PL( 14,  1)                 FG2 3740
      BB=   PL(  5,  6)+    PL(  6,  6)+    PL( 14,  6)                 FG2 3750
      B       = AA - BB                                                 FG2 3760
      GO TO 95                                                          FG2 3770
   67 AA=PL(10,6)                                                       FG2 3780
      BB=PL(10,1)                                                       FG2 3790
      B       = AA - BB                                                 FG2 3800
      GO TO 95                                                          FG2 3810
   68 AA= PL(15, 6) + PL(16,1)                                          FG2 3820
      BB= PL(15, 1) + PL(16, 6)                                         FG2 3830
      B       = AA - BB                                                 FG2 3840
      GO TO 95                                                          FG2 3850
   69 AA= PL(16, 6)                                                     FG2 3860
      BB= PL(16, 1)                                                     FG2 3870
      B       = AA - BB                                                 FG2 3880
   95 IF(IND)110,101,110                                                FG2 3890
  101 IND = 1                                                           FG2 3900
      GAMMA = 0.                                                        FG2 3910
      DO102I=1,16                                                       FG2 3920
      IF(I.GT.2)GAMMA = 1.                                              FG2 3930
      Q = (RATES(2,I) + RATES(3,I)/T)/T                                 FG2 3940
      PL(I,1) = Q*PL(I,1)                                               FG2 3950
      Q = GAMMA/RT + Q - E(I,1,L)/T1(1) - E(I,2,L)/2. - E(I,3,L)*T1(1)/3FG2 3950
     X. - E(I,4,L)*T1(2)/4. - E(I,5,L)*T1(3)/5. - E(I,6,L)/T1(2)        FG2 3960
```

```
102 PL(I,6) = Q*PL(I,6)                                                        FG2 3970
    C = B                                                                      FG2 3980
    GO TO 191                                                                  FG2 3990
110 RETURN                                                                     FG2 4000
    END                                                                        FG2 4010
```

```
      SUBROUTINE LRAD                  9999                           LRAD  10
C                                                                     LRAD  20
C                                                                     LRAD  30
C  **  THIS IS A DRIVER PROGRAM FOR SUBROUTINE TRANS WHICH CALCULATES **LRAD  40
C      THE RADIATIVE FLUX DIVERGENCE THROUGH A ONE-DIMENSIONAL SLAB   LRAD  50
C      FOR A GIVEN TEMPERATURE AND SPECIES DISTRIBUTION               LRAD  60
      COMMON /SFLUX/ QRI(3)                                           LRAD  70
      COMMON /TRN/         NUT(60). FMC(12.60). FPC(12.60).           LRAD  80
     1              FM(9.60). FP(9.60). LINES                         LRAD  90
      COMMON /TEST/ETZ(60).IEZ                                        LRAD 100
      COMMON /YL/ETA(60).YOND(60)                                     LRAD 110
      COMMON/PROP1/PI(60).RHO(60). T(60).AMW(60).C (20.60).EC(5.60)   LRAD 120
      COMMON/SIS/SY(20.60)                                            LRAD 130
      COMMON /FRSTRM/ U INF. RINF. UINF2. R . RE. LXI. ITM. IEM. NETA LRAD 140
      COMMON /DEL/ DELTA.DTIL.DTILS                                   LRAD 150
      COMMON /NON/RDZ.MUDZ.RMDZ.AKNF.HNF.CPNF                         LRAD 160
      COMMON /MAIM/KEEP.MAXE.MAXM.MAXD.   IDG.MCONV.ECONV.DCONV.LT.IAB LRAD 170
      COMMON /RFLUX/ E(60).IRAD.ITYPE                                 LRAD 180
      COMMON /NUMDEN/ SNDO2(60). SNDN2(60). SNDO(60). SNDN(60).       LRAD 190
     1                                     SNDE(60). SNDC(60).        LRAD 200
     2                 SNDH(60). SNDC2(60). SNDH2(60). SNDCO(60).     LRAD 210
     3                 SNDC3(60).SNDC2H(60)                           LRAD 220
      COMMON /SPEC/ MF. XMOL                                          LRAD 230
      COMMON/TOM/ SC(60).TO(60).PR(60).TE(60)                         LRAD 240
C                                                                     LHAD 250
      DO100 I=1.20                                                    LRAD 260
      DO100J=1.NETA                                                   LRAD 270
  100 SY(I.J) = C(I.J)                                                LRAD 280
      DO200 I=1.20                                                    LRAD 290
      DO200 J=1.NETA                                                  LRAD 300
  200 IF(C(I.J).LT.0.)C(I.J) = 1.E-20                                 LRAD 310
C                                                                     LRAD 320
C  **  NETA = NUMBER OF ETA POINTS                                    LRAD 330
C      MF   = 1  IF SPECIE  MOLE FRACTIONS ARE INPUT AND NUMBER DENSITY LRAD 340
C                TO BE COMPUTED                                       LRAD 350
C              0  IF SPECIE NUMBER DENSITIES ARE INPUT                LRAD 360
```

```
C       NS    = NUMBER OF SPECIES TO BE INPUT                           LRAD 370
C       LINES= 1  IF LINE CALCULATION IS TO BE DONE                     LRAD 380
C              0  IF ONLY CONTINUUM CALCULATION IS TO BE DONE           LRAD 390
C       IDG   = 0  ONLY FINAL PRINT IS GIVEN                            LRAD 400
C               1  PRINT IS GIVEN FOR EACH ETA                          LRAD 410
C              99  COMPLETE PRINT                                       LRAD 420
C                                                                       LRAD 430
C                                                                       LRAD 440
C   **  R     = BODY RADIUS (FT)                                        LRAD 450
C       DELTA = NONDIMENSIONAL STAND-OFF DISTANCE                       LRAD 460
C       DTIL  = TRANSFORMED STAND-OFF DISTANCE                          LRAD 470
C       XMOL  = 1.0 FOR RUN WITH MOLECULES                              LRAD 480
C               0.0 FOR RUN WITHOUT MOLECULES                           LRAD 490
C                                                                       LRAD 500
      XMOL = 0.0                                                        LRAD 510
      XMOL= 1.0                                                         LRAD 520
C                                                                       LRAD 530
C     ** DETERMINE ETZ POINTS                                           LRAD 540
      N2 = NETA-2                                                       LRAD 550
      K =0                                                              LRAD 560
      IEZ =0                                                            LRAD 570
      DO 20 I=1,N2,2                                                    LRAD 580
      K=K+1                                                             LRAD 590
 20   ETZ(K) = ETA(I)                                                   LRAD 600
      ETZ(K+1) = ETA(NETA-1)                                            LRAD 610
      ETZ(K+2) = ETA(NETA)                                              LRAD 620
      IEZ = K +1                                                        LRAD 630
C                                                                       LRAD 640
C     **  COMPUTE THE  Y  COORDINATE   **                               LRAD 650
      YOND(1) = 0.0                                                     LRAD 660
      SUM = 0.0                                                         LRAD 670
      DO 30 K=2,NETA                                                    LRAD 680
      DETA = ETA(K) -ETA(K-1)                                           LRAD 690
      SUM = SUM +DETA*(1./RHO(K) +1./RHO(K-1) )/2.0                     LRAD 700
      YOND(K) = DTIL *SUM                                               LRAD 710
 30   CONTINUE                                                          LRAD 720
```

```
      DELTA = YOND(NETA)                                                LRAD 730
      DO 40 K=1.NETA                                                    LRAD 740
      YOND(K) = YOND(K)/YOND(NETA)                                      LRAD 750
      T(K) = 0.65 * T(K)  +  0.35 * TE(K)                               LRAD 760
   40 CONTINUE                                                          LRAD 770
C                                                                       LRAD 780
      LINES= 1                                                          LRAD 790
      IDGS = IDG                                                        LRAD 800
      IDG = 0                                                           LRAD 810
      CALL TRANS(1)                                                     LRAD 820
      CALL TRANS1 (1)                                                   LRAD 830
      IDG= IDGS                                                         LRAD 840
C                                                                       LRAD 850
C  **  INDEX IS NUMBER GIVEN SPECIE FOR USE IN STORING ARRAYS **        LRAD 860
C                             1   =    O2                               LRAD 870
C                             2   =    N2                               LRAD 880
C                             3   =    O                                LRAD 890
C                             4   =    N                                LRAD 900
C                             5   =    E-                               LRAD 910
C                             6   =    C                                LRAD 920
C                             7   =    H                                LRAD 930
C                             8   =    C2                               LRAD 940
C                             9   =    H2                               LRAD 950
C                            10   =    CO                               LRAD 960
C                            11   =    C3                               LRAD 970
C                            12   =    C2H                              LRAD 980
C                                                                       LRAD 990
C                                                                       LRAD1000
      DO300I=1.20                                                       LRAD1010
      DO300J=1.NETA                                                     LRAD1020
  300 C(I.J) = SY(I.J)                                                  LRAD1030
      RETURN                                                            LRAD1040
      END                                                               LRAD1050
      SUBROUTINE RADIN                                                  RADI  10
      COMMON /DBUG/ QLC(60), QCL(60), QLL(60), DQN(60), QCC(60),        RADI  20
     1               BEEC(12,60),    FMUC(12,60),    EM(12,60),         RADI  30
     2               EP(12,60),      TAUC(12,60),    BEEL(9,60),        RADI  40
     3               QCCP(12),       WMM(9,60),      GMM(9,60),         RADI  50
     4               EEM(9,60),      XLMM(9,60),     QLCP(9),           RADI  60
     5               QCLP(9),        QLLP(9),        DELTA,    IY,  IYY, RADI  70
     6               WPP(9,60),      GPP(9,60),      EEP(9,60),         RADI  80
     7               XLPP(9,60),     FG(9,4),        GP(9,4),           RADI  90
     8               WN(9,4),        FMUL(9,60),     SSM(9,4,60),       RADI 100
     9               GGM(9,4,60),    ETAM(9,4,60),   SBM(9,4,60),       RADI 110
     A               TAUL(9,60)                                         RADI 120
C  **  GROUP 1  **                                                      RADI 130
      WN(1,1)=0.                                                        RADI 140
      FG(1,1)=0.                                                        RADI 150
      GP(1,1)=0.                                                        RADI 160
      WN(1,2)=18.                                                       RADI 170
      WN(1,3)=15.                                                       RADI 180
      WN(1,4)=5.                                                        RADI 190
C  **  GROUP 2  **                                                      RADI 200
      WN(2,1)=3.0                                                       RADI 210
      WN(2,2)=5.0                                                       RADI 220
      WN(2,3)=11.0                                                      RADI 230
      WM(2,4)=10.                                                       RADI 240
C  **  GROUP 3  **                                                      RADI 250
      WN(3,1)=0.                                                        RADI 260
      FG(3,1)=0.                                                        RADI 270
      GP(3,1)=0.                                                        RADI 280
      WN(3,2)=2.0                                                       RADI 290
      WN(3,3)=0.                                                        RADI 300
      FG(3,3)=0.                                                        RADI 310
      GP(3,3)=0.                                                        RADI 320
      WN(3,4)=0.                                                        RADI 330
      FG(3,4)=0.                                                        RADI 340
      GP(3,4)=0.                                                        RADI 350
C  **  GROUP 4  **                                                      RADI 360
```

```
      WN(4,1)=0.                                                        RADI 370
      FG(4,1)=0.                                                        RADI 380
      GP(4,1)=0.                                                        RADI 390
      WN(4,2)=8.0                                                       RADI 400
      WN(4,3)=2.0                                                       RADI 410
      WN(4,4)=0.                                                        RADI 420
      FG(4,4)=0.                                                        RADI 430
      GP(4,4)=0.                                                        RADI 440
C   **  GROUP 5   **                                                    RADI 450
      WN(5,1)=0.                                                        RADI 460
      FG(5,1)=0.                                                        RADI 470
      GP(5,1)=0.                                                        RADI 480
      WN(5,2)=14.                                                       RADI 490
      WN(5,3)=4.0                                                       RACI 500
      WN(5,4)=1.0                                                       RADI 510
C   **  GROUP 6   **                                                    RADI 520
      WN(6,1)=1.0                                                       RADI 530
      WN(6,2)=4.0                                                       RADI 540
      WN(6,3)=13.0                                                      RADI 550
      WN(6,4)=2.0                                                       RADI 560
C   **  GROUP 7   **                                                    RADI 570
      WN(7,1)=0.                                                        RADI 580
      FG(7,1)=0.                                                        RADI 590
      GP(7,1)=0.                                                        RADI 600
      WN(7,2)=6.0                                                       RADI 610
      WN(7,3)=14.0                                                      RADI 620
      WN(7,4)=3.0                                                       RADI 630
C   **  GROUP 8   **                                                    RADI 640
      WN(8,1)=2.0                                                       RADI 650
      WN(8,2)=2.0                                                       RADI 660
      WN(8,3)=11.                                                       RADI 670
      WN(8,4)=15.                                                       RADI 680
C   **  GROUP 9   **                                                    RADI 690
      WN(9,1)=0.                                                        RADI 700
      FG(9,1)=0.                                                        RACI 710
      GP(9,1)=0.                                                        RADI 720
      WN(9,2)=1.0                                                      RADI 730
      WN(9,3)=11.                                                      RADI 740
      WN(9,4)=10.                                                      RADI 750
      RETURN                                                           RADI 760
      END                                                              RADI 770
      SUBROUTINE TRANS (ISW)
C
C-----THIS IS A MODIFIED VERSION OF SUBROUTINE TRANS FROM K WILSON
C     TRANS IS DOCUMENTED IN  LMSC-687209 APRIL 69  ---------------
C
      COMMON /ZPI/ ZPO(6), ZPN(6),ZPH(2),  ZPC(7)
      COMMON /FINV/ NHVL,NIHVC,FHVC(12),DJ(9),HVJ(9),ZKZ
      COMMON /SFLUX/ QRI(3)
      COMMON /TRN/         NUT(60), FMC(12,60), FPC(12,60),
     1          FM(9,60), FP(9,60), LINES
      COMMON /YL/ETA(60),   YD(60)
      COMMON/PROP1/P (60),  R(60),  T(60),AMW(60),C (20,60),EC(5,60)
      COMMON /FRSTRM/ U INF, RINF, UINF2,XL , RE, LXI, ITM, IEM, NES
      COMMON /DEL/  W( 1),DTIL,DTILS
      COMMON /NON/RDZ,MUDZ,RMDZ,AKNF,HNF,CPNF
      COMMON /MAIN/KEEP,MAXE,MAXM,MAXD,    IDG,MCONV,ECONV,DCONV,LT,IAB
      COMMON /RFLUX/ E(60),IRAD,ITYPE
      COMMON /RH/ DUD,DPHI,TD,RZB,PD,HD,HTOTAL
      COMMON/WT/SMW(20),AWT(5)
      COMMON /TEST/ETZ(60),IEZ
      COMMON /NUMDEN/ SNDO2(60), SNDN2(60), SNDO(60), SNDN(60),
     1                                      SNDE(60), SNDC(60),
     2                SNDH(60), SNDC2(60), SNDH2(60), SNDCO(60),
     3                SNDC3(60),SNDC2H(60)
      COMMON /DBUG/ QLC(60), QCL(60), QLL(60), DQN(60), QCC(60),
     1              BEEC(12,60),   FMUC(12,60),   EM(12,60),
     2              EP(12,60),     TAUC(12,60),   BEEL(9,60),
     3              QCCP(12),      WMM(9,60),     GMM(9,60),
     4              EEM(9,60),     XLMM(9,60),    QLCP(9),
     5              QCLP(9),       QLLP(9),       DELTA,    IY,  IYY,
     6              WPP(9,60),     GPP(9,60),     EEP(9,60),
     7              XLPP(9,60),    FG(9,4),       GP(9,4),
     8              WN(9,4),       FMUL(9,60),    SSM(9,4,60),
     9              GGM(9,4,60),   ETAM(9,4,60),  SBM(9,4,60),
     A              TAUL(9,60)
      COMMON /SPEC/ MF, XMOL
      COMMON/MIKE/ NETA1.NETA2.PNF.WNF.RHOD.DP.TS.UD.VD.RW.RWJ.EPS.PHI   TRAN 370
      DIMENSION  XKT(60).          DQ(60)                                TRAN 380
C                                                                        TRAN 390
C **   BAND AVERAGE ABSORPTION CROSS SECTION (EQ.A2)   **                TRAN 400
C                                                                        TRAN 410
      SIGMA(ZH.ZA.ZB.ZG)=  ((5.0E+03*T1*ZG*ZKZ)/BE) * (EXP(ZDL/T1)      TRAN 420
     1                     *ZH*(ZA+ZB* (ZH**2)/3.0) +                    TRAN 430
     2                     T1 * (ZA+2.0*ZB*T12) -T1*EXP((ZH-ZHVP)/T1)    TRAN 440
     3                     *(ZA+ZB*(ZHVP-ZH)**2) -T1*EXP((ZH-ZHVP)/T1)   TRAN 450
     4                     *2.0*ZB*T1*(ZHVP-ZH+T1))                      TRAN 460
      SIGMA2(ZH.ZG.ZE.ZY)=7.26E-16*T1*ZG*EXP((-ZE+ZY+ZDL)/T1)/ZH**3     TRAN 470
      GAMMA(ZX)=(1.0+(1.5707963*ZX)**1.25)**(-0.4)                       TRAN 480
      XLAMB(ZX)=(1.0+ZX*EXP(-ZX))/SQRT(1.0+6.283185 *ZX)                 TRAN 490
C                                                                        TRAN 500
C **   W(GROUP)/D CORRELATION (EQ.88)   **                               TRAN 510
C                                                                        TRAN 520
      PHI1(ZX)=(ATAN(1.570796 *ZX)/1.570796 )                            TRAN 530
C                                                                        TRAN 540
C **   FLUX DIVERGENCE OVERLAPPING FUNCTION (EQ.92)   **                 TRAN 550
C                                                                        TRAN 560
      PHI2(ZX)=EXP(-ZX)                                                  TRAN 570
C                                                                        TRAN 580
      DO 400 I=1.NES                                                     TRAN 590
  400 T(I)= T(I)*TS                                                      TRAN 600
      ZHVP=5.0                                                           TRAN 610
      YI=0.0                                                             TRAN 620
      CONVER = 3.10375E+23 *R  (I) *RDZ                                  TRAN 630
      SNDE(NES) = CONVER * C( 7.NES)/SMW(7)                              TRAN 640
      XNE=SNDE(NES)                                                      TRAN 650
      FNE=(4.71E-6 * XNE**(2.0/7.0))/((T(NES)/11606.)**(1.0/7.0))        TRAN 660
      ZDL=AMIN1(0.20.FNE)                                                TRAN 670
C                                                                        TRAN 680
C **   DEBUG PRINT  **                                                   TRAN 690
C                                                                        TRAN 700
      IF (IDG.NE.0) CALL BUGPR (1)                                       TRAN 710
      DELTA=W(1) * XL * 30.48006                                         TRAN 720
      CALL BUGPR (2)                                                    TRAN 730
 6001 CONTINUE                                                          TRAN 740
      DO 91 L=1.NES                                                     TRAN 750
      XKT(L)=T(L)/11606.                                                TRAN 760
      T1=XKT(L)                                                         TRAN 770
      CALL SND(L)                                                       TRAN 780
C                                                                       TRAN 790
C **   PARTITION FUNCTIONS FOR H. C. N. O  **                           TRAN 800
C                                                                       TRAN 810
   94 IF(T(L).GT.15000.) GO TO 6                                        TRAN 820
C                                                                       TRAN 830
C **   LOW  TEMPERATURE  **                                             TRAN 840
C                                                                       TRAN 850
      SUMH=2.0                                                          TRAN 860
      SUMC=9.0   +  5.0 * EXP(-1.264/T1) + EXP(-2.684/T1) +             TRAN 870
     1              5.0 * EXP(-4.183/T1)                                TRAN 880
      SUMN=4.0 + 10.0 *EXP(-2.384/T1) + 6.0 *EXP(-3.576/T1)             TRAN 890
      SUMO= 9.0 + 5.0 * EXP(-1.975/T1)                                  TRAN 900
      GO TO 7                                                           TRAN 910
C                                                                       TRAN 920
C **   HIGH TEMPERATURE  **                                             TRAN 930
C                                                                       TRAN 940
    6 SUMH=2.0                                                          TRAN 950
      SUMC=2.71818  +  6.40677 * T(L)/1.0E4 -0.45466 * (T(L)/1.0E4)**2  TRAN 960
      SUMN=5.938216 - 0.225593 * T(L)/1.0E3 + 0.015408 * (T(L)/1.0E3)**2TRAN 970
      SUMO=11.79563 -0.317964 * T(L)/1.0E3 + 0.013765 * (T(L)/1.0E3)**2 TRAN 980
    7 CONTINUE                                                          TRAN 990
      T12=T1**2                                                         TRAN1000
      GH = 6.4994                                                       TRAN1010
      DO 5 K=1.12                                                       TRAN1020
      GF=FHVC(K)/T1                                                     TRAN1030
      GHM=GH                                                            TRAN1040
      GH=EXP(-GF)  *GF  *  (GF**2 + 3.0 *GF  +6.0  + 6.0/GF)            TRAN1050
C                                                                       TRAN1060
C **   PLANK MEAN ABSORPTION COEFFICIENT FOR BAND INTERVALS (EQ.A3)  ** TRAN1070
C                                                                       TRAN1080
```

```
      BEEC(K.L)=5.04E3  *  (T12**2)  *  (GHM-GH)                         TRAN1090
      BE=BEEC(K.L)                                                       TRAN1100
C                                                                        TRAN1110
C **   ABSORPTION CROSS SECTIONS  **                                     TRAN1120
C      SCECIES --                                                        TRAN1130
C                N       N2      CO                                      TRAN1140
C                O       O2                                              TRAN1150
C                C       C2      C2H                                     TRAN1160
C                H       H2      C3                                      TRAN1170
C                                                                        TRAN1180
      SGH=0.                                                             TRAN1190
      SGN=0.                                                             TRAN1200
      SGC=0.                                                             TRAN1210
      SGO=0.                                                             TRAN1220
      SGCO=0.                                                            TRAN1230
      SGC2=0.                                                            TRAN1240
      SGO2=0.                                                            TRAN1250
      SGN2=0.                                                            TRAN1260
      SGH2=0.                                                            TRAN1270
      SGC3=0.                                                            TRAN1280
      SGC2H = 0.0                                                        TRAN1290
      GO TO (581.582.583.584.585.586.587.588.589.590.591.592).K          TRAN1300
  581 SGH=SIGMA(2.4.1.0.0.0.1.0)  *  EXP(-13.56/T1)                      TRAN1310
      SGC=SIGMA(3.78,  0.3,   0.0488,  1.33)  * EXP(-11.26/T1)           TRAN1320
      SGN=SIG[illegible].22,  0.24,  0.0426,  4.5) * EXP(-14.54/T1)      TRAN1330
      SGO=SIGMA(4.22,  0.24,  0.0426,   .888889)  * EXP(-13.61/T1)       TRAN1340
      GO TO 38                                                           TRAN1350
  582 ZZHV=5.5                                                           TRAN1360
      SGC2=8.0E-18 * EXP(-0.5/T1)  +  3.0E-18                            TRAN1370
      SGC3=4.0E-18                                                       TRAN1380
  593 CALL ZHV(ZZHV.ZZO.ZZN.ZZI.ZZC)                                     TRAN1390
      SGC=SIGMA2(ZZHV, 1.33,  11.26,  3.78) * ZZC + SGC                  TRAN1400
      SGN=SIGMA2 (ZZHV.4.50,  14.54,  4.22) * ZZN                        TRAN1410
  594 SGO=SIGMA2 (ZZHV, .889,  13.61,  4.22) * ZZO                       TRAN1420
  595 SGH=SIGMA2 (ZZHV, 1.00,  13.56,  2.40)                             TRAN1430
      GO TO 38                                                           TRAN1440
  583 ZZHV=6.5                                                                  TRAN1450
      SGC2=1.0E-18                                                              TRAN1460
      SGCO=3.0E-18 * EXP(-0.7/T1)                                               TRAN1470
      GO TO 593                                                                 TRAN1480
  584 ZZHV=7.5                                                                  TRAN1490
      SGC=5.0E-17  * EXP(-4.18/T1)/SUMC                                         TRAN1500
      SGCO=1.9E-17  * EXP(-0.5/T1)                                              TRAN1510
      SGO2=6.0E-19                                                              TRAN1520
      SGC2H = 1.3E-18                                                           TRAN1530
      GO TO 593                                                                 TRAN1540
  585 ZZHV=8.5                                                                  TRAN1550
      SGC=5.0E-17 *EXP(-4.18/T1)/SUMC   +                                       TRAN1560
     1    2.2E-17* EXP(-2.68/T1)/SUMC                                           TRAN1570
      SGCO=2.5E-17                                                              TRAN1580
      SGO2=2.0E-19                                                              TRAN1590
      SGC2H = 8.5E-19                                                           TRAN1600
      GO TO 593                                                                 TRAN1610
  586 ZZHV=9.5                                                                  TRAN1620
      SGC=5.0E-17 * EXP(-4.18/T1)/SUMC   +                                      TRAN1630
     1    2.2E-17 * EXP(-2.68/T1)/SUMC                                          TRAN1640
      SGCO=5.0E-18                                                              TRAN1650
      SGO2=1.0E-18                                                              TRAN1660
      GO TO 593                                                                 TRAN1670
  587 SGN=3.2E-18 *T1 *EXP(-10.2/T1)/SUMN                                       TRAN1680
      SGO2=6.0E-19                                                              TRAN1690
      ZZHV=10.4                                                                 TRAN1700
      CALL ZHV(ZZHV.ZZO.ZZN.ZZI.ZZC)                                            TRAN1710
  596 SGC=(8.5E-17 *EXP(-1.26/T1)  +  2.2E-17 * EXP(-2.75/T1)                   TRAN1720
     1    +  5.0E-17 * EXP(-4.18/T1))/SUMC                                      TRAN1730
      GO TO 594                                                                 TRAN1740
  588 ZZHV=10.9                                                                 TRAN1750
      CALL ZHV(ZZHV.ZZO.ZZN.ZZI.ZZC)                                            TRAN1760
      SGN=(5.16E-17  *EXP(-3.50/T1))/SUMN                                       TRAN1770
      GO TO 596                                                                 TRAN1780
  589 ZZHV=11.6                                                                 TRAN1790
      CALL ZHV(ZZHV.ZZO.ZZN.ZZI.ZZC)                                            TRAN1800
```

```
                                                                            TRAN1810
      SGN2=1.0E-18                                                          TRAN1820
      SGN=(5.16E-17 *  EXP(-3.50))/SUMN                                     TRAN1830
  598 SGC=(9.9E-17  +  8.5E-17 * EXP(-1.26/T1)  +2.2E-17 * EXP(-2.75/T1)TRAN1840
     1      +  5.0E-17 * EXP(-4.18/T1))/SUMC                                TRAN1850
      IF (K.LT.11) GO TO 594                                                TRAN1860
      GO TO 38                                                              TRAN1870
  590 ZZHV=12.7                                                             TRAN1880
      CALL ZHV  (ZZHV.ZZO.ZZN.ZZI.ZZC)                                      TRAN1890
      SGN2=2.0E-18                                                          TRAN1900
      SGH2 = 2.7E-17                                                        TRAN1910
  599 SGN=(6.4E-17 * EXP(-2.30/T1)  +  5.16E-17 * EXP(-3.50/T1))/SUMN       TRAN1920
     1     + SGN                                                            TRAN1930
      GO TO 598                                                             TRAN1940
  591 SGH=1.18E-17/SUMH                                                     TRAN1950
      SGO=3.6E-17/SUMO                                                      TRAN1960
      SGN2=1.0E-17                                                          TRAN1970
      SGH2 = 2.7E-17                                                        TRAN1980
      GO TO 599                                                             TRAN1990
  592 SGN=3.6E-17/SUMN                                                      TRAN2000
      SGN2=1.0E-18                                                          TRAN2010
      GO TO 599                                                             TRAN2020
   38 CONTINUE                                                              TRAN2030
      FMUC(K.L)= SNDH(L)*SGH + SNDC(L)*SGC + SNDN(L)*SGN + SNDO(L)*SGO      TRAN2040
     1           + XMOL *     (SNDN2(L)*SGN2 + SNDO2(L)*SGO2 +              TRAN2050
     2           SNDC2(L)*SGC2 + SNDH2(L)*SGH2 + SNDCO(L)*SGCO +            TRAN2060
     3           SNDC3(L)*SGC3 +SNDC2H(L)*SGC2H )                           TRAN2070
      IF (L.GT.1) GO TO 8                                                   TRAN2080
      TAUC(K.L)=0.                                                          TRAN2090
      GO TO 5                                                               TRAN2100
    8 TAUC(K.L)=TAUC(K.L-1)+(YD(L)-YD(L-1))*                                TRAN2110
     1      (FMUC(K.L-1)+FMUC(K.L)) * DELTA                                 TRAN2120
    5 CONTINUE                                                              TRAN2130
      IF (LINES.EQ.0) GO TO 91                                              TRAN2140
C                                                                           TRAN2150
C **   FRACTIONAL POPULATION STATES FOR H. N. O. C  **                      TRAN2160
C
```

```
      CALL ZP (T1.SUMN.SUMO.SUMH.SUMC)                                 TRAN2170
C **   CALCULATION OF PARAMETERS FOR 9 LINE GROUPES  **                TRAN2180
C      WN -- NUMBER OF LINES                                           TRAN2190
C      FG -- EFFECTIVE F-NUMBER                                        TRAN2200
C      GP -- EFFECTIVE HALF-WIDTH                                      TRAN2210
C                                                                      TRAN2220
C GROUP 1                                                              TRAN2230
      FG(1.2)=(1.02 * ZPC(5)  +  .795 * ZPC(6)  +  0.114 * ZPC(7))     TRAN2240
     1  /WN(1.2)                                                       TRAN2250
      GP(1.2)=(8.16E-11 * SQRT(ZPC(5))  +  1.25E-10 * SQRT(ZPC(6))     TRAN2260
     1     +2.55E-10 * SQRT(ZPC(7)))**2 /(FG(1.2)* WN(1.2)**2)         TRAN2270
      FG(1.3)=(1.040 * ZPN(4)  +  1.29 * ZPN(5)  +  0.00 *ZPN(6))      TRAN2280
     1        /WN(1.3)                                                 TRAN2290
      GP(1.3)=(6.65E-11 * SQRT(ZPN(4))  +  1.71E-10 * SQRT(ZPN(5))     TRAN2300
     1        +  0.00E-10 * SQRT(ZPN(6)))**2/(FG(1.3) * WN(1.3)**2)    TRAN2310
      FG(1.4)=(1.00 * ZPO(5)  +  .978 * ZPO(6))/WN(1.4)                TRAN2320
      GP(1.4)=(3.90E-11 * SQRT(ZPO(5))  +  9.68E-11 * SQRT(ZPO(6)))**2 TRAN2330
     1        /(FG(1.4) * WN(1.4)**2)                                  TRAN2340
      FMUL( 1.L)=FMUC(1.L)                                             TRAN2350
C GROUP 2                                                              TRAN2360
      FG(2.1)=0.805 * ZPH(2)/WN(2.1)                                   TRAN2370
      GP(2.1)=2.37E-10 * 2.37E-10 * ZPH(2)/(FG(2.1) * WN(2.1)**2)      TRAN2380
      FG(2.2)=(0.00E-2 * ZPC(5)  +  6.71E-2 * ZPC(6))/WN(2.2)          TRAN2390
      GP(2.2)=(0.00E-12 * SQRT(ZPC(5))  +  7.15E-11 * SQRT(ZPC(6)))**2 TRAN2400
     1        /(FG(2.2) * WN(2.2)**2)                                  TRAN2410
      FG(2.3)=(0.047* ZPN(4)  +  2.85E-2 * ZPN(5))/WN(2.3)             TRAN2420
      GP(2.3)=(1.11E-10 * SQRT(ZPN(4))  +  6.07E-11 * SQRT(ZPN(5)))**2 TRAN2430
     1        /(FG(2.3) * WN(2.3)**2)                                  TRAN2440
      FG(2.4)=(.0217 * ZPO(4)  +  8.25E-2 * ZPO(5))/WN(2.4)            TRAN2450
      GP(2.4)=(2.61E-11 * SQRT(ZPO(4))  +  7.19E-11 * SQRT(ZPO(5)))**2 TRAN2460
     1  /(FG(2.4) * WN(2.4)**2)                                        TRAN2470
      FMUL( 2.L)=FMUC(1.L)                                             TRAN2480
C  GROUP 3                                                             TRAN2490
      FG(3.2)=(7.29E-2 * ZPC(2)  +  6.76E-2 *ZPC(3))/WN(3.2)           TRAN2500
      GP(3.2)=(9.08E-12 * SQRT(ZPC(2))  +  8.75E-12 * SQRT(ZPC(3)))**2 TRAN2510
     1        /(FG(3.2) * WN(3.2)**2)                                  TRAN2520
```

```
      FMUL(3.L)=FMUC(2.L)                                                 TRAN2530
C   GROUP 4                                                               TRAN2540
      FG(4.2)=(1.05 * ZPC(1)  +  1.10E-2 *ZPC(2)  +  0.150 * ZPC(3))      TRAN2550
     1        /WN(4.2)                                                    TRAN2560
      GP(4.2)=(9.57E-12 * SQRT(ZPC(1))  +  4.86E-12 * SQRT(ZPC(2))        TRAN2570
     1        +  5.93E-10 * SQRT(ZPC(3)))**2/(FG(4.2) * WN(4.2)**2)       TRAN2580
      FG(4.3)=( 7.40E-2  * ZPN(2)  +  6.34E-2 * ZPN(3))/WN(4.3)           TRAN2590
      GP(4.3)=(8.22E-12 * SQRT(ZPN(2))  +  7.60E-12 * SQRT(ZPN(3)))**2    TRAN2600
     1        /(FG(4.3) * WN(4.3)**2)                                     TRAN2610
      FMUL(4.L)=FMUC(4.L)                                                 TRAN2620
C   GROUP 5                                                               TRAN2630
      FG(5.2)=(0.329 * ZPC(1)  +  0.118 * ZPC(2)  +  0.226 * ZPC(4))      TRAN2640
     1        /WN(5.2)                                                    TRAN2650
      GP(5.2)=(3.65E-11 * SQRT(ZPC(1))  +  5.77E-10 * SQRT(ZPC(2))        TRAN2660
     1        +  6.56E-11 *  SQRT(ZPC(4)))**2/(FG(5.2) * WN(5.2)**2)      TRAN2670
      FG(5.3)=0.108 * ZPN(3)/WN(5.3)                                      TRAN2680
      GP(5.3)=3.09E-11 * 3.09E-11 * ZPN(3)/(FG(5.3) * WN(5.3)**2)         TRAN2690
      FG(5.4)=4.71E-2 * ZPO(1)/WN(5.4)                                    TRAN2700
      GP(5.4)=5.08E-12 * 5.08E-12 * ZPO(1)/(FG(5.4) * WN(5.4)**2)         TRAN2710
      FMUL(5.L)=FMUC(6.L)                                                 TRAN2720
C   GROUP 6                                                               TRAN2730
      FG(6.1)=0.416 * ZPH(1)/WN(6.1)                                      TRAN2740
      GP(6.1)=3.02E-11 * 3.02E-11 * ZPH(1)/(FG(6.1)* WN(6.1)**2)          TRAN2750
      FG(6.2)=8.65E-2 * ZPC(1)/WN(6.2)                                    TRAN2760
      GP(6.2)=2.35E-10 * 2.35E-10 * ZPC(1)/(FG(6.2) * WN(6.2)**2)         TRAN2770
      FG(6.3)=(0.184 * ZPN(1)  +  0.290 * ZPN(2)  +  8.52E-2 * ZPN(3))    TRAN2780
     1        /WN(6.3)                                                    TRAN2790
      GP(6.3)=(1.07E-11 * SQRT (ZPN(1))  +  4.28E-11 * SQRT(ZPN(2))       TRAN2800
     1        +  2.09E-10 * SQRT(ZPN(3)))**2/(FG(6.3) * WN(6.3)**2)       TRAN2810
      FG(6.4)=(.120 * ZPO(2)  +  0.151 * ZPO(3))/WN(6.4)                  TRAN2820
      GP(6.4)=(8.85E-12 * SQRT(ZPO(2))  +  9.93E-12 * SQRT(ZPO(3)))**2    TRAN2830
     1        /(FG(6.4) * WN(6.4)**2)                                     TRAN2840
      FMUL(6.L)=FMUC(7.L)                                                 TRAN2850
C    GROUP  7                                                             TRAN2860
      FG(7.2)=(4.51E-2 * ZPC(1)  +  0.705 * ZPC(2))/WN(7.2)               TRAN2870
      GP(7.2)=(6.07E-10 * SQRT(ZPC(1))  +  2.10E-10 * SQRT(ZPC(2)))**2    TRAN2880
```

```
1         /(FG(7,2) * WN(7,2)**2)                                       TRAN2890
  FG(7,3)=(0.454 * ZPN(1)  +  9.66E-2 * ZPN(2)                          TRAN2900
1         + 0.178 * ZPN(3))/WN(7,3)                                     TRAN2910
  GP(7,3)=(2.71E-12 * SQRT(ZPN(1))  +  2.34E-10 * SQRT(ZPN(2))          TRAN2920
1         + 2.46E-11 * SQRT(ZPN(3)))**2/(FG(7,3)* WN(7,3)**2)           TRAN2930
  FG(7,4)=4.23E-2 * ZPO(3)/WN(7,4)                                      TRAN2940
  GP(7,4)=2.52E-11 * 2.52E-11 * ZPO(3)/(FG(7,4) * WN(7,4)**2)           TRAN2950
  FMUL(7,L)=FMUC(9,L)                                                   TRAN2960
C GROUP 8                                                               TRAN2970
  FG(8,1)=0.108 * ZPH(1)/WN(8,1)                                        TRAN2980
  GP(8,1)=1.32E-10  *  1.32E-10 * ZPH(1)                                TRAN2990
1         /(FG(8,1) * WN(8,1)**2)                                       TRAN3000
  FG(8,2)=(0.379 * ZPC(1)  +  1.05 * ZPC(3))/WN(8,2)                    TRAN3010
  GP(8,2)=(1.95E-11 * SQRT(ZPC(1))  +  1.27E-10 * SQRT(ZPC(3)))**2      TRAN3020
1         /(FG(8,2) * WN(8,2)**2)                                       TRAN3030
  FG(8,3)=(0.155 * ZPN(1)  +  0.142*ZPN(2)  +  3.75E-2 * ZPN(3))        TRAN3040
1         /WN(8,3)                                                      TRAN3050
  GP(8,3)=(2.98E-11 * SQRT(ZPN(1))  +  7.08E-11 * SQRT(ZPN(2))          TRAN3060
1         + 1.33E-10 * SQRT(ZPN(3)))**2/(FG(8,3, * WN(8,3)**2)          TRAN3070
  FG(8,4)=(0.146 * ZPO(1)  +  8.61E-2*ZPO(2)                            TRAN3080
1         + 9.33E-2 * ZPO(3))/WN(8,4)                                   TRAN3090
  GP(8,4)=(1.97E-10 * SQRT(ZPO(1))  +  1.80E-11 * SQRT(ZPO(2))          TRAN3100
1         + 8.13E-11 * SQRT(ZPO(3)))**2/(FG(8,4) * WN(8,4)**2)          TRAN3110
  FMUL(8,L)=FMUC(10,L)                                                  TRAN3120
C GROUP 9                                                               TRAN3130
  FG(9,2)=2.95 * ZPC(2)/WN(9,2)                                         TRAN3140
  GP(9,2)=5.85E-12 * 5.85E-12 * ZPC(2)/(FG(9,2) * WN(9,2)**2)           TRAN3150
  FG(9,3)=(0.224 * ZPN(1)  +  2.92E-2 * ZPN(2))/WN(9,3)                 TRAN3160
  GP(9,3)=(3.41E-10 * SQRT(ZPN(1))  +  1.48E-10 * SQRT(ZPN(2)))**2      TRAN3170
1         /(FG(9,3) * WN(9,3)**2)                                       TRAN3180
  FG(9,4)=(5.24E-2 * ZPO(1)  +  7.22E-2 * ZPO(2)                        TRAN3190
1         + 6.04E-2 * ZPO(3))/WN(9,4)                                   TRAN3200
  GP(9,4)=(5.76E-12 * SQRT(ZPO(1))  +  7.20E-11 * SQRT(ZPO(2))          TRAN3210
1         + 8.05E-11 * SQRT(ZPO(3)))**2/(FG(9,4) * WN(9,4)**2)          TRAN3220
  FMUL(9,L)=FMUC(11,L)                                                  TRAN3230
C                                                                       TRAN3240
```

```
C **   PLANCK FUNCTION   **                                             TRAN3250
C                                                                       TRAN3260
      DO 9 J=1,NHVL                                                     TRAN3270
      BEEL(J,L)=5.04E3 * HVJ(J)**3 / (EXP(HVJ(J)/T1)  -  1.0)           TRAN3280
C                                                                       TRAN3290
C **   INDUCED EMISSION FACTOR (EQ 81)  **                              TRAN3300
C                                                                       TRAN3310
      SSM(J,1,L)=1.10E-16*SNDH (L)*(1.0-EXP(-HVJ(J)/T1)) * FG(J,1)      TRAN3320
      SSM(J,2,L)=1.10E-16*SNDC (L)*(1.0-EXP(-HVJ(J)/T1)) * FG(J,2)      TRAN3330
      SSM(J,3,L)=1.10E-16*SNDN (L)*(1.0-EXP(-HVJ(J)/T1)) * FG(J,3)      TRAN3340
      SSM(J,4,L)=1.10E-16*SNDO (L)*(1.0-EXP(-HVJ(J)/T1)) * FG(J,4)      TRAN3350
      DO 10 M=1,4                                                       TRAN3360
      GGM(J,M,L)=GP(J,M) * SNDE(L)   * (T(L)/1.0E4)**0.25               TRAN3370
     1         +  1.0E-6                                                TRAN3380
      IF(L.GT.1) GO TO 11                                               TRAN3390
      ETAM(J,M,1)=0.                                                    TRAN3400
      SBM (J,M,1)=0.                                                    TRAN3410
      GO TO 10                                                          TRAN3420
   11 ETAM(J,M,L)=ETAM(J,M,L-1)+  (YD(L)-YD(L-1))                       TRAN3430
     1         *(SSM(J,M,L-1) * GGM(J,M,L-1)  +  SSM(J,M,L) * GGM(J,M,L))TRAN3440
     2         * DELTA/3.14159265                                       TRAN3450
      SBM(J,M,L)=SBM(J,M,L-1)  +  (YD(L)-YD(L-1))                       TRAN3460
     1         * (SSM(J,M,L-1)+SSM(J,M,L)) * DELTA                      TRAN3470
   10 CONTINUE                                                          TRAN3480
      IF (L.GT.1) GO TO 12                                              TRAN3490
      TAUL(J,1)=0.                                                      TRAN3500
      GO TO 9                                                           TRAN3510
   12 TAUL(J,L)=TAUL(J,L-1)  +  (YD(L)-YD(L-1))                         TRAN3520
     1         * (FMUL(J,L-1)+FMUL(J,L))  * DELTA                       TRAN3530
    9 CONTINUE                                                          TRAN3540
      IF (ICG.NE.99) GO TO 91                                           TRAN3550
      CALL BUGPR (7)                                                    TRAN3560
C                                                                       TRAN3570
   91 CONTINUE                                                          TRAN3580
      IEZ=IEZ+1                                                         TRAN3590
      ETZ(IEZ)=1.0                                                      TRAN3600
```

```
C                                                                       TRAN3610
      RETURN                                                            TRAN3620
      END                                                               TRAN3630
      SUBROUTINE TRANS1 (ISW)                                          TRAN  10
C                                                                      TRAN  20
C **   CONTINUUM - CONTINUUM FLUX DIVERGENCE CALCULATION   **          TRAN  30
C                                                                      TRAN  40
      COMMON /ZPI/ ZPD(6), ZPN(6),ZPH(2),  ZPC(7)                      TRAN  50
      COMMON /FINV/ NHVL,NIHVC,FHVC(12),DJ(9),HVJ(9),ZKZ               TRAN  60
      COMMON /SFLUX/ QRI(3)                                            TRAN  70
      COMMON /TRN/        NUT(60), FMC(12,60), FPC(12,60),             TRAN  80
     1         FM(9,60), FP(9,60), LINES                               TRAN  90
      COMMON /YL/ETA(60),  YD(60)                                      TRAN 100
      COMMON/PROP1/P (60),  R(60), T(60),AMW(60),C (20,60),EC(5,60)    TRAN 110
      COMMON /FRSTRM/ U INF, RINF, UINF2,XL , RE, LXI, ITM, IEM, NES   TRAN 120
      COMMON /DEL/  W(1),DTIL,D7ILS                                    TRAN 130
      COMMON /NON/RDZ,MUDZ,RMDZ,AKNF,HNF,CPNF                          TRAN 140
      COMMON /MAIM/KEEP,MAXE,MAXM,MAXD,   IDG,MCONV,ECONV,DCONV,LT,IAB TRAN 150
      COMMON /RFLUX/ E(60),IRAD,ITYPE                                  TRAN 160
      COMMON /RH/ DUD,DPHI,TD,RZB,PD,HD,HTOTAL                         TRAN 170
      COMMON/WT/SMW(20),AWT(5)                                         TRAN 180
      COMMON /TEST/ETZ(60),IEZ                                         TRAN 190
      COMMON /NUMDEN/ SNDD2(60), SNDN2(60), SNDC(60), SNDN(60),        TRAN 200
     1                                     SNDE(60), SNDC(60),         TRAN 210
     2           SNDH(60), SNDC2(60), SNDH2(60), SNDCD(60),            TRAN 220
     3           SNDC3(60),SNDC2H(60)                                  TRAN 230
      COMMON /DBUG/ QLC(60), QCL(60), QLL(60), DQN(60), QCC(60),       TRAN 240
     1              BEEC(12,60),   FMUC(12,60),   EM(12,60),           TRAN 250
     2              EP(12,60),     TAUC(12,60),   BEEL(9,60),          TRAN 260
     3              QCCP(12),      WMM(9,60),     GMM(9,60),           TRAN 270
     4              EEM(9,60),     XLMM(9,60),    QLCP(9),             TRAN 280
     5              QCLP(9),       QLLP(9),       DELTA,    IY,  IYY,  TRAN 290
     6              WPP(9,60),     GPP(9,60),     EEP(9,60),           TRAN 300
     7              XLPP(9,60),    FG(9,4),       GP(9,4),             TRAN 310
     8              WN(9,4),       FMUL(9,60),    SSM(9,4,60),         TRAN 320
     9              GGM(9,4,60),   ETAM(9,4,60),  SBM(9,4,60),         TRAN 330
     A              TAUL(9,60)                                         TRAN 340
      COMMON /SPEC/ MF, XMOL                                           TRAN 350
      COMMON/MIKE/ NETA1,NETA2,PNF,WNF,RHOD,DP,TS,UD,VD,RW,RWD,EPS,PHI TRAN 360
      DIMENSION  XKT(60).          DQ(60)
C
C **   BAND AVERAGE ABSORPTION CROSS SECTION (EQ.A2)  **
C
      SIGMA(ZH.ZA.ZB.ZG)=  ((5.0E+03*T1*ZG*ZKZ)/BE) * (EXP(ZDL/T1)
     1                      *ZH*(ZA+ZB* (ZH**2)/3.0) +
     2                      T1 * (ZA+2.0*ZB*T12) -T1*EXP((ZH-ZHVP)/T1)
     3                      *(ZA+ZB*(ZHVP-ZH)**2) -T1*EXP((ZH-ZHVP)/T1)
     4                      *2.0*ZB*T1*(ZHVP-ZH+T1))
      SIGMA2(ZH.ZG.ZE.ZY)=7.26E-16*T1*ZG*EXP((-ZE+ZY+ZDL)/T1)/ZH**3
      GAMMA(ZX)=(1.0+(1.5707963*ZX)**1.25)**(-0.4)
      XLAMB(ZX)=(1.0+ZX*EXP(-ZX))/SQRT(1.0+6.283185 *ZX)
C
C **   W(GROUP)/D CORRELATION (EQ.88)  **
C
      PHI1(ZX)=(ATAN(1.570796 *ZX)/1.570796 )
C
C **   FLUX DIVERGENCE OVERLAPPING FUNCTION (EQ.92)  **
C
      PHI2(ZX)=EXP(-ZX)
C
C **   CONTINUUM - CONTINUUM FLUX DIVERGENCE CALCULATION  **
C
      DO 300 K=1.IEZ
      DO 31 LK=1.NES
      I=LK
      NUT(K)=I
      IF (ABS(ETZ(K)-ETA(LK)) - 1.0E-5) 300.300.31
   31 CONTINUE
  300 CONTINUE
      DO 1612 J=1.9
      QCLP(J)=0.
      QLCP(J)=0.
      QLLP(J)=0.
      DO 1612 L=1.NES
      FM(J.L)=0.
```

```
 1612 FP(J,L)=0.                                                        TRAN 730
      DO 1613 L=1,IEZ                                                   TRAN 740
      QCL(L)=0.                                                         TRAN 750
      QLC(L)=0.                                                         TRAN 760
 1613 QLL(L)=0.                                                         TRAN 770
      DO 49 IYY=1,IEZ                                                   TRAN 780
      IY=NUT(IYY)                                                       TRAN 790
      DO 20 K=1,12                                                      TRAN 800
      FMC(K,IY)=0.                                                      TRAN 810
      FPC(K,IY)=0.                                                      TRAN 820
      IF (IY.EQ.1) GO TO 44                                             TRAN 830
      DO 40 L=1,IY                                                      TRAN 840
C                                                                       TRAN 850
C **   MINUS EMISSIVITY FUNCTION (EQ 47)   *                            TRAN 860
C                                                                       TRAN 870
      EM(K,L)=1.0   -  EXP(TAUC(K,L)-TAUC(K,IY))                        TRAN 880
      IF (L.EQ.1) GO TO 40                                              TRAN 890
C                                                                       TRAN 900
C **   MINUS CONTINUUM FLUX (EQ 45)   **                                TRAN 910
C                                                                       TRAN 920
      FMC(K,IY)=FMC(K,IY)  -   (EM(K,L)-EM(K,L-1))                      TRAN 930
     1         * (BEEC(K,L-1)+BEEC(K,L))/2.                             TRAN 940
   40 CONTINUE                                                          TRAN 950
   44 IF (IY.EQ.NES ) GO TO 41                                          TRAN 960
      DO 42 L=IY,NES                                                    TRAN 970
C                                                                       TRAN 980
C **   POSITIVE EMISSIVITY FUNCTION (EQ 47)   **                        TRAN 990
C                                                                       TRAN1000
      EP(K,L)=1.0   -  EXP(TAUC(K,IY)-TAUC(K,L))                        TRAN1010
      IF (L.EQ.IY) GO TO 42                                             TRAN1020
C                                                                       TRAN1030
C **   POSITIVE EMISSIVITY CONTINUUM FLUX (EQ 46)   **                  TRAN1040
C                                                                       TRAN1050
      FPC(K,IY)=FPC(K,IY)  +   (EP(K,L)-EP(K,L-1))                      TRAN1060
     1         * (BEEC(K,L-1)+BEEC(K,L))/2.                             TRAN1070
   42 CONTINUE                                                          TRAN1080
```

```
C                                                                       TRAN1090
C **   POSITIVE EMISSIVITY CONTINUUM FLUXDIVERGENCE (EQ 51)   **        TRAN1100
C                                                                       TRAN1110
   41 QCCP(K)=6.2831853 * FMUC(K.IY) *                                  TRAN1120
     1          (FMC(K.IY)  +  FPC(K.IY)  -  2.0* BEEC(K.IY))           TRAN1130
      FMC(K.IY)=FMC(K,IY) * 3.14159265                                  TRAN1140
      FPC(K.IY)=FPC(K,IY) * 3.14159265                                  TRAN1150
   20 CONTINUE                                                          TRAN1160
C                                                                       TRAN1170
C **   DEBUG PRINT  **                                                  TRAN1180
C                                                                       TRAN1190
      IF (IDG.NE.99) GO TO 21                                           TRAN1200
      CALL BUGPR (3)                                                    TRAN1210
   21 QCC(IYY)=0.                                                       TRAN1220
      DO 24 K=1.12                                                      TRAN1230
C                                                                       TRAN1240
C **   LINE AND CROSS TERM FLUX DIVERGENCE CALCULATION  **              TRAN1250
C                                                                       TRAN1260
   24 QCC(IYY)=QCC(IYY)  +  QCCP(K)                                     TRAN1270
      IF (LINES.EQ.0) GO TO 1614                                        TRAN1280
C                                                                       TRAN1290
C **   INTEGRATION FROM 1 TO IY  **                                     TRAN1300
C                                                                       TRAN1310
      IF (IY.EQ.1) GO TO 68                                             TRAN1320
      DO 65 J=1.9                                                       TRAN1330
      DO 66 L=1.IY                                                      TRAN1340
      WIM=0.                                                            TRAN1350
      SUM1=0.                                                           TRAN1360
      SUM2=0.                                                           TRAN1370
      DO 67 M=1.4                                                       TRAN1380
      DIF=ETAM(J.M.IY)  -  ETAM(J.M.L)                                  TRAN1390
      DIFSBM =     SBM(J.M.IY)-SBM(J.M.L)                               TRAN1400
      IF(ABS(DIFSBM).LT.1.E-10)  DIFSBM = 1.E-10                        TRAN1410
      BETAM=DIF / ( DIFSBM               )  *  3.14159265               TRAN1420
      IF (L.EQ.IY) BETAM=GGM(J.M.L)                                     TRAN1430
      IF(ABS(DIF).GT.1.E-10) GO TO 9001                                 TRAN1440
      TM = 1.E-10                                                       TRAN1450
      GO TO 9002                                                        TRAN1460
 9001 CONTINUE                                                          TRAN1470
      TM=DIF/2.0/BETAM**2                                               TRAN1480
 9002 RRM=DIF/2.0/GGM(J,M,IY)**2                                        TRAN1490
      WWM=6.2831853 * WN(J,M) * BETAM * GAMMA(TM) * TM                  TRAN1500
      SUM1=SUM1  +  GAMMA(TM) * WN(J,M) * SSM(J,M,IY)                   TRAN1510
      SUM2=SUM2  +  XLAMB(RRM) * WN(J,M) * SSM(J,M,IY)                  TRAN1520
   67 WIM=WIM  +  WWM                                                   TRAN1530
      ALPHAM=WIM/DJ(J)                                                  TRAN1540
C                                                                       TRAN1550
C **   OVERLAPPING LINE CALCULATIONS  **                                TRAN1560
C                                                                       TRAN1570
C                                                                       TRAN1580
C **   GROUP EQUIVALENT WIDTHS  (EQ.88)  **                             TRAN1590
C                                                                       TRAN1600
      WMM(J,L)=DJ(J) * PHI1(ALPHAM) * EXP(TAUL(J,L)-TAUL(J,IY))         TRAN1610
C                                                                       TRAN1620
C **   GROUP GAMMA -- LINE TRANSPORT FUNCTION (EQ.92)  **               TRAN1630
C                                                                       TRAN1640
      GMM(J,L)=PHI2(ALPHAM) * SUM1                                      TRAN1650
C                                                                       TRAN1660
C **   MINUS EMISSIVITY FUNCTION FOR LINES (EQ.47)  **                  TRAN1670
C                                                                       TRAN1680
      EEM(J,L)=1.0  -  EXP(TAUL(J,L)-TAUL(J,IY))                        TRAN1690
   66 XLMM(J,L)=PHI2(ALPHAM) * SUM2                                     TRAN1700
   65 CONTINUE                                                          TRAN1710
      IF (IDG.EC.99) CALL BUGPR(1)                                      TRAN1720
      IF (IDG.EQ.99) CALL BUGPR (4)                                     TRAN1730
   68 IF (IY.EQ.NES) GO TO 72                                           TRAN1740
C                                                                       TRAN1750
C **   INTEGRATION FROM IY TO NES  **                                   TRAN1760
C                                                                       TRAN1770
      DO 69 J=1,9                                                       TRAN1780
      DO 70 L=IY,NES                                                    TRAN1790
      WIP=0.                                                            TRAN1800
      SUM1=0.
      SUM2=0.
      DO 71 M=1.4
      DIF=ETAM(J.M.L)  -  ETAM(J.M.IY)
      DIFSBM =      SBM(J.M.L)-SBM(J.M.IY)
      IF(ABS(DIFSBM).LT.1.E-10)  DIFSBM = 1.E-10
      BETAP=DIF / ( DIFSBM                  )  *  3.14159265
      IF (L.EQ.IY) BETAP=GGM(J.M.L)
      IF(ABS(DIF).GT.1.E-10) GO TO 9003
      TP = 1.E-10
      GO TO 9004
 9003 CONTINUE
      TP=DIF/2.0/BETAP**2
 9004 RRP=DIF/2.0/GGM(J.M.IY)**2
      WWP=6.2831853 * WN(J.M) * BETAP * GAMMA(TP) * TP
      SUM1=SUM1  +  GAMMA(TP) * WN(J.M) * SSM(J.M.IY)
      SUM2=SUM2  +  XLAMB(RRP) * WN(J.M) * SSM(J.M.IY)
   71 WIP=WIP+WWP
      ALPHAP=WIP/DJ(J)
      WPP(J.L)=DJ(J) * PHI1(ALPHAP) * EXP(TAUL(J.IY)-TAUL(J.L))
      GPP(J.L)=PHI2(ALPHAP) * SUM1
C
C **   POSITIVE EMISSIVITY FUNCTION FOR LINES (EQ.47)   **
C
      EEP(J.L)=1.0  -  EXP(TAUL(J.IY)-TAUL(J.L))
   70 XLPP(J.L)=PHI2(ALPHAP) * SUM2
   69 CONTINUE
C
C **   DEBUG PRINT  **
      IF (IDG.EQ.99) CALL BUGPR (5)
C
   72 DO 80 J=1.9
      ASM1=0.
      ASM2=0.
      FM(J.IY)=0.
      IF (IY.EQ.1) GO TO 81
      DO 82 L=2.IY                                                      TRAN2170
      FM(J.IY)=FM(J.IY)  -  (WMM(J.L)-WMM(J.L-1))                       TRAN2180
     1        *(BEEL(J.L-1)+BEEL(J.L)) * 1.5707963                      TRAN2190
      IF (L.EQ.IY) GO TO 82                                             TRAN2200
      ASM1=ASM1  -  (EEM(J.L)-EEM(J.L-1))                               TRAN2210
     1        * (BEEL(J.L-1) * XLMM(J.L-1) + BEEL(J.L) * XLMM(J.L))/2.  TRAN2220
      ASM2=ASM2  -  (XLMM(J.L)-XLMM(J.L-1))                             TRAN2230
     1        * (BEEL(J.L-1) * EXP(TAUL(J.L-1)-TAUL(J.IY)) + BEEL(J.L)  TRAN2240
     2        * EXP(TAUL(J.L)-TAUL(J.IY)))/2.0                          TRAN2250
   82 CONTINUE                                                          TRAN2260
   81 ASP1=0.                                                           TRAN2270
      ASP2=0.                                                           TRAN2280
      IYP=IY+1                                                          TRAN2290
      IF (IY.EQ.NES) GO TO 83                                           TRAN2300
      DO 84 L=IYP.NES                                                   TRAN2310
      FP(J.IY)=FP(J.IY)  +  (WPP(J.L)-WPP(J.L-1))                       TRAN2320
     1        * (BEEL(J.L-1)+BEEL(J.L)) * 1.5707963                     TRAN2330
      IF (L.EQ.IYP) GO TO 84                                            TRAN2340
      ASP1=ASP1  +  (EEP(J.L)-EEP(J.L-1))                               TRAN2350
     1        * (BEEL(J.L-1) * XLPP(J.L-1) + BEEL(J.L) * XLPP(J.L))/2.0 TRAN2360
      ASP2=ASP2  +  (XLPP(J.L)-XLPP(J.L-1)) *                           TRAN2370
     1        (BEEL(J.L-1) * EXP(TAUL(J.IY)-TAUL(J.L-1))  +  BEEL(J.L)  TRAN2380
     2        * EXP(TAUL(J.IY)-TAUL(J.L)))/2.0                          TRAN2390
   84 CONTINUE                                                          TRAN2400
   83 QLCP(J)=2.0 * FMUL(J.IY) * (FM(J.IY)+FP(J.IY))                    TRAN2410
      SUMS=1.0                                                          TRAN2420
      SUMT=0.                                                           TRAN2430
      DO 86 M=1.4                                                       TRAN2440
   86 SUMT=SUMT  +  SSM(J.M.IY) * WN(J.M)                               TRAN2450
      ATM1=0.                                                           TRAN2460
      IF (IY.NE.1) ATM1=(BEEL(J.IY-1)+BEEL(J.IY)) /2.0 * EEM(J.IY-1)    TRAN2470
     1        * XLMM(J.IY-1)                                            TRAN2480
      ATP1=0.                                                           TRAN2490
      IF(IY.NE.NES) ATP1=(BEEL(J.IY+1)+BEEL(J.IY))/2.0 * EEP(J.IY+1)    TRAN2500
     1        * XLPP(J.IY+1)                                            TRAN2510
      QCLP(J)=6.2831853  * SUMS * (ASM1+ASP1+ATM1+ATP1)                 TRAN2520
      IF (IY.EQ.1) ATM2=-BEEL(J,IY) * SUMT                              TRAN2530
      IF (IY.NE.1) ATM2=(BEEL(J,IY-1)-BEEL(J,IY))  *  GMM(J,IY-1)       TRAN2540
     1        -  BEEL(J,IY-1) * XLMM(J,IY-1)                            TRAN2550
      IF (IY.EQ.NES) ATP2=-BEEL(J,IY) * SUMT                            TRAN2560
      IF (IY.NE.NES)ATP2=(BEEL(J,IY+1)-BEEL(J,IY))  * GPP(J,IY+1)       TRAN2570
     1        -  BEEL(J,IY+1) * XLPP(J,IY+1)                            TRAN2580
      QLLP(J)=6.2831853 * SUMS*(-ASM2-ASP2+ATM2+ATP2)                   TRAN2590
   80 CONTINUE                                                          TRAN2600
      QCL(IYY)=0.                                                       TRAN2610
      QLC(IYY)=0.                                                       TRAN2620
      QLL(IYY)=0.                                                       TRAN2630
      DO 85 J=1,9                                                       TRAN2640
      QCL(IYY)=QCL(IYY)  +  QCLP(J)                                     TRAN2650
      QLC(IYY)=QLC(IYY)  +  QLCP(J)                                     TRAN2660
   85 QLL(IYY)=QLL(IYY)  +  QLLP(J)                                     TRAN2670
 1614 CONTINUE                                                          TRAN2680
      DQN(IYY)=-(QCC(IYY)+QCL(IYY)+QLC(IYY)+QLL(IYY))                   TRAN2690
C                                                                       TRAN2700
C **   DEBUG PRINT  **                                                  TRAN2710
C                                                                       TRAN2720
      IF (IDG.EQ.0) GO TO 49                                            TRAN2730
      CALL BUGPR(6)                                                     TRAN2740
   49 CONTINUE                                                          TRAN2750
      IEZ=IEZ-1                                                         TRAN2760
      DQ(1)=DQN(1)                                                      TRAN2770
      L=2                                                               TRAN2780
      DO 1 N=2,NES                                                      TRAN2790
      DO 2 I=2,IEZ                                                      TRAN2800
      NP=I                                                              TRAN2810
      IF (ETZ(I).GT.ETA(N)) GO TO 3                                     TRAN2820
    2 CONTINUE                                                          TRAN2830
    3 NN=NP-1                                                           TRAN2840
      AA=0.0                                                            TRAN2850
      ZB=(DQN(NN)-DQN(NP)) / (ETZ(NN)-ETZ(NP))                          TRAN2860
      CC=DQN(NN)  -  ZB * ETZ(NN)                                       TRAN2870
      DQ(N)=AA * ETA(N)**2  +  ZB * ETA(N)  +  CC                       TRAN2880
      GO TO 1                                                           TRAN2890
    4 DQ(N)=DQN(NN)                                                     TRAN2900
    1 CONTINUE                                                          TRAN2910
C                                                                       TRAN2920
C **  NON-DIMENSIONALIZE E(I)   **                                      TRAN2930
      DO 250 I=1.NES                                                    TRAN2940
      T(I) = T(I)/TS                                                    TRAN2950
  250 E(I) = ((DQ(I)*XL  )/(RDZ *UINF**3))*20866.0                      TRAN2960
      RETURN                                                            TRAN2970
      END                                                               TRAN2980
      SUBROUTINE TRANS2
      COMMON /SFLUX/ QRI(3)
      COMMON /YL/ETA(60),YOND(60)
      COMMON /FRSTRM/ U INF, RINF, UINF2, R , RE, LXI , ITM, IEM, NES
      COMMON /TRN/         MUT(60), FMC(12,60), FPC(12,60),
     1              FM(9,60), FP(9,60), LINES
      COMMON /FINV/ NHVL,NIHVC,FHVC(12),DJ(9),HVJ(9),ZKZ
      COMMON /TEST/ETZ(60),IEZ
      COMMON /NUMDEN/ SNDO2(60), SNDN2(60), SNDO(60), SNDN(60),
     1                                      SNDE(60), SNDC(60),
     2                SNDH(60), SNDC2(60), SNDH2(60), SNDCO(60),
     3                SNDC3(60),SNDC2H(60)
      COMMON /MAIM/KEEP,MAXE,MAXM,MAXD,   IDG,MCONV,ECONV,DCONV,LT,IAB
      COMMON /SPEC/ MF, XMOL
      DIMENSION ETOUT(3)
      NETA=NES
      ETOUT(1)=0.0
      ETOUT(2)=0.5
      ETOUT(3)=1.0
      NOUT=3
C
C  OUTPUT FLUX
C
      IF (IDG .GT. 0)
     XWRITE (6,600)
      IF (IDG .GT. 0)
     XWRITE (6,603) (ETA(I),SNDN2(I),SNDO2(I),SNDN(I),SNDO(I),
     1                           SNDE(I), SNDH(I),
     2                         SNDC(I),SNDC2(I),SNDH2(I),SNDCO(I),SNDC3(I),
     3                  SNDC2H(I),              I=1,NETA)
C **   CONTINUUM CONTRIBUTION TO THE SPECTRAL FLUX **
C
      IF (IDG .GT. 0)
     XWRITE (6,4103)
      DO 8040 K=1,NOUT
      DO 8041 LK=1,NES
      NUT(K )=LK
      IF (ABS(ETOUT(K)-ETA(LK)) - 1.0E-05) 8040,8040,8041
 8041 CONTINUE
 8040 CONTINUE
      L1=NUT(1)
      L2=NUT(2)
      L3=NUT(3)
      IF (IDG .GT. 0)
     XWRITE (6,8037)(ETOUT(IL),IL=1,3)
      FM1=0.0
      FP1=0.0
      FM2=0.0
      FP2=0.0
      FM3=0.0
      FP3=0.0
      DO 4104 KL=1,NIHVC
      IF (IDG .GT. 0)
     XWRITE (6,8042) KL,   FHVC(KL),   FMC(KL,L1),   FPC(KL,L1),
     1               FMC(KL,L2),   FPC(KL,L2),  FMC(KL,L3),   FPC(KL,L3)
      FM1=FM1  +  FMC(KL,L1)
      FP1=FP1  +  FPC(KL,L1)
      FM2=FM2  +  FMC(KL,L2)
      FP2=FP2  +  FPC(KL,L2)
      FM3=FM3  +  FMC(KL,L3)
      FP3=FP3  +  FPC(KL,L3)
 4104 CONTINUE
      IF (IDG .GT. 0)
     XWRITE (6,8045) FM1,   FP1,   FM2,   FP2,   FM3,   FP3
      QRI(1)=FM1+FP1
      QRI(2)=FM2+FP2
      QRI(3)=FM3+FP3
C
C **   LINE      CONTRIBUTION TO THE SPECTRAL FLUX **
C
      IF (LINES.EQ.0) RETURN
      IF (IDG .GT. 0)
      XWRITE (6.8035)                                                   TRAN 730
       IF (IDG .GT. 0)                                                  TRAN 740
      XWRITE (6.8037) (ETOUT(IL).IL=1.3)                                TRAN 750
       FM1=0.0                                                          TRAN 760
       FP1=0.0                                                          TRAN 770
       FM2=0.0                                                          TRAN 780
       FP2=0.0                                                          TRAN 790
       FM3=0.0                                                          TRAN 800
       FP3=0.0                                                          TRAN 810
C                                                                       TRAN 820
C **   TOTAL FLUX CALCULATION  **                                       TRAN 830
C                                                                       TRAN 840
       DO 8043 KL=1.NHVL                                                TRAN 850
       IF (IDG .GT. 0)                                                  TRAN 860
      XWRITE (6.8042) KL.   HVJ(KL).    FM(KL.L1).   FP(KL.L1).         TRAN 870
      1              FM(KL.L2).   FP(KL.L2).   FM(KL.L3).   FP(KL.L3)   TRAN 880
       FM1=FM1  +  FM(KL.L1)                                            TRAN 890
       FP1=FP1  +  FP(KL.L1)                                            TRAN 900
       FM2=FM2  +  FM(KL.L2)                                            TRAN 910
       FP2=FP2  +  FP(KL.L2)                                            TRAN 920
       FM3=FM3  +  FM(KL.L3)                                            TRAN 930
       FP3=FP3  +  FP(KL.L3)                                            TRAN 940
 8043 CONTINUE                                                          TRAN 950
       IF (IDG .GT. 0)                                                  TRAN 960
      XWRITE (6.8045) FM1.   FP1.   FM2.   FP2.   FM3.   FP3            TRAN 970
       QRI(1)=QRI(1)  +  FM1  +  FP1                                    TRAN 980
       QRI(2)=QRI(2)  +  FM2  +  FP2                                    TRAN 990
       QRI(3)=QRI(3)  +  FM3  +  FP3                                    TRAN1000
C                                                                       TRAN1010
  600 FORMAT (1H1.33HNUMBER DENSITIES  (PARTICLES/CM3) ///5X.3HETA. 8X. TRAN1020
      1          2HN2. 8X.2HO2. 8X.1HN. 8X.1HO. 8X. 2HE-.8X.            TRAN1030
      2 1HH.8X.1HC. 8X.2HC2. 8X.2HH2. 8X.2HCO. 8X.2HC3.8X.3HC2H///)     TRAN1040
  603 FORMAT (1P13E10.2)                                                TRAN1050
 4103 FORMAT (44H1CONTINUUM CONTRIBUTION TO THE SPECTRAL FLUX)          TRAN1060
 8035 FORMAT (39H0LINE CONTRIBUTION TO THE SPECTRAL FLUX)               TRAN1070
 8037 FORMAT (/22X.5HETA =F7.3.13X.5HETA =F7.3.13X.5HETA =F7.3//3X.1HI. TRAN1080
    1 3X,3HHNU,[illegible] 6HQMINUS,7X,5HQPLUS,8X,6HQMINUS,7X,5HQPLUS,8X,        TRAN1090
    2 6HQMINUS,7X,5HQPLUS/)                                                      TRAN1100
 8042 FORMAT (I4,F8.3,1P8E13.3)                                                  TRAN1110
 8045 FORMAT (12H0TOTAL FLUX ,1P8E13.3)                                          TRAN1120
      RETURN                                                                     TRAN1130
      END                                                                        TRAN1140
      SUBROUTINE SND(I)
      COMMON/PROP1/PI(60).RHO(60). T(60).AMW(60).C (20.60).EC(5.60)
      COMMON /RFLUX/ E(60).IRAD.ITYPE
      COMMON /NON/RDZ.MUDZ.RMDZ.AKNF.HNF.CPNF
      COMMON/WT/SMW(20).AWT(5)
      COMMON /NUMDEN/ SNDO2(60). SNDN2(60). SNDO(60). SNDN(60).
     1                                     SNDE(60). SNDC(60).
     2               SNDH(60). SNDC2(60). SNDH2(60). SNDCO(60).
     3               SNDC3(60).SNDC2H(60)
C     **  CALCULATE SPECIE NUMBER DENSITIES BASED ON MOLE FRACTIONS  **
C
      CONVER = 3.10375E+23 *RHO(I) *RDZ
C
      SNDO2(I) = CONVER * C( 1.I)/SMW( 1)
      SNDN2(I) = CONVER * C( 2.I)/SMW( 2)
      SNDO (I) = CONVER * C( 3.I)/SMW( 3)
      SNDN (I) = CONVER * C( 4.I)/SMW( 4)
      SNDE (I) = CONVER * C( 7.I)/SMW( 7)
      SNDC (I) = CONVER * C( 8.I)/SMW( 8)
      SNDH (I) = CONVER * C( 9.I)/SMW( 9)
      SNDH2(I) = CONVER * C(10.I)/SMW(10)
      SNDCO(I) = CONVER * C(11.I)/SMW(11)
      SNDC3(I) = CONVER * C(12.I)/SMW(12)
      SNDC2(I) = CONVER * C(19.I)/SMW(19)
      SNCC2H(I)= CONVER * C(14.I)/SMW(14)
      RETURN
      END
      SUBROUTINE ZP(T1.SUMN.SUMO.SUMH.SUMC)
C
C     **  FRACTIONAL POPULATION STATES FOR N. O. H. C  **
C
      COMMON /ZPI/ ZPO(6). ZPN(6).ZPH(2).  ZPC(7)
      ZPH(1)=2.0/SUMH
      ZPH(2)=8.0 * EXP(-10.20/T1)/SUMH
      ZPC(1)=9.0/SUMC
      ZPC(2)=5.0 * EXP(-1.264/T1)/SUMC
      ZPC(3)=EXP(-2.684/T1)/SUMC
      ZPC(4)=5.0 * EXP(-4.183/T1)/SUMC
      ZPC(5)=12.0 * EXP(-7.532/T1)/SUMC
      ZPC(6)=36.0*EXP(-8.722/T1)/SUMC
      ZPC(7)=60.0 * EXP(-9.724/T1)/SUMC
      ZPN(1)=4.0/SUMN
      ZPN(2)=10.0* EXP(-2.384/T1)/SUMN
      ZPN(3)=6.0 * EXP(-3.576/T1)/SUMN
      ZPN(4)=18.0 * EXP(-10.452/T1)/SUMN
      ZPN(5)=54.0 * EXP(-11.877/T1)/SUMN
      ZPN(6)=90.0 * EXP(-13.002/T1)/SUMN
      ZPO(1)=9.0/SUMO
      ZPO(2)=5.0 * EXP(-1.967/T1)/SUMO
      ZPO(3)=EXP(-4.188/T1)/SUMO
      ZPO(4)=8.0 * EXP(-9.283/T1)/SUMO
      ZPO(5)=24.0 * EXP(-10.830/T1)/SUMO
      ZPO(6)=40.0 * EXP(-12.077/T1)/SUMO
C
      RETURN
      END
      SUBROUTINE BUGPR (IDGSW)                                          BUGP  10
      COMMON /FRSTRM/ U INF, RINF, UINF2, R , RE, LXI, ITM, IEM, NES    BUGP  20
      COMMON /YL/ETA(60),  YD(60)                                       BUGP  30
      COMMON /TRN/       NUT(60), FMC(12,60), FPC(12,60),               BUGP  40
     1             FM(9,60),  FP(9,60), LINES                           BUGP  50
      COMMON /DBUG/ QLC(60), QCL(60), QLL(60), DQN(60), QCC(60),        BUGP  60
     1             BEEC(12,60),    FMUC(12,60),    EM(12,60),           BUGP  70
     2             EP(12,60),      TAUC(12,60),    BEEL(9,60),          BUGP  80
     3             QCCP(12),       WMM(9,60),      GMM(9,60),           BUGP  90
     4             EEM(9,60),      XLMM(9,60),     QLCP(9),             BUGP 100
     5             QCLP(9),        QLLP(9),        DELTA,    IY,  IYY,  BUGP 110
     6             WPP(9,60),      GPP(9,60),      EEP(9,60),           BUGP 120
     7             XLPP(9,60),     FG(9,4),        GP(9,4),             BUGP 130
     8             WN(9,4),        FMUL(9,60),     SSM(9,4,60),         BUGP 140
     9             GGM(9,4,60),    ETAM(9,4,60),   SBM(9,4,60),         BUGP 150
     A             TAUL(9,60)                                           BUGP 160
      GO TO (10,20,30,40,50,60,70), IDGSW                               BUGP 170
   10              WRITE (6,194)                                        BUGP 180
  194 FORMAT (1H1)                                                      BUGP 190
      RETURN                                                            BUGP 200
   20 WRITE (6,7182) DELTA                                              BUGP 210
 7182 FORMAT (7H0DELTA=1PE14.7,3H CM)                                   BUGP 220
      RETURN                                                            BUGP 230
   30 WRITE (6,190) IY,   YD(IY)                                        BUGP 240
  190 FORMAT (4H1IY=I3,2X,3HYD=1PE12.5//2X,1HK,2X,1HL,7X,3HETA,13X,2HYD,BUGP 250
     1 13X,2HMU,11X,3HTAU,14X,1HE,11X,3HBEE//)                          BUGP 260
      DO 22 K=1,12                                                      BUGP 270
      IF (IY.EQ.1) GO TO 23                                             BUGP 280
      WRITE(6,191) (K,   L,   ETA(L),   YD(L),   FMUC(K,L),   TAUC(K,L),BUGP 290
     1             EM(K,L),   BEEC(K,L),   L=1,IY)                      BUGP 300
  191 FORMAT (2I3,1P6E15.5)                                             BUGP 310
      WRITE (6,192)                                                     BUGP 320
  192 FORMAT (//)                                                       BUGP 330
   23 IF (IY.EQ.NES) GO TO 22                                           BUGP 340
      WRITE (6,191) (K,   L,   ETA(L),   YD(L),   FMUC(K,L),            BUGP 350
     1             TAUC(K,L),   EP(K,L),   BEEC(K,L),   L=IY,NES)       BUGP 360
 22 WRITE (6,193) FMC(K,IY),   FPC(K,IY),   QCCP(K)                   BUGP 370
193 FORMAT (5H0FIM=1PE12.5 ,2X,4HFIP=E12.5,2X,5HQCCP=E12.5)             BUGP 380
    RETURN                                                              BUGP 390
40                    WRITE (6,195) IY,   YD(IY),   ((J,   L,   YD(L),  BUGP 400
   1               WMM(J,L),   GMM(J,L),   XLMM(J,L),   EEM(J,L),       BUGP 410
   2               BEEL(J,L),   L=1,IY),   J=1,9)                       BUGP 420
195 FORMAT (4H0IY=I3,2X,3HYY=1PE12.5//2X,1HJ,2X,1HL,7X,2HYD,12X,3HWMM,BUGP 430
   1 12X,3HGMM,11X,4HXLMM,13X,3HEEM,13X,3HBEE//(2I3,6E16.5))            BUGP 440
    RETURN                                                              BUGP 450
50                    WRITE (6,196) IY,   YD(IY),   ((J,   L,   YD(L),  BUGP 460
   1          WPP(J,L),   GPP(J,L),   XLPP(J,L),   EEP(J,L),            BUGP 470
   2          BEEL(J,L),   L=IY,NES),   J=1,9)                          BUGP 480
196 FORMAT (4H0IY=I3,2X,3HYY=1PE12.5//2X,1HJ,2X,1HL,7X,2HYD,13X,3HWPP,BUGP 490
   1 2X,3HGPP,11X,4HXLPP,13X,3HEEP,13X,3HBEE//(2I3,6E16.5))             BUGP 500
    RETURN                                                              BUGP 510
60  WRITE (6,198) IY,   ETA(IY),   YD(IY)                               BUGP 520
198 FORMAT (4H0IY=I3,2X,4HETA=1PE12.5,2X,3HYY=E12.5//2X,1HJ,5X,3HQCC, BUGP 530
   1 11X,3HFMC,11X,3HFPC,11X,3HQCL,11X,3HQLC,11X,3HQLL,12X,2HFM,12X,  BUGP 540
   2 2HFP,11X,3HDQN//)                                                  BUGP 550
    WRITE (6,199) (J,   QCCP(J),   FMC(J,IY),   FPC(J,IY),              BUGP 560
   1               QCLP(J),   QLCP(J),   QLLP(J),   FM(J,IY),FP(J,IY),  BUGP 570
   2               J=1,9)                                               BUGP 580
199 FORMAT (I3,1P8E14.5)                                                BUGP 590
    WRITE (6,8069) (J,   QCCP(J),   FMC(J,IY),   FPC(J,IY),   J=10,12)BUGP 600
8069 FORMAT (I3,1P3E14.5)                                               BUGP 610
    WRITE (6,200) QCC(IYY),   QCL(IYY),   QLC(IYY),   QLL(IYY),         BUGP 620
   1               DQN(IYY)                                             BUGP 630
200 FORMAT (1H0,2X,1PE14.5,28X,3E14.5,28X,E14.5)                        BUGP 640
    RETURN                                                              BUGP 650
70  WRITE (6,197) L,   ETA(L),   YD(L),   ((J,   M,   WN(J,M),          BUGP 660
   1               FG(J,M),   GP(J,M),   FMUL(J,L),   TAUL(J,L),        BUGP 670
   2               SSM(J,M,L),   GGM(J,M,L),   ETAM(J,M,L),   SBM(J,M,L),BUGP 680
   3               M=1,4),J=1,9)                                        BUGP 690
197 FORMAT (3H0L=I3,2X,4HETA=1PE12.5,2X,3HYD=E12.5//2X,1HJ,2X,1HM,7X,  BUGP 700
   1 1HN,13X,1HF,13X,1HG,11X,3HFMU,11X,3HTAU,11X,3HSSM,11X,3HGGM,10X,  BUGP 710
   2 4HETAM,11X,3HSBM//(2I3,9E14.5))                                    BUGP 720
```

```
      RETURN                                                            BUGP 730
      END                                                               BUGP 740
      SUBROUTINE ZHV(HV.ZO.ZN.ZI.ZC)
C
C
C  **  THIS SUBROUTINE CALCULATES THE QUANTUM MECHANICAL CORRECTION
C            FACTORS GIVEN A FREQUENCY (HV) **
C
      X= HV
      X2 =X*X
      X3 =X2*X
      X4 =X3*X
      X5 =X4*X
      X6 =X5*X
      X7 =X6*X
      IF (X -9.82) 1.1.2
    1 ZO = .9999795              -.3155480*X             +2.824548 E-02*X2
     1     +6.677328 E-03*X3     -3.644585 E-03*X4       +8.058070 E-04*X5
     2     -7.708637 E-05*X6     +2.668133 E-06*X7
      GO TO 3
    2 ZO = (X/9.82)**3
    3 IF (X -8.35) 4.4.5
    4 ZN = 1.000148              - .4183535 *X           + .1680359 *X2
     1     -9.779458 E-02*X3     +3.354635 E-02*X4       -5.609353 E-03*X5
     2     +4.515535E-04*X6      -1.403585 E-05*X7
      GO TO 6
    5 ZN = (X/8.35)**3
    6 Y = X/4.0
      IF (Y-6.6) 9.9.10
    9 Y2 =Y*Y
      Y3 =Y2*Y
      Y4 =Y3*Y
      Y5 =Y4*Y
      Y6 =Y5*Y
      Y7 =Y6*Y
      ZI = 1.000379              - .2964767 *Y           +7.505242 E-02*Y2
     1     -1.702948E-02*Y3      +3.279554 E-03*Y4       -2.128469 E-04*Y5
      GO TO 11
```

```
10    ZI = (Y/6.6)**3                                                              ZHV( 370
11    IF (X-7.37) 12.12.13                                                         ZHV( 380
12    ZC =   .9974367              - .43418'2 *X        +8.531314 E-02*X2          ZHV( 390
   1     -1.393917 E-02*X3        +4.038545 E-03*X4    -5.426425 E-04*X5          ZHV( 400
   2      +2.812126 E-05*X6       -3.883530 E-07*X7                                ZHV( 410
      GO TO 14                                                                     ZHV( 420
13    ZC = (X/7.37)**3                                                             ZHV( 430
14    RETURN                                                                       ZHV( 440
      END                                                                          ZHV( 450
      SUBROUTINE FGH(N,F,G,H)                                           FGH(  10
      COMMON /VEL/ FZ(60),FC(60),Z(60),V(60)                            FGH(  20
C  **     **    FIRST DERIVATIVE    **     **     **                    FGH(  30
C------EVALUATES COEFFICIENTS FOR THREE POINT DIFFERENCE APPROXIMATION  FGH(  40
C       OF DAVIS (AIAA JR. VOL. 8, NO. 5, MAY 1970).                    FGH(  50
      COMMON /YL/ETA(60),YOND(60)                                       FGH(  60
      DN=ETA(N+1)-ETA(N)                                                FGH(  70
      DNM1=ETA(N)-ETA(N-1)                                              FGH(  80
      DEL=DN+DNM1                                                       FGH(  90
      D1=DN*DEL                                                         FGH( 100
      D2=DN*DNM1                                                        FGH( 110
      D3=DNM1*DEL                                                       FGH( 120
      F=DNM1/D1                                                         FGH( 130
      G=(DN-DNM1)/D2                                                    FGH( 140
      H=-DN/D3                                                          FGH( 150
      RETURN                                                            FGH( 160
      ENTRY       FGH2(N,F,G,H)                                         FGH( 170
C  **     **    SECOND DERIVATIVE   **     **     **                    FGH( 180
C------EVALUATES COEFFICIENTS FOR THREE POINT DIFFERENCE APPROXIMATION  FGH( 190
C       OF DAVIS (AIAA JR. VOL. 8, NO. 5, MAY 1970).                    FGH( 200
      DN=ETA(N+1)-ETA(N)                                                FGH( 210
      DNM1=ETA(N)-ETA(N-1)                                              FGH( 220
      F=2./(DN*(DN+DNM1))                                               FGH( 230
      G=-2./(DN*DNM1)                                                   FGH( 240
      H=2./(DNM1*(DN+DNM1))                                             FGH( 250
      RETURN                                                            FGH( 260
      END                                                               FGH( 270
      SUBROUTINE INTRPL(VAR.X.F.IMAX.SOM)                               INTR  10
C                                                                       INTR  20
C                                                                       INTR  30
C-----THIS PROGRAM PERFORMS LAGRANGIAN INTERPOLATION                    INTR  40
C     WITH NON-EQUAL STEP SIZE BETWEEN POINTS                           INTR  50
C     F=DEPENDANT VARIABLE                                              INTR  60
C     X=INDEPENDENT VARIABLE                                            INTR  70
C     VAR-VALUE OF X FOR WHICH CORRESPONDING VALUE OF                   INTR  80
C     F IS DESIRED BY INTERPOLATION                                     INTR  90
C     IMAX=NUMBER OF POINTS IN ARRAY X OR F                             INTR 100
C     SOM=VALUE OF INTERPOLATED DEPENDENT VARIABLE                      INTR 110
C     NPTS=NUMBER OF POINTS USED FOR INTERPOLATION                      INTR 120
C                                                                       INTR 130
      DIMENSION X(100).F(100).XN(300).FN(300)                           INTR 140
      NPTS=3                                                            INTR 150
  607 XUP=1.E30                                                         INTR 160
      DO611I=1.IMAX                                                     INTR 170
      T=VAR-X(I)                                                        INTR 180
      IF(T.GE.0.)GOTO609                                                INTR 190
  608 T=-T                                                              INTR 200
  609 IF(T.GE.XUP)GOTO611                                               INTR 210
  610 IP=I                                                              INTR 220
      XUP=T                                                             INTR 230
  611 CONTINUE                                                          INTR 240
      IN=1                                                              INTR 250
      NPP=NPTS+1                                                        INTR 260
      DO618I=1.NPP                                                      INTR 270
      FN(I)=F(IP)                                                       INTR 280
      XN(I)=X(IP)                                                       INTR 290
      IF(IN.GT.0)GOTO613                                                INTR 300
  612 IQ=IP-I                                                           INTR 310
      GOTO615                                                           INTR 320
  613 IQ=IP+I                                                           INTR 330
      IF(IMAX.GE.IQ)GOTO615                                             INTR 340
  614 IP=IP-1                                                           INTR 350
      GOTO618                                                           INTR 360
```

```
615  IF(IQ.GT.0)GOTO617                                     INTR 370
616  IP=IP+1                                                INTR 380
     GOTO618                                                INTR 390
617  IP=IQ                                                  INTR 400
     IN=-IN                                                 INTR 410
618  CONTINUE                                               INTR 420
     SOM=0.                                                 INTR 430
     FACT=1.                                                INTR 440
     DO620J=1.NPTS                                          INTR 450
     SOM=SOM+FACT*FN(1)                                     INTR 460
     DO619I=J.NPTS                                          INTR 470
     IQ=I-J+1                                               INTR 480
619  FN(IQ)=(FN(IQ+1)-FN(IQ))/(XN(I+1)-XN(IQ))              INTR 49C
620  FACT=FACT*(VAR-XN(J))                                  INTR 500
     RETURN                                                 INTR 510
     END                                                    INTR 520
```

```
      FUNCTION QUAD (X.FX.I)                                             QU   10
C                                                                        QU   20
C     **  TRAPEZOIDAL QUADRATURE FUNCTION  **                            QU   30
C                                                                        QU   40
      DIMENSION X(60).FX(60)                                             QU   50
      DX=X(I)-X(I-1)                                                     QU   60
      QUAD = (DX/2.0) * (FX(I) + FX(I-1) )                               QU   70
      RETURN                                                             QU   80
      END                                                                QU   90
      SUBROUTINE OUPPUT (N)
C
C
C     **  ROUTINE TO PRINT SHOCK LAYER SOLUTION  **
C
C
      COMMON/ID/SP(20),EL(5)
      COMMON /CONV/ FPRCT,TPRCT,DDAMP,TDAMP,PDTIL
      COMMON /DEL/ DELTA,DTIL,DTILS
      COMMON /FRSTRM/ U INF, RINF, UINF2, R , RE, LXI, ITM, IEM, NETA
      COMMON /MAIN/KEEP,MAXE,MAXM,MAXD,IDEBUG,MCONV,ECONV,DCONV,LT,IAB
      LOGICAL MCONV,ECONV,DCONV
      COMMON /NON/RDZ,MUDZ,RMDZ,AKNF,HNF,CPNF
      COMMON/NUMBER/NSP,NNS,NE,NC
      COMMON/PROP1/PI(60),RHO(60), T(60),AMW(60),C (20,60),EC(5,60)
      COMMON/PROP2/  MU(60),RM(60), AK(60)
      COMMON/PROP3/CPS(20,60),HS(20,60),CP (60),HM(60)
      COMMON /RFLUX/ E(60),IRAD,ITYPE
      COMMON /RH/ DUD,DPHI,TD,RZB,PD,HD,HTOTAL
      COMMON /SFLUX/QRI(3)
      COMMON/VECTOR/ CA(60),CB(60),CC(60),B(60)
      COMMON /VEL/ F(60),FC(60),Z(60),V(60)
      COMMON/WALL/RVW,PRW,TWOLD,FLUX(20),CWALL(20),ECWALL(5)
      COMMON /YL/ETA(60),YOND(60)
      COMMON /DD/ D(60)
      COMMON/SP1/SS,TOL,NDBUG
      COMMON/MIKE/ NETA1,NETA2,PNF,WNF,RHOD,DP,TS,UD,VD,RW,RWO,EPS,PHI
      COMMON/JOHN/ UO(60),U(60),DU(60),VO(60),RO(60),DNDX(60),DTLA,DTILO
      COMMON/BOB/ XI,DXI,YL,QLAST
      COMMON/TIT/TITLE(18)
      COMMON /BILL/ NODE(20),ISTART,IDGD,IDGF,IDGH,IDGT,IDGS,
     X   MI,NOE,NTIME,MIS
      DIMENSION BOUT(60),DQR(30)
      REAL  MU,MUDZ
      DATA HEAD1/'WALL'/ ,HEAD2/'    '/,HEAD3/'SHOC'/
      D(1) = 8.128E-8*(T(1)*TS)**1.659/PD/R/UINF
```

```
C
C     **  COMPUTE RADIATION FLUX IF UNCOUPLED PROBLEM  **
C
C
C     **  COMPUTE Y COORDINATE  **
C
      YOND(1) = 0.0
      SUM = 0.0
      DO 40 K=2.NETA
      IF(XI .GT. 0.0) Z(K-1) = U(K)/UD/DTIL
      DETA= ETA(K)-ETA(K-1)
      SUM= SUM +DETA*(1./RHO(K)+1./RHO(K-1))/2.
      YOND(K) = DTIL*SUM
   40 CONTINUE
      DELTA = YOND(NETA)
C     **  COMPUTE CONVECTIVE HEATING RATE  **
C
C WATTS/CM**2
      QC = -AK(1)*RINF*UINF*UINF2*   (T(2)-T(1))/
     1  (.88*778.28        *YOND(2)       *RZB)
C BTU/FT**2-SEC
      QCP=QC*.88
C
C     **  COMPUTE RADIATIVE FLUX TO SURFACE  **
C
      IF(ITYPE.NE.0)GOTO20
      IF (IRAC.NE.1) CALL TRANS2
   20 CONTINUE
      QR = 0.0
      IF(IRAD .EQ. 1) GO TO 445
      DO 1100 K=2.NETA
      QR = QR + QUAD(YOND.E.K)
 1100 CONTINUE
C WATTS/CM**2
      QR =-QR *RINF*UINF2*UINF *DELTA/(685.*RZB)
      IF(ITYPE.EQ.0)QR=-QRI(1)
 445  CONTINUE
C BTU/FT**2-SEC
      QRP=QR*0.88
C     **  COMPUTE DIFFUSIVE FLOW TO SURFACE  **
C WATTS/CM**2
      QD = 0.
      DO1768I=1.NSP
 1768 QD = QD + HS(I.1)*(C(I.2) - C(I.1))
      QD = - RHO(1)*D(1)*QD/(2.      *YOND(2))
      CD = RDZ *UINF*UINF2*QD/(.88*778.28)
C BTU/FT**2-SEC
      QDP = .88*QD
      QTOTAL=QC+QR+QD
      QTOTP=QTOTAL*.88
C
C        ***  CHECK FOR CONVERGENCE  ***
C
      N = 2
      ABD = ABS((QTOTAL-QLAST)/QTOTAL)
      QLAST = QTOTAL
      IF(XI .EQ. 0.0) GO TO 300
      IF(ABD .GT. 0.005) RETURN
      N = 1
  300 CONTINUE
      WRITE(6.203)
  203 FORMAT(1H1)
      DO 50 K=1.NETA
      YOND(K)= YOND(K)/DELTA
  50  CONTINUE
C
C
C     **  DIMENSIONALIZE RHO.MU.P.AND E  **
C
      DO 450 I = 1 . NETA
      RHO(I)=RHO(I)*RDZ
      MU (I)=MU(I)*MUDZ
      RM (I)=RM(I)*RMDZ                                                 OUPP1090
      AK(I) = AK(I)/AKNF                                                OUPP1100
      E(I) = E(I) * RDZ     * UINF2 * UINF / (20866.0 * R )             OUPP1110
      CP(I) = CP(I)/CPNF                                                OUPP1120
  450 CONTINUE                                                          OUPP1130
C                                                                       OUPP1140
      WRITE(6,200) TITLE                                                OUPP1150
  200 FORMAT( 10X,18A4,//)                                              OUPP1160
C                                                                       OUPP1170
C     **  PRINT SHOCK QUANTITIES AND HEATING RATE  **                   OUPP1180
C                                                                       OUPP1190
      WRITE(6,204) XI, DELTA,DTIL                                       OUPP1200
  204 FORMAT(1H0,' XI  =',F9.4 ,10X,9H DELTA = ,1PE14.6,10X,7HDTIL = ,  OUPP1210
     1    E15.6)                                                        OUPP1220
C                                                                       OUPP1230
      WRITE (6,210) EPS,  QC,QCP                                        OUPP1240
  210 FORMAT ( 1H0,' EPS =',F9.4,10X,5H QC = E15.6,2X,13H(WATTS/CM**2), OUPP1250
     1          2X,1H=,E15.6,2X,17H(BTU/FT**2 - SEC)       )            OUPP1260
      WRITE(6,212) RZB,QR,QRP                                           OUPP1270
  212 FORMAT ( 1H0,6H RB  =,F9.4,10X,5H QR = E15.6,2X,13H(WATTS/CM**2), OUPP1280
     1          2X,1H=,E15.6,2X,17H(BTU/FT**2 - SEC)       )            OUPP1290
      WRITE(6,213) RVW,QD,QDP                                           OUPP1300
  213 FORMAT ( 1H0,6H RVW =,F9.4,10X,5H QD = E15.6,2X,13H(WATTS/CM**2), OUPP1310
     1          2X,1H=,E15.6,2X,17H(BTU/FT**2 - SEC)       )            OUPP1320
C                                                                       OUPP1330
      WRITE(6,215) QTOTAL,QT,TP                                         OUPP1340
  215 FORMAT(1H0,16HTOTAL HEATING  = E15.6,2X,13H(WATTS/CM**2),         OUPP1350
     1        2X,1H=,E15.6,2X,17H(BTU/FT**2 - SEC)     )                OUPP1360
C                                                                       OUPP1370
C     **  PRINT Y/D , F AND T PROFILES  **                              OUPP1380
C                                                                       OUPP1390
      WRITE(6,205)                                                      OUPP1400
  205 FORMAT( 1H0,7X, 4H ETA, 5X, 4HY/DZ,  8X, 2HF', 8X, 3H RV, 8X ,    OUPP1410
     1        4HT/TD,  4X ,13H E(WATTS/CM3),4X,2H V, 7X,12H V (FT/SEC) , OUPP1420
     2  5X,2H G,6X,12H H (STATIC) , //)                                 OUPP1430
      FP = 0.0                                                          OUPP1440
      NS=NSP                                                            OUPP1450
C                                                                       OUPP1460
      DO 100 I=1,NETA                                                   OUPP1470
C COMPUTE ENTHALPIES                                                    OUPP1480
      HSTAT = 0.0                                                       OUPP1490
      DO 99 J=1,NS                                                      OUPP1500
 99   HSTAT = HSTAT + HS(J,I)*C(J,I)                                    OUPP1510
      G = HSTAT + V(I)**2                                               OUPP1520
C                                                                       OUPP1530
      HEAD=HEAD2                                                        OUPP1540
      IF(I .EQ. 1) HEAD=HEAD1                                           OUPP1550
      IF (I .EQ. NETA) HEAD=HEAD3                                       OUPP1560
      YDZ = YOND(I)                                                     OUPP1570
      IF(I.EQ.NETA) FP =1.0                                             OUPP1580
      RV = -FC(I)*DTIL*2.                                               OUPP1590
      RV = RHO(I)*V(I)/RDZ                                              OUPP1600
      VS = V(I) *UINF                                                   OUPP1610
      TP = T(I)/T(NETA)                                                 OUPP1620
      WRITE(6,208) HEAD,ETA(I),YDZ,FP,RV,TP  ,E(I),V(I),VS,G,HSTAT      OUPP1630
 208  FORMAT(1H ,A4,  F6.3,1P10E12.3)                                   OUPP1640
      IF(I.LT.NETA-1) FP = Z(I)*DTIL                                    OUPP1650
  100 CONTINUE                                                          OUPP1660
C                                                                       OUPP1670
C     **  WRITE OUT SHOCK LAYER GAS PROPERTIES  **                      OUPP1680
C                                                                       OUPP1690
      WRITE(6,44)                                                       OUPP1700
 44   FORMAT(1H1,48X,28H-SHOCK LAYER GAS PROPERTIES-    )               OUPP1710
C                                                                       OUPP1720
      WRITE(6,206)                                                      OUPP1730
 206  FORMAT( 1H0,3X,3HETA,8X,4H Y/D,12X,2HP ,12X,2H T,11X,3HRHO,11X,2HMUOUPP1740
     1       , 12X, 3HRMU,11X,2H K)                                     OUPP1750
C                                                                       OUPP1760
      WRITE(6,207)                                                      OUPP1770
 207  FORMAT (1H ,27X,6H(ATM.),6X,13H (DEG.KEL.)  ,12H(SLUGS/FT3) ,2X,  OUPP1780
     1       28H(LBM/FT-SEC) (LBF2-SEC3/FT6) ,16H (BTU/FT-SEC-R) ,//)   OUPP1790
C                                                                       OUPP1800
```

```
      DO 101 I=1.NETA                                                   OUPP1810
C                                                                       OUPP1820
      TP = T(I)*TS                                                      OUPP1830
      WRITE(6.8)ETA( I).YOND(I).PI(I).TP  .RHO(I).MU(I).RN (I).AK(I)    OUPP1840
C                                                                       OUPP1850
    8 FORMAT(1H 0PF7.4.1P8E14.4)                                        OUPP1860
    9 FORMAT(1H 0PF7.4.1P7E14.4)                                        OUPP1870
C                                                                       OUPP1880
  101 CONTINUE                                                          OUPP1890
C                                                                       OUPP1900
C     **  WRITE SPECIES MASS FRACTIONS  **                              OUPP1910
C                                                                       OUPP1920
      WRITE(6.230)                                                      OUPP1930
 230  FORMAT (1H1.48X.26H-SPECIES MASS FRACTIONS-   )                   OUPP1940
      WRITE(6.231)                                                      OUPP1950
 231  FORMAT (3X.•ETA•.8X.3H O2.11X.2HN2.11X.3H O .11X.3H N .11X.3H O+. OUPP1960
     1      11X.3H N+.11X.3H E-.//)                                     OUPP1970
      DO 102 I=1.NETA                                                   OUPP1980
      WRITE(6.8) ETA(I).C( 1.I).C(2.I).C(3.I).C(4.I).C(5.I).            OUPP1990
     1      C(6. I).C(7.I)                                              OUPP2000
 102  CONTINUE                                                          OUPP2010
      WRITE(6.230)                                                      OUPP2020
      WRITE(6.233) (SP(I).I=8.15)                                       OUPP2030
 233  FORMAT(2X.4H ETA.1X.8(10X.A4)//)                                  OUPP2040
      WRITE(6.8) (ETA(I).      (C(J.I).J= 8.15).I=1.NETA)               OUPP2050
      WRITE(6.230)                                                      OUPP2060
      WRITE(6.234) (SP(I).I=16.20)                                      OUPP2070
 234  FORMAT(2X.4H ETA.7X.3H CP.5(11X.A4).8X.4H AMW.//)                 OUPP2080
      WRITE(6.9) (ETA(I).CP(I).(C(J.I).J=16.20).AMW(I).I=1.NETA)        OUPP2090
C NONDIMENSIONALIZE                                                     OUPP2100
      DO1001I=1.NETA                                                    OUPP2110
      YOND(I) = YOND(I)*DELTA                                           OUPP2120
      RHO(I) = RHO(I)/RDZ                                               OUPP2130
      MU(I) = MU(I)/MUDZ                                                OUPP2140
      RM(I) = RM(I)/RMDZ                                                OUPP2150
      E(I)=((E(I)*R)/(RDZ *UINF**3))*20866.0                            OUPP2160
      CP(I)=CP(I)*CPNF                                                  OUPP2170
 1001 AK(I)=AK(I)*AKNF                                                  OUPP2180
 217  FORMAT(6E12.5)                                                    OUPP2190
 1000 CONTINUE                                                          OUPP2200
      CALL CPUTME(ITIME)                                                OUPP2210
      WRITE(6,110) ITIME                                                OUPP2220
  110 FORMAT('0',40X,'TIME LEFT =',I12,' MSEC',///)                     OUPP2230
      IF(ITIME/60000 .LT. NTIME) GO TO 301                              OUPP2240
      IF(XI .GT. 0.0) RETURN                                            OUPP2250
      IF(ABD .LT. 0.005) GO TO 301                                      OUPP2260
      RETURN                                                            OUPP2270
  301 CALL PONCH                                                        OUPP2280
      CALL EXIT                                                         OUPP2290
C                                                                       OUPP2300
      RETURN                                                            OUPP2310
      END                                                               OUPP2320
      SUBROUTINE PONCH
C
      COMMON /CONV/ FPRCT.TPRCT.DDAMP.TDAMP.PDTIL
      COMMON/CONV1/HDAMP
      COMMON /DEL/ DELTA.DTIL.DTILS
      COMMON /FRSTRM/ U INF, RINF, UINF2, R , RE, LXI, ITM, IEM, NETA
      COMMON /MAIM/KEEP.MAXE.MAXM.MAXD.IDEBUG.MCONV.ECONV.DCONV.LT.IAB
      COMMON /NON/RDZ.MUDZ.RMDZ.AKNF.HNF.CPNF
      COMMON/NUMBER/NSP.NNS.NE.NC
      COMMON/PROP1/PI(60).RHO(60). T(60).AMW(60).C (20.60).EC(5.60)
      COMMON/PROP2/  MU(60).RM(60). AK(60)
      COMMON/PROP3/CPS(20.60).HS(20.60).CP (60).HM(60)
      COMMON /RFLUX/ E(60).IRAD.ITYPE
      COMMON /RH/ DUD.DPHI.TD.RZB.PD.HD.HTOTAL
      COMMON /VEL/ F(60).FC(60).Z(60).V(60)
      COMMON/WALL/RVW.PRW.TWOLD.FLUX(20).CWALL(20).ECWALL(5)
      COMMON /YL/ETA(60).YOND(60)
      COMMON/TIT/TITLE(18)
      COMMON/SP1/SS.TOL.NDBUG
      COMMON/BOB/ XI.DXI.YL
      COMMON/MIKE/ NETA1.NETA2.PNF.WNF.RHOD.DP.TS.UD.VD.RW.RWD.EPS.PHI
      COMMON/JFB/ IPN
      REAL  MU.MUDZ
C
C        ****    PUNCH-OUT CARDS FOR RESTART    ****
C
      WRITE(7.566)TITLE.IEM
  566 FORMAT(18A4.I8)
      WRITE(7.1801) FPRCT.TPRCT.DDAMP.TDAMP.PDTIL.HDAMP
      WRITE(7.1801)DELTA.DTIL.DTILS
      WRITE(7.1802)   U INF, RINF, UINF2, R , RE, ITM, IEM, NETA
      WRITE(7.1803)KEEP.MAXE.MAXM.MAXD.IDEBUG.MCONV.ECONV.DCONV.LT.IAB
      PUNCH 1801, RDZ.MUDZ.RMDZ.AKNF.HNF.CPNF
      WRITE(7.1804) NSP.NNS.NE.NC
      WRITE(7.1801)(PI(J).RHO(J).T(J).J=1.NETA)
      WRITE(7.1801)(AMW(J).J=1.NETA)
      WRITE(7,1801)((C(I,J),J=1,NETA),I=1,NSP)                          PONC 370
      WRITE(7,1801)( HN(J),J=1,NETA)                                    PONC 380
      WRITE(7,1801) (E(J),J=1,NETA)                                     PONC 390
      WRITE(7,1804)IRAD,ITYPE                                           PONC 400
      PUNCH 1801, DUD,DPHI,TD,RZB,PD,HD,HTOTAL                          PONC 410
      WRITE(7,1801)(F(J),FC(J),Z(J),V(J),J=1,NETA)                      PONC 420
      PUNCH 1801, RVW,PRW,TWOLD                                         PONC 430
      WRITE(7,1801)(CWALL(I),I=1,NSP)                                   PONC 440
      WRITE(7,1801)(ECWALL(K),K=1,NE)                                   PONC 450
      WRITE(7,1801)(ETA(J),YOND(J),J=1,NETA)                            PONC 460
      WRITE(7,715)NDBUG,IAB,TOL                                         PONC 470
      WRITE(7,1801)((EC(K,J),J=1,NETA),K=1,NE)                          PONC 480
      WRITE(7,1801) XI,RW,TS,UD                                         PONC 490
 1801 FORMAT(6E13.5)                                                    PONC 500
 1802 FORMAT(5E12.5,3I3)                                                PONC 510
 1803 FORMAT(5I5,3L3,2I5)                                               PONC 520
 1804 FORMAT(4I4)                                                       PONC 530
  715  FORMAT(2I5,E15.6)                                                PONC 540
      RETURN                                                            PONC 550
      END                                                               PONC 560
      BLOCK DATA                                                        DATA  10
C                                                                       DATA  20
C        DATA INITIALIZATION ROUTINE                                    DATA  30
C                                                                       DATA  40
      COMMON/FINV/ NHVL,NIHVC,FHVC(12),DJ(9),HVJ(9),ZKZ                 DATA  50
      COMMON /FRSTRM/ U INF, RINF, UINF2, R , RE, LXI, ITM, IEM, NETA   DATA  60
      COMMON/GUESS/TG1(60),TG2(60)                                      DATA  70
      COMMON/PROP1/PI(60),RHO(60), T(60),AMW(60),C (20,60),EC(5,60)     DATA  80
      COMMON/PROP2/  MU(60),RM(60), AK(60)                              DATA  90
      COMMON/PROP3/CPS(20,60),HS(20,60),CP (60),HM(60)                  DATA 100
      COMMON/NUMBER/NSP,NNS,NE,NC                                       DATA 110
      COMMON/ELSP/LSP(5)                                                DATA 120
      COMMON/ID/SP(20),EL(5)                                            DATA 130
      COMMON/WT/SMW(20),AWT(5)                                          DATA 140
      COMMON /BLOCK1/V1(20),V2(20),V3(20)                               DATA 150
      COMMON/BLOCK3/K1(20),K2(20)                                       DATA 160
      COMMON/EQ1/AI(20), BI(20), CI(20), DI(20), EI(20), FI(20), GI(20),DATA 170
     X          AII(20),BII(20),CII(20),DII(20),EII(20),FII(20),GII(20) DATA 180
      COMMON/EQ2/AA(20,5),ICODE(20)                                     DATA 190
      COMMON/EG3/IA(20,5)                                               DATA 200
      REAL K1,K2                                                        DATA 210
      COMMON/CK/ISN(20),MWT(19)                                         DATA 220
      REAL MWT                                                          DATA 230
C                                                                       DATA 240
      COMMON/JTB/ CO(60,20),RED,RED2                                    DATA 250
      COMMON /YL/ETA(60),YOND(60),YO(60)                                DATA 260
      COMMON /RH/ DUD,DPHI,TD,RZB,PD,HD,HTOTAL                          DATA 270
      COMMON/WALL/RVW,PRW,TWOLD,FLUX(20),CWALL(20),ECWALL(5)            DATA 280
      COMMON /MAIM/KEEP,MAXE,MAXM,MAXD,IDEBUG,MCONV,ECONV,DCONV,LT,IAB  DATA 290
      COMMON/CONV1/HDAMP,FDAMP,CDAMP                                    DATA 300
      COMMON /CONV/ FPRCT,TPRCT,DDAMP,TDAMP,PDTIL                       DATA 310
      COMMON /RFLUX/ E(60),IRAD,ITYPE                                   DATA 320
      COMMON /DEL/ DELTA,DTIL,DTILS                                     DATA 330
      COMMON /NON/RDZ,MUDZ,RMDZ,AKNF,HNF,CPNF                           DATA 340
      COMMON/JOHN/ UD(60),U(60),DU(60),VO(60),RO(60),DNDX(60),DTLA,DTILODATA 350
      COMMON/BOB/ XI,DXI,YL,QLAST                                       DATA 360
      COMMON/MIKE/ NETA1,NETA2,PNF,WNF,RHOD,DP,TS,UD,VD,RW,RWD,EPS,PHI  DATA 370
      COMMON /BILL/ KODE(20),ISTART,IDGD,IDGF,IDGH,IDGT,IDGS,           DATA 380
     X  MI,NOE,NTIME,MIS,CSHOCK(20)                                     DATA 390
      COMMON /GEORGE/ EPSN(30),XIN(30),QWN(30)                          DATA 400
      LOGICAL MCONV,ECONV,DCONV                                         DATA 410
      REAL  MU,MUDZ                                                     DATA 420
C                                                                       DATA 430
C         ORDER OF SPECIES USED IN CHEMICAL PRODUCTION ROUTINE (FG2)    DATA 440
C                                                                       DATA 450
      DATA ISN/                                                         DATA 460
     1 11.   8.  19.  12.  20.  14.  13.  18.  10.   9.   2.   4.   6.  DATA 470
     2  3.   5.   7.  15.  16.  17.   1/                                DATA 480
C                                                                       DATA 490
C         SPECIE MOLECULAR WEIGHTS (FG2 ORDER)                          DATA 500
C                                                                       DATA 510
      DATA MWT/                                                         DATA 520
     1 28.011, 12.011, 24.022, 36.033, 12.011, 25.030, 26.019, 27.027,  DATA 530
     2 02.016, 01.008, 28.016, 14.008, 14.008, 16.000, 16.000, .0005486,DATA 540
     3 26.038, 37.041, 49.052/                                          DATA 550
      DATA NETA/59/                                                     DATA 560
C                                                                       DATA 570
C         INITIAL GUESS FOR DENSITY PROFILE                             DATA 580
C                                                                       DATA 590
      DATA RHO /25.1,14.3,8.85,6.50,4.37,3.01,2.49,2.17,1.90,1.67,1.46, DATA 600
     1          1.29,1.16,1.08,1.03,1.00,44*1.0/                        DATA 610
C                                                                       DATA 620
C         INITIAL GUESS FOR RM PROFILE                                  DATA 630
C                                                                       DATA 640
      DATA RM /10.0,7.71,5.89,5.10,4.18,3.54,3.31,3.10,2.83,2.48,2.09,  DATA 650
     1         1.72,1.42,1.22,1.09,1.02,44*1.0/                         DATA 660
C                                                                       DATA 670
C         INITIAL GUESS FOR NO BLOWING TEMPERATURE PROFILE              DATA 680
C                                                                       DATA 690
      DATA TG1 / .1033,.2294,.3531,.4719,.5777,.6531,.6867,.7034,.7145, DATA 700
     1 .7236,.7321,.7401,.7479,.7554,.7628,.7699,.7769,.7836,.7902,     DATA 710
     2 .7967,.8030,.8092,.8153,.8213,.8272,.8331,.8389,.8447,.8504,     DATA 720
     3 .8562,.8619,.8676,.8734,.8791,.8850,.8908,.8968,.9028,.9089,      DATA 730
     4 .9151,.9215,.9280,.9347,.9417,.9488,.9563,.9641,.9723,.9809,      DATA 740
     5 .9901,10*1.0/                                                     DATA 750
C                                                                        DATA 760
C        INITIAL GUESS FOR BLOWING TEMPERATURE PROFILE                   DATA 770
C                                                                        DATA 780
      DATA TG2 / .3325,.3325,.3325,.3325,.3325,.3325,.3325,.3326,.3328, DATA 790
     1 .3331,.3336,.3344,.3357,.3378,.3408,.3452,.3515,.3601,.3718,      DATA 800
     2 .3873,.4076,.4335,.4665,.5075,.5560,.6054,.6487,.6857,.7161,      DATA 810
     3 .7404,.7595,.7749,.7878,.7993,.8100,.8203,.8302,.8399,.8496,      DATA 820
     4 .8594,.8693,.8797,.8904,.9019,.9142,.9278,.9476,.9609,.9757,      DATA 830
     5 .9877,10*1.0/                                                     DATA 840
C                                                                        DATA 850
      DATA NSP,NNS,NE,NC/20,0,5,20/                                      DATA 860
C                                                                        DATA 870
C        SPECIES PRESENT                                                 DATA 880
C                                                                        DATA 890
      DATA SP/ 'O2  ',   'N2  ',   'O   ',   'N   ',   'O+  ',           DATA 900
     1         'N+  ',   'E-  ',   'C   ',   'H   ',   'H2  ',           DATA 910
     2         'CO  ',   'C3-G',   'CN  ',   'C2H ',   'C2H2',           DATA 920
     3         'C3H ',   'C4H ',   'HCN ',   'C2  ',   'C+  '/           DATA 930
C                                                                        DATA 940
C        SPECIES MOLECULAR WEIGHTS (REGULAR ORDER)                       DATA 950
C                                                                        DATA 960
      DATA SMW/32.000,   28.016,   16.000,   14.008,   16.000,           DATA 970
     1         14.008, 5.486E-4,   12.011,    1.008,    2.016,           DATA 980
     2         28.011,   36.033,   26.019,   25.030,   26.038,           DATA 990
     3         37.041,   49.052,   27.027,   24.022,   12.011/           DATA1000
C                                                                        DATA1010
C        CONSTANTS FOR POLYNOMIAL FITS OF PURE COMPONENT VISCOSITY       DATA1020
C                                                                        DATA1030
      DATA V1/0.1693E 01,0.9704E 00,0.1519E 01,0.2534E 00,0.0       ,    DATA1040
     1        0.0       ,0.0       ,0.1997E 01,0.2941E 00,-.7944E-01,    DATA1050
     2        0.2404E 01,0.2019E 01,0.2404E 01,0.2404E 01,0.1396E 01,    DATA1060
     3        0.2019E 01,0.2019E 01,0.1378E 01,0.1931E 01,0.0       /    DATA1070
C                                                                        DATA1080
```

```
      DATA V2/0.1496E-02,0.1613E-02,0.1875E-02,0.2206E-02,0.5000E-03,   DATA1090
     1        0.5000E-03,0.5000E-03,0.1772E-02,0.8893E-03,0.7907E-03,   DATA1100
     2        0.1363E-02,0.1179E-02,0.1363E-02,0.1363E-02,0.8423E-03,   DATA1110
     3        0.1179E-02,0.1179E-02,0.9651E-03,0.1393E-02,0.5000E-03/   DATA1120
C                                                                       DATA1130
      DATA V3/-.2276E-07,-.1916E-07,-.2228E-07,-.3737E-07,-.1000E-07,   DATA1140
     1        -.1000E-07,-.1000E-07,-.3378E-07,-.8111E-08,-.8864E-08,   DATA1150
     2        -.2184E-07,-.1655E-07,-.2184E-07,-.2184E-07,-.6939E-08,   DATA1160
     3        -.1655E-07,-.1655E-07,-.9481E-08,-.2575E-07,-.1000E-07/   DATA1170
C                                                                       DATA1180
C        CONSTANTS FOR POLYNOMIAL FITS OF THERMODYNAMIC DATA            DATA1190
C                                                                       DATA1200
      DATA  AI/0.3316E 01,0.3221E 01,0.2670E 01,0.2474E 01,0.2491E 01,  DATA1210
     1         0.2727E 01,0.2500E 01,0.2612E 01,0.2500E 01,0.3358E 01,  DATA1220
     2         0.3254E 01,0.4002E 01,0.3411E 01,0.3485E 01,0.3891E 01,  DATA1230
     3         0.3965E 01,0.5874E 01,0.3654E 01,0.4443E 01,0.2609E 01/  DATA1240
C                                                                       DATA1250
      DATA  BI/0.1151E-02,0.9878E-03,-.1970E-03,0.9097E-04,0.2762E-04,  DATA1260
     1         -.2820E-03,0.3440E-06,-.2030E-03,-.8243E-06,0.2794E-03,  DATA1270
     2         0.9698E-03,0.3541E-02,0.4897E-03,0.3563E-02,0.5717E-02,  DATA1280
     3         0.6200E-02,0.7403E-02,0.3444E-02,-.2885E-03,-.1393E-03/  DATA1290
C                                                                       DATA1300
      DATA  CI/-.3726E-06,-.2907E-06,0.7193E-07,-.7814E-07,-.1881E-07,  DATA1310
     1         0.1105E-06,-.1954E-09,0.1095E-06,0.6421E-09,0.9372E-07,  DATA1320
     2         -.2647E-06,-.1318E-05,0.1005E-06,-.1237E-05,-.1957E-05,  DATA1330
     3         -.2265E-05,-.2729E-05,-.1258E-05,0.3036E-06,0.5959E-07/  DATA1340
C                                                                       DATA1350
      DATA  DI/0.6186E-10,0.3938E-10,-.8901E-11,0.2218E-10,0.3807E-11,  DATA1360
     1         -.1551E-10,0.3937E-13,-.1695E-10,-.1720E-12,-.2948E-10,  DATA1370
     2         0.3037E-10,0.2064E-09,-.3473E-10,0.1866E-09,0.2931E-09,  DATA1380
     3         0.3717E-09,0.4437E-09,0.2169E-09,-.6244E-10,-.1037E-10/  DATA1390
C                                                                       DATA1400
      DATA  EI/-.3666E-14,-.2000E-14,0.4002E-15,-.1489E-14,-.1028E-15,  DATA1410
     1         0.7847E-15,-.2573E-17,0.8590E-15,0.1457E-16,0.2141E-14,  DATA1420
     2         -.1177E-14,-.1144E-13,0.2361E-14,-.1013E-13,-.1585E-13,  DATA1430
     3         -.2262E-13,-.2637E-13,-.1430E-13,0.3915E-14,0.6345E-15/  DATA1440
```

```
C                                                                    DATA1450
      DATA  FI/-.1044E 04,-.1043E 04,0.2915E 05,0.5609E 05,0.1879E 06,  DATA1460
     1        0.2254E 06,-.7450E 03,0.8542E 05,0.2547E 05,-.1018E 04,   DATA1470
     2        -.1434E 05,0.9423E 05,0.4745E 05,0.5809E 05,0.2590E 05,   DATA1480
     3        0.6283E 05,0.7605E 05,0.1442E 05,0.9787E 05,0.2168E 06/   DATA1490
C                                                                    DATA1500
      DATA  GI/0.5393E 01,0.4326E 01,0.4504E 01,0.4300E 01,0.4424E 01,  DATA1510
     1        0.3645E 01,-.1173E 02,0.4144E 01,-.4612E 00,-.3548E 01,   DATA1520
     2        0.4875E 01,0.2020E 01,0.4746E 01,0.4784E 01,0.6520E 00,   DATA1530
     3        0.3467E 01,-.4010E 01,0.2373E 01,-.1090E 01,0.3709E 01/   DATA1540
C                                                                    DATA1550
      DATA AII/0.3721E 01,0.3727E 01,0.2548E 01,0.2746E 01,0.2944E 01,  DATA1560
     1        0.2499E 01,0.2508E 01,0.2141E 01,0.3934E 01,0.3363E 01,   DATA1570
     2        0.3366E 01,0.2213E 02,0.3473E 01,0.5307E 01,0.6789E 01,   DATA1580
     3        0.3965E 01,0.5874E 01,0.3654E 01,0.4026E 01,0.2528E 01/   DATA1590
C                                                                    DATA1600
      DATA BII/0.4254E-03,0.4684E-03,-.5952E-04,-.3909E-03,-.4108E-03,  DATA1610
     1        -.3725E-05,-.6332E-05,0.3219E-03,-.1776E-02,0.4656E-03,   DATA1620
     2        0.8027E-03,-.1759E-01,0.7337E-03,0.8966E-03,0.1503E-02,   DATA1630
     3        0.6200E-02,0.7403E-02,0.3444E-02,0.4857E-03,0.4869E-05/   DATA1640
C                                                                    DATA1650
      DATA CII/-.2835E-07,-.1140E-06,0.2701E-07,0.1338E-06,0.9156E-07,  DATA1660
     1        0.1147E-07,0.1364E-08,-.5498E-07,0.6013E-06,-.5127E-07,   DATA1670
     2        -.1968E-06,0.5565E-05,-.9088E-07,-.1378E-06,-.2295E-06,   DATA1680
     3        -.2265E-05,-.2729E-05,-.1258E-05,-.7026E-07,-.7026E-08/   DATA1690
C                                                                    DATA1700
      DATA DII/0.6050E-12,0.1154E-10,-.2798E-11,-.1191E-10,-.5848E-11,  DATA1710
     1        -.1102E-11,-.1094E-12,0.3604E-11,-.7819E-10,0.2802E-11,   DATA1720
     2        0.1940E-10,-.6758E-09,0.4847E-11,0.9251E-11,0.1534E-10,   DATA1730
     3        0.3717E-09,0.4437E-09,0.2169E-09,0.4666E-11,0.1134E-11/   DATA1740
C                                                                    DATA1750
      DATA EII/-.5186E-17,-.3293E-15,0.9380E-16,0.3369E-15,0.1190E-15,  DATA1760
     1        0.3078E-16,0.2934E-17,-.5564E-16,0.3482E-14,-.4905E-16,   DATA1770
     2        -.5549E-15,0.2825E-13,-.1018E-15,-.2278E-15,-.3763E-15,   DATA1780
     3        -.2262E-13,-.2637E-13,-.1430E-13,-.1142E-15,-.3476E-16/   DATA1790
C                                                                    DATA1800
```

```
      DATA FII/-.1044E 04,-.1043E 04,0.2915E 05,0.5609E 05,0.1879E 06,  DATA1810
     1         0.2254E 06,-.7450E 03,0.8542E 05,0.2547E 05,-.1018E 04,  DATA1820
     2         -.1434E 05,0.9423E 05,0.5420E 05,0.5809E 05,0.2590E 05,  DATA1830
     3         0.6283E 05,0.7605E 05,0.1442E 05,0.9787E 05,0.2168E 06/  DATA1840
C                                                                       DATA1850
      DATA GII/0.3254E 01,0.1294E 01,0.5049E 01,0.2872E 01,0.1750E 01,  DATA1860
     1         0.4950E 01,-.1208E 02,0.6874E 01,-.8598E 01,-.3716E 01,  DATA1870
     2         0.4263E 01,-.1021E 03,0.4152E 01,-.5288E 01,-.1539E 02,  DATA1880
     3         0.3467E 01,-.4010E 01,0.2373E 01,0.1090E 01,0.4139E 01/  DATA1890
C                                                                       DATA1900
C        CONSTANTS FOR LINEAR FITS OF PURE COMPONENT THERMOCONDUCTIVITY DATA1910
C                                                                       DATA1920
      DATA K1/0.1019E 01,0.6541E 00,0.1250E 01,0.1281E 01,2.6000E 01,   DATA1930
     1        2.6000E 01,2.6000E 01,0.2506E 01,0.2496E 01,0.3211E 01,   DATA1940
     2        0.8589E 00,0.6304E 00,0.8589E 00,0.1126E 01,0.1126E 01,   DATA1950
     3        0.6304E 00,0.6304E 00,0.4855E 00,0.8589E 00,0.1000E-04/   DATA1960
C                                                                       DATA1970
      DATA K2/0.4901E-03,0.5457E-03,0.7092E-03,0.8593E-03,0.0000E-03,   DATA1980
     1        0.0000E-03,0.0000E-03,0.7479E-03,0.5129E-02,0.5344E-02,   DATA1990
     2        0.6233E-03,0.5804E-03,0.6233E-03,0.7439E-03,0.7439E-03,   DATA2000
     3        0.5804E-03,0.5804E-03,0.8714E-03,0.6233E-03,0.7350E-03/   DATA2010
C                                                                       DATA2020
      DATA ICODE/20*0/                                                  DATA2030
C                                                                       DATA2040
C        ELEMENTS                                                       DATA2050
C                                                                       DATA2060
      DATA EL/   'C',     'H',     'N',     'O',     'E'   /            DATA2070
C                                                                       DATA2080
C        ATOMIC WEIGHTS                                                 DATA2090
C                                                                       DATA2100
      DATA AWT/ 12.011,  1.008,  14.008, 16.000, 5.486E-4  /            DATA2110
C                                                                       DATA2120
      DATA IA/ 0,0,0,0,0,0,0,1,0,0,1,3,1,2,2,3,4,1,2,1,                 DATA2130
     H         0,0,0,0,0,0,0,0,1,2,0,0,0,1,2,1,1,1,0,0,                 DATA2140
     N         0,2,0,1,0,1,0,0,0,0,0,0,1,0,0,0,0,1,0,0,                 DATA2150
     O         2,0,1,0,1,0,0,0,0,0,1,0,0,0,0,0,0,0,0,0,                 DATA2160
     E        2,2,1,1,0,0,1,1,0,0,2,3,2,2,2,3,4,2,2,0/                 DATA2170
C                                                                      DATA2180
      DATA LSP/20,9,6,5,7/                                             DATA2190
      DATA NHVL /9/, NIHVC /12/                                        DATA2200
      DATA FHVC /5.0, 6.0, 7.0, 8.0, 9.0, 10.0, 10.8, 11.1,            DATA2210
     1   12.0, 13.4, 14.3, 20.0/                                       DATA2220
      DATA CJ /0.6, 2.2, 1.5, 1.65, 1.4, 1.0, 1.2, 1.4, 1.0/           DATA2230
      DATA HVJ /1.3, 2.7, 5.75, 7.57, 9.1, 10.4, 11.4, 12.7, 13.9/     DATA2240
      DATA ZKZ /7.26E-16/                                              DATA2250
C * * * * * * * * * * * * * * * * * * * * * * * * * * * * * * * * * * * DATA2260
C                                                                      DATA2270
C        VALUES FOR COLD START OF STANDARD CASE                        DATA2280
C                                                                      DATA2290
      DATA TWOLD,TS,RVW,RZB /3450.,14000.,0.05,0.06/                   DATA2300
      DATA CELTA,DTIL,DPHI,XI,RW,PNF,PD,EPS,DXI /8*0.0,0.05/           DATA2310
      DATA FDAMP,DDAMP,HDAMP,TDAMP,CDAMP/3*0.5,0.25,1.0/               DATA2320
      DATA TPRCT,FPRCT,PDTIL/2*0.005,0.001/                            DATA2330
      DATA RDZ,MUDZ,RMDZ,AKNF,CPNF,HNF,YL /7*1.0/                      DATA2340
      DATA IRAD,ITYPE /3,0/                                            DATA2350
      DATA KEEP,MAXE,MAXM,MAXD,IDEBUG,LT/0,10,15,30,0,2/               DATA2360
      DATA MCONV,ECONV,DCONV /F,F,F/                                   DATA2370
      DATA ITM,LT,KODE,ISTART,IDGD,IDGF,IDGH,IDGT,IDGS,NTIME /29*0/    DATA2380
      DATA MI,MIS,NDE /2*5,50/                                         DATA2390
      DATA U,CNDX /120*0.0/                                            DATA2400
      DATA ETA/                                                        DATA2410
     X   0.000,.0050,.0111,.0150,.0200,.0231,.0263,.0294,.0325,.0356,  DATA2420
     X   .0388,.0450,.0538,.0625,.0713,.0800,.0850,.0925,.1000,.1100,  DATA2430
     X   .1200,.1300,.1400,.1500,.1600,.1700,.1800,.2000,.2100,.2200,  DATA2440
     X   .2300,.2400,.2500,.2600,.2800,.3100,.3400,.3700,.4000,.4300,  DATA2450
     X   .4600,.4900,.5200,.5500,.5800,.6100,.6400,.6700,.7000,.7300,  DATA2460
     X   .7600,.7900,.8200,.8500,.8800,.9100,.9400,.9700,1.0,1.0/      DATA2470
      DATA CSHOCK /                                                    DATA2480
     X   1.110E-05,2.735E-05,9.583E-02,3.355E-01,1.259E-01,4.407E-01,  DATA2490
     X   2.162E-05,1.295E-04,1.010E-03,3.957E-11,1.188E-09,1.329E-38,  DATA2500
     X   1.265E-09,8.679E-22,4.401E-43,2.569E-43,1.717E-50,3.672E-18,  DATA2510
     X   1.768E-13,8.811E-04/                                          DATA2520
```

```
      DATA CWALL/                                                       DATA2530
     X    .1000E-09,.2389E-01,.1000E-09,.2000E-04,.1000E-09,.1000E-09,  DATA2540
     X    .1000E-09,.1570E-02,.1708E-01,.3277E-01,.2578E+00,.1767E-01,  DATA2550
     X    .3100E-02,.1500E-00,.8216E-01,.2037E+00,.1589E+00,.4710E-01,  DATA2560
     X    .4130E-02,.1000E-09/                                          DATA2570
      DATA RHOD,T /61*1.0/                                              DATA2580
      DATA EC,CD /1500*0.0/                                             DATA2590
      DATA C /1200*1.E-20/                                              DATA2600
      DATA EPSN,XIN     /31*0.0,.05,.1,.15,.2,.25,.3,.35,.4,.45,.5,.55, DATA2610
     X    .6,.65,.7,.75,.8,.85,.9,.95,1.,1.05,1.1,1.15,1.2,1.25,1.3,    DATA2620
     X    1.35,1.4,1.45/                                                DATA2630
      DATA QWN /1.,.98,.95,.91,.85,.76,.68,.57,.5,.42,.35,.28,.22,      DATA2640
     X     .17,.15,.12,14*.1/                                           DATA2650
      DATA QLAST/0.0/                                                   DATA2660
      DATA IAB /30/                                                     DATA2670
      END                                                               DATA2680
```

```
ENTRY MAIN
OVERLAY ONE
INSERT TRID,SOLVE,CHECK,MOLMAS,SLINIT,OUTPUT,TEMPR
OVERLAY TWO
INSERT FG2
OVERLAY THREE
INSERT SPECIE,SLMTM
OVERLAY THREE
INSERT ENERGY,INTRPL
OVERLAY TWO
INSERT XMOMTM,GLOBAL,PROPRT,DEDX
OVERLAY ONE
INSERT INPUT,OUPPUT,TRANS2,PONCH,NEXT
OVERLAY ONE
INSERT SHOCK
OVERLAY FIVE
INSERT GAS
OVERLAY ONE
INSERT LRAD,ZP,SND,BUGPR,ZHV
INSERT DBUG
OVERLAY FOUR
INSERT TRANS
OVERLAY FOUR
INSERT TRANS1
```

```
                C A S E  2     53.000 FT/SEC       2.5E-7 SLUGS/CU FT
53000.          2.5E-7        9.     0
 &ENTRY
 RVW = 0.0605
 &END
```

```
C A S E  2     53,000 FT/SEC      2.5E-7 SLUGS/CU FT


     BOUNDARY CONDITIONS AT     XI  =  0.0


                              BOW SHOCK CONDITIONS

     SHOCK TEMPERATURE (OK)    =    14541.         NORMAL VELOCITY         =   -0.0563
     SHOCK PRESSURE (ATM)      =    0.3132         TANGENTIAL VELOCITY     =    0.0
     SHOCK ANGLE, PHI (RAD)    =    0.0            ANGLE EPS (RAD)         =    0.0


                                ABLATOR SURFACE

     SURFACE TEMPERATURE (OK) =     3577.         QCOND (BTU/FT2-SEC)     =       216.
     SURFACE PRESSURE (ATM)    =    0.3132         QSUBL (BTU/FT2-SEC)     =       116.
     BLOWING RATE              =    0.0612         QRR (BTU/FT2-SEC)       =       541.
     MASS LOSS (LB/FT2-SEC)    =    0.0261         QTOTAL (BTU/FT2-SEC)    =       873.
```

ORIGINAL PAGE IS
OF POOR QUALITY

```
                    C A S E  2     53.000 FT/SEC      2.5E-7 SLUGS/CU FT


XI  =   0.0             DELTA =   3.967547E-02            DTIL =    5.820692E-02

EPS =   0.0             QC =  -0.174508E+03  (WATTS/CM**2)  =  -0.153567E+03  (BTU/FT**2 - SEC)

RN  =   0.0563          QR =  -0.763413E+03  (WATTS/CM**2)  =  -0.671803E+03  (BTU/FT**2 - SEC)

RVW =   0.0612          QD =  -0.544773E+02  (WATTS/CM**2)  =  -0.479400E+02  (BTU/FT**2 - SEC)

TOTAL HEATING  =  -0.992397E+03  (WATTS/CM**2)  =  -0.873310E+03  (BTU/FT**2 - SEC)

        ETA      Y/D2         F*           RV         T/TD     E(WATTS/CM3)     V        V (FT/SEC)       G         H (STATIC)


WALL 0.0       0.0         0.0         3.402E-03   2.460E-01  -1.681E+02   5.468E-04   2.898E+01   2.048E-01   2.048E-01
     0.005     1.191E-03   2.127E-03   3.402E-03   2.486E-01  -1.684E+02   5.581E-04   2.958E+01   2.076E-01   2.076E-01
     0.011     2.677E-03   4.774E-03   3.400E-03   2.514E-01  -1.686E+02   5.714E-04   3.029E+01   2.119E-01   2.119E-01
     0.015     3.667E-03   6.501E-03   3.397E-03   2.533E-01  -1.691E+02   5.801E-04   3.074E+01   2.148E-01   2.148E-01
     0.020     4.912E-03   8.756E-03   3.393E-03   2.557E-01  -1.695E+02   5.914E-04   3.134E+01   2.188E-01   2.188E-01
     0.023     5.710E-03   1.014E-02   3.389E-03   2.572E-01  -1.701E+02   5.985E-04   3.172E+01   2.213E-01   2.213E-01
     0.026     6.545E-03   1.167E-02   3.385E-03   2.588E-01  -1.704E+02   6.060E-04   3.212E+01   2.240E-01   2.240E-01
     0.029     7.366E-03   1.313E-02   3.381E-03   2.604E-01  -1.706E+02   6.134E-04   3.251E+01   2.267E-01   2.267E-01
     0.032     8.196E-03   1.462E-02   3.376E-03   2.620E-01  -1.708E+02   6.209E-04   3.290E+01   2.295E-01   2.295E-01
     0.036     9.034E-03   1.613E-02   3.370E-03   2.636E-01  -1.709E+02   6.285E-04   3.331E+01   2.323E-01   2.323E-01
     0.039     9.927E-03   1.771E-02   3.364E-03   2.654E-01  -1.708E+02   6.364E-04   3.373E+01   2.353E-01   2.353E-01
     0.045     1.167E-02   2.093E-02   3.350E-03   2.688E-01  -1.701E+02   6.527E-04   3.457E+01   2.413E-01   2.413E-01
     0.054     1.427E-02   2.545E-02   3.326E-03   2.740E-01  -1.693E+02   6.755E-04   3.580E+01   2.504E-01   2.504E-01
     0.063     1.688E-02   3.022E-02   3.298E-03   2.795E-01  -1.672E+02   6.996E-04   3.708E+01   2.599E-01   2.599E-01
     0.071     1.963E-02   3.529E-02   3.264E-03   2.855E-01  -1.651E+02   7.248E-04   3.842E+01   2.703E-01   2.703E-01
     0.080     2.257E-02   4.057E-02   3.226E-03   2.919E-01  -1.623E+02   7.506E-04   3.978E+01   2.812E-01   2.812E-01
     0.085     2.412E-02   4.373E-02   3.202E-03   2.958E-01  -1.607E+02   7.658E-04   4.059E+01   2.877E-01   2.877E-01
     0.092     2.701E-02   4.867E-02   3.161E-03   3.020E-01  -1.583E+02   7.888E-04   4.181E+01   2.980E-01   2.980E-01
     0.100     2.981E-02   5.386E-02   3.117E-03   3.087E-01  -1.560E+02   8.121E-04   4.304E+01   3.087E-01   3.087E-01
     0.113     3.375E-02   6.119E-02   3.050E-03   3.183E-01  -1.535E+02   8.429E-04   4.468E+01   3.235E-01   3.235E-01
     0.120     3.729E-02   6.937E-02   2.974E-03   3.290E-01  -1.510E+02   8.732E-04   4.628E+01   3.390E-01   3.390E-01
     0.133     4.224E-02   7.755E-02   2.894E-03   3.406E-01  -1.494E+02   9.011E-04   4.776E+01   3.550E-01   3.550E-01
     0.140     4.710E-02   8.664E-02   2.793E-03   3.532E-01  -1.478E+02   9.258E-04   4.907E+01   3.714E-01   3.714E-01
     0.150     5.211E-02   9.653E-02   2.686E-03   3.671E-01  -1.465E+02   9.463E-04   5.015E+01   3.894E-01   3.884E-01
     0.160     5.744E-02   1.072E-01   2.568E-03   3.818E-01  -1.451E+02   9.605E-04   5.091E+01   4.052E-01   4.062E-01
     0.170     6.310E-02   1.186E-01   2.436E-03   3.976E-01  -1.442E+02   9.680E-04   5.130E+01   4.258E-01   4.258E-01
     0.180     6.911E-02   1.319E-01   2.290E-03   4.142E-01  -1.433E+02   9.670E-04   5.125E+01   4.475E-01   4.475E-01
     0.200     8.231E-02   1.534E-01   1.953E-03   4.503E-01  -1.502E+02   9.320E-04   4.940E+01   4.986E-01   4.986E-01
     0.210     9.058E-02   1.743E-01   1.759E-03   4.704E-01  -1.567E+02   8.921E-04   4.728E+01   5.276E-01   5.276E-01
     0.220     9.726E-02   1.927E-01   1.546E-03   4.918E-01  -1.865E+02   8.318E-04   4.409E+01   5.577E-01   5.577E-01
     0.230     1.067E-01   2.050E-01   1.314E-03   5.148E-01  -2.183E+02   7.463E-04   3.955E+01   5.864E-01   5.864E-01
     0.240     1.134E-01   2.254E-01   1.062E-03   5.397E-01  -2.891E+02   6.315E-04   3.348E+01   6.113E-01   6.113E-01
     0.250     1.227E-01   2.439E-01   7.883E-04   5.657E-01  -3.593E+02   4.868E-04   2.580E+01   6.310E-01   6.310E-01
     0.260     1.319E-01   2.616E-01   4.942E-04   5.923E-01  -3.930E+02   3.135E-04   1.661E+01   6.458E-01   6.458E-01
     0.280     1.409E-01   2.954E-01  -1.541E-04   6.426E-01  -4.593E+02  -1.004E-04  -5.319E+00   6.659E-01   6.658E-01
     0.310     1.724E-01   3.377E-01  -1.260E-03   6.983E-01  -2.240E+02  -8.203E-04  -4.347E+01   6.851E-01   6.851E-01
     0.340     2.082E-01   3.727E-01  -2.500E-03   7.364E-01   1.112E+01  -1.636E-03  -8.670E+01   7.058E-01   7.058E-01
     0.370     2.376E-01   4.054E-01  -3.859E-03   7.664E-01   6.135E+01  -2.599E-03  -1.377E+02   7.337E-01   7.337E-01
     0.400     2.674E-01   4.365E-01  -5.330E-03   7.881E-01   1.114E+02  -3.733E-03  -1.979E+02   7.642E-01   7.642E-01
     0.430     2.967E-01   4.663E-01  -6.906E-03   8.030E-01   1.470E+02  -5.014E-03  -2.657E+02   7.914E-01   7.914E-01
     0.460     3.310E-01   4.952E-01  -8.596E-03   8.131E-01   1.843E+02  -6.405E-03  -3.395E+02   8.131E-01   8.131E-01
     0.490     3.646E-01   5.231E-01  -1.030E-02   8.207E-01   1.976E+02  -7.899E-03  -4.187E+02   8.311E-01   8.310E-01
     0.520     3.996E-01   5.518E-01  -1.224E-02   8.267E-01   2.110E+02  -9.496E-03  -5.033E+02   8.464E-01   8.463E-01
```

ORIGINAL PAGE IS
OF POOR QUALITY

```
     0.550    4.328E-01   5.798E-01  -1.422E-02   8.318E-01   2.178E+02  -1.120E-02  -5.935E+02   8.599E-01   8.598E-01
     0.580    4.677E-01   6.077E-01  -1.629E-02   8.362E-01   2.245E+02  -1.309E-02  -6.892E+02   8.720E-01   8.718E-01
     0.610    5.031E-01   6.356E-01  -1.846E-02   8.403E-01   2.311E+02  -1.491E-02  -7.905E+02   8.830E-01   8.828E-01
     0.640    5.390E-01   6.634E-01  -2.073E-02   8.441E-01   2.377E+02  -1.693E-02  -8.974E+02   8.930E-01   8.927E-01
     0.670    5.749E-01   6.913E-01  -2.310E-02   8.477E-01   2.454E+02  -1.906E-02  -1.010E+03   9.023E-01   9.019E-01
     0.700    6.114E-01   7.192E-01  -2.556E-02   8.512E-01   2.531E+02  -2.129E-02  -1.128E+03   9.109E-01   9.104E-01
     0.730    6.482E-01   7.471E-01  -2.812E-02   8.546E-01   2.622E+02  -2.363E-02  -1.253E+03   9.189E-01   9.183E-01
     0.760    6.854E-01   7.750E-01  -3.078E-02   8.581E-01   2.712E+02  -2.609E-02  -1.383E+03   9.265E-01   9.258E-01
     0.790    7.229E-01   8.030E-01  -3.354E-02   8.618E-01   2.858E+02  -2.867E-02  -1.520E+03   9.337E-01   9.328E-01
     0.820    7.606E-01   8.310E-01  -3.639E-02   8.661E-01   3.004E+02  -3.139E-02  -1.664E+03   9.406E-01   9.396E-01
     0.850    7.994E-01   8.591E-01  -3.934E-02   8.711E-01   3.361E+02  -3.425E-02  -1.815E+03   9.475E-01   9.463E-01
     0.880    8.379E-01   8.872E-01  -4.239E-02   8.780E-01   3.718E+02  -3.732E-02  -1.978E+03   9.546E-01   9.532E-01
     0.910    8.769E-01   9.154E-01  -4.554E-02   8.870E-01   5.417E+02  -4.063E-02  -2.153E+03   9.620E-01   9.603E-01
     0.940    9.161E-01   9.436E-01  -4.879E-02   9.054E-01   7.117E+02  -4.455E-02  -2.361E+03   9.721E-01   9.701E-01
     0.970    9.569E-01   9.718E-01  -5.213E-02   9.342E-01   1.357E+03  -4.923E-02  -2.609E+03   9.850E-01   9.828E-01
SHOC 1.000    1.000E+00   1.000E+00  -5.557E-02   1.000E+00   2.003E+03  -5.627E-02  -2.982E+03   1.010E+00   1.007E+00
```

ORIGINAL PAGE IS
OF POOR QUALITY

-SHOCK LAYER GAS PROPERTIES-

ETA	Y/D	P (ATM.)	T (DEG.KEL.)	RHO (SLUGS/FT3)	NU (LBM/FT-SEC)	RMU (LBF2-SEC3/FT6)	K (BTU/FT-SEC-R)
0.0	0.0	3.1320E-01	3.5775E+03	2.7604E-05	6.0764E-05	1.6773E-09	1.0887E-04
0.0039	[illegible]	3.1318E-01	3.6144E+03	2.7044E-05	6.1562E-05	1.6649E-09	1.0969E-04
0.0111	2.6774E-03	3.1318E-01	3.6562E+03	2.6394E-05	6.2278E-05	1.6437E-09	1.1094E-04
0.0150	[illegible]	3.1318E-01	3.6830E+03	2.5981E-05	6.2706E-05	1.6291E-09	1.1180E-04
0.0200	[illegible]	3.1318E-01	3.7180E+03	2.5451E-05	6.3249E-05	1.6098E-09	1.1296E-04
0.0231	5.7160E-03	3.1318E-01	3.7401E+03	2.5122E-05	6.3590E-05	1.5976E-09	1.1371E-04
0.0263	[illegible]	3.1318E-01	3.7633E+03	2.4783E-05	6.3948E-05	1.5848E-09	1.1449E-04
0.0294	[illegible]	3.1318E-01	3.7862E+03	2.4453E-05	6.4300E-05	1.5723E-09	1.1527E-04
0.0325	[illegible]	3.1318E-01	3.8097E+03	2.4122E-05	6.4660E-05	1.5598E-09	1.1609E-04
0.0356	[illegible]	3.1318E-01	3.8337E+03	2.3791E-05	6.5027E-05	1.5471E-09	1.1690E-04
[illegible]	[illegible]	3.1318E-01	3.8588E+03	2.3450E-05	6.5411E-05	1.5339E-09	1.1777E-04
[illegible]	[illegible]	3.1318E-01	3.9092E+03	2.2786E-05	6.6183E-05	1.5081E-09	1.1952E-04
0.0538	[illegible]	3.1318E-01	3.9848E+03	2.1845E-05	6.7332E-05	1.4709E-09	1.2218E-04
0.0625	[illegible]	3.1318E-01	4.0649E+03	2.0916E-05	6.8539E-05	1.4335E-09	1.2501E-04
0.0713	[illegible]	3.1318E-01	4.1519E+03	1.9982E-05	6.9835E-05	1.3954E-09	1.2811E-04
[illegible]	2.2580E-02	3.1318E-01	4.2448E+03	1.9068E-05	7.1196E-05	1.3576E-09	1.3143E-04
0.0950	2.4319E-02	3.1318E-01	4.3017E+03	1.8548E-05	7.2019E-05	1.3359E-09	1.3345E-04
0.0975	2.7207E-02	3.1318E-01	4.3919E+03	1.7780E-05	7.3312E-05	1.3035E-09	1.3664E-04
0.1000	2.9913E-02	3.1318E-01	4.4985E+03	1.7027E-05	7.4682E-05	1.2716E-09	1.4003E-04
0.1100	3.3752E-02	3.1318E-01	4.6283E+03	1.6052E-05	7.6647E-05	1.2303E-09	1.4482E-04
0.1200	3.7033E-02	3.1318E-01	4.7838E+03	1.5110E-05	7.8826E-05	1.1911E-09	1.4995E-04
0.1300	4.2275E-02	3.1318E-01	4.9521E+03	1.4223E-05	8.1197E-05	1.1549E-09	1.5523E-04
0.1400	4.7095E-02	3.1318E-01	5.1366E+03	1.3385E-05	8.3819E-05	1.1219E-09	1.6064E-04
0.1500	5.2112E-02	3.1318E-01	5.3383E+03	1.2595E-05	8.6710E-05	1.0921E-09	1.6611E-04
0.1600	5.7438E-02	3.1318E-01	5.5524E+03	1.1861E-05	8.9805E-05	1.0652E-09	1.7141E-04
0.1700	6.3097E-02	3.1318E-01	5.7819E+03	1.1166E-05	9.3121E-05	1.0398E-09	1.7657E-04
0.1800	6.9108E-02	3.1318E-01	6.0227E+03	1.0508E-05	9.6579E-05	1.0148E-09	1.8150E-04
0.2000	[illegible]	3.1318E-01	6.5494E+03	9.2949E-06	1.0381E-04	9.6494E-10	[illegible]
0.2100	[illegible]	3.1318E-01	6.8397E+03	8.7452E-06	1.0742E-04	9.3940E-10	1.9421E-04
0.2200	9.7196E-02	3.1318E-01	7.1509E+03	8.2464E-06	1.1083E-04	9.1400E-10	1.9737E-04
0.2300	[illegible]	3.1318E-01	7.4860E+03	7.8118E-06	1.1384E-04	8.8930E-10	1.9989E-04
0.2400	1.1304E-01	3.1318E-01	7.8472E+03	7.4548E-06	1.1614E-04	8.6584E-10	2.0175E-04
0.2500	1.2270E-01	3.1318E-01	8.2265E+03	7.1844E-06	1.1746E-04	8.4387E-10	2.0283E-04
0.2600	1.3192E-01	3.1318E-01	8.6120E+03	6.9944E-06	1.1768E-04	8.2314E-10	2.0295E-04
0.2850	[illegible]	3.1318E-01	9.3447E+03	6.8121E-06	1.1524E-04	7.8500E-10	2.0005E-04
0.3130	1.7964E-01	3.1318E-01	1.0154E+04	6.8126E-06	1.0843E-04	7.3872E-10	1.9251E-04
[illegible]	2.0417E-01	3.1318E-01	1.0708E+04	6.7812E-06	1.0250E-04	6.9507E-10	1.8947E-04
[illegible]	[illegible]	3.1318E-01	1.1144E+04	6.5878E-06	9.8210E-05	6.4700E-10	1.9190E-04
[illegible]	2.6762E-01	3.1318E-01	1.1460E+04	6.3339E-06	9.4902E-05	6.0111E-10	1.9676E-04
[illegible]	[illegible]	3.1318E-01	1.1676E+04	6.1113E-06	9.2271E-05	5.6390E-10	2.0145E-04
[illegible]	3.3140E-01	3.1318E-01	1.1823E+04	5.9473E-06	9.0118E-05	5.3596E-10	2.0514E-04
[illegible]	[illegible]	3.1318E-01	1.1934E+04	5.8214E-06	8.8314E-05	5.1411E-10	2.0811E-04
[illegible]	[illegible]	3.1318E-01	1.2021E+04	5.7199E-06	8.6742E-05	4.9617E-10	2.1060E-04
[illegible]	[illegible]	3.1318E-01	1.2095E+04	5.6337E-06	8.5368E-05	4.8094E-10	2.1276E-04
[illegible]	[illegible]	3.1318E-01	1.2160E+04	5.5590E-06	8.4151E-05	4.6780E-10	2.1465E-04
[illegible]	[illegible]	3.1318E-01	1.2219E+04	5.4925E-06	8.3070E-05	4.5627E-10	2.1635E-04
[illegible]	[illegible]	3.1318E-01	1.2274E+04	5.4326E-06	8.2105E-05	4.4605E-10	2.1787E-04
[illegible]	[illegible]	3.1318E-01	1.2326E+04	5.3777E-06	8.1241E-05	4.3689E-10	[illegible]
[illegible]	[illegible]	3.1318E-01	1.2377E+04	5.3269E-06	8.0467E-05	4.2864E-10	2.2051E-04
[illegible]	[illegible]	3.1318E-01	1.2429E+04	5.2793E-06	7.9773E-05	4.2115E-10	2.2167E-04
0.7400	[illegible]	3.1318E-01	1.2478E+04	5.2338E-06	7.9158E-05	4.1430E-10	2.2274E-04
[illegible]	[illegible]	3.1318E-01	[illegible]	5.1894E-06	7.8619E-05	4.0799E-10	2.2374E-04
[illegible]	[illegible]	3.1318E-01	1.2593E+04	5.1438E-06	7.8174E-05	4.0211E-10	2.2468E-04
[illegible]	[illegible]	3.1318E-01	1.2686E+04	5.0959E-06	7.7826E-05	3.9660E-10	2.2558E-04
[illegible]	[illegible]	3.1318E-01	1.2766E+04	5.0391E-06	7.7641E-05	3.9125E-10	2.2642E-04

ORIGINAL PAGE IS
OF POOR QUALITY

```
0.9100    8.7633E-01    3.1318E-01    1.2898E+04    4.9727E-06    7.7631E-05    3.8604E-10    2.2727E-04
0.9400    9.1606E-01    3.1318E-01    1.3168E+04    4.8583E-06    7.8201E-05    3.7992E-10    2.2826E-04
0.9700    9.5694E-01    3.1318E-01    1.3585E+04    4.6981E-06    7.9405E-05    3.7305E-10    2.2938E-04
1.0000    1.0000E+00    3.1320E-01    1.4541E+04    4.3820E-06    8.2562E-05    3.6179E-10    2.3121E-04
```

ORIGINAL PAGE IS
OF POOR QUALITY

-SPECIES MASS FRACTIONS-

ETA	O2	N2	O	N	O+	N+	E-
0.0	9.9963E-11	4.9493E-02	2.9950E-09	9.9963E-11	9.9966E-11	9.9963E-11	9.9957E-16
0.0090	[illegible]	4.9485E-02	4.0066E-07	1.4919E-07	1.0834E-06	2.6779E-05	1.0900E-09
0.0111	2.3419E-09	4.9476E-02	9.3462E-07	3.9886E-07	2.5359E-06	6.2685E-05	2.5515E-09
0.0150	3.2411E-09	4.9469E-02	1.3126E-06	6.3465E-07	3.5506E-06	8.7769E-05	3.5725E-09
0.0200	4.4909E-09	4.9459E-02	1.8488E-06	1.0593E-06	4.9588E-06	1.2258E-04	4.9894E-09
0.0231	5.3772E-09	4.9453E-02	2.2209E-06	1.4247E-06	5.8999E-06	1.4585E-04	5.9364E-09
0.0263	6.2816E-09	4.9446E-02	2.6437E-06	1.9061E-06	6.9302E-06	1.7131E-04	6.9730E-09
0.0294	7.1872E-09	4.9439E-02	3.0995E-06	2.5009E-06	7.9898E-06	1.9751E-04	8.0391E-09
0.0325	8.1897E-09	4.9431E-02	3.6111E-06	3.2552E-06	9.1147E-06	2.2531E-04	9.1707E-09
0.0356	9.2912E-09	4.9424E-02	4.1910E-06	4.2102E-06	1.0310E-05	2.5485E-04	1.0373E-08
0.0388	1.0430E-08	4.9415E-02	4.8773E-06	5.4604E-06	1.1624E-05	2.8731E-04	1.1695E-08
0.0450	1.2940E-08	4.9397E-02	6.5198E-06	8.8504E-06	1.4419E-05	3.5638E-04	1.4506E-08
0.0538	1.7083E-08	4.9367E-02	9.9113E-06	1.7055E-05	1.9053E-05	4.7081E-04	1.9164E-08
0.0625	2.2071E-08	4.9331E-02	1.5432E-05	3.2275E-05	2.4603E-05	6.0777E-04	2.4741E-08
0.0713	2.9251E-08	4.9298E-02	2.4897E-05	6.0643E-05	3.1465E-05	7.7689E-04	3.1628E-08
0.0800	3.5803E-08	4.9236E-02	4.1173E-05	1.1163E-04	3.9830E-05	9.8277E-04	4.0017E-08
0.0850	4.3900E-08	4.9201E-02	5.6185E-05	1.5891E-04	4.5556E-05	1.1235E-03	4.5751E-08
0.0925	5.0077E-08	4.9140E-02	8.9745E-05	2.6384E-04	5.5602E-05	1.3700E-03	5.5802E-08
0.1000	6.1174E-08	4.9067E-02	1.4598E-04	4.3262E-04	6.7843E-05	1.6696E-03	6.6028E-08
0.1100	7.0920E-08	4.8948E-02	2.8211E-04	8.0955E-04	8.8461E-05	2.1729E-03	8.8587E-08
0.1200	1.0448E-07	4.8793E-02	5.6386E-04	1.4742E-03	1.1580E-04	2.8373E-03	1.1577E-07
0.1300	1.3425E-07	4.8593E-02	1.1498E-03	2.5799E-03	1.5235E-04	3.7207E-03	1.5201E-07
0.1400	1.8376E-07	4.8332E-02	2.3641E-03	4.3101E-03	2.0153E-04	4.9018E-03	2.0061E-07
0.1500	2.4472E-07	4.7988E-02	4.7576E-03	6.8426E-03	2.6806E-04	6.4861E-03	2.6603E-07
0.1600	3.2744E-07	4.7531E-02	9.3338E-03	1.0349E-02	3.5834E-04	8.6140E-03	3.5424E-07
0.1700	4.3954E-07	4.6915E-02	1.6582E-02	1.5145E-02	4.8119E-04	1.1472E-02	4.7316E-07
0.1900	5.9053E-07	4.6054E-02	2.7334E-02	2.3045E-02	6.4986E-04	1.5309E-02	6.3338E-07
0.2000	1.0425E-06	4.3474E-02	6.4302E-02	4.2169E-02	1.1711E-03	2.6891E-02	1.1198E-06
0.2100	1.3906E-06	4.1377E-02	8.8458E-02	5.7416E-02	1.6071E-03	3.6000E-02	1.5067E-06
0.2200	1.8757E-06	3.8849E-02	1.1410E-01	7.7331E-02	2.1982E-03	4.7849E-02	2.0147E-06
0.2300	2.3019E-06	3.5244E-02	1.3768E-01	1.0249E-01	2.9884E-03	6.2924E-02	2.6707E-06
0.2400	3.0681E-06	3.1219E-02	1.5577E-01	1.3283E-01	4.0211E-03	8.1501E-02	3.4959E-06
0.2500	3.8497E-06	2.6753E-02	1.6741E-01	1.6735E-01	5.3276E-03	1.0343E-01	4.4939E-06
0.2600	4.7132E-06	2.2123E-02	1.7448E-01	2.0422E-01	6.9187E-03	1.2806E-01	5.6385E-06
0.2800	6.5847E-06	1.3325E-02	1.8294E-01	2.7829E-01	1.0929E-02	1.8235E-01	8.1875E-06
0.3100	9.4027E-06	4.7290E-03	1.8938E-01	3.6188E-01	1.8696E-02	2.6097E-01	1.1621E-05
0.3400	1.0311E-05	1.2725E-03	1.8850E-01	3.9600E-01	2.8031E-02	3.2260E-01	1.4078E-05
0.3700	1.0922E-05	2.6174E-04	1.8198E-01	3.9530E-01	3.8397E-02	3.6635E-01	1.5858E-05
0.4000	1.1004E-05	6.2421E-05	1.7260E-01	3.7896E-01	4.8858E-02	3.9550E-01	1.7217E-05
0.4300	1.1104E-05	3.4744E-05	1.6321E-01	3.6135E-01	5.8506E-02	4.1486E-01	1.8280E-05
0.4600	1.1104E-05	2.7931E-05	1.5466E-01	3.4733E-01	6.7062E-02	4.2985E-01	1.9124E-05
0.4900	1.1104E-05	2.3174E-05	1.4659E-01	3.3619E-01	7.4746E-02	4.4000E-01	1.9825E-05
0.5200	1.1104E-05	2.0517E-05	1.3937E-01	3.2688E-01	8.1762E-02	4.4930E-01	2.0430E-05
0.5500	1.1104E-05	1.8276E-05	1.3350E-01	3.1891E-01	8.8237E-02	4.5728E-01	2.0965E-05
0.5800	1.1104E-05	1.6554E-05	1.2750E-01	3.1196E-01	9.4243E-02	4.6423E-01	2.1444E-05
0.6100	1.1104E-05	1.5237E-05	1.2190E-01	3.0582E-01	9.9840E-02	4.7036E-01	2.1877E-05
0.6400	1.1104E-05	1.4219E-05	1.1688E-01	3.0035E-01	1.0507E-01	4.7583E-01	2.2271E-05
0.6700	1.1104E-05	1.3513E-05	1.1178E-01	2.9544E-01	1.0996E-01	4.8074E-01	2.2631E-05
0.7000	1.1104E-05	1.3031E-05	1.0719E-01	2.9101E-01	1.1455E-01	4.8517E-01	2.2963E-05
0.7300	1.1104E-05	1.2735E-05	1.0288E-01	2.8698E-01	1.1887E-01	4.8920E-01	2.3269E-05
0.7600	1.1104E-05	1.2785E-05	9.8830E-02	2.8331E-01	1.2292E-01	4.9286E-01	2.3552E-05
0.7900	1.1104E-05	1.2929E-05	9.5021E-02	2.7996E-01	1.2673E-01	4.9622E-01	2.3814E-05
0.8200	1.1104E-05	1.3449E-05	9.1442E-02	2.7689E-01	1.3031E-01	4.9928E-01	2.4058E-05
0.8500	1.1104E-05	1.4126E-05	8.8091E-02	2.7409E-01	1.3366E-01	5.0209E-01	2.4283E-05
0.8800	1.1104E-05	1.5276E-05	8.4982E-02	2.7153E-01	1.3679E-01	5.0464E-01	2.4492E-05
0.9100	1.1104E-05	1.6812E-05	8.2084E-02	2.6923E-01	1.3967E-01	5.0693E-01	2.4682E-05
0.9400	1.1104E-05	1.8311E-05	7.9458E-02	2.6719E-01	1.4230E-01	5.0897E-01	2.4854E-05

```
0.9790     1.1104E-05     2.2144E-05     7.7273E-02     2.6558E-01     1.4448E-01     5.1058E-01     2.4996E-05
1.0000     1.1103E-05     2.7353E-05     7.5560E-02     2.6447E-01     1.4620E-01     5.1168E-01     2.5102E-05
```

ORIGINAL PAGE IS
OF POOR QUALITY

-SPECIES MASS FRACTIONS-

ETA	C	H	H2	CO	C3-G	CN	C2H	C2H2
0.0	2.1042E-02	2.2092E-02	4.1334E-02	2.5689E-01	3.6933E-01	9.9961E-11	1.3871E-01	5.8879E-02
0.0055	2.1719E-02	2.4521E-02	3.7957E-02	2.5690E-01	3.6916E-01	7.3843E-05	1.6368E-01	5.8051E-02
0.0111	2.2561E-02	2.6631E-02	3.5624E-02	2.5692E-01	3.6893E-01	1.7276E-04	1.7111E-01	5.6961E-02
0.0155	2.3149E-02	2.7849E-02	3.4382E-02	2.5694E-01	3.6877E-01	2.4176E-04	1.7226E-01	5.6212E-02
0.0200	2.3967E-02	2.9462E-02	3.2879E-02	2.5696E-01	3.6855E-01	3.3736E-04	1.7202E-01	5.5190E-02
0.0231	2.4514E-02	3.0457E-02	3.1952E-02	2.5697E-01	3.6840E-01	4.0111E-04	1.7149E-01	5.4519E-02
0.0253	2.5113E-02	3.1500E-02	3.0990E-02	2.5699E-01	3.6824E-01	4.7075E-04	1.7074E-01	5.3794E-02
0.0284	[illegible]	3.2528E-02	3.0048E-02	2.5700E-01	3.6807E-01	5.4220E-04	1.6930E-01	5.3061E-02
0.0315	2.6384E-02	3.3572E-02	2.9095E-02	2.5702E-01	3.6790E-01	6.1783E-04	1.6989E-01	5.2294E-02
0.0346	2.7062E-02	3.4635E-02	2.8133E-02	2.5704E-01	3.6771E-01	6.9792E-04	1.6778E-01	5.1493E-02
0.0389	2.7849E-02	3.5749E-02	2.7129E-02	2.5706E-01	3.6751E-01	7.8559E-04	1.6651E-01	5.0629E-02
0.0450	[illegible]	3.7958E-02	2.5159E-02	2.5710E-01	3.6708E-01	9.7082E-04	1.6364E-01	4.8844E-02
0.0514	3.2185E-02	4.1190E-02	2.2327E-02	2.5717E-01	3.6637E-01	1.2731E-03	1.5845E-01	4.6041E-02
0.0575	3.5825E-02	4.4467E-02	1.9530E-02	2.5725E-01	3.6553E-01	1.6252E-03	1.5173E-01	4.2933E-02
0.0711	3.9427E-02	4.7325E-02	1.6760E-02	2.5734E-01	3.6451E-01	2.0428E-03	1.4295E-01	3.9435E-02
0.0800	4.4292E-02	5.1135E-02	1.4142E-02	2.5745E-01	3.6327E-01	2.5213E-03	1.3199E-01	3.5626E-02
0.0850	4.7608E-02	5.3000E-02	1.2717E-02	2.5751E-01	3.6243E-01	2.8257E-03	1.2461E-01	3.3289E-02
0.0925	5.1394E-02	5.5758E-02	1.0706E-02	2.5761E-01	3.6098E-01	3.3186E-03	1.1207E-01	2.9602E-02
0.1000	[illegible]	5.8326E-02	8.8718E-03	2.5771E-01	3.5924E-01	3.8426E-03	9.8003E-02	2.5745E-02
0.1100	[illegible]	6.1679E-02	6.7153E-03	2.5779E-01	3.5636E-01	4.5520E-03	7.7627E-02	2.0463E-02
0.1200	[illegible]	6.4597E-02	4.8969E-03	2.5771E-01	3.5262E-01	5.1839E-03	5.6944E-02	1.5279E-02
0.1300	1.2579E-01	6.7044E-02	3.4032E-03	2.5722E-01	3.4774E-01	5.6228E-03	3.8003E-02	1.0533E-02
0.1400	1.2937E-01	6.8921E-02	2.2188E-03	2.5579E-01	3.4132E-01	5.7620E-03	2.2563E-02	6.5575E-03
0.1500	[illegible]	7.0159E-02	1.3314E-03	2.5243E-01	3.3282E-01	5.5951E-03	1.1634E-02	3.5886E-03
0.1600	[illegible]	7.0741E-02	7.2527E-04	2.4565E-01	3.2150E-01	5.2511E-03	5.1140E-03	1.6760E-03
0.1700	[illegible]	7.0729E-02	3.5904E-04	2.3378E-01	3.0648E-01	4.7614E-03	1.8984E-03	6.4226E-04
0.1900	2.8407E-01	7.0195E-02	1.6434E-04	2.1754E-01	2.6678E-01	1.5964E-03	5.8419E-04	1.8158E-04
0.2000	[illegible]	6.7671E-02	4.7540E-05	1.5923E-01	2.2997E-01	1.5403E-03	6.0508E-05	1.3099E-05
0.2100	3.9539E-01	6.5463E-02	2.7058E-05	1.2171E-01	1.9245E-01	1.5328E-03	1.5664E-05	1.7008E-06
0.2200	4.1709E-01	6.2904E-02	1.6299E-05	8.2547E-02	1.5055E-01	1.4200E-03	4.7218E-06	1.5793E-07
0.2300	4.3403E-01	5.8723E-02	9.8742E-06	4.7681E-02	1.0768E-01	1.1730E-03	1.7280E-06	1.0410E-08
0.2400	4.4301E-01	5.4133E-02	5.8940E-06	2.2703E-02	6.8634E-02	8.3098E-04	6.9150E-07	4.9858E-10
0.2500	4.2671E-01	4.8965E-02	3.4686E-06	9.0718E-03	3.7898E-02	5.0625E-04	2.6286E-07	2.0406E-11
0.2600	[illegible]	4.1141E-02	2.0195E-06	3.2910E-03	1.7380E-02	2.8250E-04	8.5293E-08	1.1527E-12
0.2800	[illegible]	3.1168E-02	6.6604E-07	6.3627E-04	2.7040E-03	1.1074E-04	6.2042E-09	3.0240E-14
0.3100	[illegible]	[illegible]	1.1649E-07	9.9388E-05	7.9729E-05	3.2176E-05	1.2019E-10	2.0445E-16
0.3400	[illegible]	6.6871E-03	1.6108E-08	1.8155E-05	1.6859E-06	8.1166E-06	1.7773E-12	9.6090E-19
0.3700	[illegible]	[illegible]	1.7957E-09	2.6165E-06	1.9519E-08	1.4174E-06	1.7563E-14	2.7913E-21
0.4000	[illegible]	[illegible]	3.5598E-10	2.8378E-07	9.3239E-11	1.7272E-07	1.2766E-16	7.8584E-24
0.4300	[illegible]	[illegible]	2.2940E-10	7.1339E-08	3.9139E-14	4.6979E-08	8.6557E-18	4.0535E-25
0.4600	[illegible]	[illegible]	2.1280E-10	5.6016E-08	1.8468E-16	3.9109E-08	6.9041E-18	3.0524E-25
0.4900	[illegible]	[illegible]	2.0013E-10	4.5219E-08	1.5401E-18	3.3219E-08	5.4677E-18	2.2789E-25
[illegible]	[illegible]	[illegible]	1.9072E-10	3.8021E-08	5.1196E-20	2.9242E-08	4.5861E-18	1.8262E-25
[illegible]	[illegible]	[illegible]	1.8299E-10	3.2568E-08	2.6302E-20	2.6167E-08	3.9301E-18	1.5041E-25
[illegible]	[illegible]	[illegible]	1.7651E-10	2.8329E-08	2.7705E-20	2.3739E-08	3.4361E-18	1.2686E-25
0.6100	[illegible]	[illegible]	1.7082E-10	2.4854E-08	1.9621E-20	2.1708E-08	3.0379E-18	1.0841E-25
[illegible]	[illegible]	[illegible]	1.6574E-10	2.1964E-08	1.7120E-20	1.9980E-08	2.7084E-18	9.3673E-26
0.6700	[illegible]	[illegible]	1.6109E-10	1.9500E-08	1.5008E-20	1.8471E-08	2.4254E-18	8.1485E-26
0.7000	[illegible]	[illegible]	1.5677E-10	1.7372E-08	1.3191E-20	1.7133E-08	2.1778E-18	7.1239E-26
[illegible]	[illegible]	[illegible]	1.5268E-10	1.5507E-08	1.1595E-20	1.5923E-08	1.9560E-18	6.2424E-26
0.7600	[illegible]	[illegible]	1.4888E-10	1.3826E-08	1.0139E-20	1.4787E-08	1.7497E-18	5.4518E-26
0.7910	[illegible]	[illegible]	1.4468E-10	1.2283E-08	8.7757E-21	1.3693E-08	1.5535E-18	4.7241E-26
0.8200	[illegible]	[illegible]	1.4030E-10	1.0777E-08	7.3974E-21	1.2550E-08	1.3512E-18	3.9971E-26
[illegible]	[illegible]	[illegible]	1.3548E-10	9.2088E-09	6.0032E-21	1.1339E-08	1.1425E-18	3.2735E-26
[illegible]	[illegible]	[illegible]	1.2928E-10	7.6878E-09	4.4630E-21	9.8822E-09	9.0209E-19	2.4773E-26
0.9100	[illegible]	[illegible]	1.2168E-10	6.0089E-09	2.9239E-21	8.2045E-09	6.4811E-19	1.6853E-26
0.9400	[illegible]	[illegible]	1.0786E-10	3.8429E-09	1.3010E-21	5.7474E-09	3.3855E-19	7.9204E-27

[illegible]	[illegible]	[illegible]	8.8883E-11	2.0036E-09	3.9472E-22	3.3552E-09	1.2442E-19	2.4760E-27
[illegible]	[illegible]	1.0120E-03	3.9672E-11	1.1911E-09	1.3325E-38	1.2683E-09	8.7016E-22	4.4125E-43

ORIGINAL PAGE IS
OF POOR QUALITY

-SPECIES MASS FRACTIONS-

ETA	CP	C3H	C4H	HCN	C2	C+	ANW
0.0	8.[illegible]E-01	9.9957E-11	9.9557E-11	9.9962E-11	4.2184E-02	9.9963E-11	1.3347E+01
0.0050	8.[illegible]E-01	1.2929E-06	2.1260E-09	1.1727E-06	1.8421E-02	2.8125E-08	1.3212E+01
0.0111	8.[illegible]E-01	2.8848E-06	4.7839E-09	2.7371E-06	1.1541E-02	6.5709E-08	1.3044E+01
0.0150	8.[illegible]E-01	3.8910E-06	6.6357E-09	3.8182E-06	1.0601E-02	9.2000E-08	1.2934E+01
[illegible]	8.[illegible]E-01	5.2098E-06	9.1749E-09	5.2993E-06	1.1035E-02	1.2856E-07	1.2790E+01
[illegible]	7.[illegible]E-01	6.0111E-06	1.0846E-08	6.2727E-06	1.1674E-02	1.5307E-07	1.2700E+01
[illegible]	7.[illegible]E-01	6.8418E-06	1.2652E-08	7.3225E-06	1.2521E-02	1.7999E-07	1.2606E+01
[illegible]	7.[illegible]E-01	7.7076E-06	1.4481E-08	8.3833E-06	1.3473E-02	2.0780E-07	1.2514E+01
[illegible]	7.[illegible]E-01	8.5[illegible]E-06	1.6390E-08	9.4875E-06	1.4537E-02	2.3747E-07	1.2422E+01
[illegible]	7.[illegible]E-01	9.7638E-06	1.8382E-08	1.0635E-05	1.5709E-02	2.6919E-07	1.2328E+01
[illegible]	7.[illegible]E-01	1.0220E-05	2.0520E-08	1.1864E-05	1.7035E-02	3.0432E-07	1.2231E+01
[illegible]	7.[illegible]E-01	1.1977E-05	2.4948E-08	1.4372E-05	1.9967E-02	3.8003E-07	1.2040E+01
[illegible]	7.[illegible]E-01	1.4215E-05	3.1844E-08	1.8198E-05	2.5078E-02	5.0891E-07	1.1766E+01
[illegible]	7.[illegible]E-01	1.6483E-05	3.9414E-08	2.2223E-05	3.1460E-02	6.7032E-07	1.1492E+01
[illegible]	7.[illegible]E-01	1.9700E-05	4.7849E-08	2.6421E-05	3.9489E-02	8.8156E-07	1.1214E+01
0.04[illegible]	7.[illegible]E-01	2.0768E-05	5.6540E-08	3.0516E-05	4.9113E-02	1.1581E-06	1.0940E+01
[illegible]	7.111[illegible]E-01	2.1875E-05	6.2470E-08	3.2728E-05	5.5361E-02	1.3612E-06	1.0785E+01
[illegible]	7.1[illegible]E-01	2.3408E-05	7.1144E-08	3.5736E-05	6.5575E-02	1.7411E-06	1.0555E+01
0.1000	7.1[illegible]E-01	2.4728E-05	8.0140E-09	3.8131E-05	7.6361E-02	2.2484E-06	1.0330E+01
0.1100	7.1[illegible]E-01	2.6104E-05	9.2322E-08	3.9941E-05	9.0479E-02	3.2076E-06	1.0042E+01
0.1200	7.17[illegible]E-01	2.6931E-05	1.0398E-07	3.9530E-05	1.0205E-01	4.6982E-06	9.7703E+00
0.1300	7.1[illegible]E-01	2.7132E-05	1.1399E-07	3.6505E-05	1.0837E-01	7.0830E-06	9.5200E+00
0.1400	7.20[illegible]E-01	2.6650E-05	1.2094E-07	3.0981E-05	1.0731E-01	1.1006E-05	9.2929E+00
0.1500	7.220[illegible]E-01	2.5476E-05	1.2278E-07	2.3805E-05	9.8061E-02	1.7625E-05	9.0880E+00
0.1600	7.[illegible]E-01	2.3621E-05	1.1918E-07	1.6409E-05	8.1887E-02	2.9029E-05	8.9015E+00
0.1700	7.[illegible]E-01	2.1123E-05	1.0619E-07	1.0138E-05	6.1979E-02	4.8959E-05	8.7261E+00
0.1800	7.[illegible]E-01	1.8095E-05	8.7652E-08	5.8393E-06	4.2367E-02	8.3911E-05	8.5540E+00
0.2000	7.[illegible]E-01	1.0587E-05	3.5516E-08	1.8108E-06	1.4648E-02	2.5797E-04	8.2270E+00
0.2100	7.2[illegible]E-01	7.0802E-06	2.1360E-08	9.9906E-07	8.0240E-03	5.0752E-04	8.0849E+00
[illegible]	7.[illegible]E-01	4.1355E-06	9.4345E-09	5.4094E-07	4.7762E-03	9.6059E-04	7.9706E+00
[illegible]	7.1[illegible]E-01	2.0358E-06	3.2965E-09	2.6624E-07	3.2029E-03	1.7675E-03	7.9045E+00
0.2400	8.[illegible]E-01	8.1382E-07	8.8646E-10	1.1253E-07	2.2045E-03	3.1259E-03	7.9071E+00
0.2500	8.[illegible]E-01	2.5470E-07	1.8032E-10	4.0834E-08	1.3906E-03	5.1976E-03	7.9887E+00
0.2600	8.[illegible]E-01	5.9128E-08	2.2744E-11	1.3452E-08	7.4490E-04	7.9466E-03	8.1419E+00
0.2800	8.[illegible]E-01	2.0067E-09	4.5514E-13	1.9186E-09	1.3106E-04	1.4156E-02	8.6042E+00
0.3100	8.[illegible]E-01	2.2659E-11	2.3225E-15	1.4136E-10	7.9600E-06	1.5908E-02	9.3505E+00
0.3400	8.[illegible]E-01	1.5048E-[illegible]	6.8325E-18	9.0745E-12	3.9850E-07	9.8191E-03	9.8144E+00
0.3700	8.[illegible]E-01	5.[illegible]E-16	1.0828E-20	3.7590E-13	1.4263E-08	3.7336E-03	9.9234E+00
0.4100	8.[illegible]E-01	8.2328E-19	6.8246E-24	1.5359E-14	2.8023E-10	8.4712E-04	9.8112E+00
[illegible]	8.[illegible]E-01	2.2968E-22	8.0056E-28	2.7089E-15	2.6906E-11	3.6270E-04	9.6452E+00
[illegible]	8.[illegible]E-01	4.2210E-25	6.2642E-31	1.8700E-15	2.3177E-11	4.0334E-04	9.5041E+00
0.4900	8.[illegible]E-01	6.9685E-27	6.4291E-34	1.3695E-15	1.9709E-11	4.2629E-04	9.3901E+00
[illegible]	8.[illegible]E-01	5.8627E-27	1.6329E-34	1.0701E-15	1.7472E-11	4.4560E-04	9.2937E+00
[illegible]	8.[illegible]E-01	4.3272E-27	1.1034E-34	8.6324E-16	1.5709E-11	4.6156E-04	9.2102E+00
[illegible]	8.[illegible]E-01	3.3102E-27	7.8830E-35	7.1442E-16	1.4319E-11	4.7557E-04	9.1369E+00
[illegible]	8.[illegible]E-01	2.5797E-27	5.7682E-35	6.0013E-16	1.3134E-11	4.8918E-04	9.0714E+00
[illegible]	8.[illegible]E-01	2.0416E-27	4.3000E-35	5.1012E-16	1.2104E-11	4.9989E-04	9.0127E+00
[illegible]	8.[illegible]E-01	1.6301E-27	3.2435E-35	4.3697E-16	1.1182E-11	5.1112E-04	8.9597E+00
[illegible]	8.[illegible]E-01	1.3048E-27	2.4657E-35	3.7627E-16	1.0345E-11	5.2219E-04	8.9114E+00
[illegible]	8.[illegible]E-01	1.0541E-27	1.8791E-35	3.2488E-16	9.5722E-12	5.3735E-04	8.8674E+00
[illegible]	8.[illegible]E-01	8.4188E-28	1.4181E-35	2.7963E-16	8.8288E-12	5.4513E-04	8.8270E+00
[illegible]	8.[illegible]E-01	6.6204E-28	1.0498E-35	2.3899E-16	8.0923E-12	5.5794E-04	8.7899E+00
[illegible]	8.[illegible]E-01	4.9682E-28	7.3[illegible]52E-36	1.9954E-16	7.2943E-12	5.7330E-04	8.7557E+00
[illegible]	8.[illegible]E-01	3.[illegible]E-28	4.7825E-36	1.6154E-16	6.4223E-12	5.9209E-04	8.7243E+00
[illegible]	8.[illegible]E-01	2.1729E-28	2.5[illegible]E-36	1.2073E-16	5.3508E-12	6.1848E-04	8.6955E+00
[illegible]	8.[illegible]E-01	1.0[illegible]E-28	1.1038E-36	8.1555E-17	4.1199E-12	6.5480E-04	8.6694E+00
[illegible]	8.[illegible]E-01	2.7360E-29	1.9180E-37	3.6859E-17	2.4637E-12	7.1729E-04	8.6458E+00

```
0.9700    6.4[illegible]E-01   2.2504E-30   1.0994E-38   1.0204E-17   1.1128E-12   7.9416E-04   8.6266E+00
1.0000    7.1127E-01   2.5757E-43   1.7215E-50   3.6816E-18   1.7726E-13   8.8339E-04   6.6122E+00
                              TIME LEFT =     2030446 MSEC
```

```
C A S E  2     53.000 FT/SEC      2.5E-7 SLUGS/CU FT



     BOUNDARY CONDITIONS AT     XI  =  0.10


                               BOW SHOCK CONDITIONS

     SHOCK TEMPERATURE (OK)   =    14473.        NORMAL VELOCITY        =   -0.0559
     SHOCK PRESSURE (ATM)     =    0.3101        TANGENTIAL VELOCITY    =    0.0996
     SHOCK ANGLE, PHI (RAD)   =    0.0998        ANGLE EPS (RAD)        =    0.0002


                                ABLATOR SURFACE

     SURFACE TEMPERATURE (OK) =     3573.        QCOND (BTU/FT2-SEC)    =      207.
     SURFACE PRESSURE (ATM)   =    0.3090        QSUBL (BTU/FT2-SEC)    =      116.
     BLOWING RATE             =    0.0582        QRR (BTU/FT2-SEC)      =      538.
     MASS LOSS (LB/FT2-SEC)   =    0.0248        QTOTAL (BTU/FT2-SEC)   =      855.
```

```
                 C A S E  2     53.CCO FT/SEC      2.5E-7 SLUGS/CU FT


XI   =    0.100C          DELTA =    3.973309E-C2          DTIL =    5.791126E-02

EPS =     0.0032          QC =  -0.176551E+03  (WATTS/CM**2)  =  -0.155365E+03  (BTU/FT**2 - SEC)

RB   =    0.0562          QR =  -0.740401E+03  (WATTS/CM**2)  =  -0.651553E+03  (BTU/FT**2 - SEC)

RVB =     0.0552          GF =  -0.548939E+02  (WATTS/CM**2)  =  -0.483119E+02  (BTU/FT**2 - SEC)

TOTAL HEATING  =  -0.971651E+03  (WATTS/CM**2)  =  -0.855229E+03  (BTU/FT**2 - SEC)

       ETA      V/DZ        F*          RV         T/TD     E(WATTS/CM3)     V        V (FT/SEC)      G        H (STATIC)


WALL 0.0       0.0         0.0        3.277E-03  2.468E-01  -1.624E+02  5.333E-04   2.826E+01   2.047E-01   2.047E-01
     0.005     1.196E-03   2.214E-03  3.277E-03  2.494E-01  -1.626E+02  5.444E-04   2.885E+01   2.075E-01   2.075E-01
     0.011     2.6[illegible]E-03   4.471E-03  3.274E-03  2.524E-01  -1.629E+02  5.576E-04   2.955E+01   2.119E-01   2.119E-01
     0.015     3.670E-03   6.763E-03  3.272E-03  2.543E-01  -1.634E+02  5.661E-04   3.000E+01   2.149E-01   2.149E-01
     0.020     4.364E-03   9.119E-03  3.267E-03  2.568E-01   1.641E+02  5.772E-04   3.059E+01   2.189E-01   2.189E-01
     0.023     5.747E-03   1.060E-02  3.264E-03  2.583E-01  -1.644E+02  5.843E-04   3.097E+01   2.215E-01   2.215E-01
     0.026     6.5[illegible]E-03   1.215E-02  3.259E-03  2.600E-01  -1.647E+02  5.916E-04   3.136E+01   2.242E-01   2.242E-01
     0.029     7.414E-03   1.359E-02  3.255E-03  2.616E-01  -1.648E+02  5.989E-04   3.174E+01   2.269E-01   2.269E-01
     0.032     8.251E-03   1.522E-02  3.250E-03  2.632E-01  -1.650E+02  6.062E-04   3.213E+01   2.297E-01   2.297E-01
     0.036     9.107E-03   1.679E-02  3.244E-03  2.649E-01  -1.650E+02  6.137E-04   3.252E+01   2.326E-01   2.326E-01
     0.039     9.9[illegible]E-03   1.844E-02  3.237E-03  2.667E-01  -1.650E+02  6.215E-04   3.294E+01   2.356E-01   2.356E-01
     0.045     1.175E-02   2.163E-02  3.223E-03  2.702E-01  -1.644E+02  6.369E-04   3.376E+01   2.417E-01   2.417E-01
     0.054     1.414E-02   2.649E-02  3.198E-03  2.755E-01  -1.634E+02  6.596E-04   3.496E+01   2.509E-01   2.509E-01
     0.063     1.701E-02   3.146E-02  3.165E-03  2.812E-01  -1.613E+02  6.828E-04   3.619E+01   2.606E-01   2.606E-01
     0.071     1.934E-02   3.474E-02  3.134E-03  2.873E-01  -1.592E+02  7.071E-04   3.747E+01   2.711E-01   2.711E-01
     0.080     2.277E-02   4.222E-02  3.094E-03  2.938E-01  -1.564E+02  7.317E-04   3.878E+01   2.821E-01   2.821E-01
     0.085     2.452E-02   4.591E-02  3.068E-03  2.977E-01  -1.548E+02  7.461E-04   3.954E+01   2.887E-01   2.887E-01
     0.092     2.724E-02   5.0[illegible]E-02  3.026E-03  3.041E-01  -1.524E+02  7.678E-04   4.069E+01   2.990E-01   2.990E-01
     0.100     3.0[illegible]E-02   5.602E-02  2.975E-03  3.108E-01  -1.501E+02  7.895E-04   4.184E+01   3.098E-01   3.098E-01
     0.110     3.4[illegible]E-02   6.3[illegible]E-02  2.910E-03  3.206E-01  -1.476E+02  8.179E-04   4.335E+01   3.247E-01   3.247E-01
     0.120     3.827E-02   7.178E-02  2.831E-03  3.314E-01  -1.451E+02  8.452E-04   4.480E+01   3.403E-01   3.403E-01
     0.130     4.27[illegible]E-02   8.0[illegible]E-02  2.742E-03  3.431E-01  -1.436E+02  8.698E-04   4.610E+01   3.563E-01   3.563E-01
     0.140     4.753E-02   8.7[illegible]E-02  2.644E-03  3.570E-01  -1.422E+02  8.906E-04   4.720E+01   3.727E-01   3.727E-01
     0.150     5.2[illegible]E-02   1.031E-01  2.534E-03  3.700E-01  -1.412E+02  9.064E-04   4.804E+01   3.897E-01   3.897E-01
     0.160     5.7[illegible]E-02   1.119E-01  2.412E-03  3.849E-01  -1.403E+02  9.154E-04   4.852E+01   4.077E-01   4.077E-01
     0.170     6.1[illegible]E-02   1.22[illegible]E-01  2.276E-03  4.008E-01  -1.402E+02  9.168E-04   4.859E+01   4.272E-01   4.272E-01
     0.180     6.771E-02   1.3[illegible]E-01  2.127E-03  4.175E-01  -1.401E+02  9.090E-04   4.818E+01   4.489E-01   4.489E-01
     0.200     8.2[illegible]E-02   1.63[illegible]E-01  1.780E-03  4.540E-01  -1.503E+02  8.582E-04   4.549E+01   5.003E-01   5.003E-01
     0.210     9.021E-02   1.7[illegible]E-01  1.580E-03  4.742E-01  -1.554E+02  8.090E-04   4.288E+01   5.292E-01   5.292E-01
     0.220     9.7[illegible]E-02   1.9[illegible]E-01  1.364E-03  4.959E-01  -1.895E+02  7.387E-04   3.915E+01   5.588E-01   5.588E-01
     0.230     1.0[illegible]E-01   2.1[illegible]E-01  1.124E-03  5.193E-01  -2.236E+02  6.430E-04   3.408E+01   5.868E-01   5.868E-01
     0.240     1.14[illegible]E-01   2.311E-01  8.661E-04  5.444E-01  -2.927E+02  5.185E-04   2.748E+01   6.108E-01   6.108E-01
     0.250     1.219E-01   2.456E-01  5.974E-04  5.706E-01  -3.617E+02  3.644E-04   1.931E+01   6.296E-01   6.296E-01
     0.270     1.32[illegible]E-01   2.7[illegible]E-01  2.880E-04  5.971E-01  -3.867E+02  1.833E-04   9.715E+00   6.438E-01   6.438E-01
     0.280     1.51[illegible]E-01   2.9[illegible]E-01 -3.654E-04  6.470E-01  -4.366E+02 -2.412E-04  -1.278E+01   6.637E-01   6.637E-01
     0.310     1.80[illegible]E-01   3.416E-01 -1.484E-03  7.022E-01  -2.090E+02 -9.713E-04  -5.148E+01   6.840E-01   6.840E-01
     0.340     2.0[illegible]E-01   3.7[illegible]0E-01 -2.727E-03  7.398E-01   1.858E+01 -1.800E-03  -9.540E+01   7.060E-01   7.060E-01
     0.370     2.1[illegible]E-01   4.0[illegible]E-01 -4.081E-03  7.693E-01   6.342E+01 -2.780E-03  -1.474E+02   7.346E-01   7.346E-01
     0.400     2.4[illegible]E-01   4.1[illegible]E-01 -5.564E-03  7.965E-01   1.083E+02 -3.929E-03  -2.082E+02   7.648E-01   7.648E-01
     0.430     3.0[illegible]E-01   4.6[illegible]E-01 -7.107E-03  8.049E-01   1.429E+02 -5.217E-03  -2.765E+02   7.911E-01   7.911E-01
     0.465     3.1[illegible]E-01   4.7[illegible]E-01 -8.779E-03  8.147E-01   1.776E+02 -6.611E-03  -3.504E+02   8.121E-01   8.120E-01
     0.490     3.5[illegible]E-01   5.0[illegible]E-01 -1.054E-02  8.222E-01   1.903E+02 -8.106E-03  -4.296E+02   8.293E-01   8.292E-01
     0.520     3.9[illegible]E-01   5.[illegible]E-01 -1.240E-02  8.281E-01   2.030E+02 -9.702E-03  -5.142E+02   8.441E-01   8.440E-01
```

ORIGINAL PAGE IS
OF POOR QUALITY

```
     0.550    4.342E-01    5.815E-01   -1.436E-02    8.332E-01    2.102E+02   -1.140E-02   -6.042E+02    8.571E-01    8.570E-01
     0.580    4.691E-01    6.093E-01   -1.641E-02    8.377E-01    2.173E+02   -1.320E-02   -6.996E+02    8.687E-01    8.685E-01
     0.610    5.045E-01    6.370E-01   -1.856E-02    8.417E-01    2.234E+02   -1.510E-02   -8.005E+02    8.792E-01    8.790E-01
     0.640    5.403E-01    6.648E-01   -2.081E-02    8.454E-01    2.295E+02   -1.711E-02   -9.068E+02    8.887E-01    8.884E-01
     0.670    5.764E-01    6.925E-01   -2.315E-02    8.489E-01    2.361E+02   -1.922E-02   -1.019E+03    8.975E-01    8.971E-01
     0.700    6.128E-01    7.203E-01   -2.559E-02    8.523E-01    2.426E+02   -2.143E-02   -1.136E+03    9.056E-01    9.052E-01
     0.730    6.496E-01    7.481E-01   -2.812E-02    8.557E-01    2.513E+02   -2.376E-02   -1.259E+03    9.132E-01    9.126E-01
     0.760    6.867E-01    7.759E-01   -3.075E-02    8.591E-01    2.600E+02   -2.619E-02   -1.388E+03    9.203E-01    9.196E-01
     0.790    7.241E-01    8.038E-01   -3.348E-02    8.628E-01    2.750E+02   -2.874E-02   -1.523E+03    9.270E-01    9.262E-01
     0.820    7.618E-01    8.317E-01   -3.631E-02    8.671E-01    2.901E+02   -3.143E-02   -1.666E+03    9.336E-01    9.326E-01
     0.850    7.998E-01    8.597E-01   -3.923E-02    8.722E-01    3.258E+02   -3.426E-02   -1.816E+03    9.400E-01    9.388E-01
     0.880    8.382E-01    8.877E-01   -4.225E-02    8.791E-01    3.616E+02   -3.729E-02   -1.976E+03    9.466E-01    9.452E-01
     0.910    8.770E-01    9.158E-01   -4.536E-02    8.882E-01    5.271E+02   -4.055E-02   -2.149E+03    9.535E-01    9.519E-01
     0.940    9.165E-01    9.439E-01   -4.857E-02    9.064E-01    6.926E+02   -4.441E-02   -2.354E+03    9.631E-01    9.611E-01
     0.970    9.572E-01    9.719E-01   -5.188E-02    9.350E-01    1.324E+03   -4.901E-02   -2.598E+03    9.754E-01    9.730E-01
SHOC 1.000    1.000E+00    1.000E+00   -5.526E-02    1.000E+00    1.955E+03   -5.590E-02   -2.963E+03    9.993E-01    9.962E-01
```

-SHOCK LAYER GAS PROPERTIES-

ETA	Y/C	P (ATM.)	T (DEG.KEL.)	RHO (SLUGS/FT3)	MU (LBM/FT-SEC)	RMU (LBF2-SEC3/FT6)	K (BTU/FT-SEC-R)
0.0	0.0	3.0892E-01	3.5725E+03	2.7265E-05	6.0705E-05	1.6551E-09	1.0875E-04
0.0050	[illegible]	[illegible]	3.6102E+03	2.6705E-05	6.1511E-05	1.6427E-09	1.0959E-04
0.0111	[illegible]	[illegible]	3.6529E+03	2.6054E-05	6.2239E-05	1.6216E-09	1.1086E-04
0.0150	[illegible]	[illegible]	3.6803E+03	2.5640E-05	6.2674E-05	1.6070E-09	1.1174E-04
0.0200	[illegible]	[illegible]	3.7160E+03	2.5111E-05	6.3227E-05	1.5877E-09	1.1291E-04
0.0231	[illegible]	[illegible]	3.7386E+03	2.4782E-05	6.3574E-05	1.5755E-09	1.1367E-04
0.0263	[illegible]	[illegible]	3.7623E+03	2.4442E-05	6.3938E-05	1.5628E-09	1.1446E-04
0.0294	[illegible]	[illegible]	3.7857E+03	2.4113E-05	6.4296E-05	1.5503E-09	1.1525E-04
0.0325	[illegible]	[illegible]	3.8096E+03	2.3782E-05	6.4662E-05	1.5378E-09	1.1607E-04
0.0356	[illegible]	[illegible]	3.8340E+03	2.3452E-05	6.5034E-05	1.5252E-09	1.1690E-04
0.0389	[illegible]	[illegible]	3.8597E+03	2.3111E-05	6.5426E-05	1.5120E-09	1.1778E-04
0.0450	[illegible]	[illegible]	3.9110E+03	2.2445E-05	6.6208E-05	1.4863E-09	1.1955E-04
0.0538	[illegible]	[illegible]	3.9875E+03	2.1512E-05	6.7375E-05	1.4494E-09	1.2223E-04
0.0625	[illegible]	[illegible]	[illegible]	2.0580E-05	6.8597E-05	1.4124E-09	1.2509E-04
0.0713	[illegible]	[illegible]	4.1576E+03	1.9663E-05	6.9909E-05	1.3746E-09	1.2820E-04
0.0800	[illegible]	[illegible]	4.2918E+03	1.8750E-05	7.1287E-05	1.3372E-09	1.3152E-04
0.0850	[illegible]	[illegible]	4.3694E+03	1.8244E-05	7.2119E-05	1.3158E-09	1.3355E-04
0.0925	[illegible]	[illegible]	4.4007E+03	1.7485E-05	7.3425E-05	1.2839E-09	1.3674E-04
0.1000	[illegible]	[illegible]	4.4985E+03	1.6743E-05	7.4810E-05	1.2525E-09	1.4011E-04
0.1100	[illegible]	[illegible]	4.6359E+03	1.5783E-05	7.6796E-05	1.2121E-09	1.4487E-04
0.1200	[illegible]	[illegible]	4.7563E+03	1.4860E-05	7.8988E-05	1.1737E-09	1.4994E-04
0.1300	[illegible]	[illegible]	4.9664E+03	1.3989E-05	8.1383E-05	1.1365E-09	1.5515E-04
0.1400	[illegible]	[illegible]	5.1525E+03	1.3170E-05	8.4024E-05	1.1066E-09	1.6047E-04
0.1500	[illegible]	[illegible]	5.3545E+03	1.2407E-05	8.6923E-05	1.0780E-09	1.6580E-04
0.1600	[illegible]	3.0892E-01	5.5705E+03	1.1688E-05	9.0031E-05	1.0523E-09	1.7096E-04
0.1700	[illegible]	[illegible]	5.8007E+03	1.1016E-05	9.3344E-05	1.0283E-09	1.7593E-04
0.1800	[illegible]	[illegible]	6.0422E+03	1.0380E-05	9.6787E-05	1.0047E-09	1.8058E-04
0.2000	8.2970E-02	[illegible]	6.5715E+03	9.2023E-06	1.0394E-04	9.5651E-10	1.8893E-04
0.2100	9.0214E-02	[illegible]	6.8639E+03	8.6678E-06	1.0742E-04	9.3114E-10	1.9247E-04
0.2200	[illegible]	[illegible]	7.1774E+03	8.1808E-06	1.1067E-04	9.0542E-10	1.9546E-04
0.2300	[illegible]	[illegible]	7.5153E+03	7.7571E-06	1.1346E-04	8.8017E-10	1.9788E-04
0.2400	[illegible]	[illegible]	[illegible]	7.4114E-06	1.1553E-04	8.5626E-10	1.9972E-04
0.2500	[illegible]	[illegible]	8.2597E+03	7.1519E-06	1.1663E-04	8.3413E-10	2.0077E-04
0.2600	[illegible]	[illegible]	8.6416E+03	6.9712E-06	1.1669E-04	8.1347E-10	2.0088E-04
0.2800	[illegible]	[illegible]	9.3649E+03	6.7952E-06	1.1413E-04	7.7553E-10	1.9815E-04
0.3100	[illegible]	[illegible]	1.0163E+04	6.7788E-06	1.0749E-04	7.2868E-10	1.9137E-04
0.3400	[illegible]	[illegible]	1.0708E+04	6.7218E-06	1.0180E-04	6.8426E-10	1.8909E-04
0.3700	[illegible]	[illegible]	1.1135E+04	6.5128E-06	9.7706E-05	6.3634E-10	1.9196E-04
0.4000	[illegible]	[illegible]	1.1441E+04	6.2584E-06	9.4551E-05	5.9175E-10	1.9688E-04
0.4300	[illegible]	[illegible]	[illegible]	6.0438E-06	9.2045E-05	5.5631E-10	2.0144E-04
0.4600	[illegible]	[illegible]	1.1751E+04	5.8877E-06	8.9989E-05	5.2983E-10	2.0500E-04
0.4900	[illegible]	[illegible]	1.1900E+04	5.7673E-06	8.8265E-05	5.0905E-10	2.0787E-04
0.5200	[illegible]	[illegible]	1.1986E+04	5.6700E-06	8.6766E-05	4.9197E-10	2.1028E-04
0.5500	[illegible]	[illegible]	[illegible]	5.5874E-06	8.5459E-05	4.7749E-10	2.1236E-04
0.5800	[illegible]	[illegible]	[illegible]	5.5159E-06	8.4306E-05	4.6502E-10	2.1419E-04
0.6100	[illegible]	[illegible]	1.2182E+04	5.4526E-06	8.3284E-05	4.5412E-10	2.1581E-04
0.6400	[illegible]	[illegible]	[illegible]	5.3959E-06	8.2374E-05	4.4448E-10	2.1727E-04
0.6700	[illegible]	[illegible]	[illegible]	5.3443E-06	8.1562E-05	4.3590E-10	2.1859E-04
0.7000	[illegible]	[illegible]	[illegible]	5.2967E-06	8.0832E-05	4.2818E-10	2.1979E-04
0.7300	[illegible]	[illegible]	[illegible]	5.2522E-06	8.0195E-05	4.2120E-10	2.2089E-04
0.7600	[illegible]	[illegible]	[illegible]	5.2095E-06	7.9631E-05	4.1485E-10	2.2190E-04
0.7900	[illegible]	[illegible]	1.2488E+04	5.1680E-06	7.9145E-05	4.0902E-10	2.2284E-04
0.8200	[illegible]	[illegible]	[illegible]	5.1250E-06	7.8754E-05	4.0362E-10	2.2372E-04
0.8500	[illegible]	[illegible]	1.2623E+04	5.0794E-06	7.8460E-05	3.9858E-10	2.2455E-04
0.8800	8.3826E-01	[illegible]	1.2723E+04	5.0259E-06	7.8330E-05	3.9369E-10	2.2536E-04

L PAGE IS
UALITY

```
0.9100    8.7705E-01    3.0983E-01    1.2854E+04    4.9626E-06    7.8374E-05    3.8894E-10    2.2615E-04
0.9400    9.1656E-01    3.0397E-01    1.3119E+04    4.8519E-06    7.8999E-05    3.8330E-10    2.2709E-04
0.9700    9.5723E-01    3.1061E-01    1.3532E+04    4.6961E-06    8.0259E-05    3.7690E-10    2.2817E-04
1.0000    1.0000E+00    3.1011E-01    1.4473E+04    4.3856E-06    8.3480E-05    3.6611E-10    2.2998E-04
```

PAGE IS
LITY

-SPECIES MASS FRACTIONS-

ETA	O2	N2	O	N	O+	N+	E-
0.0	[illegible]	4.9472E-02	2.5590E-09	9.9963E-11	9.9967E-11	9.9963E-11	9.9957E-16
0.0050	[illegible]	[illegible]	3.2929E-07	1.8591E-07	1.3063E-06	3.2592E-05	1.3229E-09
0.0111	[illegible]	4.9473E-02	7.8661E-07	4.9615E-07	3.0547E-06	7.6219E-05	3.0938E-09
0.0150	[illegible]	4.9465E-02	1.0763E-06	7.8856E-07	4.2744E-06	1.0665E-04	4.3291E-09
0.0200	[illegible]	4.9454E-02	1.5168E-06	1.3147E-06	5.9651E-06	1.4883E-04	6.0412E-09
0.0231	[illegible]	4.9441E-02	1.8240E-06	1.7672E-06	7.0937E-06	1.7699E-04	7.1841E-09
0.0263	8.4144E-09	4.9438E-02	2.1751E-06	2.3632E-06	8.3281E-06	2.0778E-04	8.4339E-09
0.0294	[illegible]	[illegible]	2.5560E-06	3.0996E-06	9.5964E-06	2.3941E-04	9.7180E-09
0.0325	[illegible]	4.9421E-02	2.9867E-06	4.0336E-06	1.0942E-05	2.7296E-04	1.1060E-08
0.0356	1.2447E-08	4.9411E-02	3.4790E-06	5.2160E-06	1.2370E-05	3.0857E-04	1.2525E-08
0.0395	1.4611E-08	4.9401E-02	4.0666E-06	6.7640E-06	1.3938E-05	3.4766E-04	1.4112E-08
0.0450	[illegible]	[illegible]	5.4563E-06	1.0961E-05	1.7271E-05	4.3071E-04	1.7483E-08
0.0539	[illegible]	4.9342E-02	8.4895E-06	2.1117E-05	2.2783E-05	5.6794E-04	2.3054E-08
0.0625	[illegible]	[illegible]	1.3455E-05	3.9942E-05	2.9370E-05	7.3167E-04	2.9702E-08
0.0713	[illegible]	[illegible]	2.2102E-05	7.4984E-05	3.7489E-05	9.3314E-04	3.7883E-08
0.0800	[illegible]	4.9177E-02	3.7137E-05	1.3786E-04	4.7363E-05	1.1775E-03	4.7807E-08
0.0850	[illegible]	4.9132E-02	5.1109E-05	1.9608E-04	5.4105E-05	1.3440E-03	5.4569E-08
0.0925	[illegible]	4.9054E-02	8.2514E-05	3.2511E-04	6.5911E-05	1.6348E-03	6.6383E-08
0.1000	[illegible]	[illegible]	1.3547E-04	5.3232E-04	8.0259E-05	1.9870E-03	8.0695E-08
0.1100	[illegible]	4.8804E-02	2.6456E-04	9.5418E-04	1.0436E-04	2.5758E-03	1.0463E-07
0.1200	[illegible]	[illegible]	5.3391E-04	1.8065E-03	1.3619E-04	3.3456E-03	1.3606E-07
0.1300	[illegible]	[illegible]	1.1009E-03	3.1567E-03	1.7861E-04	4.3701E-03	1.7763E-07
0.1400	[illegible]	4.8025E-02	2.2557E-03	5.2663E-03	2.3550E-04	5.7272E-03	2.3291E-07
0.1500	[illegible]	[illegible]	4.7419E-03	8.3436E-03	3.1217E-04	7.5357E-03	3.0667E-07
0.1600	[illegible]	[illegible]	9.4050E-03	1.2569E-02	4.1582E-04	9.9482E-03	4.0522E-07
0.1700	[illegible]	[illegible]	1.7386E-02	1.8254E-02	5.5626E-04	1.3164E-02	5.3688E-07
0.1800	[illegible]	[illegible]	2.8096E-02	2.7436E-02	7.4685E-04	1.7446E-02	7.1266E-07
0.2000	[illegible]	[illegible]	6.7044E-02	4.2898E-02	1.3360E-03	3.0243E-02	1.2418E-06
0.2100	[illegible]	[illegible]	9.1558E-02	6.5369E-02	1.8216E-03	4.0152E-02	1.6575E-06
0.2200	[illegible]	3.7184E-02	1.1795E-01	8.6469E-02	2.4744E-03	5.2921E-02	2.1999E-06
0.2300	[illegible]	3.3714E-02	1.4135E-01	1.1269E-01	3.3384E-03	6.8984E-02	2.8940E-06
0.2400	[illegible]	[illegible]	1.5855E-01	1.4388E-01	4.4540E-03	8.8496E-02	3.7558E-06
0.2500	[illegible]	[illegible]	1.7015E-01	1.7884E-01	5.8475E-03	1.1117E-01	4.7813E-06
0.2600	[illegible]	[illegible]	1.7698E-01	2.1565E-01	7.5247E-03	1.3625E-01	5.9388E-06
0.2800	[illegible]	[illegible]	1.8506E-01	2.8807E-01	1.1694E-02	1.9352E-01	8.4684E-06
0.3100	[illegible]	[illegible]	1.9044E-01	3.6676E-01	1.9640E-02	2.6758E-01	1.1824E-05
0.3400	[illegible]	[illegible]	1.8851E-01	3.9758E-01	2.7069E-02	3.2708E-01	1.4213E-05
0.3700	[illegible]	[illegible]	1.8136E-01	3.9500E-01	3.3416E-02	3.6879E-01	1.5947E-05
0.4000	[illegible]	[illegible]	1.7191E-01	3.7846E-01	4.9746E-02	3.9636E-01	1.7269E-05
0.4300	[illegible]	[illegible]	1.6255E-01	3.6153E-01	5.9209E-02	4.1466E-01	1.8294E-05
0.4600	[illegible]	[illegible]	1.5417E-01	3.4820E-01	6.7585E-02	4.2735E-01	1.9104E-05
0.4900	[illegible]	[illegible]	1.4665E-01	3.3761E-01	7.5112E-02	4.3855E-01	1.9778E-05
0.5200	[illegible]	[illegible]	1.3578E-01	3.2878E-01	8.1981E-02	4.4738E-01	2.0360E-05
0.5500	[illegible]	[illegible]	1.3345E-01	3.2124E-01	8.8309E-02	4.5492E-01	2.0873E-05
0.5800	[illegible]	[illegible]	1.2759E-01	3.1471E-01	9.4167E-02	4.6146E-01	2.1331E-05
0.6100	[illegible]	[illegible]	1.2214E-01	3.0897E-01	9.9613E-02	4.6719E-01	2.1743E-05
0.6400	[illegible]	[illegible]	1.1707E-01	3.0389E-01	1.0469E-01	4.7227E-01	2.2116E-05
0.6700	[illegible]	[illegible]	1.1233E-01	2.9930E-01	1.0943E-01	4.7681E-01	2.2457E-05
0.7000	[illegible]	[illegible]	1.0785E-01	2.9530E-01	1.1387E-01	4.8087E-01	2.2769E-05
0.7300	[illegible]	[illegible]	1.0373E-01	2.9164E-01	1.1803E-01	4.8453E-01	2.3055E-05
0.7600	[illegible]	[illegible]	9.9237E-02	2.8833E-01	1.2192E-01	4.8784E-01	2.3319E-05
0.7900	[illegible]	[illegible]	9.6178E-02	2.8534E-01	1.2558E-01	4.9083E-01	2.3562E-05
0.8200	[illegible]	[illegible]	9.2757E-02	2.8262E-01	1.2900E-01	4.9354E-01	2.3786E-05
0.8500	[illegible]	[illegible]	8.9560E-02	2.8018E-01	1.3219E-01	4.9599E-01	2.3992E-05
0.8800	[illegible]	[illegible]	8.6598E-02	2.7798E-01	1.3516E-01	4.9818E-01	2.4181E-05
0.9100	[illegible]	[illegible]	8.3881E-02	2.7604E-01	1.3787E-01	5.0012E-01	2.4352E-05
0.9400	[illegible]	[illegible]	8.1414E-02	2.7435E-01	1.4034E-01	5.0181E-01	2.4506E-05

```
0.9700     1.1103E-05     2.3586E-05     7.9377E-02     2.7309E-01     1.4238E-01     5.0307E-01     2.4628E-05
1.0000     1.1103E-05     2.8914E-05     7.7799E-02     2.7231E-01     1.4395E-01     5.0384E-01     2.4717E-05
```

ORIGINAL PAGE IS
OF POOR QUALITY

-SPECIES MASS FRACTICNS-

ETA	C	H	H2	CO	C3-G	CN	C2H	C2H2
0.0	2.10[illegible]E-02	2.20[illegible]E-02	4.1334E-02	2.5688E-01	3.6933E-01	9.9962E-11	1.3871E-01	5.8880E-02
0.0050	2.1771E-02	2.453[illegible]E-02	3.7948E-02	2.5690E-01	3.6914E-01	9.5035E-05	1.6362E-01	5.8026E-02
0.0111	2.2681E-02	2.6654E-02	3.5597E-02	2.5692E-01	3.6889E-01	2.2214E-04	1.7103E-01	5.6902E-02
0.0150	2.3317E-02	2.7911E-02	3.4344E-02	2.5693E-01	3.6871E-01	3.1068E-04	1.7215E-01	5.6131E-02
0.0200	2.4198E-02	2.950[illegible]E-02	3.2827E-02	2.5695E-01	3.6846E-01	4.3320E-04	1.7188E-01	5.5079E-02
0.0231	2.4788E-02	3.0507E-02	3.1891E-02	2.5697E-01	3.6830E-01	5.1481E-04	1.7131E-01	5.4390E-02
0.0263	2.54[illegible]E-02	3.1557E-02	3.0920E-02	2.5698E-01	3.6812E-01	6.0388E-04	1.7053E-01	5.3640E-02
0.0294	2.6[illegible]E-02	3.2591E-02	2.9970E-02	2.5700E-01	3.6793E-01	6.9519E-04	1.6963E-01	5.2893E-02
0.0325	2.67[illegible]E-02	3.3[illegible]E-02	2.9309E-02	2.5701E-01	3.6773E-01	7.9175E-04	1.6860E-01	5.2108E-02
0.0356	2.754[illegible]E-02	3.471[illegible]E-02	2.8037E-02	2.5703E-01	3.6752E-01	8.9392E-04	1.6745E-01	5.1288E-02
0.0388	2.8367E-02	3.58[illegible]E-02	2.7025E-02	2.5705E-01	3.6730E-01	1.0057E-03	1.6613E-01	5.0405E-02
0.0450	3.0112E-02	3.8049E-02	2.5038E-02	2.5708E-01	3.6681E-01	1.2414E-03	1.6315E-01	4.8582E-02
0.0538	3.3006E-02	4.12[illegible]E-02	2.2185E-02	2.5714E-01	3.6600E-01	1.6254E-03	1.5781E-01	4.5725E-02
0.0625	3.6443E-02	4.457[illegible]E-02	1.9371E-02	2.5721E-01	3.6504E-01	2.0716E-03	1.5090E-01	4.2569E-02
0.0713	4.0694E-02	4.7[illegible]E-02	1.6589E-02	2.5728E-01	3.6385E-01	2.5993E-03	1.4191E-01	3.9025E-02
0.0800	4.5[illegible]E-02	5.121[illegible]E-02	1.3964E-02	2.5737E-01	3.6241E-01	3.2025E-03	1.3073E-01	3.5179E-02
0.0850	4.[illegible]E-02	5.3[illegible]E-02	1.2538E-02	2.5742E-01	3.6144E-01	3.5854E-03	1.2323E-01	3.2826E-02
0.0925	5.[illegible]E-02	5.[illegible]E-02	1.0530E-02	2.5749E-01	3.5973E-01	4.2043E-03	1.1052E-01	2.9123E-02
0.1060	6.2770E-02	5.826[illegible]E-02	8.7612E-03	2.5756E-01	3.5768E-01	4.8607E-03	9.6335E-02	2.5263E-02
0.1100	7.4934E-02	6.1561E-02	6.5580E-03	2.5761E-01	3.5427E-01	5.7466E-03	7.5891E-02	2.0000E-02
0.1200	9.0405E-02	6.43[illegible]E-02	4.7579E-03	2.5753E-01	3.4986E-01	6.5318E-03	5.5309E-02	1.4864E-02
0.1300	1.1003E-01	6.66[illegible]E-02	3.2865E-03	2.5709E-01	3.4413E-01	7.0659E-03	3.6609E-02	1.0189E-02
0.1400	1.3436E-01	6.841[illegible]E-02	2.1270E-03	2.5577E-01	3.3665E-01	7.2074E-03	2.1521E-02	6.3012E-03
0.1500	1.6[illegible]E-01	6.9479E-02	1.2653E-03	2.5257E-01	3.2688E-01	6.9366E-03	1.0969E-02	3.4229E-03
0.1600	1.97[illegible]E-01	6.[illegible]74E-02	6.8225E-04	2.4588E-01	3.1415E-01	6.4122E-03	4.7570E-03	1.5855E-03
0.1700	2.34[illegible]E-01	6.964[illegible]E-02	3.3406E-04	2.3388E-01	2.9764E-01	5.7061E-03	1.7396E-03	6.0265E-04
0.1800	2.74[illegible]E-01	6.[illegible]1E-02	1.5125E-04	2.1768E-01	2.7650E-01	1.8894E-03	5.2529E-04	1.6875E-04
0.2000	3.53[illegible]E-01	6.592[illegible]E-02	4.3312E-05	1.5687E-01	2.1803E-01	1.7250E-03	5.3354E-05	1.2046E-05
0.2100	3.8[illegible]E-01	6.3[illegible]E-02	2.4543E-05	1.1835E-01	1.8093E-01	1.6671E-03	1.3624E-05	1.5633E-06
0.2200	4.16[illegible]E-01	6.024[illegible]E-02	1.4694E-05	7.8855E-02	1.4031E-01	1.4982E-03	4.0643E-06	1.4555E-07
0.2300	4.33[illegible]E-01	5.6[illegible]E-02	8.8379E-06	4.4592E-02	9.9476E-02	1.1994E-03	1.4768E-06	9.6574E-09
0.2400	4.3[illegible]E-01	5.1711E-02	5.2385E-06	2.0820E-02	6.2844E-02	8.2553E-04	5.8709E-07	4.6000E-10
0.2[illegible]00	4.1[illegible]E-01	4.[illegible]E-02	3.0626E-06	8.2450E-03	3.4393E-02	4.9350E-04	2.2150E-07	1.8759E-11
0.2500	3.7[illegible]E-01	4.0[illegible]E-02	1.7723E-06	3.0109E-03	1.5614E-02	2.7369E-04	7.1112E-08	9.4362E-13
0.2800	2.[illegible]E-01	2.[illegible]E-02	5.7641E-07	5.8884E-04	1.[illegible]532E-03	1.0576E-04	5.0875E-09	2.3145E-14
0.3100	1.2[illegible]E-01	1.4[illegible]E-02	9.7518E-08	9.0524E-05	6.9558E-05	2.9649E-05	9.5064E-11	1.5224E-16
0.3400	4.1[illegible]E-02	[illegible].00[illegible]E-03	1.2942E-08	1.5932E-05	1.4256E-06	7.1749E-06	1.3[illegible]E-12	6.7726E-19
0.3700	9.7[illegible]E-03	2.21[illegible]E-03	1.4473E-09	2.2156E-06	1.5551E-08	1.2004E-06	1.1960E-14	1.8746E-21
0.4000	1.57[illegible]E-03	1.14[illegible]E-03	3.2613E-10	2.3878E-07	6.3684E-11	1.4505E-07	8.9876E-17	5.6090E-24
0.4300	6.271[illegible]E-04	1.00[illegible]E-03	2.2841E-10	7.1473E-08	7.1514E-14	4.6086E-08	8.6710E-18	4.0[illegible]E-25
0.4600	6.21[illegible]E-04	1.01[illegible]E-03	2.1332E-10	5.7630E-08	3.9166E-16	4.0065E-08	7.1348E-18	3.1195E-25
0.4900	5.9[illegible]E-04	1.01[illegible]E-03	2.0090E-10	4.6626E-08	3.5942E-18	3.4115E-08	5.6630E-18	2.3396E-25
0.5200	5.7[illegible]E-04	1.01[illegible]E-03	1.9172E-10	3.9320E-08	8.1056E-20	3.0134E-08	4.7671E-18	1.8837E-25
0.5500	5.5[illegible]E-04	1.01[illegible]E-03	1.8411E-10	3.3730E-08	2.7203E-20	2.7018E-08	4.0922E-18	1.5562E-25
0.5800	5.4[illegible]E-04	1.01[illegible]E-03	1.7774E-10	2.9391E-08	2.3916E-20	2.4564E-08	3.5833E-18	1.3180E-25
0.6100	5.3[illegible]E-04	1.01[illegible]E-03	1.7217E-10	2.5857E-08	2.0675E-20	2.2525E-08	3.1726E-18	1.1324E-25
0.6400	5.21[illegible]E-04	1.01[illegible]E-03	1.6722E-10	2.2927E-08	1.8072E-20	2.0800E-08	2.8[illegible]E-18	9.8444E-26
0.6700	5.0[illegible]E-04	1.01[illegible]E-03	1.6273E-10	2.0433E-08	1.5905E-20	1.9298E-08	2.5461E-18	8.6197E-26
0.7000	4.[illegible]E-04	1.01[illegible]E-03	1.5850E-10	1.8271E-08	1.4033E-20	1.7958E-08	2.2934E-18	7.5777E-26
0.7300	4.[illegible]E-04	1.01[illegible]E-03	1.5466E-10	1.6362E-08	1.2378E-20	1.6736E-08	2.0663E-18	6.6082E-26
0.7600	4.7[illegible]E-04	1.01[illegible]E-03	1.5069E-10	1.4625E-08	1.0850E-20	1.5577E-08	1.8530E-18	5.8396E-26
0.7900	4.[illegible]E-04	1.01[illegible]E-03	1.4674E-10	1.3021E-08	9.4037E-21	1.4449E-08	1.6483E-18	5.0684E-26
0.8200	4.[illegible]E-04	1.01[illegible]E-03	1.4241E-10	1.1448E-08	7.9258E-21	1.3263E-08	1.43[illegible]E-18	4.2941E-26
0.8500	4.27[illegible]E-04	1.01[illegible]E-03	1.3762E-10	9.8984E-09	6.4295E-21	1.2003E-08	1.2150E-18	3.5224E-26
0.8800	4.[illegible]E-04	1.01[illegible]E-03	1.3144E-10	8.2645E-09	4.7772E-21	1.0479E-08	9.6051E-19	2.6711E-26
0.9100	3.[illegible]E-04	1.01[illegible]E-03	1.2387E-10	6.4333E-09	3.1278E-21	8.7192E-09	6.9123E-19	1.8224E-26
0.9400	3.00[illegible]E-04	1.01[illegible]E-03	1.1008E-10	4.1372E-09	1.3940E-21	6.1334E-09	3.6311E-19	8.6275E-27

```
0.9700     2.2304E-04     1.0151E-03     9.1073E-11     2.1682E-09     4.2163E-22     3.5966E-09     1.3434E-19     2.7225E-27
1.0000     1.3018E-04     1.0153E-03     3.9775E-11     1.1942E-09     1.3359E-38     1.2716E-09     8.7242E-22     4.4240E-43
```

ORIGINAL PAGE IS
OF POOR QUALITY

```
                                        -SPECIES MASS FRACTIONS-
 ETA        CF          C3H         C4H         HCN          C2          C+          AMW


0.0      6.9592E-01  9.9957E-11  9.9957E-11  9.9963E-11  4.2184E-02  9.9963E-11  1.3347E+01
0.0050   6.9710E-01  1.2974E-06  2.2405E-09  1.4724E-06  1.8452E-02  2.4692E-08  1.3211E+01
0.0111   6.9822E-01  2.9037E-06  5.0902E-09  3.4332E-06  1.1553E-02  5.7623E-08  1.3040E+01
0.0153   6.9889E-01  3.9405E-06  7.0566E-09  4.7863E-06  1.0608E-02  8.0630E-08  1.2929E+01
0.0200   6.9973E-01  5.2776E-06  9.7481E-09  6.6375E-06  1.1043E-02  1.1259E-07  1.2785E+01
0.0231   7.0025E-01  6.1112E-06  1.1517E-08  7.8525E-06  1.1687E-02  1.3401E-07  1.2694E+01
0.0263   7.0078E-01  6.9745E-06  1.3426E-08  9.1614E-06  1.2541E-02  1.5752E-07  1.2599E+01
0.0294   7.0130E-01  7.8132E-06  1.5358E-08  1.0483E-05  1.3501E-02  1.8180E-07  1.2506E+01
0.0325   7.0181E-01  8.6536E-06  1.7372E-08  1.1856E-05  1.4575E-02  2.0771E-07  1.2412E+01
0.0356   7.0223E-01  9.4950E-06  1.9471E-08  1.3282E-05  1.5759E-02  2.3541E-07  1.2318E+01
0.0388   7.0286E-01  1.0264E-05  2.1730E-08  1.4807E-05  1.7098E-02  2.6609E-07  1.2220E+01
0.0450   7.0380E-01  1.2046E-05  2.6375E-08  1.7913E-05  2.0060E-02  3.3226E-07  1.2028E+01
0.0538   7.0535E-01  1.4417E-05  3.3601E-08  2.2636E-05  2.5225E-02  4.4512E-07  1.1752E+01
0.0625   7.0678E-01  1.6711E-05  4.1501E-08  2.7578E-05  3.1671E-02  5.8700E-07  1.1476E+01
0.0713   7.0822E-01  1.8942E-05  5.0258E-08  3.2702E-05  3.9769E-02  7.7364E-07  1.1198E+01
0.0800   7.0962E-01  2.1015E-05  5.9635E-08  3.7661E-05  4.9456E-02  1.0196E-06  1.0924E+01
0.0850   7.1042E-01  2.2106E-05  6.5305E-08  4.0317E-05  5.5729E-02  1.2013E-06  1.0768E+01
0.0925   7.1100E-01  2.3603E-05  7.4134E-08  4.3891E-05  6.5954E-02  1.5430E-06  1.0539E+01
0.1000   7.1277E-01  2.4888E-05  8.3196E-08  4.6675E-05  7.6697E-02  2.0026E-06  1.0315E+01
0.1100   7.1427E-01  2.6171E-05  9.5274E-08  4.8645E-05  9.0642E-02  2.8790E-06  1.0028E+01
0.1200   7.1570E-01  2.6866E-05  1.0652E-07  4.7869E-05  1.0186E-01  4.2558E-06  9.7598E+00
0.1300   7.1701E-01  2.6894E-05  1.1572E-07  4.3909E-05  1.0769E-01  6.4824E-06  9.5133E+00
0.1400   7.1817E-01  2.6212E-05  1.2136E-07  3.6969E-05  1.0603E-01  1.0185E-05  9.2913E+00
0.1500   7.1920E-01  2.4827E-05  1.2177E-07  2.8132E-05  9.6225E-02  1.6498E-05  9.0931E+00
0.1600   7.2008E-01  2.2783E-05  1.1556E-07  1.9152E-05  7.9708E-02  2.7471E-05  8.9146E+00
0.1700   7.2079E-01  2.0151E-05  1.0232E-07  1.1648E-05  5.9777E-02  4.6781E-05  8.7485E+00
0.1800   7.2838E-01  1.7028E-05  8.3210E-08  6.5810E-06  4.0447E-02  8.0766E-05  8.5870E+00
0.2000   7.2220E-01  9.7792E-06  3.6465E-08  1.9297E-06  1.3757E-02  2.5176E-04  8.2786E+00
0.2100   7.2059E-01  6.4901E-06  1.9474E-08  1.0258E-06  7.5006E-03  4.9592E-04  8.1444E+00
0.2200   7.1224E-01  3.7685E-06  8.5075E-09  5.3525E-07  4.4585E-03  9.3827E-04  8.0374E+00
0.2300   7.0190E-01  1.8473E-06  2.9421E-09  2.5404E-07  2.9788E-03  1.7222E-03  7.9793E+00
0.2400   6.9063E-01  7.1674E-07  7.8393E-10  1.0393E-07  2.0340E-03  3.0308E-03  7.9918E+00
0.2500   6.7785E-01  2.3054E-07  1.5828E-10  3.6265E-08  1.2703E-03  5.0031E-03  8.0841E+00
0.2600   6.7068E-01  4.8015E-08  1.5719E-11  1.2034E-08  6.7272E-04  7.5789E-03  8.2459E+00
0.2800   [illegible] 1.8702E-09  3.9170E-13  1.6881E-09  1.1626E-04  1.3249E-02  8.7128E+00
0.3130   6.3522E-01  2.0[illegible]E-11  2.0003E-15  1.1851E-10  6.8487E-06  1.4545E-02  9.4349E+00
0.3430   6.1506E-01  1.3721E-13  5.8557E-18  7.1740E-12  3.2115E-07  8.7103E-03  9.8582E+00
0.3730   6.0656E-01  [illegible] 5.1263E-21  2.8664E-13  1.0524E-08  3.1631E-03  9.9327E+00
0.4000   [illegible] [illegible] 5.4068E-24  1.2479E-14  2.0089E-10  7.0522E-04  9.8070E+00
0.4300   6.1778E-01  2.7504E-22  8.9528E-28  2.7519E-15  2.6627E-11  3.5324E-04  9.6432E+00
0.4600   6.2523E-01  5.0325E-25  7.5738E-31  1.9654E-15  2.3845E-11  3.9903E-04  9.5074E+00
0.4900   6.3147E-01  7.0646E-27  8.6920E-34  1.4528E-15  2.0279E-11  4.2047E-04  9.3976E+00
0.5200   6.3621E-01  6.3108E-27  1.7891E-34  1.1427E-15  1.8023E-11  4.3968E-04  9.3048E+00
0.5500   6.4177E-01  4.6062E-27  1.2133E-34  9.2567E-16  1.6210E-11  4.5547E-04  9.2245E+00
0.5800   [illegible] 3.6093E-27  8.7422E-35  7.6911E-16  1.4781E-11  4.6957E-04  9.1541E+00
0.6130   [illegible] 2.8378E-27  6.4649E-35  6.4927E-16  1.3574E-11  4.8233E-04  9.0915E+00
0.6430   [illegible] 2.2887E-27  4.8826E-35  5.5517E-16  1.2539E-11  4.9420E-04  9.0356E+00
0.6700   6.5723E-01  1.8312E-27  3.7328E-35  4.7859E-16  1.1619E-11  5.0546E-04  8.9852E+00
0.7000   6.6032E-01  1.4849E-27  2.8705E-35  4.1462E-16  1.0782E-11  5.1651E-04  8.9395E+00
0.7300   [illegible] 1.2038E-27  2.2069E-35  3.5990E-16  9.9989E-12  5.2764E-04  8.8980E+00
0.7600   [illegible] 9.6[illegible]E-28  1.6749E-35  3.1109E-16  9.2343E-12  5.3947E-04  8.8601E+00
0.7900   [illegible] 7.615[illegible]E-28  1.2437E-35  2.6678E-16  8.4678E-12  5.5249E-04  8.8254E+00
0.8200   6.7146E-01  5.7477E-28  8.7328E-36  2.2341E-16  7.6332E-12  5.6818E-04  8.7937E+00
0.8500   6.7454E-01  [illegible] 5.7012E-36  1.8145E-16  6.7208E-12  5.8742E-04  8.7647E+00
0.8800   6.7790E-01  2.5231E-28  3.1121E-36  1.3622E-16  5.6017E-12  6.1432E-04  8.7383E+00
0.8930   6.7977E-01  1.2[illegible]E-28  1.2343E-36  9.2594E-17  4.3167E-12  6.5132E-04  8.7146E+00
0.9000   [illegible] 3.2652E-29  2.3734E-37  4.2476E-17  2.5912E-12  7.1455E-04  8.6934E+00
```

```
0.9700   6.7135E-01   3.5196E-30   1.4168E-38   1.2054E-17   1.1748E-12   7.9266E-04   8.6765E+00
1.0800   7.0921E-01   2.5824E-43   1.7260E-50   3.6911E-18   1.7772E-13   8.8568E-04   8.6644E+00
                                TIME LEFT =     1211508 MSEC
```

VITA

John Frederick Balhoff was born Thursday, October 14, 1948 in Howell, Michigan about 30 miles west of Detroit to his proud but poor parents Jack and Kaye. Shortly after accepting his discharge from the hospital he made the acquaintance of his two older brothers, Mike and Tom. Little did he realize he was to be followed by six more brothers and two sisters - Bob, Don, Bill, Dick, George, Margaret, Kathleen, and Danny. At this writing it appears that no more siblings will be announced.

Elementary education was achieved at Sacred Heart and St. Aloysius parochial schools in Baton Rouge where a somewhat dubious career of academia commenced. In the Fall of 1962, secondary education was initiated at St. Joseph's Seminary in St. Benedict, Louisiana where an attempt was made to become a man of the cloth. Three years was sufficient to be convinced that the calling was no longer there and another profession would have to be pursued. The last year of secondary education was accomplished at Catholic High School in Baton Rouge and graduation came in May of 1966.

In June of 1966 the spurious career of a new chemical engineer began when the author enrolled at Louisiana State University in Baton Rouge. In May of 1970 he was awarded a Bachelor of Science in chemical engineering. Continuing his education by attending graduate school at L.S.U. in August, 1970, the author recieved his Master of Science in chemical engineering in May of 1972. Being ambitious and somewhat foolish, pursuit of a doctorate was initiated immediately following his M.S. graduation. On the 29th of October 1973, prior to completion of all the requirements of the doctoral program, he started employment at Ethyl Corporation, Baton Rouge naively assuming that in a couple of months the work on the doctorate would be finished.

Presently the author is still working for Ethyl Corporation as a Process Evaluation Engineer and plans to attend graduation in May of 1975. At this time the author is not married with no immediate prospects in sight.